Analysis of Pipeline Systems under Harmonic Forces

By

Raydin Salahifar

A dissertation

submitted in partial fulfillment of the requirements for

Doctor of Philosophy in Civil Engineering

Supervised by

Dr. Magdi Mohareb

Department of Civil Engineering

University of Ottawa

© Raydin Salahifar, Ottawa, Ontario, Canada, 2011

To my dearest mother & to the pure soul of my beloved father

Farideh & Behroox Salahifar

Abstract

Starting with tensor calculus and the variational form of the Hamiltonian functional, a generalized theory is formulated for doubly curved thin shells. The formulation avoids geometric approximations commonly adopted in other formulations. The theory is then specialized for cylindrical and toroidal shells as special cases, both of interest in the modeling of straight and elbow segments of pipeline systems.

Since the treatment avoids geometric approximations, the cylindrical shell theory is believed to be more accurate than others reported in the literature. By adopting a set of consistent geometric approximations, the present theory is shown to revert to the well known Flugge shell theory. Another set of consistent geometric approximations is shown to lead to the Donnell-Mushtari-Vlasov (DMV) theory.

A general closed form solution of the theory is developed for cylinders under general harmonic loads. The solution is then used to formulate a family of exact shape functions which are subsequently used to formulate a super-convergent finite element. The formulation efficiently and accurately captures ovalization, warping, radial expansion, and other shell behavioural modes under general static or harmonic forces either in-phase or out-of-phase. Comparisons with shell solutions available in Abaqus demonstrate the validity of the formulation and the accuracy of its predictions.

The generalized thin shell theory is then specialized for toroidal shells. Consistent sets of approximations lead to three simplified theories for toroidal shells. The first set of approximations has lead to a theory comparable to that of Sanders while the second set of

approximation has lead to a theory nearly identical to the DMV theory for toroidal shells. A closed form solution is then obtained for the governing equation. Exact shape functions are then developed and subsequently used to formulate a finite element. Comparisons with Abaqus solutions show the validity of the formulation for short elbow segments under a variety of loading conditions. Because of their efficiency, the finite elements developed are particularly suited for the analysis of long pipeline systems.

Acknowledgement

I would like to express my deepest gratitude to my supervisor Dr. Magdi Mohareb for his continuous encouragement, assistance, advice and support during the course of this research. It has been truly a great honour and a unique experience for me to work with such a distinguished professor and a leading researcher. He always offered his most sincere support with utmost generosity and walked the author throughout the challenging path of research.

I am always grateful to my beloved father, Behrooz, who passed a way in Iran while I was studying in Canada, and to my dearest mother, Farideh, for their continuous support and sacrifice for me. I am truly indebted to my parents and my sister, Rozita, for being a boundless source of love and inspiration. It was certainly their ceaseless support and unconditional love that has led me throughout all challenges of my life.

I wish to express my special gratitude to Dr. Hiroshi Tanaka and Mr. Mahmoud Badavam for their most sincere encouragement and support in initiation, progress and completion of this study.

The last but not the least, I would like to thank the Baha'i Community of Canada and the Baha'i Institute for Higher Education (BIHE) for their encouragement and support. The author would also like to extend his appreciation to all his family, Samin and Parviz Moradipour in particular, and all his friends, Rafael Flores Vera, Elham Seddigh, Lester Clark and Haleh and Farhood Nowzartash in particular, for their unforgettable and limitless support during my studies in Canada.

Table of Contents

Absract ii

Acknowledgement iv

Table of Contents v

List of Tables xv

List of Figures xvii

Chapter 1 1

Introduction 1

1.1 Description of the Problem/Motivation 1

1.2 Scope of the Research 3

1.2.1 Geometric Description 3

1.2.2 Features of the Model 4

1.2.3 Limitations of the Model 5

1.3 Other Applications 6

1.4 Literature Review 6

1.4.1 Studies on Free Vibration 7

1.4.2 Studies on Steady state Response 8

1.4.3 Studies on Finite Element Formulations 10

1.5 Thesis Overview and Methodology 13

1.6 References 16

Chapter 2 23

A Generalized Thin Shell Theory 23

2.1 Abstract 23
2.2 Introduction 23
2.3 Geometry of Curved Surfaces 25
2.3.1 The First Fundamental Tensor of a Surface 26
2.3.2 The Second Fundamental Tensor of a Surface 28
2.4 Geometry of Thin Shells 29
2.5 Strains in Thin Shells 32
2.6 Displacements of a Point within the Shell 32
2.7 Stress-Strain Relationship 36
2.8 Generalized Constitutive Elasticity Tensor for Thin Shells 37
2.9 Hamilton's Principle for Thin Shells 37
2.10 Summary and Conclusion 38
2.11 References 38
2.12 List of Symbols 40
Appendix 2.A. Contravariant Components of the Displacement 44
Appendix 2.B. Reduction of the Number of Components of the Constitutive Elasticity Tensor 46
Appendix 2.C. Expanding the Term $U_{\alpha}|_{\beta}$ 51
Appendix 2.D. Expansion of Hamilton's Principle for Thin Shells 53
2.D.1. Variation of the Kinetic Energy 53
2.D.2. Variation of the Potential Energy 54
Appendix 2.E. Proof of $U_3||_{\beta} = U_{3,\beta}$ 57
Chapter 3 60

Circular Cylindrical Thin Shell Theory 60
3.1 Abstract 60
3.2 Geometry 60
3.3 Base Vectors for Middle Surface 60
3.4 Curvature of the Middle Surface 62
3.5 Base Vectors for a General Surface 62
3.6 Differential Volume Element 63
3.7 Relating the Curvature of Middle Surface to that of a General Surface 63
3.8 Expressions for Displacements 64
3.9 Expressions for Strains 65
3.10 Expressions for the Elastic Constitutive Tensor 65
3.11 Hamilton's Principle for Thin Circular Cylindrical Shells 66
3.12 Discussion 68
3.13 Comparison of Different Theories 70
3.14 Conclusion 76
3.15 References 77
3.16 List of Symbols 78
Appendix 3.A. Generic In-plane Strain- Midsurface Displacement Relationship for Circular Cylindrical Thin Shells 83
Appendix 3.B. Explicit Expression of Hamilton's Principle for Circular Cylindrical Shells 84
3.B.1. Kinetic Energy 84
3.B.2. Internal Strain Energy 86
3.B.3. External Work 93

3.B.4. Boundary Conditions 95
3.B.5. Hamilton's Principle Expression 100
Chapter 4 103
Analysis of Circular Cylindrical Thin Shells under Harmonic Forces 103
4.1 Abstract 103
4.2 Introduction 104
4.3 Literature Review 104
4.4 Studies on Free Vibration 105
4.5 Studies on Steady state Response 105
4.6 Assumptions 108
4.7 Statement of the Problem 108
4.8 Preliminaries 109
4.9 Displacement Distribution across the Shell Thickness 109
4.10 Strain-Displacement Relations 110
4.11 Stress-Strain Relations 110
4.12 Formulation 111
4.12.1 Hamilton's Principle for Circular Cylindrical Thin Shells 111
4.12.2 Force Functions 114
4.12.3 Displacement Functions 114
4.12.4 Equilibrium Condition 116
4.12.5 Homogeneous Solution of Field Equations 118
4.12.6 Particular Solution of Field Equations 121
4.12.7 General Solution of Field Equations 122
4.12.8 Boundary Conditions 122

4.12.9 General Displacement Fields 124
4.13 Solution Steps 124
4.14 Examples 125
4.14.1 Example 1 125
4.14.2 Example 2 130
4.14.3 Example 3 132
4.14.4 Example 4 137
4.15 Summary and Conclusions 142
4.16 Acknowledgement 143
4.17 References 143
4.18 List of Symbols 147
Appendix 4.A. Expressions for Out-of-Phase Forces 152
Appendix 4.B. Coefficients of Boundary and Field Terms 154
Appendix 4.C. Constants in Characteristic Equations 156
Chapter 5 157
Finite Element for Pipes under Harmonic Forces 157
5.1 Abstract 157
5.2 Scope and Literature Review 157
5.3 Geometry and Loading 161
5.4 Assumptions 162
5.5 Variational Expression 163
5.6 Expressions for Applied Forces 165
5.7 Steady State Displacement Functions 166
5.8 Equilibrium Conditions 167

5.9 Formulating Exact Shape Functions 168
5.10 Equilibrium Equations 171
5.11 General Displacement Fields 172
5.12 Strain and Stress Fields 172
5.13 Examples 173
5.13.1 Example 1 173
5.13.2 Example 2 176
5.13.3 Example 3 179
5.13.4 Example 4 180
5.14 Conclusion 183
5.15 Acknowledgement 183
5.16 References 184
5.17 List of Symbols 188
Appendix 5.A. Coefficients of Boundary and Field Terms 193
Appendix 5.B. Constants in Characteristic Equations 195
Appendix 5.C. Entries of Stiffness Matrix and Force Vector 196
5.C.1. Stiffness Matrix 196
5.C.2. Force Vector 198
Appendix 5.D. Matlab Code for Example 1 200
Chapter 6 221
Formulation of Thin Shell Theories for Toroids 221
6.1 Abstract 221
6.2 Introduction 221
6.3 Geometry 222

6.4 Constitutive Elasticity Tensor 226
6.5 Strain-Displacement Relationships 226
6.6 Generalized Representation on Toroidal Thin Shell Theories 231
6.7 Field Equations of Toroidal Thin Shell Theories 234
6.7.1 DMV Theory 235
6.7.2 TTS-V3 Theory 235
6.7.3 TTS-V2 Theory 236
6.7.4 Sanders Theory 236
6.8 A Modified Toroidal Thin Shell Theory (TTS-V2M) for Elbows of Common Geometry 237
6.9 Conclusions and Remarks 239
6.10 References 240
6.11 List of Symbols 241
Appendix 6.A Coefficients of Various Toroidal Thin Sell Theory 245
6.A.1 Coefficients for DMV Theory 245
6.A.2 Coefficients for TTS-V3 Theory 246
6.A.3 Coefficients for TTS-V2 Theory 250
6.A.4 Coefficients for Sanders Theory 254
6.A.5 Coefficients for TTS-V2M Theory 255
Appendix 6.B Comparative Review of Various Toroidal Thin Shell Theories 259
Chapter 7 289
Finite Element Formulation for Toroidal Thin Shells 289
7.1 Abstract 289
7.2 Introduction 289

7.3 Literature Review 290
7.4 Assumptions 292
7.5 Hamilton's Principle for Toroidal Thin Shells 293
7.6 Overview of the Formulation 295
7.6.1 Displacement Function Expressions 295
7.6.2 Approximations for Coefficients Dependent on Circumferential Coordinate 296
7.6.3 Truncation of Intermodal Coupling 297
7.6.4 Equilibrium Condition in Terms of Longitudinal Coordinate 298
7.7 Formulation of the Field Equations 302
7.8 Homogeneous Solution 306
7.9 Finite Element Development 308
7.9.1 Formulation of Shape Functions 308
7.9.2 Discretized Equilibrium Equations 310
7.10 Example 317
7.11 Summary and Conclusion 321
7.12 References 322
7.13 List of Symbols 325
Appendix 7.A Coefficients for the TTS-V2 Theory 331
Appendix 7.B Coefficient Matrices in the Functional 336
7.B.1 Explicit Expressions for c_{ij} and h_{ij} 337
7.B.2 Entries of Matrices ${}_{\mathbf{v}}\mathbf{H}_{n}^{i}$, ${}_{\mathbf{v}}\mathbf{G}_{n}^{i}$, ${}_{\mathbf{v}}\mathbf{H}_{j.n}^{xw}$, ${}_{\mathbf{v}}\mathbf{G}_{j.n}^{xu}$, ${}_{\mathbf{v}}\mathbf{G}_{j.n}^{sv}$, ${}_{\mathbf{v}}\mathbf{G}_{j.n}^{zw}$, ${}_{\mathbf{v}}\mathbf{G}_{j.n}^{xw}$ and ${}_{\mathbf{v}}\mathbf{G}_{j.n}^{sw}$ 345
Chapter 8 375

Conclusions and Remarks....375
8.1 Summary and Conclusions....375
8.2 Proposed Future Work....377
Appendix A....378
Mathematical Preliminaries....378
A.1 Objective and Scope....378
A.2 Introduction....378
A.3 Conventions....379
A.4 Coordinate Transformation....379
A.4.1 Contravariant Law of Transformation....379
A.4.2 Covariant Law of Transformation....380
A.5 Tensors....382
A.5.1 Contravariant Tensors....382
A.5.2 Covariant Tensors....382
A.5.3 Mixed Tensors....383
A.6 Covariant Base Vectors....383
A.7 Reciprocal Contravariant Base Vectors....384
A.8 Algebra of Tensors....385
A.8.1 Addition and Subtraction....385
A.8.2 Outer Product....386
A.8.3 Contraction....386
A.8.4 Inner Product....386
A.8.5 Scalar Product....387
A.9 Invariant Formulation....387

A.10 The First Fundamental Tensor 388
A.11 Lowering and Raising of indices 388
A.12 Permutation Tensor 389
A.13 Determinant 389
A.14 Cross Product 390
A.15 Surface and Volume Elements 390
A.16 Christoffel Symbol 391
A.16.1 Symmetry Property 393
A.16.2 Evaluation of the Christoffel Symbol 393
A.17 Covariant Derivatives 394
A.17.1 Covariant Derivative of First Order Tensors 394
A.17.2 Covariant Derivative of Second Order Tensors 395
A.17.3 Second Covariant Derivative of First Order Covariant Tensors 395
A.18 Strain Expressions for a Continuum 396
A.18.1 Strains in Terms of First Fundamental Tensor 396
A.18.2 Strain Tensor In Terms of Displacements 397
A.19 Hamilton's Principle in Tensor Form 398
A.19.1 Kinetic Energy 399
A.19.2 Internal Strain Energy 400
A.19.3 External Work 401
A.20 Physical Components of Tensors 401
A.21 References 402
A.22 List of symbols 404

List of Tables

Table 3.1 - Comparing strain-displacement in various thin shell theories 70

Table 3.2 - Coefficients in first equilibrium equation (Eq. 3.28a) in various theories 72

Table 3.3 - Coefficients in second equilibrium equation (Eq. 3.28b) in various theories 73

Table 3.4 - Coefficients in third equilibrium equation (Eq. 3.28c) in various theories 74

Table 4.1 - Mid-span deflection at point A 128

Table 4.2 - Displacements (in $10^{-2}\ mm$) of points A, B, C and D 132

Table 4.3 - Displacements (in mm) at top of cylinder 135

Table 4.4 - Displacements at mid-span 140

Table 5.1 - Mid-surface displacement components of Point J (in mm) 183

Table 6.1 - Comparison of longitudinal strain-displacement expressions in various toroidal thin shell theories 229

Table 6.2 - Comparison of circumferential strain-displacement expressions in various toroidal thin shell theories 229

Table 6.3 - Comparison of shear strain-displacement expressions in various toroidal thin shell theories 230

Table 6.4 - Membrane (M) and flexural (F) effects in differential operators L_{ij} (Field terms). 238

Table 6.5 - Membrane (M) and flexural (F) effects in differential operators D_{ij} (Boundary terms). 239

Table 6.6 - Comparison of l_i coefficients in various toroidal thin shell theories 259

Table 6.7 - Comparison of d_i coefficients in various toroidal thin shell theories 278

Table 6.8 - Comparison of I_i^I coefficients in various toroidal thin shell theories.....288

Table 7.1 - Scenarios in the Example 318

Table 7.2 - Geometric and mechanical properties of the toroid and their equivalent in MATLAB codes 337

Table 7.3 - Font conversion between the text symbols and their equivalent in MATLAB codes 346

List of Figures

Figure 1.1 - Piping system in an Offshore Structure 3

Figure 1.2 - Piping system in a Petrochemical Plant 4

Figure 2.1 - General Curved Surface 26

Figure 2.2 - Geometry of surface 27

Figure 2.3 - Shell Geometry 30

Figure 2.4 - Deformed and Un-deformed Configurations of a Thin Shell 33

Figure 2.5 - Displacement of a generic point within the shell 36

Figure 3.1 - Cartesian and Curvilinear Coordinates 61

Figure 4.1 - Cylinder geometry and coordinate definition 109

Figure 4.2 - Cross sectional profile of the traction 126

Figure 4.3 - Radial displacements at point A 129

Figure 4.4 - Radial displacement of point A as a function of exciting frequency 130

Figure 4.5 - Wave forces on a vertical circular cylinder 133

Figure 4.6 - Transverse displacement of point A 136

Figure 4.7 - Longitudinal stresses along a generator going through point A (Solid lines denote the results from current model and dash-dotted lines denote the results from Abaqus) 137

Figure 4.8 - a) Patch Loading area and the direction of the out of phase applied tractions q_L and q_V, and b) Distribution of the vertical traction q_V 138

Figure 4.9 - a) Applied forces q_L and q_V (in KN) b) Axial response u at point J (in mm) c) Circumferential response v and radial response w at point J (in mm). In all cases abscissa is time in terms of period of excitation. 141

Figure 5.1 - Cylinder geometry and coordinate definition 162

Figure 5.2 - Example 1, Cantilever pipe with tip point load 173

Figure 5.3 - Longitudinal, circumferential and radial displacements of the generator of the beam at $s/R = 11\pi/6$ 175

Figure 5.4 - Deformed Configuration for a pipe subject to point load based on a) Current Model (solid lines denote the top and bottom generators and dash-dotted line denotes the generator at $s/R = 11\pi/6$), and b) Abaqus S4R shell model 176

Figure 5.5 - Pipe configuration 176

Figure 5.6 - Maximum stresses along the top generator for inner surface ($z = -h/2$), mid-surface ($z = 0$), and outer surface ($z = +h/2$). Solid lines denote results based on the current study and dotted lines denote results based on the Abaqus 179

Figure 5.7 - a) Patch Loading area and the direction of the out of phase applied tractions q_L and q_V, and b) Distribution of the vertical traction q_V 180

Figure 5.8 - Maximum mid-surface displacement components along the top generator 182

Figure 6.1 - Toroid geometry and coordinate definition 222

Figure 6.2 - Comparing coefficient d_{15} from various theories 282

Figure 6.3 - Comparing coefficient d_{17} from various theories 284

Figure 7.1 - Comparison of coefficients ζ^{-3} and corresponding approximate Fourier series 297

Figure 7.2 - Schematic matrices of coefficients a) Matrix of coefficients of the uncoupled system of a CCTS, b) Matrix of coefficients of the coupled system of a toroidal thin shell302

Figure 7.3 - Schematic presentation of matrices ${}^{i}\bar{\mathbf{G}}$ and ${}^{i}\mathbf{G}$ and their constructing blocks ${}^{i}\mathbf{G}_{n}$ and ${}^{i}_{\mathbf{v}}\mathbf{G}_{n}$ 304

Figure 7.4 - Schematic presentation of matrices ${}^{i}\bar{\mathbf{H}}$ and ${}^{i}\mathbf{H}$ and their constructing blocks ${}^{i}\mathbf{H}_{n}$ and ${}^{i}_{\mathbf{v}}\mathbf{H}_{n}$ 312

Figure 7.5 - Schematic presentation of matrices $\bar{\mathbf{X}}^{\mathbf{xx}}_{j}$ and $\mathbf{X}^{\mathbf{xx}}_{j}$ and their constructing blocks $\mathbf{X}^{\mathbf{xx}}_{jn}$ and ${}_{\mathbf{v}}\mathbf{X}^{\mathbf{xx}}_{jn}$.....314

Figure 7.6 - Fixed-free pipe bend in the Example 317

Figure 7.7 - Pipe bend under axial traction (Scenario a), $L = 0.15\,m$ 319

Figure 7.8 - Pipe bend under uniform torsion (Scenario b), $L = 0.15\,m$ 319

Figure 7.9 - Pipe bend under uniform radial traction (Scenario c), $L = 0.05\,m$ 320

Figure 7.10 - Pipe bend under self weight (Scenario d), $L = 0.10\,m$ 320

Figure 7.11 - Pipe bend under out-of-plain harmonic moment (Scenario e), $L = 0.05\,m$ 321

Figure 7.12 - Block diagram of the evaluation of constant matrices ${}_{\mathbf{v}}\mathbf{H}^{i}_{n}$, ${}_{\mathbf{v}}\mathbf{G}^{i}_{n}$, ${}_{\mathbf{v}}\mathbf{H}^{xw}_{j.n}$, ${}_{\mathbf{v}}\mathbf{G}^{xu}_{j.n}$, ${}_{\mathbf{v}}\mathbf{G}^{sv}_{j.n}$, ${}_{\mathbf{v}}\mathbf{G}^{zw}_{j.n}$, ${}_{\mathbf{v}}\mathbf{G}^{xw}_{j.n}$ and ${}_{\mathbf{v}}\mathbf{G}^{sw}_{j.n}$.....336

Figure A. 1 - A point defined in Two 3D curvilinear coordinate systems 380

Figure A. 2 - Infinitesimal volume element.....391

Chapter 1

Introduction

1.1 Description of the Problem/Motivation

Elevated pipeline systems in petrochemical plants and power plants are subject to a variety of loading conditions. Some of these loads are static or quasi-static and include a) gravity loads induced by self weight, weight of the fluids/gases they convey, heavy valves, etc., b) thermal effects induced by atmospheric temperature changes and temperature changes of fluid they convey, c) internal pressure of the fluids they convey.

Pipelines can also be subject to dynamic forces induced by machinery, and seismic action on the fluids they convey. Harmonic forces are one of the most common types of dynamic forces in piping systems. They can arise in machinery from the eccentricity of rotary parts in pumps, turbines, engines, generators, and propellers. Also, they arise from the beating phenomenon in pumps and conveyance systems. The oscillatory nature of internal strains and stresses caused by harmonic forces can severely shorten the life time of the structure by leading to rupture failure due to fatigue, particularly when the structures are subjected to such loads for most of their operational time.

Under these loads, the steady-state response of the pipe system needs to be determined for fatigue design consideration since it represents the sustained effect. The transient response is of little importance in the fatigue design as it tends to dampen out quickly.

Under the above loads, large diameter pipes can undergo complex shell deformational behaviour. This includes ovalization, warping, radial extensibility, and other effects that are not captured by beam models. In contrast, general shell models are capable of capturing these effects. Existing finite element softwares are equipped with shell elements capable of capturing these effects. The underlying models involve thousands of degrees of freedom to model short pipe segments.

Elevated pipeline systems can span several hundreds of meters. The use of conventional shell finite element in such a long pipe system yields an impractical large model. In these applications, shell based analytical solutions become impractical. Also, the use of conventional shell finite elements aimed at capturing localized shell effects necessitates a large number of degrees of freedom which makes them impractical as design tools.

Pipe elements bring about a promising class of finite elements for such applications. Some of these elements are based on shell behaviour. In these elements, the axi-symmetric geometry of the pipe is exploited to transform the shell problem from a 2D problem into a uni-dimensional problem, thus significantly reducing the degrees of freedoms necessary to model the problem.

In this class of finite elements, the unknown displacements fields are expressed in terms of Fourier series with respect to the circumferential coordinate. In the longitudinal direction, researchers have adopted various approximate shape functions such as Hermitian

polynomials (e.g. [1.1] and [1.2]), Lagrangian interpolation functions (e.g. [1.3] and [1.4]), Harmonic functions (e.g. [1.2] and [1.5]), or a combination thereof. The finite element mesh based on pipe elements is discretized only along the longitudinal direction of the cylinder and no discretization is needed in the circumferential direction, resulting in significant

1.2 Scope of the Research

1.2.1 Geometric Description

A pipeline system (Figure 1.1 and Figure 1.2) typically consists of straight segments, curved segments, annular flanges, hemispherical caps, and T-junctions. The present study aims at developing accurate and efficient finite element models for the analysis of two main elements of the piping systems, i.e. straight pipes and curved pipes. Other components such as annular flanges, hemispherical caps, etc. could be considered as future extensions to this work.

Figure 1.1 - Piping system in an Offshore Structure

Source: http://main.oceanus-eng.com

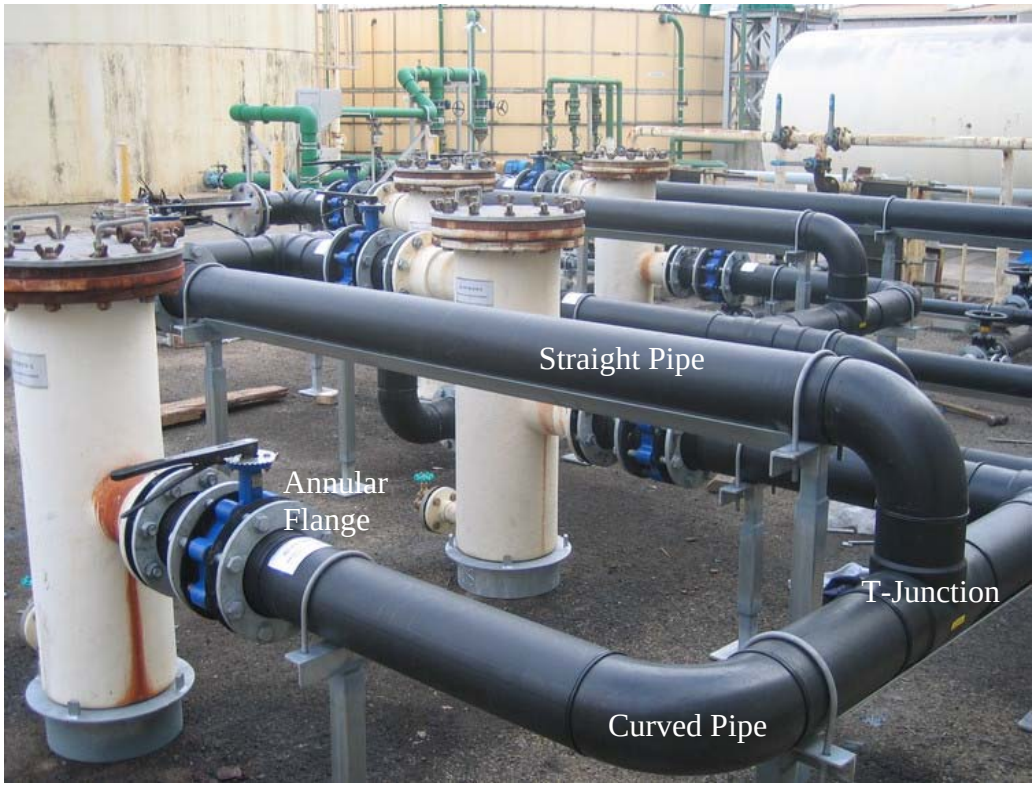

Figure 1.2 - Piping system in a Petrochemical Plant

Source: http://www.piha.com.au/what_we_do/process_pipe_work.phtml

1.2.2 Features of the Model

1) The model is to capture the steady state response of pipes under harmonic loads of general distributions including body forces, surface tractions, ring loads, line loads or point loads.

2) The applied harmonic forces can be applied in-phase or out-of-phase.

3) The model is applicable to general boundary conditions and support excitations.

4) The model is to capture full shell behaviour including ovalization, warping, and mid-surface longitudinal and circumferential extensibility. This is accomplished by avoiding common simplifying assumptions in most developments in the literature.

5) The model is capable of modelling of hysteretic damping.

The present formulation departs from previous pipe finite element formulations in the following respects:

1) It adopts a family of interpolation functions for the displacement fields based on the closed-form solution of the homogeneous form of the equilibrium equations. This feature is intended to remove the approximations arising from longitudinal descretization, in contrast to most previous work.

2) While most solutions developed in the literature focus on either the static response (e.g. [1.1], [1.2] and [1.3]) or on the free vibration (e.g. [1.6] and [1.7]), the present study extends the developments to the steady state response of straight and curved pipes under harmonic loads. The solution directly captures the steady state response without the need to extract the modal shapes and natural frequencies.

3) While most studies (e.g. [1.3], [1.4], [1.8] and [1.9]) typically use only a limited number of or certain harmonic terms, the present formulation for straight pipe segments is applicable to any number of terms. In practicality, the number of terms in a series will be truncated when the accuracy sought is reached.

1.2.3 Limitations of the Model

1) Given the frequent to permanent nature of harmonic loads in the aforementioned applications, pipe systems are normally designed to respond to harmonic effects within the linearly elastic range of their material. Thus, the present study is limited to the elastic isotropic material.

2) Material and geometric nonlinear effects are outside the scope of the formulations.

3) While multiple harmonic forces can be modelled within the present formulation, all forces need to have the same exciting frequency.

4) The formulation captures only the steady state response. The transient response is not captured within the present formulation.

1.3 Other Applications

a) Although the primary motivation of this study is the analysis of pipeline systems, the work is applicable to other applications. This includes structural members (e.g., hollow structural sections), members of offshore structures and platforms, cooling towers, aircraft fuselages, naval halls of submarines etc. In these applications, members are commonly subject to harmonic loads either due to machine loads, wave induced hydrodynamic loads, wind or water flow induced vortex shedding effects etc. The model developed herein is either applicable or expandable to these cases.

b) The model is capable of capturing the response of pipe systems under static case as a special case.

c) It is possible to extract the natural frequencies and corresponding mode shapes from the present model.

1.4 Literature Review

Several studies have focused on the dynamic analysis of shells. This includes a) solutions aimed at determining the free vibration characteristics of shells (i.e., natural frequencies and

mode shapes), b) those that are geared towards determining the closed form solution to the steady-state response of pipes, and c) finite element formulations. Studies under the above three categories are summarized in the following subsections. Other studies aimed at investigating the full dynamic response of pipes are outside of the scope of the present review.

1.4.1 Studies on Free Vibration

The monograph by Leissa [1.10] presented a compilation of studies focusing on free vibration of circular cylindrical thin shells (CCTSs) based on various kinematic assumptions and shell theories. Markus [1.11] provided a comparative study on the elastic free vibration analysis of cylindrical shells. In two companion papers, Qatu ([1.12] and [1.13]) provided a review summary of recent research advances on the dynamic response of laminated composite shells and homogeneous shells with emphasis on free vibrations. Recent developments include also the work of Xiang et al. [1.14] who investigated the vibration of CCTSs with intermediate ring supports. Jafari and Bagheri [1.15] studied the free vibration of non-uniformly ring stiffened CCTSs. Xuebin [1.16] investigated the free vibration of the CCTSs using Fourier decomposition. Rougui et al. [1.17] provided a semi-analytical solution for geometrically non-linear free vibration of simply supported CCTSs. Zhang and Xiang [1.18] developed the exact solutions for the vibration of CCTSs with step-wise thickness variations in longitudinal direction. Using a wave propagation approach, Xuebin [1.19] conducted a free vibration analysis of CCTS and Gan et al. [1.20] investigated the free vibration analysis of ring-stiffened CCTSs. In a recent paper, Matsunaga [1.21] studied the free vibration and stability of functionally graded (layered) CCTSs.

1.4.2 Studies on Steady state Response

This section focuses on dynamic solutions, with emphasis on analytical developments rather than computational solutions. Warburton [1.22] studied the response of a simply supported uniform CCTSs under a harmonic transverse point force acting at mid-span. He adopted Novozhilov's thin shell theory and applied a double Fourier series solution in the longitudinal and circumferential coordinates when expanding the displacement fields. He modelled hysteretic damping by adopting the complex form of Young's modulus. Later on, Warburton and Soni [1.23] extended their work to the case of orthotropic CCTSs.

Leissa [1.24] extended the work of Warburton [1.22] to model the response of a simply supported CCTS under harmonic radial pressure. In their solution, they postulated displacement fields with distributions similar to the applied radial pressure. Structural damping was modelled in the solution.

Beskos and Oates [1.25] used the dynamic stiffness influence coefficients approach. Using Laplace transforms, they developed a numerical solution for the analysis of the simply supported ring-stiffened CCTSs under harmonic loading. In their analysis only circular symmetric vibrations of shell segments and radial and torsional vibrations of the rings were considered.

Zarutskii [1.26] developed a closed-form solution for the response of simply supported CCTSs with longitudinal stiffeners subject to general harmonic pressure. The Kirchhoff-Love thin shell theory was adopted to model the cylinder while the Kirchhoff-Klebsch rod theory was adopted to model the longitudinal stiffeners.

By combining the method proposed by Forsberg [1.27] for free vibration analysis of shells and a general solution technique for one-dimensional forced vibration problems, Glandier et al. [1.28] developed an analytical solution for in-vacuo vibration of CCTSs with general boundary conditions subjected to harmonic point load. Using Donnell's thin shell theory, the cylinder was longitudinally subdivided into two domains. The homogenous solution of the system of differential equations was expressed for both domains. The problem was then solved by enforcing four boundary conditions at each end of the cylinder, seven continuity conditions, and one discontinuity condition at the interface of the two sub-domains.

Huang and Fuller [1.29] studied the effect of dynamic absorbers on the reduction of vibration and sound level in the enclosed acoustic field within CCTS under harmonic radial point loading and patch loading. Their analytical solution was based on the Donnell-Mushtari shell theory. Their solution was based on the substructure synthesis and modal expansion techniques. However, only the radial displacement expression is reported in their study.

Using the Lagrangian approach, Amabili [1.30] performed a comparative study on the large amplitude response of CCTS subjected to radial harmonic force by evoking Donnell's, Sanders-Koiter , Flugge-Lure-Byrne, and Novozhilov's non-linear shell theories.

Pellicano and Avramov [1.31] investigated the dynamic behaviour of vertical CCTS clamped at the bottom end and connected to a rigid disk at the top. Their study focussed on a) the free vibration of CCTSs and b) those subject to harmonically excited supports. The Sanders-Koiter non-linear theory was adopted and approximate trial functions were assumed for the displacement fields. Using the Sanders-Koiter theory and a mixed modal

decomposition of the displacement fields (trigonometric functions in circumferential direction and Chebyshev polynomials in the longitudinal direction), Pellicano [1.32] developed a solution for the linear and nonlinear, free and harmonically forced vibration of CCTSs.

Duan and Koh [1.33] developed an analytical solution method for the axisymmetric transverse vibration of cylindrical shells with variable thickness under transverse forces based on a generalized hyper-geometric function.

1.4.3 Studies on Finite Element Formulations

A comprehensive review of finite element formulations for pressure vessels and piping is provided in Mackerle [1.34]-[1.37]. The following review focuses on shell based pipe elements, either curved or straight, with this particular feature. Various studies have used different interpolation schemes in the longitudinal directions and number of harmonic modes as detailed in the following.

Based on the principle of virtual work, Ohtsubo and Watanabe [1.1] developed a ring element for small strains for torus elements. Displacement components are interpolated by Hermitian polynomials along the elbow. Their model captures both ovalization and warping effects. Takeda et al. [1.2] modified the work of Ohtsubo and Watanabe [1.1] by including the transverse shear effects in their formulation and adopting 2D Lagrangian bilinear functions to interpolate the circumferential, radial displacements, and rotations. The longitudinal displacement is interpolated using Fourier series in the circumferential direction and linear functions in the longitudinal direction.

Bathe and Almeida [1.3] developed a four node elbow finite element for in-plane flexure analysis. Based on Lagrangian cubic interpolation of the displacement fields, their model captures circumferential shear deformation and ovalization effects and neglects warping effects. They extended their model to investigate interaction effects between elbow elements and straight pipe segments [1.38]. Also, they added geometric non-linear effects to the formulation [1.39].

Militello and Huespe [1.4] extended the model by Bathe and Almeida [1.3] to capture warping deformations by adopting a Lagrangian cubic interpolation for the longitudinal displacement. The tangential and radial displacements were interpolated using harmonic functions. Abo-Elkhier [1.40] generalized the model by Bathe and Almeida [1.3] by adopting more complete displacement-strain relations into the formulation. In a ring formulation, Melo and Castro [1.41] used simple linear interpolation for displacements which captures both in-plane and out-of-plane flexure of curved pipes.

Yan et al. [1.42] developed an element for elasto-plastic limit load of pipe elbows by relaxing the pipe inextensibility assumption in the radial direction adopted in the model by Militello and Huespe [1.4]. They used cubic Lagrangian interpolation for the longitudinal displacement and Hermitian polynomials for the tangential and radial displacements.

Sivadas and Ganesan [1.43] developed a finite element method for the vibration of thin orthotropic cantilever circular cylindrical shell with variable thickness in axial direction. In their five-node element, shear deformation effects are included, fourth order Lagrangian polynomials are used to interpolate displacement components along the pipe.

Stanley and Ganesan [1.44] studied the response of cantilever CCTS with thickness discontinuities subject to harmonic axi-symmetric loads including uniform internal pressure and circular ring load acting at cantilever tip. The longitudinal and circumferential displacements were linearly interpolated while the radial displacement was interpolated using cubic Hermitian functions.

Xi et al. [1.45] developed a semi-analytical model for the vibration of composite shells of revolution based on the Reissner-Mindlin shell theory. The model is based on a two node straight conical frustum element capable of modelling shells of revolutions of general geometries.

Pinto Correia et al [1.46] developed a frustra conica finite element for the analysis of laminated axisymmetric shells based on a higher order shell theory. The radial displacements were interpolated using Hermitian polynomials while the longitudinal and circumferential displacements were interpolated using linear Lagrangian interpolation.

Karamanos [1.47] formulated an element to model buckling instability of pipes. Subsequent extension of the model involved adding plasticity and internal pressure effects (Karamanos et al. [1.48]).

Santos et al [1.49] developed a finite element model based on an axi-symmetric 3D formulation to study the bending, free vibration and buckling behaviour of shells of revolution made of laminated orthotropic elastic material. The displacement fields were linearly interpolated across the thickness and in the form of Lagrange polynomials longitudinally.

Weicker [1.50] developed a cylindrical element for elastic analysis of straight pipes under general static loads. He used the closed-form solution of the homogeneous part of the field equations to develop shape functions. A methodology similar to Weicker's work on straight pipes under static loads is evoked in the current study. However, the present work is more general in three respects: a) It is based on the more general shell theory to be developed in Chapter 2, b) It extends the work to toroidal shells and c) It extends the work to harmonic forces.

1.5 Thesis Overview and Methodology

A survey of the literature reveals the existence of multiple thin-shell theories. Circular cylindrical shell theories include those of Timoshenko [1.51], Novozhilov [1.52], Morley-Koiter[1.53], Flugge and DMV [1.54], etc and those for toroidal shells include Donnell [1.55], Sanders [1.56], Washizu [1.57], DMV [1.59], etc. The difference between various theories lies in the simplifying assumptions adopted. Some of the simplifications adopted are inconsistent. As a result, it was not clear to the candidate which theories are superior. In order to elucidate the problem, Chapter 2 focuses on developing a generalized thin shell theory in which the strain-displacement relationships are formulated based on tensor calculus within the classical thin shell assumptions as a starting point. The stress-strain relations are expressed and the Hamilton functional of the system is formulated in a tensorial form for shells of general geometries. The stationary conditions of the Hamilton functional are then evoked to recover the dynamic equilibrium equations for thin shells of general geometries. Simplifying assumptions adopted in other simplified theories are avoided and the field equations obtained from the present study are thus more general and accurate. The use of the variational approach has also led to the formulation of all possible boundary conditions. For

some theories (e.g. Flugge [1.54] for CCTSs and DMV [1.59] for TTSs), explicit expressions for boundary terms were not reported in the documents collected by the author. Within this context, the present treatment complements these theories.

In Chapter 3, the generalized thin shell theory developed in Chapter 2 is specialized to circular cylinders to obtain the equilibrium equations. Further simplifications in line with those in existing simplified theories are evoked and the existing theories are recovered as special cases of the present one (e.g. Flugge and DMV [1.54],).

The CCTS theory developed in Chapter 3 is used for the analysis of the CCTSs under harmonic forces in Chapter 4. In addition to the assumptions made in Chapter 2, it is assumed that the material is elastic isotropic and only the steady state response is sought. The field equations and the corresponding boundary conditions are expressed in terms of the three unknown displacement fields which are functions of time and two independent coordinates (longitudinal and circumferential) defined at the middle surface of the cylinder. Using the method of separation of variables with respect to time and knowing that the steady-state response of the structure is harmonic allows the elimination of time dependency of the response. By expanding the unknown displacement fields as infinite complex Fourier series in the circumferential direction, and using the orthogonal properties of the Fourier terms when integrating over the circumferential direction, the dependency of the response on the circumferential direction is also eliminated. All functions in the Hamiltonian functional become dependent only on the longitudinal direction. After taking the variation of the functional, a series of ordinary differential equations (ODEs), rather than partial DE, is obtained in terms of longitudinal coordinate. The resulting field equations are coupled and related the longitudinal, circumferential and radial displacement contributions within each

Fourier mode, while uncoupling the contributions of a given Fourier mode from those of other Fourier modes. The complete uncoupling between mode n and modes $m \neq n$ allows a separate solution for each mode with implications on computational efficiency. The solution starts with the most predominant mode and additional contributions from other modes are subsequently added until the desired convergence is obtained. The closed form solution of the homogeneous part of the obtained system of ODEs is developed. Also, a solution scheme of the particular solution for general loading is developed by decomposing the applied forces into infinite complex Fourier series of the longitudinal coordinate. The validity of the method is verified against well established shell solutions and its applicability to practical problems is illustrated through examples.

The analytical solution developed in Chapter 4 is used to develop a finite element for pipe straight segments in Chapter 5. A series of exact shape functions are formulated based on the exact solution of the field equations. The shape functions are then used to formulate a super-convergent finite element able to model long pipelines with very few degrees of freedom while predicting results in exact agreement with those based on the differential equations of equilibrium. The accuracy, efficiency and applicability of the proposed element are illustrated through examples.

In Chapter 6, the generalized thin shell theory developed in Chapter 2 is specialized to toroidal shells. The field equations and boundary conditions are obtained. By making different simplifying geometric assumptions, three different versions of toroidal thin shell theories are proposed. All three toroidal thin shell (TTS) theories are compared to those of Sanders [1.56] and DMV [1.59] theories.

Chapter 7 focuses on formulating a finite element for TTSs developed in Chapter 6. It is observed that the curvature of the torus significantly increases the complexity of the equations in two respects: a) by increasing the number of the terms in the functional and b) The coefficients of the governing equations are no longer constant and consist of trigonometric functions of the circumferential coordinate. Solution for these complexities are proposed and field equations are explicitly solved and used to develop quasi-exact shape functions. The shape functions are subsequently used to develop a finite element for the analysis of pipe elbows.

Chapter 8 provides a summary and conclusion of the work along with recommendations for possible future work.

Appendix A provides a concise review of the fundamentals of tensor calculus with emphasis on aspects relevant to shell analysis. This chapter is aimed to introduce the reader to the basics necessary to understand the developments. This chapter can be skipped by readers who are already familiar with tensor calculus.

Apart from the introductory Chapter 1 and the conclusion Chapter 8, the thesis is written in a paper format. Chapter 4 is published [1.60] and Chapter 5 is in the process of journal review for publication.

1.2 References

[1.1] H. Ohtsubo, O. Watanabe, Stress analysis of pipe bends by ring elements, J. Press. Vessel. Technol. 100 (1978) 112-122.

[1.2] H. Takeda, S. Asai, K. Kwata, A New Finite Element for Structural Analysis of Piping Systems, Proc. Fifth SMIRT Conf. Berlin, 1979.

[1.3] K.J. Bathe, C. A. Almeida, A Simple and Effective Pipe Elbow Element-Linear Analysis, Trans. ASME, J. Appl. Mech. 47 (1980) 93-100.

[1.4] C. Militello, A.E. Huespe, A displacement-based pipe elbow element, Comput. Struct. 29 (1988) 339-343.

[1.5] P.B. Goncalves, N.R.S.S. Ramos, Free Vibration Analysis of Cylindrical Tanks Partially Filled with Liquid, J. sound and Vib. 195 (1996) 429-444.

[1.6] L. Xuebin, A New Approach for Free Vibration Analysis of Thin Circular Cylindrical Shell, J. Sound Vib. 296 (2006) 91-98.

[1.7] L. Gan, X. Li, Z. Zhang, Free Vibration Analysis of Ring-Stiffened Cylindrical Shells Using Wave Propagation Approach. J. Sound Vib. doi: 10.1016/j.jsv.2009.05.001.

[1.8] E.M.M. Fonseca, F.J.M.Q. de Melo, C.A.M. Oliveira, Determination of flexibility factors in curved pipes with end restraints using a semi-analytical formulation, Int. J. Press. Vessel. Pip, 79 (2002) 829-840

[1.9] S.A. Karamanos, E. Giakoumatos, A.M. Gresnigt, Nonlinear response and failure of steel elbows under in-plane bending and pressure, J. Press. Vessel. Technol. 125 (2003) 393-402.

[1.10] A.W. Leissa, Vibration of Shells. Report LC-77-186367, NASA-SP-288, 1973, 428 pp.

[1.11] S. Markus, The Mechanics of Vibrations of Cylindrical Shells. Stud. Appli. Mech. 17, Elsevier, Amsterdam Oxford New York Tokyo, 1988.

[1.12] M.S. Qatu, Recent Research Advances in the Dynamic Behaviour of Shells: 1989-2000, Part 1: Laminated Composite Shells. ASME, Appl. Mech. Rev. 55 (2002) 325-350.

[1.13] M.S. Qatu, Recent Research Advances in the Dynamic Behaviour of Shells: 1989-2000, Part 2: Homogeneous Shells. ASME, Appl. Mech. Rev. 55 (2002) 415-434.

[1.14] Y., Xiang, Y.F. Ma, S. Kitipornchai, C.W. Lim, H. Lau, Exact Solutions for Vibration of Cylindrical Shells with Intermediate Ring Supports. Int. J. Mech. Sci. 44 (2002) 1907-1924.

[1.15] A.A. Jafari, M. Bagheri, Free Vibration of Non-uniformly Ring Stiffened cylindrical Shells Using Analytical, Experimental and Numerical Methods. Thin-Walled Struct. 44 (2006) 82-90.

[1.16] L. Xuebin, A New Approach for Free Vibration Analysis of Thin Circular Cylindrical Shell. J. Sound Vib. 296 (2006) 91-98.

[1.17] M. Rougui, F. Moussaoui, R. Benamar, Geometrically Non-Linear Free and Forced Vibrations of Simply Supported Circular Cylindrical Shells: A Semi-Analytical Approach. Int. J. Non-Linear Mech. 42 (2007) 1102-1115.

[1.18] L. Zhang, Y. Xiang, Exact Solutions for Vibration of Stepped Circular Cylindrical Shells. J. Sound Vib. 299 (2007) 948-964.

[1.19] L. Xuebin, Study on Free Vibration Analysis of Circular Cylindrical Shells Using Wave Propagation. J. Sound Vib. 311 (2008) 667-682.

[1.20] L. Gan, X. Li, Z. Zhang, Free Vibration Analysis of Ring-Stiffened Cylindrical Shells Using Wave Propagation Approach. J. Sound Vib. doi: 10.1016/j.jsv.2009.05.001.

[1.21] H. Matsunaga, Free Vibration and Stability of Functionally Graded Circular Cylindrical Shells According to a 2D Higher-Order Deformation Theory. Compos. Struct. 88 (2009) 519-531.

[1.22] G.B. Warburton, Harmonic Response of Cylindrical Shells. J. Eng. Industry, Trans. Am. Soc. Mech. Eng. 96B (1974) 994–999

[1.23] G.B. Warburton, S.R. Soni, Resonant Response of Orthotropic Cylindrical Shells. J. Sound Vib. 53 (1977) 1-23.

[1.24] A.W. Leissa, Modal Response of Circular Cylindrical Shells with Structural Damping. J. Sound Vib. 77 (1981) 1-10.

[1.25] D.E. Beskos, J.B. Oates, Dynamic Analysis of Ring-Stiffened Circular Cylindrical Shells. J. Sound Vib. 75 (1981) 1-15.

[1.26] V.A. Zarutskii, Forced Vibrations of a Longitudinally Reinforced Cylindrical Shell Supporting a Local Apparent Additional Mass. Institute of Mechanics, Academy of Science of the Ukranian SSR, Kiev. Plenum Publ. Corp., Translated from Prikladnaya Mekhanika. 18 (1982) 50-56.

[1.27] K. Forsberg, Influence of Boundary Conditions on the Modal Characteristics of Thin Cylindrical Shells. AIAA J. 2 (1963) 2150-2156.

[1.28] C.Y. Glandier, Y.H. Berthelot, J. Jarzynski, Wave-Vector Analysis of the Forced Vibrations of Cylindrical Shells of Finite Length. J. Acoust. Soc. Am.; 92(1992), Pt. 1.

[1.29] Y.M. Huang, C.R. Fuller, The Effect of Dynamic Absorbers on the Forced Vibration of a Cylindrical shell and Its Coupled Interior Sound Field. J. Sound Vib. 200(1997) 401-418.

[1.30] M. Amabili, A Comparison of Shell Theories for Large-Amplitude Vibrations of Circular Cylindrical Shells: Lagrangian Approach. J. Sound Vib. 264 (2003) 1091-1125.

[1.31] F. Pellicano, K.V. Avramov, Linear and Nonlinear Dynamic of a Circular Cylindrical Shell Connected to a Rigid Disk. Commun Nonlinear Sci. Numer. Simul. 12 (2007) 496-518.

[1.32] F. Pellicano, Vibrations of circular cylindrical shells: Theory and experiments. J. Sound Vib. 303 (2007) 154-170.

[1.33] W.H. Duan, C.G. Koh, Axisymmetric Transverse Vibrations of Circular Cylindrical Shells with Variable Thickness. J. Sound Vib. 317 (2008) 1035-1041.

[1.34] J. Mackerle, Finite elements in the analysis of pressure vessels and piping – a bibliography (1976-1996), Int. J. Press. Vessel. Pip. 69 (1996) 279-339.

[1.35] J. Mackerle, Finite elements in the analysis of pressure vessels and piping, an addendum (1996-1998)", Int. J. Press. Vessel. Pip. 76 (1999) 461-485.

[1.36] J. Mackerle, Finite elements in the analysis of pressure vessels and piping, an addendum: a bibliography (1998-2001), Int. J. Press. Vessel. Pip. 79 (2002) 1-26.

[1.37] J. Mackerle, Finite elements in the analysis of pressure vessels and piping, an addendum: a bibliography (2001-2004), Int. J. Press. Vessel. Pip. 82 (2005) 571-592.

[1.38] K.J. Bathe, C. Almeida, A simple and effective pipe elbow element – interaction effects, J. Appl. Mech. 49 (1982) 165-171.

[1.39] K.J. Bathe, C. Almeida, A simple and effective pipe elbow element – some non-linear capabilities, Comput. Struct. 17 (1983) 659-667.

[1.40] M. Abo-Elkhier, Analysis of pipe bends using pipe elbow element, Comput. Struct. 37 (1990) 9-15.

[1.41] F.J.M.Q. Melo, P.M.S.T. de Castro, The Linear Elastic Stress Analysis of curved pipes under generalized loads using a reduced integration finite element, J. Strain Anal. Eng. Des. 32 (1997) 47-59.

[1.42] A.M. Yan, R.J. Jospin, D.H. Nguyen, An enhanced pipe elbow element - application in plastic limit analysis of pipe structures, International Journal for Numerical Methods in Engineering, 46 (1999) 409-431.

[1.43] K.R. Sivadas, N. Ganesan, Dynamic Analysis of Circular Cylindrical Shells with Material Damping, J. Sound Vib. 166 (1993) 103-116.

[1.44] A.J. Stanley, N. Ganesan, Dynamic Response of Cantilever Cylindrical Shells with Discontinuity in Thickness Subjected to Axisymmetric Load, Comput. Struct. 55 (1995) 667-685.

[1.45] Z.C. Xi, L.H. Yam, T.P. Leung, Semi-Analytical Study of Free Vibration of Composite Shells of Revolution Based on the Reissner-Mindlin Assumption, Int. J. Solid. Struct. 33 (1996) 851-863.

[1.46] I.F. Pinto Correia, J.I. Barbosa, C.M. Mota Soares, C.A. Mota Soares, A Finite Element Semi-Analytical Model for Laminated Axisymmetric Shells: Static, Dynamic and Buckling, Comput. Struct. 79 (2000) 299-317.

[1.47] S.A. Karamanos, Bending Instabilities of Elastic Tubes, Int. J. Solid. and Struct. 39 (2002) 2059-2085.

[1.48] S.A.Karamanos, E. Giakoumatos, A.M. Gresnigt, Nonlinear Response and Failure of Steel Elbows under In-Plane Bending and Pressure, J. Press. Vessel Technol. 125 (2003) 393-402.

[1.49] H. Santos, C.M. Mota Soares, C.A. Mota Soares, J.N. Reddy, A Semi-Analytical Finite Element Model for the Analysis of Laminated 3D Axisymmetric Shells: Bending, Free Vibration and Buckling, Compos. Struct. 71 (2005) 273-281.

[1.50] K. Weicker, Finite Element Formulation for Analysis of Pipes based Thin Shell Theory. M.A.Sc. Thesis, Department of Civil Engineering, University of Ottawa, Ottawa, ON, Canada, 2008.

[1.51] S. Timoshenko, Theory of Plates and Shells. McGraw-Hill Book Company, New York, 1959.

[1.52] V.V. Novozhilov, Thin Shell Theory. P. Noordhoff Ltd. –Groningen-The Netherlands, 1964.

[1.53] F. I. Niordson, Shell Theory. North-Holland Series In Applied Mathematics and Mechanics, 1985.

[1.54] W. Flugge, Stresses in Shells. Springer-Verlag, New York, 1973.

[1.55] L.H. Donnell, A discussion of thin-shell theory, Proc. Fifth Int. Congr. Appl. Mech., Cambridge, Mass. 66 (1938).

[1.56] Jr.J.L. Sanders, An Improved First Approximation Theory for Thin Shells. Langley Research Center, TR-24, 1959.

[1.57] K. Washizu, Variational Methods in Elasticity and Plasticity, 3rd Edn., Pergamon, Oxford 1982.

[1.58] J.P. Dedieu and F. Tisseur, Perturbation theory for homogeneous polynomial eigenvalue problems, Linear Algebra Appl. 358 (2003) 71-94.

[1.59] D. Redekop, B. Xu, Vibration Analysis of Toroidal Panels Using the Differential Quadrature Method, J. Thin-Walled Struct. 34 (1999) 217-231.

[1.60] R. Salahifar, M. Mohareb, Analysis of Circular Cylindrical Shells under Harmonic Forces, J. Thin-Walled Struct. 48 (2010) 528-539.

Chapter 2

A Generalized Thin Shell Theory

2.1 Abstract

In this chapter the dynamic version of problem of thin shell theory is reformulated. In this regard, tensor calculus is used to preserve the accuracy and consistency of the theory within the assumptions of the thin shell theory. Using the energy approach has enabled the formulation to provide the field equations and boundary condition equations, simultaneously.

2.2 Introduction

The theory of shells is a challenging part of continuum mechanics that has been thoroughly investigated by many engineers and researchers. In general, the theory of thin shells deals with two main issues, a) developing the governing field equations and boundary conditions and b) providing the solution to the field equations to problems with specific geometries, boundary conditions, and loading. During the last century, many scientists have worked on this subject and developed different field equations. Most thin-shell formulations are based on the following assumptions:

1. Conservation of normals: All points lying on a normal to the middle surface before deformation will remain on the normal to the deformed middle surface. This implies a linear distribution of in-plane displacement across the thickness of the shell.

2. A surface at a distance x^3 from the middle surface before deformation will remain at the same distance from the middle surface after deformation.

3. All displacements are small compared to the radii of curvature of the middle surface. This signifies that the curvatures of the shell mid-surface after deformation are considered identical to the curvatures before deformation.

The differences between various shell theories are attributed to the following factors:

1. Different strain-displacement relationships

   In some cases (e.g., Flugge [2.1] and Timoshenko [2.2]) the strain-displacement relationships are obtained based on geometric inspection of an infinitesimal portion of the shell undergoing deformation. In other references (e.g., Niordson [2.3], Novozhilov [2.4] and Saada [2.5]), a vector or tensor analysis approach is utilized.

2. Methodology used in formulating the field equations

   In most cases (e.g., Flugge [2.1], Niordson [2.3], Timoshenko [2.2] and Saada [2.5]) the equilibrium equations are obtained based on the force equilibrium of an infinitesimal element of the shell, while in others (e.g., Novozhilov [2.4]), an energy approach is used in which the equilibrium equations are obtained by setting the variation of the total potential energy equal to zero.

3. Additional simplifications in some theories

   Most authors have applied different simplification in different levels of formulation process, which had implications on the final form of the governing field equations and boundary conditions. For example, Novozhilov [2.4] has neglected some terms in the expression of total potential energy compared to the other terms.

4. Inconsistency in enforcing simplifications in some theories

   Most authors (Timoshenko [2.2], Saada [2.5], Niordson [2.3], etc.) were inconsistent in their simplifications. For example, the effect of the thickness in strain expression is neglected in some terms, while it is kept in some other terms within the same formulation. This inconsistency, in most cases, arose from separating the membrane and bending strains.

Given the above discrepancies, it is difficult to assess which of the theories should be used for a given engineering problem. Within this context, the present treatment focuses on developing a thin shell theory in which the strain-displacement relationships are developed from the thin shell assumptions as a starting point. Tensor calculus is then used to develop a generalized theory. The stress-strain and strain-displacement relations are evoked. The expression for the total potential energy of the system is formulated and the stationary conditions of the total potential energy are evoked to recover the equilibrium equations.

2.3 Geometry of Curved Surfaces

In general, a three dimensional surface can be described by a vector $\mathbf{r}$ defined in a fixed spatial coordinate system $X^i\,(i=1,2,3)$. However, if we affix a two dimensional curvilinear

coordinate system x^α ($\alpha = 1,2$) to the surface (Figure 2.1), vector $\mathbf{r}$ can be defined in terms of coordinates x^α instead of coordinates X^i. All Greek subscripts and superscripts range from 1 to 2 while all Latin subscripts and superscripts range from 1 to 3.

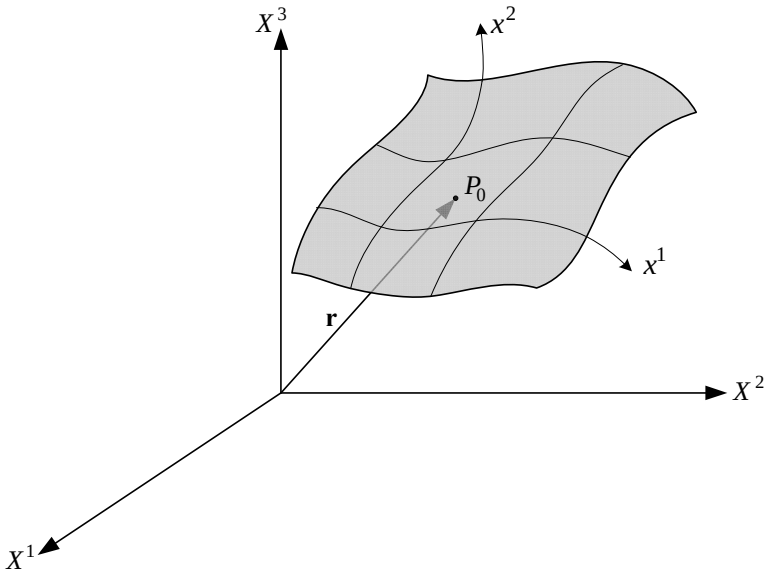

Figure 2.1 - General Curved Surface

A brief review of Tensor Calculus fundamentals is provided in Appendix A.

2.3.1 The First Fundamental Tensor of a Surface

In a three dimensional space, the position vector $\mathbf{r}$ of a point P_0 on the surface (Figure 2.2) can be written as

$$\mathbf{r} = \mathbf{r}\left(x^1, x^2\right) \qquad \Rightarrow \qquad d\mathbf{r} = \frac{\partial \mathbf{r}}{\partial x^\alpha} dx^\alpha \tag{2.1}$$

Consequently, vector $d\mathbf{r}$ (Figure 2.2) is located within the surface. One knows (Eq. A.18), base vectors $\mathbf{a}_1$, $\mathbf{a}_2$ (Figure 2.2) within the surface are

$$\mathbf{a}_\alpha = \frac{\partial \mathbf{r}}{\partial x^\alpha} \tag{2.2}$$

In order to define the curvature of the surface, one needs to express the direction of the normal to the surface. Therefore, unit vector $\mathbf{a}^3\left(x^1, x^2\right)$, defined as the normal to the plane defined by base vectors $\mathbf{a}_1$ and $\mathbf{a}_2$, is given by

$$\mathbf{a}^3 = \frac{\mathbf{a}_1 \otimes \mathbf{a}_2}{\left|\mathbf{a}_1 \otimes \mathbf{a}_2\right|} \tag{2.3}$$

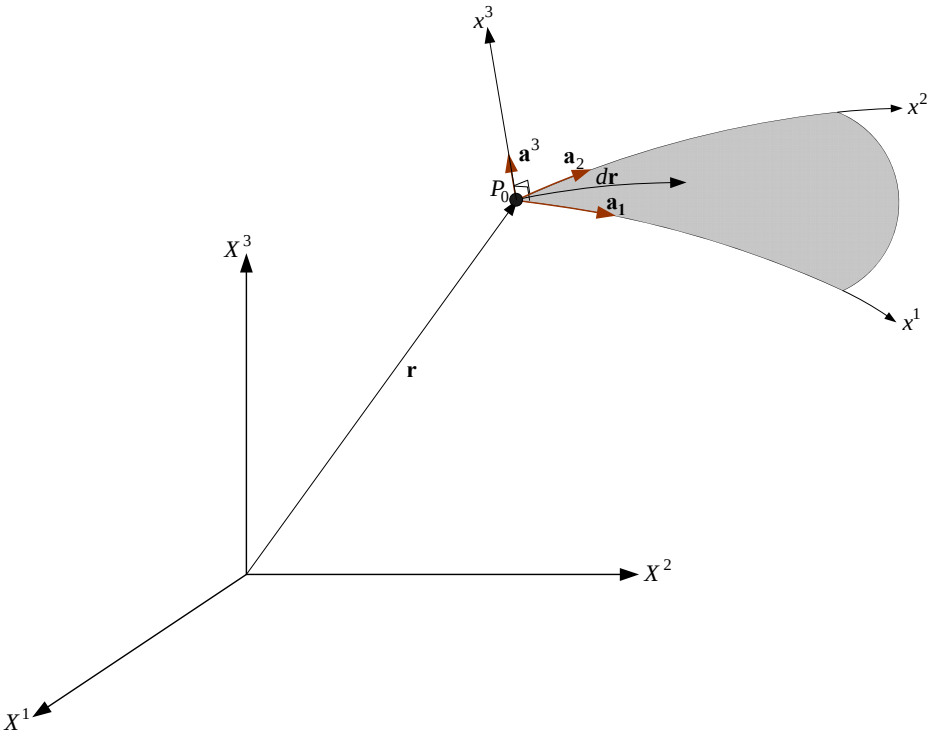

Figure 2.2 – Geometry of surface

In a tensor calculus context, one can write the following identities (by recalling Eqs. A.23, A.35, A.36, A.38, A.51, A.68). From the definition of the covariant and contravariant base vectors (Eq. A.23) one has:

$$\mathbf{a}_i \cdot \mathbf{a}^j = \delta_i^j \qquad \Rightarrow \qquad \mathbf{a}_i \cdot \mathbf{a}^i = 1 \tag{2.4a-b}$$

The fact that $\mathbf{a}^3$ is a unit vector and considering the orthogonality of the covariant base vectors and their reciprocal contravariant counterparts (Eq. 2.4a) yields

$$\mathbf{a}_3 = \mathbf{a}^3 \tag{2.5}$$

Deducting from the covariant and contravariant form of the metric tensor (Eqs. A.35 and A.36), the covariant and contravariant metric tensors of the surface are:

$$a_{\alpha\beta} = \mathbf{a}_\alpha \cdot \mathbf{a}_\beta \qquad , \qquad a^{\alpha\beta} = \mathbf{a}^\alpha \cdot \mathbf{a}^\beta \tag{2.6a-c}$$

and the determinant a of the covariant metric tensor is

$$a = \begin{vmatrix} a_{11} & a_{12} & a_{13} \\ a_{21} & a_{22} & a_{23} \\ a_{31} & a_{32} & a_{33} \end{vmatrix} \tag{2.7}$$

2.3.2 The Second Fundamental Tensor of a Surface

The curvature of the surface is equal to the change of the unit vector $d\mathbf{a}_3$ $(= d\mathbf{a}^3)$ normal to the surface with respect to small changes in its location $d\mathbf{r}$:

$$d\mathbf{a}_3 = \frac{\partial \mathbf{a}_3}{\partial x^\alpha} dx^\alpha \tag{2.8}$$

One recalls that vector $\mathbf{a}_3$ is a function only of coordinates x^α. Thus, its partial derivatives with respect to coordinates x^α, are also vectors and may be decomposed along the components of the base vectors $\mathbf{a}_\alpha$. This is performed by dot-multiplying vector $d\mathbf{a}_3$ by the vector $d\mathbf{r}$ yielding

$$d\mathbf{a}_3 \cdot d\mathbf{r} = \left(\frac{\partial \mathbf{a}_3}{\partial x^\alpha} dx^\alpha \right) \cdot \left(\frac{\partial \mathbf{r}}{\partial x^\beta} dx^\beta \right) = \mathbf{a}_{3,\alpha} \cdot \mathbf{a}_\beta dx^\alpha dx^\beta = -\bar{b}_{\alpha\beta} dx^\alpha dx^\beta \tag{2.9}$$

in which the definition

$$\bar{b}_{\alpha\beta} = \mathbf{a}_{3,\alpha} \cdot \mathbf{a}_\beta \tag{2.10}$$

has been introduced. Symbol $\bar{b}_{\alpha\beta}$ is called the second fundamental tensor of the surface or curvature tensor of the surface.

2.4 Geometry of Thin Shells

In general, thin shells can be considered as a group of parallel curved surfaces in the immediate vicinity of the middle surface. As pointed out, in general, a point P_0 on a surface can be defined by two dimensional curvilinear coordinates, which is a two dimensional subspace of the general three dimensional space. This implies that the geometry of any of those surfaces can be defined by two curvilinear coordinates x^α on the middle surface and an additional coordinate x^3 normal to the middle surface. Thus, the position vector $\mathbf{R}$ in a three dimensional space of any point P_1 (Figure 2.3) within the shell, can be defined by the position vector $\mathbf{r}$ of its projection P_0 on the middle surface and the distance x^3 as:

$$\mathbf{R}\left(x^1, x^2, x^3\right) = \mathbf{r}\left(x^1, x^2\right) + x^3 \mathbf{a_3}\left(x^1, x^2\right) \tag{2.11}$$

We recall that base vector $\mathbf{a}_3$ is the unit vector normal to the middle surface. In other words, Eq. 2.11 expresses the rule of transformation of the geometry of the shell surfaces from coordinate system x^i into coordinate system X^i. In a similar manner, the base vectors $\mathbf{g}_i$ for any general surface within the shell volume are given by

$$\mathbf{g}_i = \frac{\partial \mathbf{R}}{\partial x^i} \tag{2.12}$$

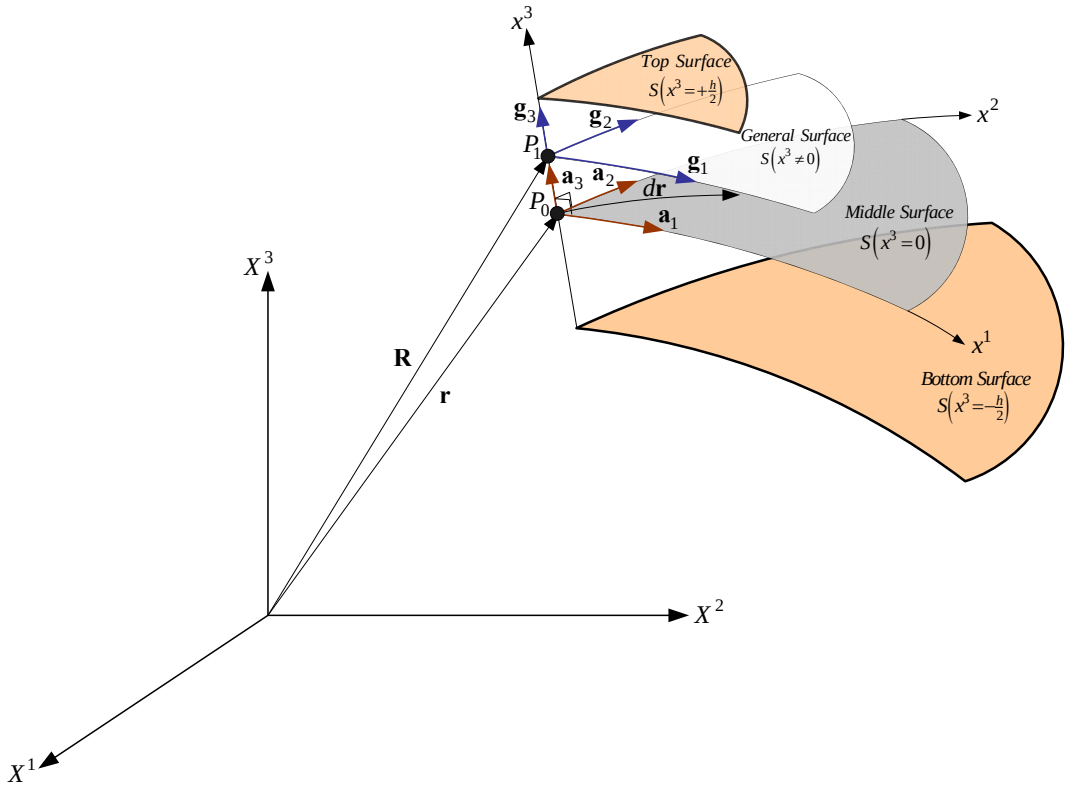

Figure 2.3 – Shell Geometry

From Eq. 2.11 by substituting into Eq. 2.12, and using Eq. 2.2, one obtains

$$\mathbf{g}_i=\frac{\partial\mathbf{R}}{\partial x^i}=\frac{\partial\mathbf{r}}{\partial x^i}+\frac{\partial}{\partial x^i}\left(x^3\mathbf{a_3}\left(x_1,x_2\right)\right)=\begin{cases}\mathbf{g}_\alpha=\dfrac{\partial\mathbf{r}}{\partial x^\alpha}+\dfrac{\partial\left(x^3\mathbf{a_3}\right)}{\partial x^\alpha}=\mathbf{a}_\alpha+x^3\mathbf{a}_{3,\alpha}\\ \mathbf{g}_3=\mathbf{a}_3\end{cases}\qquad(2.13a\text{-}b)$$

Using the operation of raising indices in Eq. 2.10 and dot-multiply by $\mathbf{a}_\rho$ yields $\mathbf{a}_{3,\alpha}=\bar{b}_\alpha^\gamma\mathbf{a}_\gamma$. By substituting into Eq. 2.13-a and using the Kronecker delta function δ_α^γ, one obtains

$$\mathbf{g}_\alpha=\mathbf{a}_\alpha+x^3\bar{\Gamma}_{3\alpha}^\gamma\mathbf{a}_\gamma=\delta_\alpha^\gamma\mathbf{a}_\gamma-x^3\bar{b}_\alpha^\gamma\mathbf{a}_\gamma=\left(\delta_\alpha^\gamma-x^3\bar{b}_\alpha^\gamma\right)\mathbf{a}_\gamma=\mu_\alpha^\gamma\mathbf{a}_\gamma\qquad(2.14)$$

in which $\bar{\Gamma}_{3\alpha}^\gamma=-\bar{b}_\alpha^\gamma$ is the Christoffel symbol for the middle surface of the shell (as a matter of convention, the presence of a bar denotes the middle surface). Thus

$$\mathbf{g}_\alpha=\mu_\alpha^\gamma\mathbf{a}_\gamma\quad,\quad\mathbf{g}_3=\mathbf{a}_3\qquad(2.15a\text{-}b)$$

in which

$$\mu_\alpha^\gamma = \delta_\alpha^\gamma - x^3 \bar{b}_\alpha^\gamma \tag{2.16}$$

Tensor μ_α^γ relates the base vectors on surfaces adjacent to the mid-surface, to the base vectors of the middle surface ($x^3 = 0$). More properties of interest are

$$\mathbf{g}_\beta \cdot \mathbf{g}^\alpha = \delta_\beta^\alpha \quad \Rightarrow \quad \mathbf{g}_\alpha \cdot \mathbf{g}^\alpha = 1 \tag{2.17a-b}$$

The contravariant counterparts of covariant base vectors are:

$$\mathbf{g}^\alpha = \lambda_\gamma^\alpha \mathbf{a}^\gamma \quad , \quad \mathbf{g}^3 = \mathbf{a}^3 \tag{2.18a-b}$$

in which

$$\lambda_\gamma^\alpha \mu_\beta^\gamma = \delta_\beta^\alpha \tag{2.19}$$

Eq. 2.19 can be proved by substitution of Eqs. 2.16-a and 2.18-a into Eq. 2.17-a and using Eq. 2.4-a. Equation 2.19 signifies that the symbol λ_γ^α is the contravariant counterpart of μ_β^γ, which may be defined in the form of a power series as

$$\lambda_\rho^\gamma = \delta_\rho^\gamma + \bar{b}_\rho^\gamma x^3 + \bar{b}_\eta^\gamma \bar{b}_\rho^\eta \left(x^3\right)^2 + \bar{b}_\eta^\gamma \bar{b}_\theta^\eta \bar{b}_\rho^\theta \left(x^3\right)^3 + \ldots \tag{2.20}$$

All superscripts outside of the brackets in Eq. 2.20 are exponents. The covariant and contravariant metric tensors parallel and adjacent to the middle surface are respectively expressed as

$$g_{\alpha\beta} = \mathbf{g}_\alpha \cdot \mathbf{g}_\beta = \mu_\alpha^\gamma \mu_\beta^\delta a_{\gamma\delta} \quad , \quad g^{\alpha\beta} = \mathbf{g}^\alpha \cdot \mathbf{g}^\beta = \lambda_\gamma^\alpha \lambda_\delta^\beta a^{\gamma\delta} \tag{2.21a-b}$$

The Jacobian g at a generic point within the shell is given by

$$g = \det\left(g_{ij}\right) \tag{2.22}$$

and represents a differential element of volume.

2.5 Strains in Thin Shells

The present study is focused on the linear response of shells and limited to small deformations. Thus, the nonlinear terms $U^k|_i\, U_k|_j$ in strain-displacement relationships (Eq. A.95) are neglected. For the special case of thin shells, the strains can be resolved into in-plane $\eta_{\alpha\beta}$ and out-of-plane components, $\eta_{\alpha 3} = \eta_{3\alpha}$ and η_{33}. These are expressed as

$$\eta_{\alpha\beta} = \tfrac{1}{2}\left(U_\alpha|_\beta + U_\beta|_\alpha\right) \tag{2.23}$$

$$\eta_{\alpha 3} = \eta_{3\alpha} = \tfrac{1}{2}\left(U_\alpha|_3 + U_3|_\alpha\right) \tag{2.24}$$

$$\eta_{33} = \tfrac{1}{2}\left(U_3|_3 + U_3|_3\right) \tag{2.25}$$

According to the second assumption in Section 2.2 the strain normal to the midsurface vanishes. Thus $\eta_{33} = \tfrac{1}{2}\left(U_3|_3 + U_3|_3\right) = 0$. Also, according to the third assumption in section 2.2 , the through thickness strains are negligible in thin shells and $\eta_{\alpha 3} = \eta_{3\alpha} = 0$.

2.6 Displacements of a Point within the Shell

In general, the displacement vector $\mathbf{U}$ at any point within a shell is

$$\mathbf{U} = U_i\left(x^1, x^2, x^3, t\right)\mathbf{g}^i = U^i\left(x^1, x^2, x^3, t\right)\mathbf{g}_i \tag{2.26}$$

where U_i and U^i are the covariant and contravariant components of the displacement vector in the x^i coordinate system. In the following, however, the displacements $\mathbf{U}$ at any point within the thin shell will be expressed in terms of the middle surface displacements.

Displacement vector $\mathbf{U} = \hat{\mathbf{R}} - \mathbf{R}$ (Eq. A.86) of a point A (Figure 2.4) offset from the middle surface can be expressed in terms of the position vector of the mid-surface and the unit vector normal to the mid-surface $\mathbf{a}_3$ as

$$\mathbf{U} = \hat{\mathbf{R}} - \mathbf{R} = \left(\hat{\mathbf{r}} + \hat{x}^3\hat{\mathbf{a}}_3\right) - \left(\mathbf{r} + x^3\mathbf{a}_3\right) = \left(\hat{\mathbf{r}} - \mathbf{r}\right) + x^3\left(\hat{\mathbf{a}}_3 - \mathbf{a}_3\right) \tag{2.27}$$

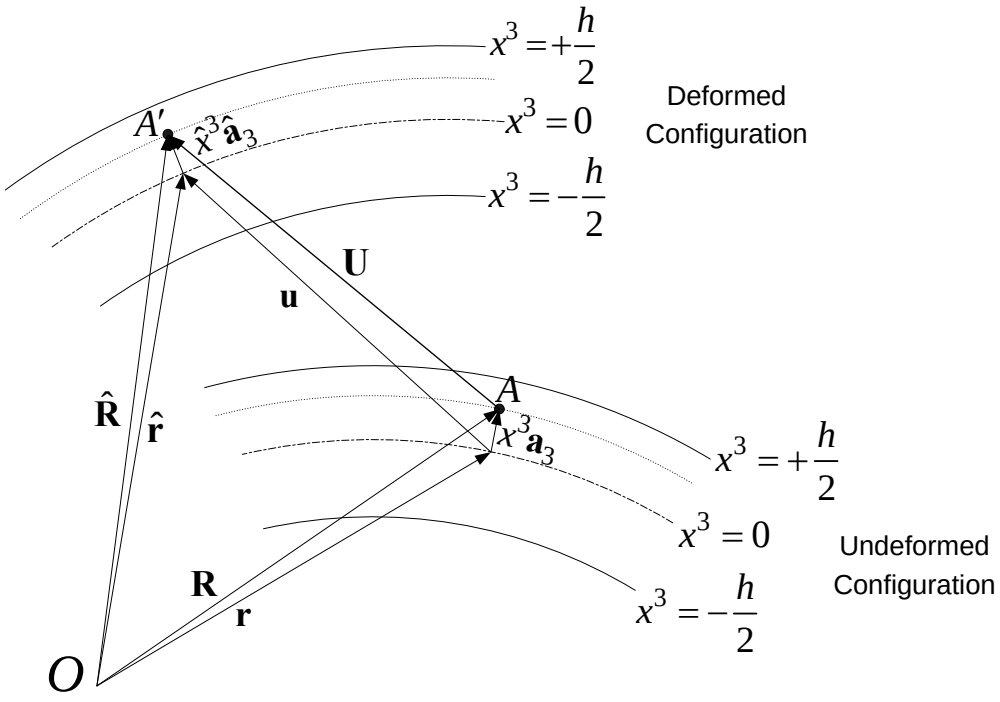

Figure 2.4 Deformed and Un-deformed Configurations of a Thin Shell

As vectors $\mathbf{r}$ and $\hat{\mathbf{r}}$ are respectively the position vectors of the corresponding point on the middle surface before and after deformation, their difference $\mathbf{u} = \hat{\mathbf{r}} - \mathbf{r}$ expresses the displacement vector at the mid-surface point. Also, $\mathbf{a}_3$ and $\hat{\mathbf{a}}_3$ are unit vectors normal to the mid-surface at the point of interest before and after deformation. Therefore, their difference $\boldsymbol{\theta} = \hat{\mathbf{a}}_3 - \mathbf{a}_3$ expresses the angle of rotation of the middle surface. Thus, Eq. 2.27 can be re-written as:

$$\mathbf{U} = \mathbf{u}\left(x^1, x^2\right) + x^3\boldsymbol{\theta}\left(x^1, x^2\right) \tag{2.28}$$

in which vectors $\mathbf{u}$ and $\boldsymbol{\theta}$ are functions only of x^α and are defined through the middle surface coordinates as

$$\mathbf{u}\left(x^1, x^2\right) = u_i\left(x^1, x^2\right)\mathbf{a}^i = u^i\left(x^1, x^2\right)\mathbf{a}_i \tag{2.29}$$

$$\boldsymbol{\theta}\left(x^1, x^2\right) = \theta_\alpha\left(x^1, x^2\right)\mathbf{a}^\alpha = \theta^\alpha\left(x^1, x^2\right)\mathbf{a}_\alpha \tag{2.30}$$

By differentiating both side of Eq. 2.27 with respect to x^3, One obtains

$$\boldsymbol{\theta} = \hat{\mathbf{a}}_3 - \mathbf{a}_3 = \frac{\partial \mathbf{U}}{\partial x^3} \tag{2.31}$$

The right hand side of Eq. 2.31 (by using Eq. A.90) can be expanded as $\partial \mathbf{U}/\partial x^3 = U_i\,|_3\,\mathbf{g}^i = U_\alpha\,|_3\,\mathbf{g}^\alpha + U_3\,|_3\,\mathbf{g}^3$. Thus,

$$\boldsymbol{\theta} = \hat{\mathbf{a}}_3 - \mathbf{a}_3 = U_i\,|_3\,\mathbf{g}^i = U_\alpha\,|_3\,\mathbf{g}^\alpha + U_3\,|_3\,\mathbf{g}^3 \tag{2.32}$$

Eq. 2.32 can be written for the middle surface as a special case, yielding

$$\boldsymbol{\theta} = \hat{\mathbf{a}}_3 - \mathbf{a}_3 = u_\alpha\,|_3\,\mathbf{a}^\alpha + \underbrace{u_3\,|_3}_{0}\mathbf{a}^3 = u_\alpha\,|_3\,\mathbf{a}^\alpha = \left(u_\alpha\,|_3 + u_3\,|_\alpha - u_3\,|_\alpha\right)\mathbf{a}^\alpha \tag{2.33}$$

In Eq. 2.33, $\mathbf{U}\left(x^3 = 0\right) = \mathbf{u}\left(x^1, x^2\right)$ as obtained from Eq. 2.28 was used. By evoking the first assumption in Section 2.2 (i.e., normal to the mid-surface remains normal after deformation, which implies zero shear strain), one obtains

$$\eta_{3\alpha} = \eta_{\alpha 3} = \tfrac{1}{2}\left(U_\alpha\,|_3 + U_3\,|_\alpha\right) = 0 \tag{2.34}$$

and

$$\varepsilon_{3\alpha} = \varepsilon_{3\alpha} = \tfrac{1}{2}\left(u_\alpha\,|_3 + u_3\,|_\alpha\right) = 0 \tag{2.35}$$

In Eq. 2.35, ε_{ij} denotes the strain tensor η_{ij} at the middle surface ($x^3 = 0$). Using Eq. 2.35, Eq. 2.33 is simplified to

$$\boldsymbol{\theta} = \hat{\mathbf{a}}_3 - \mathbf{a}_3 = -u_3\,|_\alpha\,\mathbf{a}^\alpha \tag{2.36}$$

By expanding the right hand side of Eq. 2.36 (using Eq. A.73), one obtains

$$\boldsymbol{\theta} = \hat{\mathbf{a}}_3 - \mathbf{a}_3 = -\left(u_{3,\alpha} - u_\gamma \bar{\Gamma}^\gamma_{3\alpha}\right)\mathbf{a}^\alpha = -\left(u_{3,\alpha} + u_\gamma \bar{b}^\gamma_\alpha\right)\mathbf{a}^\alpha \tag{2.37}$$

From Eqs. 2.29 and 2.37, by substituting into Eq. 2.28, one obtains

$$\mathbf{U} = u_i \mathbf{a}^i - x^3 \left(u_{3,\alpha} + u_\gamma \bar{b}_\alpha^\gamma \right) \mathbf{a}^\alpha = u_\alpha \mathbf{a}^\alpha + u_3 \mathbf{a}^3 - x^3 \left(u_{3,\alpha} + u_\gamma \bar{b}_\alpha^\gamma \right) \mathbf{a}^\alpha \tag{2.38}$$

By grouping terms with the same base vectors, one obtains

$$\mathbf{U} = \left(u_\alpha - x^3 u_{3,\alpha} - x^3 u_\gamma \bar{b}_\alpha^\gamma \right) \mathbf{a}^\alpha + u_3 \mathbf{a}^3 \tag{2.39}$$

Using the Kronecker delta tensor

$$\mathbf{U} = \left(u_\gamma \delta_\alpha^\gamma - x^3 u_{3,\alpha} - x^3 u_\gamma \bar{b}_\alpha^\gamma \right) \mathbf{a}^\alpha + u_3 \mathbf{a}^3 \tag{2.40}$$

From Eq. 2.16, by substituting in Eq. 2.40, one obtains

$$\mathbf{U} = \left[\mu_\alpha^\gamma u_\gamma - x^3 u_{3,\alpha} \right] \mathbf{a}^\alpha + u_3 \mathbf{a}^3 \tag{2.41}$$

By dot-multiplying both sides of Eq. 2.18-a by μ_α^δ, one obtains $\mathbf{a}^\delta = \mu_\alpha^\delta \mathbf{g}^\alpha$. By substituting in Eq. 2.41 and using Eq. 2.18b, one obtains

$$\mathbf{U} = \left(\mu_\delta^\gamma u_\gamma - x^3 u_{3,\delta} \right) \mu_\alpha^\delta \mathbf{g}^\alpha + u_3 \mathbf{g}^3 \tag{2.42}$$

Eq. 2.42 relates the displacement of a point within the shell to the displacement of their picture on the middle surface. Thus, Eq. 2.26 can be rewritten as

$$\mathbf{U} = U_\alpha \left(x^1, x^2, x^3, t \right) \mathbf{g}^\alpha + U_3 \left(x^1, x^2, t \right) \mathbf{g}^3 \tag{2.43}$$

and

$$\mathbf{U} = U^\alpha \left(x^1, x^2, x^3, t \right) \mathbf{g}_\alpha + U^3 \left(x^1, x^2, t \right) \mathbf{g}_3 \tag{2.44}$$

By comparing Eqs. 2.42 and 2.43, one obtains

$$U_\alpha = \left(\mu_\delta^\gamma u_\gamma - x^3 u_{3,\delta} \right) \mu_\alpha^\delta \quad , \quad U_3 = u_3 \tag{2.45a-b}$$

The geometric interpretations for $U_\alpha \mathbf{g}^\alpha$ and $U_3 \mathbf{g}^3$ are schematically shown in Figure 2.5, in which point A located at a distance $x^3 \neq 0$ from the shell mid-surface undergoes

displacements U_α parallel to the shell mid-surface and a displacement U_3 normal to the mid-surface.

The contravariant components of the displacement in terms of contravariant components of the displacement of their picture on the middle surface can be obtained in the same manner as for the covariant components (Appendix 2.A). Alternatively, the operation of raising indices $U^i = g^{ij}U_j$ is used herein in order to obtain them in terms of the covariant components of the displacements of their picture on the middle surface

$$U^\alpha = U_\beta g^{\alpha\beta} = \left(\mu_\delta^\gamma u_\gamma - x^3 u_{3,\delta}\right)\mu_\beta^\delta g^{\alpha\beta} \quad , \quad U^3 = u^3 = u_3 \tag{2.46a-b}$$

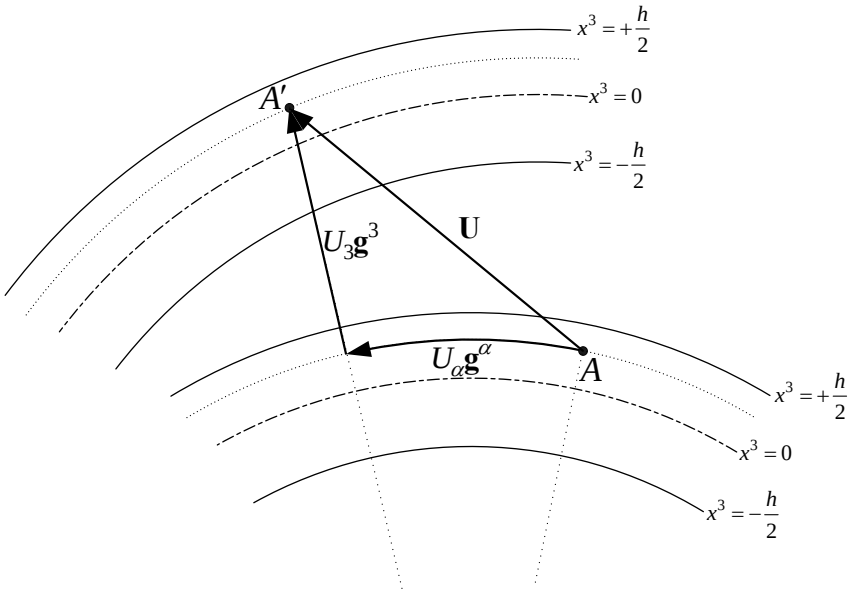

Figure 2.5 – Displacement of a generic point within the shell

2.7 Stress-Strain Relationship

The elastic stress-strain relationship in tensor form is (Flugge [2.6]):

$$\sigma^{ij} = E^{ijlm}\eta_{lm} \tag{2.47}$$

where σ^{ij} is the stress tensor, η_{lm} is the strain tensor and E^{ijlm} is the 4th order constitutive elastic tensor. The elasticity tensor E^{ijlm} has $3^4 = 81$ components. It is shown in Appendix

2.B that these constants are functions of only two independent properties (e.g., Modulus of elasticity E and Poisson's ratio ν) when the material is elastic and isotropic. The customized form of expression 2.47 for in-plane stresses is:

$$\sigma^{\alpha\beta} = E^{\alpha\beta\lambda\delta}\eta_{\lambda\delta} \tag{2.48}$$

2.8 Generalized Constitutive Elasticity Tensor for Thin Shells

The elasticity tensor for in-plane stress in Cartesian coordinate systems ([2.6]) is

$$E^{\alpha\beta\lambda\delta} = \frac{E}{2(1+\nu)}\left[\delta^{\alpha\lambda}\delta^{\beta\delta} + \delta^{\alpha\delta}\delta^{\beta\lambda} + \frac{2\nu}{1-\nu}\delta^{\alpha\beta}\delta^{\lambda\delta}\right] \tag{2.49}$$

In tensor calculus, when an equation is valid in one coordinate system, it is known to be valid in all other coordinate systems ([2.7]). Thus, Eq. 2.49 can be generalized to other coordinate systems by replacing the Kronecker deltas by the proper components of the metric tensor, i.e.,

$$E^{\alpha\beta\lambda\delta} = \frac{E}{2(1+\nu)}\left[g^{\alpha\lambda}g^{\beta\delta} + g^{\alpha\delta}g^{\beta\lambda} + \frac{2\nu}{1-\nu}g^{\alpha\beta}g^{\lambda\delta}\right] \tag{2.50}$$

2.9 Hamilton's Principle for Thin Shells

Starting with the Hamilton's principle (Eq. A.96)

$$\delta\prod = \int_{t_1}^{t_2}\delta(T^* - V^*)dt + \int_{t_1}^{t_2}\delta W^* dt = 0 \tag{2.51}$$

where

$$\delta T^* = \int_V \rho\dot{U}^i\delta\dot{U}_i dV \;,\; \delta V^* = \int_V E^{ijkl}\eta_{kl}\delta\eta_{ij}dV \;,\; \delta W^* = \int_V F^i\delta U_i dV \tag{2.52a-c}$$

In the above equations $\prod$ is the mechanical energy of the system, T^*, V^* and W^* are the kinetic energy, potential energy and external work in the system, respectively. Symbol δ denotes the variation operator and integration is performed over an arbitrary period starting

from time t_1 to time t_2 (more elaboration is provided in Appendix A). By substituting from Eq. 2.52a-c into Eq. 2.51, integrating by parts with respect to time on the kinetic energy integral term, and using the definition $U_\alpha|_\beta = U_\alpha\|_\beta - U_3 b_{\alpha\beta}$ (more elaboration is provided in Appendix 2.C) in potential strain energy integral term and integrating by parts with respect to x^β yields (the details are provided in Appendix 2.D)

$$\begin{aligned}\delta\prod = &\left[\int_V \dot{U}^i \rho \delta U_i dV\right]_{t_1}^{t_2} + \int_{t_1}^{t_2}\left\{-\int_V \ddot{U}^i \rho \delta U_i dV dt\right.\\ &-\int_A \left[\tfrac{1}{2}E^{\alpha\beta\lambda\delta}\left(U_\lambda\|_\delta + U_\delta\|_\lambda - 2U_3 b_{\lambda\delta}\right)\delta U_\alpha\right]_0^{x_\beta} dA\\ &+\int_V \left[\tfrac{1}{2}E^{\alpha\beta\lambda\delta}\left(U_\lambda\|_{\delta\beta} + U_\delta\|_{\lambda\beta} - 2U_{3,\beta}b_{\lambda\delta} - 2U_3 b_{\lambda\delta}\|_\beta\right)\right.\\ &\qquad\left.+\tfrac{1}{2}\left(E^{\alpha\beta\lambda\delta}\|_\beta\right)\left(U_\lambda\|_\delta + U_\delta\|_\lambda - 2U_3 b_{\lambda\delta}\right)\right]\delta U_\alpha dV\\ &+\int_V \tfrac{1}{2}E^{\alpha\beta\lambda\delta}\left(U_\lambda\|_\delta + U_\delta\|_\lambda - 2U_3 b_{\lambda\delta}\right)\left(b_{\alpha\beta}\delta U_3\right)dV\\ &\left.+\int_V F^i \delta U_i dV\right\} dt = 0\end{aligned} \tag{2.53}$$

2.10 Summary and Conclusion

Starting from the basic definitions of the continuum mechanics by benefiting from the exactness, consistency and conciseness of the tensor calculus a three dimensional generalized thin shell theory applicable to general static and dynamic cases is developed. The generalized theory developed in this chapter will be specialized to circular cylindrical shells in Chapter 3 and toroidal shells in Chapter 6.

2.11 References

[2.1] W. Flugge, Stresses in Shells. Springer-Verlag, New York Heidelberg Berlin, 1973.

[2.2] S. Timoshenko, Theory of Plates and Shells. McGraw-Hill Book Company, New York, 1959.

[2.3] F. I. Niordson, Shell Theory. North-Holland Series In Applied Mathematics and Mechanics, 1985.

[2.4] V.V. Novozhilov, Thin Shell Theory. P. Noordhoff Ltd. –Groningen-The Netherlands, 1964.

[2.5] A.S. Saada, Elasticity: Theory and Applications, Pergamon Press Inc., New York, 1974.

[2.6] W. Flugge, Tensor Analysis and Continuum Mechanics, Springer-Verlag, New York Heidelberg Berlin, 1972.

[2.7] I. S. Sokolnikoff, Tensor Analysis Theory And Applications To Geometry And Mechanics Of Continua, Second Edition, John Wiley & Sons, Inc., New York, 1965.

2.12 List of Symbols

$\mathbf{a}_i$	Covariant base vectors of the middle surface
a_{ij}	First fundamental tensor defined on the middle surface of a thin shell
a	Determinant of the first fundamental tensor a_{ij}
$b_{\alpha\beta}$	Curvature tensor of the surfaces parallel and adjacent to the middle surface
$\bar{b}_{\alpha\beta}$	Second fundamental tensor or curvature tensor defined on the middle surface of a thin shell
$\mathbf{a}^i$	Contravariant base vectors of the middle surface
a^{ij}	First fundamental tensor of the second kind defined on the middle surface of a thin shell
$\mathbf{g}_i$	Covariant base vectors of any surface parallel and adjacent to the middle surface
g_{ij}	First fundamental tensor defined within the shell
g	Determinant of the first fundamental tensor g_{ij}
$\mathbf{g}^i$	Contravariant base vectors of any surface parallel and adjacent to the middle surface

g^{ij}	First fundamental tensor of the second kind defined within the shell
$\mathbf{U}$	Displacement of a point within the shell
U_i	Covariant components of the displacement of a point on a surface parallel and adjacent to the middle surface along axis x^i
u_i	Covariant components of the displacement of a point on the middle surface along axis x^i
X^i	Coordinate system/Coordinates of the system
x^i	Coordinate system/Coordinates of the system
$^{\alpha}, _{\alpha}, ...$	All Greek superscripts or subscripts range from 1 to 2
$^{i}, _{i}, ...$	All Italic superscripts or subscripts range from 1 to 3
$\vec{\mathbf{i}}_i, \vec{\mathbf{j}}_i$	Covariant unit vectors along axis x^i in middle surface and adjacent surfaces, respectively
$\vec{\mathbf{i}}^i, \vec{\mathbf{j}}^i$	Contravariant unit vectors along axis x^i in middle surface and adjacent surfaces, respectively
Γ^k_{ij}	Christoffel symbols in terms of g_i and g_{ij}
$\overline{\Gamma}^k_{ij}$	Christoffel symbols in terms of a_i and a_{ij} (defined for the middle surface)

$\cdot$	Inner product
$\otimes$	Cross product
$\vert$	Covariant derivative
$\Vert$	Covariant derivative in two dimensional spaces
T^*	Kinetic energy
V^*	Potential energy
V	Volume
W^*	External work
Π	Mechanical energy of the system
ε_{ij}	Components of the strain tensor on the middle surface
η_{ij}	Components of the strain tensor adjacent to the middle surface
$\eta_{\alpha\beta}$	In-plane components of the Strain tensor
σ^{ij}	Stress tensor
$\sigma^{\alpha\beta}$	In-plane components of the stress tensor
E^{ijlm}	Generalized Hooke's Law

$E^{\alpha\beta\lambda\delta}$	In-plane components of the generalized Hooke's Law
$\cdots_{,i}$	Partial derivative with respect to x^i
δ_β^α	Kronecker delta function
μ_β^α	The covariant tensor which connects the base vectors of two different points
λ_α^γ	Contravariant counterpart of μ_β^α
ρ	Density of the mass
E	Modulus of elasticity
ν	Poisson's ratio

Appendix 2.A. Contravariant Components of the Displacement

Using the identity $\mathbf{a}^{\alpha} = a^{\alpha\rho}\mathbf{a}_{\rho}$ (operation of raising indices) in Eq. 2.37 yields

$$\boldsymbol{\theta}\left(x^1, x^2\right) = \hat{\mathbf{a}}_3 - \mathbf{a}_3 = -\left(u_{3,\alpha} + u_{\gamma}\bar{b}_{\alpha}^{\gamma}\right)a^{\alpha\rho}\mathbf{a}_{\rho} \tag{2.A.1}$$

From Eqs. 2.29 and 2.A.1, by substituting into Eq. 2.28, one obtains

$$\begin{aligned}\mathbf{U} &= u^{i}\mathbf{a}_{i} - x^{3}\left(u_{3,\alpha} + u_{\gamma}\bar{b}_{\alpha}^{\gamma}\right)a^{\alpha\rho}\mathbf{a}_{\rho} \\ &= u^{\rho}\mathbf{a}_{\rho} + u^{3}\mathbf{a}_{3} - x^{3}\left(u_{3,\alpha} + u_{\gamma}\bar{b}_{\alpha}^{\gamma}\right)a^{\alpha\rho}\mathbf{a}_{\rho}\end{aligned} \tag{2.A.2}$$

Grouping terms with the same base vectors yields

$$\mathbf{U} = \left[u^{\rho} - x^{3}\left(u_{3,\alpha} + u_{\gamma}\bar{b}_{\alpha}^{\gamma}\right)a^{\alpha\rho}\right]\mathbf{a}_{\rho} + u^{3}\mathbf{a}_{3} \tag{2.A.3}$$

Using the Kronicker delta tensor and the identity $u_{\gamma} = g_{\lambda\gamma}u^{\lambda}$ yields

$$\begin{aligned}\mathbf{U} &= \left[\delta_{\lambda}^{\rho}u^{\lambda} - x^{3}\left(u_{3,\alpha} + g_{\lambda\gamma}u^{\lambda}\bar{b}_{\alpha}^{\gamma}\right)a^{\alpha\rho}\right]\mathbf{a}_{\rho} + u^{3}\mathbf{a}_{3} \\ &= \left[\delta_{\lambda}^{\rho}u^{\lambda} - x^{3}a^{\alpha\rho}a_{\lambda\gamma}u^{\lambda}\bar{b}_{\alpha}^{\gamma} - x^{3}u_{3,\alpha}a^{\alpha\rho}\right]\mathbf{a}_{\rho} + u^{3}\mathbf{a}_{3} \\ &= \left[\delta_{\lambda}^{\rho}u^{\lambda} - x^{3}a_{\lambda}^{\alpha}a_{\gamma}^{\rho}u^{\lambda}\bar{b}_{\alpha}^{\gamma} - x^{3}u_{3,\alpha}a^{\alpha\rho}\right]\mathbf{a}_{\rho} + u^{3}\mathbf{a}_{3} \\ &= \left[\delta_{\lambda}^{\rho}u^{\lambda} - x^{3}\delta_{\lambda}^{\alpha}\delta_{\gamma}^{\rho}u^{\lambda}\bar{b}_{\alpha}^{\gamma} - x^{3}u_{3,\alpha}a^{\alpha\rho}\right]\mathbf{a}_{\rho} + u^{3}\mathbf{a}_{3} \\ &= \left[\delta_{\lambda}^{\rho}u^{\lambda} - x^{3}\bar{b}_{\lambda}^{\rho}u^{\lambda} - x^{3}u_{3,\alpha}a^{\alpha\rho}\right]\mathbf{a}_{\rho} + u^{3}\mathbf{a}_{3} \\ &= \left[\left(\delta_{\lambda}^{\rho} - x^{3}\bar{b}_{\lambda}^{\rho}\right)u^{\lambda} - x^{3}u_{3,\alpha}a^{\alpha\rho}\right]\mathbf{a}_{\rho} + u^{3}\mathbf{a}_{3}\end{aligned} \tag{2.A.4}$$

Using Eq. 2.16 in Eq. 2.A.4 yields

$$\mathbf{U} = \left(\mu_{\lambda}^{\rho}u^{\lambda} - x^{3}u_{3,\gamma}a^{\gamma\rho}\right)\mathbf{a}_{\rho} + u^{3}\mathbf{a}_{3} \tag{2.A.5}$$

By dot-multiplying both sides of Eq. 2.15-a by $\lambda_{\delta}^{\alpha}$, one obtains $\mathbf{a}_{\delta} = \lambda_{\delta}^{\alpha}\mathbf{g}_{\alpha}$. By substituting in Eq. 2.A.5 and using Eq. 2.15b, one obtains

$$\mathbf{U} = \left(\mu_{\lambda}^{\rho}u^{\lambda} - x^{3}u_{3,\gamma}a^{\gamma\rho}\right)\lambda_{\rho}^{\alpha}\mathbf{g}_{\alpha} + u^{3}\mathbf{g}_{3} \tag{2.A.6}$$

Eq. 2.A.6 relates the displacement of points within the shell to the displacement of their picture on the middle surface. Thus, Eq. 2.26 can be rewritten as

$$\mathbf{U} = U^{\alpha}\left(x^1, x^2, x^3, t\right)\mathbf{g}_{\alpha} + U^{3}\left(x^1, x^2, t\right)\mathbf{g}_3 \tag{2.A.7}$$

By comparing Eqs. 2.A.6and 2.A.7, one obtains

$$U^{\alpha} = \left(\mu_{\lambda}^{\rho} u^{\lambda} - x^3 u_{,\gamma}^{3} a^{\gamma\rho}\right)\lambda_{\rho}^{\alpha} \qquad , \qquad U^3 = u^3 \tag{2.A.8}$$

Checking the equality by equating the right hand sides of Eqs. 2.46 and 2.A.8:

$$\left(\mu_{\lambda}^{\rho} u^{\lambda} - x^3 u_{,\gamma}^{3} a^{\gamma\rho}\right)\lambda_{\rho}^{\alpha} = \left(\mu_{\delta}^{\gamma} u_{\gamma} - x^3 u_{3,\delta}\right)\mu_{\beta}^{\delta} g^{\alpha\beta} \tag{2.A.9}$$

Using the identity $u^{\lambda} = a^{\lambda\gamma} u_{\gamma}$ and changing the dummy index γ to δ in the second term on the left hand side, one obtains

$$\lambda_{\rho}^{\alpha}\mu_{\lambda}^{\rho} a^{\lambda\gamma} u_{\gamma} - x^3 u_{,\delta}^{3}\lambda_{\rho}^{\alpha} a^{\delta\rho} = \mu_{\delta}^{\gamma}\mu_{\beta}^{\delta} g^{\alpha\beta} u_{\gamma} - x^3 u_{3,\delta}\mu_{\beta}^{\delta} g^{\alpha\beta} \tag{2.A.10}$$

As $u^3 = u_3$ and u_i are independent, one can write

$$\begin{aligned}
\lambda_{\rho}^{\alpha}\mu_{\lambda}^{\rho} a^{\lambda\gamma} &= \mu_{\delta}^{\gamma}\mu_{\beta}^{\delta} g^{\alpha\beta} &,\quad & \lambda_{\rho}^{\alpha} a^{\delta\rho} = \mu_{\beta}^{\delta} g^{\alpha\beta} \\
\delta_{\lambda}^{\alpha} a^{\lambda\gamma} &= \mu_{\delta}^{\gamma}\mu_{\beta}^{\delta}\mathbf{g}^{\alpha}\cdot\mathbf{g}^{\beta} &,\quad & \lambda_{\rho}^{\alpha} a^{\delta\rho} = \mu_{\beta}^{\delta}\mathbf{g}^{\alpha}\cdot\mathbf{g}^{\beta} \\
a^{\alpha\gamma} &= \mu_{\delta}^{\gamma}\mu_{\beta}^{\delta}\left(\lambda_{\rho}^{\alpha}\mathbf{a}^{\rho}\right)\cdot\left(\lambda_{\gamma}^{\beta}\mathbf{a}^{\gamma}\right) &,\quad & \lambda_{\rho}^{\alpha} a^{\delta\rho} = \mu_{\beta}^{\delta}\left(\lambda_{\rho}^{\alpha}\mathbf{a}^{\rho}\right)\cdot\left(\lambda_{\gamma}^{\beta}\mathbf{a}^{\gamma}\right) \\
a^{\alpha\gamma} &= \mu_{\delta}^{\gamma}\mu_{\beta}^{\delta}\lambda_{\rho}^{\alpha}\lambda_{\theta}^{\beta} a^{\rho\theta} &,\quad & \lambda_{\rho}^{\alpha} a^{\delta\rho} = \mu_{\beta}^{\delta}\lambda_{\rho}^{\alpha}\lambda_{\gamma}^{\beta} a^{\rho\gamma} \\
a^{\alpha\gamma} &= \mu_{\delta}^{\gamma}\lambda_{\rho}^{\alpha}\delta_{\theta}^{\delta} a^{\rho\theta} &,\quad & \lambda_{\rho}^{\alpha} a^{\delta\rho} = \lambda_{\rho}^{\alpha}\delta_{\gamma}^{\delta} a^{\rho\gamma} \\
a^{\alpha\gamma} &= \mu_{\delta}^{\gamma}\lambda_{\rho}^{\alpha} a^{\rho\delta} &,\quad & \lambda_{\rho}^{\alpha} a^{\delta\rho} = \lambda_{\rho}^{\alpha} a^{\delta\rho} \\
a^{\alpha\gamma} &= \mu_{\delta}^{\gamma}\lambda^{\alpha\delta} \\
a^{\alpha\gamma} &= \mu_{\delta}^{\gamma}\lambda_{\rho}^{\delta} a^{\alpha\rho} \\
a^{\alpha\gamma} &= \delta_{\rho}^{\gamma} a^{\alpha\rho} \\
a^{\alpha\gamma} &= a^{\alpha\gamma}
\end{aligned} \tag{2.A.11}$$

Appendix 2.B. Reduction of the Number of Components of the Constitutive Elasticity Tensor

In general, as each of the superscripts i, j, l, m can take any of the values $1, 2, 3$, the elasticity tensor E^{ijlm} has $3^4 = 81$ components. The symmetry of the problem yields $\sigma^{ij} = \sigma^{ji}$ and $\varepsilon_{lm} = \varepsilon_{ml}$, from which it follows that

$$E^{ijlm} = E^{jilm} = E^{jiml} = E^{ijml} \tag{2.B.1}$$

which means that the order of the superscripts in each pair does not matter. Therefore, Subscripts i and j can take six possible sets of pairs of values: $(1,1);(1,2);(1,3);(2,2);(2,3);(3,3)$. A similar argument can be extended to subscripts l and m resulting in six possible combinations. This reduces the number of independent constitutive terms E^{ijlm} to $6^2 = 36$.

It will now be shown that the order of the pairs ij and lm is interchangeable as well. The strain energy in an infinitesimal element is

$$v^* = \tfrac{1}{2}\sigma^{ij}\varepsilon_{ij} \tag{2.B.2}$$

Thus, the differential change in the internal strain energy density is

$$dv^* = \tfrac{1}{2}d\left(\sigma^{ij}\varepsilon_{ij}\right) = \tfrac{1}{2}d\sigma^{ij}\varepsilon_{ij} + \tfrac{1}{2}\sigma^{ij}d\varepsilon_{ij} \tag{2.B.3}$$

By using Eq. 2.47) to substitute $E^{ijlm}\varepsilon_{lm}$ for σ^{ij} and interchanging the dummy indices ij and lm in the first term, one obtains

$$\begin{aligned} dv^* &= \tfrac{1}{2}E^{ijlm}d\varepsilon_{lm}\varepsilon_{ij} + \tfrac{1}{2}E^{ijlm}\varepsilon_{lm}d\varepsilon_{ij} = \tfrac{1}{2}E^{lmij}\varepsilon_{lm}d\varepsilon_{ij} + \tfrac{1}{2}E^{ijlm}\varepsilon_{lm}d\varepsilon_{ij} \\ &= \tfrac{1}{2}\left(E^{lmij} + E^{ijlm}\right)\varepsilon_{lm}d\varepsilon_{ij} \end{aligned} \tag{2.B.4}$$

The differential change in the internal strain energy dv^* can also be expressed as the work done by existing stress along the increment of the strains, i.e.,

$$dv^* = \sigma^{ij} d\varepsilon_{ij} = E^{ijlm} \varepsilon_{ij} d\varepsilon_{ij} \tag{2.B.5}$$

By equating Eqs. 2.B.4 and 2.B.5 , one obtains

$$E^{ijlm} = E^{lmij} \tag{2.B.6}$$

This means that the order of pairs ij and lm is interchangeable, which reduces the number of independent components of E^{ijlm} from 36 to 21.

In isotropic materials with infinite number of planes of material properties symmetry, it will be shown that those 21 components are functions only of two independent material properties (E and ν). To do so, we first consider the implications of the symmetry about the x^1x^2 plane in coordinate system x^i by introducing a new coordinate system $\hat{x}^i$ with the following transformation law to coordinate system x^i

	x^1	x^2	x^3
$\hat{x}^1$	1	0	0
$\hat{x}^2$	0	1	0
$\hat{x}^3$	0	0	−1

The transformed stress tensor from coordinate system x^i to $\hat{x}^i$ is

$$\hat{\sigma}^{ij} = \frac{\partial \hat{x}^i}{\partial x^m} \frac{\partial \hat{x}^j}{\partial x^n} \sigma^{mn} = \beta_m^{\hat{i}} \beta_n^{\hat{j}} \sigma^{mn}$$

For component $\hat{\sigma}^{11}$, one has

$$\begin{aligned} \hat{\sigma}^{11} &= \beta_1^{\hat{1}} \beta_n^{\hat{1}} \sigma^{1n} + \cancelto{0}{\beta_2^{\hat{1}}} \beta_n^{\hat{1}} \sigma^{2n} + \cancelto{0}{\beta_3^{\hat{1}}} \beta_n^{\hat{1}} \sigma^{3n} \\ &= \cancelto{1}{\beta_1^{\hat{1}}} \cancelto{1}{\beta_1^{\hat{1}}} \sigma^{11} \\ &= \sigma^{11} \end{aligned} \tag{2.B.7a}$$

In a similar manner, one obtains

$$\hat{\sigma}^{12} = \sigma^{12}, \hat{\sigma}^{22} = \sigma^{22} \quad , \hat{\sigma}^{13} = -\sigma^{13}, \hat{\sigma}^{33} = \sigma^{33}, \hat{\sigma}^{23} = -\sigma^{23} \tag{2.B.7b-f}$$

Also,

$$\begin{aligned} \hat{\varepsilon}_{11} &= \varepsilon_{11} \quad , \quad \hat{\varepsilon}_{12} = -\varepsilon_{12} \\ \hat{\varepsilon}_{22} &= \varepsilon_{22} \quad , \quad \hat{\varepsilon}_{13} = -\varepsilon_{13} \\ \hat{\varepsilon}_{33} &= \varepsilon_{33} \quad , \quad \hat{\varepsilon}_{23} = \varepsilon_{23} \end{aligned} \tag{2.B.8a-f}$$

By expanding the constitutive equation $\sigma^{ij} = E^{ijlm}\varepsilon_{lm}$ for σ^{11} and $\hat{\sigma}^{11}$ and using the identities in Eqs. 2.B.8, one obtains

$$\begin{aligned} \sigma^{11} &= E^{1111}\varepsilon_{11} + E^{1112}\varepsilon_{12} + E^{1113}\varepsilon_{13} + E^{1122}\varepsilon_{22} + E^{1123}\varepsilon_{23} + E^{1133}\varepsilon_{33} \\ \hat{\sigma}^{11} &= E^{1111}\hat{\varepsilon}_{11} + E^{1112}\hat{\varepsilon}_{12} + E^{1113}\hat{\varepsilon}_{13} + E^{1122}\hat{\varepsilon}_{22} + E^{1123}\hat{\varepsilon}_{23} + E^{1133}\hat{\varepsilon}_{33} \\ &= E^{1111}\varepsilon_{11} + E^{1112}\varepsilon_{12} - E^{1113}\varepsilon_{13} + E^{1122}\varepsilon_{22} - E^{1123}\varepsilon_{23} + E^{1133}\varepsilon_{33} \end{aligned}$$

Recalling the identity $\hat{\sigma}^{11} = \sigma^{11}$ in Eq. 2.B.7a, one obtains

$$E^{1113} = E^{1123} = 0 \tag{2.B.9}$$

Repeating the procedure for the remaining stress components will result in

$$E^{2213} = E^{2223} = E^{3313} = E^{3323} = E^{2313} = 0 \tag{2.B.10}$$

and the number of independent components of the constitutive tensor is reduced from 21 to 13. A material with only one plane of material property symmetry is called monoclinic.

In the same manner, by assuming material symmetry about planes x^1x^3 one obtains the following additional relationships

$$E^{1112} = E^{2212} = E^{3312} = E^{2312} = E^{1312} = 0 \tag{2.B.11}$$

and the number of independent components of the constitutive tensor is reduced to nine.

By considering symmetry about the x^2x^3 plane, the relations obtained are found to be identically satisfied and no additional reductions in the number of independent components

is obtained. A material with three orthogonal planes of material property symmetry is called orthotropic.

Let us consider the axis of symmetry x^1 for plane of symmetry x^2x^3 by defining three new coordinate systems $\hat{x}^i$ with the following transformation laws to coordinate system x^i

	x^1	x^2	x^3
$\hat{x}^1$	1	0	0
$\hat{x}^2$	0	0	1
$\hat{x}^3$	0	−1	0

,

	x^1	x^2	x^3
$\hat{x}^1$	1	0	0
$\hat{x}^2$	0	−1	0
$\hat{x}^3$	0	0	−1

,

	x^1	x^2	x^3
$\hat{x}^1$	$\sqrt{2}/2$	$\sqrt{2}/2$	0
$\hat{x}^2$	$-\sqrt{2}/2$	$\sqrt{2}/2$	0
$\hat{x}^3$	0	0	1

One can show that the stress transformation between the old and new coordinate systems will yield the following additional relationships

$$E^{1122} = E^{1133}$$
$$E^{2222} = E^{3333}$$
$$E^{1313} = E^{1212}$$

,

$$E^{1111} = E^{2222}$$
$$E^{2233} = E^{1133}$$
$$E^{2323} = E^{1313}$$

and

$$E^{1212} = \frac{1}{2}\left(E^{1111} - E^{1122}\right) \qquad \text{(2.B.12a-g)}$$

respectively.

The seven equations 2.B.12a-g reduce the number of independent components from nine to two. An elastic material with only two independent constitutive constants is called isotropic. Conventionally, these are the Elasticity modulus and Poisson ratio or the Lame's constants. The elasticity tensor of an isotropic material in Cartesian coordinate system can be written as ([2.6])

$$E^{ijlm} = \frac{E}{2(1+\nu)}\left[\delta^{il}\delta^{jm} + \delta^{im}\delta^{jl} + \frac{2\nu}{1-2\nu}\delta^{ij}\delta^{lm}\right] \tag{2.B.13}$$

The validity of Eq. 2.B.13 can be simply investigated by expanding it into its components and comparing the results with the relationships obtained in this Appendix (Eqs. 2.B.1, 2.B.6 , 2.B.9, 2.B.10, 2.B.11 and 2.B.12a-g).

Appendix 2.C. Expanding the Term $U_\alpha|_\beta$

In this section it will be shown that in thin shells the covariant derivative of in-plane components of the displacement are expressible in terms of the properties and displacements of the middle surface.

The covariant derivative of U_α with respect to coordinates x^β, on a general surface (i.e., a surface parallel and offset from the middle surface) in a three dimensional space is

$$U_\alpha|_\beta = U_{\alpha,\beta} - U_k\Gamma^k_{\alpha\beta} = U_{\alpha,\beta} - U_\gamma\Gamma^\gamma_{\alpha\beta} - U_3\Gamma^3_{\alpha\beta} \tag{2.C.1}$$

where $\Gamma^\gamma_{\alpha\beta}$ and $\Gamma^3_{\alpha\beta}$ are the Christoffel symbols on the surface of interest. A new definition $U_\alpha\|_\beta = U_{\alpha,\beta} - U_\gamma\Gamma^\gamma_{\alpha\beta}$ is introduced to express Eq. 2.C.1 in a two dimensional form

$$U_\alpha|_\beta = U_\alpha\|_\beta - U_3\Gamma^3_{\alpha\beta} = U_\alpha\|_\beta - U_3 b_{\alpha\beta} \tag{2.C.2}$$

in which the symbol "||" is a two dimensional counterpart of the three dimensional covariant derivative symbol "|". By dot-multiplying Eq. A.54 by the base vector $\mathbf{g}^l$, one obtains

$$\Gamma^l_{ij} = \mathbf{g}_{i,j}\cdot\mathbf{g}^l \quad \Rightarrow \quad \Gamma^\gamma_{\alpha\beta} = \mathbf{g}_{\alpha,\beta}\cdot\mathbf{g}^\gamma \quad \Rightarrow \quad \overline{\Gamma}^\gamma_{\alpha\beta} = \mathbf{a}_{\alpha,\beta}\cdot\mathbf{a}^\gamma \tag{2.C.3a-c}$$

Form Eqs. 2.16a and 2.18a, substituting into Eq. 2.C.3b yields

$$\Gamma^\gamma_{\alpha\beta} = \left(\mu^\xi_\alpha\mathbf{a}_\xi\right)_{,\beta}\cdot\left(\lambda^\gamma_\rho\mathbf{a}^\rho\right) = \left(\mu^\xi_{\alpha,\beta}\mathbf{a}_\xi + \mu^\xi_\alpha\mathbf{a}_{\xi,\beta}\right)\cdot\left(\lambda^\gamma_\rho\mathbf{a}^\rho\right) = \lambda^\gamma_\rho\left(\mu^\xi_{\alpha,\beta}\delta^\rho_\xi + \mu^\xi_\alpha\mathbf{a}_{\xi,\beta}\cdot\mathbf{a}^\rho\right) \tag{2.C.4}$$

From Eq. 2.C.3c, substituting into the second term of Eq. 2.C.4 yields

$$\Gamma^\gamma_{\alpha\beta} = \lambda^\gamma_\rho\left(\mu^\rho_{\alpha,\beta} + \mu^\xi_\alpha\overline{\Gamma}^\rho_{\xi\beta}\right) \tag{2.C.5}$$

As μ_α^ξ is a second rank plane tensor defined on the middle surface, by considering the definition of covariant derivative (Eq. A.78), one may write

$$\mu_\alpha^\rho \|_\beta = \mu_{\alpha,\beta}^\rho + \mu_\alpha^\xi \overline{\Gamma}_{\xi\beta}^\rho - \mu_\xi^\rho \overline{\Gamma}_{\alpha\beta}^\xi \tag{2.C.6}$$

From Eq. 2.C.6, substituting into Eq. 2.C.5 yields

$$\Gamma_{\alpha\beta}^\gamma = \lambda_\rho^\gamma \left(\mu_\alpha^\rho \|_\beta + \mu_\xi^\rho \overline{\Gamma}_{\alpha\beta}^\xi \right) \tag{2.C.7}$$

Using the identity $\lambda_\gamma^\alpha \mu_\beta^\gamma = \delta_\beta^\alpha$ (Eq. 2.19) in Eq. 2.C.7 yields

$$\Gamma_{\alpha\beta}^\gamma = \lambda_\rho^\gamma \mu_\alpha^\rho \|_\beta + \overline{\Gamma}_{\alpha\beta}^\gamma \tag{2.C.8}$$

In the same manner, considering Eq. 2.C.3a, one writes

$$\Gamma_{\alpha\beta}^3 = \mathbf{g}_{\alpha,\beta} \cdot \mathbf{g}^3 \tag{2.C.9}$$

Substituting the identities $\mathbf{g}_\alpha = \mu_\alpha^\gamma \mathbf{a}_\gamma$ and $\mathbf{g}^3 = \mathbf{a}^3$ (Eqs. 2.15a and 2.18b) into Eq. 2.C.9 yields

$$\Gamma_{\alpha\beta}^3 = \left(\mu_\alpha^\gamma \mathbf{a}_\gamma \right)_{,\beta} \cdot \left(\mathbf{a}^3 \right) = \left(\mu_{\alpha,\beta}^\gamma \mathbf{a}_\gamma + \mu_\alpha^\gamma \mathbf{a}_{\gamma,\beta} \right) \cdot \left(\mathbf{a}^3 \right) = \mu_\alpha^\gamma \mathbf{a}_{\gamma,\beta} \cdot \mathbf{a}^3 \tag{2.C.10}$$

From Eq. 2.C.3c, substituting into Eq. 2.C.10 yields

$$\Gamma_{\alpha\beta}^3 = \mu_\alpha^\gamma \overline{\Gamma}_{\gamma\beta}^3 = \mu_\alpha^\gamma \overline{b}_{\gamma\beta} \tag{2.C.11}$$

Equation 2.C.11 relates the curvature of surfaces parallel and adjacent to the middle surface to the curvature of the middle surface. By substituting Eqs. 2.C.8 and 2.C.11 into Eq. 2.C.1, one obtains

$$U_\alpha|_\beta = U_{\alpha,\beta} - U_\gamma \left(\lambda_\rho^\gamma \mu_\alpha^\rho \|_\beta + \overline{\Gamma}_{\alpha\beta}^\gamma \right) - U_3 \mu_\alpha^\gamma \overline{\Gamma}_{\gamma\beta}^3 \tag{2.C.12}$$

By substituting the identities $U_\alpha = \left(\mu_\delta^\gamma u_\gamma - z u_{3,\delta} \right) \mu_\alpha^\delta$ and $U_3 = u_3$ (Eq. 2.45) into Eq. 2.C.12 , one obtains

$$U_\alpha|_\beta = \left[\left(\mu_\delta^\gamma u_\gamma - z u_{3,\delta} \right) \mu_\alpha^\delta \right]_{,\beta} - \left(\mu_\delta^\psi u_\psi - z u_{3,\delta} \right) \mu_\gamma^\delta \left(\lambda_\rho^\gamma \mu_\alpha^\rho \|_\beta + \overline{\Gamma}_{\alpha\beta}^\gamma \right) - u_3 \mu_\alpha^\gamma \overline{\Gamma}_{\gamma\beta}^3 \tag{2.C.13}$$

Appendix 2.D. Expansion of Hamilton's Principle for Thin Shells

2.D.1. Variation of the Kinetic Energy

Recalling Eq. 2.52a, integrating by parts with respect to time yields

$$\int_{t_1}^{t_2} \delta T^* dt = \int_{t_1}^{t_2} \int_V \dot{U}^i \rho \delta \dot{U}_i dV dt$$
$$= \int_V \int_{t_1}^{t_2} \dot{U}^i \rho \delta \dot{U}_i dt dV = \int_V \left(\left[\dot{U}^i \rho \delta U_i \right]_{t_1}^{t_2} - \int_{t_1}^{t_2} \ddot{U}^i \rho \delta U_i dt \right) dV \tag{2.D.1}$$

$$\int_{t_1}^{t_2} \delta T^* dt = \left[\int_V \dot{U}^i \rho \delta U_i dV \right]_{t_1}^{t_2} - \int_{t_1}^{t_2} \int_V \ddot{U}^i \rho \delta U_i dV dt \tag{2.D.2}$$

The following definition is introduced

$$\int_{t_1}^{t_2} \delta T^* dt = \delta T^*_{I.F.C.} + \int_{t_1}^{t_2} \delta T^*_{F.E.} dt \tag{2.D.3}$$

where,

$$\delta T^*_{\text{I.F.C.}} = \left[\int_V \dot{U}^i \rho \delta U_i dV \right]_{t_1}^{t_2} \tag{2.D.4}$$

$$\delta T^*_{\text{F.E.}} = -\int_V \ddot{U}^i \rho \delta U_i dV \tag{2.D.5}$$

It is noted that $\delta T^*_{\text{I.F.C.}}$ contributes to initial and final conditions (I.F.C.) of the problem and $\delta T^*_{\text{F.E.}}$ contributes to the field equations (F.E.).

2.D.2. Variation of the Potential Energy

Using the in-plane component of the strain-displacement relationship $\eta_{\alpha\beta} = \frac{1}{2}\left(U_\alpha|_\beta + U_\beta|_\alpha\right)$ (Eq. 2.23) in the expression for the internal strain energy (Eq.2.52b) yields

$$\delta V^* = \int_V E^{\alpha\beta\lambda\delta}\left[\tfrac{1}{2}\left(U_\lambda|_\delta + U_\delta|_\lambda\right)\right]\delta\left[\tfrac{1}{2}\left(U_\alpha|_\beta + U_\beta|_\alpha\right)\right]dV \tag{2.D.6}$$

It should be noted that the material is considered uniform and homogeneous. It is defined in Appendix 2.C that $U_\alpha|_\beta = U_\alpha\|_\beta - U_3 b_{\alpha\beta}$, thus Eq. 2.D.6 is expanded as

$$\begin{aligned}
\delta V^* &= \int_V \tfrac{1}{4} E^{\alpha\beta\lambda\delta}\left(U_\lambda\|_\delta + U_\delta\|_\lambda - 2U_3 b_{\lambda\delta}\right)\delta\left(U_\alpha\|_\beta + U_\beta\|_\alpha - 2U_3 b_{\alpha\beta}\right)dV \\
&= \int_V \tfrac{1}{4} E^{\alpha\beta\lambda\delta}\left(U_\lambda\|_\delta + U_\delta\|_\lambda - 2U_3 b_{\lambda\delta}\right)\left[\delta\left(U_\alpha\|_\beta\right) + \delta\left(U_\beta\|_\alpha\right) - \delta\left(2U_3 b_{\alpha\beta}\right)\right]dV \\
&= \int_V \tfrac{1}{4} E^{\alpha\beta\lambda\delta}\left(U_\lambda\|_\delta + U_\delta\|_\lambda - 2U_3 b_{\lambda\delta}\right)\left[\left(\delta U_\alpha\right)\|_\beta + \left(\delta U_\beta\right)\|_\alpha - 2b_{\alpha\beta}\delta U_3\right]dV \\
&= \int_V \tfrac{1}{4} E^{\alpha\beta\lambda\delta}\left(U_\lambda\|_\delta + U_\delta\|_\lambda - 2U_3 b_{\lambda\delta}\right)\left(\delta U_\alpha\right)\|_\beta \, dV \\
&\quad + \int_V \tfrac{1}{4} E^{\alpha\beta\lambda\delta}\left(U_\lambda\|_\delta + U_\delta\|_\lambda - 2U_3 b_{\lambda\delta}\right)\left(\delta U_\beta\right)\|_\alpha \, dV \\
&\quad + \int_V \tfrac{1}{4} E^{\alpha\beta\lambda\delta}\left(U_\lambda\|_\delta + U_\delta\|_\lambda - 2U_3 b_{\lambda\delta}\right)\left(-2b_{\alpha\beta}\delta U_3\right)dV
\end{aligned} \tag{2.D.7}$$

By interchanging the dummy indices α and β in the second integral term, and using the identity $E^{\beta\alpha\lambda\delta} = E^{\alpha\beta\lambda\delta}$ (Eq. 2.B.1), one obtains

$$\begin{aligned}
\delta V^* &= \int_V \tfrac{1}{2} E^{\alpha\beta\lambda\delta}\left(U_\lambda\|_\delta + U_\delta\|_\lambda - 2U_3 b_{\lambda\delta}\right)\left(\delta U_\alpha\right)\|_\beta \, dV \\
&\quad + \int_V \tfrac{1}{2} E^{\alpha\beta\lambda\delta}\left(U_\lambda\|_\delta + U_\delta\|_\lambda - 2U_3 b_{\lambda\delta}\right)\left(-b_{\alpha\beta}\delta U_3\right)dV
\end{aligned} \tag{2.D.8}$$

Integrating by parts with respect to β in the first integral term yields

$$\begin{aligned}\delta V^* = &\int_A \left[\tfrac{1}{2}E^{\alpha\beta\lambda\delta}\left(U_\lambda\|_\delta + U_\delta\|_\lambda - 2U_3 b_{\lambda\delta}\right)\delta U_\alpha\right]_0^{x_\beta} dA \\ &-\int_V \left\{\tfrac{1}{2}E^{\alpha\beta\lambda\delta}\left[U_\lambda\|_{\delta\beta} + U_\delta\|_{\lambda\beta} - \left(2U_3 b_{\lambda\delta}\right)\|_\beta\right]\right. \\ &\qquad \left. + \tfrac{1}{2}\left(E^{\alpha\beta\lambda\delta}\|_\beta\right)\left[U_\lambda\|_\delta + U_\delta\|_\lambda - \left(2U_3 b_{\lambda\delta}\right)\right]\right\}\delta U_\alpha dV \\ &-\int_V \tfrac{1}{2}E^{\alpha\beta\lambda\delta}\left(U_\lambda\|_\delta + U_\delta\|_\lambda - 2U_3 b_{\lambda\delta}\right)\left(b_{\alpha\beta}\delta U_3\right)dV\end{aligned} \tag{2.D.9}$$

It should be noted that the elasticity tensor $E^{\alpha\beta\lambda\delta}$ is defined in terms of base vectors $\mathbf{g}^\alpha$, thus in general, its covariant derivative with respect to x^β ($E^{\alpha\beta\lambda\delta}\|_\beta$) is different from zero. Using the relationship $U_3\|_\beta = U_{3,\beta}$ proved in Appendix 2.E, Eq. 2.D.9 is simplified to

$$\begin{aligned}\delta V^* = &\int_A \left[\tfrac{1}{2}E^{\alpha\beta\lambda\delta}\left(U_\lambda\|_\delta + U_\delta\|_\lambda - 2U_3 b_{\lambda\delta}\right)\delta U_\alpha\right]_0^{x_\beta} dA \\ &-\int_V \left[\tfrac{1}{2}E^{\alpha\beta\lambda\delta}\left(U_\lambda\|_{\delta\beta} + U_\delta\|_{\lambda\beta} - 2U_{3,\beta}b_{\lambda\delta} - 2U_3 b_{\lambda\delta}\|_\beta\right)\right. \\ &\qquad \left. + \tfrac{1}{2}\left(E^{\alpha\beta\lambda\delta}\|_\beta\right)\left(U_\lambda\|_\delta + U_\delta\|_\lambda - 2U_3 b_{\lambda\delta}\right)\right]\delta U_\alpha dV \\ &-\int_V \tfrac{1}{2}E^{\alpha\beta\lambda\delta}\left(U_\lambda\|_\delta + U_\delta\|_\lambda - 2U_3 b_{\lambda\delta}\right)\left(b_{\alpha\beta}\delta U_3\right)dV\end{aligned} \tag{2.D.10}$$

The following definition is introduced

$$\delta V^* = \delta V^*_{B.C.} + \delta V^*_{F.E.} \tag{2.D.11}$$

where

$$\delta V^*_{B.C.} = \int_A \left[\tfrac{1}{2}E^{\alpha\beta\lambda\delta}\left(U_\lambda\|_\delta + U_\delta\|_\lambda - 2U_3 b_{\lambda\delta}\right)\delta U_\alpha\right]_0^{x_\beta} dA \tag{2.D.12}$$

$$\begin{aligned}\delta V^*_{F.E.} = &-\int_V \left[\tfrac{1}{2}E^{\alpha\beta\lambda\delta}\left(U_\lambda\|_{\delta\beta} + U_\delta\|_{\lambda\beta} - 2U_{3,\beta}b_{\lambda\delta} - 2U_3 b_{\lambda\delta}\|_\beta\right)\right. \\ &\qquad \left. + \tfrac{1}{2}\left(E^{\alpha\beta\lambda\delta}\|_\beta\right)\left(U_\lambda\|_\delta + U_\delta\|_\lambda - 2U_3 b_{\lambda\delta}\right)\right]\delta U_\alpha dV \\ &-\int_V \tfrac{1}{2}E^{\alpha\beta\lambda\delta}\left(U_\lambda\|_\delta + U_\delta\|_\lambda - 2U_3 b_{\lambda\delta}\right)\left(b_{\alpha\beta}\delta U_3\right)dV\end{aligned} \tag{2.D.13}$$

It is noted that $\delta V^*_{B.C.}$ contributes to the boundary conditions (B.C.) of the problem and $\delta V^*_{F.E.}$ contributes to the field equations (F.E.).

Appendix 2.E. Proof of $U_3\|_\beta = U_{3,\beta}$

Calling Eq. A.79, the second covariant derivative of a first rank tensor is

$$U_\lambda|_{\delta\beta} = \left(U_{\lambda,\delta} - U_m\Gamma^m_{\lambda\delta}\right)_{,\beta} - \left(U_{l,\delta} - U_m\Gamma^m_{l\delta}\right)\Gamma^l_{\lambda\beta} - \left(U_{\lambda,l} - U_m\Gamma^m_{\lambda l}\right)\Gamma^l_{\beta\delta} \tag{2.E.1}$$

Thus, one can write

$$\begin{aligned}
U_\lambda|_{\delta\beta} + U_\delta|_{\lambda\beta} &= \left(U_{\lambda,\delta} - U_m\Gamma^m_{\lambda\delta}\right)_{,\beta} - \left(U_{l,\delta} - U_m\Gamma^m_{l\delta}\right)\Gamma^l_{\lambda\beta} - \left(U_{\lambda,l} - U_m\Gamma^m_{\lambda l}\right)\Gamma^l_{\beta\delta} \\
&\quad + \left(U_{\delta,\lambda} - U_m\Gamma^m_{\delta\lambda}\right)_{,\beta} - \left(U_{l,\lambda} - U_m\Gamma^m_{l\lambda}\right)\Gamma^l_{\delta\beta} - \left(U_{\delta,l} - U_m\Gamma^m_{\delta l}\right)\Gamma^l_{\beta\lambda} \\
&= \left(U_{\lambda,\delta} - U_m\Gamma^m_{\lambda\delta}\right)_{,\beta} - \left(U_{\rho,\delta} - U_m\Gamma^m_{\rho\delta}\right)\Gamma^\rho_{\lambda\beta} - \left(U_{3,\delta} - U_m\Gamma^m_{3\delta}\right)\Gamma^3_{\lambda\beta} \\
&\quad - \left(U_{\lambda,\rho} - U_m\Gamma^m_{\lambda\rho}\right)\Gamma^\rho_{\beta\delta} - \left(U_{\lambda,3} - U_m\Gamma^m_{\lambda 3}\right)\Gamma^3_{\beta\delta} \\
&\quad + \left(U_{\delta,\lambda} - U_m\Gamma^m_{\delta\lambda}\right)_{,\beta} - \left(U_{\rho,\lambda} - U_m\Gamma^m_{\rho\lambda}\right)\Gamma^\rho_{\delta\beta} - \left(U_{3,\lambda} - U_m\Gamma^m_{3\lambda}\right)\Gamma^3_{\delta\beta} \\
&\quad - \left(U_{\delta,\rho} - U_m\Gamma^m_{\delta\rho}\right)\Gamma^\rho_{\beta\lambda} - \left(U_{\delta,3} - U_m\Gamma^m_{\delta 3}\right)\Gamma^3_{\beta\lambda} \\
&= \left(U_{\lambda,\delta} - U_\gamma\Gamma^\gamma_{\lambda\delta} - U_3\Gamma^3_{\lambda\delta}\right)_{,\beta} - \left(U_{\rho,\delta} - U_\gamma\Gamma^\gamma_{\rho\delta} - U_3\Gamma^3_{\rho\delta}\right)\Gamma^\rho_{\lambda\beta} \\
&\quad - \left(U_{3,\delta} - U_\gamma\Gamma^\gamma_{3\delta} - U_3\Gamma^3_{3\delta}\right)\Gamma^3_{\lambda\beta} - \left(U_{\lambda,\rho} - U_\gamma\Gamma^\gamma_{\lambda\rho} - U_3\Gamma^3_{\lambda\rho}\right)\Gamma^\rho_{\beta\delta} \\
&\quad - \left(U_{\lambda,3} - U_\gamma\Gamma^\gamma_{\lambda 3} - U_3\Gamma^3_{\lambda 3}\right)\Gamma^3_{\beta\delta} \\
&\quad + \left(U_{\delta,\lambda} - U_\gamma\Gamma^\gamma_{\delta\lambda} - U_3\Gamma^3_{\delta\lambda}\right)_{,\beta} - \left(U_{\rho,\lambda} - U_\gamma\Gamma^\gamma_{\rho\lambda} - U_3\Gamma^3_{\rho\lambda}\right)\Gamma^\rho_{\delta\beta} \\
&\quad - \left(U_{3,\lambda} - U_\gamma\Gamma^\gamma_{3\lambda} - U_3\Gamma^3_{3\lambda}\right)\Gamma^3_{\delta\beta} - \left(U_{\delta,\rho} - U_\gamma\Gamma^\gamma_{\delta\rho} - U_3\Gamma^3_{\delta\rho}\right)\Gamma^\rho_{\beta\lambda} \\
&\quad - \left(U_{\delta,3} - U_\gamma\Gamma^\gamma_{\delta 3} - U_3\Gamma^3_{\delta 3}\right)\Gamma^3_{\beta\lambda}
\end{aligned}$$

to be continued ⟶

continued →

$$
\begin{aligned}
&= \left(U_{\lambda,\delta} - U_{\gamma}\Gamma^{\gamma}_{\lambda\delta}\right)_{,\beta} - \left(U_{3}\Gamma^{3}_{\lambda\delta}\right)_{,\beta} - \left(U_{\rho,\delta} - U_{\gamma}\Gamma^{\gamma}_{\rho\delta}\right)\Gamma^{\rho}_{\lambda\beta} + \left(U_{3}\Gamma^{3}_{\rho\delta}\right)\Gamma^{\rho}_{\lambda\beta} \\
&\quad - \left(U_{3,\delta} - U_{\gamma}\Gamma^{\gamma}_{3\delta} - U_{3}\Gamma^{3}_{3\delta}\right)\Gamma^{3}_{\lambda\beta} - \left(U_{\lambda,\rho} - U_{\gamma}\Gamma^{\gamma}_{\lambda\rho}\right)\Gamma^{\rho}_{\beta\delta} + \left(U_{3}\Gamma^{3}_{\lambda\rho}\right)\Gamma^{\rho}_{\beta\delta} \\
&\quad - \left(U_{\lambda,3} - U_{\gamma}\Gamma^{\gamma}_{\lambda 3} - U_{3}\Gamma^{3}_{\lambda 3}\right)\Gamma^{3}_{\beta\delta} \\
&\quad + \left(U_{\delta,\lambda} - U_{\gamma}\Gamma^{\gamma}_{\delta\lambda}\right)_{,\beta} - \left(U_{3}\Gamma^{3}_{\delta\lambda}\right)_{,\beta} - \left(U_{\rho,\lambda} - U_{\gamma}\Gamma^{\gamma}_{\rho\lambda}\right)\Gamma^{\rho}_{\delta\beta} + \left(U_{3}\Gamma^{3}_{\rho\lambda}\right)\Gamma^{\rho}_{\delta\beta} \\
&\quad - \left(U_{3,\lambda} - U_{\gamma}\Gamma^{\gamma}_{3\lambda} - U_{3}\Gamma^{3}_{3\lambda}\right)\Gamma^{3}_{\delta\beta} - \left(U_{\delta,\rho} - U_{\gamma}\Gamma^{\gamma}_{\delta\rho}\right)\Gamma^{\rho}_{\beta\lambda} + \left(U_{3}\Gamma^{3}_{\delta\rho}\right)\Gamma^{\rho}_{\beta\lambda} \\
&\quad - \left(U_{\delta,3} - U_{\gamma}\Gamma^{\gamma}_{\delta 3} - U_{3}\Gamma^{3}_{\delta 3}\right)\Gamma^{3}_{\beta\lambda}
\end{aligned}
\tag{2.E.2}
$$

Reorganizing the terms

$$
\begin{aligned}
U_{\lambda}|_{\delta\beta} + U_{\delta}|_{\lambda\beta} &= \left(U_{\lambda,\delta} - U_{\gamma}\Gamma^{\gamma}_{\lambda\delta}\right)_{,\beta} - \left(U_{\lambda,\rho} - U_{\gamma}\Gamma^{\gamma}_{\lambda\rho}\right)\Gamma^{\rho}_{\beta\delta} - \left(U_{\rho,\delta} - U_{\gamma}\Gamma^{\gamma}_{\rho\delta}\right)\Gamma^{\rho}_{\lambda\beta} \\
&\quad + \left(U_{\delta,\lambda} - U_{\gamma}\Gamma^{\gamma}_{\delta\lambda}\right)_{,\beta} - \left(U_{\delta,\rho} - U_{\gamma}\Gamma^{\gamma}_{\delta\rho}\right)\Gamma^{\rho}_{\beta\lambda} - \left(U_{\rho,\lambda} - U_{\gamma}\Gamma^{\gamma}_{\rho\lambda}\right)\Gamma^{\rho}_{\delta\beta} \\
&\quad - \left(U_{3,\lambda} - U_{\gamma}\Gamma^{\gamma}_{3\lambda} - U_{3}\Gamma^{3}_{3\lambda}\right)\Gamma^{3}_{\delta\beta} - \left(U_{\lambda,3} - U_{\gamma}\Gamma^{\gamma}_{\lambda 3} - U_{3}\Gamma^{3}_{\lambda 3}\right)\Gamma^{3}_{\beta\delta} \\
&\quad - \left(U_{3,\delta} - U_{\gamma}\Gamma^{\gamma}_{3\delta} - U_{3}\Gamma^{3}_{3\delta}\right)\Gamma^{3}_{\lambda\beta} - \left(U_{\delta,3} - U_{\gamma}\Gamma^{\gamma}_{\delta 3} - U_{3}\Gamma^{3}_{\delta 3}\right)\Gamma^{3}_{\beta\lambda} \\
&\quad - \left(U_{3}\Gamma^{3}_{\lambda\delta}\right)_{,\beta} + \left(U_{3}\Gamma^{3}_{\rho\delta}\right)\Gamma^{\rho}_{\lambda\beta} + \left(U_{3}\Gamma^{3}_{\lambda\rho}\right)\Gamma^{\rho}_{\beta\delta} \\
&\quad - \left(U_{3}\Gamma^{3}_{\delta\lambda}\right)_{,\beta} + \left(U_{3}\Gamma^{3}_{\rho\lambda}\right)\Gamma^{\rho}_{\delta\beta} + \left(U_{3}\Gamma^{3}_{\delta\rho}\right)\Gamma^{\rho}_{\beta\lambda} \\
&= U_{\lambda}\|_{\delta\beta} + U_{\delta}\|_{\lambda\beta} \\
&\quad - \left(\cancel{U_{3,\lambda} + U_{\lambda,3} - 2U_{\gamma}\Gamma^{\gamma}_{3\lambda}}^{\,0} - 2U_{3}\cancel{\Gamma^{3}_{3\lambda}}^{\,0}\right)\Gamma^{3}_{\delta\beta} \\
&\quad - \left(\cancel{U_{3,\delta} + U_{\delta,3} - 2U_{\gamma}\Gamma^{\gamma}_{3\delta}}^{\,0} - 2U_{3}\cancel{\Gamma^{3}_{\delta 3}}^{\,0}\right)\Gamma^{3}_{\lambda\beta} \\
&\quad - \left(U_{3}\Gamma^{3}_{\lambda\delta}\right)_{,\beta} + \left(U_{3}\Gamma^{3}_{\rho\delta}\right)\Gamma^{\rho}_{\lambda\beta} + \left(U_{3}\Gamma^{3}_{\lambda\rho}\right)\Gamma^{\rho}_{\beta\delta} \\
&\quad - \left(U_{3}\Gamma^{3}_{\delta\lambda}\right)_{,\beta} + \left(U_{3}\Gamma^{3}_{\rho\lambda}\right)\Gamma^{\rho}_{\delta\beta} + \left(U_{3}\Gamma^{3}_{\delta\rho}\right)\Gamma^{\rho}_{\beta\lambda} \\
&= U_{\lambda}\|_{\delta\beta} + U_{\delta}\|_{\lambda\beta} - 2\left[\left(U_{3}\Gamma^{3}_{\lambda\delta}\right)_{,\beta} + \left(U_{3}\Gamma^{3}_{\rho\delta}\right)\Gamma^{\rho}_{\lambda\beta} + \left(U_{3}\Gamma^{3}_{\lambda\rho}\right)\Gamma^{\rho}_{\beta\delta}\right] \\
&= U_{\lambda}\|_{\delta\beta} + U_{\delta}\|_{\lambda\beta} - 2\left[U_{3,\beta}\Gamma^{3}_{\lambda\delta} + \left(U_{3}\Gamma^{3}_{\lambda\delta,\beta} + U_{3}\Gamma^{3}_{\rho\delta}\Gamma^{\rho}_{\lambda\beta} + U_{3}\Gamma^{3}_{\lambda\rho}\Gamma^{\rho}_{\beta\delta}\right)\right]
\end{aligned}
\tag{2.E.3}
$$

Thus, we have

$$U_{\lambda}|_{\delta\beta}+U_{\delta}|_{\lambda\beta}=U_{\lambda}\|_{\delta\beta}+U_{\delta}\|_{\lambda\beta}-2\left[U_{3,\beta}\Gamma^{3}_{\lambda\delta}+\left(U_{3}\Gamma^{3}_{\lambda\delta,\beta}-U_{3}\Gamma^{3}_{\rho\delta}\Gamma^{\rho}_{\lambda\beta}-U_{3}\Gamma^{3}_{\lambda\rho}\Gamma^{\rho}_{\beta\delta}\right)\right] \quad (2.E.4)$$

Also, Eq. 2.C.2 yields

$$U_{\lambda}|_{\delta}+U_{\delta}|_{\lambda}=U_{\lambda}\|_{\delta}+U_{\delta}\|_{\lambda}-2U_{3}\Gamma^{3}_{\lambda\delta} \quad (2.E.5)$$

Thus we can write

$$\left(U_{\lambda}|_{\delta}+U_{\delta}|_{\lambda}\right)\|_{\beta}=\left(U_{\lambda}\|_{\delta}+U_{\delta}\|_{\lambda}-2\left(U_{3}\Gamma^{3}_{\lambda\delta}\right)\right)\|_{\beta}=U_{\lambda}\|_{\delta\beta}+U_{\delta}\|_{\lambda\beta}-2\left(U_{3}\Gamma^{3}_{\lambda\delta}\right)\|_{\beta} \quad (2.E.6)$$

Based on the chain rule in derivation we have

$$\begin{aligned}\left(U_{3}\Gamma^{3}_{\lambda\delta}\right)\|_{\beta}&=U_{3}\|_{\beta}\,\Gamma^{3}_{\lambda\delta}+U_{3}\Gamma^{3}_{\lambda\delta}\|_{\beta}\\&=U_{3}\|_{\beta}\,\Gamma^{3}_{\lambda\delta}+U_{3}\left(\Gamma^{3}_{\lambda\delta,\beta}-\Gamma^{3}_{\lambda\rho}\Gamma^{\rho}_{\beta\delta}-\Gamma^{3}_{\rho\delta}\Gamma^{\rho}_{\lambda\beta}\right)\\&=U_{3}\|_{\beta}\,\Gamma^{3}_{\lambda\delta}+\left(U_{3}\Gamma^{3}_{\lambda\delta,\beta}-U_{3}\Gamma^{3}_{\lambda\rho}\Gamma^{\rho}_{\beta\delta}-U_{3}\Gamma^{3}_{\rho\delta}\Gamma^{\rho}_{\lambda\beta}\right)\end{aligned} \quad (2.E.7)$$

From Eq. 2.E.7, by substituting into Eq. 2.E.6, one obtains

$$\begin{aligned}\left(U_{\lambda}|_{\delta}+U_{\delta}|_{\lambda}\right)\|_{\beta}&=\left(U_{\lambda}\|_{\delta}+U_{\delta}\|_{\lambda}-2\left(U_{3}\Gamma^{3}_{\lambda\delta}\right)\right)\|_{\beta}=U_{\lambda}\|_{\delta\beta}+U_{\delta}\|_{\lambda\beta}-2\left(U_{3}\Gamma^{3}_{\lambda\delta}\right)\|_{\beta}\\&=U_{\lambda}\|_{\delta\beta}+U_{\delta}\|_{\lambda\beta}-2\left[U_{3}\|_{\beta}\,\Gamma^{3}_{\lambda\delta}+\left(U_{3}\Gamma^{3}_{\lambda\delta}-U_{3}\Gamma^{3}_{\lambda\rho}\Gamma^{\rho}_{\beta\delta}-U_{3}\Gamma^{3}_{\rho\delta}\Gamma^{\rho}_{\lambda\beta}\right)\right]\end{aligned} \quad (2.E.8)$$

Comparing Eqs. 2.E.4 and 2.E.8 yields

$$U_{3}\|_{\beta}=U_{3,\beta} \quad (2.E.9)$$

Chapter 3

Circular Cylindrical Thin Shell Theory

3.1 Abstract

The generalized thin shell theory developed in Chapter 2 is specialized to circular cylinders. The dynamic version of variational form of the Hamilton's functional for CCTSs is obtained, in which the explicit form of field equations and corresponding boundary condition equations of the system are expressed in terms of midsureface displacement fields. Well-known theories are recovered as special cases from the current generalized formulation. Some comparison with other theories is provided.

3.2 Geometry

Position vector $\mathbf{r}$ of a general point lying on the middle surface (Figure 3.1) of a circular cylinder is expressed in terms of the unit vectors $\vec{\mathbf{I}}_i$ which correspond to the Cartesian coordinate system X^i and in terms of the curvilinear coordinates system x^i as

$$\mathbf{r}\left(x^1, x^2\right) = \left(x^1\right)\vec{\mathbf{I}}_1 + \left(R\sin\frac{x^2}{R}\right)\vec{\mathbf{I}}_2 + \left(R\cos\frac{x^2}{R}\right)\vec{\mathbf{I}}_3 \tag{3.1}$$

3.3 Base Vectors for Middle Surface

Since coordinate system X^i is orthonormal, one has

$$\vec{\mathbf{I}}^{\,i} = \vec{\mathbf{I}}_i \tag{3.2}$$

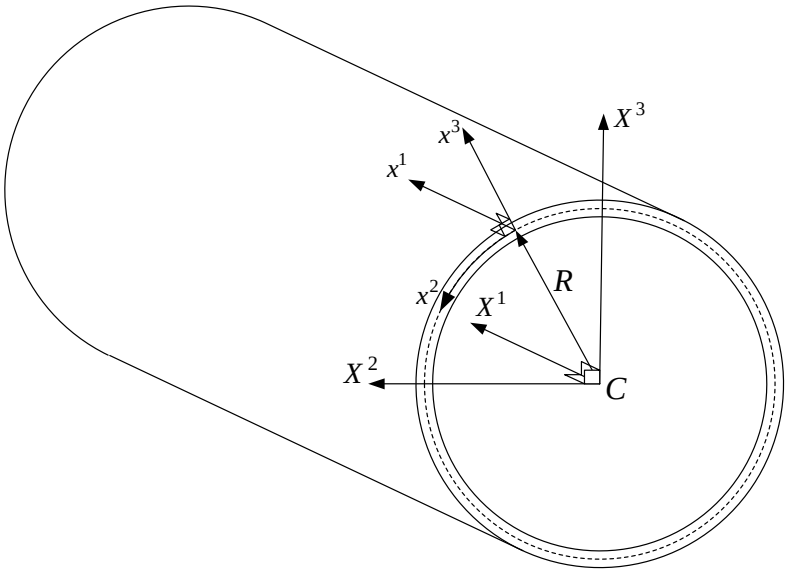

Figure 3.1 - Cartesian and Curvilinear Coordinates

From this point on, symbols x, s, z will be used instead of x^1, x^2, x^3. From Eq. 3.1 and recalling the relation $\mathbf{a}_\alpha = \partial \mathbf{r} / \partial x^\alpha$ in Eq. 2.2, one obtains

$$\begin{aligned} \mathbf{a}_1 &= 1\vec{\mathbf{I}}_1 = 1\vec{\mathbf{i}}_1 \\ \mathbf{a}_2 &= \cos\frac{s}{R}\vec{\mathbf{I}}_2 - \sin\frac{s}{R}\vec{\mathbf{I}}_3 = 1\vec{\mathbf{i}}_2 \end{aligned} \tag{3.3a-b}$$

in which, $\vec{\mathbf{i}}_i$ are the covariant unit vectors associated with $\mathbf{a}_i$. From Eqs. 3.3, by substituting into the $\mathbf{a}^3 = \mathbf{a}_1 \otimes \mathbf{a}_2 / |\mathbf{a}_1 \otimes \mathbf{a}_2|$ given in Eq. 2.3 and considering the orthonormality relationship between all base vectors, one has $\mathbf{a}_3 = \mathbf{a}^3$ and $\vec{\mathbf{I}}^{\,i} = \vec{\mathbf{I}}_i$ (Eqs. 2.5 and 3.2), and thus

$$\mathbf{a}_3 = \mathbf{a}^3 = \sin\frac{s}{R}\vec{\mathbf{I}}_2 + \cos\frac{s}{R}\vec{\mathbf{I}}_3 = 1\vec{\mathbf{i}}_3 = 1\vec{\mathbf{i}}^{\,3} \tag{3.4}$$

From Eq. 3.3, by substituting into Eq. 2.6-a yields

$$a_{11} = a_{22} = a_{33} = 1 \quad , \quad a_{ij} = 0 \text{ for } i \neq j \quad , \quad a = \det\left(a_{ij}\right) = 1 \tag{3.5}$$

Using Eqs.3.3, and based on Eq. 2.4-b, one obtains the contravariant unit vectors associated with $\mathbf{a}^i$ as

$$\mathbf{a}^1 = 1\bar{\mathbf{i}}^1 \quad , \quad \mathbf{a}^2 = 1\bar{\mathbf{i}}^2 \tag{3.6}$$

By applying the relation $\mathbf{U} = U_i\mathbf{g}^i = U^i\mathbf{g}_i$ (Eq. 2.26) to the middle surface, Eqs. 3.3 and 3.6 yield

$$u_i = u^i \tag{3.7}$$

Substitution of Eq. 3.6 into Eq. 2.6-b yields

$$a^{11} = a^{22} = a^{33} = 1 \quad , \quad a^{ij} = 0; \text{if } i \neq j \tag{3.8}$$

3.4 Curvature of the Middle Surface

From Eqs 3.3 and 3.4, by substituting into Eq. 2.10 ($\bar{b}_{\alpha\beta} = \mathbf{a}_{3,\alpha} \cdot \mathbf{a}_\beta$), one obtains

$$\bar{b}_{11} = \bar{b}_{12} = \bar{b}_{21} = 0 \quad , \quad \bar{b}_{22} = -\frac{1}{R} \tag{3.9}$$

Using the operation of raising indices, $\bar{b}_\beta^\alpha = a^{\alpha\gamma}\bar{b}_{\gamma\beta}$, one obtains

$$\bar{b}_1^1 = \bar{b}_1^2 = \bar{b}_2^1 = 0 \quad , \quad \bar{b}_2^2 = -\frac{1}{R} \tag{3.10}$$

3.5 Base Vectors for a General Surface

From Eq. 3.10, substituting into Eqs. 2.16 and 2.19 yields

$$\begin{aligned} &\mu_1^1 = 1 \quad , \quad \mu_1^2 = \mu_2^1 = 0 \quad , \quad \mu_2^2 = 1 + \frac{z}{R} \\ &\lambda_1^1 = 1 \quad , \quad \lambda_1^2 = \lambda_2^1 = 0 \quad , \quad \lambda_2^2 = \frac{1}{1 + \frac{z}{R}} \end{aligned} \tag{3.11}$$

From Eqs. 3.3, 3.6, 3.10 and 3.11, by substituting into Eqs. 2.15 and 2.18, the covariant and contravariant base vectors $\mathbf{g}_i$ and $\mathbf{g}^i$ are obtained as

$$\mathbf{g}_1 = 1\vec{\mathbf{j}}_1 \quad , \quad \mathbf{g}_2 = \left(1+\frac{z}{R}\right)\vec{\mathbf{j}}_2 \quad , \quad \mathbf{g}_3 = 1\vec{\mathbf{j}}_3 \tag{3.12}$$

$$\mathbf{g}^1 = 1\vec{\mathbf{j}}^1 \quad , \quad \mathbf{g}^2 = \frac{1}{\left(1+\frac{z}{R}\right)}\vec{\mathbf{j}}^2 \quad , \quad \mathbf{g}^3 = 1\vec{\mathbf{j}}^3 \tag{3.13}$$

In Eqs. 3.12 and 3.13, $\vec{\mathbf{j}}_i$ and $\vec{\mathbf{j}}^i$ are the covariant and contravariant unit vectors associated with base vectors $\mathbf{g}_i$ and $\mathbf{g}^i$, respectively. From Eqs. 3.12 and 3.13, by substituting into Eqs. 2.21 ($g_{\alpha\beta} = \mathbf{g}_\alpha \cdot \mathbf{g}_\beta$ and $g^{\alpha\beta} = \mathbf{g}^\alpha \cdot \mathbf{g}^\beta$), the components of the covariant and contravariant metric tensors are obtained as

$$\begin{aligned} &g_{11} = g_{33} = 1 \quad , \quad g_{22} = \left(1+\frac{z}{R}\right)^2 \quad , \quad g_{ij} = 0 \ \ (i \neq j) \\ &g^{11} = g^{33} = 1 \quad , \quad g^{22} = \frac{1}{\left(1+\frac{z}{R}\right)^2} \quad , \quad g^{ij} = 0 \ \ (i \neq j) \end{aligned} \tag{3.14}$$

$$g = \det\left(g_{ij}\right) = \left(1+\frac{z}{R}\right)^2 \tag{3.15}$$

3.6 Differential Volume Element

The determinant of the metric tensor g is used to express for the volume of an infinitesimal element $dV = \sqrt{g}\, dr^1 ds^2 dt^3$ (Eq. A.52) yielding

$$dV = \left(1+\frac{z}{R}\right) dz ds dx \tag{3.16}$$

3.7 Relating the Curvature of Middle Surface to that of a General Surface

Eq. 2.C.11 in Appendix 2.C , relates the Christoffel symbol $\Gamma^3_{\alpha\beta}$ of a surface parallel and adjacent to the middle surface to that of the middle surface $\overline{\Gamma}^3_{\gamma\beta} = \overline{b}_{\gamma\beta}$ through

$$\Gamma^3_{\alpha\beta} = b_{\gamma\beta} = \mu^{\gamma}_{\alpha}\bar{\Gamma}^3_{\gamma\beta} = \mu^{\gamma}_{\alpha}\bar{b}_{\gamma\beta} \tag{3.17}$$

From Eq. 3.9, by substituting into Eq. 3.17, one obtains

$$b_{11} = b_{12} = b_{21} = 0 \quad , \quad b_{22} = -\left(1+\frac{z}{R}\right)\frac{1}{R} \tag{3.18}$$

Using the operation of raising indices, $b^{\alpha}_{\beta} = g^{\alpha\gamma}b_{\gamma\beta}$, yields the components of the mixed curvature tensor as

$$b^1_1 = b^2_1 = b^1_2 = 0 \quad , \quad b^2_2 = -\frac{1}{R}\frac{1}{\left(1+\frac{z}{R}\right)} \tag{3.19}$$

3.8 Expressions for Displacements

Considering the geometric properties (Eqs. 3.10 and 3.11) developed in previous sections and recalling Eqs. 2.45 and 2.46, the covariant components of the displacement U_i are

$$\begin{aligned} U_1 &= u - zw_{,1} \\ U_2 &= \left(1+\frac{z}{R}\right)^2 v - z\left(1+\frac{z}{R}\right)w_{,2} \\ U_3 &= w \end{aligned} \tag{3.20a-c}$$

and those of the contravariant components U^i are

$$\begin{aligned} U^1 &= u - zw_{,1} \\ U^2 &= v - z\frac{1}{\left(1+\frac{z}{R}\right)}w_{,2} \\ U^3 &= w \end{aligned} \tag{3.21a-c}$$

The physical components of the covariant components of the displacement (Appendix A, Section A.20) can be recovered by multiplying them by the length of their corresponding contravariant base vector (i.e. $\bar{U}_i = \sqrt{g^{ii}}U_i$). In the same manner, the physical components

of the contravariant components of the displacement are $\bar{U}^i = \sqrt{g_{ii}}U^i$. It is noted that the covariant and contravariant components of the displacement have the same magnitude at $z = 0$.

3.9 Expressions for Strains

From Eq. 3.19, 3.11 and 2.45, substituting into Eq. 2.23 ($\eta_{\alpha\beta} = \frac{1}{2}\left(U_\alpha|_\beta + U_\beta|_\alpha\right)$), the physical components of the strain tensor can be expressed as

$$\eta_{11} = u_{,1} - zw_{,11}$$

$$\eta_{22} = v_{,2} + \frac{1}{R}\frac{1}{\left(1+\frac{z}{R}\right)}w - z\frac{1}{\left(1+\frac{z}{R}\right)}w_{,22} \tag{3.22a-c}$$

$$\eta_{12} = \eta_{21} = \frac{1}{2}\left\{\frac{1}{\left(1+\frac{z}{R}\right)}u_{,2} + \left(1+\frac{z}{R}\right)v_{,1} - z\left[1+\frac{1}{\left(1+\frac{z}{R}\right)}\right]w_{,12}\right\}$$

A generic in-plane strain-midsurface displacement relationship for CCTSs is developed in Appendix 3.A

3.10 Expressions for the Elastic Constitutive Tensor

Using Eqs. 3.14 in Eq. 2.50 yields the following non-zero components of the elasticity tensor

$$E^{1111} = \frac{E}{1-\nu^2} g^{11} g^{11} = \frac{E}{1-\nu^2}$$

$$E^{2222} = \frac{E}{1-\nu^2} g^{22} g^{22} = \frac{E}{1-\nu^2} \frac{1}{\left(1+\frac{z}{R}\right)^4}$$

$$E^{1122} = E^{2211} = \frac{E}{1-\nu^2} \nu g^{11} g^{22} = \frac{E}{1-\nu^2} \nu \frac{1}{\left(1+\frac{z}{R}\right)^2} \qquad \text{(3.23a-d)}$$

$$E^{1212} = E^{1221} = E^{2112} = E^{2121} = \frac{E}{1-\nu^2}\left(\frac{1-\nu}{2}\right) g^{11} g^{22} = \frac{E}{1-\nu^2}\left(\frac{1-\nu}{2}\right) \frac{1}{\left(1+\frac{z}{R}\right)^2}$$

3.11 Hamilton's Principle for Thin Circular Cylindrical Shells

From Eqs. 3.20, 3.21 and 3.23, by substituting into the variation of the Hamilton's principle, integrating with respect to z, grouping terms with the same coefficients (δu, δv, δw, $\delta w_{,1}$, $\delta w_{,2}$), integrating by parts with respect to x and s in all terms with coefficients $\delta w_{,1}$ and $\delta w_{,2}$, respectively, yields (details are provided in Appendix 3.A)

$$\delta\prod=\int_{t_1}^{t_2}\Bigg\{\int_s\Bigg\{\Bigg[-\frac{Eh}{1-\nu^2}\left(u_{,1}+\nu v_{,2}+\frac{\nu}{R}w-\frac{h^2}{12R}w_{,11}\right)\delta u$$

$$-\frac{Eh}{1-\nu^2}\left\{\frac{1-\nu}{2}\left[u_{,2}+\left(1+\frac{h^2}{4R^2}\right)v_{,1}-\frac{h^2}{4R}w_{,12}\right]\right\}\delta v$$

$$+\Bigg[\Bigg[\frac{Eh}{1-\nu^2}\Bigg\langle-\frac{h^2}{12R}u_{,11}+R\left[\frac{R}{h}\ln\left(\frac{2R+h}{2R-h}\right)-1\right]\frac{1-\nu}{2}u_{,22}-\frac{h^2}{12R}\left(\frac{3-\nu}{2}\right)v_{,12}$$

$$+\frac{h^2}{12}w_{,111}+\left\{\frac{h^2}{12}\left(\frac{3-\nu}{2}\right)+R^2\left[\frac{R}{h}\ln\left(\frac{2R+h}{2R-h}\right)-1\right]\frac{1-\nu}{2}\right\}w_{,122}\Bigg\rangle$$

$$-\rho h\left(-\frac{h^2}{12R}\ddot{u}+\frac{h^2}{12}\ddot{w}_{,1}\right)+f^{xw}\Bigg]\Bigg]\delta w$$

$$-\frac{Eh}{1-\nu^2}\left(-\frac{h^2}{12R}u_{,1}-\frac{h^2}{12R}\nu v_{,2}+\frac{h^2}{12}w_{,11}+\frac{h^2}{12}\nu w_{,22}\right)\delta w_{,1}\Bigg]\Bigg]_0^x ds$$

$$+\int_A\Bigg\{\Bigg[\Bigg\langle\frac{Eh}{1-\nu^2}\Bigg\{u_{,11}+\frac{R}{h}\ln\left(\frac{2R+h}{2R-h}\right)\frac{1-\nu}{2}u_{,22}+\frac{1+\nu}{2}v_{,12}+\frac{\nu}{R}w_{,1}$$

$$-\frac{h^2}{12R}w_{,111}+R\left[\frac{R}{h}\ln\left(\frac{2R+h}{2R-h}\right)-1\right]\frac{1-\nu}{2}w_{,122}\Bigg\}-\rho h\left(\ddot{u}-\frac{h^2}{12R}\ddot{w}_{,1}\right)+f^{xu}\Bigg\rangle\delta u$$

$$+\Bigg\langle\frac{Eh}{1-\nu^2}\left[\frac{1+\nu}{2}u_{,12}+\left(1+\frac{h^2}{4R^2}\right)\frac{1-\nu}{2}v_{,11}+v_{,22}+\frac{1}{R}w_{,2}-\frac{h^2}{12R}\left(\frac{3-\nu}{2}\right)w_{,112}\right]$$

$$-\rho h\left[\ddot{v}\left(1+\frac{h^2}{12R^2}\right)-2\frac{h^2}{12R}\ddot{w}_{,2}\right]+f^{sv}\Bigg\rangle\delta v$$

$$+\Bigg[\Bigg[-\frac{Eh}{1-\nu^2}\Bigg\langle\frac{\nu}{R}u_{,1}+\frac{1}{R}v_{,2}+\frac{1}{R^2}\left[\frac{R}{h}\ln\left(\frac{2R+h}{2R-h}\right)\right]w+2\left[\frac{R}{h}\ln\left(\frac{2R+h}{2R-h}\right)-1\right]w_{,22}$$

$$-\frac{h^2}{12R}u_{,111}+R\left[\frac{R}{h}\ln\left(\frac{2R+h}{2R-h}\right)-1\right]\frac{1-\nu}{2}u_{,122}-\frac{h^2}{12R}\left(\frac{3-\nu}{2}\right)v_{,112}+\frac{h^2}{12}w_{,1111}$$

$$+\left\{\frac{h^2}{12}\left(\frac{3+\nu}{2}\right)+R^2\left[\frac{R}{h}\ln\left(\frac{2R+h}{2R-h}\right)-1\right]\frac{1-\nu}{2}\right\}w_{,1122}$$

$$+R^2\left[\frac{R}{h}\ln\left(\frac{2R+h}{2R-h}\right)-1\right]w_{,2222}\Bigg\rangle-\rho h\left[\ddot{w}-\frac{h^2}{12}\left(\ddot{w}_{,11}+\ddot{w}_{,22}\right)+\frac{h^2}{12R}\left(\ddot{u}_{,1}+2\ddot{v}_{,2}\right)\right] \quad (3.24)$$

$$+\left(-f_{,1}^{xw}-f_{,2}^{sw}+f^{zw}\right)\Bigg]\Bigg]\delta w\Bigg\}\Bigg\}dsdx\Bigg\}dt=0$$

In Eq. 3.24, the sequence $\Big\| \Big\| \Big[\Big[\Big\langle \big\{ \big[(...) \big] \big\} \Big\rangle \Big] \Big] \Big\| \Big\|$ of nested brackets was adopted.

3.12 Discussion

Equation 3.24 expresses the field equations and corresponding boundary conditions for circular cylindrical thin shells that are fully consistent with the assumptions of thin shell theory postulated in Section 2.2 . In order to provide simpler approximate forms of the field equations the logarithmic coefficients can be replaced by a truncated power series expansion

$$\frac{R}{h}\ln\left(\frac{2R+h}{2R-h}\right) \approx 1+\frac{1}{12}\left(\frac{h}{R}\right)^2+\frac{1}{80}\left(\frac{h}{R}\right)^4+\cdots \tag{3.25}$$

where h and R are the thickness and radius of the CCTS, respectively. By omitting all time dependent terms, considering the applied loads as tractions applied to the middle surface and using the series approximation in Eq. 3.25 up to the second term, the field equations in Flugge's theory [2.1] are recovered as a special case of the present formulation. A simpler theory can be obtained by replacing all terms appearing in the formulation in the form $(1+z/R)^n$, in which n is an integer, by the linear approximation $(1+z/R)^n \approx 1+n(z/R)$. The corresponding strain expressions are provided in Table 3.1. An even simpler version of the theory can be obtained by neglecting z/R compared to unity $(1+z/R \approx 1)$ in strain expressions, base vectors and the Jacobian. The resulting field equations (Eq. 3.26) are found to be identical to those of Donnell-Mushtari-Vlasov theory (DMV) reported in [2.1]. The strain expressions corresponding to this simplification are also provided in Table 3.1. In general, as the thickness $1+z/R \to 1$ all three simplifications converge to the present generalized theory.

$$
\begin{aligned}
\delta\Pi = \int_{t_1}^{t_2} \Bigg[\int_s \Bigg\langle & \left[-\frac{Eh}{1-\nu^2}\left(u_{,1} + \nu v_{,2} + \frac{\nu}{R} w \right) \right] \delta u \\
& + \left\{ -\frac{Eh}{1-\nu^2}\left[\left(\frac{1-\nu}{2} \right)\left(u_{,2} + v_{,1} \right) \right] \right\} \delta v \\
& + \left\{ \frac{Eh}{1-\nu^2}\left[\frac{h^2}{12} w_{,111} + \frac{h^2}{12}\left(2-\nu \right) w_{,122} \right] - \rho h \frac{h^2}{12} \ddot{w}_{,1} + f^{xw} \right\} \delta w \\
& + \left[-\frac{Eh}{1-\nu^2}\left(\frac{h^2}{12} w_{,11} + \frac{h^2}{12} \nu w_{,22} \right) \right] \delta w_{,1} \Bigg\rangle_0^x ds \\
+ \int_{x,s} \Bigg\langle & \left[\frac{Eh}{1-\nu^2}\left(u_{,11} + \frac{1-\nu}{2} u_{,22} + \frac{1+\nu}{2} v_{,12} + \frac{\nu}{R} w_{,1} \right) - \rho h \ddot{u} + f^{xu} \right] \delta u \\
& + \left[\frac{Eh}{1-\nu^2}\left(\frac{1+\nu}{2} u_{,12} + \frac{1-\nu}{2} v_{,11} + v_{,22} + \frac{1}{R} w_{,2} \right) - \rho h \ddot{v} + f^{sv} \right] \delta v \\
& + \left\{ -\frac{Eh}{1-\nu^2}\left[\frac{\nu}{R} u_{,1} + \frac{1}{R} v_{,2} + \frac{1}{R^2} w + \frac{h^2}{12}\left(w_{,1111} + 2w_{,1122} + w_{,2222} \right) \right] \right. \\
& \qquad - \rho h \left[\ddot{w} - \frac{h^2}{12}\left(\ddot{w}_{,11} + \ddot{w}_{,22} \right) \right] \\
& \qquad \left. + \left(-f_{,1}^{xw} - f_{,2}^{sw} + f^{zw} \right) \right\} \delta w \Bigg\rangle ds dx \Bigg] dt = 0
\end{aligned}
\tag{3.26}
$$

where

$$
\begin{aligned}
f^{xu} &= \int_{-\frac{h}{2}}^{+\frac{h}{2}} p^x dz \qquad , \qquad f^{xw} = -\int_{-\frac{h}{2}}^{+\frac{h}{2}} p^x z dz \\
f^{sv} &= \int_{-\frac{h}{2}}^{+\frac{h}{2}} p^s dz \qquad , \qquad f^{sw} = -\int_{-\frac{h}{2}}^{+\frac{h}{2}} p^s z dz \\
f^{zw} &= \int_{-\frac{h}{2}}^{+\frac{h}{2}} p^z dz
\end{aligned}
\tag{3.27}
$$

3.13 Comparison of Different Theories

The strain expressions, which are used in well known theories as well as those derived as part of the present study, are provided in Table 3.1. The longitudinal strain $\eta_{11} = u_{,1} - zw_{,11}$ is identical in all theories. In all theories, the Jacobian determinant is taken as unity except those two proposed in this study and in the Theory of Flugge's in which the Jacobian determinant is taken as $(1+z/R)^2$ (Eq. 3.15).

Table 3.1 – Comparing strain-displacement in various thin shell theories

Theory	Strain Expressions	
	η_{22}	η_{12}
Present Study	$v_{,2} + \frac{1}{R}\frac{1}{\left(1+\frac{z}{R}\right)}w - z\frac{1}{\left(1+\frac{z}{R}\right)}w_{,22}$	$\frac{1}{2}\left\{\frac{1}{\left(1+\frac{z}{R}\right)}u_{,2} + \left(1+\frac{z}{R}\right)v_{,1} - z\left[1+\frac{1}{\left(1+\frac{z}{R}\right)}\right]w_{,12}\right\}$
Flugge [3.1]	$v_{,2} + \frac{1}{R}\frac{1}{\left(1+\frac{z}{R}\right)}w - z\frac{1}{\left(1+\frac{z}{R}\right)}w_{,22}$	$\frac{1}{2}\left\{\frac{1}{\left(1+\frac{z}{R}\right)}u_{,2} + \left(1+\frac{z}{R}\right)v_{,1} - z\left[1+\frac{1}{\left(1+\frac{z}{R}\right)}\right]w_{,12}\right\}$
Proposed Linear Approximation	$v_{,2} + \frac{1}{R}\left(1-\frac{z}{R}\right)w - z\left(1-\frac{z}{R}\right)w_{,22}$	$\frac{1}{2}\left\{\left(1-\frac{z}{R}\right)u_{,2} + \left(1+\frac{z}{R}\right)v_{,1} - z\left[1+\left(1-\frac{z}{R}\right)\right]w_{,12}\right\}$
DMV	$v_{,2} + \frac{1}{R}w - zw_{,22}$	$\frac{1}{2}\left(u_{,2} + v_{,1} - 2zw_{,12}\right)$
Novozhilov [3.4]	$v_{,2} + \frac{1}{R}\left(1-\frac{z}{R}\right)w - zw_{,22}$	$\frac{1}{2}\left[\left(1-\frac{z}{R}\right)u_{,2} + \left(1+\frac{z}{R}\right)v_{,1} - 2zw_{,12}\right]$
Timoshenko [3.2]	$\left(1+\frac{z}{R}\right)v_{,2} + \frac{1}{R}w - zw_{,22}$	$\frac{1}{2}\left[u_{,2} + \left(1+2\frac{z}{R}\right)v_{,1} - 2zw_{,12}\right]$
Saada [3.5]	$\left(1+\frac{z}{R}\right)v_{,2} + \frac{1}{R}w - zw_{,22}$	$\frac{1}{2}\left[u_{,2} + \left(1+\frac{z}{R}\right)v_{,1} - 2zw_{,12}\right]$
Morley-Koiter, Niordson [3.3]	$\left(1+2\frac{z}{R}\right)v_{,2} + \frac{1}{R}\left(1+\frac{z}{R}\right)w - zw_{,22}$	$\frac{1}{2}\left[u_{,2} + \left(1+2\frac{z}{R}\right)v_{,1} - 2zw_{,12}\right]$

Table 3.1 shows that the strain expressions in Flugge's theory are consistent with those based on the present theory. The strain expressions of Novozhilov's and Donnell-Mushtari-Vlasov's can be considered as approximations of the present theory. In contrast, the strain expressions in the theories of Timoshenko, Saada, Morley-Koiter and Niordson include additional terms which do not arise in the present tensor based approach. These additional terms stem from additional approximations that were avoided in the present treatment.

A comparison of the field equations of the above theories are provided in Table 3.2 to Table 3.4. All field equations take the form

$$\begin{aligned}
&A_1u_{,11}+A_2u_{,22}+A_3v_{,12}+A_4w_{,1}+A_5w_{,111}+A_6w_{,122}=0\\
&B_1u_{,12}+B_2v_{,11}+B_3v_{,22}+B_4w_{,2}+B_5w_{,112}+B_6w_{,222}=0\\
&C_1u_{,1}+C_2v_{,2}+C_3w+C_4w_{,11}+C_5w_{,22}+C_6u_{,111}+C_7u_{,122}+C_8v_{,112}+C_9w_{,222}\\
&\qquad\qquad +C_{10}w_{,1111}+C_{11}w_{,1122}+C_{12}w_{,2222}=0
\end{aligned} \tag{3.28a-c}$$

in which the constant coefficients $A_1,...,C_{12}$ are provided in Tables 2-5 and constant $\Phi=\Phi\left(h/R\right)=\ln\left[\left(2+h/R\right)/\left(2-h/R\right)\right]\Big/\left(h/R\right)$ has been introduced.

Table 3.2 – Coefficients in first equilibrium equation (Eq. 3.28a) in various theories

Theory	Coefficients					
	A_1	A_2	A_3	A_4	A_5	A_6
Present Study	1	$\Phi\left(\frac{1-\nu}{2}\right)$	$\left(\frac{1+\nu}{2}\right)$	$\frac{\nu}{R}$	$-\frac{h^2}{12R}$	$R(\Phi-1)\left(\frac{1-\nu}{2}\right)$
Flugge	1	$\left(1+\frac{h^2}{12R^2}\right)\left(\frac{1-\nu}{2}\right)$	$\left(\frac{1+\nu}{2}\right)$	$\frac{\nu}{R}$	$-\frac{h^2}{12R}$	$\frac{h^2}{12R}\left(\frac{1-\nu}{2}\right)$
Linear	1	$\left(\frac{1-\nu}{2}\right)$	$\left(\frac{1+\nu}{2}\right)$	$\frac{\nu}{R}$	$-\frac{h^2}{12R}$	$\frac{h^2}{12R}\left(\frac{1-\nu}{2}\right)$
DMV	1	$\left(\frac{1-\nu}{2}\right)$	$\left(\frac{1+\nu}{2}\right)$	$\frac{\nu}{R}$	-	-
Novozhilov	1	$\left(\frac{1-\nu}{2}\right)$	$\left(\frac{1+\nu}{2}\right)$	$\frac{\nu}{R}$	-	-
Timoshenko	1	$\left(\frac{1-\nu}{2}\right)$	$\left(\frac{1+\nu}{2}\right)$	$\frac{\nu}{R}$	-	-
Saada	1	$\left(\frac{1-\nu}{2}\right)$	$\left(\frac{1+\nu}{2}\right)$	$\frac{\nu}{R}$	-	-
Morley-Koiter Niordson	1	$\left(\frac{1-\nu}{2}\right)$	$\left(\frac{1+\nu}{2}\right)$	$\frac{\nu}{R}$	-	-

Table 3.3 - Coefficients in second equilibrium equation (Eq. 3.28b) in various theories

Theory	Coefficients					
	B_1	B_2	B_3	B_4	B_5	B_6
Present Study	$\frac{1+\nu}{2}$	$\left(1+3\frac{h^2}{12R^2}\right)\left(\frac{1-\nu}{2}\right)$	1	$\frac{1}{R}$	$-\frac{h^2}{12R}\left(\frac{3-\nu}{2}\right)$	-
Flugge	$\frac{1+\nu}{2}$	$\left(1+3\frac{h^2}{12R^2}\right)\left(\frac{1-\nu}{2}\right)$	1	$\frac{1}{R}$	$-\frac{h^2}{12R}\left(\frac{3-\nu}{2}\right)$	-
Linear	$\frac{1+\nu}{2}$	$\left(\frac{1-\nu}{2}\right)$	1	$\frac{1}{R}$	$-\frac{h^2}{12R}\left(\frac{3-\nu}{2}\right)$	-
DMV	$\frac{1+\nu}{2}$	$\left(\frac{1-\nu}{2}\right)$	1	$\frac{1}{R}$	-	-
Novozhilov	$\frac{1+\nu}{2}$	$\left(1+4\frac{h^2}{12R^2}\right)\left(\frac{1-\nu}{2}\right)$	$\left(1+\frac{h^2}{12R^2}\right)$	$\frac{1}{R}$	$-\frac{h^2}{12R}(2-\nu)$	$-\frac{h^2}{12R}$
Timoshenko	$\frac{1+\nu}{2}$	$\left(1+2\frac{h^2}{12R^2}\right)\left(\frac{1-\nu}{2}\right)$	$\left(1+\frac{h^2}{12R^2}\right)$	$\frac{1}{R}$	$-\frac{h^2}{12R}$	$-\frac{h^2}{12R}$
Saada	$\frac{1+\nu}{2}$	$\left(1+\frac{h^2}{12R^2}\right)\left(\frac{1-\nu}{2}\right)$	$\left(1+\frac{h^2}{12R^2}\right)$	$\frac{1}{R}$	$-\frac{h^2}{12R}$	$-\frac{h^2}{12R}$
Morley-Koiter Niordson	$\frac{1+\nu}{2}$	$\left(\frac{1-\nu}{2}\right)$	1	$\frac{1}{R}$	-	-

Table 3.4 - Coefficients in third equilibrium equation (Eq. 3.28c) in various theories (part 1)

Theory	Coefficients						
	C_1	C_2	C_3	C_4	C_5	C_6	C_7
Present Study	$\frac{\nu}{R}$	$\frac{1}{R}$	$\frac{1}{R^2}\Phi$	-	$2(\Phi-1)$	$-\frac{h^2}{12R}$	$R(\Phi-1)\left(\frac{1-\nu}{2}\right)$
Flugge	$\frac{\nu}{R}$	$\frac{1}{R}$	$\frac{1}{R^2}\left(1+\frac{h^2}{12R^2}\right)$	-	$2\frac{h^2}{12R^2}$	$-\frac{h^2}{12R}$	$\frac{h^2}{12R}\left(\frac{1-\nu}{2}\right)$
Linear	$\frac{\nu}{R}$	$\frac{1}{R}$	$\frac{1}{R^2}$	-	$2\frac{h^2}{12R^2}$	$-\frac{h^2}{12R}$	$\frac{h^2}{12R}\left(\frac{1-\nu}{2}\right)$
DMV	$\frac{\nu}{R}$	$\frac{1}{R}$	$\frac{1}{R^2}$	-	-	-	-
Novozhilov	$\frac{\nu}{R}$	$\frac{1}{R}$	$\frac{1}{R^2}$	-	-	-	-
Timoshenko	$\frac{\nu}{R}$	$\frac{1}{R}$	$\frac{1}{R^2}$	-	-	-	-
Saada	$\frac{\nu}{R}$	$\frac{1}{R}$	$\frac{1}{R^2}$	-	-	-	-
Morley-Koiter Niordson	$\frac{\nu}{R}$	$\frac{1}{R}$	$\frac{1}{R^2}\left(1+\frac{h^2}{12R^2}\right)$	$2\frac{h^2}{12R^2}$	$2\frac{h^2}{12R^2}$	-	-

Table 3.4 - Coefficients in third equilibrium equation (Eq. 3.28c) in various theories (part 1) (part 2)

Theory	Coefficients				
	C_8	C_9	C_{10}	C_{11}	C_{12}
Present Study	$-\frac{h^2}{12R}\left(\frac{3-\nu}{2}\right)$	-	$\frac{h^2}{12}$	$\frac{h^2}{12}\left(\frac{3+\nu}{2}\right)+R^2\left(\Phi-1\right)\left(\frac{1-\nu}{2}\right)$	$R^2\left(\Phi-1\right)$
Flugge	$-\frac{h^2}{12R}\left(\frac{3-\nu}{2}\right)$	-	$\frac{h^2}{12}$	$2\frac{h^2}{12}$	$\frac{h^2}{12}$
Linear	$-\frac{h^2}{12R}\left(\frac{3-\nu}{2}\right)$	-	$\frac{h^2}{12}$	$2\frac{h^2}{12}$	$\frac{h^2}{12}$
DMV	-	-	$\frac{h^2}{12}$	$2\frac{h^2}{12}$	$\frac{h^2}{12}$
Novozhilov	$-\frac{h^2}{12R}\left(2-\nu\right)$	$-\frac{h^2}{12R}$	$\frac{h^2}{12}$	$2\frac{h^2}{12}$	$\frac{h^2}{12}$
Timoshenko	$-\frac{h^2}{12R}\left(2-\nu\right)$	$-\frac{h^2}{12R}$	$\frac{h^2}{12}$	$2\frac{h^2}{12}$	$\frac{h^2}{12}$
Saada	$-\frac{h^2}{12R}$	$-\frac{h^2}{12R}$	$\frac{h^2}{12}$	$2\frac{h^2}{12}$	$\frac{h^2}{12}$
Morley-Koiter Niordson	-	-	$\frac{h^2}{12}$	$2\frac{h^2}{12}$	$\frac{h^2}{12}$

As can be observed in Table 3.2-4, the adoption of different simplifications and approximations by various authors, has led to the elimination of terms in some cases, and to the creation of additional terms (such as C_9) in other cases compared to the present tensor-based theory. For other coefficients, such as for C_{10}, these simplifications/approximations did not affect the expressions of these coefficients. It is observed that the simplifications implied in the Flugge's and DMV theories are consistent with the present tensor based approach. The DMV theory has the simplest expressions while providing a consistent approximation.

3.14 Conclusion

The theories above can be classified into two groups, based on whether or not they adopt approximations that are consistent with the above tensor based approach.

a) Theories that adopt consistent approximations and are thus derivable from the present thoery. These are Flugge's theory, the linear approximation proposed, and the DMV theory.

b) Theories that adopt approximations that are inconsistent with the present approach. These are Novozhilov's, Timoshenko's, Saada's, Morley-Koiter and Niordson's.

Also, it is observed that the field equations for all theories approach those of the DMV as the thickness to radius ratio become negligible compared to unity.

Depending on the desired level of accuracy the following theories are recommended

- Present Theory (most accurate, most complex)/Flugge's theory
- Linear approximation
- DMV theory (least accurate, simplest)

The above recommendation is based on the following criteria:

- They preserve the symmetry of the differential operator matrix of the field equation.
- Consistency and uniformity in applying the simplifications in the whole process
- The uniform simplifications are extensible without ambiguity to boundary condition terms.

The theory developed in this Chapter will be evoked in Chapter 4 for analysis of circular cylindrical thin shells under general harmonic forces with general boundary conditions.

3.15 References

[3.1] W. Flugge, Stresses in Shells. Springer-Verlag, New York Heidelberg Berlin, 1973.

[3.2] S. Timoshenko, Theory of Plates and Shells. McGraw-Hill Book Company, New York, 1959.

[3.3] F. I. Niordson, Shell Theory. North-Holland Series In Applied Mathematics and Mechanics, 1985.

[3.4] V.V. Novozhilov, Thin Shell Theory. P. Noordhoff Ltd. –Groningen-The Netherlands, 1964.

[3.5] A.S. Saada, Elasticity: Theory and Applications, Pergamon Press Inc., New York, 1974.

[3.6] W. Flugge, Tensor Analysis and Continuum Mechanics, Springer-Verlag, New York Heidelberg Berlin, 1972.

[3.7] I. S. Sokolnikoff, Tensor Analysis Theory And Applications To Geometry And Mechanics Of Continua, Second Edition, John Wiley & Sons, Inc., New York, 1965.

3.16 List of Symbols

$\mathbf{a}_i$	Covariant base vectors of the middle surface
a_{ij}	First fundamental tensor defined on the middle surface of a thin shell
a	Determinant of the first fundamental tensor a_{ij}
$b_{\alpha\beta}$	Curvature tensor of the surfaces parallel and adjacent to the middle surface
$\overline{b}_{\alpha\beta}$	Second fundamental tensor or curvature tensor defined on the middle surface of a thin shell
$\mathbf{a}^i$	Contravariant base vectors of the middle surface
a^{ij}	First fundamental tensor of the second kind defined on the middle surface of a thin shell
$\mathbf{g}_i$	Covariant base vectors of any surface parallel and adjacent to the middle surface
g_{ij}	First fundamental tensor defined within the shell
g	Determinant of the first fundamental tensor g_{ij}
$\mathbf{g}^i$	Contravariant base vectors of any surface parallel and adjacent to the middle surface

g^{ij}	First fundamental tensor of the second kind defined within the shell
$\mathbf{U}$	Displacement of a point within the shell
U_i	Covariant components of the displacement of a point on a surface parallel and adjacent to the middle surface along axis x^i
u_i	Covariant components of the displacement of a point on the middle surface along axis x^i
u, v, w	Components of the displacement of a point on the middle surface along axes x^1, x^2 and x^3, respectively
X^i	Coordinate system/Coordinates of the system
x^i	Coordinate system/Coordinates of the system
x, s, z	Coordinates of the system, equivalent to x^1, x^2 and x^3, respectively
$^{\alpha}, _{\alpha}, ...$	All Greek superscripts or subscripts range from 1 to 2
$^{i}, _{i}, ...$	All Italic superscripts or subscripts range from 1 to 3
$\vec{\mathbf{i}}_i, \vec{\mathbf{j}}_i$	Covariant unit vectors along axis x^i in middle surface and adjacent surfaces, respectively

$\vec{\mathbf{i}}^{\,i}, \vec{\mathbf{j}}^{\,i}$	Contravariant unit vectors along axis x^i in middle surface and adjacent surfaces, respectively
Γ_{ij}^{k}	Christoffel symbols in terms of g_i and g_{ij}
$\overline{\Gamma}_{ij}^{k}$	Christoffel symbols in terms of a_i and a_{ij} (defined for the middle surface)
$\cdot$	Inner product
$\otimes$	Cross product
$\vert$	Covariant derivative
$\Vert$	Covariant derivative in two dimensional spaces
T^*	Kinetic energy
V^*	Potential energy
V	Volume
W^*	External work
Π	Mechanical energy of the system
ε_{ij}	Components of the strain tensor on the middle surface
η_{ij}	Components of the strain tensor adjacent to the middle surface

$\eta_{\alpha\beta}$	In-plane components of the Strain tensor
σ^{ij}	Stress tensor
$\sigma^{\alpha\beta}$	In-plane components of the stress tensor
E^{ijlm}	Generalized Hooke's Law
$E^{\alpha\beta\lambda\delta}$	In-plane components of the generalized Hooke's Law
$\cdots_{,i}$	Partial derivative with respect to x^i
δ^{α}_{β}	Kronecker delta function
μ^{α}_{β}	The covariant tensor which connects the base vectors of two different points
$\lambda^{\gamma}_{\alpha}$	Contravariant counterpart of μ^{α}_{β}
ρ	Density of the mass
E	Modulus of elasticity
ν	Poisson's ratio

A_i, B_i, C_i Coefficients representative of constants in the field equations of the system

Appendix 3.A. Generic In-plane Strain- Midsurface Displacement Relationship for Circular Cylindrical Thin Shells

Considering Eq. 2.C.13 and using the results from Eqs. 3.3-3.19, the covariant derivative of displacement can be simplified as

$$\begin{aligned} U_\alpha\,|_\beta &= \left[\left(\mu_\delta^\gamma u_\gamma - z u_{3,\delta}\right)\mu_\alpha^\delta\right]_{,\beta} - \left(\mu_\delta^\psi u_\psi - z u_{3,\delta}\right)\mu_\gamma^\delta\left(\lambda_\rho^\gamma \underbrace{\mu_\alpha^\rho\,\|_\beta}_{0} + \underbrace{\bar{\Gamma}_{\alpha\beta}^\gamma}_{0}\right) - u_3\mu_\alpha^\gamma\bar{\Gamma}_{\gamma\beta}^3 \\ &= \left[\left(\mu_\delta^\gamma u_\gamma - z u_{3,\delta}\right)\mu_\alpha^\delta\right]_{,\beta} - \mu_\alpha^\gamma u_3\bar{b}_{\gamma\beta} \\ &= \mu_\alpha^\delta\mu_\delta^\gamma u_{\gamma,\beta} - z\mu_\alpha^\delta u_{3,\delta\beta} - \mu_\alpha^\gamma u_3\bar{b}_{\gamma\beta} \end{aligned} \tag{3.A.1}$$

Therefore, after substitution of Eq. 3.A.1 into Eq. 2.23, the linear in-plane part of strain-displacement relationship is expressed as

$$\eta_{\alpha\beta} = \tfrac{1}{2}\left(\mu_\alpha^\delta\mu_\delta^\gamma u_{\gamma,\beta} - z\mu_\alpha^\delta u_{3,\delta\beta} - \mu_\alpha^\gamma u_3\bar{b}_{\gamma\beta} + \mu_\beta^\delta\mu_\delta^\gamma u_{\gamma,\alpha} - z\mu_\beta^\delta u_{3,\delta\alpha} - \mu_\beta^\gamma u_3\bar{b}_{\gamma\alpha}\right) \tag{3.A.2}$$

Appendix 3.B. Explicit Expression of Hamilton's Principle for Circular Cylindrical Shells

3.B.1. Kinetic Energy

Recalling Eq. 2.D.5

$$\delta T^*_{\text{F.E.}} = -\int_V \ddot{U}^i \rho \delta U_i dV \tag{3.B.1}$$

By Expanding and substituting the displacement expressions from Eqs. 3.20 and 3.21, one obtains

$$\begin{aligned}
\delta T^*_{\text{F.E.}} &= -\int_V \rho \ddot{U}^1 \delta U_1 dV - \int_V \rho \ddot{U}^2 \delta U_2 dV - \int_V \rho \ddot{U}^3 \delta U_3 dV \\
&= -\int_V \rho\left(\ddot{u} - z\ddot{w}_{,1}\right)\delta\left(u - z w_{,1}\right) dV \\
&-\int_V \rho\left[\ddot{v} - z\frac{1}{\left(1+\frac{z}{R}\right)}\ddot{w}_{,2}\right]\delta\left[\left(1+\frac{z}{R}\right)^2 v - z\left(1+\frac{z}{R}\right)w_{,2}\right] dV - \int_V \rho \ddot{w}\delta w dV
\end{aligned} \tag{3.B.2}$$

From Eq. 3.16, substituting into equation above for the volume of an infinitesimal element and separating the terms multiplied by δu, $\delta w_{,1}$, δv, $\delta w_{,2}$ and δw yields

$$\delta T^*_{\text{F.E.}} = -\int_x \int_s \int_{-\frac{h}{2}}^{+\frac{h}{2}} \rho\left(\ddot{u} - z\ddot{w}_{,1}\right)\delta u\left(1+\frac{z}{R}\right)dzdsdx$$
$$-\int_x \int_s \int_{-\frac{h}{2}}^{+\frac{h}{2}} \rho\left(\ddot{u} - z\ddot{w}_{,1}\right)(-z)\delta w_{,1}\left(1+\frac{z}{R}\right)dzdsdx$$
$$-\int_x \int_s \int_{-\frac{h}{2}}^{+\frac{h}{2}} \rho\left[\ddot{v} - z\frac{1}{\left(1+\frac{z}{R}\right)}\ddot{w}_{,2}\right]\left(1+\frac{z}{R}\right)^2 \delta v\left(1+\frac{z}{R}\right)dzdsdx$$
$$-\int_x \int_s \int_{-\frac{h}{2}}^{+\frac{h}{2}} \rho\left[\ddot{v} - z\frac{1}{\left(1+\frac{z}{R}\right)}\ddot{w}_{,2}\right](-z)\left(1+\frac{z}{R}\right)\delta w_{,2}\left(1+\frac{z}{R}\right)dzdsdx$$
$$-\int_x \int_s \int_{-\frac{h}{2}}^{+\frac{h}{2}} \rho\ddot{w}\delta w dzdsdx \qquad (3.B.3)$$

By performing the integral across the shell thickness, one obtains

$$\delta T^*_{\text{F.E.}} = -\int_x \int_s \rho h\left(\ddot{u} - \frac{h^2}{12R}\ddot{w}_{,1}\right)\delta u dsdx - \int_x \int_s \rho h\left(-\frac{h^2}{12R}\ddot{u} + \frac{h^2}{12}\ddot{w}_{,1}\right)\delta w_{,1} dsdx$$
$$-\int_x \int_s \rho h\left[\left(1+\frac{h^2}{4R^2}\right)\ddot{v} - \frac{h^2}{6R}\ddot{w}_{,2}\right]\delta v dsdx - \int_x \int_s \rho h\left(-\frac{h^2}{6R}\ddot{v} + \frac{h^2}{12}\ddot{w}_{,2}\right)\delta w_{,2} dsdx \qquad (3.B.4)$$
$$-\int_x \int_s \rho h\ddot{w}\delta w dsdx$$

Finally, integration by parts with respect to x and s in the second and forth integral terms, respectively, yields

$$
\begin{aligned}
\delta T^{*}{}_{\text{F.E.}} &= -\int_x\int_s \rho h\left(\ddot{u}-\frac{h^2}{12R}\ddot{w}_{,1}\right)\delta u ds dx - \int_s\left[\rho h\left(-\frac{h^2}{12R}\ddot{u}+\frac{h^2}{12}\ddot{w}_{,1}\right)\delta w\right]_0^x ds \\
&+\int_x\int_s\left[\rho h\left(-\frac{h^2}{12R}\ddot{u}_{,1}+\frac{h^2}{12}\ddot{w}_{,11}\right)\delta w\right]ds dx - \int_x\int_s \rho h\left[\left(1+\frac{h^2}{4R^2}\right)\ddot{v}-\frac{h^2}{6R}\ddot{w}_{,2}\right]\delta v ds dx \\
&-\int_x\left[\rho h\left(-\frac{h^2}{6R}\ddot{v}+\frac{h^2}{12}\ddot{w}_{,2}\right)\delta w\right]_0^s dx + \int_x\int_s\left[\rho h\left(-\frac{h^2}{6R}\ddot{v}_{,2}+\frac{h^2}{12}\ddot{w}_{,22}\right)\delta w\right]ds dx \\
&-\int_x\int_s \rho h\ddot{w}\delta w ds dx
\end{aligned}
\tag{3.B.5}
$$

It should be noted that the second and fifth integral terms in the equation above contribute to the boundary condition terms.

3.B.2. Internal Strain Energy

Recalling Eq. 2.D.13

$$
\begin{aligned}
\delta V^{*} = -\int_V \Big[&\tfrac{1}{2}E^{\alpha\beta\lambda\delta}\left(U_\lambda\|_{\delta\beta}+U_\delta\|_{\lambda\beta}-2U_{3,\beta}b_{\lambda\delta}-2U_3 b_{\lambda\delta}\|_\beta\right) \\
&+\tfrac{1}{2}\left(E^{\alpha\beta\lambda\delta}\|_\beta\right)\left(U_\lambda\|_\delta+U_\delta\|_\lambda-2U_3 b_{\lambda\delta}\right)\Big]\delta U_\alpha dV \\
&-\int_V \tfrac{1}{2}E^{\alpha\beta\lambda\delta}\left(U_\lambda\|_\delta+U_\delta\|_\lambda-2U_3 b_{\lambda\delta}\right)\left(b_{\alpha\beta}\delta U_3\right)dV
\end{aligned}
\tag{3.B.6}
$$

The following relationships are valid in circular cylindrical shells.

$$
\begin{aligned}
&\Gamma^{\gamma}_{\lambda\delta}=0 \quad , \quad U_\lambda\|_\delta = U_{\lambda,\delta} \\
&b_{\lambda\delta}\|_\beta = 0 \quad , \quad U_\lambda\|_{\delta\beta} = U_{\lambda,\delta\beta} \\
&E^{\alpha\beta\lambda\delta}\|_\beta = 0
\end{aligned}
\tag{3.B.7}
$$

Thus, Eq. 3.B.6 is simplified to

$$
\begin{aligned}
\int_{t_1}^{t_2}\delta V^{*}dt = &-\int_{t_1}^{t_2}\frac{1}{2}\int_V E^{\alpha\beta\lambda\delta}\left(U_{\lambda,\delta\beta}+U_{\delta,\lambda\beta}-2U_{3,\beta}b_{\lambda\delta}\right)\delta U_\alpha dV dt \\
&-\int_{t_1}^{t_2}\frac{1}{2}\int_V E^{\alpha\beta\lambda\delta}\left(U_{\lambda,\delta}+U_{\delta,\lambda}-2U_3 b_{\lambda\delta}\right)b_{\alpha\beta}\delta U_3 dV dt
\end{aligned}
\tag{3.B.8}
$$

or

$$\begin{aligned}\delta V^{*}{}_{\text{F.E.}} = &-\frac{1}{2}\int_V E^{\alpha\beta\lambda\delta}\left(U_{\lambda,\delta\beta}+U_{\delta,\lambda\beta}-2U_{3,\beta}b_{\lambda\delta}\right)\delta U_\alpha dV \\ &-\frac{1}{2}\int_V E^{\alpha\beta\lambda\delta}\left(U_{\lambda,\delta}+U_{\delta,\lambda}-2U_3 b_{\lambda\delta}\right)b_{\alpha\beta}\delta U_3 dV\end{aligned} \tag{3.B.9}$$

By expanding the first term we get

$$\begin{aligned}\delta V^{*}{}_{\text{F.E.}} = &-\frac{1}{2}\int_V E^{1\beta\lambda\delta}\left(U_{\lambda,\delta\beta}+U_{\delta,\lambda\beta}-2U_{3,\beta}b_{\lambda\delta}\right)\delta U_1 dV \\ &-\frac{1}{2}\int_V E^{2\beta\lambda\delta}\left(U_{\lambda,\delta\beta}+U_{\delta,\lambda\beta}-2U_{3,\beta}b_{\lambda\delta}\right)\delta U_2 dV \\ &-\frac{1}{2}\int_V E^{\alpha\beta\lambda\delta}\left(U_{\lambda,\delta}+U_{\delta,\lambda}-2U_3 b_{\lambda\delta}\right)b_{\alpha\beta}\delta U_3 dV\end{aligned} \tag{3.B.10}$$

Expansion of the first integral term of Eq. 3.B.10 gives

$$\begin{aligned}\delta V^{*}{}_{\text{F.E.1}} &= -\frac{1}{2}\int_V E^{1\beta\lambda\delta}\left(U_{\lambda,\delta\beta}+U_{\delta,\lambda\beta}-2U_{3,\beta}b_{\lambda\delta}\right)\delta U_1 dV \\ &= -\int_V\left[E^{1111}U_{1,11}+E^{1122}\left(U_{2,21}-U_{3,1}b_{22}\right)+E^{1212}\left(U_{1,22}+U_{2,12}\right)\right]\delta U_1 dV\end{aligned} \tag{3.B.11}$$

Substituting the displacement expressions (Eqs. 3.20), elasticity tensor (Eq. 3.23) and the expression for the volume of an infinitesimal element (Eq. 3.16) into Eq. 3.B.11 and separating the terms multiplied by δu and δw_1 yields

$$\delta V^{*}_{\text{F.E.1}} = -\int_x\int_s\int_{-\frac{h}{2}}^{+\frac{h}{2}} \frac{E}{1-\nu^2}\Bigg[\Bigg[\left(u - zw_{,1}\right)_{,11}$$

$$+\nu\frac{1}{\left(1+\frac{z}{R}\right)^2}\left\{\left[\left(1+\frac{z}{R}\right)^2 v - z\left(1+\frac{z}{R}\right)w_{,2}\right]_{,12} + w_{,1}\left(1+\frac{z}{R}\right)\frac{1}{R}\right\}$$

$$+\frac{1-\nu}{2}\frac{1}{\left(1+\frac{z}{R}\right)^2}\left\{\left(u - zw_{,1}\right)_{,22} + \left[\left(1+\frac{z}{R}\right)^2 v - z\left(1+\frac{z}{R}\right)w_{,2}\right]_{,12}\right\}\Bigg]\Bigg]\delta u\left(1+\frac{z}{R}\right)dzdsdx$$

$$-\int_x\int_s\int_{-\frac{h}{2}}^{+\frac{h}{2}} \frac{E}{1-\nu^2}\Bigg[\Bigg[\left(u - zw_{,1}\right)_{,11}$$

$$+\nu\frac{1}{\left(1+\frac{z}{R}\right)^2}\left\{\left[\left(1+\frac{z}{R}\right)^2 v - z\left(1+\frac{z}{R}\right)w_{,2}\right]_{,12} + w_{,1}\left(1+\frac{z}{R}\right)\frac{1}{R}\right\}$$

$$+\frac{1-\nu}{2}\frac{1}{\left(1+\frac{z}{R}\right)^2}\left\{\left(u - zw_{,1}\right)_{,22} + \left[\left(1+\frac{z}{R}\right)^2 v - z\left(1+\frac{z}{R}\right)w_{,2}\right]_{,12}\right\}\Bigg]\Bigg] \qquad (3.B.12)$$

$$(-z)\delta w_{,1}\left(1+\frac{z}{R}\right)dzdsdx$$

Performing the integral across the thickness of the shell yields

$$\begin{aligned}\delta V^*_{\text{F.E.1}} = &-\int_x\int_s \frac{Eh}{1-\nu^2}\left\{u_{,11}+\frac{R}{h}\ln\left(\frac{2R+h}{2R-h}\right)\left(\frac{1-\nu}{2}\right)u_{,22}+\left(\frac{1+\nu}{2}\right)v_{,12}\right.\\ &\left.+\frac{\nu}{R}w_{,1}-\frac{h^2}{12R}w_{,111}+R\left[\frac{R}{h}\ln\left(\frac{2R+h}{2R-h}\right)-1\right]\left(\frac{1-\nu}{2}\right)w_{,122}\right\}\delta u ds dx\\ &-\int_x\int_s \frac{Eh}{1-\nu^2}\left[\!\!\left[-\frac{h^2}{12R}u_{,11}+R\left[\frac{R}{h}\ln\left(\frac{2R+h}{2R-h}\right)-1\right]\left(\frac{1-\nu}{2}\right)u_{,22}\right.\right.\\ &-\frac{h^2}{12R}\left(\frac{1+\nu}{2}\right)v_{,12}+\frac{h^2}{12}w_{,111}\\ &\left.\left.+\left\{\frac{h^2}{12}\left(\frac{1+\nu}{2}\right)+R^2\left[\frac{R}{h}\ln\left(\frac{2R+h}{2R-h}\right)-1\right]\left(\frac{1-\nu}{2}\right)\right\}w_{,122}\right]\!\!\right]\delta w_{,1} ds dx\end{aligned} \tag{3.B.13}$$

Integrating by parts with respect to x, in second integral term, yields

$$\begin{aligned}\delta V^*_{\text{F.E.1}} = &-\int_x\int_s \frac{Eh}{1-\nu^2}\left\{u_{,11}+\frac{R}{h}\ln\left(\frac{2R+h}{2R-h}\right)\left(\frac{1-\nu}{2}\right)u_{,22}+\left(\frac{1+\nu}{2}\right)v_{,12}\right.\\ &+\frac{\nu}{R}w_{,1}-\frac{h^2}{12R}w_{,111}\\ &\left.+R\left[\frac{R}{h}\ln\left(\frac{2R+h}{2R-h}\right)-1\right]\left(\frac{1-\nu}{2}\right)w_{,122}\right\}\delta u ds dx\\ &-\int_s\left\langle \frac{Eh}{1-\nu^2}\left[\!\!\left[-\frac{h^2}{12R}u_{,11}+R\left[\frac{R}{h}\ln\left(\frac{2R+h}{2R-h}\right)-1\right]\left(\frac{1-\nu}{2}\right)u_{,22}\right.\right.\right.\\ &-\frac{h^2}{12R}\left(\frac{1+\nu}{2}\right)v_{,12}+\frac{h^2}{12}w_{,111}\\ &\left.\left.\left.+\left\{\frac{h^2}{12}\left(\frac{1+\nu}{2}\right)+R^2\left[\frac{R}{h}\ln\left(\frac{2R+h}{2R-h}\right)-1\right]\left(\frac{1-\nu}{2}\right)\right\}w_{,122}\right]\!\!\right]\delta w\right\rangle_0^x ds\\ &+\int_x\int_s \frac{Eh}{1-\nu^2}\left[\!\!\left[-\frac{h^2}{12R}u_{,111}+R\left[\frac{R}{h}\ln\left(\frac{2R+h}{2R-h}\right)-1\right]\left(\frac{1-\nu}{2}\right)u_{,122}\right.\right.\\ &-\frac{h^2}{12R}\left(\frac{1+\nu}{2}\right)v_{,112}+\frac{h^2}{12}w_{,1111}\\ &\left.\left.+\left\{\frac{h^2}{12}\left(\frac{1+\nu}{2}\right)+R^2\left[\frac{R}{h}\ln\left(\frac{2R+h}{2R-h}\right)-1\right]\left(\frac{1-\nu}{2}\right)\right\}w_{,1122}\right]\!\!\right]\delta w ds dx\end{aligned} \tag{3.B.14}$$

Expansion of the second integral term of Eq. 3.B.10 gives

$$\delta V^*_{\text{F.E.2}} = -\frac{1}{2}\int_V E^{2\beta\lambda\delta}\left(U_{\lambda,\delta\beta} + U_{\delta,\lambda\beta} - 2U_{3,\beta}b_{\lambda\delta}\right)\delta U_2 dV \tag{3.B.15}$$

$$\begin{aligned}\delta V^*_{\text{F.E.2}} = -\frac{1}{2}\int_V \Bigg[& E^{2112}\left(U_{1,21} + U_{2,11} - \underbrace{2U_{3,1}b_{12}}_{0}\right) + E^{2121}\left(U_{2,11} + U_{1,21} - \underbrace{2U_{3,1}b_{21}}_{0}\right) \\ & + E^{2211}\left(U_{1,12} + U_{1,12} - \underbrace{2U_{3,2}b_{11}}_{0}\right) + E^{2222}\left(U_{2,22} + U_{2,22} - 2U_{3,2}b_{22}\right)\Bigg]\delta U_2 dV\end{aligned} \tag{3.B.16}$$

$$\delta V^*_{\text{F.E.2}} = -\int_V \left[E^{2112}\left(U_{1,21} + U_{2,11}\right) + E^{2211}U_{1,12} + E^{2222}\left(U_{2,22} - U_{3,2}b_{22}\right)\right]\delta U_2 dV \tag{3.B.17}$$

Substituting the displacement expressions (Eqs. 3.20), elasticity tensor (Eq. 3.23) and the expression for the volume of an infinitesimal element (Eq. 3.16) into Eq. 3.B.17 and separating the terms multiplied by δv and δw_2 yields

$$\delta V^{*}_{\text{F.E.2}} = -\int_x \int_s \int_{-\frac{h}{2}}^{+\frac{h}{2}} \frac{E}{1-\nu^2} \left[\!\!\left[\frac{1-\nu}{2} \frac{1}{\left(1+\frac{z}{R}\right)^2} \right.\right.$$

$$\left\{ \left(u - zw_{,1}\right)_{,12} + \left[\left(1+\frac{z}{R}\right)^2 \nu - z\left(1+\frac{z}{R}\right) w_{,2} \right]_{,11} \right\} + \nu \frac{1}{\left(1+\frac{z}{R}\right)^2} \left(u - zw_{,1}\right)_{,12}$$

$$\left. \left. + \frac{1}{\left(1+\frac{z}{R}\right)^4} \left\{ \left[\left(1+\frac{z}{R}\right)^2 \nu - z\left(1+\frac{z}{R}\right) w_{,2} \right]_{,22} + w_{,2}\left(1+\frac{z}{R}\right)\frac{1}{R} \right\} \right]\!\!\right] \left(1+\frac{z}{R}\right)^3 \delta v dz ds dx$$

$$- \int_x \int_s \int_{-\frac{h}{2}}^{+\frac{h}{2}} \frac{E}{1-\nu^2} \left[\!\!\left[\frac{1-\nu}{2} \frac{1}{\left(1+\frac{z}{R}\right)^2} \right.\right. \left\{ \left(u - zw_{,1}\right)_{,12} + \left[\left(1+\frac{z}{R}\right)^2 \nu - z\left(1+\frac{z}{R}\right) w_{,2} \right]_{,11} \right\}$$

$$+ \nu \frac{1}{\left(1+\frac{z}{R}\right)^2} \left(u - zw_{,1}\right)_{,12}$$

$$\left. \left. + \frac{1}{\left(1+\frac{z}{R}\right)^4} \left\{ \left[\left(1+\frac{z}{R}\right)^2 \nu - z\left(1+\frac{z}{R}\right) w_{,2} \right]_{,22} + w_{,2}\left(1+\frac{z}{R}\right)\frac{1}{R} \right\} \right]\!\!\right]$$

$$(-z)\left(1+\frac{z}{R}\right)^2 \delta w_{,2} dz ds dx \qquad (3.B.18)$$

Performing the integral across the thickness of the shell yields

$$\begin{aligned}\delta V^*_{\text{F.E.2}} = &-\int_x\int_s \frac{Eh}{1-\nu^2}\left[\frac{1+\nu}{2}u_{,12}+\left(1+\frac{h^2}{4R^2}\right)\left(\frac{1-\nu}{2}\right)v_{,11}\right.\\ &\left.+v_{,22}+\frac{1}{R}w_{,2}-\frac{h^2}{12R}\left(\frac{3-\nu}{2}\right)w_{,112}\right]\delta v\,ds\,dx\\ &-\int_x\int_s \frac{Eh}{1-\nu^2}\left\{-\frac{h^2}{6R}\frac{1-\nu}{2}v_{,11}+\left[\frac{R}{h}\ln\left(\frac{2R+h}{2R-h}\right)-1\right]w_{,2}\,\delta w_{,2}\right.\\ &\left.+\frac{h^2}{12}w_{,112}+R^2\left[\frac{R}{h}\ln\left(\frac{2R+h}{2R-h}\right)-1\right]w_{,222}\right\}ds\,dx\end{aligned} \tag{3.B.19}$$

Integrating by parts with respect to s, gives:

$$\begin{aligned}\delta V^*_{\text{F.E.2}} = &-\int_x\int_s \frac{Eh}{1-\nu^2}\left[\frac{1+\nu}{2}u_{,12}+\left(1+\frac{h^2}{4R^2}\right)\left(\frac{1-\nu}{2}\right)v_{,11}\right.\\ &\left.+v_{,22}+\frac{1}{R}w_{,2}-\frac{h^2}{12R}\left(\frac{3-\nu}{2}\right)w_{,112}\right]\delta v\,ds\,dx\\ &-\int_x\left[\left[\frac{Eh}{1-\nu^2}\left\{-\frac{h^2}{6R}\frac{1-\nu}{2}v_{,11}+\left[\frac{R}{h}\ln\left(\frac{2R+h}{2R-h}\right)-1\right]w_{,2}\right.\right.\right.\\ &\left.\left.\left.+\frac{h^2}{12}w_{,112}+R^2\left[\frac{R}{h}\ln\left(\frac{2R+h}{2R-h}\right)-1\right]w_{,222}\right]\delta w\right]_0^s dx\\ &+\int_x\int_s \frac{Eh}{1-\nu^2}\left\{-\frac{h^2}{6R}\frac{1-\nu}{2}v_{,112}+\left[\frac{R}{h}\ln\left(\frac{2R+h}{2R-h}\right)-1\right]w_{,22}\right.\\ &\left.+\frac{h^2}{12}w_{,1122}+R^2\left[\frac{R}{h}\ln\left(\frac{2R+h}{2R-h}\right)-1\right]w_{,2222}\delta w\right\}ds\,dx\end{aligned} \tag{3.B.20}$$

It should be noted that the second integral term should be added to the boundary condition terms.

In the last integral term of Eq. 3.B.10, we know that $\bar{b}_{22}\neq 0$ only if $\alpha=\beta=2$ (in circular cylinders), therefore, we can write:

$$\delta V^*_{\text{F.E.3}} = -\frac{1}{2}\int_V E^{\alpha\beta\lambda\delta}\left(U_{\lambda,\delta}+U_{\delta,\lambda}-2U_3 b_{\lambda\delta}\right)b_{\alpha\beta}\delta U_3\,dV \tag{3.B.21}$$

$$\delta V^*_{\text{F.E.3}} = -\frac{1}{2}\int_V E^{22\lambda\delta}\left(U_{\lambda,\delta}+U_{\delta,\lambda}-2U_3 b_{\lambda\delta}\right)b_{22}\delta U_3 dV \tag{3.B.22}$$

By expanding the equation above, one obtains

$$\begin{aligned}\delta V^*_{\text{F.E.3}} = -\frac{1}{2}\int_V \Bigg[& E^{2211}\left(U_{1,1}+U_{1,1}-\underbrace{2U_3 b_{11}}_{0}\right)b_{22}\delta U_3 dV \\ & +E^{2222}\left(U_{2,2}+U_{2,2}-2U_3 b_{22}\right)\Bigg]b_{22}\delta U_3 dV \\ = -\int_V & \left[E^{2211}U_{1,1}+E^{2222}\left(U_{2,2}-U_3 b_{22}\right)\right]b_{22}\delta U_3 dV\end{aligned} \tag{3.B.23}$$

Substituting the displacement expressions (Eqs. 3.20), elasticity tensor (Eq. 3.23) and the expression for the volume of an infinitesimal element (Eq. 3.16) into Eq. 3.B.23, yields

$$\begin{aligned}\delta V^*_{\text{F.E.3}} = -\int_x\int_s\int_{-\frac{h}{2}}^{+\frac{h}{2}}\frac{E}{1-\nu^2}\Bigg[\Bigg[& \nu\frac{1}{\left(1+\frac{z}{R}\right)^2}\left(u-zw_{,1}\right)_{,1} \\ & +\frac{1}{\left(1+\frac{z}{R}\right)^4}\left\{\left[\left(1+\frac{z}{R}\right)^2\nu-z\left(1+\frac{z}{R}\right)w_{,2}\right]_{,2}+w\left[\left(1+\frac{z}{R}\right)\frac{1}{R}\right]\right\}\Bigg]\Bigg] \\ & \times\left[-\left(1+\frac{z}{R}\right)^2\frac{1}{R}\right]\delta w dz ds dx\end{aligned} \tag{3.B.24}$$

Performing the integral across the thickness of the shell yields

$$\begin{aligned}\delta V^*_{\text{F.E.3}} = -\int_x\int_s\frac{Eh}{1-\nu^2}\Bigg\{ & -\frac{\nu}{R}u_{,1}-\frac{1}{R}v_{,2}-\frac{1}{Rh}\ln\left(\frac{2R+h}{2R-h}\right)w \\ & -\left[\frac{R}{h}\ln\left(\frac{2R+h}{2R-h}\right)-1\right]w_{,22}\Bigg\}\delta w ds dx\end{aligned} \tag{3.B.25}$$

3.B.3. External Work

Recalling Eq. A.109

$$\delta W^* = \int_V F^i \delta U_i dV = \int_V \left(F^1 \delta U_1 + F^2 \delta U_2 + F^3 \delta U_3 \right) dV \tag{3.B.26}$$

The tractions in contravariant form can be defined as below:

$$\begin{aligned} F^1 &= F^x(x,s,z,t) = p^x \\ F^2 &= F^s(x,s,z,t) = p^s \frac{1}{\left(1+\frac{z}{R}\right)} \\ F^3 &= F^z(x,s,z,t) = p^z \end{aligned} \tag{3.B.27}$$

It should be noted that p^x, p^s and p^z (functions of x, s, z and t) are scalars and not the contravariant tensors. From Eqs. 3.20 and 3.B.27 and , substituting the displacmenet expressions and force functions and expression for the volume of an infinitesimal element, respectively, into Eq. 3.B.26 yields and separating the terms multiplied by δu, δw_1, δv, δw_2 and δw, yields

$$\begin{aligned} \delta W^* = &\int_x \int_s \int_{-\frac{h}{2}}^{+\frac{h}{2}} p^x \delta u \left(1+\frac{z}{R}\right) dzdsdx + \int_x \int_s \int_{-\frac{h}{2}}^{+\frac{h}{2}} p^x (-z) \delta w_{,1} \left(1+\frac{z}{R}\right) dzdsdx \\ &+ \int_x \int_s \int_{-\frac{h}{2}}^{+\frac{h}{2}} p^s \left(1+\frac{z}{R}\right) \delta v \left(1+\frac{z}{R}\right) dzdsdx + \int_x \int_s \int_{-\frac{h}{2}}^{+\frac{h}{2}} p^s (-z) \delta w_{,2} \left(1+\frac{z}{R}\right) dzdsdx \\ &\int_x \int_s \int_{-\frac{h}{2}}^{+\frac{h}{2}} p^z \delta w \left(1+\frac{z}{R}\right) dzdsdx \end{aligned} \tag{3.B.28}$$

To keep the generality of the theory, the following definitions are introduced.

$$f^{xu} = \int_{-\frac{h}{2}}^{+\frac{h}{2}} p^x \left(1+\frac{z}{R}\right) dz \qquad , \qquad f^{xw} = \int_{-\frac{h}{2}}^{+\frac{h}{2}} p^x (-z)\left(1+\frac{z}{R}\right) dz$$
$$f^{sv} = \int_{-\frac{h}{2}}^{+\frac{h}{2}} p^s \left(1+\frac{z}{R}\right)^2 dz \qquad , \qquad f^{sw} = \int_{-\frac{h}{2}}^{+\frac{h}{2}} p^s (-z)\left(1+\frac{z}{R}\right) dz \tag{3.B.29}$$
$$f^{zw} = \int_{-\frac{h}{2}}^{+\frac{h}{2}} p^z \left(1+\frac{z}{R}\right) dz$$

Performing the integral across the thickness of the shell yields

$$\delta W^* = \int_x \int_s f^{xu} \delta u ds dx + \int_x \int_s f^{xw} \delta w_{,1} ds dx + \int_x \int_s f^{sv} \delta v ds dx$$
$$+ \int_x \int_s f^{sw} \delta w_{,2} ds dx + \int_x \int_s f^{zw} \delta w ds dx \tag{3.B.30}$$

Integrating by parts with respect to x yields

$$\delta W^* = \int_x \int_s f^{xu} \delta u ds dx + \int_s \left[f^{xw} \delta w \right]_0^x ds - \int_x \int_s f^{xw}_{,1} \delta w ds dx$$
$$\int_x \int_s f^{sv} \delta v ds dx + \int_x \left[f^{sw} \delta w \right]_0^s dx - \int_x \int_s f^{sw}_{,2} \delta w ds dx + \int_x \int_s f^{zw} \delta w ds dx \tag{3.B.31}$$

It should be noted that the second and fifth integral terms in Eqs. 3.B.31 contribute to the boundary condition terms.

3.B.4. Boundary Conditions

During the development of the variation of the mechanical energy, different boundary condition terms are obtained, which are listed below.

$$\delta T^*_{\text{I.F.C.}} = \left[\int_V \dot{U}^i \rho \delta U_i dV \right]_{t_1}^{t_2} \tag{3.B.32}$$

$$\delta T^*_{\text{B.C.1}} = -\int_s \left[\rho h \left(-\frac{h^2}{12R} \ddot{u} + \frac{h^2}{12} \ddot{w}_{,1} \right) \delta w \right]_0^x ds \tag{3.B.33}$$

$$\delta T^*_{\text{B.C.2}} = -\int_x \left[\rho h \left(-\frac{h^2}{6R}\ddot{v} + \frac{h^2}{12}\ddot{w}_{,2} \right) \delta w \right]_0^s dx \tag{3.B.34}$$

$$\delta V^*_{\text{B.C.}} = \frac{1}{2}\int_A \left[E^{\alpha\beta\lambda\delta} \left(U_{\lambda,\delta} + U_{\delta,\lambda} - 2U_3 \bar{b}_{\lambda\delta} \right) \delta U_\alpha \right]_0^{x_\beta} dA \tag{3.B.35}$$

$$\begin{aligned} \delta V^*_{\text{F.E.1.B.C}} = -\int_s \Bigg\langle \frac{Eh}{1-\nu^2} \Bigg[& -\frac{h^2}{12R} u_{,11} + R\left[\frac{R}{h}\ln\left(\frac{2R+h}{2R-h} \right) - 1 \right]\left(\frac{1-\nu}{2} \right) u_{,22} \\ & - \frac{h^2}{12R}\left(\frac{1+\nu}{2} \right) v_{,12} + \frac{h^2}{12} w_{,111} \\ & + \left\{ \frac{h^2}{12}\left(\frac{1+\nu}{2} \right) + R^2 \left[\frac{R}{h}\ln\left(\frac{2R+h}{2R-h} \right) - 1 \right]\left(\frac{1-\nu}{2} \right) \right\} w_{,122} \Bigg] \delta w \Bigg\rangle_0^x ds \end{aligned} \tag{3.B.36}$$

$$\begin{aligned} \delta V^*_{\text{F.E.2.B.C}} = -\int_x \Bigg[\frac{Eh}{1-\nu^2} \Bigg\{ & -\frac{h^2}{6R}\frac{1-\nu}{2} v_{,11} + \left[\frac{R}{h}\ln\left(\frac{2R+h}{2R-h} \right) - 1 \right] w_{,2} + \frac{h^2}{12} w_{,112} \\ & + R^2 \left[\frac{R}{h}\ln\left(\frac{2R+h}{2R-h} \right) - 1 \right] w_{,222} \Bigg] \delta w \Bigg]_0^s dx \end{aligned} \tag{3.B.37}$$

$$\delta W^*_{\text{1.B.C.}} = \int_s \left[f^{xw} \delta w \right]_0^x ds \tag{3.B.38}$$

$$\delta W^*_{\text{2.B.C.}} = \int_x \left[f^{sw} \delta w \right]_0^s dx \tag{3.B.39}$$

In the set of eight equations above, the first equation, 3.B.32, can be considered equal to zero, if the solution to the free vibration is not desired. The third, 3.B.34, the sixth, 3.B.37, and the eighth, 3.B.39, equations are equal to zero for the specific case of closed section circular cylindrical shells (rather than panels). The second, 3.B.33, the fifth, 3.B.36, and the seventh, 3.B.38, equations are ready to be used. Thus, we only need to expand the fourth equation, 3.B.35,

$$\begin{aligned} \delta V^*_{\text{B.C.}} = & \frac{1}{2}\int_A \left[E^{\alpha 1\lambda\delta} \left(U_{\lambda,\delta} + U_{\delta,\lambda} - 2U_3 b_{\lambda\delta} \right) \delta U_\alpha \right]_0^{x_1} dA \\ & + \frac{1}{2}\int_A \left[E^{\alpha 2\lambda\delta} \left(U_{\lambda,\delta} + U_{\delta,\lambda} - 2U_3 b_{\lambda\delta} \right) \delta U_\alpha \right]_0^{x_2} dA \end{aligned} \tag{3.B.40}$$

Based on the same reasoning in previous paragraph, the second integral term in Eq. 3.B.40 equals zero, thus

$$\begin{aligned}\delta V^{*}{}_{\text{B.C.}} = &\frac{1}{2}\int_A \left[E^{11\lambda\delta}\left(U_{\lambda,\delta}+U_{\delta,\lambda}-2U_3 b_{\lambda\delta}\right)\delta U_1 \right]_0^x dA \\ &+\frac{1}{2}\int_A \left[E^{21\lambda\delta}\left(U_{\lambda,\delta}+U_{\delta,\lambda}-2U_3 b_{\lambda\delta}\right)\delta U_2 \right]_0^x dA\end{aligned} \tag{3.B.41}$$

Expanding the first integral term in Eq. 3.B.41 yields

$$\begin{aligned}\delta V^{*}{}_{\text{B.C.1}} &= \frac{1}{2}\int_A \left[E^{11\lambda\delta}\left(U_{\lambda,\delta}+U_{\delta,\lambda}-2U_3 b_{\lambda\delta}\right)\delta U_1 \right]_0^{x_1} dA \\ &= \frac{1}{2}\int_A \left\{ \left[E^{1111}\left(U_{1,1}+U_{1,1}\right)+E^{1122}\left(U_{2,2}+U_{2,2}-2U_3 b_{22}\right)\right]\delta U_1 \right\}_0^{x_1} dA\end{aligned} \tag{3.B.42}$$

Substituting the displacement expressions (Eqs. 3.20), elasticity tensor (Eq. 3.23) and the expression for the volume of an infinitesimal element (Eq. 3.16) into Eq. 3.B.42 and separating the terms multiplied by δu and δw_1 yields

$$\begin{aligned}\delta V^{*}{}_{\text{B.C.1}} = \int_s \int_{-\frac{h}{2}}^{+\frac{h}{2}} \Bigg\langle \frac{E}{1-\nu^2} \Bigg[\!\!\Bigg[\left(u - zw_{,1}\right)_{,1} \\ + \nu \frac{1}{\left(1+\frac{z}{R}\right)^2} \Bigg\{ \Bigg[\left(1+\frac{z}{R}\right)^2 v - z\left(1+\frac{z}{R}\right) w_{,2} \Bigg]_{,2} \\ + w\left(1+\frac{z}{R}\right)\frac{1}{R} \Bigg\} \Bigg]\!\!\Bigg] \delta u \Bigg\rangle_0^x \left(1+\frac{z}{R}\right) dzds \\ + \int_s \int_{-\frac{h}{2}}^{+\frac{h}{2}} \Bigg\langle \frac{E}{1-\nu^2} \Bigg[\!\!\Bigg[\left(u - zw_{,1}\right)_{,1} \\ + \nu \frac{1}{\left(1+\frac{z}{R}\right)^2} \Bigg\{ \Bigg[\left(1+\frac{z}{R}\right)^2 v - z\left(1+\frac{z}{R}\right) w_{,2} \Bigg]_{,2} \\ + w\left(1+\frac{z}{R}\right)\frac{1}{R} \Bigg\} \Bigg]\!\!\Bigg] (-z)\delta\left(w_{,1}\right) \Bigg\rangle_0^x \left(1+\frac{z}{R}\right) dzds \end{aligned} \tag{3.B.43}$$

By performing the integral across the thickness of the shell, one obtains

$$\begin{aligned}\delta V^{*}{}_{\text{B.C.1}} = \int_s \left[\frac{Eh}{1-\nu^2} \left(u_{,1} + \nu v_{,2} + \frac{\nu}{R} w - \frac{h^2}{12R} w_{,11} \right) \delta u \right]_0^x ds \\ + \int_s \left[\frac{Eh}{1-\nu^2} \left(-\frac{h^2}{12R} u_{,1} - \frac{h^2}{12R} \nu v_{,2} + \frac{h^2}{12} w_{,11} + \frac{h^2}{12} \nu w_{,22} \right) \delta w_1 \right]_0^x ds \end{aligned} \tag{3.B.44}$$

Expanding the second integral term in Eq. 3.B.41 yields

$$\begin{aligned}\delta V^{*}{}_{\text{B.C.2}} &= \frac{1}{2} \int_A \left[E^{21\lambda\delta} \left(U_{\lambda,\delta} + U_{\delta,\lambda} - 2U_3 b_{\lambda\delta} \right) \delta U_2 \right]_0^{x_1} dA \\ &= \frac{1}{2} \int_A \left\{ \left[E^{2112} \left(U_{1,2} + U_{2,1} \right) + E^{2121} \left(U_{2,1} + U_{1,2} \right) \right] \delta U_2 \right\}_0^{x_1} dA \end{aligned} \tag{3.B.45}$$

Substituting the displacement expressions (Eqs. 3.20), elasticity tensor (Eq. 3.23) and the expression for the surface of an infinitesimal element ($dA = \sqrt{g}\,dxdsdz$) into Eq. 3.B.45 and separating the terms multiplied by δv and δw_2 yields

$$\begin{aligned}
\delta V^{*}{}_{\text{B.C.2}} = \int_A \Bigg\langle \frac{E}{1-\nu^2} \Bigg[\!\!\Bigg[\left(\frac{1-\nu}{2}\right) \frac{1}{\left(1+\frac{z}{R}\right)^2} \\
\times \left\{ \left(u - z w_{,1}\right)_{,2} + \left[\left(1+\frac{z}{R}\right)^2 \nu - z\left(1+\frac{z}{R}\right) w_{,2} \right]_{,1} \right\} \Bigg]\!\!\Bigg] \\
\times \left(1+\frac{z}{R}\right)^2 \delta v \Bigg\rangle_0^x \left(1+\frac{z}{R}\right) dzds \\
+ \int_A \Bigg\langle \frac{E}{1-\nu^2} \Bigg[\!\!\Bigg[\left(\frac{1-\nu}{2}\right) \frac{1}{\left(1+\frac{z}{R}\right)^2} \\
\times \left\{ \left(u - z w_{,1}\right)_{,2} + \left[\left(1+\frac{z}{R}\right)^2 \nu - z\left(1+\frac{z}{R}\right) w_{,2} \right]_{,1} \right\} \Bigg]\!\!\Bigg] \\
\times (-z)\left(1+\frac{z}{R}\right) \delta w_{,2} \Bigg\rangle_0^x \left(1+\frac{z}{R}\right) dzds
\end{aligned} \tag{3.B.46}$$

By performing the integral across the thickness of the shell, one obtains

$$\delta V^*_{\text{B.C.2}} = \int_s \left[\frac{Eh}{1-\nu^2} \left\{ \left(\frac{1-\nu}{2} \right) \left[u_{,2} + \left(1 + \frac{h^2}{4R^2} \right) v_{,1} - \frac{h^2}{4R} w_{,12} \right] \right\} \delta u \right]_0^x ds + \int_s \left[\frac{Eh}{1-\nu^2} \left(\frac{1-\nu}{2} \right) \left(-\frac{h^2}{6R} v_{,1} + \frac{h^2}{6} w_{,12} \right) \delta w_{,2} \right]_0^x ds \tag{3.B.47}$$

Integrating by parts in the second integral term with respect to s yields

$$\delta V^*_{\text{B.C.2}} = \int_s \left[\frac{Eh}{1-\nu^2} \left\{ \left(\frac{1-\nu}{2} \right) \left[u_{,2} + \left(1 + \frac{h^2}{4R^2} \right) v_{,1} - \frac{h^2}{4R} w_{,12} \right] \right\} \delta v \right]_0^x ds + \left\{ \left[\frac{Eh}{1-\nu^2} \left(\frac{1-\nu}{2} \right) \left(-\frac{h^2}{6R} v_{,1} + \frac{h^2}{6} w_{,12} \right) \delta w \right]_0^x \right\}_0^s - \int_s \left[\frac{Eh}{1-\nu^2} \left(\frac{1-\nu}{2} \right) \left(-\frac{h^2}{6R} v_{,12} + \frac{h^2}{6} w_{,122} \right) \delta w \right]_0^x ds \tag{3.B.48}$$

As the outer lower and upper limits of the second term in Eq. 3.B.48 coincide, that term is equal to zero, thus

$$\delta V^*_{\text{B.C.2}} = \int_s \left[\frac{Eh}{1-\nu^2} \left\{ \left(\frac{1-\nu}{2} \right) \left[u_{,2} + \left(1 + \frac{h^2}{4R^2} \right) v_{,1} - \frac{h^2}{4R} w_{,12} \right] \right\} \delta v \right]_0^x ds - \int_s \left[\frac{Eh}{1-\nu^2} \left(\frac{1-\nu}{2} \right) \left(-\frac{h^2}{6R} v_{,12} + \frac{h^2}{6} w_{,122} \right) \delta w \right]_0^x ds \tag{3.B.49}$$

3.B.5. Hamilton's Principle Expression

Collecting all terms from Eqs. 3.B.5, 3.B.14, 3.B.20 and 3.B.25 which contribute to the field equations and adding the boundary condition terms from Eqs. 3.B.33, 3.B.36, 3.B.38, 3.B.44 and 3.B.49 and substituting into the Hamilton's Principle results

$$\delta\prod=\int_{t_1}^{t_2}\Bigg\{\int_s\Bigg\{\Bigg[-\frac{Eh}{1-\nu^2}\left(u_{,1}+\nu v_{,2}+\frac{\nu}{R}w-\frac{h^2}{12R}w_{,11}\right)\delta u$$

$$-\frac{Eh}{1-\nu^2}\left\{\left(\frac{1-\nu}{2}\right)\left[u_{,2}+\left(1+\frac{h^2}{4R^2}\right)v_{,1}-\frac{h^2}{4R}w_{,12}\right]\right\}\delta v$$

$$+\Bigg[\frac{Eh}{1-\nu^2}\Bigg\langle-\frac{h^2}{12R}u_{,11}+R\left[\frac{R}{h}\ln\left(\frac{2R+h}{2R-h}\right)-1\right]\left(\frac{1-\nu}{2}\right)u_{,22}-\frac{h^2}{12R}\left(\frac{3-\nu}{2}\right)v_{,12}$$

$$+\frac{h^2}{12}w_{,111}+\left\{\frac{h^2}{12}\left(\frac{3-\nu}{2}\right)+R^2\left[\frac{R}{h}\ln\left(\frac{2R+h}{2R-h}\right)-1\right]\left(\frac{1-\nu}{2}\right)\right\}w_{,122}\Bigg\rangle$$

$$-\rho h\left(-\frac{h^2}{12R}\ddot{u}+\frac{h^2}{12}\ddot{w}_{,1}\right)+f^{xw}\Bigg]\delta w$$

$$-\left[\frac{Eh}{1-\nu^2}\left(-\frac{h^2}{12R}u_{,1}-\frac{h^2}{12R}\nu v_{,2}+\frac{h^2}{12}w_{,11}+\frac{h^2}{12}\nu w_{,22}\right)\delta w_{,1}\right]\Bigg]\Bigg\}_0^x ds$$

to be continued →

continued →

$$
\begin{aligned}
+\int_A \Bigg\| \Bigg[& \left\langle \frac{Eh}{1-\nu^2}\left\{ u_{,11} + \frac{R}{h}\ln\left(\frac{2R+h}{2R-h}\right)\frac{1-\nu}{2}u_{,22} + \frac{1+\nu}{2}v_{,12} + \frac{\nu}{R}w_{,1} - \frac{h^2}{12R}w_{,111} \right.\right. \\
& \left.\left. + R\left[\frac{R}{h}\ln\left(\frac{2R+h}{2R-h}\right)-1\right]\frac{1-\nu}{2}w_{,122}\right\} - \rho h\left(\ddot{u} - \frac{h^2}{12R}\ddot{w}_{,1}\right) + f^{xu}\right\rangle \delta u \\
& + \left\langle \frac{Eh}{1-\nu^2}\left[\frac{1+\nu}{2}u_{,12} + \left(1+\frac{h^2}{4R^2}\right)\frac{1-\nu}{2}v_{,11} + v_{,22} + \frac{1}{R}w_{,2} - \frac{h^2}{12R}\left(\frac{3-\nu}{2}\right)w_{,112}\right] \right. \\
& \left. - \rho h\left[\ddot{v}\left(1+\frac{h^2}{12R^2}\right) - 2\frac{h^2}{12R}\ddot{w}_{,2}\right] + f^{sv}\right\rangle \delta v \\
& + \Bigg\| -\frac{Eh}{1-\nu^2}\left\langle \frac{\nu}{R}u_{,1} + \frac{1}{R}v_{,2} + \frac{1}{R^2}\left[\frac{R}{h}\ln\left(\frac{2R+h}{2R-h}\right)\right]w + 2\left[\frac{R}{h}\ln\left(\frac{2R+h}{2R-h}\right)-1\right]w_{,22} \right. \\
& \quad - \frac{h^2}{12R}u_{,111} + R\left[\frac{R}{h}\ln\left(\frac{2R+h}{2R-h}\right)-1\right]\frac{1-\nu}{2}u_{,122} - \frac{h^2}{12R}\left(\frac{3-\nu}{2}\right)v_{,112} \\
& \quad + \frac{h^2}{12}w_{,1111} + \left\{\frac{h^2}{12}\left(\frac{3+\nu}{2}\right) + R^2\left[\frac{R}{h}\ln\left(\frac{2R+h}{2R-h}\right)-1\right]\frac{1-\nu}{2}\right\}w_{,1122} \\
& \quad \left. + R^2\left[\frac{R}{h}\ln\left(\frac{2R+h}{2R-h}\right)-1\right]w_{,2222}\right\rangle + \left(-f_{,1}^{xw} - f_{,2}^{sw} + f^{zw}\right)\Bigg\| \delta w \Bigg] \Bigg\| ds dx \Bigg\| dt = 0
\end{aligned}
\tag{3.B.50}
$$

Chapter 4

Analysis of Circular Cylindrical Thin Shells under Harmonic Forces

4.1 Abstract

A generalized thin shell theory for the stress-deformation analysis of thin-walled circular cylindrical shells is formulated based on Hamilton's variational principle. The theory is applicable to multiple in-phase and out-of phase harmonic forces and general boundary conditions. The stationary conditions of the Hamilton functional are then evoked to recover the equations of motion and boundary conditions of the problem. Other theories such as Flugge's and DMV are recovered as special cases of the present theory. The unknown displacement fields are expanded as infinite complex Fourier series in the circumferential coordinate. The resulting field equations are observed to couple the radial, tangential, and longitudinal displacement contributions within each mode, while uncoupling the contributions of a given Fourier mode from those of other Fourier modes. A general solution for the obtained field equations is developed for harmonic loading of general spatial distribution. The method developed is verified against well established solutions and its applicability to practical problems is illustrated through examples.

4.2 Introduction

Circular cylindrical thin shells (CCTSs) are commonly used as structural members (e.g., hollow structural sections), piping systems, members of offshore platforms, cooling towers, aircraft fuselages, naval halls of submarines etc. In these applications, CCTSs are commonly subjected to dynamic loads due to machinery, fluids flow, etc.. Harmonic forces can arise in machinery from the eccentricity of rotary parts in turbines, engines, generators, and propellers. Also, they arise from beating in pumps and conveyance systems and in wave induced hydrodynamic loads and wind or water flow induced vortex shedding effects. In such systems, the steady-state response of the structure is of particular importance in fatigue design since it is the sustained effect. The transient response of the structure is of little importance in fatigue design as it tends to dampen out quickly.

Within the above context, the present study aims at developing an analytical solution for the analysis of CCTSs under harmonic loads, in which the time dependency of the response is eliminated in order to efficiently isolate the steady state response of CCTSs. Given the frequent to permanent nature of harmonic loads in the aforementioned applications, they are normally designed to respond to harmonic effects within their linearly elastic range. Thus, the present study focuses on the elastic response of CCTSs.

4.3 Literature Review

Several studies have focused on the dynamic analysis of shells. This includes a) solutions aimed at determining the free vibration characteristics of shells (i.e., natural frequencies and mode shapes), b) those that are geared towards determining the steady-state response of CCTSs. Studies under the above two categories are summarized in the following

subsections. Other studies aimed at investigating the full dynamic response of CCTSs are outside of the scope of the present review.

4.4 Studies on Free Vibration

The monograph by Leissa [4.1] presented a compilation of studies focusing on free vibration of CCTSs based on various kinematic assumptions and shell theories. Markus [4.2] provided a comparative study on the elastic free vibration analysis of cylindrical shells. In two companion papers, Qatu ([4.3] and [4.4]) provided a review summary of recent research advances on the dynamic response of laminated composite shells and homogeneous shells with emphasis on free vibrations. Recent developments include also the work of Xiang et al. [4.5] who investigated the vibration of CCTSs with intermediate ring supports. Jafari and Bagheri [4.6] studied the free vibration of non-uniformly ring stiffened CCTSs. Xuebin [4.7] investigated the free vibration of the CCTSs using Fourier decomposition. Rougui et al. [4.8] provided a semi-analytical solution for geometrically non-linear free vibration of simply supported CCTSs. Zhang and Xiang [4.9] developed the exact solutions for the vibration of CCTSs with step-wise thickness variations in longitudinal direction. Using a wave propagation approach, Xuebin [4.10] conducted a free vibration analysis of CCTS and Gan et al. [4.11] investigated the free vibration analysis of ring-stiffened CCTSs. In a recent paper, Matsunaga [4.12] studied the free vibration and stability of functionally graded (layered) CCTSs.

4.5 Studies on Steady state Response

This section focuses on dynamic solutions, with emphasis on analytical developments rather than computational solutions. Warburton [4.13] studied the response of a simply supported

uniform CCTSs under a harmonic transverse point force acting at mid-span. He adopted Novozhilov's thin shell theory and applied a double Fourier series solution in the longitudinal and circumferential coordinates when expanding the displacement fields. He modelled hysteretic damping by adopting the complex form of Young's modulus. Later on, Warburton and Soni [4.14] extended their work to the case of orthotropic CCTSs.

Leissa [4.15] extended the work of Warburton [4.13] to model the response of a simply supported CCTS under harmonic radial pressure. In their solution, they postulated displacement fields with distributions similar to the applied radial pressure. Structural damping was modelled in the solution.

Beskos and Oates [4.16] used the dynamic stiffness influence coefficients approach. Using Laplace transforms, they developed a numerical solution for the analysis of the simply supported ring-stiffened CCTSs under harmonic loading. In their analysis only circular symmetric vibrations of shell segments and radial and torsional vibrations of the rings were considered.

Zarutskii [4.17] developed a closed-form solution for the response of simply supported CCTSs with longitudinal stiffeners subject to general harmonic pressure. The Kirchhoff-Love thin shell theory was adopted to model the cylinder while the Kirchhoff-Klebsch rod theory was adopted to model the longitudinal stiffeners.

By combining the method proposed by Forsberg [4.18] for free vibration analysis of shells and a general solution technique for one-dimensional forced vibration problems, Glandier et al. [4.19] developed an analytical solution for in-vacuo vibration of CCTSs with general boundary conditions subjected to harmonic point load. Using Donnell's thin shell theory, the

cylinder was longitudinally subdivided into two domains. The homogenous solution of the system of differential equations was expressed for both domains. The problem was then solved by enforcing four boundary conditions at each end of the cylinder, seven continuity conditions, and one discontinuity condition at the interface of the two sub-domains.

Huang and Fuller [4.20] studied the effect of dynamic absorbers on the reduction of vibration and sound level in the enclosed acoustic field within CCTS under harmonic radial point loading and patch loading. Their analytical solution was based on the Donnell-Mushtari shell theory. Their solution was based on the substructure synthesis and modal expansion techniques. However, only the radial displacement expression is reported in their study.

Using the Lagrangian approach, Amabili [4.21] performed a comparative study on the large amplitude response of CCTS subjected to radial harmonic force by evoking Donnell's, Sanders-Koiter , Flugge-Lure-Byrne, and Novozhilov's non-linear shell theories.

Pellicano and Avramov [4.22] investigated the dynamic behaviour of vertical CCTS clamped at the bottom end and connected to a rigid disk at the top. Their study focussed on a) the free vibration of CCTSs and b) those subject to harmonically excited supports. The Sanders-Koiter non-linear theory was adopted and approximate trial functions were assumed for the displacement fields. Using the Sanders-Koiter theory and a mixed modal decomposition of the displacement fields (trigonometric functions in circumferential direction and Chebyshev polynomials in the longitudinal direction), Pellicano [4.23] developed a solution for the linear and nonlinear, free and harmonically forced vibration of CCTSs.

Duan and Koh [4.24] developed an analytical solution method for the axisymmetric transverse vibration of cylindrical shells with variable thickness under transverse forces based on a generalized hyper-geometric function.

4.6 Assumptions

The main assumptions of the formulation are:

- A straight fibre normal to the shell mid-surface before deformation remains straight, un-stretched and normal to the mid-surface throughout deformation.
- All displacements are small compared to the radius of curvature of the middle surface.
- Normal stresses perpendicular to the middle surface are negligible compared to the in-plane stresses.
- The through thickness shear strains are negligible.
- Material is elastic isotropic.
- Only the steady state response is sought.

4.7 Statement of the Problem

A circular cylinder with mid-surface radius R, length L and constant thickness h is considered. The cylinder is subject to general body forces F^i (in a contravariant form). Other external forces such as surface forces that may act within the shell volume can be conceived as lumped body forces. The cylinder has general boundary conditions. It is required to develop expressions for the response of the cylinder.

4.8 Preliminaries

The cylinder can be conceived as a group of parallel curved surfaces in the immediate vicinity of the mid-surface. The position of a point within the shell volume is defined by two curvilinear coordinates x^{α} (As a convention all subscripts/superscripts in Greek letters range from 1 to 2 and those in Latin letters from 1 to 3) on the mid-surface and an additional coordinate $-h/2 \le x^3 \le +h/2$ normal to the mid-surface. The sign convention for the x^i coordinates is illustrated in Figure 4.1.

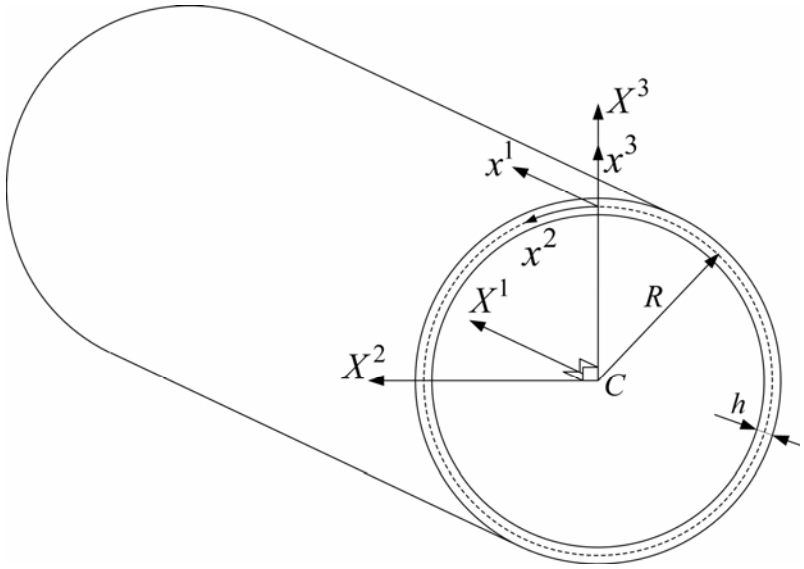

Figure 4.1 – Cylinder geometry and coordinate definition

4.9 Displacement Distribution across the Shell Thickness

Based on the assumptions in Section 4.6 , the covariant components of the displacement U_i of a point within the thin shell with a coordinate x^3 from the mid-surface can be expressed in terms of the covariant components of the displacement u_i of its projection on the mid-surface as

$$U_{\alpha} = \left(\mu_{\delta}^{\gamma} u_{\gamma} - x^3 u_{3,\delta}\right)\mu_{\alpha}^{\delta} \quad , \quad U_3 = u_3 \qquad (4.1a,b)$$

in which subscripts "$,\delta$" denote differentiation with respect to x^{δ}, and μ_{α}^{δ} are the components of the shifter tensor [4.25] defined as

$$\mu_{\alpha}^{\delta} = \delta_{\alpha}^{\delta} - x^3 b_{\alpha}^{\delta} \tag{4.2}$$

and b_{α}^{δ} are the components of the curvature tensor.

4.10 Strain-Displacement Relations

The present study is focused on the linear response of circular cylindrical thin shells under small deformations, in which the through thickness strains $\eta_{\alpha 3} = \eta_{3\alpha}$ (assumption 4) and the strains normal to the mid-surface η_{33} (assumption 1) are assumed negligible. The linear part of the in-plane covariant components of the Green-Lagrange strain-displacement relationships [4.25] are

$$\eta_{11} = \left[u_{1,1} - x^3 u_{3,11} \right] \quad , \quad \eta_{22} = \left[u_{2,2} + \frac{1}{R + x^3} u_3 - x^3 \frac{R}{R + x^3} u_{3,22} \right] \left(\frac{R + x^3}{R} \right)^2$$
$$\eta_{12} = \eta_{21} = \left[\frac{1}{2} \left(\frac{R}{R + x^3} u_{1,2} + \frac{R + x^3}{R} u_{2,1} - x^3 \frac{2R + x^3}{R + x^3} u_{3,12} \right) \right] \frac{R + x^3}{R} \tag{4.3a-c}$$

The expressions inside the square brackets in Eqs. 4.3a-c express the physical components of the corresponding covariant component as presented by Flugge [4.26].

4.11 Stress-Strain Relations

The in-plane contravariant stress tensor $\sigma^{\alpha\beta}$ is related to the covariant strain tensor $\eta_{\lambda\delta}$ through

$$\sigma^{\alpha\beta} = E^{\alpha\beta\lambda\delta} \eta_{\lambda\delta} \tag{4.4}$$

in which $E^{\alpha\beta\lambda\delta}$ is the 4th order contravariant constitutive elasticity tensor. Under elastic isotropic material assumptions, the constitutive contravariant elasticity tensor, takes the form [4.25]

$$E^{\alpha\beta\lambda\delta} = \frac{E}{2(1+\nu)}\left(g^{\alpha\lambda}g^{\beta\delta} + g^{\alpha\delta}g^{\beta\lambda} + \frac{2\nu}{1-\nu} g^{\alpha\beta}g^{\lambda\delta} \right) \tag{4.5}$$

Symbols E and ν are Young's modulus of elasticity and Poisson's ratio, respectively, and $g^{\alpha\lambda}$ are the components of the contravariant metric tensor defined as

$$g^{11} = 1 \quad , \quad g^{22} = \left(\frac{R}{R+x^3} \right)^2 \quad , \quad g^{12} = \frac{R}{R+x^3} \tag{4.6a-c}$$

4.12 Formulation

4.12.1 Hamilton's Principle for Circular Cylindrical Thin Shells

In general, the variational form of Hamilton's principle is expressed as

$$\delta \prod = \int_{t_1}^{t_2} \delta(T^* - V^*)dt + \int_{t_1}^{t_2} \delta W^* dt = 0 \tag{4.7}$$

in which T^* is the kinetic energy, V^* is the internal strain energy and W^* is the external work on the system. The integration is performed between arbitrary time limits t_1 and t_2. For thin shells, the variations δT^*, δV^* and δW^* are

$$\delta T^* = \int_V \rho \dot{U}^i \delta \dot{U}_i dV \quad , \quad \delta V^* = \int_V E^{\alpha\beta\lambda\delta}\eta_{\lambda\delta}\delta\eta_{\alpha\beta}dV \quad , \quad \delta W^* = \int_V F^i \delta U_i dV \tag{4.8a-c}$$

in which ρ is the density of the cylinder material and $U^i = g^{ij}U_j$ are the contravariant components of the displacements. All dots denote differentiation with respect to time and all integrations are performed over the volume of the shell. From Eqs. 4.1-4.5, by substituting

into Eq. 4.8 and then in Eq. 4.7, and introducing the dimensionless parameter $\Phi(h/R)=\ln\left[(2+h/R)/(2-h/R)\right]\Big/(h/R)$ one obtains [4.27]

$$
\begin{aligned}
\delta\prod=\int_{t_1}^{t_2}\Bigg[\int_s\Bigg[&-\frac{Eh}{1-\nu^2}\left(u_{,1}+\nu v_{,2}+\frac{\nu}{R}w-\frac{h^2}{12R}w_{,11}\right)\delta u\\
&-\frac{Eh}{1-\nu^2}\left\{\frac{1-\nu}{2}\left[u_{,2}+\left(1+\frac{h^2}{4R^2}\right)v_{,1}-\frac{h^2}{4R}w_{,12}\right]\right\}\delta v\\
&+\left\langle\frac{Eh}{1-\nu^2}\left\{-\frac{h^2}{12R}u_{,11}+R(\Phi-1)\frac{1-\nu}{2}u_{,22}-\frac{h^2}{12R}\left(\frac{3-\nu}{2}\right)v_{,12}+\frac{h^2}{12}w_{,111}\right.\right.\\
&\left.\left.+\left[\frac{h^2}{12}\left(\frac{3-\nu}{2}\right)+R^2(\Phi-1)\frac{1-\nu}{2}\right]w_{,122}\right\}-\rho h\left(-\frac{h^2}{12R}\ddot{u}+\frac{h^2}{12}\ddot{w}_{,1}\right)+f^{xw}\right\rangle\delta w\\
&-\frac{Eh}{1-\nu^2}\left(-\frac{h^2}{12R}u_{,1}-\frac{h^2}{12R}\nu v_{,2}+\frac{h^2}{12}w_{,11}+\frac{h^2}{12}\nu w_{,22}\right)\delta w_{,1}\Bigg]_0^x ds\\
+\int_A\Bigg[&\left\langle\frac{Eh}{1-\nu^2}\left\{u_{,11}+\Phi\frac{1-\nu}{2}u_{,22}+\frac{1+\nu}{2}v_{,12}+\frac{\nu}{R}w_{,1}\right.\right.\\
&\left.\left.-\frac{h^2}{12R}w_{,111}+R(\Phi-1)\frac{1-\nu}{2}w_{,122}\right\}-\rho h\left(\ddot{u}-\frac{h^2}{12R}\ddot{w}_{,1}\right)+f^{xu}\right\rangle\delta u\\
&+\left\langle\frac{Eh}{1-\nu^2}\left[\frac{1+\nu}{2}u_{,12}+\left(1+\frac{h^2}{4R^2}\right)\frac{1-\nu}{2}v_{,11}+v_{,22}+\frac{1}{R}w_{,2}-\frac{h^2}{12R}\left(\frac{3-\nu}{2}\right)w_{,112}\right]\right.\\
&\left.-\rho h\left[\ddot{v}\left(1+\frac{h^2}{12R^2}\right)-2\frac{h^2}{12R}\ddot{w}_{,2}\right]+f^{sv}\right\rangle\delta v\\
&-\left\langle\frac{Eh}{1-\nu^2}\left\{\frac{\nu}{R}u_{,1}+\frac{1}{R}v_{,2}+\frac{1}{R^2}\Phi w+2(\Phi-1)w_{,22}-\frac{h^2}{12R}u_{,111}+R(\Phi-1)\frac{1-\nu}{2}u_{,122}\right.\right.\\
&-\frac{h^2}{12R}\left(\frac{3-\nu}{2}\right)v_{,112}+\frac{h^2}{12}w_{,1111}+\left[\frac{h^2}{12}\left(\frac{3+\nu}{2}\right)+R^2(\Phi-1)\frac{1-\nu}{2}\right]w_{,1122}\\
&\left.\left.+R^2(\Phi-1)w_{,2222}\right\}+\rho h\left[\ddot{w}-\frac{h^2}{12}\left(\ddot{w}_{,11}+\ddot{w}_{,22}\right)+\frac{h^2}{12R}\left(\ddot{u}_{,1}+2\ddot{v}_{,2}\right)\right]\right.\\
&\left.-\left(-f_{,1}^{xw}-f_{,2}^{sw}+f^{zw}\right)\right\rangle\delta w\Bigg]dsdx\Bigg]dt=0
\end{aligned}
\tag{4.9}
$$

in which

$$f^{xu} = \int_{-\frac{h}{2}}^{+\frac{h}{2}} p^x \left(1+\frac{z}{R}\right) dz \qquad f^{xw} = -\int_{-\frac{h}{2}}^{+\frac{h}{2}} p^x \, z \left(1+\frac{z}{R}\right) dz$$

$$f^{sv} = \int_{-\frac{h}{2}}^{+\frac{h}{2}} p^s \left(1+\frac{z}{R}\right)^2 dz \qquad f^{sw} = -\int_{-\frac{h}{2}}^{+\frac{h}{2}} p^s \, z \left(1+\frac{z}{R}\right) dz \qquad (4.10a\text{-}e)$$

$$f^{zw} = \int_{-\frac{h}{2}}^{+\frac{h}{2}} p^z \left(1+\frac{z}{R}\right) dz$$

where functions p^x, p^s and p^z are physical components of the contravariant force components F^1, F^2 and F^3. In Eq. 4.9, the sequence $\left\| \left[\left[\left\langle \left\{ \left[(...) \right] \right\} \right\rangle \right] \right] \right\|$ of nested brackets was adopted.

It is of interest to note that by performing a Taylor expansion of the term $\Phi\left(h/R\right)$ $(=1+\frac{1}{12}\left(h/R\right)^2+\frac{1}{80}\left(h/R\right)^4+\cdots)$ and retaining only the first two terms, and omitting the dynamic terms, the field equations in Eq. 4.9 revert to Flugge's theory [4.26]. Also, by adopting the approximation $1+z/R \approx 1$ before integration through the thickness, Eq. 4.9 reverts to the field equations of the DMV shell theory [4.26]. Other theories such as Timoshenko's [4.28], Novozhilov's [4.29] and Morley-Koiter [4.30] can all be obtained from the present theory by making other approximations [4.27]. Another point of interest is that not all theories have reported the energy consistent boundary conditions. Within this context, the boundary terms in Eq. 4.9 provides the boundary conditions under each theory [4.27].

4.12.2 Force Functions

A general expression for harmonic body forces of frequency $\bar{\omega}$ is given by

$$p^x(x,s,z,t)=\bar{p}^x(x,s,z)e^{i\bar{\omega}t},\ p^s(x,s,z,t)=\bar{p}^s(x,s,z)e^{i\bar{\omega}t},\ p^z(x,s,z,t)=\bar{p}^z(x,s,z)e^{i\bar{\omega}t}$$

(4.11a-c)

Other load distributions such as surface tractions, ring loads, line loads, point loads etc. can always be conceived as special cases of Eqs. 4.11a-c using the Heaviside and Dirac Delta functions as needed. When the applied forces are real and in-phase, the loading function takes the form

$$\left[p^x(x,s,z,t),p^s(x,s,z,t),p^z(x,s,z,t)\right]=\left[\bar{p}^x(x,s,z),\bar{p}^s(x,s,z),\bar{p}^z(x,s,z)\right]\mathrm{Re}\left(e^{i\bar{\omega}t}\right)$$

in which $\bar{p}^x(x,s,z)$, $\bar{p}^s(x,s,z)$ and $\bar{p}^z(x,s,z)$ are real functions. When the applied forces are real but out-of-phase, it can be shown (Appendix 4.A) that the force functions in Eq. 4.11a-c are still valid. However, functions $\bar{p}^x(x,s,z)$, $\bar{p}^s(x,s,z)$ and $\bar{p}^z(x,s,z)$ become complex in these cases. Given the continuity of the shell in the circumferential direction, a general expression for harmonic loading is

$$\left[\bar{p}^x(x,s,z),\bar{p}^s(x,s,z),\bar{p}^z(x,s,z)\right]=\left[\left(\sum_{n=-\infty}^{+\infty}\bar{p}_n^x(x,z)e^{ins/R}\right),\left(\sum_{n=-\infty}^{+\infty}\bar{p}_n^s(x,z)e^{ins/R}\right),\left(\sum_{n=-\infty}^{+\infty}\bar{p}_n^z(x,z)e^{ins/R}\right)\right] \quad (4.12)$$

4.12.3 Displacement Functions

In the absence of damping, the steady state displacements at the mid-surface are harmonic and in-phase with the applied body forces, i.e.,

$$u(x,s,t)=\bar{u}(x,s)e^{i\bar{\omega}t},\quad v(x,s,t)=\bar{v}(x,s)e^{i\bar{\omega}t},\quad v(x,s,t)=\bar{w}(x,s)e^{i\bar{\omega}t} \quad (4.13a\text{-}c)$$

Related to the discussion in Sec. 4.12.2 , when the applied forces $\bar{p}^x(x,s,z)$, $\bar{p}^s(x,s,z)$ and $\bar{p}^z(x,s,z)$ are real functions (e.g., in-phase real forces), the corresponding displacement fields $\bar{u}(x,s)$, $\bar{v}(x,s)$ and $\bar{w}(x,s)$ are real functions. Conversely, when the applied forces are complex functions (i.e., out-of-phase), the corresponding displacement fields are complex.

Given the continuity of the displacement fields in the circumferential direction, the general expressions for $\bar{u}(x,s)$, $\bar{v}(x,s)$ and $\bar{w}(x,s)$ can be decomposed into their Fourier series expansion in the circumferential direction. The corresponding displacement expressions are:

$$u(x,s,t)=\sum_{n=-\infty}^{+\infty}A_n(x)e^{ins/R}e^{i\bar{\omega}t}$$
$$v(x,s,t)=\sum_{n=-\infty}^{+\infty}B_n(x)e^{ins/R}e^{i\bar{\omega}t} \qquad \text{(4.14a-c)}$$
$$w(x,s,t)=\sum_{n=-\infty}^{+\infty}C_n(x)e^{ins/R}e^{i\bar{\omega}t}$$

The displacement expressions in Eqs. 4.14a-c are quite general. The terms corresponding to $n=0$ represent the axi-symmetric components of the displacements (i.e., $A_0(x)$ represents the longitudinal displacement characteristic of a cylinder under longitudinal end traction uniformly distributed around the circumference, $B_0(x)$ is the tangential displacement characteristic of a cylinder under St. Venant torsion, and $C_0(x)$ is the radial extensibility characteristic of a cylinder under internal or external pressure).

The terms $n=\pm 1$ represent beam-like displacements: a) Combinations of displacements v and w based on $n=\pm 1$ were observed to yield a nearly circular deformed cross-sections,

and b) the deformed configuration of the cylinder cross-section undergoing the longitudinal displacement u based on $n=\pm 1$ remain co-planar, in line with conventional beam theories.

The terms $|n|\geq 2$ represent cross-sectional distortions (specifically, displacements v and w based on $n=\pm 2$ represent the cross-section ovalization, while higher order terms represent higher modes of cross-section distortions). Also, displacement u with $|n|\geq 2$ represent the deviations from the co-planar behaviour represented by mode $n=\pm 1$ and thus represent warping deformations.

4.12.4 Equilibrium Condition

From Eqs. 4.11, 4.12 and 4.14, by substituting into Eq. 4.9 and integrating with respect to time t and the circumferential coordinate s yields

$$\sum_{n=-\infty}^{+\infty}\left(\frac{2\pi REh}{1-\nu^2}\left\langle \delta A_{-n}(x) \quad \delta B_{-n}(x) \quad \delta C_{-n}(x) \quad \delta C'_{-n}(x)\right\rangle \times\left[\left[\begin{array}{c|c|c} {}^{1}_{1}HD & {}^{1}_{2}H_n & {}^{1}_{3}H+{}^{1}_{4}HD^2 \\ \hline {}^{2}_{1}H_n & {}^{2}_{2}HD & {}^{2}_{3}H_nD \\ \hline {}^{3}_{1}H_n+{}^{3}_{2}HD^2 & {}^{3}_{3}H_nD & {}^{3}_{4}H_nD+{}^{3}_{5}HD^3 \\ \hline {}^{4}_{1}HD & {}^{4}_{2}H_n & {}^{4}_{3}H_n+{}^{4}_{4}HD^2 \end{array}\right]\left\{\begin{array}{c} A_n(x) \\ B_n(x) \\ C_n(x)\end{array}\right\}+\left\{\begin{array}{c} 0 \\ 0 \\ {}^{3}_{6}Hf_n^{xw}(x) \\ 0\end{array}\right\}\right]\right]_0^L\right) +$$

$$\sum_{n=-\infty}^{+\infty}\int_0^L\left(\frac{2\pi REh}{1-\nu^2}\left\langle \delta A_{-n}(x) \quad \delta B_{-n}(x) \quad \delta C_{-n}(x)\right\rangle \times\left[\left[\begin{array}{c|c|c} {}^{1}_{1}G_n+{}^{1}_{2}GD^2 & {}^{1}_{3}G_nD & {}^{1}_{4}G_nD+{}^{1}_{5}GD^3 \\ \hline {}^{2}_{1}G_nD & {}^{2}_{2}G_n+{}^{2}_{3}GD^2 & {}^{2}_{4}G_n+{}^{2}_{5}G_nD^2 \\ \hline {}^{3}_{1}G_nD+{}^{3}_{2}GD^3 & {}^{3}_{3}G_n+{}^{3}_{4}G_nD^2 & {}^{3}_{5}G_n+{}^{3}_{6}G_nD^2+{}^{3}_{7}GD^4 \end{array}\right]\times\left\{\begin{array}{c} A_n(x) \\ B_n(x) \\ C_n(x)\end{array}\right\}\right]\right]dx=0$$

$$+\left\{\begin{array}{c} {}^{1}_{6}Gf_n^{xu}(x) \\ {}^{2}_{6}Gf_n^{sv}(x) \\ {}^{3}_{8}GDf_n^{xw}(x)+{}^{3}_{9}G_nf_n^{sw}(x)+{}^{3}_{10}Gf_n^{zw}(x)\end{array}\right\}\Bigg]\Bigg]\Bigg) \qquad (4.15)$$

in which

$$f_n^{xu}(x)=\int_{-\frac{h}{2}}^{+\frac{h}{2}}\bar{p}_n^x(x,z)\left(1+\frac{z}{R}\right)dz \quad , \qquad f_n^{xw}(x)=-\int_{-\frac{h}{2}}^{+\frac{h}{2}}\bar{p}_n^x(x,z)\,z\left(1+\frac{z}{R}\right)dz$$

$$f_n^{sv}(x)=\int_{-\frac{h}{2}}^{+\frac{h}{2}}\bar{p}_n^s(x,z)\left(1+\frac{z}{R}\right)^2 dz \quad , \qquad f_n^{sw}(x)=-\int_{-\frac{h}{2}}^{+\frac{h}{2}}\bar{p}_n^s(x,z)\,z\left(1+\frac{z}{R}\right)dz \quad (4.16a\text{-}e)$$

$$f_n^{zw}(x)=\int_{-\frac{h}{2}}^{+\frac{h}{2}}\bar{p}_n^z(x,z)\left(1+\frac{z}{R}\right)dz$$

In Eq. 4.15, symbols D^d ($d=1,2,3,4$) denote the dth derivative of the argument functions with respect to x and constants ${}_j^iH$, ${}_j^iH_n$, ${}_j^iG$ and ${}_j^iG_n$ are defined in Appendix 4.B. As a convention, the left superscript i ($i=1,...,4$) of constants ${}_j^iH$, ${}_j^iH_n$, ${}_j^iG$ and ${}_j^iG_n$ denotes the constants are related to the ith boundary or integral term, as applicable. The left subscript j denotes the jth coefficient of ith boundary or integral term. The presence of subscript n in constants ${}_j^iH_n$ and ${}_j^iG_n$ denotes that the constants are dependent on the circumferential mode number n.

As an equilibrium requirement, the variation of the total potential energy in Eq. 4.15 must vanish. As a result, the integral term yields the field equations of the system and results into coupled ordinary differential equations in the unknown functions $A_n(x)$, $B_n(x)$ and $C_n(x)$. The boundary term yields all possible boundary conditions of the system. One obtains only eight boundary conditions per mode. These will be treated in Section 4.12.8 From Eq. 4.15 and noting that $\delta A_{-n}(x)$, $\delta B_{-n}(x)$ and $\delta C_{-n}(x)$ are arbitrary functions, one recovers the following set of field equations for each mode n.

$$\left[\begin{array}{c|c|c} {}_1^1G_n + {}_2^1GD^2 & {}_3^1G_nD & {}_4^1G_nD + {}_5^1GD^3 \\ \hline {}_1^2G_nD & {}_2^2G_n + {}_3^2GD^2 & {}_4^2G_n + {}_5^2G_nD^2 \\ \hline {}_1^3G_nD + {}_2^3GD^3 & {}_3^3G_n + {}_4^3G_nD^2 & {}_5^3G_n + {}_6^3G_nD^2 + {}_7^3GD^4 \end{array}\right]\left\{\begin{array}{c} A_n(x) \\ B_n(x) \\ C_n(x) \end{array}\right\} = -\left\{\begin{array}{c} {}_6^1Gf_n^{xu}(x) \\ {}_6^2Gf_n^{sv}(x) \\ {}_8^3GDf_n^{xw}(x) + {}_9^3G_n f_n^{sw}(x) + {}_{10}^3Gf_n^{zw}(x) \end{array}\right\} \tag{4.17}$$

The solution of the above system consists of two components: homogenous and particular.

4.12.5 Homogeneous Solution of Field Equations

The homogeneous solution to the field equations is obtained by setting the right hand side of Eq. 4.17 equal to zero. The unknown functions are assumed to take the following form

$$A_{nh}(x) = A_n e^{m_n x} \quad , \quad B_{nh}(x) = B_n e^{m_n x} \quad , \quad C_{nh}(x) = C_n e^{m_n x} \tag{4.18a-c}$$

which yields

$$\left[\begin{array}{c|c|c} {}_1^1G_n + {}_2^1Gm_n^2 & {}_3^1G_nm_n & {}_4^1G_nm_n + {}_5^1Gm_n^3 \\ \hline {}_1^2G_nm_n & {}_2^2G_n + {}_3^2Gm_n^2 & {}_4^2G_n + {}_5^2G_nm_n^2 \\ \hline {}_1^3G_nm_n + {}_2^3Gm_n^3 & {}_3^3G_n + {}_4^3G_nm_n^2 & {}_5^3G_n + {}_6^3G_nm_n^2 + {}_7^3Gm_n^4 \end{array}\right]\left\{\begin{array}{c} A_n \\ B_n \\ C_n \end{array}\right\} = 0 \tag{4.19}$$

The nontrivial solution of Eq. 4.19 is to be obtained by setting the determinant of the matrix in Eq. 4.19 equal to zero. In general, for modes $n \neq 0$, the system of differential equations in Eq. 4.19 is entirely coupled. This case is treated in Section 4.12.5.1 . For mode $n = 0$ however, one can verify that ${}_3^1G_0 = {}_1^2G_0 = {}_4^2G_0 = {}_5^2G_0 = {}_3^3G_0 = {}_4^3G_0 = 0$, which uncouples the second equation from the other two. A separate treatment is needed for this case and is provided in Section 4.12.5.2 .

4.12.5.1 Solution for Case $n \neq 0$:

For $n \neq 0$, the characteristic equation of the system yields a bi-quartic polynomial in m_n of the form $a_n m_n^8 + b_n m_n^6 + c_n m_n^4 + d_n m_n^2 + e_n = 0$, where the constants $a_n, ..., e_n$ are defined in Appendix 4.C. By setting $M_n = m_n^2$ one obtains $a_n M_n^4 + b_n M_n^3 + c_n M_n^2 + d_n M_n + e_n = 0$. The four complex roots M_{0i} $(i = 1, ..., 4)$ of the quartic are then obtained. The eight roots of the characteristic equation are obtained as $m_{0j} = \pm\sqrt{M_{0i}}$ $(j = 1, ..., 8)$. Thus, the homogeneous part of the displacement functions $A_{nh}(x)$, $B_{nh}(x)$ and $A_{nh}(x)$ is

$$A_{nh}(x) = \sum_{j=1}^{8} A_{nj}\bar{A}_{nj}e^{m_{nj}x} \;,\; B_{nh}(x) = \sum_{j=1}^{8} A_{nj}\bar{B}_{nj}e^{m_{nj}x} \;,\; C_{nh}(x) = \sum_{j=1}^{8} A_{nj}\bar{C}_{nj}e^{m_{nj}x} \quad (4.20a\text{-}c)$$

in which

$$\bar{A}_{nj} = 1 \quad , \quad \bar{B}_{nj} = \frac{{}_3^1K_{nj}\,{}_1^2K_{nj} - {}_1^1K_{nj}\,{}_3^2K_{nj}}{{}_2^1K_{nj}\,{}_3^2K_{nj} - {}_3^1K_{nj}\,{}_2^2K_{nj}} \quad , \quad \bar{C}_{n,j} = \frac{{}_1^1K_{nj}\,{}_2^2K_{nj} - {}_2^1K_{nj}\,{}_1^2K_{nj}}{{}_2^1K_{nj}\,{}_3^2K_{nj} - {}_3^1K_{nj}\,{}_2^2K_{nj}} \quad (4.21)$$

and

$$\begin{aligned}
&{}_1^1K_{nj} = {}_1^1G_n + {}_2^1Gm_{nj}^2 \quad , \quad && {}_2^1K_{nj} = {}_1^2K_{n,j} = {}_3^1G_n m_{nj} \\
&{}_3^1K_{nj} = {}_1^3K_{nj} = {}_4^1G_n m_{nj} + {}_5^1Gm_{nj}^3 \quad , \quad && {}_2^2K_{nj} = {}_2^2G_n + {}_3^2Gm_{nj}^2 \\
&{}_3^2K_{nj} = {}_2^3K_{nj} = {}_4^2G_n + {}_5^2G_n m_{nj}^2 \quad , \quad && {}_3^3K_{nj} = {}_5^3G_n + {}_6^3G_n m_{nj}^2 + {}_7^3Gm_{nj}^4
\end{aligned} \quad (4.22a\text{-}f)$$

In the characteristic equation $a_n M_n^4 + b_n M_n^3 + c_n M_n^2 + d_n M_n + e_n = 0$, it can be verified that $a_n = a_{-n}$, $b_n = b_{-n}$, $c_n = c_{-n}$, $d_n = d_{-n}$ and $e_n = e_{-n}$. Therefore, the roots of the characteristic equation for mode n and mode $-n$ happen to be identical.

4.12.5.2 Case $n = 0$

For $n = 0$, the second equation is uncoupled from the first and the third one and leads to a bi-cubic characteristic equation in the form of $b_0 m_0^6 + c_0 m_0^4 + d_0 m_0^2 + e_0 = 0$, where constants

$b_0,...,e_0$ are defined in Appendix 4.C. By setting $M_0 = m_0^2$, one obtains $b_0 M_0^3 + c_0 M_0^2 + d_0 M_0 + e_0 = 0$. The three complex roots M_{0i} $(i = 1,2,3)$ of the cubic polynomial are then obtained and the six roots of the characteristic equation are $m_{0j} = \pm\sqrt{M_{0i}}$ $(j = 1,...,6)$. Thus, the homogeneous part of the displacement functions $A_{0h}(x)$ and $C_{0h}(x)$ are

$$A_{0h}(x) = \sum_{j=1}^{6} A_{0j} e^{m_{0j}x} \quad , \quad C_{0h}(x) = \sum_{j=1}^{6} A_{0j} \bar{C}_{0j} e^{m_{0j}x} \qquad (4.23a,b)$$

$$\bar{C}_{0j} = -\frac{{}_1^1K_{0j}}{{}_3^1K_{0j}}$$

where symbols ${}_1^1K_{0j}$ and ${}_3^1K_{0j}$ were defined in Eq. 4.22. The second (uncoupled) equation leads to a quadratic characteristic equation with two distinct roots $m_{0j} = \pm\sqrt{-{}_2^2G_0 / {}_3^2G}$ $(j = 7,8)$. Thus, the homogeneous part of $B_{0h}(x)$ is

$$B_{0h}(x) = \sum_{j=7}^{8} A_{0j} e^{m_{0j}x} \qquad (4.24)$$

Equations 4.23 and 4.24 can be cast in the same form as Eq. 4.20, i.e.,

$$A_{0h}(x) = \sum_{j=1}^{8} A_{0j} \bar{A}_{0j} e^{m_{0j}x} \,,\; B_{0h}(x) = \sum_{j=1}^{8} A_{0j} \bar{B}_{0j} e^{m_{0j}x} \,,\; C_{0h}(x) = \sum_{j=1}^{8} A_{0j} \bar{C}_{0j} e^{m_{0j}x} \quad (4.25a\text{-}c)$$

in which

$$\bar{A}_{0j} = \begin{cases} 1 & j = 1,...,6 \\ 0 & j = 7,8 \end{cases} \quad , \quad \bar{B}_{0j} = \begin{cases} 0 & j = 1,...,6 \\ 1 & j = 7,8 \end{cases} \quad , \quad \bar{C}_{0j} = \begin{cases} -\dfrac{{}_1^1K_{0j}}{{}_3^1K_{0j}} & j = 1,...,6 \\ 0 & j = 7,8 \end{cases} \quad (4.26a\text{-}c)$$

4.12.6 Particular Solution of Field Equations

The load functions $f_n^{xu}(x)$, $f_n^{xw}(x)$, $f_n^{sv}(x)$, $f_n^{sw}(x)$ and $f_n^{zw}(x)$ can be expanded as Fourier series yielding

$$f_n^{xu}(x)=\sum_{k=-\infty}^{+\infty} f_{nk}^{xu} e^{2\pi ikx/L},\quad f_n^{sv}(x)=\sum_{k=-\infty}^{+\infty} f_{nk}^{sv} e^{2\pi ikx/L}$$
$$f_n^{zw}(x)=\sum_{k=-\infty}^{+\infty} f_{nk}^{zw} e^{2\pi ikx/L},\quad f_n^{xw}(x)=\sum_{k=-\infty}^{+\infty} f_{nk}^{xw} e^{2\pi ikx/L} \qquad (4.27a\text{-}e)$$
$$f_n^{sw}(x)=\sum_{k=-\infty}^{+\infty} f_{nk}^{sw} e^{2\pi ikx/L}$$

in which constants f_{nk}^{xu}, f_{nk}^{sv}, f_{nk}^{zw}, f_{nk}^{xw} and f_{nk}^{sw} are the Fourier coefficients of the loading functions and are given by

$$f_{nk}^{xu}=\int_0^1 f_n^{xu}(x)e^{-2\pi ikx/L}dx,\quad f_{nk}^{xw}=\int_0^1 f_n^{xw}(x)e^{-2\pi ikx/L}dx$$
$$f_{nk}^{sv}=\int_0^1 f_n^{sv}(x)e^{-2\pi ikx/L}dx,\quad f_{nk}^{sw}=\int_0^1 f_n^{sw}(x)e^{-2\pi ikx/L}dx \qquad (4.28a\text{-}e)$$
$$f_{nk}^{zw}=\int_0^1 f_n^{zw}(x)e^{-2\pi ikx/L}dx$$

For most load patterns, a limited number of Fourier terms are enough to properly describe the load. For a given longitudinal Fourier series term k and circumferential mode n, in the expansion series above (Eq. 4.27) the particular solution is assumed to take the form

$$A_{nkp}(x)=R_{nk}e^{2\pi ikx/L},\quad B_{nkp}(x)=S_{nk}e^{2\pi ikx/L},\quad C_{nkp}(x)=T_{nk}e^{2\pi ikx/L} \qquad (4.29a\text{-}c)$$

In Eq. 4.29, symbols R_{nk}, S_{nk} and T_{nk} are unknown constants to be determined by substituting into the field equations (Eq. 4.17) while retaining the right hand sides. From Eqs. 4.29, by substituting into Eq. 4.17 and equating the terms with identical powers in both sides of each equation, one obtains

$$\begin{bmatrix} {}_1^1G_n + {}_2^1G\left(2\pi ik/L\right)^2 & {}_3^1G_n\left(2\pi ik/L\right) & {}_4^1G_n\left(2\pi ik/L\right)+8\pi^3\ {}_5^1G\left(2\pi ik/L\right)^3 \\ {}_1^2G_n\left(2\pi ik/L\right) & {}_2^2G_n + {}_3^2G\left(2\pi ik/L\right)^2 & {}_4^2G_n + {}_5^2G_n\left(2\pi ik/L\right)^2 \\ {}_1^3G_n\left(2\pi ik/L\right)\ + {}_2^3G\left(2\pi ik/L\right)^3 & {}_3^3G_n + {}_4^3G_n\left(2\pi ik/L\right)^2 & {}_5^3G_n + {}_6^3G_n\left(2\pi ik/L\right)^2 + {}_7^3G\left(2\pi ik/L\right)^4 \end{bmatrix}$$

$$\times\begin{Bmatrix} R_{nk} \\ S_{nk} \\ T_{nk} \end{Bmatrix} = -\begin{Bmatrix} {}_6^1Gf_{nk}^{xu} \\ {}_6^2Gf_{nk}^{sv} \\ {}_8^3G\left(2\pi ik\right)f_{nk}^{xw} + {}_9^3G_n f_{nk}^{sw} + {}_{10}^3Gf_{nk}^{zw} \end{Bmatrix} \tag{4.30}$$

The system of equations in Eq. 4.30 is solved for all relevant n and k values to yield coefficients R_{nk}, S_{nk}, and T_{nk}. Finally, the particular solution for mode n is the summation of the individual contributions of the Fourier longitudinal modes k, yielding

$$A_{np}(x) = \sum_{k=-\infty}^{+\infty} R_{nk}e^{2\pi ikx/L}, \quad B_{np}(x) = \sum_{k=-\infty}^{+\infty} S_{nk}e^{2\pi ikx/L}, \quad C_{np}(x) = \sum_{k=-\infty}^{+\infty} T_{nk}e^{2\pi ikx/L} \tag{4.31a-c}$$

4.12.7 General Solution of Field Equations

The general solution for mode n is the summation of the homogeneous solution (Eqs. 4.20 and 4.25) and the particular solutions (Eq. 4.31), i.e.,

$$\begin{aligned} A_n(x) &= \sum_{j=1}^{8} A_{nj}\bar{A}_{nj}e^{m_{nj}x} + \sum_{k=-\infty}^{+\infty} R_{nk}e^{2\pi ikx/L} \\ B_n(x) &= \sum_{j=1}^{8} A_{nj}\bar{B}_{nj}e^{m_{nj}x} + \sum_{k=-\infty}^{+\infty} S_{nk}e^{2\pi ikx/L} \\ C_n(x) &= \sum_{j=1}^{8} A_{nj}\bar{C}_{nj}e^{m_{nj}x} + \sum_{k=-\infty}^{+\infty} T_{nk}e^{2\pi ikx/L} \end{aligned} \tag{4.32a-c}$$

4.12.8 Boundary Conditions

The first summation over n in Eq. 4.15 yields the boundary conditions of the system. From Eq. 4.32, by substituting into the set of boundary conditions , one obtains

$$\sum_{n=-\infty}^{+\infty}\Bigg[\delta A_{-n}(x)\times\Bigg\{\sum_{j=1}^{8}\Big({}_1^1Hm_{nj}\bar{A}_{nj}+{}_2^1H_n\bar{B}_{nj}+{}_3^1H\bar{C}_{nj}+{}_4^1Hm_{nj}^2\bar{C}_{nj}\Big)A_{nj}e^{m_{nj}x}$$
$$+\Big[{}_1^1HA'_{np}(x)+{}_2^1H_nB_{np}(x)+{}_3^1HC_{np}(x)+{}_4^1HC''_{np}(x)\Big]\Bigg\}$$
$$+\delta B_{-n}(x)\times\Bigg\{\sum_{j=1}^{8}\Big({}_1^2H_n\bar{A}_{nj}+{}_2^2Hm_{nj}\bar{B}_{nj}+{}_3^2H_nm_{nj}\bar{C}_{nj}\Big)A_{nj}e^{m_{nj}x}$$
$$+\Big[{}_1^2H_nA_{np}(x)+{}_2^2HB'_{np}(x)+{}_3^2H_nC'_{np}(x)\Big]\Bigg\}$$
$$+\delta C_{-n}(x)\times\Bigg\{\sum_{j=1}^{8}\Big({}_1^3H_n\bar{A}_{nj}+{}_2^3Hm_{nj}^2\bar{A}_{nj}+{}_3^3H_nm_{nj}\bar{B}_{nj}+{}_4^3H_nm_{nj}\bar{C}_{nj}+{}_5^3Hm_{nj}^3\bar{C}_{nj}\Big)A_{nj}e^{m_{nj}x}$$
$$+\Big[{}_1^3H_nA_{np}(x)+{}_2^3HA''_{np}(x)+{}_3^3H_nB'_{np}(x)+{}_4^3H_nC'_{np}(x)+{}_5^3HC'''_{np}(x)+{}_6^3Hf_n^{xw}(x)\Big]\Bigg\}$$
$$+\delta C'_{-n}(x)\times\Bigg\{\sum_{j=1}^{8}\Big({}_1^4Hm_{nj}\bar{A}_{nj}+{}_2^4H_n\bar{B}_{nj}+{}_3^4H_n\bar{C}_{nj}+{}_4^4Hm_{nj}^2\bar{C}_{nj}\Big)A_{nj}e^{m_{nj}x}$$
$$+\Big[{}_1^4HA'_{np}(x)+{}_2^4H_nB_{np}(x)+{}_3^4H_nC_{np}(x)+{}_4^4HC''_{np}(x)\Big]\Bigg\}\Bigg]_0^L=0 \tag{4.33}$$

In which symbol "'" denotes the derivative with respect to x in the same way as symbol "D". In Eq. 4.33, depending on the boundary conditions of the problem, either the variations $\delta A_{-n}(0)$, $\delta A_{-n}(L)$, $\delta B_{-n}(0)$, $\delta B_{-n}(L)$, $\delta C_{-n}(0)$, $\delta C_{-n}(L)$, $\delta C'_{-n}(0)$, $\delta C'_{-n}(L)$ are equal to zero or the corresponding bracketed terms must vanish. This leads to the eight boundary conditions for each mode n necessary to determine the unknown integration constants A_{nj}.

4.12.9 General Displacement Fields

By summation over n in Eqs. 4.32 and substitution into Eqs. 4.1, one obtains the total response $\tilde{U},\tilde{V},\tilde{W}$ of any point within the shell volume in the form of

$$\tilde{U}\left(x,s,z,t\right)=\sum_{n=-\infty}^{+\infty}\left[\left(\sum_{j=1}^{8}A_{nj}\left(\bar{A}_{nj}-zm_{nj}\bar{C}_{nj}\right)e^{m_{nj}x}\right)+\sum_{k=-\infty}^{+\infty}\left(R_{nk}-z\frac{2\pi ik}{L}T_{nk}\right)e^{2\pi ikx}\right]e^{ins/R}e^{i\bar{\omega}t}$$

$$\tilde{V}\left(x,s,z,t\right)=\sum_{n=-\infty}^{+\infty}\left[\left(\sum_{j=1}^{8}A_{nj}\left(\bar{B}_{nj}-z\frac{in}{R}\bar{C}_{nj}\right)e^{m_{nj}x}\right)+\sum_{k=-\infty}^{+\infty}\left(S_{nk}-z\frac{in}{R}T_{nk}\right)e^{2\pi ikx/L}\right]\left(1+\frac{z}{R}\right)e^{ins/R}e^{i\bar{\omega}t}$$

$$\tilde{W}\left(x,s,z,t\right)=\sum_{n=-\infty}^{+\infty}\left[\left(\sum_{j=1}^{8}A_{nj}\bar{C}_{nj}e^{m_{nj}x}\right)+\sum_{k=-\infty}^{+\infty}T_{nk}e^{2\pi ikx/L}\right]e^{ins/R}e^{i\bar{\omega}t} \qquad (4.34a\text{-}c)$$

4.13 Solution Steps

Given the pipe dimensions h, R and L, its material properties E, ν and ρ, applied harmonic body forces $\bar{p}^{x}\left(x,s,z\right)$, $\bar{p}^{s}\left(x,s,z\right)$, $\bar{p}^{z}\left(x,s,z\right)$, and exciting frequency $\bar{\omega}$, the following steps are performed to solve any problem.

1. Body forces $\bar{p}^{x},\bar{p}^{s},\bar{p}^{z}$ are decomposed with respect to the circumferential coordinate into their Fourier series form using Eq. 4.12.
2. Constants f_{nk}^{xu}, f_{nk}^{sv}, f_{nk}^{xw}, f_{nk}^{sw} and f_{nk}^{zw} are calculated by substituting the results of step 1 into Eqs. 4.16, and then into Eqs. 4.28.
3. The particular solution for each mode n and Fourier term k are obtained by solving Eq. 4.30 for R_{nk}, S_{nk}, T_{nk}.
4. The roots of the characteristic equation, Eq. 4.19, are determined for the relevant modes identified in step 1. While an exact solution involves an infinite number of terms, an approximate solution is obtained by truncating the series. This provides the homogeneous solution for the contributing modes.
5. Constants $\bar{A}_{nj}$, $\bar{B}_{nj}$ and $\bar{C}_{nj}$ are then calculated from Eqs. 4.21 and 4.26.

6. The boundary conditions relevant to the problem are expressed by selecting either the essential or natural boundary conditions in Eq. 4.33.
7. The integration constants A_{nj} are determined by solving the corresponding n sets of eight boundary condition equations in Eq. 4.33.
8. From steps 2, 4, 5 and 7, by substituting into Eq. 4.34, one obtains the closed form solution of the displacement fields for the shell.

4.14 Examples

4.14.1 Example 1

A circular cylinder is fixed at both ends. The cross-section thickness h is $0.005m$, its radius R is $0.25m$. The beam span L is $5m$. Material is steel with Young's modulus $E = 200GPa$, Poisson's ratio $\nu = 0.3$ and density $\rho = 7{,}850\,Kg/m^3$. The cylinder is subject to a harmonic radial traction $t^z(x,s,t) = P^z \cos(s/R)\cos\bar{\omega}t$ (force per square length units) acting on the outer surface $z = h/2$, in which $P^z = -1{,}000\,N/m^2$ and $\bar{\omega} = 200\,rad/s$ (Figure 4.2). The given loading pattern could be conceived as a simplification of vortex shedding effects. It is required to determine the steady state response of the cylinder under the given loads.

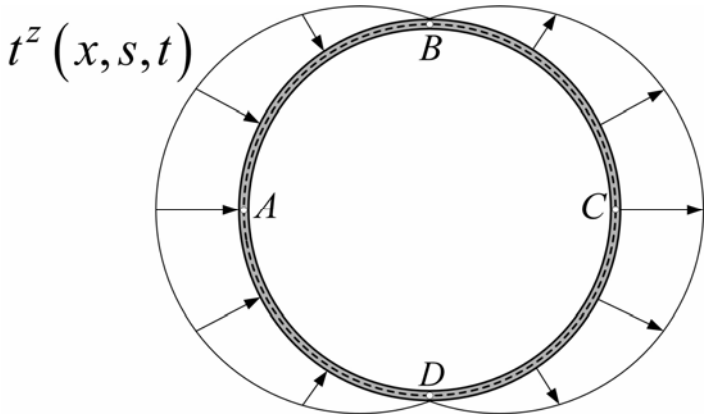

Figure 4.2 – Cross sectional profile of the traction

4.14.1.1 Developments Specific to the Problem

In order to formulate the particular solution of the problem, the applied traction is cast into a force per unit volume format using the Dirac delta function

$$\begin{aligned} p^z\left(x,s,z,t\right) &= P^z \mathrm{Dirac}\left(z-h/2\right)\cos\left(s/R\right)\cos\bar{\omega}t \\ &= P^z \mathrm{Dirac}\left(z-h/2\right)\left(\frac{e^{is/R}+e^{-is/R}}{2}\right)\mathrm{Re}\left(e^{i\bar{\omega}t}\right) \end{aligned} \tag{4.35}$$

in which function Re denotes the real part of the argument function. From Eq. 4.35, it is observed that the Fourier series expansion of the forces per unit volume have only two non-zero terms, i.e.,

$$\bar{p}_n^z\left(x,z\right) = \begin{cases} \dfrac{P^z}{2}\mathrm{Dirac}\left(z-h/2\right) & ; \quad n=-1,+1 \\ 0 & ; \quad n\neq -1,+1 \end{cases} \tag{4.36}$$

From Eq. 4.36, by substituting into Eqs. 4.16, one recovers the following Fourier coefficients for the equivalent tractions

$$\begin{aligned} f_n^{zw}\left(x\right) &= \int_{-\frac{h}{2}}^{+\frac{h}{2}} \bar{p}_n^z\left(1+\frac{z}{R}\right)dz \\ &= \begin{cases} \displaystyle\int_{-\frac{h}{2}}^{+\frac{h}{2}} \frac{P^z}{2}\mathrm{Dirac}\left(z-h/2\right)\left(1+\frac{z}{R}\right)dz = \frac{P^z}{2}\left(1+\frac{h}{2R}\right) & ; n=-1,+1 \\ 0 & ; n\neq -1,+1 \end{cases} \end{aligned} \tag{4.37}$$

In the present problem, the absence of the longitudinal and circumferential body forces implies that $f_n^{xu} = f_n^{xw} = f_n^{sv} = f_n^{sw} = 0$. In Eq. 4.37, the magnitude of the traction contributions f_{-1}^{zw}, f_1^{zw} is observed to be larger than the applied traction P^z since f_{-1}^{zw}, f_1^{zw}

are referred to the mid-surface, while the given applied traction P^z is applied to the outer surface.

Since the given radial load is constant along longitudinal coordinate $\bar{x}$, only the zero modal components ($k=0$) in Eq. 4.31 contribute to the particular solution. Thus, only components $R_{-1,0}$, $S_{-1,0}$, $T_{-1,0}$ $R_{1,0}$, $S_{1,0}$, and $T_{1,0}$ need to be determined. This is done by solving Eq. 4.30. All other R_{nk}, S_{nk}, T_{nk} coefficients happen to vanish in the present problem. The solution then proceeds according to Steps 4 through 8 outlined in Section 4.13 . When applying the boundary conditions as per Step 6, the boundary conditions of the problem are $\delta A_{-n}(0) = \delta A_{-n}(L) = \delta B_{-n}(0) = \delta B_{-n}(L) = \delta C_{-n}(0) = \delta C_{-n}(L) = \delta C'_{-n}(0) = \delta C'_{-n}(L) = 0$.

4.14.1.2 Results

Four points A, B, C and D on the mid-surface at the beam mid-span are considered (Figure 4.2). The radial displacement at points A and C, and the circumferential displacements at points B and D are -3.7248×10^{-2}, $+3.7248\times10^{-2}$, $+3.7533\times10^{-2}$ and -3.7533×10^{-2} mm, respectively, i.e., all four points undergo essentially the same vertical displacement. All other displacement components are zero. For comparison, the vertical displacement of point A at the same section is calculated based on a) the Euler-Bernoulli beam theory and b) a shell finite element analysis based on Abaqus. In the Abaqus model, the shell element S4R (4-node doubly curved shell element with five integration points across the thickness) is used. Five different meshes are investigated. The specifics of the meshes used and a comparison of the results are presented in Table 4.1.

Table 4.1 – Mid-span deflection at point A

	Current Study (CS)	Abaqus					Euler-Bernoulli
		Number of Elements					
		8×25 $=200$	16×50 $=800$	32×102 $=3,264$	80×254 $=20,320$	160×510 $=81,600$	
Displacement (mm)	0.03725	0.04239	0.03842	0.03753	0.03730	0.03726	0.02808
% Difference from CS	-	13.8%	3.16%	0.74%	0.13%	0.04%	-24.6%

There is a 24.6% difference between the result from Euler-Bernoulli solution and that of the current study. This is particularly because the Euler-Bernoulli beam theory does not capture the localized effects. The results from Abaqus based on the finest mesh show excellent agreement with the present solution. Essentially, the current study provides results in very close agreement with Abaqus with far fewer degrees of freedom. The Abaqus displacement is 0.04% larger than that based on the present study since the Abaqus S4R shell element captures the transverse shear effects which are neglected in the present formulation (Assumption 1). A graphical comparison of various solutions is provided in Figure 4.3.

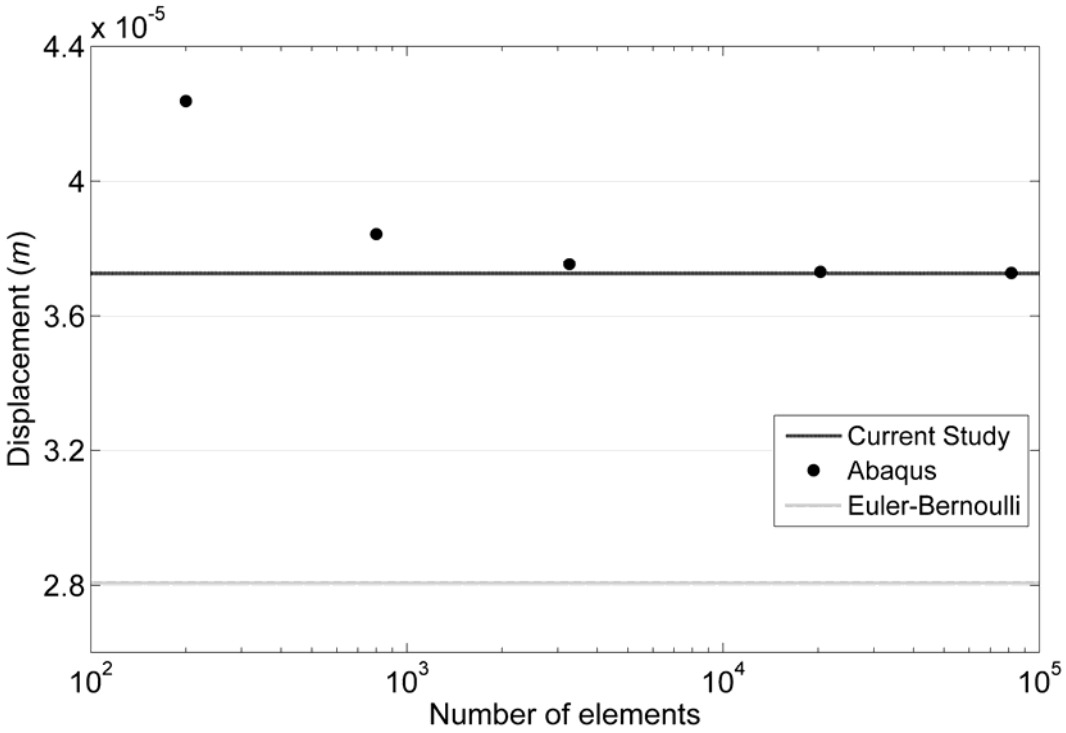

Figure 4.3 – Radial displacements at point A

It is noted that, as the number of elements in Abaqus increases, the results based on Abaqus is observed to converge from above. This contrasts to static finite element analyses, which tend to converge from below. The dynamic nature of the analysis is believed to be the reason for this phenomenon. A further comparison between the results of the current study and those based on Abaqus is provided in Figure 4.4 for a wide range of frequencies ranging from zero to $3,200\,Hz$. The figure shows excellent agreement between both solutions.

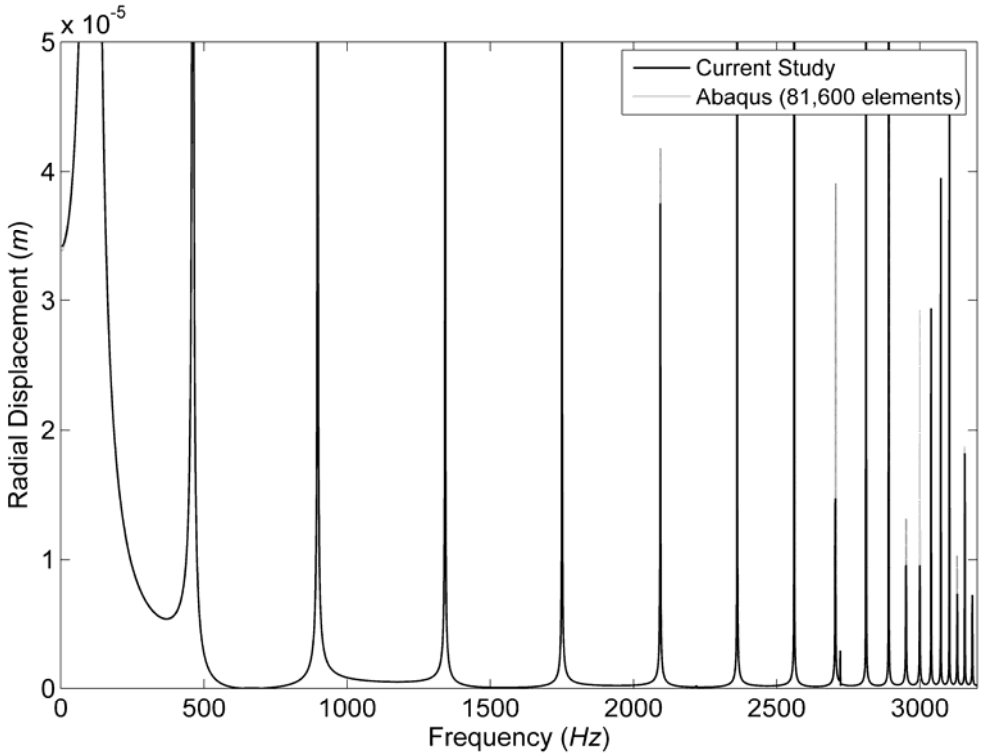

Figure 4.4 - Radial displacement of point A as a function of exciting frequency

4.14.2 Example 2

A horizontal cantilever beam with a cylindrical cross-section has a thickness $h = 0.006\,m$, mid-surface radius $R = 0.2\,m$, span $L = 4\,m$, Poisson's ratio $\nu = 0.3$, Young's modulus $E = 200\,GPa$, density $\rho = 7{,}850\,Kg/m^3$ is subject to gravity force. It is required to determine the deflection of the beam under its self weight. This example was considered by Weicker [4.31] and is solved here as a verification example.

4.14.2.1 Solution

The static gravity loading in the present problem can be approached as a harmonic load with very low frequency (compared to the first natural frequency). The corresponding load functions are $p^x(x,s,z,t) = 0$, $p^s(x,s,z,t) = \rho g \sin(s/R) e^{i\bar{\omega}t}$ and

$p^z(x,s,z,t) = -\rho g \cos(s/R) e^{i\bar{\omega}t}$ $g = 9.81 m/s^2$. Given that the first natural frequency of the cylinder ω_1 is around $25 rad/s$, an exciting frequency of $\bar{\omega} = 0.01 rad/s$ is judged suitable to capture the static response of the structure.

Similar to Example 1, the circumferential modes $n = \pm 1$ and the longitudinal mode $k = 0$ are the only non-zero term needed to express the self weight.

4.14.2.2 Enforcing Boundary Conditions

At the cantilever root ($x = 0$), all displacements vanish, i.e., $A_{-n}(0) = B_{-n}(0) = C_{-n}(0) = C'_{-n}(0) = 0$. At the free end ($x = L$), the natural boundary conditions in Eqs. 4.33 must vanish, leading to the following conditions for $n = -1, +1$

$$\sum_{j=1}^{8} \left({}_1^1 H m_{nj} \bar{A}_{nj} + {}_2^1 H_n \bar{B}_{nj} + {}_3^1 H \bar{C}_{nj} + {}_4^1 H m_{nj}^2 \bar{C}_{nj} \right) A_{nj} e^{m_{nj}} + \left[{}_1^1 H A'_{np}(L) + {}_2^1 H_n B_{np}(L) + {}_3^1 H C_{np}(L) + {}_4^1 H C''_{np}(L) \right] = 0$$

$$\sum_{j=1}^{8} \left({}_1^2 H_n \bar{A}_{nj} + {}_2^2 H m_{nj} \bar{B}_{nj} + {}_3^2 H_n m_{nj} \bar{C}_{nj} \right) A_{nj} e^{m_{nj}} + \left[{}_1^2 H_n A_{np}(L) + {}_2^2 H B'_{np}(L) + {}_3^2 H_n C'_{np}(L) \right] = 0$$

$$\sum_{j=1}^{8} \left({}_1^3 H_n \bar{A}_{nj} + {}_2^3 H m_{nj}^2 \bar{A}_{nj} + {}_3^3 H_n m_{nj} \bar{B}_{nj} + {}_4^3 H_n m_{nj} \bar{C}_{nj} + {}_5^3 H m_{nj}^3 \bar{C}_{nj} \right) A_{nj} e^{m_{nj}} + \left[{}_1^3 H_n A_{np}(L) + {}_2^3 H A''_{np}(L) + {}_3^3 H_n B'_{np}(L) + {}_4^3 H_n C'_{np}(L) + {}_5^3 H C'''_{np}(L) + {}_6^3 H f_n^{xw} \right] = 0$$

$$\sum_{j=1}^{8} \left({}_1^4 H m_{nj} \bar{A}_{nj} + {}_2^4 H_n \bar{B}_{nj} + {}_3^4 H_n \bar{C}_{nj} + {}_4^4 H m_{nj}^2 \bar{C}_{nj} \right) A_{nj} e^{m_{nj}} + \left[{}_1^4 H A'_{np}(L) + {}_2^4 H_n B_{np}(L) + {}_3^4 H_n C_{np}(L) + {}_4^4 H C''_{np}(L) \right] = 0$$

Integration constants A_{nj} are determined by solving the set of eight boundary conditions for each of modes $n = -1, +1$.

4.14.2.3 Results

Considering four points A, B, C and D similar to Example 1, (the gravity force is acting in the AC direction), the absolute values of the nonzero components of the displacement are given in Table 4.2. Excellent agreement is achieved between the results based on the current study and those based on Abaqus FEA and shell analysis. A $100 \times 313 = 31,300$ S4R element mesh is adopted in the Abaqus model. The present solution agrees with Weicker's shell analysis [4.31] within 1.3% and with Abaqus FEA model within 0.1%.

Table 4.2 – Displacements (in 10^{-2} mm) of points A, B, C and D

	Absolute Value of Displacements (mm)		
	Axial	Circumferential	Radial
	Points A, C	Points B, D	Points A, C
Current Study	0.04107	0.6312	0.6312
Weicker's shell analysis	0.04161	0.6395	0.6395
Abaqus	0.04112	0.6320	0.6320

4.14.3 Example 3

It is required to investigate the steady state response of a single offshore pier, holding a light platform subjected to hydrodynamic wave forces. The pier is made of a steel cylindrical thin

shell with thickness $h = 0.004\,m$, radius $R = 0.1\,m$ and submerged length $L = 10\,m$ (from seabed to still water level). The material properties are identical to those in Example 1. According to Rahman [4.32], the dynamic pressure on vertical circular cylinders under wave loads Figure 4.5 can be approximated by

$$t^z(x,s,t) = \rho_w g H k_w \left(R + \frac{h}{2}\right) \frac{\cosh\left[k_w x\right]}{\cosh\left(k_w h_w\right)} \cos\left(s/R\right) e^{i\bar{\omega}t} \qquad ; x = 0 \text{ to } h_w \quad ,$$

in which, the water density ρ_w is taken as $1{,}000\,Kg/m^3$, H, the wave height, is taken $1m$, $k_w = 2\pi / L_w$, the wave number is expressed in terms of the wave length (in meters) as $L_w = 8.7T_w + 21.3$ [4.33] and T_w (in seconds) is the wave period (normally ranging from 8 to 15 seconds). The wave period is related to the exciting frequency through $\bar{\omega} = 2\pi / T_w$ (corresponding to practical wave frequencies in the 0.42 - $0.79 Hz$ range).

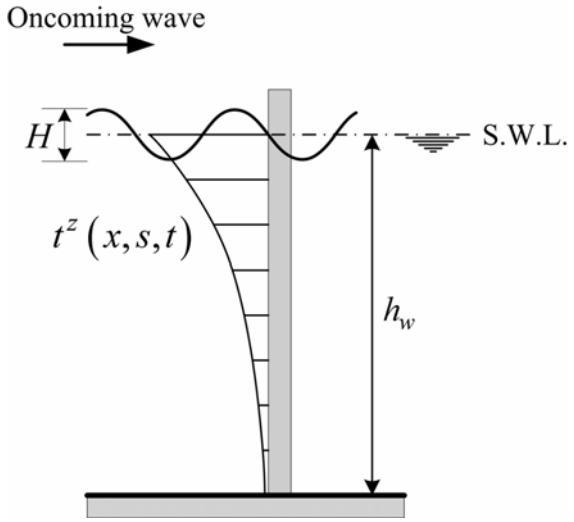

Figure 4.5 – Wave forces on a vertical circular cylinder

4.14.3.1 Solution

The applied pressure is cast into a force per unit volume format using the Dirac delta function as

$$\begin{aligned} p^z\left(x,s,z,t\right) &= \rho_w g H k_w \left(R+\frac{h}{2}\right)\frac{\cosh\left(k_w h_w x\right)}{\cosh\left(k_w h_w\right)}\cos\left(s/R\right)e^{i\bar{\omega}t} \\ &= \mathrm{Re}\left[\rho_w g H k_w \left(R+h/2\right)\mathrm{Dirac}\left(z-h/2\right)\frac{\cosh\left(k_w x\right)}{\cosh\left(k_w h_w\right)}\left(\frac{e^{is/R}+e^{-is/R}}{2}\right)e^{i\bar{\omega}t}\right] \end{aligned} \quad (4.38)$$

Similar to Example 1, $n=-1,+1$ are the only non-zero circumferential force modes. Unlike examples 1 and 2, the given load is variable along the longitudinal coordinate x. Thus, an exact representation of the load requires an infinite number of longitudinal modes. Practically, a finite number of longitudinal modes are taken. In Figure 4.6 three solutions are provided. The first considers the longitudinal modes $-1\le k\le+1$. The second solution takes the modes $-8\le k\le+8$ while the third solution takes the modes $-15\le k\le+15$. Overlaid on the same figure is a steady state solution based on Abaqus FEA (Using $100\times1,566=156,600$ shell elements) for comparison. The problem is also solved for hypothetical static loading ($-7\le k\le+7$) with the same longitudinal distribution (by setting $\bar{\omega}=0.01\,\mathrm{rad/sec}$). The boundary conditions are identical to those of Example 2, i.e. all essential boundary conditions vanish at $x=0$ and all natural boundary conditions vanish at $x=L$.

4.14.3.2 Results

Table 4.3 provides the transverse displacement at point A (defined as in Example 1) at the top of the cylinder. Two solutions are provided, one based on the current study and the other based on Abaqus shell FEA.

Table 4.3 – Displacements (in mm) at top of cylinder

Models	Details	$T_w = 2\,\text{sec}$	$T_w = 12\,\text{sec}$
Current Study	Hypothetical static: $-7 \le k \le +7$	18.25	7.563
	Dynamic: $-1 \le k \le +1$	18.24	7.522
	Dynamic: $-8 \le k \le +8$	19.51	7.582
	Dynamic: $-15 \le k \le +15$	19.64	7.594
Abaqus	Dynamic: $100 \times 1,566 =$ $156,600$ elements	19.83	7.612

The results are depicted in Figure 4.6. For the practical range of wave periods (8 to 15 seconds) it is shown that, for the current problem, all four solutions are in excellent agreements. The static solution appears to be adequate to predict the structure steady state displacements in the same range.

For lower wave periods, the solution based on the dynamic analysis departs significantly from the static solution. This is because the exciting frequency is approaching the natural frequencies of the structure and the problem becomes highly sensitive to forced vibration. Also, with lower wave periods, more Fourier terms are needed to converge to the dynamic solution. This is apparent by the fact that solutions based on $-8 \le k \le +8$, $-15 \le k \le +15$, and Abaqus are in excellent agreement but depart from the solution based on $-1 \le k \le +1$.

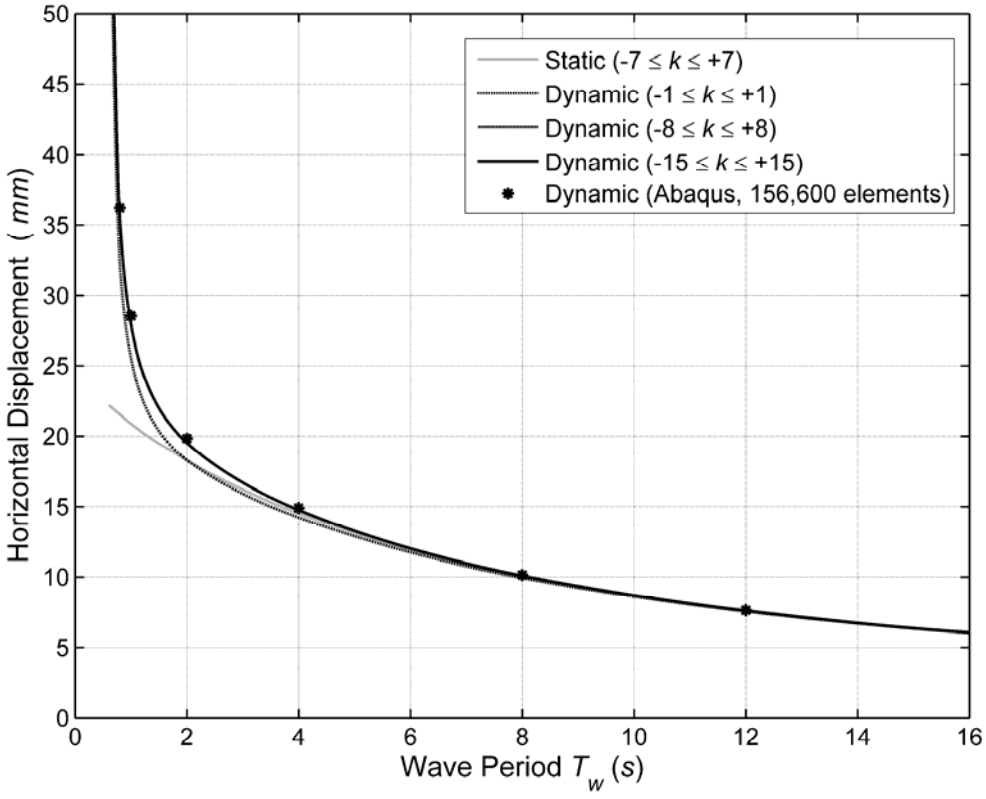

Figure 4.6 - Transverse displacement of point A

Also, the distributions of longitudinal stresses along a generator going through point A (Figure 4.7) is provided at the inside and outside fibres ($z=-h/2$ and $z=+h/2$, respectively) are plotted in Figure 4.7. Results from Abaqus are shown for comparison. Apart from a localized effect near the root of the pier, the results from current model essentially coincide with those based on Abaqus. Closer agreement in the localized region between stresses in both models was obtained by further refining the Abaqus mesh near the root area.

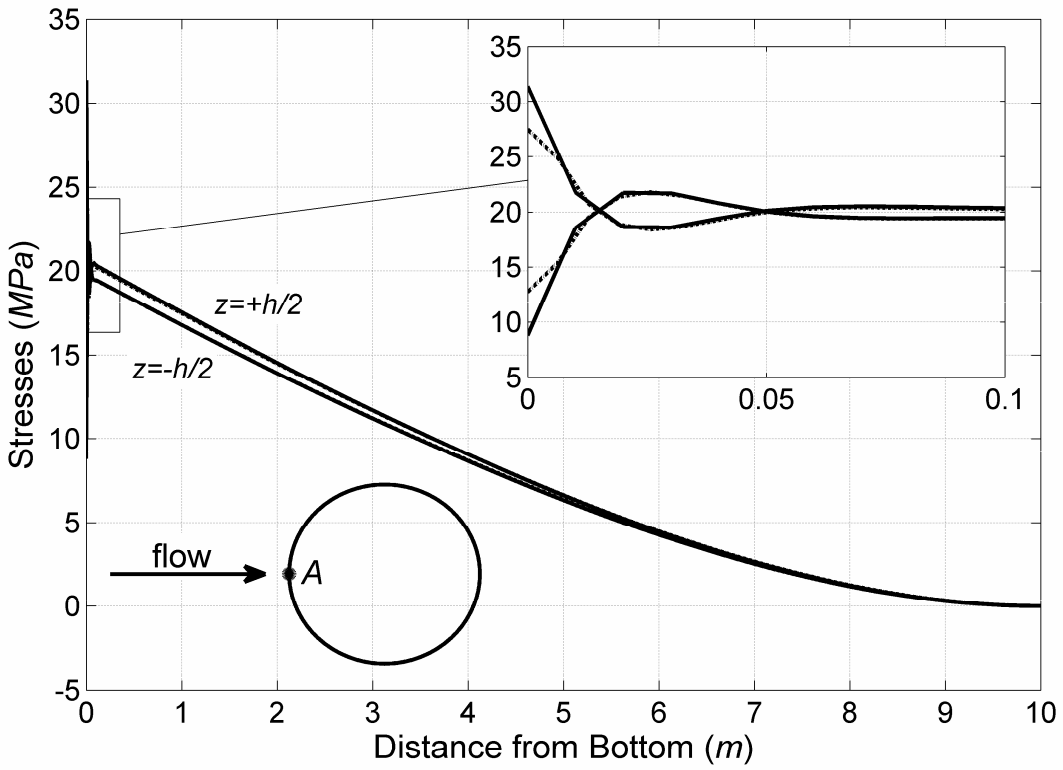

Figure 4.7 – Longitudinal stresses along a generator going through point A (Solid lines denote the results from current model and dash-dotted lines denote the results from Abaqus)

4.14.4 Example 4

A horizontal cylindrical thin shell of span $L = 6\,m$, radius $R = 0.1\,m$ and thickness $h = 0.003\,m$ is simply supported at both ends. The shell is subject to a distributed harmonic patch load acting at mid-span within a rectangular area bounded with the lines $s/R = \pm\pi/8$ and $x = 3 \pm 0.06$ (Figure 4.8a). Two types of loads act on the patch: a) A vertical traction load $q_V = 1{,}000\,e^{i\bar{\omega}t}\ KN/m^2$ and b) a longitudinal load $q_L = 1{,}000\,e^{i(\bar{\omega}t+\theta_1)}\ KN/m^2$ which is θ_1 out-of-phase relative to q_V. Such loading may be induced by rotary equipment with an eccentric mass. It is required to determine the steady state displacements under the combined

effect of the two given loads under two scenarios: $\theta_1 = \pi/4\ rad$ and $\theta_1 = \pi/2\ rad$. The exciting frequency is $\bar{\omega} = 2\pi \times 60\, rad/s$.

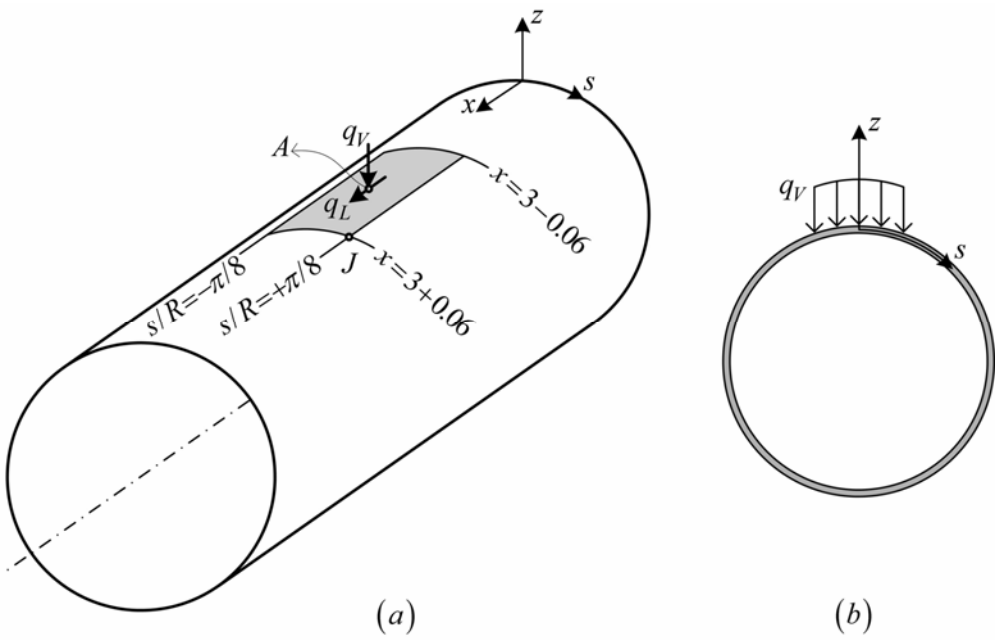

Figure 4.8 –a) Patch Loading area and the direction of the out of phase applied tractions q_L and q_V, and b) Distribution of the vertical traction q_V

The mathematical expressions of the corresponding body forces are

$$\begin{aligned} p^x(x,s,z,t) &= P_q(x,s,z)\, q_L\, e^{i(\bar{\omega}t+\theta_1)} \\ p^s(x,s,z,t) &= P_q(x,s,z)\left[q_V \sin(s/R)\right] e^{i\bar{\omega}t} \\ p^z(x,s,z,t) &= P_q(x,s,z)\left[-q_V \cos(s/R)\right] e^{i\bar{\omega}t} \end{aligned} \tag{4.39}$$

in which,

$$P_q(x,s,z) = \left[H(x-2.94) - H(x-3.06)\right]\left[1 - H(s-\pi R/8) + H(s-15\pi R/8)\right]\mathrm{Dirac}(z-h/2)$$

and H is the Heaviside unit step function. It is noted that circumferential and radial components of the applied forces result from decomposing the vertical traction force (Figure 4.8b) into the radial and tangential directions. Based on the discussion in Appendix 4.A the out-of-phase loads in axial direction can be cast in the form of Eq. 4.11a, in which

$\overline{p}^x(x,s,z) = q_L P_q(x,s,z) e^{i\theta_1}$ is complex while the other loading functions $\overline{p}^s(x,s,z) = \left[q_V \sin(s/R)\right] P_q(x,s,z)$ and $\overline{p}^z(x,s,z) = -\left[q_V \cos(s/R)\right] P_q(x,s,z)$ are real. Through numeric experimentation, it was determined that the number of terms needed to expand the loads in the circumferential direction is 15 ($-7 \le n \le +7$). Also, the number of terms needed in the longitudinal direction is 29 ($-14 \le k \le +14$). Additional terms were observed to have negligible contributions. The mid-surface displacement components for points A and J (Figure 4.8a) respectively located at the center and the corner of the patch are provided and compared to the results based on Abaqus in Table 4.4. The Abaqus shell model consisted of $96 \times 800 = 76{,}800$ S4R elements. J. Table 4.4 shows very good agreement between the results from current study and those based on Abaqus. The difference in the displacement magnitudes were within 2.4%.

Table 4.4 – Displacements at mid-span

Phase angle	Points	Model	Displacement components		
			Axial	Circumferential	Radial
$\theta_1 = \frac{\pi}{4}$	*A*	Current Study	$0.0458e^{i0.7854}$	0	4.891
		Abaqus	$0.0463e^{i0.7854}$	0	4.774
		Difference	+1.2%	-	-2.4%
	J	Current Study	$0.0489e^{i0.6500}$	$1.926e^{i3.139}$	$4.862e^{-i0.0017}$
		Abaqus	$0.0485e^{i0.6481}$	$1.901e^{i3.141}$	$4.797e^{-i0.0019}$
		Difference	-0.8%	-1.3%	-1.3%
$\theta_1 = \frac{\pi}{2}$	*A*	Current Study	$0.04580e^{i1.571}$	0	4.891
		Abaqus	$0.04633e^{i1.571}$	$0.002729e^{i3.142}$	4.774
		Difference	+1.2%	-	-2.4%
	J	Current Study	$0.0428e^{i1.351}$	$1.9300e^{i3.138}$	$4.871e^{-i0.0023}$
		Abaqus	$0.0424e^{i1.348}$	$1.896e^{i3.138}$	$4.789e^{-i0.0023}$
		Difference	-0.9%	-1.8%	-1.7%

The resulting displacements are complex since they generally are out-of-phase from the applied loads. The displacements are conveniently expressed in a polar form in the Table. The magnitude of the displacement denotes the maximum displacement attained and the exponent denotes the phase angle. The applied loads and corresponding response are plotted as a function of time in Figure 4.9 for the case $\theta_1 = \pi/4$ at point J. It can be clearly seen that the displacement components are in different phase angles.

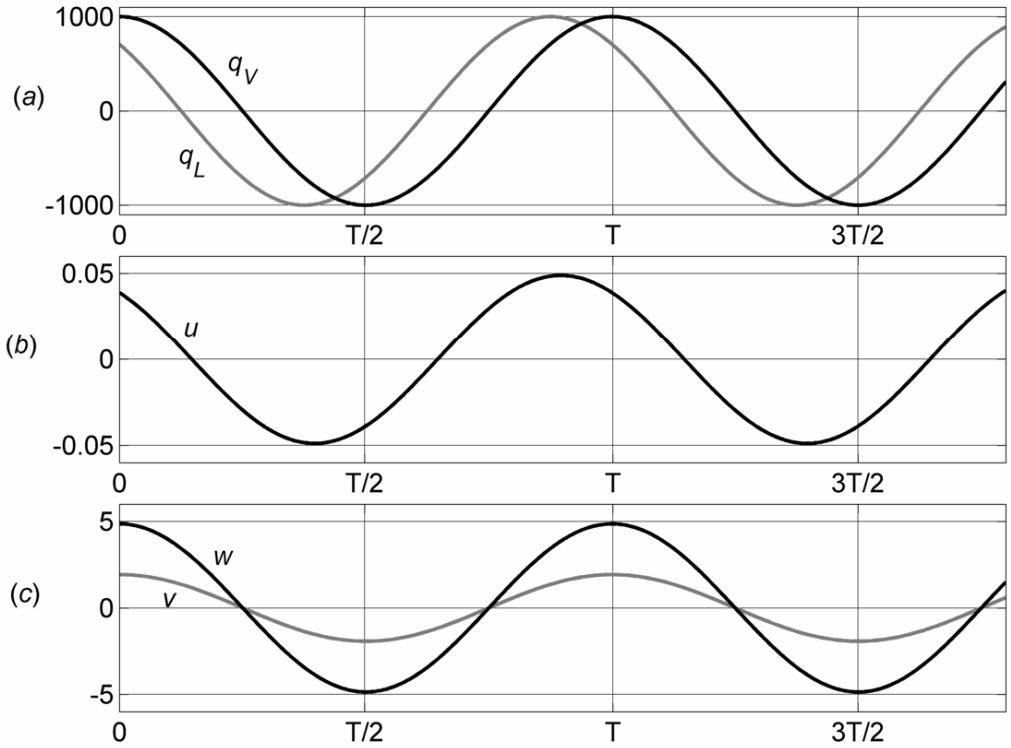

Figure 4.9 - a) Applied forces q_L and q_V (in KN) b) Axial response u at point J (in mm) c) Circumferential response v and radial response w at point J (in mm). In all cases abscissa is time in terms of period of excitation.

4.15 Summary and Conclusions

Based on the variational form of Hamilton's principle, the field equations and boundary conditions are formulated for circular cylindrical thin shells under general in-phase and out-of- phase harmonic loads. The resulting field equations are solved in a closed form for general loading and boundary conditions.

Through Fourier decomposition of the body forces in the longitudinal direction, a technique for developing the particular solution for general harmonic loading was developed.

Through four examples, the results based on the current formulation are shown to be in consistent agreement with those based on established shell models in Abaqus.

The solution developed herein is efficient for two reasons. Firstly, the contribution of each circumferential mode n is independently solved from other modes. This allows the analyst to calculate the individual contributions separately and adding them to obtain the total response. Secondly, for most practical problems, only a few transverse and longitudinal modes need to be considered in order to accurately capture the structure response.

While the formulation is geared towards computing the steady state response of cylinders under general harmonic force, it is also able to capture the natural frequencies as illustrated in Example 1.

The solution method provided in this chapter will be used in Chapter 5 to develop a super convergent finite element for analysis of circular cylindrical thin shells under general harmonic forces.

4.16 Acknowledgement

The authors would like to express their deepest gratitude to the Bahai Institute for Higher Education (BIHE) for its encouragement and support to the first author. Financial support from the Natural Science and Engineering Research Council (NSERC) to the second author is gratefully acknowledged.

4.17 References

[4.1] A.W. Leissa, Vibration of Shells. Report LC-77-186367, NASA-SP-288, 1973,

[4.2] S. Markus, The Mechanics of Vibrations of Cylindrical Shells. Stud. Appli. Mech. 17, Elsevier, Amsterdam Oxford 1988.

[4.3] M.S. Qatu, Recent Research Advances in the Dynamic Behaviour of Shells: 1989-2000, Part 1: Laminated Composite Shells. ASME, Appl. Mech. Rev.

[4.4] M.S. Qatu, Recent Research Advances in the Dynamic Behaviour of Shells: 1989-2000, Part 2: Homogeneous Shells. ASME, Appl. Mech. Rev. 2002

[4.5] Y., Xiang, Y.F. Ma, S. Kitipornchai, C.W. Lim, H. Lau, Exact Solutions for Vibration of Cylindrical Shells with Intermediate Ring Supports. Int. J. Mech. Sci. 44 2002 1907-1924.

[4.6] A.A. Jafari, M. Bagheri, Free Vibration of Non-uniformly Ring Stiffened cylindrical Shells Using Analytical, Experimental and Numerical Methods. Thin-Walled Struct. 44 (2006) 82-90.

[4.7] L. Xuebin, A New Approach for Free Vibration Analysis of Thin Circular Cylindrical Shell. J. Sound Vib. 296 (2006) 91-98.

[4.8] M. Rougui, F. Moussaoui, R. Benamar, Geometrically Non-Linear Free and Forced Vibrations of Simply Supported Circular Cylindrical Shells: A Semi-Analytical Approach. Int. J. Non-Linear Mech. 42 2007 1102-1115.

[4.9] L. Zhang, Y. Xiang, Exact Solutions for Vibration of Stepped Circular Cylindrical Shells. J. Sound Vib. 299 2007 948-964.

[4.10] L. Xuebin, Study on Free Vibration Analysis of Circular Cylindrical Shells Using Wave Propagation. J. Sound Vib. 311 2008 667-682.

[4.11] L. Gan, X. Li, Z. Zhang, Free Vibration Analysis of Ring-Stiffened Cylindrical Shells Using Wave Propagation Approach. J. Sound Vib. doi: 10.1016/j.jsv.2009.05.001.

[4.12] H. Matsunaga, Free Vibration and Stability of Functionally Graded Circular Cylindrical Shells According to a 2D Higher-Order Deformation Theory. Compos. Struct. 88 2009519-531.

[4.13] G.B. Warburton, Harmonic Response of Cylindrical Shells. J. Eng. Industry, Trans. Am. Soc. Mech. Eng. 96B (1974) 994–999

[4.14] G.B. Warburton, S.R. Soni, Resonant Response of Orthotropic Cylindrical Shells. J. Sound Vib. 53 1977 1-23.

[4.15] A.W. Leissa, Modal Response of Circular Cylindrical Shells with Structural Damping. J. Sound Vib. 77 (1981) 1-10.

[4.16] D.E. Beskos, J.B. Oates, Dynamic Analysis of Ring-Stiffened Circular Cylindrical Shells. J. Sound Vib. 75 (1981) 1-15.

[4.17] V.A. Zarutskii, Forced Vibrations of a Longitudinally Reinforced Cylindrical Shell Supporting a Local Apparent Additional Mass. Institute of Mechanics, Academy of Science of the Ukranian SSR, Kiev. Plenum Publ. Corp., Translated from Prikladnaya Mekhanika. 1982 50-56.

[4.18] K. Forsberg, Influence of Boundary Conditions on the Modal Characteristics of Thin Cylindrical Shells. AIAA J. 2 (1963) 2150-2156.

[4.19] C.Y. Glandier, Y.H. Berthelot, J. Jarzynski, Wave-Vector Analysis of the Forced Vibrations of Cylindrical Shells of Finite Length. J. Acoust. Soc. Am.; 92(1992), Pt. 1.

[4.20] Y.M. Huang, C.R. Fuller, The Effect of Dynamic Absorbers on the Forced Vibration of a Cylindrical shell and Its Coupled Interior Sound Field. J. Sound Vib. 200(1997) 401-418.

[4.21] M. Amabili, A Comparison of Shell Theories for Large-Amplitude Vibrations of Circular Cylindrical Shells: Lagrangian Approach. J. Sound Vib. 264 (2003) 1091-1125.

[4.22] F. Pellicano, K.V. Avramov, Linear and Nonlinear Dynamic of a Circular Cylindrical Shell Connected to a Rigid Disk. Commun Nonlinear Sci. Numer. Simul. 12 2007 496-518.

[4.23] F. Pellicano, Vibrations of circular cylindrical shells: Theory and experiments. J. Sound Vib. 303 (2007) 154-170.

[4.24] W.H. Duan, C.G. Koh, Axisymmetric Transverse Vibrations of Circular Cylindrical Shells with Variable Thickness. J. Sound Vib. 317 (2008) 1035-1041.

[4.25] W. Flugge, Tensor Analysis and Continuum Mechanics, Springer-Verlag, New York Heidelberg Berlin, 1972.

[4.26] W. Flugge, Stresses in Shells. Springer-Verlag, New York Heidelberg Berlin, 1973.

[4.27] R. Salahifar, Analysis of Thin Shells under Harmonic Loads. Ph.D. Thesis, Department of Civil Engineering, University of Ottawa, Ottawa, ON, Canada, 2010.

[4.28] S. Timoshenko, Theory of Plates and Shells. McGraw-Hill Book Company, New York, 1959.

[4.29] V.V. Novozhilov, Thin Shell Theory. P. Noordhoff Ltd. –Groningen-The Netherlands, 1964.

[4.30] F. I. Niordson, Shell Theory. North-Holland Series In Applied Mathematics and Mechanics, 1985.

[4.31] K. Weicker, Finite Element Formulation for Analysis of Pipes based Thin Shell Theory. M.A.Sc. Thesis, Department of Civil Engineering, University of Ottawa, Ottawa, ON, Canada, 2008.

[4.32] M. Rahman, Nonlinear Hydrodynamic Loading on Offshore Structures. Theo. Comput. Fluid Dyn. 10 1998 323-347.

[4.33] J.F. Anthoni, www.seafriends.org.nz/oceano/waves.htm , 2000 (Accessed 20 August 2009)

4.18 List of Symbols

$A_n(x), B_n(x), C_n(x)$	Contributions of circumferential mode n to mid-surface displacements u, v, w, respectively
$A_{nh}(x), B_{nh}(x), C_{nh}(x)$	Homogeneous part of functions $A_n(x)$, $B_n(x)$ and $C_n(x)$, respectively
$A_{np}(x), B_{np}(x), C_{np}(x)$	Particular part of functions $A_n(x)$, $B_n(x)$ and $C_n(x)$, respectively
$A_{nkp}(x), B_{nkp}(x), C_{nkp}(x)$	kth term of the functions $A_{np}(x)$, $B_{np}(x)$ and $C_{np}(x)$, respectively, in their Fourier series form in longitudinal direction
A_{nj}, B_{nj}, C_{nj}	j th integration constant in the assumed displacement field functions $A_n(x)$, $B_n(x)$ and $C_n(x)$, respectively, corresponding to mode n
$\bar{A}_{nj}$, $\bar{B}_{nj}$, $\bar{C}_{nj}$	Constants relating constants A_{nj}, B_{nj} and C_{nj}
D^d	The dth derivative with respect to the axial coordinate x
E	Modulus of elasticity
E^{ijlm}	Generalized constitutive elasticity tensor

$E^{\alpha\beta\lambda\delta}$	In-plane components of the generalized constitutive elasticity tensor E^{ijlm}
F^i	Contravariant component of applied forces along x^i coordinate
${}^i_j G_n$	Coefficient of jth term in ith field equation of mode number n
${}^i_j G$	Coefficient of jth term in ith field equation independent of mode number n
${}^i_j H_n$	Coefficient of jth term in ith boundary equation of mode number n
${}^i_j H_n$	Coefficient of jth term in ith boundary equation independent of mode number n
L	Length of the cylinder
R	Radius of the cylinder
R_{nk}, S_{nk}, T_{nk}	kth coefficient of functions $A_{np}(x)$, $B_{np}(x)$ and $C_{np}(x)$, respectively, in their Fourier series form in longitudinal direction for circumferential mode n
$\mathrm{Re}(...)$	Real part of argument

T^*	Kinetic energy
U_i	Covariant component of displacement of any point within the shell along x^i coordinate
U^i	Contravariant component of displacement of any point within the shell along x^i coordinate
$\tilde{U},\tilde{V},\tilde{W}$	Physical components of the longitudinal, circumferential and radial displacement of a point within the shell, respectively
V^*	Internal Strain energy
V	Volume
W^*	External work
X^i	Cartesian coordinate
b_α^δ	Curvature tensor
f^{xu}, f^{xw} f^{sv}, f^{sw} f^{zw}	Contributions to the forces induced by the applied body forces (after integration across the thickness of the shell) as functions of coordinates x, s and time t
$f_n^{xu}(x), f_n^{xw}(x)$ $f_n^{sv}(x), f_n^{sw}(x)$ $f_n^{zw}(x)$	Respective force contributions of f^{xu}, f^{xw}, f^{sv}, f^{sw} and f^{zw} based on mode n as functions of coordinate x

f_{nk}^{xu}, f_{nk}^{sv} f_{nk}^{xw}, f_{nk}^{sw} f_{nk}^{zw}	kth term of the force contributions $f_n^{xu}(x)$, $f_n^{xw}(x)$, $f_n^{sv}(x)$, $f_n^{sw}(x)$ and $f_n^{zw}(x)$, respectively, in their Fourier series form in longitudinal direction
g_{ij}	Covariant components of the metric tensor
g^{ij}	Contravariant components of the metric tensor
h	Thickness of the cylinder
$\cdots_{,i}$	Partial derivative with respect to x^i
m_{nj}	j th root of the characteristic equation for mode n
p^x, p^s, p^z	Physical components of applied body forces F^1, F^2 and F^3, respectively, as functions of coordinates x, s, z and time t
$\bar{p}^x$, $\bar{p}^s$, $\bar{p}^z$	Axial, circumferential and radial components of applied body forces, respectively, as functions of coordinates x, s, z
u_i	Covariant components of the mid-surface displacement along coordinate x^i

u, v, w	Components of the displacement of a point on the middle surface along coordinates x, s and z, respectively
$\bar{u}$, $\bar{v}$, $\bar{w}$	Axial, circumferential and radial components of the displacement of a point on the middle surface as a function of coordinates x and s
x^i	Curvilinear Coordinate
η_{ij}	Covariant components of the strain tensor for an infinitesimal element within the shell volume η_{ij}
$\eta_{\alpha\beta}$	In-plane components of the strain tensor
Π	Mechanical energy of the system
ν	Poisson's ratio
ρ	Density of the material
σ^{ij}	Contravariant components of the stress tensor
μ_α^δ	Shifter tensor
Φ	Non-dimensional coefficient defined as

$$\Phi\left(h/R\right)=\ln\left[\left(2+h/R\right)/\left(2-h/R\right)\right]\Big/\left(h/R\right)$$

Appendix 4.A. Expressions for Out-of-Phase Forces

In practice, it is common to have several harmonic forces, with the same angular frequency $\bar{\omega}$ and different phase angles. The corresponding body force expressions are

$$p^x(x,s,z,t)=\sum_{l=1}^{Q_x} p_l^x(x,s,z)e^{i(\bar{\omega}t+\theta_l)}$$

$$p^s(x,s,z,t)=\sum_{q=1}^{Q_s} p_q^s(x,s,z)e^{i(\bar{\omega}t+\varphi_q)} \qquad \text{(4.A.1a-c)}$$

$$p^z(x,s,z,t)=\sum_{r=1}^{Q_z} p_r^z(x,s,z)e^{i(\bar{\omega}t+\psi_r)}$$

in which θ_l, φ_q and ψ_r are the phase angles in longitudinal, circumferential and radial direction, respectively. Equation 4.A.1a-c can be cast in the form of Eq. 4.11 as follows.

$$p^x(x,s,z,t)=\sum_{l=1}^{Q_x} p_l^x(x,s,z)e^{i(\bar{\omega}t+\theta_l)}=\left(\sum_{l=1}^{Q_x} p_l^x(x,s,z)e^{i\theta_l}\right)e^{i\bar{\omega}t}$$

$$p_t^s(x,s,z,t)=\sum_{q=1}^{Q_s} p_q^s(x,s,z)e^{i(\bar{\omega}t+\varphi_q)}=\left(\sum_{q=1}^{Q_x} p_q^s(x,s,z)e^{i\varphi_q}\right)e^{i\bar{\omega}t} \qquad \text{(4.A.2a-c)}$$

$$p_t^z(x,s,z,t)=\sum_{r=1}^{Q_z} p_r^z(x,s,z)e^{i(\bar{\omega}t+\psi_r)}=\left(\sum_{r=1}^{Q_x} p_r^z(x,s,z)e^{i\psi_r}\right)e^{i\bar{\omega}t}$$

By terming the bracketed term in the right hand side of Eq. 4.A.2a-c as $\bar{p}^x(x,s,z)$, $\bar{p}^s(x,s,z)$ and $\bar{p}^z(x,s,z)$, respectively, one recovers a form identical to Eq. 4.11a-c. The only difference is that $\bar{p}^x(x,s,z)$, $\bar{p}^s(x,s,z)$ and $\bar{p}^z(x,s,z)$ are now complex functions. It is noted that, in general, all out-of-phase forces reduce into two orthogonal components.

Mathematically, these are represented by the real and imaginary components of the body forces and the resulting displacement fields.

Appendix 4.B. Coefficients of Boundary and Field Terms

The coefficients of the boundary and field terms in Eq. 4.9 are defined below. We recall that $i=\sqrt{-1}$, $\Phi\left(h/R\right)=\ln\left[\left(2+h/R\right)/\left(2-h/R\right)\right]\Big/\left(h/R\right)$ and n is the circumferential mode number.

$$
{}^{1}_{1}H=-1 \quad , \quad {}^{1}_{2}H_n=-\frac{\nu}{R}in \quad , \quad {}^{1}_{3}H=-\frac{\nu}{R} \quad , \quad {}^{1}_{4}H=\frac{h^2}{12R}
$$

$$
{}^{2}_{1}H_n=-\frac{1-\nu}{2}\frac{1}{R}in \quad , \quad {}^{2}_{2}H=-\frac{1-\nu}{2}\left(1+\frac{h^2}{4R^2}\right) \quad , \quad {}^{2}_{3}H_n=\frac{1-\nu}{2}\frac{h^2}{4R^2}in
$$

$$
{}^{3}_{1}H_n=-\frac{1}{R}\left(\Phi-1\right)\frac{1-\nu}{2}n^2-\rho\bar{\omega}^2\frac{1-\nu^2}{E}\frac{h^2}{12R} \quad , \quad {}^{3}_{2}H=-\frac{h^2}{12R}
$$

$$
{}^{3}_{3}H_n=-\frac{h^2}{12R^2}\left(\frac{3-\nu}{2}\right)in
$$

$$
{}^{3}_{4}H_n=-\left\{\frac{h^2}{12R^2}\frac{3-\nu}{2}+\left(\Phi-1\right)\frac{1-\nu}{2}\right\}n^2+\rho\bar{\omega}^2\frac{1-\nu^2}{E}\frac{h^2}{12}
$$

$$
{}^{3}_{5}H=\frac{h^2}{12} \quad , \quad {}^{3}_{6}H=\frac{1-\nu^2}{Eh}
$$

$$
{}^{4}_{1}H=\frac{h^2}{12R} \quad , \quad {}^{4}_{2}H_n=\frac{h^2}{12R^2}\nu in \quad , \quad {}^{4}_{3}H_n=\frac{h^2}{12R^2}\nu n^2 \quad , \quad {}^{4}_{4}H=-\frac{h^2}{12} \qquad \text{(4.B.1a-q)}
$$

$$
{}^{1}_{1}G_n=-\frac{1}{R^2}\Phi\frac{1-\nu}{2}n^2+\frac{1-\nu^2}{E}\rho\bar{\omega}^2 \quad , \quad {}^{1}_{2}G=1 \quad , \quad {}^{1}_{3}G_n=\frac{1}{R}\frac{1+\nu}{2}in
$$

$$
{}^{1}_{4}G_n=\frac{\nu}{R}-\frac{1}{R}\left(\Phi-1\right)\frac{1-\nu}{2}n^2-\frac{1-\nu^2}{E}\rho\bar{\omega}^2\frac{h^2}{12R} \quad , \quad {}^{1}_{5}G=-\frac{h^2}{12R}
$$

$$
{}^{1}_{6}G=\frac{1-\nu^2}{Eh}
$$

$$
{}^{2}_{1}G_n = \frac{1}{R}\frac{1+\nu}{2} in \quad , \quad {}^{2}_{2}G_n = -\frac{1}{R^2} n^2 + \frac{1-\nu^2}{E}\rho\bar{\omega}^2\left(1+\frac{h^2}{12R^2}\right)
$$

$$
{}^{2}_{3}G = \left(1+\frac{h^2}{4R^2}\right)\frac{1-\nu}{2} \quad , \quad {}^{2}_{4}G_n = \frac{1}{R^2} in - \frac{1-\nu^2}{E}\rho\bar{\omega}^2\frac{h^2}{6R^2} in
$$

$$
{}^{2}_{5}G_n = -\frac{h^2}{12R^2}\frac{3-\nu}{2} in \quad , \quad {}^{2}_{6}G = \frac{1-\nu^2}{Eh}
$$

$$
{}^{3}_{1}G_n = -\frac{\nu}{R} + \frac{1}{R}(\Phi-1)\frac{1-\nu}{2} n^2 + \frac{1-\nu^2}{E}\rho\bar{\omega}^2\frac{h^2}{12R} \quad , \quad {}^{3}_{2}G = \frac{h^2}{12R}
$$

$$
{}^{3}_{3}G_n = -\frac{1}{R^2} in + \frac{1-\nu^2}{E}\rho\bar{\omega}^2\frac{h^2}{6R^2} in \quad , \quad {}^{3}_{4}G_n = \frac{h^2}{12R^2}\frac{3-\nu}{2} in
$$

$$
{}^{3}_{5}G_n = -\frac{1}{R^2}\Phi + \frac{2}{R^2}(\Phi-1) n^2 - \frac{1}{R^2}(\Phi-1) n^4 + \frac{1-\nu^2}{E}\rho\bar{\omega}^2 + \frac{1-\nu^2}{E}\rho\bar{\omega}^2\frac{h^2}{12R^2} n^2 \quad \text{(4.B.2a-q)}
$$

$$
{}^{3}_{6}G_n = \left[\frac{h^2}{12R^2}\frac{3+\nu}{2} + (\Phi-1)\frac{1-\nu}{2}\right] n^2 - \frac{1-\nu^2}{E}\rho\bar{\omega}^2\frac{h^2}{12}
$$

$$
{}^{3}_{7}G = -\frac{h^2}{12} \quad , \quad {}^{3}_{8}G = -\frac{1-\nu^2}{Eh} \quad , \quad {}^{3}_{9}G_n = -\frac{1-\nu^2}{EhR} in \quad , \quad {}^{3}_{10}G = \frac{1-\nu^2}{Eh}
$$

Since the matrix of coefficients of field equations is symmetric, one has

$$
{}^{2}_{1}G_n = {}^{1}_{3}G_n \quad , \quad {}^{3}_{1}G_n = {}^{1}_{4}G_n \quad , \quad {}^{3}_{2}G = {}^{1}_{5}G \quad , \quad {}^{3}_{3}G_n = {}^{2}_{4}G_n \quad , \quad {}^{3}_{4}G_n = {}^{2}_{5}G_n \qquad \text{(4.B.3)}
$$

Appendix 4.C. Constants in Characteristic Equations

The coefficients in characteristic equation of the system discussed in sections 4.12.5.1 and 4.12.5.2 are defined below.

For $n = 0$

$$
\begin{aligned}
b_0 &= \left({}^{1}_{1}G_n\right)\left({}^{3}_{5}G_n\right) \\
c_0 &= -\left({}^{1}_{4}G_n\right)^2 + \left({}^{1}_{2}G\right)\left({}^{3}_{5}G_n\right) + \left({}^{1}_{1}G_n\right)\left({}^{3}_{6}G_n\right) \\
d_0 &= \left({}^{1}_{2}G\right)\left({}^{3}_{6}G_n\right) - 2\left({}^{1}_{5}G\right)\left({}^{1}_{4}G_n\right) + \left({}^{3}_{7}G\right)\left({}^{1}_{1}G_n\right) \\
e_0 &= \left({}^{1}_{2}G\right)\left({}^{3}_{7}G\right) - \left({}^{1}_{5}G\right)^2
\end{aligned}
\qquad \text{(4.C.1a-f)}
$$

For $n \neq 0$

$$
\begin{aligned}
a_n &= \left({}^{1}_{1}G_n\right)\left({}^{2}_{2}G_n\right)\left({}^{3}_{5}G_n\right) - \left({}^{1}_{1}G_n\right)\left({}^{2}_{4}G_n\right)^2 \\
b_n &= \Big[-\left({}^{3}_{5}G_n\right)\left({}^{1}_{3}G_n\right)^2 + 2\left({}^{1}_{3}G_n\right)\left({}^{1}_{4}G_n\right)\left({}^{2}_{4}G_n\right) - \left({}^{2}_{2}G_n\right)\left({}^{1}_{4}G_n\right)^2 - \left({}^{1}_{2}G\right)\left({}^{2}_{4}G_n\right)^2 \\
&\quad - 2\left({}^{1}_{1}G_n\right)\left({}^{2}_{5}G_n\right)\left({}^{2}_{4}G_n\right) + \left({}^{1}_{2}G\right)\left({}^{2}_{2}G_n\right)\left({}^{3}_{5}G_n\right) + \left({}^{2}_{3}G\right)\left({}^{1}_{1}G_n\right)\left({}^{3}_{5}G_n\right) \\
&\quad + \left({}^{1}_{1}G_n\right)\left({}^{2}_{2}G_n\right)\left({}^{3}_{6}G_n\right) \Big] \\
c_n &= \Big[-\left({}^{3}_{6}G_n\right)\left({}^{1}_{3}G_n\right)^2 + 2\left({}^{1}_{3}G_n\right)\left({}^{1}_{4}G_n\right)\left({}^{2}_{5}G_n\right) + 2\left({}^{1}_{5}G\right)\left({}^{2}_{4}G_n\right)\left({}^{1}_{3}G_n\right) \\
&\quad - \left({}^{2}_{3}G\right)\left({}^{1}_{4}G_n\right)^2 - 2\left({}^{1}_{5}G\right)\left({}^{2}_{2}G_n\right)\left({}^{1}_{4}G_n\right) - \left({}^{1}_{1}G_n\right)\left({}^{2}_{5}G_n\right)^2 \\
&\quad - 2\left({}^{1}_{2}G\right)\left({}^{2}_{4}G_n\right)\left({}^{2}_{5}G_n\right) + \left({}^{1}_{2}G\right)\left({}^{2}_{3}G\right)\left({}^{3}_{5}G_n\right) \\
&\quad + \left({}^{1}_{2}G\right)\left({}^{2}_{2}G_n\right)\left({}^{3}_{6}G_n\right) + \left({}^{2}_{3}G\right)\left({}^{1}_{1}G_n\right)\left({}^{3}_{6}G_n\right) + \left({}^{3}_{7}G\right)\left({}^{1}_{1}G_n\right)\left({}^{2}_{2}G_n\right) \Big] \\
d_n &= \Big[-\left({}^{2}_{2}G_n\right)\left({}^{1}_{5}G\right)^2 + 2\left({}^{1}_{5}G\right)\left({}^{1}_{3}G_n\right)\left({}^{2}_{5}G_n\right) - 2\left({}^{2}_{3}G\right)\left({}^{1}_{4}G_n\right)\left({}^{1}_{5}G\right) - \left({}^{3}_{7}G\right)\left({}^{1}_{3}G_n\right)^2 \\
&\quad - \left({}^{1}_{2}G\right)\left({}^{2}_{5}G_n\right)^2 + \left({}^{1}_{2}G\right)\left({}^{2}_{3}G\right)\left({}^{3}_{6}G_n\right) + \left({}^{1}_{2}G\right)\left({}^{3}_{7}G\right)\left({}^{2}_{2}G_n\right) + \left({}^{2}_{3}G\right)\left({}^{3}_{7}G\right)\left({}^{1}_{1}G_n\right) \Big] \\
e_n &= -\left({}^{1}_{5}G\right)^2\left({}^{2}_{3}G\right) + \left({}^{1}_{2}G\right)\left({}^{2}_{3}G\right)\left({}^{3}_{7}G\right)
\end{aligned}
\qquad \text{(4.C.2a-e)}
$$

Chapter 5

Finite Element for Pipes under Harmonic Forces

5.1 Abstract

A super-convergent finite element is developed for the steady state analysis of pipes under general harmonic forces based on shell theory. Simplifying assumptions in previous formulations are avoided and the resulting model is capable of capturing warping, ovalization, and radial extensibility. A series of exact shape functions are then developed based on the exact solution of the field equations and used to formulate a pipe finite element capable of capturing shell behaviour with very few degrees of freedom. Through examples, the element is shown to efficiently model pipe problems subject to in-phase and out-of phase harmonic loading and support excitation.

5.2 Scope and Literature Review

Circular cylindrical thin shells (CCTSs) are commonly used as structural members and as mechanical components. Also, they are key components of piping and conveyance systems. In these applications, CCTSs are commonly subjected to harmonic excitations induced by pumps, turbines, generators, etc. Under these loads, the steady-state response of the structure needs to be determined for fatigue design considerations since it represents the sustained

effect. In contrast, the transient response of the structure is of little importance in fatigue design as it tends to dampen out quickly.

In complex systems (e.g., long pipeline systems), shell based analytical solutions become impractical. Also, in such systems, finite element models based on conventional shell elements aimed at capturing localized shell effects necessitate a large number of degrees of freedom and are impractical as design tools. A promising class of finite element developments expresses the unknown displacement fields in terms of Fourier series with respect to the circumferential coordinate. In the longitudinal direction, various researchers have adopted different approximate shape functions such as Hermitian polynomials (e.g. [5.1] and [5.2]), Lagrangian interpolation functions (e.g. [5.3] and [5.4]), Harmonic functions (e.g. [5.2]and [5.5]), or a combination thereof. In this class of finite elements, the mesh is discretized only along the longitudinal direction of the cylinder and no discretization is needed in the circumferential direction, resulting in significant computational efficiency. The present formulation lies in this category. It departs from previous finite element formulations in the following respects:

1 It adopts a family of interpolation functions for the displacement fields based on the closed form solution of the homogeneous form of the equilibrium equations.

2 While most of the solutions developed focus on either the static response (e.g. [5.1], [5.2] and [5.3]) or on the free vibration (e.g. [5.6]and [5.7]), the present study extends the developments to the steady state response of CCTSs under harmonic loads. The solution directly captures the steady state response without the need to extract the modal shapes and natural frequencies.

3 While most studies (e.g. [5.3], [5.4], [5.8] and [5.9]) typically use only a limited number of or certain harmonic terms, the present formulation is applicable to any number of terms. In practicality, the number of terms in a series will be truncated when the accuracy sought is reached.

A comprehensive review of finite element formulations for pressure vessels and piping is provided in Mackerle [5.10]-[5.13]. The present formulation is aimed at developing a pipe element based on shell formulation. In this class of elements, the displacement fields are harmonic in the circumferential direction in order to enforce the continuity of displacements around the circumference. Hence, the following review focuses on shell based pipe elements, either curved or straight, with this particular feature. Various studies have used different interpolation schemes in the longitudinal directions and number of harmonic modes as detailed in the following.

Based on the principle of virtual work, Ohtsubo and Watanabe [5.1] developed a ring element for small strains for torus elements. Displacement components are interpolated by Hermitian polynomials along the elbow. Their model captures both ovalization and warping effects. Takeda et al. [5.2] modified the work of Ohtsubo and Watanabe [5.1] by including the transverse shear effects in their formulation and adopting 2D Lagrangian bilinear functions to interpolate the circumferential, radial displacements, and rotations. The longitudinal displacement is interpolated using Fourier series in the circumferential direction and linear functions in the longitudinal direction.

Bathe and Almeida [5.3] developed a four node elbow finite element for in-plane flexure analysis. Based on Lagrangian cubic interpolation of the displacement fields, their model

captures circumferential shear deformation and ovalization effects and neglects warping effects. They extended their model to investigate interaction effects between elbow elements and straight pipe segments [5.17]. Also, they added geometric non-linear effects to the formulation [5.18].

Militello and Huespe [5.4] extended the model by Bathe and Almeida [5.3] to capture warping deformations by adopting a Lagrangian cubic interpolation for the longitudinal displacement. The tangential and radial displacements were interpolated using harmonic functions. Abo-Elkhier [5.19] generalized the model by Bathe and Almeida [5.3] by adopting more complete displacement-strain relations into the formulation. In a ring formulation, Melo and Castro [5.20] used simple linear interpolation for displacements which captures both in-plane and out-of-plane flexure of curved pipes.

Yan et al. [5.21] developed an element for elasto-plastic limit load of pipe elbows by relaxing the pipe inextensibility assumption in the radial direction adopted in the model by Militello and Huespe [5.4]. They used cubic Lagrangian interpolation for the longitudinal displacement and Hermitian polynomials for the tangential and radial displacements.

Sivadas and Ganesan [5.22] developed a finite element method for the vibration of thin orthotropic cantilever circular cylindrical shell with variable thickness in axial direction. In their five-node element, shear deformation effects are included, fourth order Lagrangian polynomials are used to interpolate displacement components along the pipe.

Stanley and Ganesan [5.23] studied the response of cantilever CCTS with thickness discontinuities subject to harmonic axisymmetric loads including uniform internal pressure and circular ring load acting at cantilever tip. The longitudinal and circumferential

displacements were linearly interpolated while the radial displacement was interpolated using cubic Hermitian functions.

Xi et al. [5.24] developed a semi-analytical model for the vibration of composite shells of revolution based on the Reissner-Mindlin shell theory. The model is based on a two node straight conical frustum element capable of modelling shells of revolutions of general geometries.

Pinto Correia et al [5.25] developed a frustra conica finite element for the analysis of laminated axisymmetric shells based on a higher order shell theory. The radial displacements were interpolated using Hermitian polynomials while the longitudinal and circumferential displacements were interpolated using linear Lagrangian interpolation.

Karamanos [5.26] formulated an element to model buckling instability of pipes. Subsequent extension of the model involved adding plasticity and internal pressure effects (Karamanos et al. [5.27]).

Santos et al [5.28] developed a finite element model based on an axi-symmetric 3D formulation to study the bending, free vibration and buckling behaviour of shells of revolution made of laminated orthotropic elastic material. The displacement fields were linearly interpolated across the thickness and in the form of Lagrange polynomials longitudinally.

5.3 Geometry and Loading

A circular cylindrical thin shell with mid-surface radius R, length L and constant thickness h is subjected to body forces p^x, p^s and p^z along axial ($0 \le x \le L$), circumferential

($0 \le s \le 2\pi R$) and radial ($-h/2 \le z \le h/2$) axes, respectively. Under the given forces, it is assumed to undergo displacements u, v and w along the x, s and z coordinates, respectively. The sign convention adopted for the coordinates is illustrated in Figure 5.1

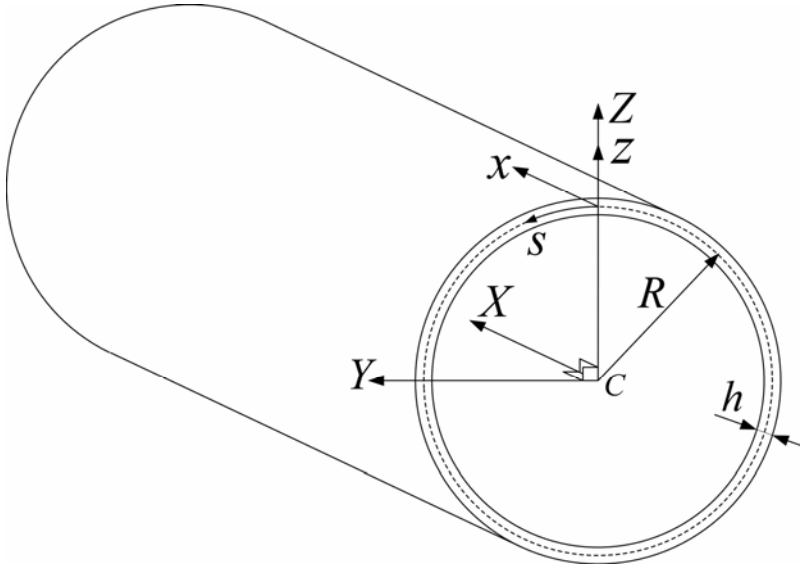

Figure 5.1 – Cylinder geometry and coordinate definition

5.4 Assumptions

Given the frequent to permanent nature of harmonic loads in the aforementioned applications, CCTSs are normally designed to respond to harmonic effects within the linearly elastic range of their material. Thus, the present study focuses on the elastic response of CCTSs. Pipe material is assumed to be linearly elastic. The Love-Kirchoff kinematic assumption for thin shells is adopted.

Displacements and strains are assumed small. Stresses normal to the shell mid-surface and transverse shear stress are neglected. The formulation is general in that it captures all membrane and bending stresses, cross-sectional distortions (such as ovalization), and warping effects under general loads and boundary conditions.

5.5 Variational Expression

Based on the above assumptions, using the variational form of Hamilton's principle, and performing all integrations across the thickness of the shell, it can be shown [5.29] that the stationarity condition of the system is

$$\delta\Pi=\int_{t_1}^{t_2}\Bigg\{\Bigg[\int_s\Bigg\{-\frac{Eh}{1-\nu^2}\left(u_{,1}+\nu v_{,2}+\frac{\nu}{R}w-\frac{h^2}{12R}w_{,11}\right)\delta u$$
$$-\frac{Eh}{1-\nu^2}\left\{\frac{1-\nu}{2}\left[u_{,2}+\left(1+\frac{h^2}{4R^2}\right)v_{,1}-\frac{h^2}{4R}w_{,12}\right]\right\}\delta v$$
$$+\left\langle\frac{Eh}{1-\nu^2}\left\{-\frac{h^2}{12R}u_{,11}+R(\Phi-1)\frac{1-\nu}{2}u_{,22}-\frac{h^2}{12R}\left(\frac{3-\nu}{2}\right)v_{,12}+\frac{h^2}{12}w_{,111}\right.\right.$$
$$\left.\left.+\left[\frac{h^2}{12}\left(\frac{3-\nu}{2}\right)+R^2(\Phi-1)\frac{1-\nu}{2}\right]w_{,122}\right\}-\rho h\left(-\frac{h^2}{12R}\ddot{u}+\frac{h^2}{12}\ddot{w}_{,1}\right)+f^{xw}\right\rangle\delta w$$
$$-\frac{Eh}{1-\nu^2}\left(-\frac{h^2}{12R}u_{,1}-\frac{h^2}{12R}\nu v_{,2}+\frac{h^2}{12}w_{,11}+\frac{h^2}{12}\nu w_{,22}\right)\delta w_{,1}\Bigg\}\Bigg]_0^x ds$$
$$+\int_A\Bigg\{\Bigg\langle\frac{Eh}{1-\nu^2}\Bigg\{u_{,11}+\Phi\frac{1-\nu}{2}u_{,22}+\frac{1+\nu}{2}v_{,12}+\frac{\nu}{R}w_{,1}$$
$$\left.-\frac{h^2}{12R}w_{,111}+R(\Phi-1)\frac{1-\nu}{2}w_{,122}\right\}-\rho h\left(\ddot{u}-\frac{h^2}{12R}\ddot{w}_{,1}\right)+f^{xu}\Bigg\rangle\delta u$$
$$+\left\langle\frac{Eh}{1-\nu^2}\left[\frac{1+\nu}{2}u_{,12}+\left(1+\frac{h^2}{4R^2}\right)\frac{1-\nu}{2}v_{,11}+v_{,22}+\frac{1}{R}w_{,2}-\frac{h^2}{12R}\left(\frac{3-\nu}{2}\right)w_{,112}\right]\right.$$
$$\left.-\rho h\left[\ddot{v}\left(1+\frac{h^2}{12R^2}\right)-2\frac{h^2}{12R}\ddot{w}_{,2}\right]+f^{sv}\right\rangle\delta v$$
$$-\Bigg\langle\frac{Eh}{1-\nu^2}\Bigg\{\frac{\nu}{R}u_{,1}+\frac{1}{R}v_{,2}+\frac{1}{R^2}\Phi w+2(\Phi-1)w_{,22}-\frac{h^2}{12R}u_{,111}+R(\Phi-1)\frac{1-\nu}{2}u_{,122}$$
$$-\frac{h^2}{12R}\left(\frac{3-\nu}{2}\right)v_{,112}+\frac{h^2}{12}w_{,1111}+\left[\frac{h^2}{12}\left(\frac{3+\nu}{2}\right)+R^2(\Phi-1)\frac{1-\nu}{2}\right]w_{,1122}$$
$$+R^2(\Phi-1)w_{,2222}\Bigg\}+\rho h\left[\ddot{w}-\frac{h^2}{12}\left(\ddot{w}_{,11}+\ddot{w}_{,22}\right)+\frac{h^2}{12R}\left(\ddot{u}_{,1}+2\ddot{v}_{,2}\right)\right]$$
$$\left.-\left(-f_{,1}^{xw}-f_{,2}^{sw}+f^{zw}\right)\Bigg\rangle\delta w\Bigg\}dsdx\Bigg\}dt=0 \qquad (5.1)$$

in which the parameter $\Phi(h/R)=\ln\left[(2+h/R)/(2-h/R)\right]/(h/R)$ was used, and the following loading terms are defined.

$$f^{xu} = \int_{-\frac{h}{2}}^{+\frac{h}{2}} p^x \left(1+\frac{z}{R}\right) dz \qquad f^{xw} = -\int_{-\frac{h}{2}}^{+\frac{h}{2}} p^x \, z \left(1+\frac{z}{R}\right) dz$$

$$f^{sv} = \int_{-\frac{h}{2}}^{+\frac{h}{2}} p^s \left(1+\frac{z}{R}\right)^2 dz \qquad f^{sw} = -\int_{-\frac{h}{2}}^{+\frac{h}{2}} p^s \, z \left(1+\frac{z}{R}\right) dz \qquad \text{(5.2a-e)}$$

$$f^{zw} = \int_{-\frac{h}{2}}^{+\frac{h}{2}} p^z \left(1+\frac{z}{R}\right) dz$$

In Eq. 5.1, the sequence $\left\| \left[\left[\left\langle \left\{ \left[(...) \right] \right\} \right\rangle \right] \right] \right\|$ of nested brackets was adopted. It is of interest to note that by performing a Taylor expansion of the term $\Phi\left(h/R\right)$ $(=1+\frac{1}{12}\left(h/R\right)^2+\frac{1}{80}\left(h/R\right)^4+\cdots)$ and retaining only the first two terms, and omitting the dynamic terms, the field equations in Eq. 5.1 revert to Flugge's theory [5.30]. Also, by adopting the approximation $1+z/R\approx 1$ before integration through the thickness, Eq. 5.1 reverts to the field equations of the DMV shell theory [5.30]. Other theories such as Timoshenko's [5.31], Novozhilov's [5.32] and Morley-Koiter [5.33] can all be obtained from the present theory by making other approximations [5.29]. Another point of interest is not all theories have reported the energy consistent boundary conditions. Within this context, the boundary terms in Eq. 5.1 provides the boundary conditions under each theory.

5.6 Expressions for Applied Forces

Harmonic body forces applied to a cylindrical shell are expressed as

$$p^x(x,s,z,t) = \bar{p}^x(x,s,z)e^{i\bar{\omega}t} = \sum_{n=-\infty}^{+\infty} \bar{p}_n^x(x,z)e^{ins/R}e^{i\bar{\omega}t}$$

$$p^s(x,s,z,t) = \bar{p}^s(x,s,z)e^{i\bar{\omega}t} = \sum_{n=-\infty}^{+\infty} \bar{p}_n^s(x,z)e^{ins/R}e^{i\bar{\omega}t} \qquad \text{(5.3a-c)}$$

$$p^z(x,s,z,t) = \bar{p}^z(x,s,z)e^{i\bar{\omega}t} = \sum_{n=-\infty}^{+\infty} \bar{p}_n^z(x,z)e^{ins/R}e^{i\bar{\omega}t}$$

in which, $\bar{\omega}$ is the exciting angular frequency. In Eqs. 5.3a-c, the continuity of the applied body forces in the circumferential direction is ensured by assuming the dependency of p^x, p^s, p^z on the circumferential coordinate s to take the harmonic form $e^{ins/R}$. Other load distributions such as surface tractions, ring loads, line loads or point loads can always be conceived as special cases of Eqs. 5.3a-c using the Dirac Delta function as needed. When the acting forces are in phase, force distributions $\bar{p}^x(x,s,z)$, $\bar{p}^s(x,s,z)$, $\bar{p}^z(x,s,z)$ are functions with real values. However, the current model is capable of taking complex force distributions, in order to model forces with the same angular frequency $\bar{\omega}$ but different phase angles.

5.7 Steady State Displacement Functions

The present study is aimed at capturing only the steady state response of the system. Under the given harmonic forces, the mid-surface displacements corresponding to the steady state response are also harmonic, i.e.,

$$u(x,s,t)=\bar{u}(x,s)e^{i\bar{\omega}t}=\left(\sum_{n=-\infty}^{+\infty}A_n(x)e^{ins/R}\right)e^{i\bar{\omega}t}$$
$$v(x,s,t)=\bar{v}(x,s)e^{i\bar{\omega}t}=\left(\sum_{n=-\infty}^{+\infty}B_n(x)e^{ins/R}\right)e^{i\bar{\omega}t} \qquad (5.4a\text{-}c)$$
$$v(x,s,t)=\bar{w}(x,s)e^{i\bar{\omega}t}=\left(\sum_{n=-\infty}^{+\infty}C_n(x)e^{ins/R}\right)e^{i\bar{\omega}t}$$

5.8 Equilibrium Conditions

From Eqs. 5.3 and 5.4 by substituting into Eq. 5.1 and performing the integrations with respect to time t and circumferential coordinate s yields

$$\sum_{n=-\infty}^{+\infty}\left[\frac{2\pi EhR}{1-\nu^2}\left\langle\delta A_{-n}(x)\quad\delta B_{-n}(x)\quad\delta C_{-n}(x)\quad\delta C'_{-n}(x)\right\rangle\times\right.$$
$$\left.\left[\begin{array}{c|c|c}{}^{1}_{1}HD & {}^{1}_{2}H_n & {}^{1}_{3}H+{}^{1}_{4}HD^2\\ \hline {}^{2}_{1}H_n & {}^{2}_{2}HD & {}^{2}_{3}H_nD\\ \hline {}^{3}_{1}H_n+{}^{3}_{2}HD^2 & {}^{3}_{3}H_nD & {}^{3}_{4}H_nD+{}^{3}_{5}HD^3\\ \hline {}^{4}_{1}HD & {}^{4}_{2}H_n & {}^{4}_{3}H_n+{}^{4}_{4}HD^2\end{array}\right]\left\{\begin{array}{c}A_n(x)\\B_n(x)\\C_n(x)\end{array}\right\}\right]_0^L$$
$$+\sum_{n=-\infty}^{+\infty}\left[\frac{2\pi EhR}{1-\nu^2}\delta C_{-n}(x)\,{}^{3}_{6}Hf_n^{xw}\right]_0^L$$
$$+\sum_{n=-\infty}^{+\infty}\int_0^L\left[\frac{2\pi EhR}{1-\nu^2}\left\langle\delta A_{-n}(x)\quad\delta B_{-n}(x)\quad\delta C_{-n}(x)\right\rangle\right.$$
$$\left.\left[\begin{array}{c|c|c}{}^{1}_{1}G_n+{}^{1}_{2}GD^2 & {}^{1}_{3}G_nD & {}^{1}_{4}G_nD+{}^{1}_{5}GD^3\\ \hline {}^{2}_{1}G_nD & {}^{2}_{2}G_n+{}^{2}_{3}GD^2 & {}^{2}_{4}G_n+{}^{2}_{5}G_nD^2\\ \hline {}^{3}_{1}G_nD+{}^{3}_{2}GD^3 & {}^{3}_{3}G_n+{}^{3}_{4}G_nD^2 & {}^{3}_{5}G_n+{}^{3}_{6}G_nD^2+{}^{3}_{7}GD^4\end{array}\right]\left\{\begin{array}{c}A_n(x)\\B_n(x)\\C_n(x)\end{array}\right\}\right]dx$$
$$+\sum_{n=-\infty}^{+\infty}\int_0^L\left\{\frac{2\pi EhR}{1-\nu^2}\left\langle\delta A_{-n}(x)\quad\delta B_{-n}(x)\quad\delta C_{-n}(x)\right\rangle\right.$$
$$\left.\left\{\begin{array}{c}{}^{1}_{6}Gf_n^{xu}(x)\\ {}^{2}_{6}Gf_n^{sv}(x)\\ {}^{3}_{8}G\,Df_n^{xw}(x)+{}^{3}_{9}G_n f_n^{sw}(x)+{}^{3}_{10}Gf_n^{zw}(x)\end{array}\right\}\right]dx=0 \qquad (5.5)$$

in which

$$f_n^{xu} = \int_{-\frac{h}{2}}^{+\frac{h}{2}} \overline{p}_n^x \left(1+\frac{z}{R}\right) dz \qquad , \qquad f_n^{xw} = -\int_{-\frac{h}{2}}^{+\frac{h}{2}} \overline{p}_n^x z \left(1+\frac{z}{R}\right) dz$$

$$f_n^{sv} = \int_{-\frac{h}{2}}^{+\frac{h}{2}} \overline{p}_n^s \left(1+\frac{z}{R}\right)^2 dz \qquad , \qquad f_n^{sw} = -\int_{-\frac{h}{2}}^{+\frac{h}{2}} \overline{p}_n^s z \left(1+\frac{z}{R}\right) dz \qquad \text{(5.6a-e)}$$

$$f_n^{zw} = \int_{-\frac{h}{2}}^{+\frac{h}{2}} \overline{p}_n^z \left(1+\frac{z}{R}\right) dz$$

In Eq. 5.5, symbols D^d ($d = 1,2,3,4$) denote the dth derivative of the argument functions with respect to $\overline{x}$ and constants ${}_j^iH$, ${}_j^iH_n$, ${}_j^iG$ and ${}_j^iG_n$ are defined in Appendix 5.A. As a convention, the left superscript i ($i = 1,...,4$) of constants ${}_j^iH$, ${}_j^iH_n$, ${}_j^iG$ and ${}_j^iG_n$ indicates the constants are related to the ith boundary or integral term, as applicable. The left subscript j denotes the jth coefficient of ith boundary or integral term. The presence of subscript n in constants ${}_j^iH_n$ and ${}_j^iG_n$ denotes that the constants are dependent on the circumferential mode number n.

5.9 Formulating Exact Shape Functions

In Eq. 5.4, functions $A_n(x)$, $B_n(x)$ and $C_n(x)$ are unknown. Conventionally, approximate interpolation functions would be used at this stage to relate functions $A_n(x)$, $B_n(x)$ and $C_n(x)$ to nodal displacements. The present study departs from this convention by adopting interpolation functions which exactly satisfy the homogeneous part of the field equations (Eq. 5.5), i.e.,

$$\left[\begin{array}{c|c|c} {}_1^1G_n + {}_2^1GD^2 & {}_3^1G_nD & {}_4^1G_nD + {}_5^1GD^3 \\ \hline {}_1^2G_nD & {}_2^2G_n + {}_3^2GD^2 & {}_4^2G_n + {}_5^2G_nD^2 \\ \hline {}_1^3G_nD + {}_2^3GD^3 & {}_3^3G_n + {}_4^3G_nD^2 & {}_5^3G_n + {}_6^3G_nD^2 + {}_7^3GD^4 \end{array}\right] \times \begin{Bmatrix} A_n(x) \\ B_n(x) \\ C_n(x) \end{Bmatrix} = \{0\} \tag{5.7}$$

It can be shown [5.29] that the solution of Eqs. 7 is

$$A_n(x) = \sum_{j=1}^{8} A_{nj}\bar{A}_{nj}e^{m_{nj}x} \quad , \quad B_n(x) = \sum_{j=1}^{8} A_{nj}\bar{B}_{nj}e^{m_{nj}x} \quad , \quad C_n(x) = \sum_{j=1}^{8} A_{nj}\bar{C}_{nj}e^{m_{nj}x} \tag{5.8}$$

in which subscript n is the mode number in Fourier expansion series in circumferential direction (Eq. 5.4). Integration constants A_{nj} ($j = 1,...,8$) are unknowns to be determined from boundary conditions and m_{nj} are the eight roots of the characteristic equation $a_n m_n^8 + b_n m_n^6 + c_n m_n^4 + d_n m_n^2 + e_n = 0$ in which coefficients $a_n,...,e_n$ are defined in Appendix 5.B. It is observed that the characteristic roots of modes n and $-n$ are identical. Constants $\bar{A}_{nj}$, $\bar{B}_{nj}$ and $\bar{C}_{nj}$ are defined as

$$\bar{A}_{nj} = \begin{cases} 1 & ;n = 0,\ j = 1,...,6 \\ 0 & ;n = 0,\ j = 7,8 \\ 1 & ;n \neq 0,\ j = 1,...,8 \end{cases} \tag{5.9}$$

$$\bar{B}_{nj} = \begin{cases} 0 & ;n = 0,\ j = 1,...,6 \\ 1 & ;n = 0,\ j = 7,8 \\ \dfrac{K_{nj.13}K_{nj.21} - K_{nj.11}K_{nj.23}}{K_{nj.12}K_{nj.23} - K_{nj.13}K_{nj.22}} & ;n \neq 0,\ j = 1,...,8 \end{cases} \tag{5.10}$$

$$\bar{C}_{nj} = \begin{cases} 1 & ;n = 0,\ j = 1,...,6 \\ 0 & ;n = 0,\ j = 7,8 \\ \dfrac{K_{nj.11}K_{nj.22} - K_{nj.12}K_{nj.21}}{K_{nj.12}K_{nj.23} - K_{nj.13}K_{nj.22}} & ;n \neq 0,\ j = 1,...,8 \end{cases} \tag{5.11}$$

in which

$$
\begin{aligned}
&{}^{1}_{1}K_{nj} = {}^{1}_{1}G_n + {}^{1}_{2}Gm^2_{nj} \quad , \quad {}^{1}_{2}K_{nj} = {}^{2}_{1}K_{n,j} = {}^{1}_{3}G_n m_{nj} \\
&{}^{1}_{3}K_{nj} = {}^{3}_{1}K_{nj} = {}^{1}_{4}G_n m_{nj} + {}^{1}_{5}Gm^3_{nj} \quad , \quad {}^{2}_{2}K_{nj} = {}^{2}_{2}G_n + {}^{2}_{3}Gm^2_{nj} \\
&{}^{2}_{3}K_{nj} = {}^{3}_{2}K_{nj} = {}^{2}_{4}G_n + {}^{2}_{5}G_n m^2_{nj} \quad , \quad {}^{3}_{3}K_{nj} = {}^{3}_{5}G_n + {}^{3}_{6}G_n m^2_{nj} + {}^{3}_{7}Gm^4_{nj}
\end{aligned}
\tag{5.12a-f}
$$

In a matrix form, Eqs. 5.8 are expressed as

$$
\begin{aligned}
A_n(x) &= \left\langle \mathbf{S}_{\mathbf{A}n}(x) \right\rangle_{1\times 8} \left\{ \mathbf{A}_n \right\}_{8\times 1} \\
B_n(x) &= \left\langle \mathbf{S}_{\mathbf{B}n}(x) \right\rangle_{1\times 8} \left\{ \mathbf{A}_n \right\}_{8\times 1} \\
C_n(x) &= \left\langle \mathbf{S}_{\mathbf{C}n}(x) \right\rangle_{1\times 8} \left\{ \mathbf{A}_n \right\}_{8\times 1}
\end{aligned}
\tag{5.13a-c}
$$

in which

$$
\begin{aligned}
\left\langle \mathbf{S}_{\mathbf{A}n}(x) \right\rangle_{1\times 8} &= \left\langle \bar{A}_{n1}e^{m_{n1}x} \middle| \bar{A}_{n2}e^{m_{n2}x} \middle| \bar{A}_{n3}e^{m_{n3}x} \middle| \bar{A}_{n4}e^{m_{n4}x} \middle| \bar{A}_{n5}e^{m_{n5}x} \middle| \bar{A}_{n6}e^{m_{n6}x} \middle| \bar{A}_{n7}e^{m_{n7}x} \middle| \bar{A}_{n8}e^{m_{n8}x} \right\rangle \\
\left\langle \mathbf{S}_{\mathbf{B}n}(x) \right\rangle_{1\times 8} &= \left\langle \bar{B}_{n1}e^{m_{n1}x} \middle| \bar{B}_{n2}e^{m_{n2}x} \middle| \bar{B}_{n3}e^{m_{n3}x} \middle| \bar{B}_{n4}e^{m_{n4}x} \middle| \bar{B}_{n5}e^{m_{n5}x} \middle| \bar{B}_{n6}e^{m_{n6}x} \middle| \bar{B}_{n7}e^{m_{n7}x} \middle| \bar{B}_{n8}e^{m_{n8}x} \right\rangle \\
\left\langle \mathbf{S}_{\mathbf{C}n}(x) \right\rangle_{1\times 8} &= \left\langle \bar{C}_{n1}e^{m_{n1}x} \middle| \bar{C}_{n2}e^{m_{n2}x} \middle| \bar{C}_{n3}e^{m_{n3}x} \middle| \bar{C}_{n4}e^{m_{n4}x} \middle| \bar{C}_{n5}e^{m_{n5}x} \middle| \bar{C}_{n6}e^{m_{n6}x} \middle| \bar{C}_{n7}e^{m_{n7}x} \middle| \bar{C}_{n8}e^{m_{n8}x} \right\rangle
\end{aligned}
\tag{5.14a-c}
$$

and

$$
\left\{ \mathbf{A}_n \right\}_{8\times 1} = \left\langle A_{n1} \middle| A_{n2} \middle| A_{n3} \middle| A_{n4} \middle| A_{n5} \middle| A_{n6} \middle| A_{n7} \middle| A_{n8} \right\rangle^T \tag{5.15}
$$

In a finite element context, all unknown coefficients $\left\{ \mathbf{A}_n \right\}_{8\times 1}$ are to be expressed in terms of nodal displacements $A_n(0)$, $B_n(0)$, $C_n(0)$, $C'_n(0)$, $A_n(L)$, $B_n(L)$, $C_n(L)$ and $C'_n(L)$. From Eqs. 5.13, one has

$$
\left\{ \mathbf{\Delta}_n \right\}_{8\times 1} = \left[\mathbf{L}_n \right]_{8\times 8} \left\{ \mathbf{A}_n \right\}_{8\times 1} \tag{5.16}
$$

in which

$$
\left\{ \mathbf{\Delta}_n \right\}_{8\times 1} = \left\langle A_n(0) \middle| B_n(0) \middle| C_n(0) \middle| C'_n(0) \middle| A_n(L) \middle| B_n(L) \middle| C_n(L) \middle| C'_n(L) \right\rangle^T \tag{5.17}
$$

and

$$
\left[\mathbf{L}_n \right]_{8\times 8} = \left[\mathbf{L}_{n1} \middle| \mathbf{L}_{n2} \middle| \mathbf{L}_{n3} \middle| \mathbf{L}_{n4} \middle| \mathbf{L}_{n5} \middle| \mathbf{L}_{n6} \middle| \mathbf{L}_{n7} \middle| \mathbf{L}_{n8} \right] \tag{5.18}
$$

where

$$\left\{\mathbf{L}_{nj}\right\}_{8\times1}=\left\langle \bar{A}_{nj}\ \middle|\ \bar{B}_{nj}\ \middle|\ \bar{C}_{nj}\ \middle|\ m_{nj}\bar{C}_{nj}\ \middle|\ \bar{A}_{nj}e^{m_{nj}L}\ \middle|\ \bar{B}_{nj}e^{m_{nj}L}\ \middle|\ \bar{C}_{nj}e^{m_{nj}L}\ \middle|\ m_{nj}\bar{C}_{nj}e^{m_{nj}L}\right\rangle^{T}\quad ;\ j=1,...,8 \tag{5.19}$$

Solving Eq. 5.16 for the unknown coefficients $\left\{\mathbf{A}_n\right\}_{8\times1}$ yields

$$\left\{\mathbf{A}_n\right\}_{8\times1}=\left[\mathbf{L}_n\right]_{8\times8}^{-1}\left\{\mathbf{\Delta}_n\right\}_{8\times1} \tag{5.20}$$

By substituting Eq. 5.20 into Eqs. 5.14, one obtains

$$\begin{aligned} A_n(x)&=\left\langle \mathbf{N}_{\mathbf{A}n}(x)\right\rangle_{1\times8}\left\{\mathbf{\Delta}_n\right\}_{8\times1}\\ B_n(x)&=\left\langle \mathbf{N}_{\mathbf{B}n}(x)\right\rangle_{1\times8}\left\{\mathbf{\Delta}_n\right\}_{8\times1}\\ C_n(x)&=\left\langle \mathbf{N}_{\mathbf{C}n}(x)\right\rangle_{1\times8}\left\{\mathbf{\Delta}_n\right\}_{8\times1} \end{aligned} \tag{5.21a-c}$$

in which

$$\begin{aligned} \left\langle \mathbf{N}_{\mathbf{A}n}(x)\right\rangle_{1\times8}&=\left\langle \mathbf{S}_{\mathbf{A}n}(x)\right\rangle_{1\times8}\left[\mathbf{L}_n\right]_{8\times8}^{-1}\\ \left\langle \mathbf{N}_{\mathbf{B}n}(x)\right\rangle_{1\times8}&=\left\langle \mathbf{S}_{\mathbf{B}n}(x)\right\rangle_{1\times8}\left[\mathbf{L}_n\right]_{8\times8}^{-1}\\ \left\langle \mathbf{N}_{\mathbf{C}n}(x)\right\rangle_{1\times8}&=\left\langle \mathbf{S}_{\mathbf{C}n}(x)\right\rangle_{1\times8}\left[\mathbf{L}_n\right]_{8\times8}^{-1} \end{aligned} \tag{5.22a-c}$$

It is noted that $\left\langle \mathbf{N}_{\mathbf{A}n}(x)\right\rangle_{1\times8}$, $\left\langle \mathbf{N}_{\mathbf{B}n}(x)\right\rangle_{1\times8}$ and $\left\langle \mathbf{N}_{\mathbf{C}n}(x)\right\rangle_{1\times8}$ are the exact shape function row vectors.

5.10 Equilibrium Equations

From Eqs. 5.22a-c, by substituting into Eq. 5.5, and noting that the shape functions derived exactly satisfy the homogeneous part of the field equations, (i.e. the third term in Eq. 5.5 vanishes), one obtains

in which the entries of the *n*th stiffness matrix contribution $\left[\mathbf{K}_n\right]_{8\times 8}$ and the *n*th energy equivalent load vector $\left\{\mathbf{F}_n\right\}_{8\times 1}$ are defined in Appendix 5.C.

5.11 General Displacement Fields

The steady state displacements of a generic point within the shell volume are expressed as

$$\tilde{U}\left(x,s,z,t\right)=\sum_{n=-\infty}^{+\infty}\left[\left(\left\langle \mathbf{N}_{\mathbf{A}n}\left(x\right)\right\rangle_{1\times 8}-z\left\langle \mathbf{N}'_{\mathbf{C}n}\left(x\right)\right\rangle_{1\times 8}\right)\left\{\boldsymbol{\Delta}_n\right\}_{8\times 1}\right]e^{ins/R}e^{i\bar{\omega}t}$$

$$\tilde{V}\left(x,s,z,t\right)=\sum_{n=-\infty}^{+\infty}\left[\left(\left\langle \mathbf{N}_{\mathbf{B}n}\left(x\right)\right\rangle_{1\times 8}-z\frac{in}{R}\left\langle \mathbf{N}_{\mathbf{C}n}\left(x\right)\right\rangle_{1\times 8}\right)\left\{\boldsymbol{\Delta}_n\right\}_{8\times 1}\right]\left(1+\frac{z}{R}\right)e^{ins/R}e^{i\bar{\omega}t}$$

$$\tilde{W}\left(x,s,z,t\right)=\sum_{n=-\infty}^{+\infty}\left[\left\langle \mathbf{N}_{\mathbf{C}n}\left(x\right)\right\rangle_{1\times 8}\left\{\boldsymbol{\Delta}_n\right\}_{8\times 1}\right]e^{ins/R}e^{i\bar{\omega}t} \qquad (5.24a\text{-}c)$$

5.12 Strain and Stress Fields

Recalling the strain-displacement relations $\bar{\eta}_{11}=u_{,1}-zw_{,11}$,

$\bar{\eta}_{22}=v_{,2}+w/\left(R+z\right)-zRw_{,22}/\left(R+z\right)$ and

$\bar{\eta}_{12}=\left[Ru_{,2}/\left(R+z\right)+\left(R+z\right)v_{,1}/R-z\left(2R+z\right)w_{,12}/\left(R+z\right)\right]/2$ [5.29] the physical components of the strain at any point within the shell are expressed as

$$\bar{\eta}_{11}=\sum_{n=-\infty}^{+\infty}\left[\left(\left\langle \mathbf{N}'_{\mathbf{A}n}\left(\bar{x}\right)\right\rangle_{1\times 8}-z\left\langle \mathbf{N}''_{\mathbf{C}n}\left(\bar{x}\right)\right\rangle_{1\times 8}\right)\left\{\boldsymbol{\Delta}_n\right\}_{8\times 1}\right]e^{in\bar{s}}e^{i\bar{\omega}t}$$

$$\bar{\eta}_{22}=\sum_{n=-\infty}^{+\infty}\left[\left(\frac{in}{R}\left\langle \mathbf{N}_{\mathbf{B}n}\left(\bar{x}\right)\right\rangle_{1\times 8}+\frac{1}{R+z}\left\langle \mathbf{N}_{\mathbf{C}n}\left(\bar{x}\right)\right\rangle_{1\times 8}+z\frac{n^2}{R\left(R+z\right)}\left\langle \mathbf{N}_{\mathbf{C}n}\left(\bar{x}\right)\right\rangle_{1\times 8}\right)\left\{\boldsymbol{\Delta}_n\right\}_{8\times 1}\right]e^{in\bar{s}}e^{i\bar{\omega}t}$$

$$\bar{\eta}_{12}=\sum_{n=-\infty}^{+\infty}\left[\frac{1}{2}\left(\frac{in}{R+z}\left\langle \mathbf{N}_{\mathbf{A}n}\left(\bar{x}\right)\right\rangle_{1\times 8}+\frac{R+z}{R}\left\langle \mathbf{N}'_{\mathbf{B}n}\left(\bar{x}\right)\right\rangle_{1\times 8}\right.\right.$$
$$\left.\left.-z\frac{2R+z}{R+z}\frac{in}{R}\left\langle \mathbf{N}'_{\mathbf{C}n}\left(\bar{x}\right)\right\rangle_{1\times 8}\right)\left\{\boldsymbol{\Delta}_n\right\}_{8\times 1}\right]e^{in\bar{s}}e^{i\bar{\omega}t} \qquad (5.25a\text{-}c)$$

The corresponding stress components are

$$\bar{\sigma}^{11}=\frac{E}{1-\nu^2}\left(\bar{\eta}_{11}+\nu\bar{\eta}_{22}\right)\quad,\quad \bar{\sigma}^{22}=\frac{E}{1-\nu^2}\left(\bar{\eta}_{22}+\nu\bar{\eta}_{11}\right)\quad,\quad \bar{\sigma}^{12}=\frac{E}{1+\nu}\bar{\eta}_{12} \qquad (5.26a\text{-}c)$$

5.13 Examples

5.13.1 Example 1

A $5\,m$ long cantilever beam composed of two cylindrical segments of radius $R=0.2\,m$ is subject to a harmonic point load $P_q\sin\bar{\omega}t$ assumed to act on the middle surface (Figure 5.2), with an exciting frequency $\bar{\omega}=10\times 2\pi\ rad/s$ and $P_q=1000\,N$. Dimensions are given on Figure 5.2. It is required to calculate the mid-surface displacements of the generator of the beam at $\alpha=30^\circ$ (i.e., $s/R=11\pi/6$). For the present and following examples, material is steel with $E=200\,GPa$ and $\nu=0.30$.

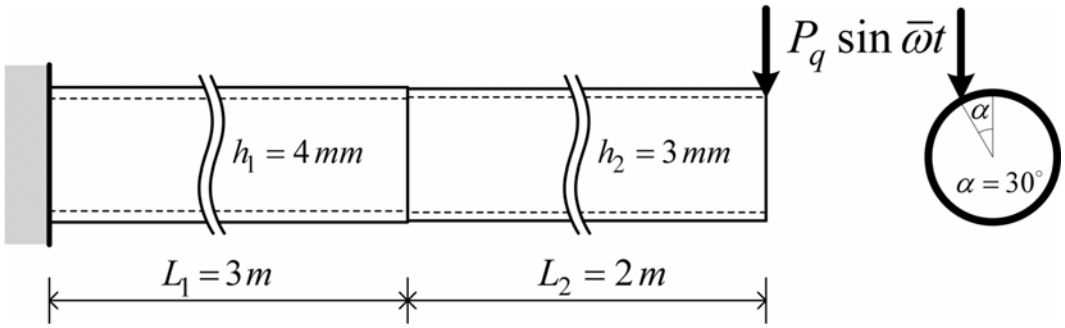

Figure 5.2 - Example 1, Cantilever pipe with tip point load

Considering the coordinate configuration defined in Figure 5.1, the time-independent contributions of the applied body forces are $\bar{p}^x\left(x,s,z\right)=0$,

$\bar{p}^s(x,s,z) = -P_q \sin\alpha\,\delta(x-5)\,\delta(s-11\pi R/6)\,\delta(z)$ and

$\bar{p}^z(x,s,z) = -P_q \cos\alpha\,\delta(x-5)\,\delta(s-11\pi R/6)\,\delta(z)$. One element is used for each segment in order to model the change in thickness. The problem is solved twice: for $-7 \le n \le +7$ and $-10 \le n \le +10$. The mid-surface displacements of the generator at $s/R = 11\pi/6$ are plotted in Figure 5.3 and compared to the results based on the Abaqus model. In the Abaqus model two different meshes are used, a coarser mesh consisting of $72 \times 287 = 20,664$ S4R shell elements and a finer mesh consisting of $144 \times 573 = 82,512$ elements. Figure 5.3 shows that all four solutions are indistinguishable. The model developed in the present study is highly accurate and efficient with far fewer degrees of freedom (64 DOF for $-7 \le n \le +7$). The Matlab code written for the evaluation of this example is provided in Appendix 5.D.

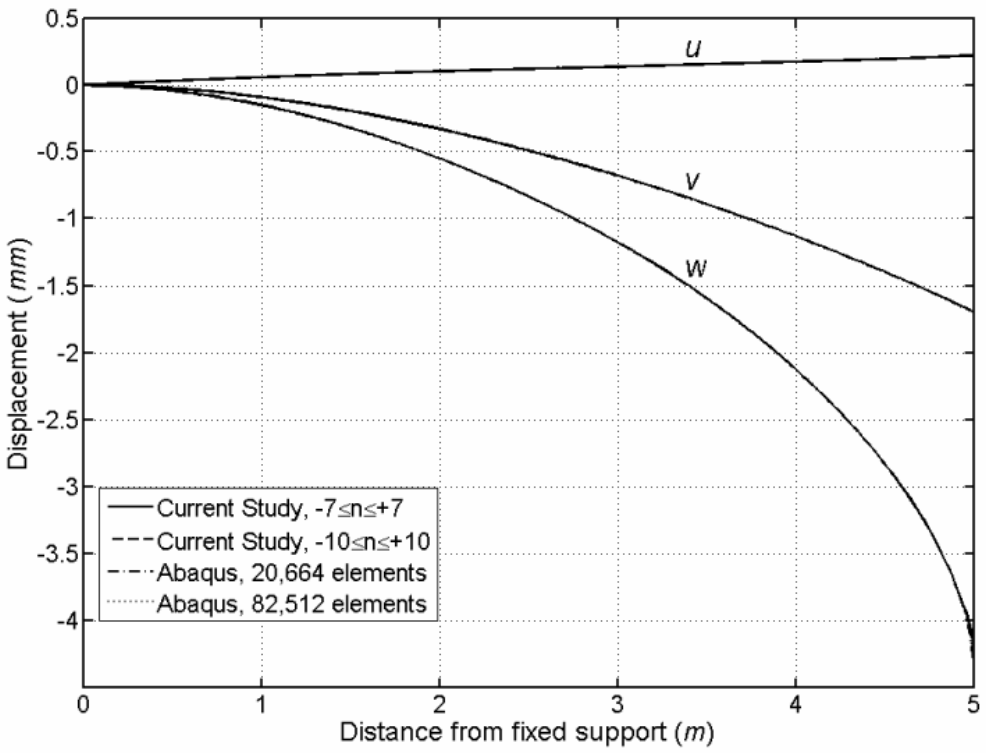

Figure 5.3 - Longitudinal, circumferential and radial displacements of the generator of the beam at $s/R = 11\pi/6$

A 3D plot of the deformed configuration of the pipe based on the current model is shown in Figure 5.4a. A plot based on the finer Abaqus mesh is also shown on Figure 5.4b for comparison. It is noted that the fine mesh depicted in Figure 5.4a is provided for a clear visualization of the deformed configuration and is no indicator of the number of degrees of freedom adopted in the solution.

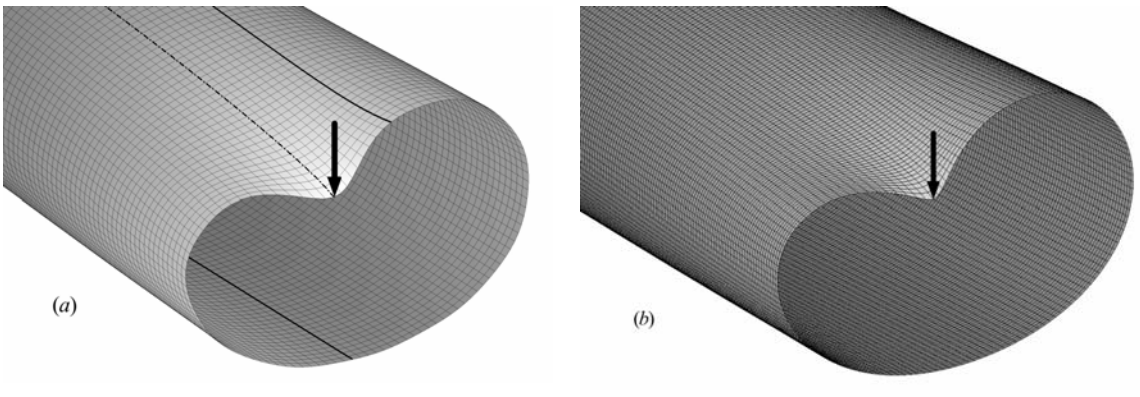

Figure 5.4 – Deformed Configuration for a pipe subject to point load based on a) Current Model (solid lines denote the top and bottom generators and dash-dotted line denotes the generator at $s/R = 11\pi/6$), and b) Abaqus S4R shell model

5.13.2 Example 2

A steel pipe (Figure 5.5) of radius $R = 0.25\,m$ and thickness $h = 5\,mm$ is subject to a vertical harmonic excitation of frequency $\bar{\omega} = 20 \times 2\pi\ rad/s$ and $10\,mm$ amplitude at its right end. The left support is fixed. It is required to determine the response of the system.

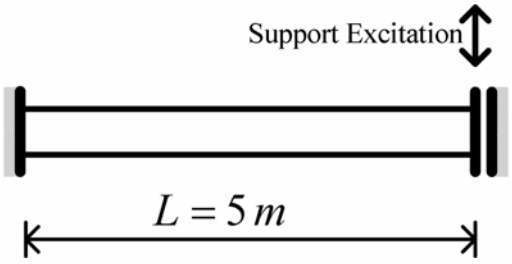

Figure 5.5 – Pipe configuration

The given harmonic support excitation induces vertical direction has the displacement components $v(x=5,s,t) = \left[0.01\sin(s/R)\right]e^{i\bar{\omega}t}$, $w(x=5,s,t) = \left[-0.01\cos(s/R)\right]e^{i\bar{\omega}t}$, and thus only contribute to modes $n = \pm 1$. The longitudinal and circumferential stresses at the top three generators (inner surface $z = -h/2$, mid-surface $z = 0$ and outer surface $z = +h/2$) of the beam are plotted in Figure 5.6a,b and the maximum shear stresses at the

beam mid-height plotted in Figure 5.6c. In all cases, comparisons are made to Abaqus results. The difference between both sets of results is indistinguishable within the scale of the figures. It is noted that the current model has reached this accuracy by using only eight degrees of freedom.

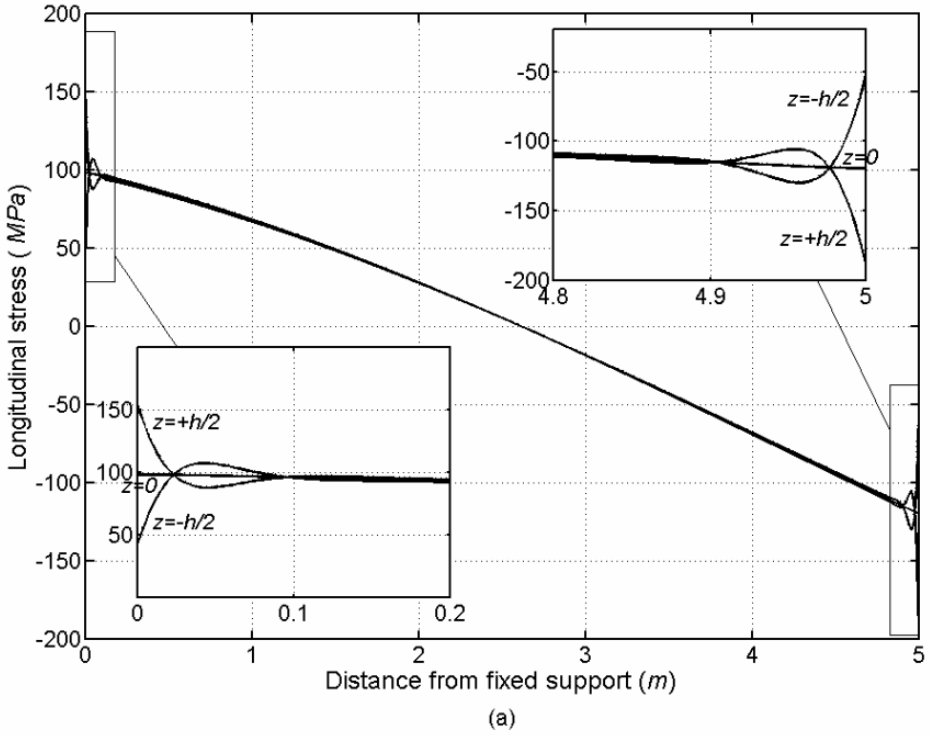

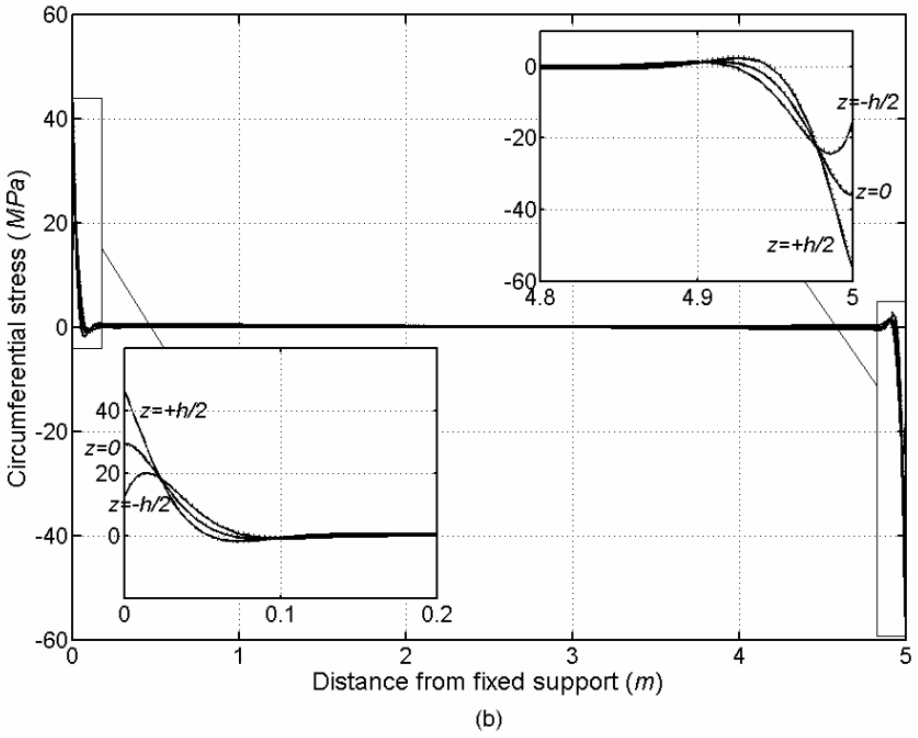
Circumferential stress (MPa)
Distance from fixed support (m)
z=+h/2
z=0
z=-h/2
z=-h/2
z=0
z=+h/2

(b)

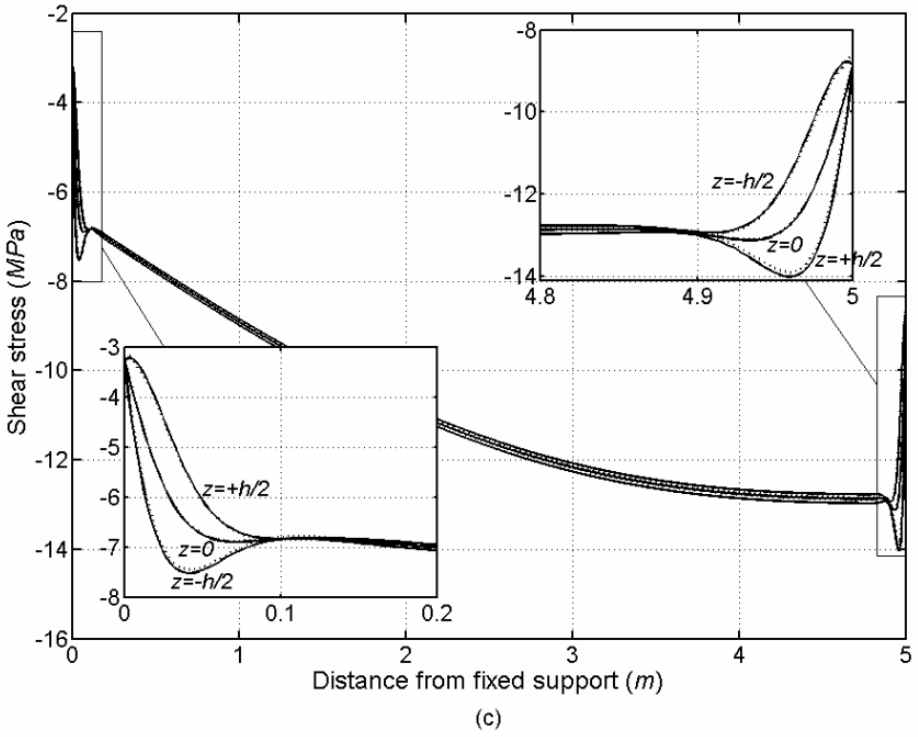

Figure 5.6 – Maximum stresses along the top generator for inner surface ($z = -h/2$), mid-surface ($z = 0$), and outer surface ($z = +h/2$). Solid lines denote results based on the current study and dotted lines denote results based on the Abaqus .

5.13.3 Example 3

It is required to obtain the static response of a fixed-fixed horizontal pipe, with the same dimensions and material properties as in Example 2, to its self weight. A very low exciting frequency of $\bar{\omega} = 2\pi \; rad/s$ (which is less than 1% of the first natural frequency of the pipe) is considered close enough to simulate the static loading case. The mid-span vertical deflection at the mid-surface for a point lying on top generator was found to be $-0.0260\,mm$ which is identical to that based on a static analysis in Abaqus with $81,600$ S4R shell element. The excellent agreement obtained is an indication of the ability of the formulation to capture the static response as a special case.

5.13.4 Example 4

A horizontal cylindrical thin shell of span $L = 6\,m$, radius $R = 0.1\,m$ and thickness $h = 0.003\,m$ is fixed at both ends. The shell is subject to a distributed harmonic patch load acting at mid-span within a rectangular area bounded with the lines $s/R = \pm\pi/8$ and $x = 3 \pm 0.06$ (Figure 5.7a). Two types of uniform harmonic loads act on the patch: a) A vertical traction load $q_V = 1{,}000\,e^{i\bar{\omega}t}\ KN/m^2$ and b) a longitudinal load $q_L = 1{,}000\,e^{i(\bar{\omega}t+\theta_1)}\ KN/m^2$ which is θ_1 out-of-phase relative to q_V. Such out-of-phase loading may be induced by rotary equipment with an eccentric mass. It is required to determine the steady state displacements under the combined effect of the two given loads with $\theta_1 = \pi/4\ rad$. The exciting frequency is $\bar{\omega} = 2\pi \times 60\,rad/s$.

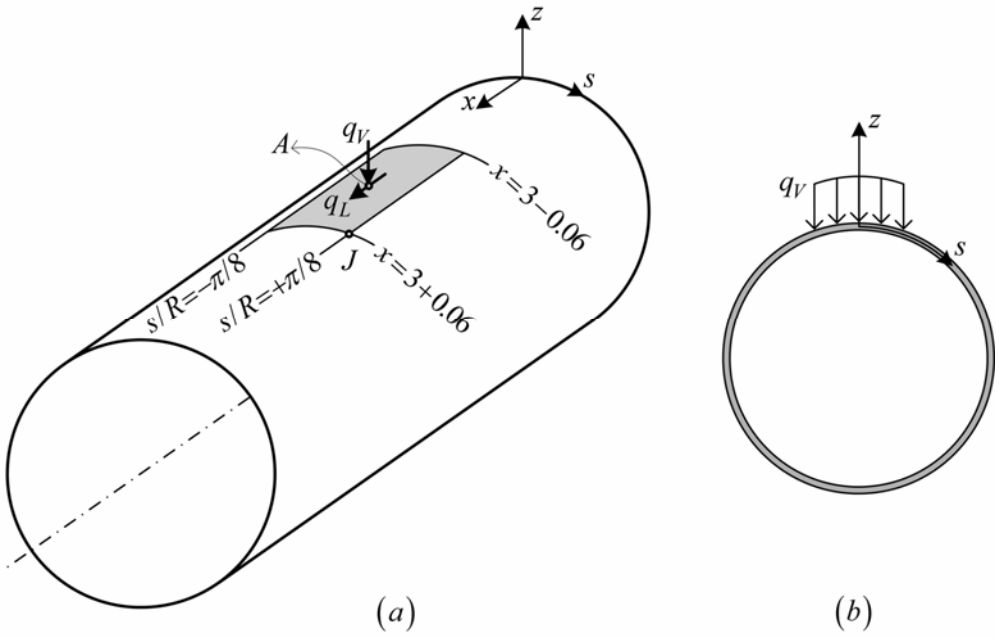

Figure 5.7 - a) Patch Loading area and the direction of the out of phase applied tractions q_L and q_V, and b) Distribution of the vertical traction q_V

The mathematical expressions of the corresponding body forces are

$$
\begin{aligned}
p^x\left(x,s,z,t\right) &= P_q\left(x,s,z\right) q_L\, e^{i\left(\bar{\omega}t+\theta_1\right)} \\
p^s\left(x,s,z,t\right) &= P_q\left(x,s,z\right)\left[q_V \sin\left(s/R\right)\right] e^{i\bar{\omega}t} \\
p^z\left(x,s,z,t\right) &= P_q\left(x,s,z\right)\left[-q_V \cos\left(s/R\right)\right] e^{i\bar{\omega}t}
\end{aligned}
\tag{5.27}
$$

in which,

$$P_q\left(x,s,z\right) = \left[H\left(x-2.94\right)-H\left(x-3.06\right)\right]\left[1-H\left(s-\pi R/8\right)+H\left(s-15\pi R/8\right)\right]\delta\left(z-h/2\right)$$

and H is the Heaviside unit step function. It is noted that circumferential and radial components of the applied forces result from decomposing the vertical traction force (Figure 5.7b) into the radial and tangential directions. The time-independent parts of the body forces are $\bar{p}^x\left(x,s,z\right) = q_L\, P_q\left(x,s,z\right) e^{i\theta_1}$, $\bar{p}^s\left(x,s,z\right) = \left[q_V \sin\left(s/R\right)\right] P_q\left(\bar{x},\bar{s},z\right)$ and $\bar{p}^z\left(x,s,z\right) = -\left[q_V \cos\left(s/R\right)\right] P_q\left(x,s,z\right)$. The number of Fourier terms needed to expand the loads in the circumferential direction was numerically found to be 15 ($-7 \le n \le +7$). The real components of the mid-surface displacement components along the top generator are plotted and compared to the results based on Abaqus in Figure 5.8. The Abaqus shell model consisted of $96 \times 916 = 87{,}936$ S4R shell elements. In the solution based on the current study, two meshes are used; a) A single element along the patch load area and an element on each side of the patch load b) Two elements along the patch load area and an element on each side of the patch load.

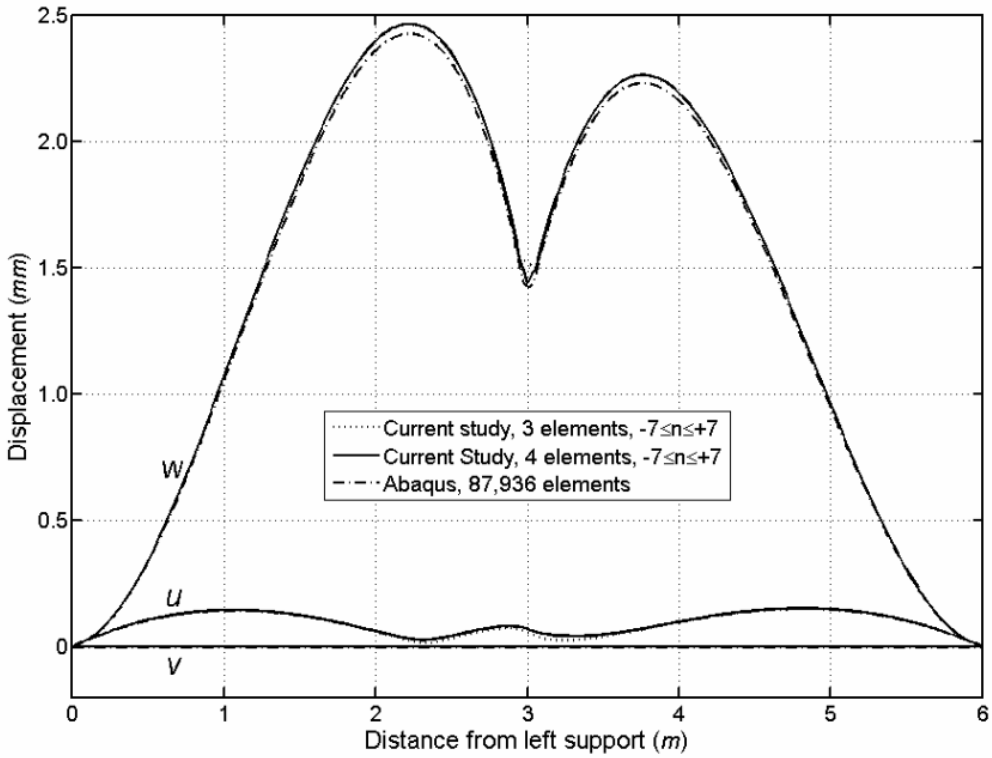

Figure 5.8 – Maximum mid-surface displacement components along the top generator

The components of displacement of point J on the mid-surface at the corner of the patch load (Figure 5.7a) are given and compared to those based on the Abaqus in Table 5.1. The magnitude of the imaginary exponent represents the out-of-phase angle with the applied tractions p^s and p^z. It is of interest to note that in the present example and all previous ones, the computational time based on the present study is three orders of magnitude faster than the solutions provided by Abaqus, while attaining the same degree of accuracy.

Table 5.1 – Mid-surface displacement components of Point J (in mm)

	Longitudinal	Circumferential	Radial
Current study	$0.0600e^{0.857i}$	$0.629e^{3.127i}$	$1.781e^{6.275i}$
Abaqus	$0.0586e^{0.859i}$	$0.621e^{3.128i}$	$1.754e^{6.275i}$
Magnitude Difference	2.3%	1.3%	1.5%

5.14 Conclusion

A family of shape functions is formulated based on the exact solution of the differential equations of equilibrium of cylindrical shells subjected to harmonic forces. A super-convergent pipe finite element is developed based on the shape functions developed. The element efficiently captures the response of pipe systems under general harmonic forces, boundary conditions, and support excitations with very few degrees of freedom. Through four examples, the model is shown to predict the displacements and stresses in excellent agreement with those based on established shell finite element solutions. The computational efficiency of the element makes it particularly suitable for the analysis of long pipeline systems subject to harmonic forces.

5.15 Acknowledgement

The authors would like to express their deepest gratitude to the Bahai Institute for Higher Education (BIHE) for its encouragement and support to the first author. Financial support from the Natural Science and Engineering Research Council (NSERC) to the second author is gratefully acknowledged.

5.16 References

[5.1] H. Ohtsubo, O. Watanabe, Stress analysis of pipe bends by ring elements, J. Press. Vessel. Technol. 100 (1978) 112-122.

[5.2] H. Takeda, S. Asai, K. Kwata, A New Finite Element for Structural Analysis of Piping Systems, Proc. Fifth SMIRT Conf. Berlin, 1979.

[5.3] K.J. Bathe, C. A. Almeida, A Simple and Effective Pipe Elbow Element-Linear Analysis, Trans. ASME, J. Appl. Mech. 47 (1980) 93-100.

[5.4] C. Militello, A.E. Huespe, A displacement-based pipe elbow element, Comput. Struct. 29 (1988) 339-343.

[5.5] P.B. Goncalves, N.R.S.S. Ramos, Free Vibration Analysis of Cylindrical Tanks Partially Filled with Liquid, J. sound and Vib. 195 (1996) 429-444.

[5.6] L. Xuebin, A New Approach for Free Vibration Analysis of Thin Circular Cylindrical Shell, J. Sound Vib. 296 (2006) 91-98.

[5.7] L. Gan, X. Li, Z. Zhang, Free Vibration Analysis of Ring-Stiffened Cylindrical Shells Using Wave Propagation Approach. J. Sound Vib. doi: 10.1016/j.jsv.2009.05.001.

[5.8] E.M.M. Fonseca, F.J.M.Q. de Melo, C.A.M. Oliveira, Determination of flexibility factors in curved pipes with end restraints using a semi-analytical formulation, Int. J. Press. Vessel. Pip, 79 (2002) 829-840

[5.9] S.A. Karamanos, E. Giakoumatos, A.M. Gresnigt, Nonlinear response and failure of steel elbows under in-plane bending and pressure, J. Press. Vessel. Technol. 125 (2003) 393-402.

[5.10] J. Mackerle, Finite elements in the analysis of pressure vessels and piping – a bibliography (1976-1996), Int. J. Press. Vessel. Pip. 69 (1996) 279-339.

[5.11] J. Mackerle, Finite elements in the analysis of pressure vessels and piping, an addendum (1996-1998)", Int. J. Press. Vessel. Pip. 76 (1999) 461-485.

[5.12] J. Mackerle, Finite elements in the analysis of pressure vessels and piping, an addendum: a bibliography (1998-2001), Int. J. Press. Vessel. Pip. 79 (2002) 1-26.

[5.13] J. Mackerle, Finite elements in the analysis of pressure vessels and piping, an addendum: a bibliography (2001-2004), Int. J. Press. Vessel. Pip. 82 (2005) 571-592.

[5.14] H.D. Hibbitt, Special Structural Elements of Piping Analysis, Pressure Vessels and Piping; Analysis and Computers, ASME, New York, 1974.

[5.15] T. J. R. Hughes, W.K. Liu, Nonlinear Finite Element Analysis of Shells, Part I: Three-Dimensional Shells, Comput. Method. Appl. Mech. Eng. 26 (1981) 331-362.

[5.16] T. J. R. Hughes, W.K. Liu, Nonlinear Finite Element Analysis of Shells, Part II: Two-Dimensional Shells, Comput. Method. Appl. Mech. Eng. 27 (1981) 167-181.

[5.17] K.J. Bathe, C. Almeida, A simple and effective pipe elbow element – interaction effects, J. Appl. Mech. 49 (1982) 165-171.

[5.18] K.J. Bathe, C. Almeida, A simple and effective pipe elbow element – some non-linear capabilities, Comput. Struct. 17 (1983) 659-667.

[5.19] M. Abo-Elkhier, Analysis of pipe bends using pipe elbow element, Comput. Struct. 37 (1990) 9-15.

[5.20] F.J.M.Q. Melo, P.M.S.T. de Castro, The Linear Elastic Stress Analysis of curved pipes under generalized loads using a reduced integration finite element, J. Strain Anal. Eng. Des. 32 (1997) 47-59.

[5.21] A.M. Yan, R.J. Jospin, D.H. Nguyen, An enhanced pipe elbow element - application in plastic limit analysis of pipe structures, International Journal for Numerical Methods in Engineering, 46 (1999) 409-431.

[5.22] K.R. Sivadas, N. Ganesan, Dynamic Analysis of Circular Cylindrical Shells with Material Damping, J. Sound Vib. 166 (1993) 103-116.

[5.23] A.J. Stanley, N. Ganesan, Dynamic Response of Cantilever Cylindrical Shells with Discontinuity in Thickness Subjected to Axisymmetric Load, Comput. Struct. 55 (1995) 667-685.

[5.24] Z.C. Xi, L.H. Yam, T.P. Leung, Semi-Analytical Study of Free Vibration of Composite Shells of Revolution Based on the Reissner-Mindlin Assumption, Int. J. Solid. Struct. 33 (1996) 851-863.

[5.25] I.F. Pinto Correia, J.I. Barbosa, C.M. Mota Soares, C.A. Mota Soares, A Finite Element Semi-Analytical Model for Laminated Axisymmetric Shells: Static, Dynamic and Buckling, Comput. Struct. 79 (2000) 299-317.

[5.26] S.A. Karamanos, Bending Instabilities of Elastic Tubes", Int. J. Solid. and Struct. 39 (2002) 2059-2085.

[5.27] S.A.Karamanos, E. Giakoumatos, A.M. Gresnigt, Nonlinear Response and Failure of Steel Elbows under In-Plane Bending and Pressure, J. Press. Vessel Technol. 125 (2003) 393-402.

[5.28] H. Santos, C.M. Mota Soares, C.A. Mota Soares, J.N. Reddy, A Semi-Analytical Finite Element Model for the Analysis of Laminated 3D Axisymmetric Shells: Bending, Free Vibration and Buckling, Compos. Struct. 71 (2005) 273-281.

[5.29] R. Salahifar, Analysis of Thin Shells under Harmonic Loads. Ph.D. Thesis, Department of Civil Engineering, University of Ottawa, Ottawa, ON, Canada, 2010.

[5.30] W. Flugge, Stresses in Shells. Springer-Verlag, New York, 1973.

[5.31] S. Timoshenko, Theory of Plates and Shells. McGraw-Hill Book Company, New York, 1959.

[5.32] V.V. Novozhilov, Thin Shell Theory. P. Noordhoff Ltd. - Groningen-The Netherlands, 1964.

[5.33] F. I. Niordson, Shell Theory. North-Holland Series In Applied Mathematics and Mechanics, 1985.

5.17 List of Symbols

$A_n(x), B_n(x), C_n(x)$	Contributions of circumferential mode n to mid-surface displacements u, v, w, respectively
A_{nj}, B_{nj}, C_{nj}	jth integration constant in the assumed displacement field functions $A_n(x)$, $B_n(x)$ and $C_n(x)$, respectively, corresponding to mode n
$\bar{A}_{nj}$, $\bar{B}_{nj}$, $\bar{C}_{nj}$	Constants relating constants A_{nj}, B_{nj} and C_{nj}
D^d	The dth derivative with respect to the axial coordinate x
E	Modulus of elasticity
${}^i_j G_n$	Coefficient of jth term in ith field equation of mode number n
${}^i_j G$	Coefficient of jth term in ith field equation independent of mode number n
${}^i_j H_n$	Coefficient of jth term in ith boundary equation of mode number n
${}^i_j H_n$	Coefficient of jth term in ith boundary equation independent of mode number n
L	Length of the cylinder

R	Radius of the cylinder
$\tilde{U},\tilde{V},\tilde{W}$	Physical components of the longitudinal, circumferential and radial displacement of a point within the shell, respectively
V	Volume
f^{xu}, f^{xw} f^{sv}, f^{sw} f^{zw}	Contributions to the forces induced by the applied body forces (after integration across the thickness of the shell) as functions of coordinates x, s and time t
$f_n^{xu}(x), f_n^{xw}(x)$ $f_n^{sv}(x), f_n^{sw}(x)$ $f_n^{zw}(x)$	Respective force contributions of f^{xu}, f^{xw}, f^{sv}, f^{sw} and f^{zw} based on mode n as functions of coordinate x
h	Thickness of the cylinder
$\ldots_{,i}$	Partial derivative with respect to x for $i=1$ and to s for $i=2$
m_{nj}	j th root of the characteristic equation for mode n
p^x, p^s, p^z	Longitudinal, circumferential and radial components of the applied body forces, as functions of coordinates x, s, z and time t

$\bar{p}^x$, $\bar{p}^s$, $\bar{p}^z$	Time-independent components of the applied body forces p^x, p^s and p^z, respectively, as functions of coordinates x, s, z
u, v, w	Longitudinal, circumferential and radial components of the displacement of a point on the middle surface along coordinates x, s and z, respectively
$\bar{u}$, $\bar{v}$, $\bar{w}$	Time-independent components of the displacement components u, v and w, of a point on the middle surface as a function of coordinates x and s
$\{\mathbf{A}_n\}_{8\times1}$	Integration constant vector
$\{\mathbf{F}_n\}_{8\times1}$	Total force vector corresponding to mode n
$[\mathbf{K}_n]_{8\times8}$	Total stiffness matrix corresponding to mode n
$[\mathbf{L}_n]_{8\times8}$	Matrix relating the integration constants vector $\{\mathbf{A}_n\}_{8\times1}$ to nodal displacement vector $\{\mathbf{\Delta}_n\}_{8\times1}$
$\langle\mathbf{N}_{An}(x)\rangle_{1\times8}$ $\langle\mathbf{N}_{Bn}(x)\rangle_{1\times8}$ $\langle\mathbf{N}_{Cn}(x)\rangle_{1\times8}$	Exact shape functions defining the axial, circumferential and radial displacements corresponding to mode n, respectively

$\langle \mathbf{S}_{An}(x) \rangle_{1\times 8}$ $\langle \mathbf{S}_{Bn}(x) \rangle_{1\times 8}$ $\langle \mathbf{S}_{Cn}(x) \rangle_{1\times 8}$	Row matrices relating the integration constants vector $\{\mathbf{A}_n\}_{8\times 1}$ to displacement functions $A_n(x)$, $B_n(x)$ and $C_n(x)$, respectively
$\left\{ {}_j^i\mathbf{f}_n \right\}_{8\times 1}$	Contributions to the total force vector of terms that are multiplied by ${}_6^3H$ or ${}_j^iG_n$ in the equation of energy corresponding to mode n
$\left[{}_j^i\mathbf{k}_n \right]_{8\times 8}$	Contribution to the total stiffness matrix of the term multiplied by ${}_j^iH$ or ${}_j^iH_n$ in the equation of energy corresponding to mode n
$\{\mathbf{\Delta}_n\}_{8\times 1}$	Nodal displacement vector corresponding to mode n
Π	Mechanical energy of the system
ν	Poisson's ratio
ρ	Density of the material
$\overline{\eta}_{11}$, $\overline{\eta}_{22}$, $\overline{\eta}_{12}$	Longitudinal, circumferential and shear strain components, respectively

$\bar{\sigma}^{11}$, $\bar{\sigma}^{22}$, $\bar{\sigma}^{12}$	Longitudinal, circumferential and shear stress components, respectively

Appendix 5.A. Coefficients of Boundary and Field Terms

The coefficients of the boundary and field terms in Eq. 5.5 are defined below. We recall that $i=\sqrt{-1}$, $\Phi\left(h/R\right)=\ln\left[\left(2+h/R\right)/\left(2-h/R\right)\right]\Big/\left(h/R\right)$ and n is the circumferential mode number.

$$
{}^{1}_{1}H=-1 \quad , \quad {}^{1}_{2}H_n=-\frac{\nu}{R}in \quad , \quad {}^{1}_{3}H=-\frac{\nu}{R} \quad , \quad {}^{1}_{4}H=\frac{h^2}{12R}
$$

$$
{}^{2}_{1}H_n=-\frac{1-\nu}{2}\frac{1}{R}in \quad , \quad {}^{2}_{2}H=-\frac{1-\nu}{2}\left(1+\frac{h^2}{4R^2}\right) \quad , \quad {}^{2}_{3}H_n=\frac{1-\nu}{2}\frac{h^2}{4R^2}in
$$

$$
{}^{3}_{1}H_n=-\frac{1}{R}\left(\Phi-1\right)\frac{1-\nu}{2}n^2-\rho\bar{\omega}^2\frac{1-\nu^2}{E}\frac{h^2}{12R} \quad , \quad {}^{3}_{2}H=-\frac{h^2}{12R}
$$

$$
{}^{3}_{3}H_n=-\frac{h^2}{12R^2}\left(\frac{3-\nu}{2}\right)in
$$

$$
{}^{3}_{4}H_n=-\left\{\frac{h^2}{12R^2}\frac{3-\nu}{2}+\left(\Phi-1\right)\frac{1-\nu}{2}\right\}n^2+\rho\bar{\omega}^2\frac{1-\nu^2}{E}\frac{h^2}{12}
$$

$$
{}^{3}_{5}H=\frac{h^2}{12} \quad , \quad {}^{3}_{6}H=\frac{1-\nu^2}{Eh}
$$

$$
{}^{4}_{1}H=\frac{h^2}{12R} \quad , \quad {}^{4}_{2}H_n=\frac{h^2}{12R^2}\nu in \quad , \quad {}^{4}_{3}H_n=\frac{h^2}{12R^2}\nu n^2 \quad , \quad {}^{4}_{4}H=-\frac{h^2}{12} \qquad \text{(5.A.1a-q)}
$$

$$
{}^{1}_{1}G_n=-\frac{1}{R^2}\Phi\frac{1-\nu}{2}n^2+\frac{1-\nu^2}{E}\rho\bar{\omega}^2 \quad , \quad {}^{1}_{2}G=1 \quad , \quad {}^{1}_{3}G_n=\frac{1}{R}\frac{1+\nu}{2}in
$$

$$
{}^{1}_{4}G_n=\frac{\nu}{R}-\frac{1}{R}\left(\Phi-1\right)\frac{1-\nu}{2}n^2-\frac{1-\nu^2}{E}\rho\bar{\omega}^2\frac{h^2}{12R} \quad , \quad {}^{1}_{5}G=-\frac{h^2}{12R}
$$

$$
{}^{1}_{6}G=\frac{1-\nu^2}{Eh}
$$

$$ {}^{2}_{1}G_n = \frac{1}{R}\frac{1+\nu}{2} in \quad , \quad {}^{2}_{2}G_n = -\frac{1}{R^2} n^2 + \frac{1-\nu^2}{E}\rho\bar{\omega}^2\left(1+\frac{h^2}{12R^2}\right) $$

$$ {}^{2}_{3}G = \left(1+\frac{h^2}{4R^2}\right)\frac{1-\nu}{2} \quad , \quad {}^{2}_{4}G_n = \frac{1}{R^2} in - \frac{1-\nu^2}{E}\rho\bar{\omega}^2\frac{h^2}{6R^2} in $$

$$ {}^{2}_{5}G_n = -\frac{h^2}{12R^2}\frac{3-\nu}{2} in \quad , \quad {}^{2}_{6}G = \frac{1-\nu^2}{Eh} $$

$$ {}^{3}_{1}G_n = -\frac{\nu}{R} + \frac{1}{R}(\Phi-1)\frac{1-\nu}{2} n^2 + \frac{1-\nu^2}{E}\rho\bar{\omega}^2\frac{h^2}{12R} \quad , \quad {}^{3}_{2}G = \frac{h^2}{12R} $$

$$ {}^{3}_{3}G_n = -\frac{1}{R^2} in + \frac{1-\nu^2}{E}\rho\bar{\omega}^2\frac{h^2}{6R^2} in \quad , \quad {}^{3}_{4}G_n = \frac{h^2}{12R^2}\frac{3-\nu}{2} in $$

$$ {}^{3}_{5}G_n = -\frac{1}{R^2}\Phi + \frac{2}{R^2}(\Phi-1) n^2 - \frac{1}{R^2}(\Phi-1) n^4 + \frac{1-\nu^2}{E}\rho\bar{\omega}^2 + \frac{1-\nu^2}{E}\rho\bar{\omega}^2\frac{h^2}{12R^2} n^2 \quad \text{(5.A.2a-v)} $$

$$ {}^{3}_{6}G_n = \left[\frac{h^2}{12R^2}\frac{3+\nu}{2} + (\Phi-1)\frac{1-\nu}{2}\right] n^2 - \frac{1-\nu^2}{E}\rho\bar{\omega}^2\frac{h^2}{12} $$

$$ {}^{3}_{7}G = -\frac{h^2}{12} \quad , \quad {}^{3}_{8}G = -\frac{1-\nu^2}{Eh} \quad , \quad {}^{3}_{9}G_n = -\frac{1-\nu^2}{EhR} in \quad , \quad {}^{3}_{10}G = \frac{1-\nu^2}{Eh} $$

Since the matrix of coefficients of field equations is symmetric, one has

$$ {}^{2}_{1}G_n = {}^{1}_{3}G_n \quad , \quad {}^{3}_{1}G_n = {}^{1}_{4}G_n \quad , \quad {}^{3}_{2}G = {}^{1}_{5}G \quad , \quad {}^{3}_{3}G_n = {}^{2}_{4}G_n \quad , \quad {}^{3}_{4}G_n = {}^{2}_{5}G_n \qquad (5.A.3) $$

Appendix 5.B. Constants in Characteristic Equations

The coefficients in characteristic equation of the system discussed in sections 5.9 are defined below.

$$
\begin{aligned}
a_n &= \left({}^{1}_{1}G_n\right)\left({}^{2}_{2}G_n\right)\left({}^{3}_{5}G_n\right)-\left({}^{1}_{1}G_n\right)\left({}^{2}_{4}G_n\right)^2 \\
b_n &= \Big[-\left({}^{3}_{5}G_n\right)\left({}^{1}_{3}G_n\right)^2+2\left({}^{1}_{3}G_n\right)\left({}^{1}_{4}G_n\right)\left({}^{2}_{4}G_n\right)-\left({}^{2}_{2}G_n\right)\left({}^{1}_{4}G_n\right)^2-\left({}^{1}_{2}G\right)\left({}^{2}_{4}G_n\right)^2 \\
&\quad -2\left({}^{1}_{1}G_n\right)\left({}^{2}_{5}G_n\right)\left({}^{2}_{4}G_n\right)+\left({}^{1}_{2}G\right)\left({}^{2}_{2}G_n\right)\left({}^{3}_{5}G_n\right)+\left({}^{2}_{3}G\right)\left({}^{1}_{1}G_n\right)\left({}^{3}_{5}G_n\right) \\
&\quad +\left({}^{1}_{1}G_n\right)\left({}^{2}_{2}G_n\right)\left({}^{3}_{6}G_n\right)\Big] \\
c_n &= \Big[-\left({}^{3}_{6}G_n\right)\left({}^{1}_{3}G_n\right)^2+2\left({}^{1}_{3}G_n\right)\left({}^{1}_{4}G_n\right)\left({}^{2}_{5}G_n\right)+2\left({}^{1}_{5}G\right)\left({}^{2}_{4}G_n\right)\left({}^{1}_{3}G_n\right) \\
&\quad -\left({}^{2}_{3}G\right)\left({}^{1}_{4}G_n\right)^2-2\left({}^{1}_{5}G\right)\left({}^{2}_{2}G_n\right)\left({}^{1}_{4}G_n\right)-\left({}^{1}_{1}G_n\right)\left({}^{2}_{5}G_n\right)^2 \\
&\quad -2\left({}^{1}_{2}G\right)\left({}^{2}_{4}G_n\right)\left({}^{2}_{5}G_n\right)+\left({}^{1}_{2}G\right)\left({}^{2}_{3}G\right)\left({}^{3}_{5}G_n\right) \\
&\quad +\left({}^{1}_{2}G\right)\left({}^{2}_{2}G_n\right)\left({}^{3}_{6}G_n\right)+\left({}^{2}_{3}G\right)\left({}^{1}_{1}G_n\right)\left({}^{3}_{6}G_n\right)+\left({}^{3}_{7}G\right)\left({}^{1}_{1}G_n\right)\left({}^{2}_{2}G_n\right)\Big] \\
d_n &= \Big[-\left({}^{2}_{2}G_n\right)\left({}^{1}_{5}G\right)^2+2\left({}^{1}_{5}G\right)\left({}^{1}_{3}G_n\right)\left({}^{2}_{5}G_n\right)-2\left({}^{2}_{3}G\right)\left({}^{1}_{4}G_n\right)\left({}^{1}_{5}G\right)-\left({}^{3}_{7}G\right)\left({}^{1}_{3}G_n\right)^2 \\
&\quad -\left({}^{1}_{2}G\right)\left({}^{2}_{5}G_n\right)^2+\left({}^{1}_{2}G\right)\left({}^{2}_{3}G\right)\left({}^{3}_{6}G_n\right)+\left({}^{1}_{2}G\right)\left({}^{3}_{7}G\right)\left({}^{2}_{2}G_n\right)+\left({}^{2}_{3}G\right)\left({}^{3}_{7}G\right)\left({}^{1}_{1}G_n\right)\Big] \\
e_n &= -\left({}^{1}_{5}G\right)^2\left({}^{2}_{3}G\right)+\left({}^{1}_{2}G\right)\left({}^{2}_{3}G\right)\left({}^{3}_{7}G\right)
\end{aligned}
\qquad \text{(5.B.1a-e)}
$$

Appendix 5.C. Entries of Stiffness Matrix and Force Vector

5.C.1. Stiffness Matrix

The entries of the stiffness matrix contribution corresponding to mode n result from the expansion of the nth terms in the first summation of Eq. 5.5. For each mode n, there are 12 contributions resulting from the matrix multiplication

$$\left[\left\langle \delta A_{-n}(\bar{x}) \quad \delta B_{-n}(\bar{x}) \quad \delta C_{-n}(\bar{x}) \quad \delta C'_{-n}(\bar{x}) \right\rangle \begin{bmatrix} {}^1_1HD & {}^1_2H_n & {}^1_3H + {}^1_4HD^2 \\ {}^2_1H_n & {}^2_2HD & {}^2_3H_nD \\ {}^3_1H_n + {}^3_2HD^2 & {}^3_3H_nD & {}^3_4H_nD + {}^3_5HD^3 \\ {}^4_1HD & {}^4_2H_n & {}^4_3H_n + {}^4_4HD^2 \end{bmatrix} \begin{Bmatrix} A_n(x) \\ B_n(x) \\ C_n(x) \end{Bmatrix}\right]_0^L$$

The first of the 12 terms is

$$\begin{aligned} \left[{}^1_1H\delta\left(A_{-n}(x)\right)A'_n(x)\right]_0^L &= \left[{}^1_1H\left(\delta\{\boldsymbol{\Delta}_{-n}\}^T_{1\times 8}\left\langle \mathbf{N}_{\mathbf{A}-n}(x)\right\rangle^T_{8\times 1}\right)\left(\left\langle \mathbf{N}'_{\mathbf{A}n}(x)\right\rangle_{1\times 8}\{\boldsymbol{\Delta}_n\}_{8\times 1}\right)\right]_0^L \\ &= \delta\{\boldsymbol{\Delta}_{-n}\}^T_{1\times 8}\left[{}^1_1H\left\langle \mathbf{N}_{\mathbf{A}-n}(x)\right\rangle^T_{8\times 1}\left\langle \mathbf{N}'_{\mathbf{A}n}(x)\right\rangle_{1\times 8}\right]_0^L\{\boldsymbol{\Delta}_n\}_{8\times 1} \\ &= \delta\{\boldsymbol{\Delta}_{-n}\}^T_{1\times 8}\left[{}^1_1\mathbf{k}_n\right]_{8\times 8}\{\boldsymbol{\Delta}_n\}_{8\times 1} \end{aligned}$$

where

$$\left[{}^1_1\mathbf{k}_n\right]_{8\times 8} = \left[{}^1_1H\left\langle \mathbf{N}_{\mathbf{A}-n}(x)\right\rangle^T_{8\times 1}\left\langle \mathbf{N}'_{\mathbf{A}n}(x)\right\rangle_{1\times 8}\right]_0^L$$

In a similar manner

$$\left[{}^1_2\mathbf{k}_n\right]_{8\times 8} = \left[{}^1_2H_n\left\langle \mathbf{N}_{\mathbf{A}-n}(x)\right\rangle^T_{8\times 1}\left\langle \mathbf{N}_{\mathbf{B}n}(x)\right\rangle_{1\times 8}\right]_0^L$$

$$\left[{}^1_3\mathbf{k}_n\right]_{8\times 8} = \left[{}^1_3H \quad \left\langle \mathbf{N}_{\mathbf{A}-n}(x)\right\rangle^T_{8\times 1}\left\langle \mathbf{N}_{\mathbf{C}n}(x)\right\rangle_{1\times 8}\right]_0^L$$

$$\left[{}^1_4\mathbf{k}_n\right]_{8\times 8} = \left[{}^1_4H \quad \left\langle \mathbf{N}_{\mathbf{A}-n}(x)\right\rangle^T_{8\times 1}\left\langle \mathbf{N}''_{\mathbf{C}n}(x)\right\rangle_{1\times 8}\right]_0^L$$

$$\left[{}^{2}_{1}\mathbf{k}_n \right]_{8\times 8} = \left[{}^{2}_{1}H_n \left\langle \mathbf{N}_{\mathbf{B}-n}(x) \right\rangle^{T}_{8\times 1} \left\langle \mathbf{N}_{\mathbf{A}n}(x) \right\rangle_{1\times 8} \right]_0^L$$

$$\left[{}^{2}_{2}\mathbf{k}_n \right]_{8\times 8} = \left[{}^{2}_{2}H \left\langle \mathbf{N}_{\mathbf{B}-n}(x) \right\rangle^{T}_{8\times 1} \left\langle \mathbf{N}'_{\mathbf{B}n}(x) \right\rangle_{1\times 8} \right]_0^L$$

$$\left[{}^{2}_{3}\mathbf{k}_n \right]_{8\times 8} = \left[{}^{2}_{3}H_n \left\langle \mathbf{N}_{\mathbf{B}-n}(x) \right\rangle^{T}_{8\times 1} \left\langle \mathbf{N}'_{\mathbf{C}n}(x) \right\rangle_{1\times 8} \right]_0^L$$

$$\left[{}^{3}_{1}\mathbf{k}_n \right]_{8\times 8} = \left[{}^{3}_{1}H_n \left\langle \mathbf{N}_{\mathbf{C}-n}(x) \right\rangle^{T}_{8\times 1} \left\langle \mathbf{N}_{\mathbf{A}n}(x) \right\rangle_{1\times 8} \right]_0^L$$

$$\left[{}^{3}_{2}\mathbf{k}_n \right]_{8\times 8} = \left[{}^{3}_{2}H \left\langle \mathbf{N}_{\mathbf{C}-n}(x) \right\rangle^{T}_{8\times 1} \left\langle \mathbf{N}''_{\mathbf{A}n}(x) \right\rangle_{1\times 8} \right]_0^L$$

$$\left[{}^{3}_{3}\mathbf{k}_n \right]_{8\times 8} = \left[{}^{3}_{3}H_n \left\langle \mathbf{N}_{\mathbf{C}-n}(x) \right\rangle^{T}_{8\times 1} \left\langle \mathbf{N}'_{\mathbf{B}n}(x) \right\rangle_{1\times 8} \right]_0^L$$

$$\left[{}^{3}_{4}\mathbf{k}_n \right]_{8\times 8} = \left[{}^{3}_{4}H_n \left\langle \mathbf{N}_{\mathbf{C}-n}(x) \right\rangle^{T}_{8\times 1} \left\langle \mathbf{N}'_{\mathbf{C}n}(x) \right\rangle_{1\times 8} \right]_0^L$$

$$\left[{}^{3}_{5}\mathbf{k}_n \right]_{8\times 8} = \left[{}^{3}_{5}H \left\langle \mathbf{N}_{\mathbf{C}-n}(x) \right\rangle^{T}_{8\times 1} \left\langle \mathbf{N}'''_{\mathbf{C}n}(x) \right\rangle_{1\times 8} \right]_0^L$$

$$\left[{}^{4}_{1}\mathbf{k}_n \right]_{8\times 8} = \left[{}^{4}_{1}H \left\langle \mathbf{N}'_{\mathbf{C}-n}(x) \right\rangle^{T}_{8\times 1} \left\langle \mathbf{N}'_{\mathbf{A}n}(x) \right\rangle_{1\times 8} \right]_0^L$$

$$\left[{}^{4}_{2}\mathbf{k}_n \right]_{8\times 8} = \left[{}^{4}_{2}H_n \left\langle \mathbf{N}'_{\mathbf{C}-n}(x) \right\rangle^{T}_{8\times 1} \left\langle \mathbf{N}_{\mathbf{B}n}(x) \right\rangle_{1\times 8} \right]_0^L$$

$$\left[{}^{4}_{3}\mathbf{k}_n \right]_{8\times 8} = \left[{}^{4}_{3}H_n \left\langle \mathbf{N}'_{\mathbf{C}-n}(x) \right\rangle^{T}_{8\times 1} \left\langle \mathbf{N}_{\mathbf{C}n}(x) \right\rangle_{1\times 8} \right]_0^L$$

$$\left[{}^{4}_{4}\mathbf{k}_n \right]_{8\times 8} = \left[{}^{4}_{4}H \left\langle \mathbf{N}'_{\mathbf{C}-n}(x) \right\rangle^{T}_{8\times 1} \left\langle \mathbf{N}''_{\mathbf{C}n}(x) \right\rangle_{1\times 8} \right]_0^L \qquad \text{(5.C.1a-p)}$$

The total stiffness matrix contribution to mode n is then

$$\left[\mathbf{K}_n\right]_{8\times 8} = \frac{2\pi EhR}{1-\nu^2} \sum_{i=1}^{i=3} \sum_{j=1}^{j=4} \left[{}^{i}_{j}\mathbf{k}_n \right]_{8\times 8} \qquad \text{(5.C.2)}$$

5.C.2. Force Vector

The force vector results from the second term and revolution of the second integral term in Eq. 5.5. The second term of Eq. 5.5 which is the only non-homogenous part of the boundary terms can be expressed as

$$\left[{}_6^3H\delta C_{-n}(x)\, f_n^{xw}(x) \right]_0^L = \left[{}_6^3H \left(\delta \{\boldsymbol{\Delta}_{-n}\}_{1\times 8}^T \left\langle \mathbf{N}_{\mathbf{C}-n}(x) \right\rangle_{8\times 1}^T \right) f_n^{xw}(x) \right]_0^L$$

$$= \left[\delta \{\boldsymbol{\Delta}_{-n}\}_{1\times 8}^T \left({}_6^3H \left\langle \mathbf{N}_{\mathbf{C}-n}(x) \right\rangle_{8\times 1}^T f_n^{xw}(x) \right) \right]_0^L$$

$$= \delta \{\boldsymbol{\Delta}_{-n}\}_{1\times 8}^T \left\{ {}_6^3\mathbf{f}_n \right\}_{8\times 1}$$

where

$$\left\{ {}_6^3\mathbf{f}_n \right\}_{8\times 1} = \left[{}_6^3H \left\langle \mathbf{N}_{\mathbf{C}-n}(x) \right\rangle_{8\times 1}^T f_n^{xw}(x) \right]_0^1 \tag{5.C.3}$$

The first integral of the fourth summation in Eq. 5.5 is

$$\int_0^L {}_6^1G\delta A_{-n}(x)\, f_n^{xu}(x)\, d\overline{x} = \int_0^L {}_6^1G \left(\delta \{\boldsymbol{\Delta}_{-n}\}_{1\times 8}^T \left\langle \mathbf{N}_{\mathbf{A}-n}(x) \right\rangle_{8\times 1}^T \right) f_n^{xu}(x)\, dx$$

$$= \delta \{\boldsymbol{\Delta}_{-n}\}_{1\times 8}^T \left\{ {}_6^1\mathbf{f}_n \right\}_{8\times 1}$$

where

$$\left\{ {}_6^1\mathbf{f}_n \right\}_{8\times 1} = {}_6^1G \int_0^L \left\langle \mathbf{N}_{\mathbf{A}-n}(x) \right\rangle_{8\times 1}^T f_n^{xu}(x)\, dx$$

In the same manner other similar terms yield

$$\left\{ {}_6^2\mathbf{f}_n \right\}_{8\times 1} = {}_6^2G \int_0^L \left\langle \mathbf{N}_{\mathbf{B}-n}(x) \right\rangle_{8\times 1}^T f_n^{sv}(x)\, dx$$

$$\left\{ {}_8^3\mathbf{f}_n \right\}_{8\times 1} = {}_8^3G_n \int_0^L \left\langle \mathbf{N}_{\mathbf{C}-n}(x) \right\rangle_{8\times 1}^T f_n^{xw\prime}(x)\, dx$$

$$\left\{ {}_9^3\mathbf{f}_n \right\}_{8\times 1} = {}_9^3G_n \int_0^L \left\langle \mathbf{N}_{\mathbf{C}-n}(x) \right\rangle_{8\times 1}^T f_n^{sw}(x)\, dx$$

$$\left\{ {}_{10}^{3}\mathbf{f}_n \right\}_{8\times 1} = {}_{10}^{3}G \int_0^L \left\langle \mathbf{N}_{\mathbf{C}-n}(x) \right\rangle_{8\times 1}^T f_n^{zw}(x)\, dx \qquad \text{(5.C.4a-e)}$$

The summation of Eqs. 5.C.3 and 5.C.4a-e yields the force vector

$$\left\{ \mathbf{F}_n \right\}_{8\times 1} = \frac{2\pi EhR}{1-\nu^2} \left\{ {}_{6}^{3}\mathbf{f}_n \right\} + \frac{2\pi EhR}{1-\nu^2} \left(\left\{ {}_{6}^{1}\mathbf{f}_n \right\} + \left\{ {}_{6}^{2}\mathbf{f}_n \right\} + \left\{ {}_{8}^{3}\mathbf{f}_n \right\} + \left\{ {}_{9}^{3}\mathbf{f}_n \right\} + \left\{ {}_{10}^{3}\mathbf{f}_n \right\} \right) \qquad \text{(5.C.5)}$$

Appendix 5.D. Matlab Code for Example 1

```
%%%%%%%%%%%%%%%%%%%%%%%%%%%%%%%%%%%%%%%%%%%%%%%%%%%%%%%%%%%%%%%%%%%%%%%%%%%%
%%%%%%%%%%%%%%%%%%%%%%%%%%% Initialization %%%%%%%%%%%%%%%%%%%%%%%%%%%%%%%%%
%%%%%%%%%%%%%%%%%%%%%%%%%%%%%%%%%%%%%%%%%%%%%%%%%%%%%%%%%%%%%%%%%%%%%%%%%%%%

clc
clear all
close all
format short eng

%%%%%%%%%%%%%%%%%%%%%%%%%%%%%%%%%%%%%%%%%%%%%%%%%%%%%%%%%%%%%%%%%%%%%%%%%%%%
%%%%%%%%%%%%%%%%%%%%%%%%%%%% Input %%%%%%%%%%%%%%%%%%%%%%%%%%%%%%%%%%%%%%%%%
%%%%%%%%%%%%%%%%%%%%%%%%%%%%%%%%%%%%%%%%%%%%%%%%%%%%%%%%%%%%%%%%%%%%%%%%%%%%

%%%-------------------------Material properties-------------------------
%%%     hS is the vector of the thicknesses of the cylinders
%%%     RS is the vector of the radii of the cylindera
%%%     LS is the vector of the lengths of the cylindera
%%%     v is the Poisson's ratio
%%%     E is the modulus of elasticity
%%%     Ro is the mass density
%%%     omega is the angular frequency of the excitation
%%%     N is the number of modes that should be considered in the
%%%      analysis
%%%---------------------------------------------------------------------
NE=2
section=201
hS=[0.004,.003,0,0,0]
RS=[0.2,0.2,0,0,0]
LS=[3,2,0,0,0]
nu=0.3
E=200e9*(1)
Ro=7850

N=10

omega=10*2*pi


%%%-------------------------Boundary conditions-------------------------
%%%     The order of the boundaries:
%%%     BoundaryConditions=[du0, dv0, dw0, dw10, du1, dv1, dw1, dw11]
%%%     du0 and du1 denote the axial B.C.s at the begining and the end of
%%%         the beam, respectively.
%%%     dv0 and dv1 denote the circumferential B.C. at the begining and
%%%          endof the beam, respectively.
%%%     dw0 and dw1 denote the radial B.C. at the begining and end of the
%%%         beam, respectively.
%%%     dw10 and dw11 denote the derivative of the radial B.C. with
%%%         respectto axial coordinate at the begining and the end of
%%%         the beam.
%%%     0 denotes clamped boundary
%%%     1 denotes free boundary
```

```
%%%-------------------------------------------------------------------------
BoundaryConditions=[0,0,0,0,1,1,1,1,1,1,1,1,1,1,1,1,1,1,1,1,1,1,1,1];


%% %%%%%%%%%%%%%%%%%%%%%%%%%%%%%%%%%%%%%%%%%%%%%%%%%%%%%%%%%%%%%%%%%%%%%%%
%%%%%%%%%%%%%%%%%%%%%%%%%%%%%% Load decomposition %%%%%%%%%%%%%%%%%%%%%%
%%%%%%%%%%%%%%%%%%%%%%%%%%%%%%%%%%%%%%%%%%%%%%%%%%%%%%%%%%%%%%%%%%%%%%%%%

%%%------------------ Loads in terms of ( x , s , z ) -------------------
%%%     x denotes the nondimentional axial coordinate variates
%%%         from 0 to 1
%%%     s denotes the nondimentional circumferential coordinate varies
%%%         from 0 to 2*pi
%%%     z denotes the dimansional radial coordinate varies
%%%         from -h/2 to h/2
%%%-------------------------------------------------------------------------

%%%-------------------------------------------------------------------------
%%%     pxx is the x component of the axial load function
%%%     pxs is the s component of the axial load function
%%%     pxz is the z component of the axial load function
%%%
%%%     psx is the x component of the circumferential load function
%%%     pss is the s component of the circumferential load function
%%%     psz is the z component of the circumferential load function
%%%
%%%     pzx is the x component of the radial load function
%%%     pzs is the s component of the radial load function
%%%     pzz is the z component of the radial load function
%%%
%%%     AppliedForcesOrSupportExcitation determines if we have applied
%%%     forces support excitation. 1 is for applied forces and 0 for
%%%     support excitation.
%%%-------------------------------------------------------------------------
syms x s z

AppliedForcesOrSupportExcitation=1;

BoundaryDisplacements=[0,0,0,0,0,0,0,0,0,0,0,0,0,0,0,0,0,0,0,0,0,0,0,0];

Pq=1000

pxxS=[0,0,0,0];
pxsS=[0,0,0,0,0];
pxzS=[0,0,0,0,0];

psxS=[0,-Pq*sin(pi/6)*2*dirac(x-LS(2)),0,0];
pssS=[0,dirac(s-RS(2)*11*pi/6),0,0];
pszS=[0,dirac(z),0,0,0];

pzxS=[0,-Pq*cos(pi/6)*2*dirac(x-LS(2)),0,0];
pzsS=[0,dirac(s-RS(2)*11*pi/6),0,0];
pzzS=[0,dirac(z),0,0,0];


%------------------- Nodal forces -----------------------------------------
FxsS=[0,0,0,0,0,0];
```

```
FssS=[0,0,0,0,0,0];
FzsS=[0,0,0,0,0,0];
FmsS=[0,0,0,0,0,0];



%-------------------------------------------------------------------------
% This should be mentioned here that Heaviside step function in MATLAB
% yields 1/2 for x=0. Also we know that the integral of Dirac delta
% functions is in term of Heaviside step function. When we are using
% Diracdelta function in load distributions, just in the boundaries of
% theintegration range, it applies a 1/2 factor in corresponding integral
% terms. Thus, an additional factor of 2 should be applied to the
% corresponding term.
%-------------------------------------------------------------------------

%%%----- Prescribed Boundary Conditions ---------------------------------
ConS=zeros(4*(NE+1),2*N+1);           % Determined non-zero displacments

sizeBCs=size(BoundaryConditions);

R=RS(1);
for i=1:4*(NE+1)
    if BoundaryConditions(i)~=0
        if BoundaryDisplacements(i)~=0
            fn=BoundaryDisplacements(i);
            for n=-N:N
                ConS(i,N+n+1)= 1/(2*pi*R) * int(fn * exp(-1i*n*s/R),...
                    s,0,2*pi*R);
            end
        end
    end
end

%%%----- Loads in terms of (x,s) after integration along z axis and then
%%%----- decomposing into Fourier series --------------------------------

CzxuS=  zeros(1,NE);
CzxwS=  zeros(1,NE);
Czxw1S= zeros(1,NE);
CzsvS=  zeros(1,NE);
CzswS=  zeros(1,NE);
Czsw2S= zeros(1,NE);
CzzwS=  zeros(1,NE);

Cnxu= zeros(2*N+1,NE);
Cnxw= zeros(2*N+1,NE);
Cnxw1=zeros(2*N+1,NE);
Cnsv= zeros(2*N+1,NE);
Cnsw= zeros(2*N+1,NE);
Cnsw2=zeros(2*N+1,NE);
Cnzw= zeros(2*N+1,NE);

for ne=1:NE

    h=hS(1,ne);
    R=RS(1,ne);
```

```
    L=LS(1,ne);

    pxs=pxsS(1,ne);
    pxz=pxzS(1,ne);

    pss=pssS(1,ne);
    psz=pszS(1,ne);

    pzs=pzsS(1,ne);
    pzz=pzzS(1,ne);

    CzxuS(1,ne)=  int(pxz*(1+z/R),z,-h/2,h/2);
    CzxwS(1,ne)=  int(pxz*(-z)*(1+z/R),z,-h/2,h/2);
    Czxw1S(1,ne)= CzxwS(ne);
    CzsvS(1,ne)=  int(psz*(1+z/R)^2,z,-h/2,h/2);
    CzswS(1,ne)=  int(psz*(-z)*(1+z/R),z,-h/2,h/2);
    Czsw2S(1,ne)= CzswS(ne);
    CzzwS(1,ne)=  int(pzz*(1+z/R),z,-h/2,h/2);


    for n=-N:N
        Cnxu(N+n+1,ne)=    1/(2*pi*R) * int(pxs * exp(-1i*n*s/R),s,0,...
                              2*pi*R);
        Cnxw(N+n+1,ne)=    1/(2*pi*R) * int(pxs * exp(-1i*n*s/R),s,0,...
                              2*pi*R);
        Cnxw1(N+n+1,ne)=   1/(2*pi*R) * int(pxs * exp(-1i*n*s/R),s,0,...
                              2*pi*R);
        Cnsv(N+n+1,ne)=    1/(2*pi*R) * int(pss * exp(-1i*n*s/R),s,0,...
                              2*pi*R);
        Cnsw(N+n+1,ne)=    1/(2*pi*R) * int(pss * exp(-1i*n*s/R),s,0,...
                              2*pi*R);
        Cnsw2(N+n+1,ne)=   1/(2*pi*R) * int(pss * exp(-1i*n*s/R),s,0,...
                              2*pi*R);
        Cnzw(N+n+1,ne)=    1/(2*pi*R) * int(pzs * exp(-1i*n*s/R),s,0,...
                              2*pi*R);
    end
end


Dnx= zeros(2*N+1,NE+1);
Dns= zeros(2*N+1,NE+1);
Dnz= zeros(2*N+1,NE+1);
Dnm= zeros(2*N+1,NE+1);

for nN=1:NE+1

    fxs=FxsS(1,nN);
    fss=FssS(1,nN);
    fzs=FzsS(1,nN);
    fms=FmsS(1,nN);

    for n=-N:N
        Dnx(N+n+1,nN)= 1/(2*pi*R) * int(fxs * exp(-1i*n*s/R),s,0,2*pi*R);
        Dns(N+n+1,nN)= 1/(2*pi*R) * int(fss * exp(-1i*n*s/R),s,0,2*pi*R);
        Dnz(N+n+1,nN)= 1/(2*pi*R) * int(fzs * exp(-1i*n*s/R),s,0,2*pi*R);
        Dnm(N+n+1,nN)= 1/(2*pi*R) * int(fms * exp(-1i*n*s/R),s,0,2*pi*R);
    end
```

```
end


%%%------Determining the modes which have contribution to the solution---
modecontribution=zeros(1,2*N+1);

if AppliedForcesOrSupportExcitation==0;
    for n=-N:N
        for nn=1:4*(NE+1)
            if ConS(nn,N+n+1)~=0
                modecontribution(N+n+1)=1;
            end
        end
    end
else
    for n=-N:N
        for ne=1:NE
            if (Cnxu(N+n+1,ne)~=0) || (Cnxw1(N+n+1,ne)~=0) ||...
                   (Cnsv(N+n+1,ne)~=0) ||  (Cnsw2(N+n+1,ne)~=0) ||...
                   (Cnzw(N+n+1,ne)~=0)
                modecontribution(N+n+1)=1;
            end
        end
        for nN=1:NE+1
            if (Dnx(N+n+1,nN)~=0) || (Dns(N+n+1,nN)~=0) ||...
                   (Dnz(N+n+1,nN)~=0) || (Dnm(N+n+1,nN)~=0)
                modecontribution(N+n+1)=1;
            end
        end
    end
end

clear s z
display(modecontribution)


%% %%%%
```

```
G12 =1;
Gn13=1/R*(1+nu)/2*1i*n;
Gn14=nu/R - 1/R*(FI - 1)*(1-nu)/2*n^2 - lan*h^2/12/R;
G15 =-h^2/12/R;

Gn21=1/R*(1+nu)/2*1i*n;
Gn22=-1/R^2*n^2 + lan*(1+h^2/12/R^2) ;
G23 =(1+h^2/4/R^2)*(1-nu)/2;
Gn24=1/R^2*1i*n - lan*h^2/6/R^2*1i*n;
Gn25=-h^2/12/R^2*(3-nu)/2*1i*n;

Gn31=nu/R - 1/R*(FI - 1)*(1-nu)/2*n^2 - lan*h^2/12/R;
G32 =-h^2/12/R;
Gn33=1/R^2*1i*n - lan*h^2/6/R^2*1i*n;
Gn34=-h^2/12/R^2*(3-nu)/2*1i*n;
Gn35=1/R^2*FI - 2/R^2*(FI-1)*n^2 + 1/R^2*(FI-1)*n^4 - lan...
       - lan*h^2/12/R^2*n^2;
Gn36=-(h^2/12/R^2*(3+nu)/2 + (FI-1)*(1-nu)/2)*n^2 +...
       lan*h^2/12;
G37 =h^2/12;

if n==0
    % Finding the roots for axial and radial displacements
    % for which the differential equations are coupled
    % together
    c0=(Gn11*Gn35);
    c2=(Gn11*Gn36-Gn14*Gn31+G12*Gn35);
    c4=(G12*Gn36+Gn11*G37-Gn14*G32-G15*Gn31);
    c6=(G12*G37-G15*G32);
    c=subs([c6,c4,c2,c0]);
    M=roots(c);
    for i=1:3
        mr(2*i-1,N+n+1,ne)=sqrt(M(i));
        mr(2*i,N+n+1,ne)= -sqrt(M(i));
    end
    % Finding the other two roots for circumferential
    % displacement for which the differential equation is
    % uncoupled from the other two displacements
    mr(7,N+n+1,ne)=sqrt(-Gn22/G23);
    mr(8,N+n+1,ne)= -sqrt(-Gn22/G23);
else
    c0=(-Gn11*Gn24*Gn33+Gn11*Gn22*Gn35);
    c2=(G12*Gn22*Gn35-G12*Gn24*Gn33-Gn31*Gn14*Gn22-...
            Gn11*Gn24*Gn34+Gn11*G23*Gn35+...
            Gn31*Gn13*Gn24+Gn11*Gn22*Gn36-...
            Gn21*Gn13*Gn35+Gn21*Gn14*Gn33-...
            Gn11*Gn25*Gn33);
    c4=(G12*G23*Gn35-G12*Gn24*Gn34-Gn11*Gn25*Gn34+...
            Gn11*Gn22*G37+G12*Gn22*Gn36+Gn21*G15*Gn33-...
            Gn21*Gn13*Gn36-G32*Gn14*Gn22-G12*Gn25*Gn33+...
            Gn11*G23*Gn36+G32*Gn13*Gn24-Gn31*Gn14*G23-...
            Gn31*G15*Gn22+Gn31*Gn13*Gn25+Gn21*Gn14*Gn34);
    c6=(G12*Gn22*G37+Gn11*G23*G37-Gn31*G15*G23+...
            G12*G23*Gn36+G32*Gn13*Gn25+Gn21*G15*Gn34-...
            G32*Gn14*G23-G12*Gn25*Gn34-...
            Gn21*Gn13*G37-G32*G15*Gn22);
    c8=(-G32*G15*G23+G12*G23*G37);
```

```
                % For modes n~1 , the differential equations for all
                % three displacements are coupled
                c=[c8,c6,c4,c2,c0];
                M=roots(c);
                for i=1:4
                    mr(2*i-1,N+n+1,ne)=sqrt(M(i));
                    mr(2*i,N+n+1,ne)=-sqrt(M(i));
                end
            end
            if n~=0 %%%--------------------------- n~0 -------------
                for j=1:8
                    m=mr(j,N+n+1,ne);
                    k11=Gn11+G12*m^2;
                    k12=Gn13*m;
                    k13=Gn14*m+G15*m^3;
                    k21=Gn21*m;
                    k22=Gn22+G23*m^2;
                    k23=Gn24+Gn25*m^2;
                    k31=Gn31*m+G32*m^3;
                    k32=Gn33+Gn34*m^2;
                    k33=Gn35+Gn36*m^2+G37*m^4;
                    Ab(j,N+n+1,ne)=1;
                    Bb(j,N+n+1,ne)=-(k33*k21-k32*k31)/(k22*k33-k23*k32);
                    Cb(j,N+n+1,ne)=-(-k23*k21+k22*k31)/(k22*k33-k23*k32);
                end
            else    %%%----------------------------n=0-----------------
                for j=1:6
                    m=mr(j,N+n+1,ne);
                    k11=Gn11+G12*m^2;
                    k12=Gn14*m+G15*m^3;
                    k21=Gn31*m+G32*m^3;
                    k22=Gn35+Gn36*m^2+G37*m^4;
                    Ab(j,N+n+1,ne)=1;
                    Bb(j,N+n+1,ne)=0;
                    Cb(j,N+n+1,ne)=-k11/k12;
                end
                Ab(7,N+n+1,ne)=0;
                Ab(8,N+n+1,ne)=0;
                Bb(7,N+n+1,ne)=1;
                Bb(8,N+n+1,ne)=1;
                Cb(7,N+n+1,ne)=0;
                Cb(8,N+n+1,ne)=0;
            end
        end
    end
end
mr

%%%%%%%%%%%%%%%%%%%%%%%%%%%%%%%%%%%%%%%%%%%%%%%%%%%%%%%%%%%%%%%%%%%%%%%%%%%%%%%%
%%%%%%%%%%%%%%%%%%%%%%%%%%%% Finite element %%%%%%%%%%%%%%%%%%%%%%%%%%%%
%%%%%%%%%%%%%%%%%%%%%%%%%%%%%%%%%%%%%%%%%%%%%%%%%%%%%%%%%%%%%%%%%%%%%%%%%%%%%%%%

LniS=zeros(8,8,2*N+1,NE);
LnjS=zeros(8,8,2*N+1,NE);

invLniS=zeros(8,8,2*N+1,NE);
invLnjS=zeros(8,8,2*N+1,NE);
```

```
BB1=zeros(8,NE);
BB2=zeros(8,NE);
BB3=zeros(8,NE);
BB4=zeros(8,NE);

FFA0fxun=  zeros(8,1);
FFB0fsvn=  zeros(8,1);
FFC0fxw1n= zeros(8,1);
FFC0fsw2n= zeros(8,1);
FFC0fzwn=  zeros(8,1);
FFC0fxwn=  zeros(8,1);

ii=0;
for i=1:4*(NE+1)
    if BoundaryConditions(1,i)~=0
        ii=ii+1;
    end
end
Bc=zeros(ii,ii,2*N+1);
Dc=zeros(ii,1,2*N+1);
Fc=zeros(ii,1,2*N+1);

Anj=zeros(8,2*N+1,NE);

BS=zeros(4*(NE+1),4*(NE+1),2*N+1);
FS=zeros(4*(NE+1),1,2*N+1);
DS=zeros(8,2*N+1,NE);
for n=-N:N
    if modecontribution(1,N+n+1)==1
        for ne=1:NE

            h=hS(1,ne);
            R=RS(1,ne);
            L=LS(1,ne);

            FI= R/h*log((2*R+h)/(2*R-h));
            lan=Ro*omega^2*(1-nu^2)/E;

            pxx=pxxS(1,ne);
            pxx1=diff(pxx,x);
            psx=psxS(1,ne);
            pzx=pzxS(1,ne);


            Czxu=  CzxuS(1,ne);
            Czxw=  CzxwS(1,ne);
            Czxw1= Czxw1S(1,ne);
            Czsv=  CzsvS(1,ne);
            Czsw=  CzswS(1,ne);
            Czsw2= Czsw2S(1,ne);
            Czzw=  CzzwS(1,ne);

            H11 =-1;
            Hn12 =-nu/R*1i*n;
            H13 =-nu/R;
            H14 =h^2/12/R;
```

```
Hn21 =-(1-nu)/2/R*1i*n;
H22 =-(1-nu)/2*(1+h^2/4/R^2);
Hn23 =(1-nu)/2*h^2/4/R^2*1i*n;
Hn31 =-1/R*(FI - 1)*(1-nu)/2*n^2 - lan*h^2/12/R;
H32 =-h^2/12/R;
Hn33 =-h^2/12/R^2*(3-nu)/2*1i*n;
Hn34 =-(h^2/12/R^2*(3-nu)/2 + (FI - 1)*(1-nu)/2)*n^2+...
           lan*h^2/12;
H35 =h^2/12;
H36 =(1-nu^2)/E/h;
H41 =h^2/12/R;
Hn42 =h^2/12/R^2*nu*1i*n;
Hn43 =h^2/12/R^2*nu*n^2;
H44 =-h^2/12;

G16 =(1-nu^2)/E/h;
G26 =(1-nu^2)/E/h;
G38 =-(1-nu^2)/E/h;
Gn39=-(1-nu^2)/E/h/R*1i*n;
G310=(1-nu^2)/E/h;


Cnxun=  Cnxu(N+n+1,ne);
Cnsvn=  Cnsv(N+n+1,ne);
Cnzwn=  Cnzw(N+n+1,ne);
Cnxwn=  Cnxw(N+n+1,ne);
Cnxw1n= Cnxw1(N+n+1,ne);
Cnsw2n= Cnsw2(N+n+1,ne);

for i=1:8
    mni=mr(i,N-n+1,ne);
    emni=exp(mni*L);
    Abni=Ab(i,N-n+1,ne);
    Bbni=Bb(i,N-n+1,ne);
    Cbni=Cb(i,N-n+1,ne);
    LniS(1,i,N-n+1,ne)=Abni;
    LniS(2,i,N-n+1,ne)=Bbni;
    LniS(3,i,N-n+1,ne)=Cbni;
    LniS(4,i,N-n+1,ne)=mni*Cbni;
    LniS(5,i,N-n+1,ne)=emni*Abni;
    LniS(6,i,N-n+1,ne)=emni*Bbni;
    LniS(7,i,N-n+1,ne)=emni*Cbni;
    LniS(8,i,N-n+1,ne)=mni*emni*Cbni;

    mnj=mr(i,N+n+1,ne);
    emnj=exp(mnj*L);
    Abnj=Ab(i,N+n+1,ne);
    Bbnj=Bb(i,N+n+1,ne);
    Cbnj=Cb(i,N+n+1,ne);
    LnjS(1,i,N+n+1,ne)=Abnj;
    LnjS(2,i,N+n+1,ne)=Bbnj;
    LnjS(3,i,N+n+1,ne)=Cbnj;
    LnjS(4,i,N+n+1,ne)=mnj*Cbnj;
    LnjS(5,i,N+n+1,ne)=emnj*Abnj;
    LnjS(6,i,N+n+1,ne)=emnj*Bbnj;
    LnjS(7,i,N+n+1,ne)=emnj*Cbnj;
    LnjS(8,i,N+n+1,ne)=mnj*emnj*Cbnj;
```

```
            end
            UnitDiag=ones(1,8);
            I=diag(UnitDiag);
            invLniS(:,:,N-n+1,ne)=LniS(:,:,N-n+1,ne)\I;
            invLnjS(:,:,N+n+1,ne)=LnjS(:,:,N+n+1,ne)\I;

%             invLni=Lni(:,:,ne)\I;
%             invLnj=Lnj(:,:,ne)\I;

            invLni=invLniS(:,:,N-n+1,ne);
            invLnj=invLnjS(:,:,N+n+1,ne);
            TinvLni=invLni.';

            %%% Calculating the displacements--------------------

            for ii=1:8
                mni=mr(ii,N-n+1,ne);
                emni=exp(mni*L);
                Abni=Ab(ii,N-n+1,ne);
                Bbni=Bb(ii,N-n+1,ne);
                Cbni=Cb(ii,N-n+1,ne);
                for j=1:8
                    mnj=mr(j,N+n+1,ne);
                    emnj=exp(mnj*L);
                    Abnj=Ab(j,N+n+1,ne);
                    Bbnj=Bb(j,N+n+1,ne);
                    Cbnj=Cb(j,N+n+1,ne);

                    Fbnij=(exp((mni+mnj)*L)-1);

                    BB1(ii,j)=Abni*((H11*mnj^1)*Abnj + (Hn12)*Bbnj +...
                                    (H13 + H14*mnj^2)*Cbnj)*Fbnij;
                    BB2(ii,j)=Bbni*((Hn21)*Abnj + (H22*mnj^1)*Bbnj +...
                                    (Hn23*mnj^1)*Cbnj)*Fbnij;
                    BB3(ii,j)=Cbni*((Hn31+H32*mnj^2)*Abnj +...
                                    (Hn33*mnj^1)*Bbnj +...
                                    (Hn34*mnj^1+H35*mnj^3)*Cbnj)*Fbnij;
                    BB4(ii,j)=mni*Cbni*((H41*mnj^1)*Abnj +...
                                    (Hn42)*Bbnj +...
                                    (Hn43+H44*mnj^2)*Cbnj)*Fbnij;
                end

                FFA0fxun(ii,1)=  Abni * (G16  * Cnxun  * Czxu)  *...
                                int( exp(mni * x) * pxx  , x, 0, L );
                FFB0fsvn(ii,1)=  Bbni * (G26  * Cnsvn  * Czsv)  *...
                                int( exp(mni * x) * psx  , x, 0, L );
                FFC0fxw1n(ii,1)= Cbni * (G38  * Cnxw1n * Czxw1) *...
                                int( exp(mni * x) * pxx1 , x, 0, L );
                FFC0fsw2n(ii,1)= R*Cbni * (Gn39 * Cnsw2n * Czsw2) *...
                                int( exp(mni * x) * psx  , x, 0, L );
                FFC0fzwn(ii,1)=  Cbni * (G310 * Cnzwn  * Czzw)  *...
                                int( exp(mni * x) * pzx  , x, 0, L );

                % This term comes from the third sets of boundary
                % conditions
                fxwAt0=subs(exp(mni * x) * pxx,x,0);
                fxwAtL=subs(exp(mni * x) * pxx,x,L);
```

```
                FFC0fxwn(ii,1)=  Cbni * (H36  * Cnxwn  * Czxw)  *...
                                (fxwAtL-fxwAt0);

            end

            BB= 2*pi*R*E*h/(1-nu^2) * (BB1+BB2+BB3+BB4);
            B= TinvLni * BB * invLnj;
            BS(4*ne-3:4*ne+4,4*ne-3:4*ne+4,N+n+1)= B +...
                   BS(4*ne-3:4*ne+4,4*ne-3:4*ne+4,N+n+1);

            FF= (2*pi*R*E*h/(1-nu^2)) * (FFA0fxun+FFB0fsvn+FFC0fxw1n+...
                FFC0fsw2n+FFC0fzwn) + 2*pi*R*E*h/(1-nu^2) * FFC0fxwn;
            F= TinvLni * FF;
            FS(4*ne-3:4*ne+4,1,N+n+1)= F + FS(4*ne-3:4*ne+4,1,N+n+1);
        end

%         for nN=1:NE+1
%
%             R=RS(1)
%             invLni=invLniS(:,:,N-n+1,ne);
%
%             TinvLni=invLni.';%             Dnxn=  Dnx(N+n+1,nN);
% %             Dnsn=  Dns(N+n+1,nN);
% %             Dnzn=  Dnz(N+n+1,nN);
% %             Dnmn=  Dnm(N+n+1,nN);
%             for ii=1:8
%                 mni=mr(ii,N-n+1,ne);
%                 emni=exp(mni*L);
%                 Abni=Ab(ii,N-n+1,ne);
%                 Bbni=Bb(ii,N-n+1,ne);
%                 Cbni=Cb(ii,N-n+1,ne);
%                 ffff(ii,1)=  Cbni * Dnz(N+n+1,nN) * exp(mni * L);
% %             FS(nN*4-3,1,N+n+1)= 2 * pi * R * Dnxn +...
% %                                 FS(nN*4-3,1,N+n+1);
% %             FS(nN*4-2,1,N+n+1)= 2 * pi * R * Dnsn +...
% %                                 FS(nN*4-2,1,N+n+1);
%             end
%             FS(:,1,N+n+1)= 2 * pi * R * TinvLni * ffff + FS(:,1,N+n+1)
% %             FS(nN*4  ,1,N+n+1)= 2 * pi * R * Dnmn +...
% %                                 FS(nN*4  ,1,N+n+1);
%         end


%         for nN=1:NE+1
%
%             R=RS(1)
%
%             Dnxn=  Dnx(N+n+1,nN);
%             Dnsn=  Dns(N+n+1,nN);
%             Dnzn=  Dnz(N+n+1,nN);
%             Dnmn=  Dnm(N+n+1,nN);
%
%             FS(nN*4-3,1,N+n+1)= 2 * pi * R * Dnxn + FS(nN*4-3,1,N+n+1);
%             FS(nN*4-2,1,N+n+1)= 2 * pi * R * Dnsn + FS(nN*4-2,1,N+n+1);
%             FS(nN*4-1,1,N+n+1)= 2 * pi * R * Dnzn + FS(nN*4-1,1,N+n+1);
%             FS(nN*4  ,1,N+n+1)= 2 * pi * R * Dnmn + FS(nN*4  ,1,N+n+1);
%         end
```

```
        CMAX=10^20*abs(max(max(BS(:,:,N+n+1))));
        for nn=1:4*(NE+1);
            if BoundaryConditions(1,nn)~=0
                if BoundaryDisplacements(1,nn)~=0
                    BS(nn,nn,N+n+1)= BS(nn,nn,N+n+1) + CMAX;
                    FS(nn,1,N+n+1)=  CMAX * ConS(nn,N+n+1);
                end
            end
        end
        iii=1;
        for ii=1:4*(NE+1);
            if BoundaryConditions(1,ii)~=0
                jjj=1;
                for jj=1:4*(NE+1)
                    if BoundaryConditions(1,jj)~=0
                        Bc(iii,jjj,N+n+1)=BS(ii,jj,N+n+1);
                        jjj=jjj+1;
                    end
                end
                Fc(iii,1,N+n+1)=FS(ii,1,N+n+1);
                iii=iii+1;
            end
        end
        Dc(:,1,N+n+1)=Bc(:,:,N+n+1)\(-Fc(:,1,N+n+1));

        D=zeros(4*(NE+1),1);
        iii=1;
        for ii=1:4*(NE+1)
            if BoundaryConditions(1,ii)~=0
                D(ii,1)=Dc(iii,1,N+n+1);
                iii=iii+1;
            else
                D(ii,1)=0;
            end
        end
        for ne=1:NE
            DS(:,N+n+1,ne)=D(4*ne-3:4*ne+4,1);
        end
    end
end

clear x

for n=-N:N
    for ne=1:NE
        if AppliedForcesOrSupportExcitation==1
            Anj(:,N+n+1,ne)=invLnjS(:,:,N+n+1,ne)*DS(:,N+n+1,ne);
        end
    end
end


%%%%%%%%%%%%%%%%%%%%%%%%%%%%%%%%%%%%%%%%%%%%%%%%%%%%%%%%%%%%%%%%%%%%%%%%%%%%%%%
%%%%%%%%%%%%%%%%%%%%%%%%%%%%%%%% Response %%%%%%%%%%%%%%%%%%%%%%%%%%%%%%%%
```

```
%%%%%%%%%%%%%%%%%%%%%%%%%%%%%%%%%%%%%%%%%%%%%%%%%%%%%%%%%%%%%%%%%%%%%%%%%%%%%%%

x=0:1/100:1;
s=0:2*pi/108:2*pi;
[x,s]=meshgrid(x,s);
sizex=size(x);
%----------------------------- Displacements ----------------------------



u=zeros(sizex(1),sizex(2),NE);
v=zeros(sizex(1),sizex(2),NE);
w=zeros(sizex(1),sizex(2),NE);

U=zeros(sizex(1),NE*sizex(2)-(NE-1));
V=zeros(sizex(1),NE*sizex(2)-(NE-1));
W=zeros(sizex(1),NE*sizex(2)-(NE-1));

for ne=1:NE

    L=LS(ne);
    R=RS(ne);

    xe=L*x;
    se=R*s;

    for n=-N:N
        if modecontribution(1,N+n+1)==1
            for j=1:8
                mnj=  (mr(j,N+n+1,ne));
                Abnj= (Ab(j,N+n+1,ne));
                Bbnj= (Bb(j,N+n+1,ne));
                Cbnj= (Cb(j,N+n+1,ne));
                u(:,:,ne)= u(:,:,ne) + Abnj.*(Anj(j,N+n+1,ne)).*...
                                exp(mnj.*xe).*exp(1i*n.*se/R);
                v(:,:,ne)= v(:,:,ne) + Bbnj.*(Anj(j,N+n+1,ne)).*...
                                exp(mnj.*xe).*exp(1i*n.*se/R);
                w(:,:,ne)= w(:,:,ne) + Cbnj.*(Anj(j,N+n+1,ne)).*...
                                exp(mnj.*xe).*exp(1i*n.*se/R);
            end
        end
    end
    U(:,ne*sizex(2)-(ne-1)-(sizex(2)-1):ne*sizex(2)-(ne-1))=u(:,:,ne);
    V(:,ne*sizex(2)-(ne-1)-(sizex(2)-1):ne*sizex(2)-(ne-1))=v(:,:,ne);
    W(:,ne*sizex(2)-(ne-1)-(sizex(2)-1):ne*sizex(2)-(ne-1))=w(:,:,ne);
end


%----------------------------- Strains --------------------------------

SAn=   zeros(sizex(1),sizex(2),8,2*N+1,NE);
SAn1=  zeros(sizex(1),sizex(2),8,2*N+1,NE);
SBn=   zeros(sizex(1),sizex(2),8,2*N+1,NE);
SBn1=  zeros(sizex(1),sizex(2),8,2*N+1,NE);
SCn=   zeros(sizex(1),sizex(2),8,2*N+1,NE);
SCn1=  zeros(sizex(1),sizex(2),8,2*N+1,NE);
SCn11= zeros(sizex(1),sizex(2),8,2*N+1,NE);
```

```
n11S= zeros(sizex(1),sizex(2),2*N+1,NE);
n22S= zeros(sizex(1),sizex(2),2*N+1,NE);
n12S= zeros(sizex(1),sizex(2),2*N+1,NE);

n11NE= zeros(sizex(1),sizex(2),NE);
n22NE= zeros(sizex(1),sizex(2),NE);
n12NE= zeros(sizex(1),sizex(2),NE);


SAnr=zeros(1,8);
SAn1r=zeros(1,8);
SBnr=zeros(1,8);
SBn1r=zeros(1,8);
SCnr=zeros(1,8);
SCn1r=zeros(1,8);
SCn11r=zeros(1,8);

n11T=zeros(sizex(1),NE*sizex(2)-(NE-1));
n22T=zeros(sizex(1),NE*sizex(2)-(NE-1));
n12T=zeros(sizex(1),NE*sizex(2)-(NE-1));

for ne=1:NE

    z=hS(1,ne)/2;
    h=hS(1,ne);
    L=LS(ne);
    R=RS(ne);

    xe=L*x;

    for n=-N:N
        if modecontribution(1,N+n+1)==1
            for j=1:8
                mnj=  (mr(j,N+n+1,ne));
                Abnj= (Ab(j,N+n+1,ne));
                Bbnj= (Bb(j,N+n+1,ne));
                Cbnj= (Cb(j,N+n+1,ne));

                SAn(:,:,j,N+n+1,ne)=   Abnj * exp(mnj * xe);
                SAn1(:,:,j,N+n+1,ne)=  Abnj * exp(mnj * xe) * mnj;
                SBn(:,:,j,N+n+1,ne)=   Bbnj * exp(mnj * xe);
                SBn1(:,:,j,N+n+1,ne)=  Bbnj * exp(mnj * xe) * mnj;
                SCn(:,:,j,N+n+1,ne)=   Cbnj * exp(mnj * xe);
                SCn1(:,:,j,N+n+1,ne)=  Cbnj * exp(mnj * xe) * mnj;
                SCn11(:,:,j,N+n+1,ne)= Cbnj * exp(mnj * xe) * mnj^2;
            end
            for i=1:sizex(1)
                for j=1:sizex(2)

                    SAnr(:,:)=   SAn(i,j,:,N+n+1,ne);
                    SAn1r(:,:)=  SAn1(i,j,:,N+n+1,ne);
                    SBnr(:,:)=   SBn(i,j,:,N+n+1,ne);
                    SBn1r(:,:)=  SBn1(i,j,:,N+n+1,ne);
                    SCnr(:,:)=   SCn(i,j,:,N+n+1,ne);
                    SCn1r(:,:)=  SCn1(i,j,:,N+n+1,ne);
                    SCn11r(:,:)= SCn11(i,j,:,N+n+1,ne);
```

```
                    n11S(i,j,N+n+1,ne)=(( SAn1r - z * SCn11r ) *...
                        (invLnjS(:,:,N+n+1,ne) * DS(:,N+n+1,ne))) *...
                         exp(1i * n * s(i,j));
                    n22S(i,j,N+n+1,ne)=(( 1i * n / R * SBnr +...
                               1/(R+z) * SCnr + z * 1/R/(R+z) * n^2 *...
                               SCnr ) * (invLnjS(:,:,N+n+1,ne) *...
                               (DS(:,N+n+1,ne)))) * exp(1i * n * s(i,j));
                    n12S(i,j,N+n+1,ne)=1/2 * (( 1/(R+z) * 1i * n *...
                                     SAnr + (R+z)/R * SBn1r...
                                          - z * (2*R+z)...
                                         /R/(R+z)* 1i * n * SCn1r) *...
                                    (invLnjS(:,:,N+n+1,ne) *...
                                    (DS(:,N+n+1,ne)))) *...
                                    exp(1i * n * s(i,j));

                end
            end

            n11NE(:,:,ne)= n11NE(:,:,ne) + n11S(:,:,N+n+1,ne);
            n22NE(:,:,ne)= n22NE(:,:,ne) + n22S(:,:,N+n+1,ne);
            n12NE(:,:,ne)= n12NE(:,:,ne) + n12S(:,:,N+n+1,ne);

        end
    end

    n11T(:,ne*sizex(2)-(ne-1)-(sizex(2)-1):ne*sizex(2)-...
                        (ne-1))= n11NE(:,:,ne);
    n22T(:,ne*sizex(2)-(ne-1)-(sizex(2)-1):ne*sizex(2)-...
                        (ne-1))= n22NE(:,:,ne);
    n12T(:,ne*sizex(2)-(ne-1)-(sizex(2)-1):ne*sizex(2)-...
                        (ne-1))= n12NE(:,:,ne);

end


%------------------------------ Stresses --------------------------------

sigma11= E/(1-nu^2) * ( n11T + nu * n22T);
sigma22= E/(1-nu^2) * ( n22T + nu * n11T);
sigma12= E/(1+nu)   * n12T;

%%%%%%%%%%%%%%%%%%%%%%%%%%%%%%%%%%%%%%%%%%%%%%%%%%%%%%%%%%%%%%%%%%%%%%%%%%%
%%%%%%%%%%%%%%%%%%%%%%%%%%%% Plotting the results %%%%%%%%%%%%%%%%%%%%%%%%%
%%%%%%%%%%%%%%%%%%%%%%%%%%%%%%%%%%%%%%%%%%%%%%%%%%%%%%%%%%%%%%%%%%%%%%%%%%%

%---------------------------- Displacements ----------------------------

size(x)
size(W)
DisplacementsABCD(1,1)=U(1,section);
DisplacementsABCD(1,2)=V(1,section);
DisplacementsABCD(1,3)=W(1,section);
DisplacementsABCD(2,1)=U(26,section);
DisplacementsABCD(2,2)=V(26,section);
DisplacementsABCD(2,3)=W(26,section);
DisplacementsABCD(3,1)=U(51,section);
```

```
DisplacementsABCD(3,2)=V(51,section);
DisplacementsABCD(3,3)=W(51,section);
DisplacementsABCD(4,1)=U(76,section);
DisplacementsABCD(4,2)=V(76,section);
DisplacementsABCD(4,3)=W(76,section);
display(DisplacementsABCD)

%%%--------Using a factor to magnify the displacement to be visualized---
L0=0;
X=zeros(sizex(1),NE*sizex(2)-(NE-1));
S=zeros(sizex(1),NE*sizex(2)-(NE-1));
for ne=1:NE
    X(:,ne*sizex(2)-(ne-1)-(sizex(2)-1):ne*sizex(2)-...
                  (ne-1))=LS(1,ne).*x+L0;
    L0=L0+LS(ne);
    S(:,ne*sizex(2)-(ne-1)-(sizex(2)-1):ne*sizex(2)-(ne-1))=s;
end

x=X;
s=S;

facu=70;
facv=70;
facw=70;

us=double(real(U));
vs=double(real(V));
ws=double(real(W));

fus=facu*us;
fvvs=facv*vs;
fws=facw*ws;

R=RS(1)
%------------------------------Displacement u ---------------------------
figure3=figure('Position', [100 80 800 650], 'Name', 'Displacement u');
colormap jet
axes1=axes('Position', [.10 .15 .80 .75], 'Parent', figure3);
j=x+fus;
k=(R).*sin(s);
l=(R).*cos(s);
plotus=surf(j,k,l,us, 'Parent', axes1, 'FaceColor', 'interp',...
      'edgeAlpha',.1);
axis equal
xlabel('X1','FontSize',12,'FontWeight','bold')
ylabel('X2','FontSize',12,'FontWeight','bold')
zlabel('X3','Rotation',0,'FontSize',12,'FontWeight','bold')
title('Displacement u','FontSize',20,'FontWeight','bold')
colorbar('peer',axes1)

%------------------------------Displacement v ---------------------------
figure4=figure('Position', [100 80 800 650], 'Name', 'Displacement v');
colormap jet
axes1=axes('Position', [.10 .15 .80 .75], 'Parent', figure4);
j=x;
% k=R*sin(s)+fvvs.*cos(s);
k=R*sin(s+fvvs./R);
```

```
% l=R*cos(s)-fvvs.*sin(s);
l=R*cos(s+fvvs./R);
plotvvs=surf(j,k,l,vs, 'Parent', axes1, 'FaceColor', 'interp',...
      'edgeAlpha',.1);
axis equal
xlabel('X1','FontSize',12,'FontWeight','bold')
ylabel('X2','FontSize',12,'FontWeight','bold')
zlabel('X3','Rotation',0,'FontSize',12,'FontWeight','bold')
title('Displacement v','FontSize',20,'FontWeight','bold')
colorbar('peer',axes1)

%------------------------------Displacement w ---------------------------
figure5=figure('Position', [100 80 800 650], 'Name', 'Displacement w');
colormap jet
axes1=axes('Position', [.10 .15 .80 .75], 'Parent', figure5);
j=x;
k=(R+fws).*sin(s);
l=(R+fws).*cos(s);
plotws=surf(j,k,l,ws, 'Parent', axes1, 'FaceColor', 'interp',...
      'edgeAlpha',.1);
axis equal
xlabel('X1','FontSize',12,'FontWeight','bold')
ylabel('X2','FontSize',12,'FontWeight','bold')
zlabel('X3','Rotation',0,'FontSize',12,'FontWeight','bold')
title('Displacement w','FontSize',20,'FontWeight','bold')
colorbar('peer',axes1)

%------------------------------Total Displacement ------------------------
figure6=figure('Position', [100 80 800 650], 'Name',...
       'Total Displacement');
colormap gray

axes1=axes('Position', [.10 .15 .80 .75], 'Parent', figure6);

j=x+fus;
k=R*sin(s)+(fws.*sin(s)+fvvs.*cos(s));
l=R*cos(s)+(fws.*cos(s)-fvvs.*sin(s));
plotusvvsws=surf(j,k,l,((us.^2+vs.^2+ws.^2).^.5),'Parent',axes1,...
    'FaceColor','interp','edgeAlpha',.4);
hold on
plot3(j(1,:),k(1,:),l(1,:),'Parent',axes1,'linestyle','-','color',...
      [0 0 0],'linewidth',2);
plot3(j(55,:),k(55,:),l(55,:),'Parent',axes1,'linestyle','-',...
      'color',[0 0 0],'linewidth',2);
plot3(j(100,:),k(100,:),l(100,:),'Parent',axes1,'linestyle',...
      '-.','color',[0 0 0],'linewidth',2);
axis equal
xlim([0 6])
ylim([-1 1])
zlim([-1 1])
xlabel('X1','FontSize',12,'FontWeight','bold')
ylabel('X2','FontSize',12,'FontWeight','bold')
zlabel('X3','Rotation',0,'FontSize',12,'FontWeight','bold')
title('Total Displacement','FontSize',20,'FontWeight','bold')
% colorbar('peer',axes1)
set(gca,'GridLineStyle','none','CameraPosition',[150 -70 10])
```

```
%=========================================================================
%=========================================================================
%=========================================================================
%---------------------------- Stresses --------------------------------

sigma11s=(real(sigma11));
sigma22s=(real(sigma22));
sigma12s=(real(sigma12));

%---------------------------- n11 -------------------------------------
figure7=figure('Position', [100 80 800 650], 'Name', 'Axial Stresses');
colormap jet
axes1=axes('Position', [.10 .15 .80 .75], 'Parent', figure7);
j=x;
% k=R*sin(s)+(fws.*sin(s)+fvvs.*cos(s));
k=R.*sin(s);
% l=R*cos(s)+(fws.*cos(s)-fvvs.*sin(s));
l=R.*cos(s);
plotsigma11s=surf(j,k,l,sigma11s,'Parent',axes1,...
    'FaceColor','interp','edgeAlpha',.1);
hold on
colormap(jet)
axis equal
xlabel('X1','FontSize',12,'FontWeight','bold')
ylabel('X2','FontSize',12,'FontWeight','bold')
zlabel('X3','Rotation',0,'FontSize',12,'FontWeight','bold')
title('Axial stress','FontSize',20,'FontWeight','bold')
colorbar('peer',axes1)

%---------------------------- n22 -------------------------------------
figure8=figure('Position', [100 80 800 650], 'Name', 'Hoop Stresses');
colormap jet
axes1=axes('Position', [.10 .15 .80 .75], 'Parent', figure8);
j=x;
% k=R*sin(s)+(fws.*sin(s)+fvvs.*cos(s));
k=R.*sin(s);
% l=R*cos(s)+(fws.*cos(s)-fvvs.*sin(s));
l=R.*cos(s);
plotsigma22s=surf(j,k,l,sigma22s,'Parent',axes1,...
    'FaceColor','interp','edgeAlpha',.1);

axis equal
xlabel('X1','FontSize',12,'FontWeight','bold')
ylabel('X2','FontSize',12,'FontWeight','bold')
zlabel('X3','Rotation',0,'FontSize',12,'FontWeight','bold')
title('Hoop stress','FontSize',20,'FontWeight','bold')
colorbar('peer',axes1)

%---------------------------- n12 -------------------------------------
figure8=figure('Position', [100 80 800 650], 'Name', 'Shear Stresses');
colormap jet
axes1=axes('Position', [.10 .15 .80 .75], 'Parent', figure8);
j=x;
% k=R*sin(s)+(fws.*sin(s)+fvvs.*cos(s));
k=R.*sin(s);
% l=R*cos(s)+(fws.*cos(s)-fvvs.*sin(s));
```

```
l=R.*cos(s);
plotsigma12s=surf(j,k,l,sigma12s,'Parent',axes1,...
    'FaceColor','interp','edgeAlpha',.1);

axis equal
xlabel('X1','FontSize',12,'FontWeight','bold')
ylabel('X2','FontSize',12,'FontWeight','bold')
zlabel('X3','Rotation',0,'FontSize',12,'FontWeight','bold')
title('Shear stress','FontSize',20,'FontWeight','bold')
colorbar('peer',axes1)

%----------------------------- Special Plots -----------------------------
figure10=figure('Position', [100 80 800 650], 'Name', 'Special Plot');
colormap jet
axes1=axes('Position', [.10 .15 .80 .75], 'Parent', figure10);
j=x(1,:);
k=sigma12s(26,:);
Zout=k.';
plotSP=plot(j,k,'Parent',axes1);

xlabel('X1','FontSize',12,'FontWeight','bold')
ylabel('X2','FontSize',12,'FontWeight','bold')

title('Special Plot','FontSize',20,'FontWeight','bold')

%-------------------------------------------------------------------------
%-------------------------------------------------------------------------
%-------------------------------------------------------------------------
%-------------------------------------------------------------------------
sizex=size(x);
xL=x(1,:);
sC=s(:,1);
sig11TL=sigma11s(1,:);
sig22TL=sigma22s(1,:);
sig12TL=sigma12s(26,:);

% sig11S001=sigma11s(:,1);
% sig11S200=sigma11s(:,200);
% sig11S201=sigma11s(:,201);
% sig11S300=sigma11s(:,300);
% sig11S396=sigma11s(:,396);
% sig11S400=sigma11s(:,400);
% sig11S401=sigma11s(:,401);

plot(xL,sig11TL)
hold on
xlim([2,5])
plot(xL,sig22TL)
plot(xL,sig12TL)
hold off

% plot(sC,sig11S001,sC,sig11S200,sC,sig11S201,sC,sig11S300,sC,...
      sig11S396,sC,sig11S400,sC,sig11S401)

plot(xL,W(1,:))
```

```
%% ------------------- Contour plots -----------------------------------

xcom=[x(1:100,:);x];
scom=[s(1:100,:);2*pi+s];
sigma11scom=1e-6*[sigma11s(1:100,:);sigma11s];

%------------------------ S11 ----------------------------------------
v1=[-24;-22;-18;-16;-14;-12;-8;-6;-4;-2;2;4;6;8;12;14;16;18;22;24];

v2=-20:10:20;
v2=v2.';

figure12=figure('Position', [100 80 800 650]);
axes1=axes('Position', [.12 .15 .80 .75], 'Parent', figure12);
contour(xcom,scom,sigma11scom,v1,'-k');
hold on
[C,h]=contour(xcom,scom,sigma11scom,v2,'-k','linewidth', 2);

ylim([pi,3*pi])
set(gca,'xtick',[0,1,2,3,4,5],'xticklabel',{'0';'1';'2';'3';'4';'5'},...
      'ytick',[pi,3*pi/2,2*pi,5*pi/2,3*pi],'yticklabel',...
      {'-180';'-90';'0';'90';'180'}, 'fontsize', 14);
clabel(C,h,'FontSize',14,'LabelSpacing',800);
xlabel('Distance from Left Support (\itm\rm)','FontSize',16,...
      'FontWeight','normal')
ylabel('Angle from Top Fiber (\itDegree\rm)','FontSize',16,...
      'FontWeight','normal')

% axes2=axes('Position', [.15 .20 .4 .3], 'Parent', figure12);
% contour(xcom,scom,sigma11scom,v1,'-k');
% xlim([4,5])
% ylim([11*pi/6-pi/3,11*pi/6+pi/3])


%------------------------------ S22 ----------------------------------
figure
contour(x,s,sigma22s,20,'-k')

%------------------------------ S12 ----------------------------------
sigma12scom=1e-6*[sigma12s(1:100,:);sigma12s];

v1=[-9;-8;-7;-6;-4;-3;-2;-1;1;2;3;4;6;7;8;9];

v2=-10e6:5e6:10e6;
v2=1e-6*v2.';

figure14=figure('Position', [100 80 800 650]);
axes1=axes('Position', [.12 .15 .80 .75], 'Parent', figure14);
contour(xcom,scom,sigma12scom,v1,'-k');
hold on
[C,h]=contour(xcom,scom,sigma12scom,v2,'-k','linewidth', 2);

ylim([pi,3*pi])
set(gca,'xtick',[0,1,2,3,4,5],'xticklabel',{'0';'1';'2';'3';'4';'5'},...
      'ytick',[pi,3*pi/2,2*pi,5*pi/2,3*pi],'yticklabel',...
      {'-pi';'-pi/2';'0';'pi/2';'pi'}, 'fontsize', 14);
clabel(C,h,'FontSize',14,'LabelSpacing',800);
```

```
xlabel('Distance from Left Support (\itm\rm)','FontSize',16,...
      'FontWeight','normal')
ylabel('Angle from Top Fiber (\itrad\rm)','FontSize',16,...
      'FontWeight','normal')

% axes2=axes('Position', [.15 .20 .4 .3], 'Parent', figure14);
% contour(xcom,scom,sigma12scom,v1,'-k');
% xlim([4,5])
% ylim([11*pi/6-pi/3,11*pi/6+pi/3])

% figure
% contour(x,s,sigma12s,15,'-k')

%------------- saving the files----------------------------------------
xlswrite('x.xls',x.')
xlswrite('s.xls',s.')
xlswrite('U.xls',U.')
xlswrite('V.xls',V.')
xlswrite('W.xls',W.')


xlswrite('xn10.xls',x.')
xlswrite('sn10.xls',s.')
xlswrite('Un10.xls',U.')
xlswrite('Vn10.xls',V.')
xlswrite('Wn10.xls',W.')
```

Chapter 6

Formulation of Thin Shell Theories for Toroids

6.1 Abstract

The generalized thin shell theory developed in Chapter 2 is specialized to toroids. By applying two sets of consistent geometric simplifications, two sets of governing field equations and corresponding boundary conditions are recovered for the problem. Several comparisons are made with other toroidal thin shell theories. A third toroidal thin shell theory is proposed for pipe bends of common geometries. The simplification essentially preserves the accuracy of the solution while reducing its complexity.

6.2 Introduction

Recalling the discussions about all the discrepancies among thin shell theories provided in Chapter 2, this chapter is centered on developing a toroidal thin shell (TTS) theory by using the generalized thin shell theory developed in Chapter 2. It is attempted to express the formulation in a generic form so that other toroidal shell theories (e.g., DMV [6.1] and Sanders [6.2]) can be expressed as special cases from the generic form. The formulation details are similar to that in Chapter 3 (for the case of CCTSs).

6.3 Geometry

Position vector $\mathbf{r}$ of a general point lying on the middle surface of a torus with cross-sectional radius R and of torus radius $\Re$ (Figure 6.1) in terms of the unit vectors $\vec{\mathbf{I}}_i$, which correspond to the Cartesian coordinate system X^i, and the curvilinear coordinate system x^i is

$$\mathbf{r}\left(x^1, x^2\right) = \left[\left(\Re + R\cos\frac{x^2}{R}\right)\sin\frac{x^1}{\Re}\right]\vec{\mathbf{I}}^1 + \left(R\sin\frac{x^2}{R}\right)\vec{\mathbf{I}}^2 + \left[\left(\Re + R\cos\frac{x^2}{R}\right)\cos\frac{x^1}{\Re}\right]\vec{\mathbf{I}}^3 \qquad (6.1)$$

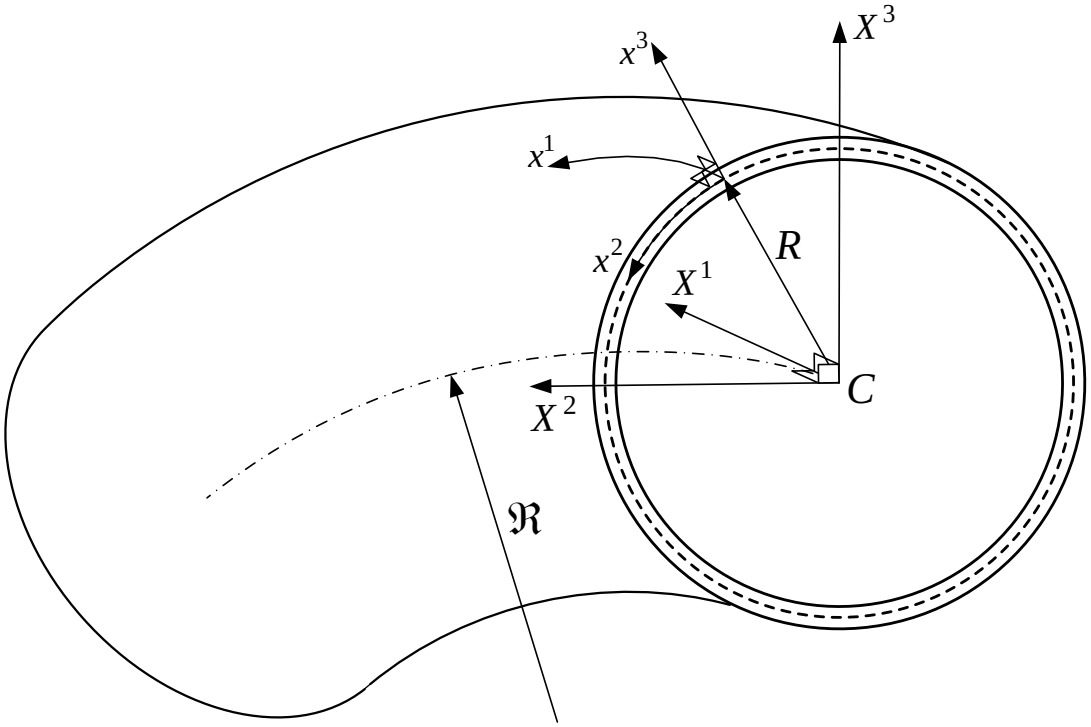

Figure 6.1 – Toroid geometry and coordinate definition

In the following, symbols x, s, z will be used instead of x^1, x^2, x^3. We define the non-dimensional parameters

$$\gamma = R/\Re \quad , \quad \chi = 1 + \frac{z}{R} \quad , \quad \theta = \frac{s}{R}$$
$$\zeta = 1 + \gamma\cos\theta \quad , \quad \xi = 1 + \gamma\chi\cos\theta \qquad (6.2)$$

In a manner similar to that in Chapter 3, the covariant base vectors are

$$\mathbf{g}_1 = \xi \vec{\mathbf{j}}_1 \quad , \quad \mathbf{g}_2 = \chi \vec{\mathbf{j}}_2 \quad , \quad \mathbf{g}_3 = 1\vec{\mathbf{j}}_3 \tag{6.3}$$

All other geometric properties of the toroidal shell necessary in the formulation are given below.

From Eq. 2.10, by using the raising indices technique, the mixed components of the curvature tensor on the middle surface ($\bar{b}_\beta^\alpha = a^{\alpha\gamma}\mathbf{a}_{3,\gamma}\cdot\mathbf{a}_\beta$) are

$$\bar{b}_1^1 = -\frac{1}{\Re}\frac{\cos\theta}{\zeta} \quad , \quad \bar{b}_1^2 = \bar{b}_2^1 = 0 \quad , \quad \bar{b}_2^2 = -\frac{1}{R} \tag{6.4}$$

The components of the Christoffel symbol ($\bar{\Gamma}_{ij}^k = \frac{1}{2}a^{kl}\left(a_{li,j} + a_{lj,i} - a_{ij,l}\right)$) on the mid-surface are (for more elaboration refer to Eq. A.68)

$$\begin{aligned} &\bar{\Gamma}_{11}^3 = \bar{b}_{11} = -\frac{1}{\Re}\zeta\cos\theta \quad , \quad \bar{\Gamma}_{12}^3 = \bar{b}_{12} = 0 \quad , \quad \bar{\Gamma}_{21}^3 = \bar{b}_{21} = 0 \\ &\bar{\Gamma}_{22}^3 = \bar{b}_{22} = -\frac{1}{R} \quad , \quad \bar{\Gamma}_{12}^1 = \bar{\Gamma}_{21}^1 = -\frac{1}{\Re}\frac{\sin\theta}{\zeta} \quad , \quad \bar{\Gamma}_{11}^2 = \frac{1}{\Re}\zeta\sin\theta \end{aligned} \tag{6.5}$$

The covariant components of the curvature tensor across the shell ($b_{\alpha\beta} = \Gamma_{\alpha\beta}^3$) are

$$b_{11} = -\frac{1}{\Re}\xi\cos\theta \quad , \quad b_{12} = b_{21} = 0 \quad , \quad b_{22} = -\frac{1}{R}\chi \tag{6.6}$$

From Eq. 6.4, by substituting into Eq. 3.16, one obtains the components of the shifter tensor as

$$\begin{aligned} &\mu_1^1 = 1 + \frac{z}{\Re}\frac{\cos\theta}{\zeta} = \frac{\xi}{\zeta} \quad , \quad \mu_2^2 = \chi \\ &\mu_1^1\,|\,|_2 = -z\frac{1}{\Re}\frac{\sin\theta}{\zeta^2} \quad , \quad \mu_2^2\,|\,|_2 = 0 \end{aligned} \tag{6.7}$$

The components of the Christoffel symbol Γ_{ij}^k across the thickness are

$$\Gamma^1_{12}=\Gamma^1_{21}=\frac{1}{2}g^{11}g_{11,2}=-\frac{1}{\Re}\frac{\chi\sin\theta}{\xi} \quad , \quad \Gamma^1_{13}=\Gamma^1_{31}=\frac{1}{2}g^{11}g_{11,3}=\frac{1}{\Re}\frac{\cos\theta}{\xi}$$
$$\Gamma^2_{11}=-\frac{1}{2}g^{22}g_{11,2}=\frac{1}{\Re}\frac{\xi\sin\theta}{\chi} \quad , \quad \Gamma^2_{23}=\Gamma^2_{32}=\frac{1}{R}\frac{1}{\chi} \qquad (6.8)$$
$$\Gamma^3_{11}=-\frac{1}{\Re}\xi\cos\theta \quad , \quad \Gamma^3_{22}=-\frac{1}{R}\chi$$

The two dimensional covariant derivative of curvature tensor ($b_{\alpha\beta}\|_\gamma$) is

$$b_{11}\|_2=b_{11,2}-2b_{11}\Gamma^1_{12} \qquad (6.9)$$

From Eq. 3.45, the displacement components U_i in terms of the mid-surface displacements u_i are

$$U_1=\left(\mu^1_1\right)^2u_1-x^3\mu^1_1u_{3,1} \quad , \quad U_2=\left(\mu^2_2\right)^2u_2-x^3\mu^2_2u_{3,2} \quad , \quad U_3=u_3 \qquad (6.10)$$

Using the chain rule, the derivatives of the displacement components U_i, required in the formulation, in terms of the mid-surface displacements u_i are

$$U_{1,1}=\left(\mu^1_1\right)^2u_{1,1}-x^3\mu^1_1u_{3,11} \quad , \quad U_{1,11}=\left(\mu^1_1\right)^2u_{1,11}-x^3\mu^1_1u_{3,111}$$
$$U_{1,12}=2\mu^1_1\mu^1_{1,2}u_{1,1}+\left(\mu^1_1\right)^2u_{1,12}-x^3\mu^1_{1,2}u_{3,11}-x^3\mu^1_1u_{3,112}$$
$$U_{1,2}=2\mu^1_1\mu^1_{1,2}u_1+\left(\mu^1_1\right)^2u_{1,2}-x^3\mu^1_{1,2}u_{3,1}-x^3\mu^1_1u_{3,12}$$
$$U_{1,22}=2\mu^1_{1,2}\mu^1_{1,2}u_1+2\mu^1_1\mu^1_{1,22}u_1+4\mu^1_1\mu^1_{1,2}u_{1,2}+\left(\mu^1_1\right)^2u_{1,22}$$
$$-x^3\mu^1_{1,22}u_{3,1}-2x^3\mu^1_{1,2}u_{3,12}-x^3\mu^1_1u_{3,122}$$
$$U_{2,1}=\left(\mu^2_2\right)^2u_{2,1}-x^3\mu^2_2u_{3,12} \quad , \quad U_{2,2}=\left(\mu^2_2\right)^2u_{2,2}-x^3\mu^2_2u_{3,22}$$
$$U_{2,11}=\left(\mu^2_2\right)^2u_{2,11}-x^3\mu^2_2u_{3,112} \quad , \quad U_{2,12}=\left(\mu^2_2\right)^2u_{2,12}-x^3\mu^2_2u_{3,122}$$
$$U_{2,22}=\left(\mu^2_2\right)^2u_{2,22}-x^3\mu^2_2u_{3,222}$$
$$U_{3,1}=u_{3,1} \quad , \quad U_{3,2}=u_{3,2} \qquad (6.11)$$

By using the relationship $U_\alpha \|_\beta = U_{\alpha,\beta} - U_\gamma \Gamma^\gamma_{\alpha\beta}$, defined in Appendix 2.C., the components of the covariant derivative of the displacement components ($U_\lambda \|_\delta$) are

$$\begin{aligned} U_1 \|_1 &= U_{1,1} - U_2 \Gamma^2_{11} \quad , \quad U_1 \|_2 = U_{1,2} - U_1 \Gamma^1_{12} \\ U_2 \|_1 &= U_{2,1} - U_1 \Gamma^1_{21} \quad , \quad U_2 \|_2 = U_{2,2} \end{aligned} \tag{6.12}$$

The in plain components of the second covariant derivatives of the displacement components ($U_\lambda \|_{\delta\beta}$) are

$$\begin{aligned} U_1 \|_{11} &= U_{1,11} - 2U_{2,1}\Gamma^2_{11} - U_{1,2}\Gamma^2_{11} + 2U_1\Gamma^1_{12}\Gamma^2_{11} \\ U_1 \|_{12} &= U_{1,12} - U_{2,2}\Gamma^2_{11} - U_2\Gamma^2_{11,2} - 2U_{1,1}\Gamma^1_{12} + 2U_2\Gamma^2_{11}\Gamma^1_{12} \\ U_1 \|_{21} &= U_{1,12} - 2U_{1,1}\Gamma^1_{12} - U_{2,2}\Gamma^2_{11} + U_2\Gamma^2_{11}\Gamma^1_{12} \\ U_1 \|_{22} &= U_{1,22} - 2U_{1,2}\Gamma^1_{12} - U_1\Gamma^1_{12,2} + U_1\Gamma^1_{12}\Gamma^1_{12} \\ U_2 \|_{11} &= U_{2,11} - 2U_{1,1}\Gamma^1_{21} + U_2\Gamma^2_{11}\Gamma^1_{21} - U_{2,2}\Gamma^2_{11} \\ U_2 \|_{12} &= U_{2,12} - U_{1,2}\Gamma^1_{21} - U_1\Gamma^1_{21,2} - U_{2,1}\Gamma^1_{21} + U_1\Gamma^1_{21}\Gamma^1_{21} \\ U_2 \|_{21} &= U_{2,12} - U_{1,2}\Gamma^1_{21} - U_{2,1}\Gamma^1_{21} + 2U_1\Gamma^1_{12}\Gamma^1_{21} \\ U_2 \|_{22} &= U_{2,22} \end{aligned} \tag{6.13}$$

All components of the covariant derivative of the metric tensor $g^{\alpha\beta} \|_\gamma$ and consequently all components of the covariant derivative of the constitutive tensor $E^{\alpha\beta\lambda\delta} \|_\beta$ are zero.

It should be reminded that the mid-surface displacement components $u(x,s)$, $v(x,s)$ and $w(x,s)$ appear in the expressions above are in a covariant form. Although for the case of TTSs, the covariant, contravariant and physical form of the mid-surface displacement components $v(x,s)$ and $w(x,s)$ have equal magnitudes, this is not the case for mid-surface displacement component $u(x,s)$. Thus, the following relationships should be used to relate

the covariant displacement components u, v and w to their counterpart physical components $\bar{u}$, $\bar{v}$ and $\bar{w}$.

$$u = \zeta \bar{u} \quad , \quad v = \bar{v} \quad , \quad w = \bar{w} \tag{6.14}$$

where we recall from Eq. 6.2 that $\zeta = 1 + \gamma \cos\theta$ is a function of coordinate θ $(= s/R)$. Thus, one has

$$\begin{aligned} u_{,2} &= \zeta_{,2}\bar{u} + \zeta \bar{u}_{,2} = -\frac{\gamma}{R}\sin\theta \bar{u} + \zeta \bar{u}_{,2} \\ u_{,22} &= \zeta_{,22}\bar{u} + \zeta_{,2}\bar{u}_{,2} + \zeta \bar{u}_{,22} = -\frac{\gamma}{R^2}\cos\theta \bar{u} - 2\frac{\gamma}{R}\sin\theta \bar{u}_{,2} + \zeta \bar{u}_{,22} \end{aligned} \tag{6.15}$$

6.4 Constitutive Elasticity Tensor

From Eq. 6.3, by substituting into Eq. 2.50, one obtains

$$\begin{aligned} E^{1111} &= \frac{E}{1-\nu^2} g^{11} g^{11} = \frac{E}{1-\nu^2}\frac{1}{\xi^4} \\ E^{2222} &= \frac{E}{1-\nu^2} g^{22} g^{22} = \frac{E}{1-\nu^2}\frac{1}{\chi^4} \\ E^{1122} &= E^{2211} = \frac{E}{1-\nu^2}\nu g^{11} g^{22} = \frac{E}{1-\nu^2}\nu\frac{1}{\xi^2\chi^2} \\ E^{1212} &= E^{1221} = E^{2112} = E^{2121} = \frac{E}{1-\nu^2}\left(\frac{1-\nu}{2}\right) g^{11} g^{22} = \frac{E}{1-\nu^2}\left(\frac{1-\nu}{2}\right)\frac{1}{\xi^2\chi^2} \end{aligned} \tag{6.16}$$

6.5 Strain-Displacement Relationships

From Eq. 6.12, by substituting into Eq. 2.23, the covariant components of the strains $\eta_{\alpha\beta}$ in terms of covariant components of the mid-surface displacement are

$$\eta_{11} = \frac{1}{\zeta^2} u_{,1} - \frac{\gamma\chi \sin\theta}{R\xi} v + \frac{\gamma \cos\theta}{R\xi} w + z \frac{\gamma \sin\theta}{R\xi} w_{,2} - z \frac{1}{\zeta\xi} w_{,11}$$

$$\eta_{22} = v_{,2} + \frac{1}{R\chi} w - z \frac{1}{\chi} w_{,22}$$

$$\eta_{12} = \eta_{21} = \frac{1}{2}\left\{ \frac{2\gamma \sin\theta}{R\zeta^2}\left(1 - z\frac{1}{R\chi\zeta}\right)u + \frac{\xi}{\chi\zeta^2} u_{,2} + \frac{\chi}{\xi} v_{,1} - z\frac{\gamma \sin\theta}{R\zeta\xi}\left(2 - z\frac{1}{R\chi\zeta}\right) w_{,1} - z\left(\frac{1}{\xi} + \frac{1}{\chi\zeta}\right) w_{,12} \right\} \quad (6.17a\text{-}c)$$

From Eq. 6.14, by substituting into Eq. 6.17, the physical components of the strains $\overline{\eta}_{\alpha\beta}$ are expressed in terms of the physical components of the mid-surface displacement

$$\overline{\eta}_{11} = \left[\frac{1}{\zeta} \overline{u}_{,1} - z \frac{1}{\zeta\xi} \overline{w}_{,11} \right] + \left[\frac{\gamma}{R\xi}\left(-\chi \sin\theta \overline{v} + \cos\theta \overline{w} + z \sin\theta \overline{w}_{,2} \right) \right]$$

$$\overline{\eta}_{22} = \overline{v}_{,2} + \frac{1}{R\chi} \overline{w} - z \frac{1}{\chi} \overline{w}_{,22}$$

$$\overline{\eta}_{12} = \frac{1}{2}\left\langle \left[\frac{\xi}{\chi\zeta} \overline{u}_{,2} + \frac{\chi}{\xi} \overline{v}_{,1} - z\left(\frac{1}{\xi} + \frac{1}{\chi\zeta}\right) \overline{w}_{,12} \right] + \frac{\gamma}{R} \frac{\sin\theta}{\zeta} \left\{ \left[\frac{1}{\chi}\left(2 - \frac{\xi}{\zeta}\right) + 2\frac{z}{R}\frac{\gamma\cos\theta}{\zeta} \right] \overline{u} - z\left[\frac{1}{\chi}\left(1 + 2\frac{z}{R}\right) + \frac{\gamma\cos\theta}{\zeta} \right] \frac{1}{\xi} \overline{w}_{,1} \right\} \right\rangle \quad (6.18a\text{-}c)$$

Among thin shell theories, the DMV theory [6.1] is commonly used for analysis of toroidal shells in the literature. In DMV, most effects related to the flexural stiffness are neglected. Sander's theory [6.2] provides a more exact representation, in which strains are assumed to linearly vary across the thickness. Three versions of the strain-displacement relationships (namely, TTS-V1, TTS-V2 and TTS-V3) are proposed based on three sets of approximations of Eq. 6.18a-c and are compared to those of DMV and Sanders in Table 6.1 through Table 6.3.

The TTS-V1 theory is the most accurate and does not involve additional approximations and simplifications beyond those given in Chapter 2. The TTS-V2 theory is based on the simplifications

$$\begin{aligned} \chi^n &= \left(1+\frac{z}{R}\right)^n \simeq 1+n\frac{z}{R} \qquad ;\ n=0,\pm1,\pm2,\pm3 \\ \xi^n &= \left(1+\gamma\chi\cos\theta\right)^n \simeq \zeta^n\left(1+n\frac{z}{R}\frac{\gamma\cos\theta}{\zeta}\right) \qquad ;\ n=0,\pm1,\pm2,\pm3 \end{aligned} \tag{6.19}$$

The maximum error in this approximation (Eq. 6.19) within the practical geometric ranges of thin shells (say $z/R \le 0.05$) and practical range of torus geometries $R/\Re$ (say $R/\Re \le 0.5$) in the worst case ($n=-3$) is within 1.5% .

The TTS-V3 theory is based on the further simplifications

$$\xi^n \simeq \zeta^n \quad , \quad \chi^n \simeq 1 \quad ; \quad n=0,\pm1,\pm2,\pm3 \tag{6.20}$$

i.e., by neglecting the ratio (z/R) compared to unity, $1+z/R \simeq 1$. For the same range of z/R and $R/\Re$ as above, the maximum error, introduced into the approximate expressions (Eq. 6.20), in the worst case ($n=-3$) is within 17% .

Both simplified strain-displacement relationships (TTS-V2 and TTS-V3) lead to comparable expressions to those of Sanders and DMV theories for toroidal shells as illustrated in Table 6.1.

Table 6.1 – Comparison of longitudinal strain-displacement expressions in various toroidal thin shell theories

Theory	Longitudinal Strain $\overline{\eta}_{11}$
TTS-V1	$\left[\frac{1}{\zeta}\overline{u}_{,1} - z\frac{1}{\zeta\xi}\overline{w}_{,11}\right] + \left[\frac{\gamma}{R\xi}\left(-\chi\sin\theta\overline{v} + \cos\theta\overline{w} + z\sin\theta\overline{w}_{,2}\right)\right]$
TTS-V3	$\left[\frac{1}{\zeta}\overline{u}_{,1} - z\frac{1}{\zeta^2}\overline{w}_{,11}\right] + \left[\frac{\gamma}{R\zeta}\left(-\sin\theta\overline{v} + \cos\theta\overline{w} + z\sin\theta\overline{w}_{,2}\right)\right]$
DMV	$\left[\frac{\xi}{\zeta^2}\overline{u}_{,1} - z\frac{1}{\zeta^2}\overline{w}_{,11}\right] + \left[\frac{\gamma}{R\zeta}\left(-\chi\sin\theta\overline{v} + \cos\theta\overline{w} + z\sin\theta\overline{w}_{,2}\right)\right]$
Sanders	$\left[\frac{\xi}{\zeta^2}\overline{u}_{,1} - z\frac{1}{\zeta^2}\overline{w}_{,11}\right] + \left[\frac{\gamma}{R\zeta}\left(-\chi\sin\theta\overline{v} + \cos\theta\overline{w} + z\sin\theta\overline{w}_{,2}\right)\right]$
TTS-V2	$\left[\frac{1}{\zeta}\overline{u}_{,1} - z\frac{1}{\zeta^2}\left(1 - \frac{z}{R}\frac{\gamma\cos\theta}{\zeta}\right)\overline{w}_{,11}\right] + \left[\frac{\gamma}{R\zeta}\left(1 - \frac{z}{R}\frac{\gamma\cos\theta}{\zeta}\right)\left(-\chi\sin\theta\overline{v} + \cos\theta\overline{w} + z\sin\theta\overline{w}_{,2}\right)\right]$

Table 6.2 - Comparison of circumferential strain-displacement expressions in various toroidal thin shell theories

Theory	Meridional Strain $\overline{\eta}_{22}$
TTS-V1	$\overline{v}_{,2} + \frac{1}{R\chi}\overline{w} - z\frac{1}{\chi}\overline{w}_{,22}$
TTS-V3	$\overline{v}_{,2} + \frac{1}{R}\overline{w} - z\overline{w}_{,22}$
DMV	$\chi\overline{v}_{,2} + \frac{1}{R}\overline{w} - z\overline{w}_{,22}$
Sanders	$\chi\overline{v}_{,2} + \frac{1}{R}\overline{w} - z\overline{w}_{,22}$
TTS-V2	$\overline{v}_{,2} + \frac{1}{R}\left(1 - \frac{z}{R}\right)\overline{w} - z\left(1 - \frac{z}{R}\right)\overline{w}_{,22}$

Table 6.3 – Comparison of shear strain-displacement expressions in various toroidal thin shell theories

Theory	Shear Strain $\bar{\eta}_{12}$
TTS-V1	$\frac{1}{2}\left\langle\left[\frac{\xi}{\chi\zeta}\bar{u}_{,2}+\frac{\chi}{\xi}\bar{v}_{,1}-z\left(\frac{1}{\xi}+\frac{1}{\chi\zeta}\right)\bar{w}_{,12}\right]+\frac{\gamma}{R}\frac{\sin\theta}{\zeta}\left\{\left[\frac{1}{\chi}\left(2-\frac{\xi}{\zeta}\right)+2\frac{z}{R}\frac{\gamma\cos\theta}{\zeta}\right]\bar{u}-z\left[\frac{1}{\chi}\left(1+2\frac{z}{R}\right)+\frac{\gamma\cos\theta}{\zeta}\right]\frac{1}{\xi}\bar{w}_{,1}\right\}\right\rangle$
TTS-V3	$\frac{1}{2}\left\{\left(\bar{u}_{,2}+\frac{1}{\zeta}\bar{v}_{,1}-2z\frac{1}{\zeta}\bar{w}_{,12}\right)+\frac{\gamma}{R}\frac{\sin\theta}{\zeta}\left[\left(1+2\frac{z}{R}\frac{\gamma\cos\theta}{\zeta}\right)\bar{u}-z\left(1+\frac{\gamma\cos\theta}{\zeta}\right)\frac{1}{\zeta}\bar{w}_{,1}\right]\right\}$
DMV	$\frac{1}{2}\left\{\left(1+2\frac{z}{R}\gamma\frac{\cos\theta}{\zeta}\right)\bar{u}_{,2}+\frac{1}{\zeta}\left(1+2\frac{z}{R}\right)\bar{v}_{,1}-2z\frac{1}{\zeta}\bar{w}_{,12}+\frac{\gamma}{R}\frac{\sin\theta}{\zeta}\left[\left(1+2\frac{z}{R}\frac{\gamma\cos\theta}{\zeta}\right)\bar{u}-2z\frac{1}{\zeta}\bar{w}_{,1}\right]\right\}$
Sanders	$\frac{1}{2}\left\langle\left[1+\frac{z}{R}\left(\gamma\cos\theta-\frac{1}{2}\right)\right]\bar{u}_{,2}+\frac{1}{\zeta}\left[1+\frac{z}{R}\left(\frac{1+2\zeta}{2\zeta}\right)\right]\bar{v}_{,1}-2z\frac{1}{\zeta}\bar{w}_{,12}+\frac{\gamma}{R}\frac{\sin\theta}{\zeta}\left\{\left[\left(1-\frac{z}{R}\frac{1}{\zeta}\right)+2\frac{z}{R}\frac{\gamma\cos\theta}{\zeta}\right]\bar{u}-2z\frac{1}{\zeta}\bar{w}_{,1}\right\}\right\rangle$
TTS-V2	$\frac{1}{2}\left[\left\{\left(1-\frac{z}{R}\right)\left(1+\frac{z}{R}\frac{\gamma\cos\theta}{\zeta}\right)\bar{u}_{,2}+\frac{\chi}{\zeta}\left(1-\frac{z}{R}\frac{\gamma\cos\theta}{\zeta}\right)\bar{v}_{,1}-z\frac{1}{\zeta}\left[\left(1-\frac{z}{R}\frac{\gamma\cos\theta}{\zeta}\right)+\left(1-\frac{z}{R}\right)\right]\bar{w}_{,12}\right\}+\frac{\gamma}{R}\frac{\sin\theta}{\zeta}\left\langle\left\{\left(1-\frac{z}{R}\right)\left[2-\left(1+\frac{z}{R}\frac{\gamma\cos\theta}{\zeta}\right)\right]+2\frac{z}{R}\frac{\gamma\cos\theta}{\zeta}\right\}\bar{u}_{,1}-z\frac{1}{\zeta}\left[\left(1-\frac{z}{R}\right)\left(1+2\frac{z}{R}\right)+\frac{\gamma\cos\theta}{\zeta}\right]\left(1-\frac{z}{R}\frac{\gamma\cos\theta}{\zeta}\right)\bar{w}\right\rangle\right]$

It is noted that while for the case of longitudinal and shear strains, $\bar{\eta}_{11}$ and $\bar{\eta}_{12}$, there are some new differential terms in addition to those from straight pipes, the circumferential strain $\bar{\eta}_{22}$ is not a function of and affected by the radius of the torus $\Re$ $(=R/\gamma)$, nor the cross-sectional angle of rotation θ $(=s/R)$. The hoop strains defined in Sanders and DMV differ from those of TTS-V1 by a factor of $1/\chi$. For $h/R=1/20$, this will yield a 5%

difference in strains at the outer and inner surfaces. Considering the degree of complexity of the various terms in TTS theory, the strain-displacement relationships based on TTS-V1, TTS-V2, Sander's and DMV could be considered very close.

6.6 Generalized Representation on Toroidal Thin Shell Theories

By modifying the generalized thin shell theory developed in Chapter 2 to toroidal shells, the governing field equations and corresponding boundary conditions were obtained. Using the geometric and mechanical properties of TTSs previously developed in Sections 6.3 and 6.4 in the same manner as in Chapter 3 (for the case of CCTSs) and after proper simplifications, the stationary condition of the Hamilton's functional is expressed as

$$\delta\Pi = \left[\left[\int_0^{2\pi R} \left(\left\langle \delta u(x,s)\ \ \delta v(x,s)\ \ \delta w(x,s)\ \ \delta w_{,1}(x,s) \right\rangle \times \left(\left[\begin{array}{c|c|c} D_{11} & D_{12} & D_{13} \\ \hline D_{21} & D_{22} & D_{23} \\ \hline D_{31} & D_{32} & D_{33} \\ \hline D_{41} & D_{42} & D_{43} \end{array}\right] \left\{\begin{array}{c} u(x,s) \\ v(x,s) \\ w(x,s) \end{array}\right\} + \left\{\begin{array}{c} 0 \\ 0 \\ F_{BC}^{w} \\ 0 \end{array}\right\} \right) \right) ds \right]\right]_0^L \right.$$

$$+ \int_0^L \int_0^{2\pi R} \left(\left\langle \delta u(x,s)\ \ \delta v(x,s)\ \ \delta w(x,s) \right\rangle \times \left(\left[\begin{array}{c|c|c} L_{11} & L_{12} & L_{13} \\ \hline L_{21} & L_{22} & L_{23} \\ \hline L_{31} & L_{32} & L_{33} \end{array}\right] \left\{\begin{array}{c} u(x,s) \\ v(x,s) \\ w(x,s) \end{array}\right\} + \left\{\begin{array}{c} F_{FE}^{u} \\ F_{FE}^{v} \\ F_{FE}^{w} \end{array}\right\} \right) \right) ds dx = 0 \tag{6.21}$$

where the differential operators D_{ij} and L_{ij} are

$$\begin{aligned} D_{11} &= d_1 \frac{\partial}{\partial x} \\ D_{12} &= d_2 \frac{\partial}{\partial s} + d_3 \\ D_{13} &= d_4 \frac{\partial^2}{\partial x^2} + d_5 \frac{\partial^2}{\partial s^2} + d_6 \frac{\partial}{\partial s} + d_7 \end{aligned} \tag{6.22}$$

$$
\begin{aligned}
D_{21} &= d_8 \frac{\partial}{\partial s} + d_9 \\
D_{22} &= d_{10} \frac{\partial}{\partial x} \\
D_{23} &= d_{11} \frac{\partial^2}{\partial x \partial s} + d_{12} \frac{\partial}{\partial x}
\end{aligned}
\tag{6.23}
$$

$$
\begin{aligned}
D_{31} &= d_{13} \frac{\partial^2}{\partial x^2} + d_{14} \frac{\partial^2}{\partial s^2} + d_{15} \frac{\partial}{\partial s} + \left(d_{16} + d_{16}^I \frac{\partial^2}{\partial t^2} \right) \\
D_{32} &= d_{17} \frac{\partial^2}{\partial x \partial s} + d_{18} \frac{\partial}{\partial x} \\
D_{33} &= d_{19} \frac{\partial^3}{\partial x^3} + d_{20} \frac{\partial^3}{\partial x \partial s^2} + d_{21} \frac{\partial^2}{\partial x \partial s} + \left(d_{22} + d_{22}^I \frac{\partial^2}{\partial t^2} \right) \frac{\partial}{\partial x}
\end{aligned}
\tag{6.24}
$$

$$
\begin{aligned}
D_{41} &= d_{23} \frac{\partial}{\partial x} \\
D_{42} &= d_{24} \frac{\partial}{\partial s} + d_{25} \\
D_{43} &= d_{26} \frac{\partial^2}{\partial x^2} + d_{27} \frac{\partial^2}{\partial s^2} + d_{28} \frac{\partial}{\partial s} + d_{29}
\end{aligned}
\tag{6.25}
$$

$$
\begin{aligned}
L_{11} &= l_1 \frac{\partial^2}{\partial x^2} + l_2 \frac{\partial^2}{\partial s^2} + l_3 \frac{\partial}{\partial s} + \left(l_4 + l_4^I \frac{\partial^2}{\partial t^2} \right) \\
L_{12} &= l_5 \frac{\partial^2}{\partial x \partial s} + l_6 \frac{\partial}{\partial x} \\
L_{13} &= l_7 \frac{\partial^3}{\partial x^3} + l_8 \frac{\partial^3}{\partial x \partial s^2} + l_9 \frac{\partial^2}{\partial x \partial s} + \left(l_{10} + l_{10}^I \frac{\partial^2}{\partial t^2} \right) \frac{\partial}{\partial x}
\end{aligned}
\tag{6.26}
$$

$$
\begin{aligned}
L_{21} &= l_{11} \frac{\partial^2}{\partial x \partial s} + l_{12} \frac{\partial}{\partial x} \\
L_{22} &= l_{13} \frac{\partial^2}{\partial x^2} + l_{14} \frac{\partial^2}{\partial s^2} + l_{15} \frac{\partial}{\partial s} + \left(l_{16} + l_{16}^I \frac{\partial^2}{\partial t^2} \right) \\
L_{23} &= l_{17} \frac{\partial^3}{\partial s^3} + l_{18} \frac{\partial^3}{\partial x^2 \partial s} + l_{19} \frac{\partial^2}{\partial x^2} + l_{20} \frac{\partial^2}{\partial s^2} + \left(l_{21} + l_{21}^I \frac{\partial^2}{\partial t^2} \right) \frac{\partial}{\partial s} + l_{22}
\end{aligned}
\tag{6.27}
$$

$$
\begin{aligned}
L_{31} &= l_{23}\frac{\partial^3}{\partial x^3} + l_{24}\frac{\partial^3}{\partial x \partial s^2} + l_{25}\frac{\partial^2}{\partial x \partial s} + \left(l_{26} + l_{26}^I \frac{\partial^2}{\partial t^2}\right)\frac{\partial}{\partial x} \\
L_{32} &= l_{27}\frac{\partial^3}{\partial s^3} + l_{28}\frac{\partial^3}{\partial x^2 \partial s} + l_{29}\frac{\partial^2}{\partial x^2} + l_{30}\frac{\partial^2}{\partial s^2} + \left(l_{31} + l_{31}^I \frac{\partial^2}{\partial t^2}\right)\frac{\partial}{\partial s} + \left(l_{32} + l_{32}^I \frac{\partial^2}{\partial t^2}\right) \\
L_{33} &= l_{33}\frac{\partial^4}{\partial x^4} + l_{34}\frac{\partial^4}{\partial s^4} + l_{35}\frac{\partial^4}{\partial x^2 \partial s^2} + l_{36}\frac{\partial^3}{\partial s^3} + l_{37}\frac{\partial^3}{\partial x^2 \partial s} + \left(l_{38} + l_{38}^I \frac{\partial^2}{\partial t^2}\right)\frac{\partial^2}{\partial x^2} \\
&\quad + \left(l_{39} + l_{39}^I \frac{\partial^2}{\partial t^2}\right)\frac{\partial^2}{\partial s^2} + \left(l_{40} + l_{40}^I \frac{\partial^2}{\partial t^2}\right)\frac{\partial}{\partial s} + \left(l_{41} + l_{41}^I \frac{\partial^2}{\partial t^2}\right)
\end{aligned}
\tag{6.28}
$$

and generic force terms F_{BC}^w, F_{FE}^u, F_{FE}^v and F_{FE}^w are defined as

$$
\begin{aligned}
F_{BC}^w &= f_1^F f_1^{xw} + f_2^F f_2^{xw} \\
F_{FE}^u &= f_3^F f_1^{xu} + f_4^F f_2^{xu} \\
F_{FE}^v &= f_5^F f_1^{sv} + f_6^F f_2^{sv} \\
F_{FE}^w &= f_7^F f_1^{zw} + f_8^F f_2^{zw} + f_9^F \frac{\partial}{\partial x} f_1^{xw} + f_{10}^F \frac{\partial}{\partial x} f_2^{xw} + \left(f_{11}^F \frac{\partial}{\partial s} + f_{12}^F\right) f_1^{sw} + f_{13}^F \frac{\partial}{\partial s} f_2^{sw}
\end{aligned}
\tag{6.29}
$$

It is noted that the differential operators D_{ij} and L_{ij} and force terms F_{BC}^w, F_{FE}^u, F_{FE}^v and F_{FE}^w include distinct differential terms depending on the degree of simplification made. However, the generic format in Eq. 6.21 empowers us to extract any of the TTS-V2, TTS-V3, Sander's and DMV theories as special cases by defining distinct coefficients d_i, d_i^I, l_i, l_i^I, f_i^F for each theory and setting the coefficients of the non-relevant terms equal to zero. Coefficients d_i, d_i^I, l_i, l_i^I, f_i^F and forces f_1^{xu}, f_2^{xu}, f_1^{sv}, f_2^{sv}, f_1^{zw}, f_2^{zw}, f_1^{xw}, f_2^{xw}, f_1^{sw} and f_2^{sw} are provided in Appendix 6.A for the TTS-V2 and TTS-V3 theories. Also given are the coefficients l_i corresponding to Sanders and DMV theories for comparison. It is noted that, in general, all coefficients d_i, d_i^I, l_i, l_i^I, f_i^F are functions of s $(= R\theta)$.

6.7 Field Equations of Toroidal Thin Shell Theories

This section provides a basis for comparing the toroidal thin shell theories TTS-V1, TTS-V2, Sander's and DMV in terms of differential terms participating in the field equations. This comparison is limited to the static part of the field equations in the absence of inertial terms and an explicit form of the boundary conditions in Sander's and DMV theories. Table 6.6 in Appendix 6.B provides a detailed term by term comparison between the four theories. It is convenient to define the following generic differential operator matrices as they will be used in upcoming sections (6.7.1 through 6.7.4).

$$\mathbf{L}_1(theory)=\begin{bmatrix} l_1\frac{\partial^2}{\partial x^2}+l_2\frac{\partial^2}{\partial s^2}+l_3\frac{\partial}{\partial s}+l_4 & l_6\frac{\partial^2}{\partial x\partial s}+l_7\frac{\partial}{\partial x} & l_{10}\frac{\partial}{\partial x} \\ l_{11}\frac{\partial^2}{\partial x\partial s}+l_{12}\frac{\partial}{\partial x} & l_{13}\frac{\partial^2}{\partial x^2}+l_{14}\frac{\partial^2}{\partial s^2}+l_{15}\frac{\partial}{\partial s}+l_{16} & l_{21}\frac{\partial}{\partial s}+l_{22} \\ l_{26}\frac{\partial}{\partial x} & l_{31}\frac{\partial}{\partial s}+l_{32} & l_{33}\frac{\partial^4}{\partial x^4}+l_{34}\frac{\partial^4}{\partial s^4}+l_{35}\frac{\partial^4}{\partial x^2\partial s^2}+l_{36}\frac{\partial^3}{\partial s^3}+l_{37}\frac{\partial^3}{\partial x^2\partial s}+l_{38}\frac{\partial^2}{\partial x^2}+l_{39}\frac{\partial^2}{\partial s^2}+l_{41} \end{bmatrix} \tag{6.30}$$

$$\mathbf{L}_2(theory)=\begin{bmatrix} 0 & 0 & l_9\frac{\partial^2}{\partial x\partial s} \\ 0 & 0 & l_{19}\frac{\partial^2}{\partial x^2} \\ l_{25}\frac{\partial^2}{\partial x\partial s} & 0 & 0 \end{bmatrix} \tag{6.31}$$

$$\mathbf{L}_3\left(theory\right)=\left[\begin{array}{c|c|c} 0 & 0 & l_7\frac{\partial^3}{\partial x^3}+l_8\frac{\partial^3}{\partial x\partial s^2} \\ \hline 0 & 0 & l_{17}\frac{\partial^3}{\partial s^3}+l_{18}\frac{\partial^3}{\partial x^2\partial s}+l_{20}\frac{\partial^2}{\partial s^2} \\ \hline l_{23}\frac{\partial^3}{\partial x^3}+l_{24}\frac{\partial^3}{\partial x\partial s^2} & l_{27}\frac{\partial^3}{\partial s^3}+l_{28}\frac{\partial^3}{\partial x^2\partial s}+l_{29}\frac{\partial^2}{\partial x^2}+l_{30}\frac{\partial^2}{\partial s^2} & l_{40}\frac{\partial}{\partial s} \end{array}\right] \tag{6.32}$$

where the argument "*theory*" denotes various theories and takes the values DMV, TTS-V3, TTS-V2, or Sanders as applicable in the following sections. The coefficients of matrices $\mathbf{L}_1\left(theory\right)$, $\mathbf{L}_2\left(theory\right)$ and $\mathbf{L}_3\left(theory\right)$ are presented for each of the four theories in the subsequent subsections.

6.7.1 DMV Theory

The homogenous part of the differential equations of the system based on DMV theory can be written as

$$\mathbf{L}_{DMV}\left\{\begin{matrix} u \\ v \\ w \end{matrix}\right\}=0 \tag{6.33}$$

where the operator matrix $\mathbf{L}_{DMV}=\mathbf{L}_1\left(DMV\right)$ in which the coefficients $l_i=l_i\left(DMV\right)$ are provided in Section 6.A.1 of Appendix 6.A . The operator matrix $\mathbf{L}_{DMV}$ includes only the membrane effects of the displacement components except for the entry $\mathbf{L}_{DMV}\left(3,3\right)$ which involves the flexural effect of the radial displacement.

6.7.2 TTS-V3 Theory

The TTS-V3 theory is the most simplified theory based on the current study. The system of ODEs developed for TTS-V3 take the form

$$\mathbf{L}_{TTS-V3}\begin{Bmatrix} u \\ v \\ w \end{Bmatrix} = \left[\mathbf{L}_1\left(TTS-V3\right)+\mathbf{L}_2\left(TTS-V3\right)\right]\begin{Bmatrix} u \\ v \\ w \end{Bmatrix} \tag{6.34}$$

where, $\mathbf{L}_1\left(TTS-V3\right)$ and $\mathbf{L}_2\left(TTS-V3\right)$ are evaluated based on the coefficients $l_i\left(TTS-V3\right)$ defined in TTS-V3 theory provided in Section 6.A.2 of Appendix 6.A . Although all non-zero entries in the operator matrix $\mathbf{L}_2\left(TTS-V3\right)$ are related to flexural effects, a study of the expressions l_i indicates that the TTS-V3 theory does not capture any flexural effect arising from the circumferential displacement component v. Also, in the coefficients of the second field equation (L_{2j}), the radial displacement component w is the only component for which the flexural effects are included.

6.7.3 TTS-V2 Theory

The TTS-V2 theory is a more accurate representative of the toroidal thin shell behaviour. The system of ODEs based on TTS-V2 takes the form

$$\mathbf{L}_{TTS-V2}\begin{Bmatrix} u \\ v \\ w \end{Bmatrix} = \left[\mathbf{L}_1\left(TTS-V2\right)+\mathbf{L}_2\left(TTS-V2\right)+\mathbf{L}_3\left(TTS-V2\right)\right]\begin{Bmatrix} u \\ v \\ w \end{Bmatrix} \tag{6.35}$$

where $\mathbf{L}_1\left(TTS-V2\right)$, $\mathbf{L}_2\left(TTS-V2\right)$ and $\mathbf{L}_3\left(TTS-V2\right)$ are evaluated based on the coefficients $l_i\left(TTS-V2\right)$ defined in TTS-V2 theory provided in Section 6.A.3 of Appendix 6.A . The entries in the differential operator matrices $\mathbf{L}_2\left(TTS-V2\right)$ and $\mathbf{L}_3\left(TTS-V2\right)$ represent only flexural effects. The expressions l_i indicate that the TTS-V2 theory includes both membrane and flexural effects for all three components of the displacement field.

6.7.4 Sanders Theory

The system of ODEs based on Sander's theory takes the form

$$\mathbf{L}_{Sanders}\begin{Bmatrix} u \\ v \\ w \end{Bmatrix} = \left[\mathbf{L}_1\left(Sanders\right) + \mathbf{L}_2\left(Sanders\right) + \mathbf{L}_3\left(Sanders\right)\right]\begin{Bmatrix} u \\ v \\ w \end{Bmatrix} \tag{6.36}$$

where $\mathbf{L}_1\left(Sanders\right)$, $\mathbf{L}_2\left(Sanders\right)$ and $\mathbf{L}_3\left(Sanders\right)$ are evaluated based on the coefficients $l_i\left(Sanders\right)$ provided in Section 6.A.4 of Appendix 6.A . Similar to the TTS-V2 theory, all the non-zero entries in the differential operator matrices $\mathbf{L}_2\left(Sanders\right)$ and $\mathbf{L}_3\left(Sanders\right)$ represent only flexural effects. Sanders theory includes both membrane and flexural effects due to all three components of the displacement field. However as shown in Appendix 6.B , although most terms in the TTS-V2 theory and those of Sanders are comparable, they are not always identical.

6.8 A Modified Toroidal Thin Shell Theory (TTS-V2M) for Elbows of Common Geometry

Considering the complexity of TTS-V2 and Sanders theories in one hand and the large approximation involved in the TTS-V3 and DMV theories on the other hand, another modified toroidal thin shell theory is developed for pipe bends of common geometries. The theory nearly retains the accuracy of the former two theories while involving simpler expressions. In determining the coefficients in the modified newer theory (termed as TTS-V2M), all differential terms in TTS-V2 are retained except those terms that are clearly negligible compared to other terms. The geometric assumptions $h/R \le 1/20$ and $R/\Re \le 1/2$ are made. These should be valid for most pipe bends. Coefficients $d_i\left(TTS-V2M\right)$, $d_i^I\left(TTS-V2M\right)$, $l_i\left(TTS-V2M\right)$ and $l_i^I\left(TTS-V2M\right)$ are then numerically evaluated under the postulated geometric assumptions. This procedure has led to several simplifications in the various coefficients of the differential equations. These are detailed in

Appendix 6.B . The coefficients for TTS-V2M are provided in Section 6.A.5 of Appendix 6.A .

Table 6.4 provides a comparative summary for the L_{ij} differential operators between various theories. Those differential terms involving only membrane terms are marked "M" while those involving only flexural terms are denoted "F". A term involving both membrane and flexural effects are denoted "M+F". A similar comparison for the differential operators D_{ij} in provided in Table 6.5. Table 6.4 may suggest that the flexural effects due to longitudinal and circumferential displacement components, u and v, have minor contribution in coefficients L_{1j} and L_{2j}. Table 6.5 indicates that while the flexural effects of all three displacement components have minor contributions on the longitudinal (D_{1j}) and circumferential (D_{2j}) natural boundary conditions, it is only their flexural effects that participates in radial (D_{3j}) and rotational (D_{4j}) natural boundary contributions.

Table 6.4 – Membrane (M) and flexural (F) effects in differential operators L_{ij} (Field terms).

Theory	L_{11}	L_{12}	L_{13}	L_{21}	L_{22}	L_{23}	L_{31}	L_{32}	L_{33}
TTS-V2	M+F	M+F	M+F	M+F	M+F	M+F	M+F	M+F	M+F
Sanders	M+F	M+F	M+F	M+F	M+F	M+F	M+F	M+F	M+F
TTS-V2M	M	M	M+F	M	M	M+F	M+F	M+F	M+F
TTS-V3	M+F	M	M+F	M	M	M+F	M+F	M	M+F
DMV	M	M	M	M	M	M	M	M	M+F

Table 6.5 – Membrane (M) and flexural (F) effects in differential operators D_{ij} (Boundary terms).

Theory	D_{11}	D_{12}	D_{13}	D_{21}	D_{22}	D_{23}	D_{31}	D_{32}	D_{33}	D_{41}	D_{42}	D_{43}
TTS-V2	M+F	M+F	M+F	M+F	M+F	F	F	F	F	F	F	F
TTS-V2M	M	M	M+F	M	M	M+F	F	F	F	F	F	F
TTS-V3	M	M	M	M	M	F	F	-	F	-	-	F

6.9 Conclusions and Remarks

The generalized thin shell theory developed in Chapter 2 was specialized to toroidal shells. Two different versions (TTS-V2 and TTS-V3) of the governing field equations and corresponding boundary conditions were obtained based on different simplifications. By comparing both versions with those of the Sanders and DMV theories for toroidal shells and some numerical evaluation for toroids of practical geometries, a third theory (TTS-V2M) was proposed.

Although the DMV strain-displacement relationships were not much different from those of TTS-V2 and Sanders, the significant difference between the field equations is believed to have arisen from the further simplifications in the process of developing the field equations in DMV theory.

It is noted that the terms of the DMV theory are a subset of those of the TTS-V3 theory. Also the terms of the TTS-V3 theory are a subset of the TTS-V2 theory. The TTS-V2 and Sanders theory are similar in terms of participation of the differential terms. However, the TTS-V2 theory has the following advantages

1. It is based on consistent simplifications.

2. It includes the inertial and dynamic effects.

3. It includes body force terms.

4. It provides expressions for the boundary conditions, which are consistent and compatible with the field equations.

The above facts are also valid for TTS-V3 theory over DMV theory. Based on the detailed study provided, the TTS-V2M theory is proposed for the pipe bends of common geometries as an alternative for Sanders, DMV, TTS-V2 and TTS-V3 with the advantage of relative simplicity of the coefficients involved while capturing all significant membrane and flexural effects.

The TTS-V2 toroidal thin shell theory developed in this chapter is used as a basis to develop a toroidal finite element in the next chapter.

6.10 References

[6.1] D. Redekop, B. Xu, Vibration Analysis of Toroidal Panels Using the Differential Quadrature Method, J. Thin-Walled Struct. 34 (1999) 217-231

[6.2] Jr.J.L. Sanders, An Improved First Approximation Theory for Thin Shells. Langley Research Center, TR-24, 1959.

[6.3] F. Zhang, D. Redecop, Surface Loading of a Thin-Walled Toroidal Shell, Comp. Struct. 43 (1992) 1019-1028.

[6.4]

6.11 List of Symbols

$\mathbf{a}_i$	Covariant base vectors of the middle surface
a_{ij}	First fundamental tensor defined on the middle surface of a thin shell
a	Determinant of the first fundamental tensor a_{ij}
$b_{\alpha\beta}$	Curvature tensor of the surfaces parallel and adjacent to the middle surface
$\overline{b}_{\alpha\beta}$	Second fundamental tensor or curvature tensor defined on the middle surface of a thin shell
$\mathbf{a}^i$	Contravariant base vectors of the middle surface
a^{ij}	First fundamental tensor of the second kind defined on the middle surface of a thin shell
$\mathbf{g}_i$	Covariant base vectors of any surface parallel and adjacent to the middle surface
g_{ij}	First fundamental tensor defined within the shell
g	Determinant of the first fundamental tensor g_{ij}
$\mathbf{g}^i$	Contravariant base vectors of any surface parallel and adjacent to the middle surface
g^{ij}	First fundamental tensor of the second kind defined within the shell
$\mathbf{U}$	Displacement of a point within the shell
U_i	Covariant components of the displacement of a point on a surface parallel and adjacent to the middle surface along axis x^i
u_i	Covariant components of the displacement of a point on the middle surface along axis x^i
u, v, w	Covariant components of the displacement of a point on the middle surface along axes x^1, x^2 and x^3, respectively
$\overline{u}, \overline{v}, \overline{w}$	Physical components of the covariant displacement components u, v, w, respectively

X^i	Coordinate system/Coordinates of the system
x^i	Coordinate system/Coordinates of the system
x, s, z	Coordinates of the system, equivalent to x^1, x^2 and x^3, respectively
$^{\alpha}, _{\alpha}, \ldots$	All Greek superscripts or subscripts range from 1 to 2
$^{i}, _{i}, \ldots$	All Italic superscripts or subscripts range from 1 to 3
$\vec{\mathbf{i}}_i, \vec{\mathbf{j}}_i$	Covariant unit vectors along axis x^i in middle surface and adjacent surfaces, respectively
$\vec{\mathbf{i}}^i, \vec{\mathbf{j}}^i$	Contravariant unit vectors along axis x^i in middle surface and adjacent surfaces, respectively
Γ_{ij}^k	Christoffel symbols in terms of g_i and g_{ij}
$\overline{\Gamma}_{ij}^k$	Christoffel symbols in terms of a_i and a_{ij} (defined for the middle surface)
$\cdot$	Inner product
$\otimes$	Cross product
$\vert$	Covariant derivative
$\Vert$	Covariant derivative in two dimensional spaces
T^*	Kinetic energy
V^*	Potential energy
V	Volume
W^*	External work
$\prod$	Mechanical energy of the system
ε_{ij}	Components of the strain tensor on the middle surface
η_{ij}	Components of the strain tensor adjacent to the middle surface

$\eta_{\alpha\beta}$	In-plane components of the Strain tensor
σ^{ij}	Stress tensor
$\sigma^{\alpha\beta}$	In-plane components of the stress tensor
E^{ijlm}	Generalized Hooke's Law
$E^{\alpha\beta\lambda\delta}$	In-plane components of the generalized Hooke's Law
$\cdots_{,i}$	Partial derivative with respect to x^i
δ^{α}_{β}	Kronecker delta function
μ^{α}_{β}	The covariant tensor which connects the base vectors of two different points
$\lambda^{\gamma}_{\alpha}$	Contravariant counterpart of μ^{α}_{β}
ρ	Density of the mass
E	Modulus of elasticity
ν	Poisson's ratio
$\mathbf{r}$	Position vector of a general point lying on the middle surface of a torus
R	Cross-sectional radius of torus
$\Re$	Torus radius
$\vec{\mathbf{I}}_i$	Unit vector in the Cartesian coordinate system X^i
γ	$R/\Re$
χ	$1+z/R$
θ	s/R
ζ	$1+\gamma\cos\theta$
ξ	$1+\gamma\chi\cos\theta$
D_{ij}	Differential operators in boundary condition equations

L_{ij}	Differential operators in field equations
F_{FE}^{u} , F_{FE}^{v} , F_{FE}^{w} , F_{BC}^{w}	Generic force terms in the functional
f_i^F $(i=1,...,13)$	Constants in defining the generic force terms F_{FE}^{u} , F_{FE}^{v} , F_{FE}^{w} , F_{BC}^{w} in the functional
f_j^{xu} , f_j^{sv} , f_j^{xw} f_j^{sw}, f_j^{zw} $(j=1,2)$	Tractions in defining the generic force terms F_{FE}^{u} , F_{FE}^{v} , F_{FE}^{w} , F_{BC}^{w} in the functional as a function of x and s

Appendix 6.A Coefficients of Various Toroidal Thin Sell Theory

The objective of this appendix is to provide the explicit expressions for coefficients d_i, d_i^I, l_i, l_i^I, f_i^F and forces f_1^{xu}, f_2^{xu}, f_1^{sv}, f_2^{sv}, f_1^{zw}, f_2^{zw}, f_1^{xw}, f_2^{xw}, f_1^{sw} and f_2^{sw} introduced in Eqs. 6.22-6.29 in defining the differential operators D_{ij} and L_{ij} used in Eq. 6.21. These coefficients and forces are provided for the TTS-V2, TTS-V2M, TTS-V3, Sanders and DMV theories in the following subsections. In case of the DMV and Sanders theories, however, in the absence of inertial terms and an explicit form of the boundary conditions and applied loads only l_i coefficients are provided.

6.A.1 Coefficients for DMV Theory

Coefficients $l_i(DMV)$ (called as l_i in this section for brevity) introduced in Eqs. 6.26-6.28 in defining the differential operators of the homogeneous part of the field equations of the DMV theory are defined as [6.1]

$$l_1 = \zeta^{-1} \quad , \quad l_2 = \frac{1-\nu}{2}\zeta$$

$$l_3 = -\frac{1}{R}\frac{1-\nu}{2}\gamma\sin\theta \quad , \quad l_4 = \frac{1}{R^2}\frac{1-\nu}{2}\left(\gamma\cos\theta - \gamma^2\zeta^{-1}\sin^2\theta\right)$$

$$l_5 = \frac{1+\nu}{2} \quad , \quad l_6 = -\frac{1}{R}\frac{3-\nu}{2}\gamma\zeta^{-1}\sin\theta$$

$$l_7 = 0 \quad , \quad l_8 = 0$$

$$l_9 = 0 \quad , \quad l_{10} = \frac{1}{R}\left(\nu + \gamma\zeta^{-1}\cos\theta\right)$$

$$l_{11}=\frac{1+\nu}{2} \quad , \quad l_{12}=\frac{3-\nu}{2}\gamma\zeta^{-1}\sin\theta$$
$$l_{13}=\frac{1-\nu}{2}\zeta^{-1} \quad , \quad l_{14}=\zeta$$
$$l_{15}=-\frac{1}{R}\gamma\sin\theta \quad , \quad l_{16}=-\frac{1}{R^2}\left(\nu\gamma\cos\theta+\gamma^2\zeta^{-1}\sin^2\theta\right)$$
$$l_{17}=0 \quad , \quad l_{18}=0$$
$$l_{19}=0 \quad , \quad l_{20}=0$$
$$l_{21}=\frac{1}{R}\left(\zeta+\nu\gamma\cos\theta\right) \quad , \quad l_{22}=-\frac{1}{R^2}\gamma\zeta^{-1}\sin\theta$$

$$l_{23}=0 \quad , \quad l_{24}=0$$
$$l_{25}=0 \quad , \quad l_{26}=-\frac{1}{R}\left(\nu+\gamma\zeta^{-1}\cos\theta\right)$$
$$l_{27}=0 \quad , \quad l_{28}=0$$
$$l_{29}=0 \quad , \quad l_{30}=0$$
$$l_{31}=-\frac{1}{R}\left(\zeta+\nu\gamma\cos\theta\right) \quad , \quad l_{32}=\frac{1}{R^2}\left(\nu\gamma\sin\theta+\gamma^2\zeta^{-1}\sin\theta\cos\theta\right)$$
$$l_{33}=-R^2\kappa\zeta^{-3} \quad , \quad l_{34}=-R^2\kappa\zeta$$
$$l_{35}=-2R^2\kappa\zeta^{-1} \quad , \quad l_{36}=2R\kappa\gamma\sin\theta$$
$$l_{37}=-2R\kappa\gamma\zeta^{-2}\sin\theta \quad , \quad l_{38}=-2\kappa\zeta^{-3}\left[\gamma^2+\gamma\cos\theta+\gamma^2\sin^2\theta\right]$$
$$l_{39}=\kappa\gamma\left(\gamma\zeta^{-1}+2\zeta^{-1}\cos\theta+\gamma\zeta^{-1}\cos^2\theta\right), \quad l_{40}=0$$
$$l_{41}=-\frac{1}{R^2}\left(2\nu\gamma\cos\theta+\gamma^2\zeta^{-1}\cos^2\theta\right)$$

6.A.2 Coefficients for TTS-V3 Theory

Coefficients $d_i\left(TTs-V3\right)$ and $d_i^I\left(TTs-V3\right)$ (called in this section as d_i and d_i^I, respectively, for brevity) introduced in Eqs. 6.22-6.25 in defining the differential operators of the boundary condition equations of the TTS-V3 theory are defined as

$$d_1=-\zeta^{-1} \quad , \quad d_2=-\nu$$
$$d_3=\frac{1}{R}\gamma\zeta^{-1}\sin\theta \quad , \quad d_4=0$$
$$d_5=0 \quad , \quad d_6=0$$
$$d_7=-\frac{1}{R}\left(\nu+\gamma\zeta^{-1}\cos\theta\right)$$

$$d_8 = -\frac{1-\nu}{2} \quad , \quad d_9 = -\frac{1}{R}\frac{1-\nu}{2}\gamma\zeta^{-1}\sin\theta$$
$$d_{10} = -\frac{1-\nu}{2}\zeta^{-1} \quad , \quad d_{11} = 0$$
$$d_{12} = -\frac{1-\nu}{2}\kappa\gamma\zeta^{-3}\sin\theta$$

$$d_{13} = 0 \quad , \quad d_{14} = 0$$
$$d_{15} = 3(1-\nu)\kappa\gamma\zeta^{-1}\sin\theta \quad , \quad d_{16} = \frac{1}{R}(1-\nu)\kappa\gamma\zeta^{-3}\left(2\gamma + 2\cos\theta + \gamma\sin^2\theta\right)$$
$$d_{16}^I = 0 \quad , \quad d_{17} = 0$$
$$d_{18} = 0 \quad , \quad d_{19} = R^2\kappa\zeta^{-3}$$
$$d_{20} = R^2(2-\nu)\kappa\zeta^{-1} \quad , \quad d_{21} = R(1-2\nu)\kappa\gamma\zeta^{-2}\sin\theta$$
$$d_{22} = 2(1-\nu)\kappa\gamma\zeta^{-3}(\gamma + \cos\theta) \quad , \quad d_{22}^I = -\frac{1-\nu^2}{E}\rho R^2\kappa\zeta$$

$$d_{23} = 0 \quad , \quad d_{24} = 0$$
$$d_{25} = 0 \quad , \quad d_{26} = -R^2\kappa\zeta^{-3}$$
$$d_{27} = -\nu R^2\kappa\zeta^{-1} \quad , \quad d_{28} = R\kappa\gamma\zeta^{-2}\sin\theta$$
$$d_{29} = 0$$

Coefficients $l_i(TTs-V3)$ and $l_i^I(TTs-V3)$ (called as l_i and l_i^I in this section for brevity) introduced in Eqs. 6.26-6.28 in defining the differential operators of the field equations of the TTS-V3 theory are defined as

$$l_1 = \zeta^{-1} \quad , \quad l_2 = \left(\frac{1-\nu}{2}\right)\zeta$$
$$l_3 = -\left(\frac{1-\nu}{2}\right)\frac{\gamma}{R}\sin\theta$$
$$l_4 = \frac{1}{R^2}\left(\frac{1-\nu}{2}\right)\Big[\gamma\cos\theta - (1-2\kappa)\gamma^2\zeta^{-1}\sin^2\theta - 4\kappa\gamma^3\zeta^{-2}\sin^2\theta\cos\theta + 2\kappa\gamma^4\zeta^{-3}\sin^2\theta\cos^2\theta\Big]$$
$$l_4^I = -\frac{1-\nu^2}{E}\rho\zeta^3 \quad , \quad l_5 = \left(\frac{1+\nu}{2}\right)$$
$$l_6 = -\left(\frac{3-\nu}{2}\right)\frac{\gamma}{R}\zeta^{-1}\sin\theta \quad , \quad l_7 = 0$$
$$l_8 = 0 \quad , \quad l_9 = (1-\nu)\kappa\gamma\zeta^{-2}\sin\theta$$

$$l_{10} = \frac{1}{R}\Big[\nu + \Big(1+\kappa\frac{1-\nu}{2}\Big)\gamma\zeta^{-1}\cos\theta - 4\Big(\frac{1-\nu}{2}\Big)\kappa\gamma^2\zeta^{-2}\cos^2\theta + 3\Big(\frac{1-\nu}{2}\Big)\kappa\gamma^2\zeta^{-2} - 3\Big(\frac{1-\nu}{2}\Big)\kappa\gamma^3\zeta^{-3}\sin^2\theta\cos\theta\Big]$$

$$l_{10}^I = 0$$

$$l_{11} = \Big(\frac{1+\nu}{2}\Big) \quad , \quad l_{12} = \Big(\frac{3-\nu}{2}\Big)\frac{\gamma}{R}\zeta^{-1}\sin\theta$$

$$l_{13} = \Big(\frac{1-\nu}{2}\Big)\zeta^{-1} \quad , \quad l_{14} = \zeta$$

$$l_{15} = -\frac{\gamma}{R}\sin\theta \quad , \quad l_{16} = -\frac{1}{R^2}\Big(\nu\gamma\cos\theta + \gamma^2\zeta^{-1}\sin^2\theta\Big)$$

$$l_{16}^I = -\frac{1-\nu^2}{E}\rho\zeta \quad , \quad l_{17} = 0$$

$$l_{18} = 0 \quad , \quad l_{19} = \kappa\gamma\zeta^{-3}\sin\theta\Big(\frac{1+\nu}{2}\Big)$$

$$l_{20} = \Big(\frac{1+\nu}{2}\Big)\kappa\gamma\zeta^{-3}\sin\theta \quad , \quad l_{21} = \frac{1}{R}\Big[1+(1+\nu)\gamma\cos\theta\Big]$$

$$l_{21}^I = 0 \quad , \quad l_{22} = -\frac{\nu\gamma}{R^2}\zeta^{-1}\sin\theta$$

$$l_{23} = 0 \quad , \quad l_{24} = 0$$

$$l_{25} = -\Big[(3-\nu)\kappa\gamma\zeta^{-1}\sin\theta - (3-\nu)\kappa\gamma^2\zeta^{-2}\sin\theta\cos\theta\Big]$$

$$l_{26} = -\frac{1}{R}\Big[\nu + \gamma\zeta^{-1}\cos\theta + (3-\nu)\kappa\gamma\zeta^{-1}\cos\theta + (3+\nu)\kappa\gamma^2\zeta^{-2}\sin^2\theta - 2\kappa\gamma^2\zeta^{-2}\cos^2\theta - (3+\nu)\kappa\gamma^3\zeta^{-3}\sin^2\theta\cos\theta\Big]$$

$$l_{26}^I = 0 \quad , \quad l_{27} = 0$$

$$l_{28} = 0 \quad , \quad l_{29} = 0$$

$$l_{30} = 0 \quad , \quad l_{31} = -\frac{1}{R}\Big[1+(1+\nu)\gamma\cos\theta\Big]$$

$$l_{31}^I = 0$$

$$l_{32} = \frac{1}{R^2}\Big[\nu(1+\kappa)\gamma\sin\theta + (1-4\kappa)\gamma^2\zeta^{-1}\sin\theta\cos\theta - \kappa\gamma^3\zeta^{-2}\sin\theta + \kappa\gamma^3\zeta^{-2}\sin\theta\cos^2\theta - 2\kappa\gamma^3\zeta^{-3}\sin\theta + 2\kappa\gamma^3\zeta^{-3}\sin\theta\cos^2\theta\Big]$$

$$l_{32}^I = 0 \quad , \quad l_{33} = -R^2\kappa\zeta^{-3}$$

$$l_{34} = -R^2\kappa\zeta \quad , \quad l_{35} = -2R^2\kappa\zeta^{-1}$$

$$l_{36} = 2R\kappa\gamma\sin\theta \quad , \quad l_{37} = -2R\kappa\gamma\zeta^{-2}\sin\theta$$

$$l_{38} = -\Big[(3-\nu)\kappa\gamma\zeta^{-2}\cos\theta + 4\kappa\gamma^2\zeta^{-3}\sin^2\theta\Big]$$

$$l_{38}^I = \frac{1-\nu^2}{E}\rho R^2\kappa\zeta$$

$$l_{39}=\left[\left(1+\nu\right)\kappa\gamma\cos\theta+\kappa\gamma^2\zeta^{-1}\sin^2\theta\right],\qquad l_{39}^{I}=\frac{1-\nu^2}{E}\rho R^2\kappa\zeta$$

$$l_{40}=\frac{1}{R}\left(-\nu\kappa\gamma\sin\theta+2\kappa\gamma^2\zeta^{-1}\sin\theta\cos\theta+\kappa\gamma^3\zeta^{-2}\sin\theta-\kappa\gamma^3\zeta^{-2}\sin\theta\cos^2\theta\right)$$

$$l_{40}^{I}=-\frac{1-\nu^2}{E}R\rho\kappa\gamma\sin\theta\quad,\qquad l_{41}=-\frac{1}{R^2}\left[1+\left(1+2\nu\right)\gamma\cos\theta+\gamma^2\zeta^{-1}\cos^2\theta\right]$$

$$l_{41}^{I}=-\frac{1-\nu^2}{E}\rho\zeta$$

Coefficients f_i^F and forces f_1^{xu}, f_2^{xu}, f_1^{sv}, f_2^{sv}, f_1^{zw}, f_2^{zw}, f_1^{xw}, f_2^{xw}, f_1^{sw} and f_2^{sw} introduced in Eq. 6.29 in defining the differential operators of the applied forces of the TTS-V2 theory are defined as

$$f_1^F=-\frac{1-\nu^2}{Eh}\quad,\qquad f_2^F=0$$

$$f_3^F=\frac{1-\nu^2}{Eh}\zeta\quad,\qquad f_4^F=0$$

$$f_5^F=\frac{1-\nu^2}{Eh}\quad,\qquad f_6^F=\frac{1-\nu^2}{Eh}\gamma\cos\theta$$

$$f_7^F=\frac{1-\nu^2}{Eh}\quad,\qquad f_8^F=\frac{1-\nu^2}{Eh}\gamma\cos\theta$$

$$f_9^F=\frac{1-\nu^2}{Eh}\quad,\qquad f_{10}^F=0$$

$$f_{11}^F=\frac{1-\nu^2}{Eh}\gamma\cos\theta\quad,\qquad f_{12}^F=-\frac{1-\nu^2}{Eh}\frac{1}{R}\gamma\sin\theta$$

$$f_{13}^F=\frac{1-\nu^2}{Eh}$$

$$f_1^{xu}=\int_{-\frac{h}{2}}^{\frac{h}{2}}p^x dz\quad,\qquad f_2^{xu}=0$$

$$f_1^{xw}=\int_{-\frac{h}{2}}^{\frac{h}{2}}p^x z dz\quad,\qquad f_2^{xw}=0$$

$$f_1^{sv}=f_2^{sv}=\int_{-\frac{h}{2}}^{\frac{h}{2}}p^s dz\quad,\qquad f_1^{sw}=f_2^{sw}=\int_{-\frac{h}{2}}^{\frac{h}{2}}p^s z dz$$

$$f_1^{zw}=f_2^{zw}=\int_{-\frac{h}{2}}^{\frac{h}{2}}p^z dz$$

6.A.3 Coefficients for TTS-V2 Theory

Coefficients $d_i\left(TTS-V2\right)$ and $d_i^I\left(TTS-V2\right)$ (called in this section as d_i and d_i^I, respectively, for brevity) introduced in Eqs. 6.22-6.25 in defining the differential operators of the boundary condition equations of the TTS-V2 theory are defined as

$$d_1=-\zeta^{-1}\left(1+\kappa\gamma\zeta^{-1}\cos\theta\right) \quad , \quad d_2=-\nu\left(1+\kappa\gamma\zeta^{-1}\cos\theta\right)$$
$$d_3=\frac{1}{R}\gamma\zeta^{-1}\sin\theta \quad , \quad d_4=R\kappa\zeta^{-2}$$
$$d_5=R\nu\kappa\gamma\zeta^{-1}\cos\theta \quad , \quad d_6=-\kappa\gamma\zeta^{-1}\sin\theta$$
$$d_7=-\frac{1}{R}\left(\nu+\gamma\zeta^{-1}\cos\theta\right)$$

$$d_8=-\frac{1-\nu}{2}\left(1+\kappa\gamma\zeta^{-1}\cos\theta\right)$$
$$d_9=-\frac{1}{R}\frac{1-\nu}{2}\gamma\zeta^{-1}\sin\theta\left[1-\kappa\left(2-\gamma\zeta^{-1}\cos\theta\right)\right]$$
$$d_{10}=-\frac{1-\nu}{2}\zeta^{-1}\left(1-3\kappa\gamma\zeta^{-1}\cos\theta\right) \quad , \quad d_{11}=R\frac{1-\nu}{2}\kappa\zeta^{-1}\left(3-\gamma\zeta^{-1}\cos\theta\right)$$
$$d_{12}=\frac{1-\nu}{2}\kappa\gamma\zeta^{-2}\sin\theta\left(3-\gamma\zeta^{-1}\cos\theta\right)$$

$$d_{13}=-R\kappa\zeta^{-2} \quad , \quad d_{14}=R\frac{1-\nu}{2}\kappa\left(1-3\gamma\zeta^{-1}\cos\theta\right)$$
$$d_{15}=3\frac{1-\nu}{2}\kappa\gamma\zeta^{-1}\sin\theta\left(1-\gamma\zeta^{-1}\cos\theta\right)$$
$$d_{16}=\frac{1}{R}\frac{1-\nu}{2}\kappa\gamma\zeta^{-1}\left[\cos\theta+3\gamma\zeta^{-1}\left(\sin^2\theta-\cos^2\theta-\gamma\zeta^{-1}\sin^2\theta\cos\theta\right)\right]$$
$$d_{16}^I=\frac{1-\nu^2}{E}R\rho\kappa\left(1+4\gamma\cos\theta+3\gamma^2\cos^2\theta\right)$$

$$d_{17}=-R\kappa\zeta^{-1}\left(\frac{3-\nu}{2}-\frac{1-\nu}{2}\gamma\zeta^{-1}\cos\theta\right)$$
$$d_{18}=\kappa\gamma\zeta^{-2}\sin\theta\left(\frac{3+\nu}{2}-\frac{1+\nu}{2}\gamma\zeta^{-1}\sin\theta\cos\theta\right)$$
$$d_{19}=R^2\kappa\zeta^{-3} \quad , \quad d_{20}=R^2\left(2-\nu\right)\kappa\zeta^{-1}$$
$$d_{21}=R\left(1-2\nu\right)\kappa\gamma\zeta^{-2}\sin\theta$$
$$d_{22}=2\left(1-\nu\right)\kappa\gamma\zeta^{-3}\left(\gamma+\frac{1-2\nu}{2-2\nu}\cos\theta\right)$$
$$d_{22}^I=-\frac{1-\nu^2}{E}R^2\rho\kappa\zeta$$

$$d_{23} = R\kappa\zeta^{-2} \quad , \quad d_{24} = R\nu\kappa\zeta^{-1}$$
$$d_{25} = -\kappa\gamma\zeta^{-2}\sin\theta\left(2-\gamma\zeta^{-1}\cos\theta\right) \quad , \quad d_{26} = -R^2\kappa\zeta^{-3}$$
$$d_{27} = -R^2\nu\kappa\zeta^{-1} \quad , \quad d_{28} = R\kappa\gamma\zeta^{-2}\sin\theta$$
$$d_{29} = \kappa\gamma\zeta^{-2}\cos\theta\left(1-\gamma\zeta^{-1}\cos\theta\right)$$

Coefficients $l_i\left(TTS-V2\right)$ and $l_i^I\left(TTS-V2\right)$ (called in this section as l_i and l_i^I, respectively, for brevity) introduced in Eqs. 6.26-6.28 in defining the differential operators of the field equations of the TTS-V2 theory are defined as

$$l_1 = \left(\zeta^{-1}+\kappa\gamma\zeta^{-2}\sin\theta\cos^2\theta\right) \quad , \quad l_2 = \left(\frac{1-\nu}{2}\right)\left[1+\left(1-3\kappa\right)\gamma\cos\theta\right]$$
$$l_3 = \frac{1}{R}\left(\frac{1-\nu}{2}\right)\left[\left(-1+4\kappa\right)\gamma\sin\theta-6\kappa\gamma^2\zeta^{-1}\sin\theta\cos\theta+8\kappa\gamma^3\zeta^{-2}\sin\theta\cos^2\theta\right]$$
$$l_4 = \frac{1}{R^2}\left(\frac{1-\nu}{2}\right)\left[\left(1+2\kappa\right)\gamma\cos\theta-\left(1-2\kappa\right)\gamma^2\zeta^{-1}\sin^2\theta-3\kappa\gamma^2\zeta^{-1}\cos^2\theta\right.$$
$$\left.+4\kappa\gamma^3\zeta^{-2}\cos\theta-10\kappa\gamma^3\zeta^{-2}\sin^2\theta\cos\theta+4\kappa\gamma^4\zeta^{-3}\sin^2\theta\cos^2\theta\right]$$
$$l_4^I = -\frac{1-\nu^2}{E}\rho\left\{1+\left[2+\left(1+\kappa\right)\left(1+\gamma^2\right)\right]\gamma\cos\theta+\left(3+2\kappa\right)\gamma^2\cos^2\theta\right.$$
$$\left.-\left(1+\kappa\right)\gamma^3\sin^2\theta\cos\theta\right\}$$
$$l_5 = \left(\frac{1+\nu}{2}\right)\left(1+\kappa\gamma\zeta^{-1}\cos\theta\right) \quad , \quad l_6 = -\left(\frac{3-\nu}{2}\right)\frac{\gamma}{R}\zeta^{-1}\sin\theta$$
$$l_7 = -R\kappa\zeta^{-2} \quad , \quad l_8 = R\left[\left(\frac{1-\nu}{2}\right)\kappa\zeta^{-1}-\kappa\gamma\zeta^{-1}\cos\theta\right]$$
$$l_9 = \left(\frac{5-3\nu}{2}\right)\kappa\gamma\zeta^{-2}\sin\theta+\kappa\gamma^2\zeta^{-2}\sin\theta\cos\theta$$
$$l_{10} = \frac{1}{R}\left[\nu+\left(1+\kappa\frac{1-\nu}{2}\right)\gamma\zeta^{-1}\cos\theta+3\left(\frac{1-\nu}{2}\right)\kappa\gamma^2\zeta^{-2}\sin^2\theta-3\left(\frac{1-\nu}{2}\right)\kappa\gamma^2\zeta^{-2}\cos^2\theta\right.$$
$$\left.-3\left(\frac{1-\nu}{2}\right)\kappa\gamma^3\zeta^{-3}\sin^2\theta\cos\theta\right]$$
$$l_{10}^I = \frac{1-\nu^2}{E}R\rho\kappa\left(1+4\gamma\cos\theta+3\gamma^2\cos^2\theta\right)$$

$$l_{11} = \left(\frac{1+\nu}{2}\right)\left(1+\kappa\gamma\zeta^{-1}\cos\theta\right)$$
$$l_{12} = \frac{1}{R}\left[\left(\frac{3-\nu}{2}\right)\gamma\zeta^{-1}\sin\theta-\left(1+\nu\right)\kappa\gamma\zeta^{-2}\sin\theta-\left(\frac{1+\nu}{2}\right)\kappa\gamma^2\zeta^{-2}\sin\theta\cos\theta\right]$$
$$l_{13} = \left(\frac{1-\nu}{2}\right)\left(\zeta^{-1}-3\kappa\gamma\zeta^{-2}\cos\theta\right) \quad , \quad l_{14} = \left[1+\left(1+\kappa\right)\gamma\cos\theta\right]$$

$$l_{15} = -\frac{\gamma}{R}\sin\theta$$

$$l_{16} = -\frac{1}{R^2}\left(\nu\gamma\cos\theta + \gamma^2\zeta^{-1}\sin^2\theta - 3\kappa\gamma^3\zeta^{-2}\sin^2\theta\cos\theta\right)$$

$$l_{16}^I = -\frac{1-\nu^2}{E}\rho\left[1+\left(1+3\kappa\right)\gamma\cos\theta\right] \quad , \qquad l_{17} = -R\kappa\gamma\cos\theta$$

$$l_{18} = -R\left[\left(\frac{3-\nu}{2}\right)\kappa\zeta^{-1} - \left(\frac{1-\nu}{2}\right)\kappa\gamma\zeta^{-2}\cos\theta\right]$$

$$l_{19} = -\left[\left(\frac{7-\nu}{2}\right)\kappa\gamma\zeta^{-3}\sin\theta + 2\kappa\gamma^2\zeta^{-3}\sin\theta\cos\theta\right]$$

$$l_{20} = \kappa\gamma\sin\theta$$

$$l_{21} = \frac{1}{R}\left\{1+\left[1+\nu\left(1+\kappa\right)\right]\gamma\cos\theta + 2\kappa\gamma^2\zeta^{-1}\sin^2\theta - \kappa\gamma^3\zeta^{-2}\sin^2\theta\cos\theta\right\}$$

$$l_{21}^I = \frac{1-\nu^2}{E}R\rho\kappa\left(2+3\gamma\cos\theta\right)$$

$$l_{22} = -\frac{1}{R^2}\left(\nu\gamma\zeta^{-1}\sin\theta - \nu\kappa\gamma^2\zeta^{-2}\sin\theta\cos\theta\right)$$

$$l_{23} = R\kappa\zeta^{-2} \quad , \qquad l_{24} = R\left[-\left(\frac{1-\nu}{2}\right)\kappa + \left(\frac{3-\nu}{2}\right)\kappa\gamma\zeta^{-1}\cos\theta\right]$$

$$l_{25} = \left[-\left(\frac{1+\nu}{2}\right)\kappa\gamma\zeta^{-1}\sin\theta + \left(\frac{3+\nu}{2}\right)\kappa\gamma^2\zeta^{-2}\sin\theta\cos\theta\right]$$

$$l_{26} = \frac{1}{R}\left\{-\nu - \left[1+\left(\frac{1-\nu}{2}\right)\kappa\right]\gamma\zeta^{-1}\cos\theta + \left(\frac{3-\nu}{2}\right)\kappa\gamma^2\zeta^{-2} + 2\kappa\gamma^2\zeta^{-2}\sin^2\theta \right.$$
$$\left. + \left(\frac{3+\nu}{2}\right)\kappa\gamma^3\zeta^{-3}\sin^2\theta\cos\theta \right\}$$

$$l_{26}^I = -\frac{1-\nu^2}{E}R\rho\kappa\left(1+4\gamma\cos\theta+3\gamma^2\cos^2\theta\right) \quad , \qquad l_{27} = R\kappa\gamma\cos\theta$$

$$l_{28} = R\left[\left(\frac{3-\nu}{2}\right)\kappa\zeta^{-1} - \left(\frac{1-\nu}{2}\right)\kappa\gamma\zeta^{-2}\cos\theta\right]$$

$$l_{29} = \left[-\left(\frac{3+\nu}{2}\right)\kappa\gamma\zeta^{-2}\sin\theta + \left(\frac{1+\nu}{2}\right)\kappa\gamma^2\zeta^{-3}\sin\theta\cos\theta\right]$$

$$l_{30} = -2\kappa\gamma\sin\theta$$

$$l_{31} = \frac{1}{R}\left[-1-\left(1+\nu\right)\left(1+\kappa\right)\gamma\cos\theta - 2\kappa\gamma^2\zeta^{-1}\sin^2\theta + \kappa\gamma^3\zeta^{-2}\sin^2\theta\cos\theta\right]$$

$$l_{31}^I = -\frac{1-\nu^2}{E}R\rho\kappa\left(2+3\gamma\cos\theta\right)$$

$$l_{32} = \frac{1}{R^2}\left[\nu\left(1+\kappa\right)\gamma\sin\theta + \left(1-4\kappa\right)\gamma^2\zeta^{-1}\sin\theta\cos\theta - \kappa\gamma^3\zeta^{-2}\sin\theta \right.$$
$$\left. + \kappa\gamma^3\zeta^{-2}\sin\theta\cos^2\theta - 2\kappa\gamma^3\zeta^{-3}\sin\theta + 2\kappa\gamma^3\zeta^{-3}\sin\theta\cos^2\theta\right]$$

$$l_{32}^I = \frac{1-\nu^2}{E}3\rho\kappa\gamma\sin\theta \quad , \qquad l_{33} = -R^2\kappa\zeta^{-3}$$

$$l_{34} = -R^2\kappa\zeta \quad , \qquad l_{35} = -2R^2\kappa\zeta^{-1}$$

$$l_{36} = 2R\kappa\gamma\sin\theta \quad , \quad l_{37} = -2R\kappa\gamma\zeta^{-2}\sin\theta$$
$$l_{38} = \left[-(1-\nu)\kappa\gamma\zeta^{-2}\cos\theta - 2\kappa\gamma^2\zeta^{-3} - 2\kappa\gamma^2\zeta^{-3}\sin^2\theta\right]$$
$$l_{38}^I = \frac{1-\nu^2}{E}R^2\rho\kappa\zeta$$
$$l_{39} = \left[-2\kappa + (1+\nu)\kappa\gamma\cos\theta + \kappa\gamma^2\zeta^{-1}\sin^2\theta\right] \quad , \quad l_{39}^I = \frac{1-\nu^2}{E}R^2\rho\kappa\zeta$$
$$l_{40} = \frac{1}{R}\left(-\nu\kappa\gamma\sin\theta + \kappa\gamma^2\zeta^{-1}\sin\theta\cos\theta + \kappa\gamma^3\zeta^{-2}\sin\theta + \nu\kappa\gamma^2\zeta^{-2}\sin\theta\cos\theta\right)$$
$$l_{40}^I = -\frac{1-\nu^2}{E}R\rho\kappa\gamma\sin\theta$$
$$l_{41} = \frac{1}{R^2}\left[-1-(1+2\nu-\kappa)\gamma\cos\theta - \gamma^2\zeta^{-1}\cos^2\theta - \nu\kappa\gamma^2\zeta^{-2} + 2\nu\kappa\gamma^2\zeta^{-2}\cos^2\theta\right.$$
$$\left. + \kappa\gamma^3\zeta^{-2}\cos\theta - \kappa\gamma^3\zeta^{-2}\sin^2\theta\cos\theta + 2\nu\kappa\gamma^3\zeta^{-3}\sin^2\theta\cos\theta\right]$$
$$l_{41}^I = -\frac{1-\nu^2}{E}\rho\left[1+(1+\kappa)\gamma\cos\theta\right]$$

Coefficients f_i^F and forces f_1^{xu}, f_2^{xu}, f_1^{sv}, f_2^{sv}, f_1^{zw}, f_2^{zw}, f_1^{xw}, f_2^{xw}, f_1^{sw} and f_2^{sw} introduced in Eq. 6.29 in defining the differential operators of the applied forces of the TTS-V2 theory are defined as

$$f_1^F = -\frac{1-\nu^2}{Eh} \quad , \quad f_2^F = -\frac{1-\nu^2}{Eh}\frac{1}{R}\gamma\zeta^{-1}\cos\theta$$
$$f_3^F = \frac{1-\nu^2}{Eh}\zeta \quad , \quad f_4^F = \frac{1-\nu^2}{Eh}\frac{2}{R}\gamma\cos\theta$$
$$f_5^F = \frac{1-\nu^2}{Eh} \quad , \quad f_6^F = \frac{1-\nu^2}{Eh}\gamma\cos\theta$$
$$f_7^F = \frac{1-\nu^2}{Eh} \quad , \quad f_8^F = \frac{1-\nu^2}{Eh}\gamma\cos\theta$$
$$f_9^F = \frac{1-\nu^2}{Eh} \quad , \quad f_{10}^F = \frac{1-\nu^2}{Eh}\frac{1}{R}\gamma\zeta^{-1}\cos\theta$$
$$f_{11}^F = \frac{1-\nu^2}{Eh}\gamma\cos\theta \quad , \quad f_{12}^F = -\frac{1-\nu^2}{Eh}\frac{1}{R}\gamma\sin\theta$$
$$f_{13}^F = \frac{1-\nu^2}{Eh}$$

$$f_1^{xu} = \int_{-\frac{h}{2}}^{\frac{h}{2}} p^x\left(1+\frac{z}{R}\right)dz \quad , \quad f_2^{xu} = \int_{-\frac{h}{2}}^{\frac{h}{2}} p^x z\left(1+\frac{z}{R}\right)dz$$
$$f_1^{xw} = \int_{-\frac{h}{2}}^{\frac{h}{2}} p^x z\left(1+\frac{z}{R}\right)dz \quad , \quad f_2^{xw} = \int_{-\frac{h}{2}}^{\frac{h}{2}} p^x z^2\left(1+\frac{z}{R}\right)dz$$

$$f_1^{sv}=\int_{-\frac{h}{2}}^{\frac{h}{2}} p^s\left(1+2\frac{z}{R}\right)dz \qquad , \qquad f_2^{sv}=\int_{-\frac{h}{2}}^{\frac{h}{2}} p^s\left(1+3\frac{z}{R}\right)dz$$

$$f_1^{sw}=\int_{-\frac{h}{2}}^{\frac{h}{2}} p^s z\left(1+2\frac{z}{R}\right)dz \qquad , \qquad f_2^{sw}=\int_{-\frac{h}{2}}^{\frac{h}{2}} p^s z\left(1+\frac{z}{R}\right)dz$$

$$f_1^{zw}=\int_{-\frac{h}{2}}^{\frac{h}{2}} p^z\left(1+\frac{z}{R}\right)dz \qquad , \qquad f_2^{zw}=\int_{-\frac{h}{2}}^{\frac{h}{2}} p^z\left(1+2\frac{z}{R}\right)dz$$

6.A.4 Coefficients for Sanders Theory

Coefficients $l_i\left(Sanders\right)$ (called as l_i in this section for brevity) introduced in Eqs. 6.26-6.28 in defining the differential operators of the homogeneous part of the field equations of the Sanders theory [6.3] are defined as

$$l_1=\zeta^{-1}\left(1+\kappa\gamma^2\zeta^{-2}\cos^2\theta\right)$$

$$l_2=\frac{1-\nu}{2}\zeta\left[1-\kappa\gamma\zeta^{-1}\cos\theta+\kappa\zeta^{-2}\left(2\gamma^2\cos^2\theta+\frac{1}{4}\right)\right]$$

$$l_3=-\frac{1}{R}\frac{1-\nu}{2}\gamma\sin\theta\left[1-\frac{1}{2}\kappa\zeta^{-1}\left(1-2\gamma\cos\theta\right)\left(1+\frac{3}{2}\zeta^{-1}\right)\right]$$

$$l_4=\frac{1}{R^2}\frac{1-\nu}{2}\left\langle\gamma\cos\theta\left\{1+\frac{\kappa\zeta^{-2}}{4}\left[\zeta^{-1}\left(1+8\gamma^2\cos^2\theta\right)-4\gamma\zeta\cos\theta\right]\right\}\right.$$
$$\left.-\gamma^2\zeta^{-1}\sin^2\theta\left[1+\frac{\kappa\zeta^{-2}}{4}\left(7+8\gamma\cos\theta+4\gamma^2\cos^2\theta\right)\right]\right\rangle$$

$$l_5=\frac{1+\nu}{2}\left(1+\kappa\gamma\zeta^{-1}\cos\theta\right)-\frac{3}{8}\left(1-\nu\right)\kappa\zeta^{-2}$$

$$l_6=-\frac{1}{R}\frac{3-\nu}{2}\gamma\zeta^{-1}\sin\theta\left\{1+\kappa\zeta^{-1}\left[\gamma\cos\theta-\frac{1-\nu}{3-\nu}\left(1+\frac{3}{4}\zeta^{-1}\right)\right]\right\}$$

$$l_7=-R\kappa\zeta^{-2}\left(\gamma\zeta^{-1}\cos\theta\right) \qquad , \qquad l_8=R\kappa\zeta^{-1}\left(\frac{1-\nu}{2}-\gamma\cos\theta\right)$$

$$l_9=\kappa\gamma\zeta^{-2}\left(\frac{3-3\nu}{2}\sin\theta+\gamma\sin\theta\cos\theta\right)$$

$$l_{10}=\frac{1}{R}\left\{\nu\left(1+3\frac{1-\nu}{2\nu}\kappa\gamma^2\zeta^{-3}\right)+\gamma\zeta^{-1}\cos\theta\left[1+\frac{1-\nu}{2}\kappa\zeta^{-2}\left(1-4\gamma\cos\theta-2\gamma^2\cos^2\theta\right)\right]\right\}$$

$$l_{11}=\frac{1+\nu}{2}\left(1+\kappa\gamma\zeta^{-1}\cos\theta\right)-\frac{3}{4}\left(\frac{1-\nu}{2}\right)\kappa\zeta^{-2}$$

$$l_{12}=\frac{1}{R}\left\{\frac{3-\nu}{2}\gamma\zeta^{-1}\sin\theta-\kappa\gamma\zeta^{-2}\sin\theta\left[\frac{1+\nu}{2}-\frac{3-\nu}{2}\gamma\cos\theta-\frac{1-\nu}{8}\left(1+3\gamma\zeta^{-1}\cos\theta\right)\right]\right\}$$

$$l_{13}=\frac{1-\nu}{2}\zeta^{-1}\left[(1+\kappa)+\kappa\zeta^{-1}\left(1+\frac{1}{4}\zeta^{-1}\right)\right],\qquad l_{14}=\zeta(1+\kappa)$$

$$l_{15}=-\frac{1}{R}\gamma\sin\theta(1+\kappa)\quad,\qquad l_{16}=-\frac{1}{R^2}\left(\nu\gamma\cos\theta+\gamma^2\zeta^{-1}\sin^2\theta\right)(1+\kappa)$$

$$l_{17}=-R\kappa\zeta\quad,\qquad l_{18}=-R\kappa\zeta^{-1}\left(1+\frac{1-\nu}{2}\zeta^{-1}\right)$$

$$l_{19}=\kappa\gamma\zeta^{-3}\sin\theta\left(-\frac{5-\nu}{2}-2\gamma\cos\theta\right)\quad,\qquad l_{20}=\kappa\gamma\sin\theta$$

$$l_{21}=\frac{1}{R}\left[\zeta+\nu\gamma\cos\theta(1+\kappa)+\kappa\gamma^2\zeta^{-1}\sin^2\theta\right],\ l_{22}=-\frac{1}{R^2}\gamma\zeta^{-1}\sin\theta$$

$$l_{23}=R\kappa\zeta^{-2}\left(\gamma\zeta^{-1}\cos\theta\right)\quad,\qquad l_{24}=R\kappa\zeta^{-1}\left(\gamma\cos\theta-\frac{1-\nu}{2}\right)$$

$$l_{25}=-\kappa\gamma\zeta^{-2}\left(\frac{3-\nu}{2}\sin\theta-\gamma\sin\theta\cos\theta\right),\qquad l_{26}=-\frac{1}{R}\left[\left[\nu\left(1-\frac{5+\nu}{2\nu}\kappa\gamma^2\zeta^{-3}\right)\right.\right.$$

$$\left.\left.+\gamma\zeta^{-1}\cos\theta\left\langle 1-\kappa\left\{1-\zeta^{-2}\left[\frac{1-\nu}{2}+\gamma^2\sin^2\theta+3(2-\nu)\gamma\cos\theta+3(1-\nu)\gamma^2\cos^2\theta\right]\right\}\right\rangle\right]\right]$$

$$l_{27}=R\kappa\zeta\quad,\qquad l_{28}=R\kappa\zeta^{-2}\left(\zeta+\frac{1-\nu}{2}\right)$$

$$l_{29}=-\kappa\gamma\zeta^{-3}\sin\theta\left(\zeta-\frac{1-\nu}{2}\right)\quad,\qquad l_{30}=-2\kappa\gamma\sin\theta$$

$$l_{31}=-\frac{1}{R}\left[\zeta\left(1+\kappa\gamma^2\zeta^{-2}\right)+\nu\gamma\cos\theta\left(1+\frac{1+\nu}{\nu}\kappa\cos\theta\right)\right]$$

$$l_{32}=\frac{1}{R^2}\left\langle\nu\gamma\sin\theta\left[1+\kappa\left(1-\frac{1}{\nu}\gamma^2\zeta^{-2}\sin^2\theta\right)\right]+(1-2\kappa)\gamma^2\zeta^{-1}\sin\theta\cos\theta\right\rangle$$

$$l_{33}=-R^2\kappa\zeta^{-3}\quad,\qquad l_{34}=-R^2\kappa\zeta$$

$$l_{35}=-2R^2\kappa\zeta^{-1}\quad,\qquad l_{36}=2R\kappa\gamma\sin\theta$$

$$l_{37}=-2R\kappa\gamma\zeta^{-2}\sin\theta\quad,\qquad l_{38}=-\kappa\zeta^{-2}\left[(3-\nu)\gamma\cos\theta+4\gamma^2\zeta^{-1}\sin^2\theta\right]$$

$$l_{39}=\kappa\gamma\left[\gamma\zeta^{-1}\sin^2\theta+(1+\nu)\cos\theta\right]$$

$$l_{40}=\frac{1}{R}\kappa\zeta^{-2}\left(-\nu\gamma\zeta^2\sin\theta+\gamma^2\zeta\sin\theta\cos\theta+\gamma^3\sin\theta+\gamma^2\sin\theta\cos\theta\right)$$

$$l_{41}=-\frac{1}{R^2}\left(2\nu\gamma\cos\theta+\gamma^2\zeta^{-1}\cos^2\theta+\zeta\right)$$

6.A.5 Coefficients for TTS-V2M Theory

The coefficients $d_i\left(TTS-V2M\right)$ and $d_i^I\left(TTS-V2M\right)$ (called as d_i and d_i^I in this section, respectively, for brevity) introduced in Eqs. 6.22-6.25 in defining the differential operators of the boundary condition equations of the TTS-V2M theory are defined as

$$d_1 = -\zeta^{-1} \quad , \quad d_2 = -\nu$$
$$d_3 = \frac{1}{R}\gamma\zeta^{-1}\sin\theta \quad , \quad d_4 = R\kappa\zeta^{-2}$$
$$d_5 = R\nu\kappa\gamma\zeta^{-1}\cos\theta \quad , \quad d_6 = -\kappa\gamma\zeta^{-1}\sin\theta$$
$$d_7 = -\frac{1}{R}\left(\nu + \gamma\zeta^{-1}\cos\theta\right)$$

$$d_8 = -\frac{1-\nu}{2} \quad , \quad d_9 = -\frac{1}{R}\frac{1-\nu}{2}\gamma\zeta^{-1}\sin\theta$$
$$d_{10} = -\frac{1-\nu}{2}\zeta^{-1} \quad , \quad d_{11} = R\frac{1-\nu}{2}\kappa\zeta^{-1}\left(3-\gamma\zeta^{-1}\cos\theta\right)$$
$$d_{12} = \frac{1-\nu}{2}\kappa\gamma\zeta^{-2}\sin\theta\left(3-\gamma\zeta^{-1}\cos\theta\right)$$

$$d_{13} = -R\kappa\zeta^{-2} \quad , \quad d_{14} = R\frac{1-\nu}{2}\kappa\left(1-3\gamma\zeta^{-1}\cos\theta\right)$$
$$d_{15} = 3\frac{1-\nu}{2}\kappa\gamma\zeta^{-1}\sin\theta\left(1-\gamma\zeta^{-1}\cos\theta\right)$$
$$d_{16} = \frac{1}{R}\frac{1-\nu}{2}\kappa\gamma\zeta^{-1}\left[\cos\theta + 3\gamma\zeta^{-1}\left(\sin^2\theta - \cos^2\theta - \gamma\zeta^{-1}\sin^2\theta\cos\theta\right)\right]$$
$$d_{16}^I = \frac{1-\nu^2}{E}R\rho\kappa\zeta\left(1+3\gamma\cos\theta\right) \quad , \quad d_{17} = -R\kappa\zeta^{-1}\left(\frac{3-\nu}{2} - \frac{1-\nu}{2}\gamma\zeta^{-1}\cos\theta\right)$$
$$d_{18} = \kappa\gamma\zeta^{-2}\sin\theta\left(\frac{3+\nu}{2} - \frac{1+\nu}{2}\gamma\zeta^{-1}\cos\theta\right) \quad , \quad d_{19} = R^2\kappa\zeta^{-3}$$
$$d_{20} = R^2\left(2-\nu\right)\kappa\zeta^{-1} \quad , \quad d_{21} = R\left(1-2\nu\right)\kappa\gamma\zeta^{-2}\sin\theta$$
$$d_{22} = 2\left(1-\nu\right)\kappa\gamma\zeta^{-3}\left(\gamma + \frac{1-2\nu}{2-2\nu}\cos\theta\right)$$
$$d_{22}^I = -\frac{1-\nu^2}{E}R^2\rho\kappa\zeta$$

$$d_{23} = R\kappa\zeta^{-2} \quad , \quad d_{24} = R\nu\kappa\zeta^{-1}$$
$$d_{25} = -\kappa\gamma\zeta^{-2}\sin\theta\left(2-\gamma\zeta^{-1}\cos\theta\right) \quad , \quad d_{26} = -R^2\kappa\zeta^{-3}$$
$$d_{27} = -R^2\nu\kappa\zeta^{-1} \quad , \quad d_{28} = R\kappa\gamma\zeta^{-2}\sin\theta$$
$$d_{29} = \kappa\gamma\zeta^{-2}\cos\theta\left(1-\gamma\zeta^{-1}\cos\theta\right)$$

The coefficients $l_i\left(TTS-V2M\right)$ and $l_i^I\left(TTS-V2M\right)$ (called as l_i and l_i^I in this section, respectively, for brevity) introduced in Eqs. 6.26-6.28 in defining the differential operators of the field equations of the TTS-V2 theory are defined as

$$l_1=\zeta^{-1} \quad , \quad l_2=\frac{1-\nu}{2}\zeta$$

$$l_3=-\frac{1}{R}\frac{1-\nu}{2}\gamma\sin\theta \quad , \quad l_4=\frac{1}{R^2}\frac{1-\nu}{2}\left(\gamma\cos\theta-\gamma^2\zeta^{-1}\sin^2\theta\right)$$

$$l_4^I=-\frac{1-\nu^2}{E}\rho\zeta^3 \quad , \quad l_5=\frac{1+\nu}{2}$$

$$l_6=-\frac{1}{R}\frac{3-\nu}{2}\gamma\zeta^{-1}\sin\theta \quad , \quad l_7=-R\kappa\zeta^{-2}$$

$$l_8=R\kappa\zeta^{-1}\left(\frac{1-\nu}{2}-\gamma\cos\theta\right) \quad , \quad l_9=\kappa\gamma\zeta^{-2}\sin\theta\left(\frac{5-3\nu}{2}+\gamma\cos\theta\right)$$

$$l_{10}=\frac{1}{R}\left(\nu+\gamma\zeta^{-1}\cos\theta\right) \quad , \quad l_{10}^I=\frac{1-\nu^2}{E}R\rho\kappa\left(1+4\gamma\cos\theta+3\gamma^2\cos^2\theta\right)$$

$$l_{11}=\frac{1+\nu}{2} \quad , \quad l_{12}=\frac{1}{R}\frac{3-\nu}{2}\gamma\zeta^{-1}\sin\theta$$

$$l_{13}=\frac{1-\nu}{2}\zeta^{-1} \quad , \quad l_{14}=\zeta$$

$$l_{15}=-\frac{1}{R}\gamma\sin\theta \quad , \quad l_{16}=-\frac{1}{R^2}\left(\nu\gamma\cos\theta+\gamma^2\zeta^{-1}\sin^2\theta\right)$$

$$l_{16}^I=-\frac{1-\nu^2}{E}\rho\zeta \quad , \quad l_{17}=-R\kappa\gamma\cos\theta$$

$$l_{18}=-R\kappa\zeta^{-1}\left(1+\frac{1-\nu}{2}\zeta^{-1}\right) \quad , \quad l_{19}=\kappa\gamma\zeta^{-3}\sin\theta\left(-\frac{7-\nu}{2}-2\gamma\cos\theta\right)$$

$$l_{20}=\kappa\gamma\sin\theta \quad , \quad l_{21}=\frac{1}{R}\left(\zeta+\nu\gamma\cos\theta\right)$$

$$l_{21}^I=\frac{1-\nu^2}{E}R\rho\kappa\left(2+3\gamma\cos\theta\right) \quad , \quad l_{22}=-\frac{1}{R^2}\nu\gamma\zeta^{-1}\sin\theta$$

$$l_{23}=R\kappa\zeta^{-2} \quad , \quad l_{24}=R\kappa\zeta^{-1}\left(\gamma\cos\theta-\frac{1-\nu}{2}\right)$$

$$l_{25}=-\kappa\gamma\zeta^{-2}\left(\frac{1+\nu}{2}\sin\theta-\gamma\sin\theta\cos\theta\right), \quad l_{26}=-\frac{1}{R}\left(\nu+\gamma\zeta^{-1}\cos\theta\right)$$

$$l_{26}^I=-\frac{1-\nu^2}{E}R\rho\kappa\left(1+4\gamma\cos\theta+3\gamma^2\cos^2\theta\right), \quad l_{27}=R\kappa\gamma\cos\theta$$

$$l_{28}=R\kappa\zeta^{-2}\left(\zeta+\frac{1-\nu}{2}\right) \quad , \quad l_{29}=-\kappa\gamma\zeta^{-3}\sin\theta\left(\zeta+\frac{1+\nu}{2}\right)$$

$$l_{30}=-2\kappa\gamma\sin\theta \quad , \quad l_{31}=-\frac{1}{R}\left(\zeta+\nu\gamma\cos\theta\right)$$

$$l_{31}^I=-\frac{1-\nu^2}{E}R\rho\kappa\left(2+3\gamma\cos\theta\right) \quad , \quad l_{32}=\frac{1}{R^2}\left(\nu\gamma\sin\theta+\gamma^2\zeta^{-1}\sin\theta\cos\theta\right)$$

$$l_{32}^I=\frac{1-\nu^2}{E}3\rho\kappa\gamma\sin\theta \quad , \quad l_{33}=-R^2\kappa\zeta^{-3}$$

$$l_{34}=-R^2\kappa\zeta \quad , \quad l_{35}=-2R^2\kappa\zeta^{-1}$$

$$l_{36}=2R\kappa\gamma\sin\theta \quad , \quad l_{37}=-2R\kappa\gamma\zeta^{-2}\sin\theta$$

$$l_{38}=-\kappa\zeta^{-2}\left[\left(1-\nu\right)\gamma\cos\theta+4\gamma^2\zeta^{-1}\sin^2\theta+2\gamma^2\zeta^{-1}\cos^2\theta\right]$$

$$l_{38}^I=\frac{1-\nu^2}{E}R^2\rho\kappa\zeta \quad , \quad l_{39}=\kappa\gamma\left[\gamma\zeta^{-1}\sin^2\theta+\left(1+\nu\right)\cos\theta\right]-2\kappa$$

$$l_{39}^{I} = \frac{1-\nu^2}{E} R^2 \rho\kappa\zeta$$

$$l_{40} = \frac{1}{R}\kappa\gamma\zeta^{-2}\sin\theta\left(-\nu\zeta^2 + \gamma\zeta\cos\theta + \gamma^2 + \nu\gamma\cos\theta\right)$$

$$l_{40}^{I} = -\frac{1-\nu^2}{E} R\rho\kappa\gamma\sin\theta \qquad , \qquad l_{41} = -\frac{1}{R^2}\left(2\nu\gamma\cos\theta + \gamma^2\zeta^{-1}\cos^2\theta + \zeta\right)$$

$$l_{41}^{I} = -\frac{1-\nu^2}{E}\rho\zeta$$

The force terms and corresponding coefficients remain identical to those of the TTS-V2 theory (Appendix 6.A.3).

Appendix 6.B Comparative Review of Various Toroidal Thin Shell Theories

Coefficients l_i from the TTS-V2, TTS-V3, Sanders and DMV theories are compared in a term by term basis in Table 6.6. Symbols α and β are generic terms of negligible magnitudes in each coefficient, when applicable. In Table 6.7, however, in the absence of inertial terms and an explicit form for boundary conditions in case of Sanders and DMV theories, comparison is made only between TTS-V2 and TTS-V3 for coefficients d_i and l_i^I. In both tables, the upper and lower bounds of negligible terms are numerically evaluated to provide a better perspective. This is done by considering the upper bound values $h/R \le 1/20$ and $\gamma \le 1/2$, which yields $1/2 \le \zeta \le 3/2$. The simplifications applied within the geometric limitations given above significantly decreases the number of operations for numerical evaluation of the equations while keeps the accuracy of the solution within a reasonable range.

Proper sign, symbol and coordinate adjustments are made to express all four theories in a unified format and make it comparable.

Table 6.6 - Comparison of l_i coefficients in various toroidal thin shell theories

Coefficient l_1				
Theory	Expression	Numeric evaluation of negligible terms		Proposed Simplification
		Compact Exp.	Range of negligible terms	
TTS-V2	$\zeta^{-1}\left(1+\kappa\gamma\zeta^{-1}\sin\theta\cos^2\theta\right)$	$\zeta^{-1}\left(1+\alpha\right)$	$-3.4\times10^{-4} \le \alpha \le 6.9\times10^{-5}$	ζ^{-1}
Sanders	$\zeta^{-1}\left(1+\kappa\gamma^2\zeta^{-2}\cos^2\theta\right)$	$\zeta^{-1}\left(1+\alpha\right)$	$0 \le \alpha \le \frac{1}{4800}$	
TTS-V3	ζ^{-1}	-	-	
DMV	ζ^{-1}	-	-	

Table 6.6 - Comparison of l_i coefficients in various toroidal thin shell theories (continued)

Coefficient l_2				
Theory	Expression	Numeric evaluation of negligible terms		Proposed Simplification
		Compact Exp.	Range of negligible terms	
TTS-V2	$\frac{1-\nu}{2}\zeta\left(1-3\kappa\gamma\zeta^{-1}\cos\theta\right)$	$\frac{1-\nu}{2}\zeta\left(1+\alpha\right)$	$-\frac{1}{4800}\le\alpha\le\frac{1}{1600}$	$\frac{1-\nu}{2}\zeta$
Sanders	$\frac{1-\nu}{2}\zeta\left[1-\kappa\gamma\zeta^{-1}\cos\theta+\kappa\zeta^{-2}\left(2\gamma^2\cos^2\theta+\frac{1}{4}\right)\right]$	$\frac{1-\nu}{2}\zeta\left(1+\alpha\right)$	$0\le\alpha\le\frac{1}{1200}$	
TTS-V3	$\frac{1-\nu}{2}\zeta$	-	-	
DMV	$\frac{1-\nu}{2}\zeta$	-	-	

Coefficient l_3				
Theory	Expression	Numeric evaluation of negligible terms		Proposed Simplification
		Compact Exp.	Range of negligible terms	
TTS-V2	$-\frac{1}{R}\frac{1-\nu}{2}\gamma\sin\theta\times\left[1-2\kappa\left(2-3\gamma\zeta^{-1}\cos\theta+4\gamma^2\zeta^{-2}\cos^2\theta\right)\right]$	$-\frac{1}{R}\frac{1-\nu}{2}\gamma\sin\theta\times\left(1+\alpha\right)$	$-\frac{1}{267}\le\alpha\le-\frac{1}{1662}$	$-\frac{1}{R}\frac{1-\nu}{2}\gamma\sin\theta$
Sanders	$-\frac{1}{R}\frac{1-\nu}{2}\gamma\sin\theta\times\left[1-\frac{1}{2}\kappa\zeta^{-1}\left(1-2\gamma\cos\theta\right)\times\left(1+\frac{3}{2}\zeta^{-1}\right)\right]$	$-\frac{1}{R}\frac{1-\nu}{2}\gamma\sin\theta\times\left(1+\alpha\right)$	$-\frac{1}{600}\le\alpha\le0$	
TTS-V3	$-\frac{1}{R}\frac{1-\nu}{2}\gamma\sin\theta$	-	-	
DMV	$-\frac{1}{R}\frac{1-\nu}{2}\gamma\sin\theta$	-	-	

Table 6.6 - Comparison of l_i coefficients in various toroidal thin shell theories (continued)

Coefficient l_4				
Theory	Expression	Numeric evaluation of negligible terms		Proposed Simplification
		Compact Exp.	Range of negligible terms	
TTS-V2	$\frac{1}{R^2}\frac{1-\nu}{2}\langle\gamma\cos\theta\times\left\{1+\kappa\left[2+\gamma\zeta^{-1}\cos\theta\times\left(4\gamma^2\zeta^{-1}-3\right)\right]\right\}-\gamma^2\zeta^{-1}\sin^2\theta\times\left\{1-\kappa\left[2+\gamma\zeta^{-2}\cos\theta\times(10+6\gamma\cos\theta)\right]\right\}\rangle$	$\frac{1}{R^2}\frac{1-\nu}{2}[\gamma\cos\theta\times(1+\alpha)-\gamma^2\zeta^{-1}\sin^2\theta\times(1+\beta)]$	$\frac{1}{3927}\le\alpha\le\frac{1}{1600}$ $-\frac{1}{982}\le\beta\le\frac{1}{400}$	$\frac{1}{R^2}\frac{1-\nu}{2}\left(\gamma\cos\theta-\gamma^2\zeta^{-1}\sin^2\theta\right)$
Sanders	$\frac{1}{R^2}\frac{1-\nu}{2}\langle\gamma\cos\theta\times\left\{1+\frac{\kappa\zeta^{-2}}{4}\left[\zeta^{-1}\times\left(1+8\gamma^2\cos^2\theta\right)-4\gamma\zeta\cos\theta\right]\right\}-\gamma^2\zeta^{-1}\sin^2\theta\times\left\{1+\frac{\kappa\zeta^{-2}}{4}\left(7+8\gamma\cos\theta+4\gamma^2\cos^2\theta\right)\right\}\rangle$	$\frac{1}{R^2}\frac{1-\nu}{2}[\gamma\cos\theta\times(1+\alpha)-\gamma^2\zeta^{-1}\sin^2\theta\times(1+\beta)]$	$-\frac{1}{43200}\le\alpha\le\frac{1}{686}$ $\frac{1}{3600}\le\beta\le\frac{1}{1200}$	
TTS-V3	$\frac{1}{R^2}\frac{1-\nu}{2}[\gamma\cos\theta-\gamma^2\zeta^{-1}\sin^2\theta\left(1-\kappa\zeta^{-2}\right)]$	$\frac{1}{R^2}\frac{1-\nu}{2}[\gamma\cos\theta-\gamma^2\zeta^{-1}\sin^2\theta\times(1+\beta)]$	$-\frac{1}{1200}\le\beta\le-\frac{1}{10800}$	
DMV	$\frac{1}{R^2}\frac{1-\nu}{2}\left(\gamma\cos\theta-\gamma^2\zeta^{-1}\sin^2\theta\right)$	-	-	

Table 6.6 - Comparison of l_i coefficients in various toroidal thin shell theories (continued)

Coefficient l_5				
Theory	Expression	Numeric evaluation of negligible terms		Proposed Simplification
		Compact Exp.	Range of negligible terms	
TTS-V2	$\frac{1+\nu}{2}\left(1+\kappa\gamma\zeta^{-1}\cos\theta\right)$	$\frac{1+\nu}{2}(1+\alpha)$	$-\frac{1}{4800}\le\alpha\le\frac{1}{14400}$	$\frac{1+\nu}{2}$
Sanders	$\frac{1+\nu}{2}\left(1+\kappa\gamma\zeta^{-1}\cos\theta\right)$ $-\frac{3}{8}(1-\nu)\kappa\zeta^{-2}$	$\frac{1+\nu}{2}(1+\alpha)$	$-\frac{1}{1835}\le\alpha\le\frac{1}{31200}$	
TTS-V3	$\frac{1+\nu}{2}$	-	-	
DMV	$\frac{1+\nu}{2}$	-	-	

Coefficient l_6				
Theory	Expression	Numeric evaluation of negligible terms		Proposed Simplification
		Compact Exp.	Range of negligible terms	
TTS-V2	$-\frac{1}{R}\frac{3-\nu}{2}\gamma\zeta^{-1}\sin\theta$	-	-	$-\frac{1}{R}\frac{3-\nu}{2}\gamma\zeta^{-1}\sin\theta$
Sanders	$-\frac{1}{R}\frac{3-\nu}{2}\gamma\zeta^{-1}\sin\theta\times$ $\left\{1+\kappa\zeta^{-1}\times\right.$ $\left.\left[\gamma\cos\theta-\frac{1-\nu}{3-\nu}\left(1+\frac{3}{4}\zeta^{-1}\right)\right]\right\}$	$-\frac{1}{R}\frac{3-\nu}{2}\gamma\zeta^{-1}$ $\times\sin\theta(1+\alpha)$	$-\frac{1}{2090}\le\alpha\le\frac{1}{64800}$	
TTS-V3	$-\frac{1}{R}\frac{3-\nu}{2}\gamma\zeta^{-1}\sin\theta$	-	-	
DMV	$-\frac{1}{R}\frac{3-\nu}{2}\gamma\zeta^{-1}\sin\theta$	-	-	

Coefficient l_7				
Theory	Expression	Numeric evaluation of negligible terms		Proposed Simplification
		Compact Exp.	Range of negligible terms	
TTS-V2	$-R\kappa\zeta^{-2}$	-	-	$-R\kappa\zeta^{-2}$
Sanders	$-R\kappa\zeta^{-2}\left(\gamma\zeta^{-1}\cos\theta\right)$	$-R\kappa\zeta^{-2}\alpha$	$-\frac{1}{3}\le\alpha\le1$	
TTS-V3	0	-	-	
DMV	0	-	-	

Table 6.6 - Comparison of l_i coefficients in various toroidal thin shell theories (continued)

Coefficient l_8				
Theory	Expression	Numeric evaluation of negligible terms		Proposed Simplification
		Compact Exp.	Range of negligible terms	
TTS-V2	$R\kappa\zeta^{-1}\left(\frac{1-\nu}{2}-\gamma\cos\theta\right)$	-	-	$R\kappa\zeta^{-1}\left(\frac{1-\nu}{2}-\gamma\cos\theta\right)$
Sanders	$R\kappa\zeta^{-1}\left(\frac{1-\nu}{2}-\gamma\cos\theta\right)$	-	-	
TTS-V3	0	-	-	
DMV	0	-	-	

Coefficient l_9				
Theory	Expression	Numeric evaluation of negligible terms		Proposed Simplification
		Compact Exp.	Range of negligible terms	
TTS-V2	$\kappa\gamma\zeta^{-2}\left(\frac{5-3\nu}{2}\sin\theta+\gamma\sin\theta\cos\theta\right)$	-	-	$\kappa\gamma\zeta^{-2}\left(\frac{5-3\nu}{2}\sin\theta+\gamma\sin\theta\cos\theta\right)$
Sanders	$\kappa\gamma\zeta^{-2}\left(\frac{3-3\nu}{2}\sin\theta+\gamma\sin\theta\cos\theta\right)$	-	-	
TTS-V3	$\kappa\gamma\zeta^{-2}\left(1-\nu\right)\sin\theta$	-	-	
DMV	0	-	-	

Table 6.6 - Comparison of l_i coefficients in various toroidal thin shell theories (continued)

Coefficient l_{10}				
Theory	Expression	Numeric evaluation of negligible terms		Proposed Simplification
		Compact Exp.	Range of negligible terms	
TTS-V2	$\frac{1}{R}\left\langle \nu\left(1+3\frac{1-\nu}{2\nu}\kappa\gamma^2\zeta^{-2}\right) +\gamma\zeta^{-1}\cos\theta \times\left\{1+\frac{1-\nu}{2}\kappa\left[1-3\gamma\zeta^{-2} \times\left(2\zeta\cos\theta+\gamma\sin^2\theta\right)\right]\right\}\right\rangle$	$\frac{1}{R}\left[\nu\left(1+\alpha\right)+ \gamma\zeta^{-1}\cos\theta\times \left(1+\beta\right)\right]$	$\frac{1}{12343}\le\alpha\le\frac{1}{1371}$ $-\frac{1}{13714}\le\beta\le\frac{1}{1959}$	$\frac{1}{R}\left(\nu+\gamma\zeta^{-1}\cos\theta\right)$
Sanders	$\frac{1}{R}\left\langle \nu\left(1+3\frac{1-\nu}{2\nu}\kappa\gamma^2\zeta^{-3}\right) +\gamma\zeta^{-1}\cos\theta \times\left[1+\frac{1-\nu}{2}\kappa\zeta^{-2} \times\left(1-4\gamma\cos\theta -2\gamma^2\cos^2\theta\right)\right]\right\rangle$	$\frac{1}{R}\left[\nu\left(1+\alpha\right)+ \gamma\zeta^{-1}\cos\theta\times \left(1+\beta\right)\right]$	$\frac{1}{18514}\le\alpha\le\frac{1}{686}$ $-\frac{1}{20571}\le\beta\le\frac{1}{1371}$	
TTS-V3	$\frac{1}{R}\left\langle \nu\left(1+3\frac{1-\nu}{2\nu}\kappa\gamma^2\zeta^{-3}\right) +\gamma\zeta^{-1}\cos\theta\times\left\{1+\frac{1-\nu}{2}\kappa\zeta^{-2} \times\left[\gamma^2-\left(4\gamma+2\gamma^3\right)\cos\theta -\left(\gamma^2+\gamma^4\right)\cos^2\theta\right]\right\}\right\rangle$	$\frac{1}{R}\left[\nu\left(1+\alpha\right)+ \gamma\zeta^{-1}\cos\theta\times \left(1+\beta\right)\right]$	$\frac{1}{18514}\le\alpha\le\frac{1}{686}$ $-\frac{1}{13344}\le\beta\le\frac{1}{1567}$	
DMV	$\frac{1}{R}\left(\nu+\gamma\zeta^{-1}\cos\theta\right)$	$\frac{1}{R}\left(\nu +\gamma\zeta^{-1}\cos\theta\right)$	-	

Coefficient l_{11}				
Theory	Expression	Numeric evaluation of negligible terms		Proposed Simplification
		Compact Exp.	Range of negligible terms	
TTS-V2	$\frac{1+\nu}{2}\left(1+\kappa\gamma\zeta^{-1}\cos\theta\right)$	$\frac{1+\nu}{2}\left(1+\alpha\right)$	$-\frac{1}{4800}\le\alpha\le\frac{1}{14400}$	$\frac{1+\nu}{2}$
Sanders	$\frac{1+\nu}{2}\left(1+\kappa\gamma\zeta^{-1}\cos\theta\right) -\frac{3}{4}\left(\frac{1-\nu}{2}\right)\kappa\zeta^{-2}$	$\frac{1+\nu}{2}\left(1+\alpha\right)\left(1+\beta\right)$	$-\frac{1}{4800}\le\alpha\le\frac{1}{14400}$ $-\frac{1}{2971}\le\beta\le-\frac{1}{26745}$	
TTS-V3	$\frac{1+\nu}{2}$	-	-	
DMV	$\frac{1+\nu}{2}$	-	-	

Table 6.6 - Comparison of l_i coefficients in various toroidal thin shell theories (continued)

Coefficient l_{12}				
Theory	Expression	Numeric evaluation of negligible terms		Proposed Simplification
		Compact Exp.	Range of negligible terms	
TTS-V2	$\frac{1}{R}\left[\frac{3-\nu}{2}\gamma\zeta^{-1}\sin\theta - \frac{1+\nu}{2}\kappa\gamma\zeta^{-2}\sin\theta\left(1+\zeta\right)\right]$	$\frac{1}{R}\frac{3-\nu}{2}\gamma\zeta^{-1} \times\sin\theta \times\left(1+\alpha\right)$	$-\frac{1}{3323}\le\alpha\le-\frac{1}{5982}$	$\frac{1}{R}\left(\frac{3-\nu}{2}\gamma\zeta^{-1}\sin\theta\right)$
Sanders	$\frac{1}{R}\left\{\frac{3-\nu}{2}\gamma\zeta^{-1}\sin\theta - \kappa\gamma\zeta^{-2}\sin\theta\times \left[\frac{1+\nu}{2}-\frac{3-\nu}{2}\gamma\cos\theta - \frac{1-\nu}{8}\left(1+3\gamma\zeta^{-1}\cos\theta\right)\right]\right\}$	$\frac{1}{R}\frac{3-\nu}{2}\gamma\zeta^{-1} \times\sin\theta \times\left(1+\alpha\right)$	$-\frac{1}{1600}\le\alpha\le\frac{1}{13407}$	
TTS-V3	$\frac{1}{R}\left(\frac{3-\nu}{2}\gamma\zeta^{-1}\sin\theta\right)$	-	-	
DMV	$\frac{1}{R}\left(\frac{3-\nu}{2}\gamma\zeta^{-1}\sin\theta\right)$	-	-	

Coefficient l_{13}				
Theory	Expression	Numeric evaluation of negligible terms		Proposed Simplification
		Compact Exp.	Range of negligible terms	
TTS-V2	$\frac{1-\nu}{2}\zeta^{-1}\left(1-3\kappa\gamma\zeta^{-1}\cos\theta\right)$	$\frac{1-\nu}{2}\zeta^{-1}\left(1+\alpha\right)$	$-\frac{1}{4800}\le\alpha\le\frac{1}{1600}$	$\frac{1-\nu}{2}\zeta^{-1}$
Sanders	$\frac{1-\nu}{2}\zeta^{-1}\left[\left(1+\kappa\right) + \kappa\zeta^{-1}\left(1+\frac{1}{4}\zeta^{-1}\right)\right]$	$\frac{1-\nu}{2}\zeta^{-1}\left(1+\alpha\right)$	$\frac{1}{2700}\le\alpha\le\frac{1}{1200}$	
TTS-V3	$\frac{1-\nu}{2}\zeta^{-1}$	-	-	
DMV	$\frac{1-\nu}{2}\zeta^{-1}$	-	-	

Table 6.6 - Comparison of l_i coefficients in various toroidal thin shell theories (continued)

Coefficient l_{14}				
Theory	Expression	Numeric evaluation of negligible terms		Proposed Simplification
		Compact Exp.	Range of negligible terms	
TTS-V2	$\zeta(1+\kappa)-\kappa$	$\zeta(1+\kappa)(1+\alpha)$	$\alpha=-\frac{1}{7202}$	ζ
Sanders	$\zeta(1+\kappa)$	-	-	
TTS-V3	ζ	-	-	
DMV	ζ	-	-	

Coefficient l_{15}				
Theory	Expression	Numeric evaluation of negligible terms		Proposed Simplification
		Compact Exp.	Range of negligible terms	
TTS-V2	$-\frac{1}{R}\gamma\sin\theta$	-	-	$-\frac{1}{R}\gamma\sin\theta$
Sanders	$-\frac{1}{R}\gamma\sin\theta(1+\kappa)$	-	-	
TTS-V3	$-\frac{1}{R}\gamma\sin\theta$	-	-	
DMV	$-\frac{1}{R}\gamma\sin\theta$	-	-	

Table 6.6 - Comparison of l_i coefficients in various toroidal thin shell theories (continued)

Coefficient l_{16}				
Theory	Expression	Numeric evaluation of negligible terms		Proposed simplification
		Compact Exp.	Range of negligible terms	
TTS-V2	$-\frac{1}{R^2}\left[\nu\gamma\cos\theta+\gamma^2\zeta^{-1}\sin^2\theta\times\left(1-3\kappa\gamma\zeta^{-1}\cos\theta\right)\right]$	$-\frac{1}{R^2}\left[\nu\gamma\cos\theta+\gamma^2\zeta^{-1}\sin^2\theta\times(1+\alpha)\right]$	$-\frac{1}{4800}\le\alpha\le\frac{1}{1600}$	$-\frac{1}{R^2}\left(\nu\gamma\cos\theta+\gamma^2\zeta^{-1}\sin^2\theta\right)$
Sanders	$-\frac{1}{R^2}\left(\nu\gamma\cos\theta+\gamma^2\zeta^{-1}\sin^2\theta\right)\times(1+\kappa)$	-	-	
TTS-V3	$-\frac{1}{R^2}\left(\nu\gamma\cos\theta+\gamma^2\zeta^{-1}\sin^2\theta\right)$	-	-	
DMV	$-\frac{1}{R^2}\left(\nu\gamma\cos\theta+\gamma^2\zeta^{-1}\sin^2\theta\right)$	-	-	

Coefficient l_{17}				
Theory	Expression	Numeric evaluation of negligible terms		Proposed Simplification
		Compact Exp.	Range of negligible terms	
TTS-V2	$-R\kappa\gamma\cos\theta$	-	-	$-R\kappa\gamma\cos\theta$
Sanders	$-R\kappa\zeta$	-	-	
TTS-V3	0	-	-	
DMV	0	-	-	

Coefficient l_{18}				
Theory	Expression	Numeric evaluation of negligible terms		Proposed Simplification
		Compact Exp.	Range of negligible terms	
TTS-V2	$-R\kappa\zeta^{-1}\left(1+\frac{1-\nu}{2}\zeta^{-1}\right)$	-	-	$-R\kappa\zeta^{-1}\left(1+\frac{1-\nu}{2}\zeta^{-1}\right)$
Sanders	$-R\kappa\zeta^{-1}\left(1+\frac{1-\nu}{2}\zeta^{-1}\right)$	-	-	
TTS-V3	0	-	-	
DMV	0	-	-	

Table 6.6 - Comparison of l_i coefficients in various toroidal thin shell theories (continued)

Coefficient l_{19}				
Theory	Expression	Numeric evaluation of negligible terms		Proposed simplification
		Compact Exp.	Range of Negligible terms	
TTS-V2	$\kappa\gamma\zeta^{-3}\sin\theta\left(-\frac{7-\nu}{2}-2\gamma\cos\theta\right)$	-	-	$\kappa\gamma\zeta^{-3}\sin\theta\left(-\frac{7-\nu}{2}-2\gamma\cos\theta\right)$
Sanders	$\kappa\gamma\zeta^{-3}\sin\theta\left(-\frac{5-\nu}{2}-2\gamma\cos\theta\right)$	-	-	
TTS-V3	$\kappa\gamma\zeta^{-3}\sin\theta\left(\frac{1+\nu}{2}\right)$	-	-	
DMV	0	-	-	

Coefficient l_{20}				
Theory	Expression	Numeric evaluation of negligible terms		Proposed Simplification
		Compact Exp.	Range of negligible terms	
TTS-V2	$\kappa\gamma\sin\theta$	-	-	$\kappa\gamma\sin\theta$
Sanders	$\kappa\gamma\sin\theta$	-	-	
TTS-V3	0	-	-	
DMV	0	-	-	

Coefficient l_{21}				
Theory	Expression	Numeric evaluation of negligible terms		Proposed Simplification
		Compact Exp.	Range of Negligible terms	
TTS-V2	$\frac{1}{R}\left[\zeta+\nu\gamma\cos\theta(1+\kappa)+\kappa\gamma^2\zeta^{-1}\sin^2\theta\left(1+\zeta^{-1}\right)\right]$	$\frac{1}{R}\left[\zeta+\nu\gamma\cos\theta(1+\kappa)\right]\times(1+\alpha)$	$0\le\alpha\le\frac{1}{5221}$	$\frac{1}{R}(\zeta+\nu\gamma\cos\theta)$
Sanders	$\frac{1}{R}\left[\zeta+\nu\gamma\cos\theta(1+\kappa)+\kappa\gamma^2\zeta^{-1}\sin^2\theta\right]$	$\frac{1}{R}\left[\zeta+\nu\gamma\cos\theta(1+\kappa)\right]\times(1+\alpha)$	$0\le\alpha\le\frac{1}{12799}$	
TTS-V3	$\frac{1}{R}(\zeta+\nu\gamma\cos\theta)$	-	-	
DMV	$\frac{1}{R}(\zeta+\nu\gamma\cos\theta)$	-	-	

Table 6.6 - Comparison of l_i coefficients in various toroidal thin shell theories (continued)

Coefficient l_{22}				
Theory	Expression	Numeric evaluation of negligible terms		Proposed Simplification
		Compact Exp.	Range of negligible terms	
TTS-V2	$-\frac{1}{R^2}\nu\gamma\zeta^{-1}\sin\theta\times\left(\frac{1+(1-\kappa)\gamma\cos\theta}{\zeta}\right)$	$-\frac{1}{R^2}\nu\gamma\zeta^{-1}\sin\theta\times\alpha$	$\frac{14399}{14400}\le\alpha\le\frac{4801}{4800}$	$-\frac{1}{R^2}\nu\gamma\zeta^{-1}\sin\theta$
Sanders	$-\frac{1}{R^2}\gamma\zeta^{-1}\sin\theta$	-	-	
TTS-V3	$-\frac{1}{R^2}\nu\gamma\zeta^{-1}\sin\theta$	-	-	
DMV	$-\frac{1}{R^2}\gamma\zeta^{-1}\sin\theta$	-	-	

Coefficient l_{23}				
Theory	Expression	Numeric evaluation of negligible terms		Proposed Simplification
		Compact Exp.	Range of negligible terms	
TTS-V2	$R\kappa\zeta^{-2}$	-	-	$R\kappa\zeta^{-2}$
Sanders	$R\kappa\zeta^{-2}\left(\gamma\zeta^{-1}\cos\theta\right)$	$R\kappa\zeta^{-2}\alpha$	$-1\le\alpha\le\frac{1}{3}$	
TTS-V3	0	-	-	
DMV	0	-	-	

Coefficient l_{24}				
Theory	Expression	Numeric evaluation of negligible terms		Proposed Simplification
		Compact Exp.	Range of negligible terms	
TTS-V2	$R\kappa\zeta^{-1}\left(\gamma\cos\theta-\frac{1-\nu}{2}\right)$	-	-	$R\kappa\zeta^{-1}\left(\gamma\cos\theta-\frac{1-\nu}{2}\right)$
Sanders	$R\kappa\zeta^{-1}\left(\gamma\cos\theta-\frac{1-\nu}{2}\right)$	-	-	
TTS-V3	0	-	-	
DMV	0	-	-	

Table 6.6 - Comparison of l_i coefficients in various toroidal thin shell theories (continued)

Coefficient l_{25}				
Theory	Expression	Numeric evaluation of negligible terms		Proposed Simplification
		Compact Exp.	Range of negligible terms	
TTS-V2	$-\kappa\gamma\zeta^{-2}\left(\frac{1+\nu}{2}\sin\theta-\gamma\sin\theta\cos\theta\right)$	-	-	$-\kappa\gamma\zeta^{-2}\left(\frac{1+\nu}{2}\sin\theta-\gamma\sin\theta\cos\theta\right)$
Sanders	$-\kappa\gamma\zeta^{-2}\left(\frac{3-\nu}{2}\sin\theta-\gamma\sin\theta\cos\theta\right)$	-	-	
TTS-V3	$-\kappa\gamma\zeta^{-2}\left(\frac{3-\nu}{2}\right)\sin\theta$	-	-	
DMV	0	-	-	

Coefficient l_{26}				
Theory	Expression	Numeric evaluation of negligible terms		Proposed simplification
		Compact Exp.	Range of Negligible terms	
TTS-V2	$-\frac{1}{R}\left\langle\nu\left(1-\kappa\gamma^2\zeta^{-3}\frac{7-\nu}{2\nu}\right)+\gamma\zeta^{-1}\cos\theta\times\left\{1+\kappa\left[\frac{1-\nu}{2}+\gamma\zeta^{-2}\times\left(-\frac{3-\nu}{2}\gamma^2+2\gamma\cos\theta-\frac{7+\nu}{2}\gamma\sin^2\theta\right)\right]\right\}\right\rangle$	$-\frac{1}{R}\left[\nu(1+\alpha)+\gamma\zeta^{-1}\cos\theta\times(1+\beta)\right]$	$-\frac{1}{215}\le\alpha\le-\frac{1}{5803}$ $-\frac{1}{2065}\le\beta\le\frac{1}{9654}$	$-\frac{1}{R}\left(\nu+\gamma\zeta^{-1}\cos\theta\right)$
Sanders	$-\frac{1}{R}\left[\left[\nu\left(1-\frac{5+\nu}{2\nu}\kappa\gamma^2\zeta^{-3}\right)+\gamma\zeta^{-1}\cos\theta\left\langle1-\kappa\left\{1-\zeta^{-2}\times\left[\frac{1-\nu}{2}+\gamma^2\sin^2\theta+3(2-\nu)\gamma\cos\theta+3(1-\nu)\gamma^2\cos^2\theta\right]\right\}\right\rangle\right]\right]$	$-\frac{1}{R}\left[\nu(1+\alpha)+\gamma\zeta^{-1}\cos\theta\times(1+\beta)\right]$	$-\frac{1}{272}\le\alpha\le-\frac{1}{7336}$ $-\frac{1}{623}\le\beta\le\frac{1}{9191}$	
TTS-V3	$-\frac{1}{R}\left\{\nu\left[1+3(1-\nu)\kappa\gamma^2\zeta^{-3}\right]+\gamma\zeta^{-1}\cos\theta\left[1+(1-\nu)\times\kappa\zeta^{-2}(1-2\gamma\cos\theta)\right]\right\}$	$-\frac{1}{R}\left[\nu(1+\alpha)+\gamma\zeta^{-1}\cos\theta\times(1+\beta)\right]$	$\frac{1}{30857}\le\alpha\le\frac{1}{1143}$ $0\le\beta\le\frac{1}{857}$	
DMV	$-\frac{1}{R}\left(\nu+\gamma\zeta^{-1}\cos\theta\right)$	-	-	

Table 6.6 - Comparison of l_i coefficients in various toroidal thin shell theories (continued)

Coefficient l_{27}				
Theory	Expression	Numeric evaluation of negligible terms		Proposed Simplification
		Compact Exp.	Range of negligible terms	
TTS-V2	$R\kappa\gamma\cos\theta$	-	-	$R\kappa\gamma\cos\theta$
Sanders	$R\kappa\zeta$	-	-	
TTS-V3	0	-	-	
DMV	0	-	-	

Coefficient l_{28}				
Theory	Expression	Numeric evaluation of negligible terms		Proposed Simplification
		Compact Exp.	Range of negligible terms	
TTS-V2	$R\kappa\zeta^{-2}\left(\zeta+\frac{1-\nu}{2}\right)$	-	-	$R\kappa\zeta^{-2}\left(\zeta+\frac{1-\nu}{2}\right)$
Sanders	$R\kappa\zeta^{-2}\left(\zeta+\frac{1-\nu}{2}\right)$	-	-	
TTS-V3	0	-	-	
DMV	0	-	-	

Coefficient l_{29}				
Theory	Expression	Numeric evaluation of negligible terms		Proposed Simplification
		Compact Exp.	Range of negligible terms	
TTS-V2	$-\kappa\gamma\zeta^{-3}\sin\theta\left(\zeta+\frac{1+\nu}{2}\right)$	-	-	$-\kappa\gamma\zeta^{-3}\sin\theta\left(\zeta+\frac{1+\nu}{2}\right)$
Sanders	$-\kappa\gamma\zeta^{-3}\sin\theta\left(\zeta-\frac{1-\nu}{2}\right)$	-	-	
TTS-V3	0	-	-	
DMV	0	-	-	

Coefficient l_{30}				
Theory	Expression	Numeric evaluation of negligible terms		Proposed Simplification
		Compact Exp.	Range of negligible terms	
TTS-V2	$-2\kappa\gamma\sin\theta$	-	-	$-2\kappa\gamma\sin\theta$
Sanders	$-2\kappa\gamma\sin\theta$	-	-	
TTS-V3	0	-	-	
DMV	0	-	-	

Table 6.6 - Comparison of l_i coefficients in various toroidal thin shell theories (continued)

Coefficient l_{31}				
Theory	Expression	Numeric evaluation of negligible terms		Proposed Simplification
		Compact Exp.	Range of Negligible terms	
TTS-V2	$-\frac{1}{R}\left\langle \zeta\left[1+\kappa\gamma^2\zeta^{-2}\left(1+\zeta^{-1}\right)\right] +\nu\gamma\cos\theta\left\{1+\kappa\left[1-\frac{\gamma}{\nu}\zeta^{-1} \times\cos\theta\left(1+\zeta^{-1}\right)\right]\right\}\right\rangle$	$-\frac{1}{R}\left[\zeta\left(1+\alpha\right) +\nu\gamma\cos\theta \times\left(1+\beta\right)\right]$	$\frac{1}{25920}\le\alpha\le\frac{1}{1600}$ $-\frac{1}{5635}\le\beta\le\frac{1}{436}$	$-\frac{1}{R}\left(\zeta+\nu\gamma\cos\theta\right)$
Sanders	$-\frac{1}{R}\left[\zeta\left(1+\kappa\gamma^2\zeta^{-2}\right)+\nu\gamma\cos\theta \times\left(1+\frac{1+\nu}{\nu}\kappa\cos\theta\right)\right]$	$-\frac{1}{R}\left[\zeta\left(1+\alpha\right) +\nu\gamma\cos\theta \times\left(1+\beta\right)\right]$	$\frac{1}{43200}\le\alpha\le\frac{1}{4800}$ $-\frac{1}{1108}\le\beta\le\frac{1}{1108}$	
TTS-V3	$-\frac{1}{R}\left(\zeta+\nu\gamma\cos\theta\right)$	-	-	
DMV	$-\frac{1}{R}\left(\zeta+\nu\gamma\cos\theta\right)$	-	-	

Table 6.6 - Comparison of l_i coefficients in various toroidal thin shell theories (continued)

Coefficient l_{32}				
Theory	Expression	Numeric evaluation of negligible terms		Proposed Simplification
		Compact Exp.	Range of Negligible terms	
TTS-V2	$\frac{1}{R^2}\langle \nu\gamma \sin\theta \times \{1+\kappa[1-\gamma^2\zeta^{-2}\sin^2\theta \times(1+2\zeta^{-1})]\}+(1-4\kappa) \times\gamma^2\zeta^{-1}\sin\theta\cos\theta\rangle$	$\frac{1}{R^2}[\nu\gamma\sin\theta \times(1+\alpha) +(1-4\kappa)\gamma^2\zeta^{-1} \times\sin\theta\cos\theta]$	$-\frac{1}{18441}\le\alpha\le\frac{1}{4800}$	$\frac{1}{R^2}(\nu\gamma\sin\theta +\gamma^2\zeta^{-1}\sin\theta\cos\theta)$
Sanders	$\frac{1}{R^2}\langle \nu\gamma\sin\theta[1+\kappa \left(1-\frac{1}{\nu}\gamma^2\zeta^{-2}\sin^2\theta\right)] +(1-2\kappa)\gamma^2\zeta^{-1}\sin\theta\cos\theta\rangle$	$\frac{1}{R^2}[\nu\gamma\sin\theta \times(1+\alpha) +(1-2\kappa)\gamma^2\zeta^{-1} \times\sin\theta\cos\theta]$	$-\frac{1}{43200}\le\alpha\le\frac{1}{4800}$	
TTS-V3	$\frac{1}{R^2}(\nu\gamma\sin\theta +\gamma^2\zeta^{-1}\sin\theta\cos\theta)$	-	-	
DMV	$\frac{1}{R^2}(\nu\gamma\sin\theta +\gamma^2\zeta^{-1}\sin\theta\cos\theta)$	-	-	

Coefficient l_{33}				
Theory	Expression	Numeric evaluation of negligible terms		Proposed Simplification
		Compact Exp.	Range of negligible terms	
TTS-V2	$-R^2\kappa\zeta^{-3}$	-	-	$-R^2\kappa\zeta^{-3}$
Sanders	$-R^2\kappa\zeta^{-3}$	-	-	
TTS-V3	$-R^2\kappa\zeta^{-3}$	-	-	
DMV	$-R^2\kappa\zeta^{-3}$	-	-	

Table 6.6 - Comparison of l_i coefficients in various toroidal thin shell theories (continued)

Coefficient l_{34}				
Theory	Expression	Numeric evaluation of negligible terms		Proposed Simplification
		Compact Exp.	Range of negligible terms	
TTS-V2	$-R^2\kappa\zeta$	-	-	$-R^2\kappa\zeta$
Sanders	$-R^2\kappa\zeta$	-	-	
TTS-V3	$-R^2\kappa\zeta$	-	-	
DMV	$-R^2\kappa\zeta$	-	-	

Coefficient l_{35}				
Theory	Expression	Numeric evaluation of negligible terms		Proposed Simplification
		Compact Exp.	Range of negligible terms	
TTS-V2	$-2R^2\kappa\zeta^{-1}$	-	-	$-2R^2\kappa\zeta^{-1}$
Sanders	$-2R^2\kappa\zeta^{-1}$	-	-	
TTS-V3	$-2R^2\kappa\zeta^{-1}$	-	-	
DMV	$-2R^2\kappa\zeta^{-1}$	-	-	

Coefficient l_{36}				
Theory	Expression	Numeric evaluation of negligible terms		Proposed Simplification
		Compact Exp.	Range of negligible terms	
TTS-V2	$2R\kappa\gamma\sin\theta$	-	-	$2R\kappa\gamma\sin\theta$
Sanders	$2R\kappa\gamma\sin\theta$	-	-	
TTS-V3	$R\kappa\gamma\sin\theta$	-	-	
DMV	$2R\kappa\gamma\sin\theta$	-	-	

Table 6.6 - Comparison of l_i coefficients in various toroidal thin shell theories (continued)

Coefficient l_{37}				
Theory	Expression	Numeric evaluation of negligible terms		Proposed Simplification
		Compact Exp.	Range of negligible terms	
TTS-V2	$-2R\kappa\gamma\zeta^{-2}\sin\theta$	-	-	$-2R\kappa\gamma\zeta^{-2}\sin\theta$
Sanders	$-2R\kappa\gamma\zeta^{-2}\sin\theta$	-	-	
TTS-V3	$-R\kappa\gamma\zeta^{-2}\sin\theta$	-	-	
DMV	$-2R\kappa\gamma\zeta^{-2}\sin\theta$	-	-	

Coefficient l_{38}				
Theory	Expression	Numeric evaluation of negligible terms		Proposed Simplification
		Compact Exp.	Range of negligible terms	
TTS-V2	$-\kappa\zeta^{-2}\left[(1-\nu)\gamma\cos\theta + 4\gamma^2\zeta^{-1}\sin^2\theta + 2\gamma^2\zeta^{-1}\cos^2\theta\right]$	-	-	$-\kappa\zeta^{-2}\left[(1-\nu)\gamma\cos\theta + 4\gamma^2\zeta^{-1}\sin^2\theta + 2\gamma^2\zeta^{-1}\cos^2\theta\right]$
Sanders	$-\kappa\zeta^{-2}\left[(3-\nu)\gamma\cos\theta + 4\gamma^2\zeta^{-1}\sin^2\theta\right]$	-	-	
TTS-V3	$-\kappa\zeta^{-2}(1-\nu)\gamma\cos\theta$	-	-	
DMV	$-2\kappa\zeta^{-3}\left[\gamma^2 + \gamma\cos\theta + \gamma^2\sin^2\theta\right]$	-	-	

Table 6.6 - Comparison of l_i coefficients in various toroidal thin shell theories (continued)

Coefficient l_{39}				
Theory	Expression	Numeric evaluation of negligible terms		Proposed Simplification
		Compact Exp.	Range of Negligible terms	
TTS-V2	$\kappa\gamma\left[\gamma\zeta^{-1}\sin^2\theta+(1+\nu)\cos\theta\right]-2\kappa$	-	-	$\kappa\gamma\left[\gamma\zeta^{-1}\sin^2\theta+(1+\nu)\cos\theta\right]-2\kappa$
Sanders	$\kappa\gamma\left[\gamma\zeta^{-1}\sin^2\theta+(1+\nu)\cos\theta\right]$	-	-	
TTS-V3	$\kappa\gamma\left(\gamma\zeta^{-1}\sin^2\theta+\nu\cos\theta\right)$	-	-	
DMV	$\kappa\gamma\left(\gamma\zeta^{-1}+2\zeta^{-1}\cos\theta+\gamma\zeta^{-1}\cos^2\theta\right)$	-	-	

Coefficient l_{40}				
Theory	Expression	Numeric evaluation of negligible terms		Proposed simplification
		Compact Exp.	Range of negligible terms	
TTS-V2	$\frac{1}{R}\kappa\zeta^{-2}\left(-\nu\gamma\zeta^2\sin\theta+\gamma^2\zeta\sin\theta\cos\theta+\gamma^3\sin\theta+\nu\gamma^2\sin\theta\cos\theta\right)$	-	-	$\frac{1}{R}\kappa\gamma\zeta^{-2}\sin\theta\left(-\nu\zeta^2+\gamma\zeta\cos\theta+\gamma^2+\nu\gamma\cos\theta\right)$
Sanders	$\frac{1}{R}\kappa\zeta^{-2}\left(-\nu\gamma\zeta^2\sin\theta+\gamma^2\zeta\sin\theta\cos\theta+\gamma^3\sin\theta+\gamma^2\sin\theta\cos\theta\right)$	-	-	
TTS-V3	0	-	-	
DMV	0	-	-	

Table 6.6 - Comparison of l_i coefficients in various toroidal thin shell theories (continued)

Coefficient l_{41}				
Theory	Expression	Numeric evaluation of negligible terms		Proposed simplification
		Compact Exp.	Range of Negligible terms	
TTS-V2	$-\frac{1}{R^2}\left[\left[2\nu\gamma\cos\theta\left\langle 1-\frac{\kappa}{2\nu}\times\left\{1+\gamma\zeta^{-2}\times\left[\gamma\cos^2\theta+2\nu\left(1+\gamma\right)\zeta^{-1}\right]\right\}\right\rangle+\gamma^2\zeta^{-1}\cos^2\theta+\zeta\left(1+\nu\kappa\gamma^2\zeta^{-3}\right)\right]\right]$	$-\frac{1}{R^2}\left[2\nu\gamma\cos\theta\times\left(1+\alpha\right)+\gamma^2\zeta^{-1}\cos^2\theta+\zeta\left(1+\beta\right)\right]$	$-\frac{1}{563}\le\alpha\le-\frac{1}{2354}$ $-\frac{1}{216000}\le\beta\le\frac{1}{8000}$	$-\frac{1}{R^2}\left(2\nu\gamma\cos\theta+\gamma^2\zeta^{-1}\cos^2\theta+\zeta\right)$
Sanders	$-\frac{1}{R^2}\left(2\nu\gamma\cos\theta+\gamma^2\zeta^{-1}\cos^2\theta+\zeta\right)$	-	-	
TTS-V3	$-\frac{1}{R^2}\left(2\nu\gamma\cos\theta+\gamma^2\zeta^{-1}\cos^2\theta+\zeta\right)$	-	-	
DMV	$-\frac{1}{R^2}\left(2\nu\gamma\cos\theta+\gamma^2\zeta^{-1}\cos^2\theta\right)$	-	-	

Table 6.7 - Comparison of d_i coefficients in various toroidal thin shell theories

Coefficient d_1				
Theory	Expression	Numeric evaluation of negligible terms		Proposed simplification
		Compact Exp.	Range of Negligible terms	
TTS-V2	$-\zeta^{-1}\left(1+\kappa\gamma\zeta^{-1}\cos\theta\right)$	$-\zeta^{-1}\left(1+\alpha\right)$	$-\frac{1}{4800}\le\alpha\le\frac{1}{14400}$	$-\zeta^{-1}$
Sanders	$-\zeta^{-1}\left(1+\kappa\gamma^{2}\zeta^{-3}\cos^{2}\theta\right)$	$-\zeta^{-1}\left(1+\alpha\right)$	$0\le\alpha\le\frac{1}{2400}$	
TTS-V3	$-\zeta^{-1}$	-	-	

Coefficient d_2				
Theory	Expression	Numeric evaluation of negligible terms		Proposed simplification
		Compact Exp.	Range of Negligible terms	
TTS-V2	$-\nu\left(1+\kappa\gamma\zeta^{-1}\cos\theta\right)$	$-\nu\left(1+\alpha\right)$	$-\frac{1}{4800}\le\alpha\le\frac{1}{14400}$	$-\nu$
Sanders	$-\nu\left(1+\kappa\gamma\zeta^{-1}\cos\theta\right)$	$-\nu\left(1+\alpha\right)$	$-\frac{1}{4800}\le\alpha\le\frac{1}{14400}$	
TTS-V3	$-\nu$	-	-	

Coefficient d_3				
Theory	Expression	Numeric evaluation of negligible terms		Proposed simplification
		Compact Exp.	Range of Negligible terms	
TTS-V2	$\frac{1}{R}\gamma\zeta^{-1}\sin\theta$	-	-	$\frac{1}{R}\gamma\zeta^{-1}\sin\theta$
Sanders	$\frac{1}{R}\gamma\zeta^{-1}\sin\theta\left(1+\kappa\gamma\zeta^{-1}\cos\theta\right)$	$\frac{1}{R}\gamma\zeta^{-1}\sin\theta\left(1+\alpha\right)$	$-\frac{1}{4800}\le\alpha\le\frac{1}{14400}$	
TTS-V3	$\frac{1}{R}\gamma\zeta^{-1}\sin\theta$	-	-	

Table 6.7 - Comparison of d_i coefficients in various toroidal thin shell theories (continued)

Coefficient d_4				
Theory	Expression	Numeric evaluation of negligible terms		Proposed simplification
		Compact Exp.	Range of Negligible terms	
TTS-V2	$R\kappa\zeta^{-2}$	-	-	$R\kappa\zeta^{-2}$
Sanders	$R\kappa\zeta^{-2}\left(\gamma\zeta^{-1}\cos\theta\right)$	-	-	
TTS-V3	0	-	-	

Coefficient d_5				
Theory	Expression	Numeric evaluation of negligible terms		Proposed simplification
		Compact Exp.	Range of Negligible terms	
TTS-V2	$R\nu\kappa\gamma\zeta^{-1}\cos\theta$	-	-	$R\nu\kappa\gamma\zeta^{-1}\cos\theta$
Sanders	$R\nu\kappa\gamma\zeta^{-1}\cos\theta$	-	-	
TTS-V3	0	-	-	

Coefficient d_6				
Theory	Expression	Numeric evaluation of negligible terms		Proposed simplification
		Compact Exp.	Range of Negligible terms	
TTS-V2	$-\kappa\gamma\zeta^{-1}\sin\theta$	-	-	$-\kappa\gamma\zeta^{-1}\sin\theta$
Sanders	$-\kappa\gamma\zeta^{-1}\sin\theta\left(\gamma\zeta^{-1}\cos\theta\right)$	-	-	
TTS-V3	0	-	-	

Coefficient d_7				
Theory	Expression	Numeric evaluation of negligible terms		Proposed simplification
		Compact Exp.	Range of Negligible terms	
TTS-V2	$-\frac{1}{R}\left(\nu+\gamma\zeta^{-1}\cos\theta\right)$	-	-	$-\frac{1}{R}\left(\nu+\gamma\zeta^{-1}\cos\theta\right)$
Sanders	$-\frac{1}{R}\left(\nu+\gamma\zeta^{-1}\cos\theta\right)$	-	-	
TTS-V3	$-\frac{1}{R}\left(\nu+\gamma\zeta^{-1}\cos\theta\right)$	-	-	

Table 6.7 - Comparison of d_i coefficients in various toroidal thin shell theories (continued)

Coefficient d_8				
Theory	Expression	Numeric evaluation of negligible terms		Proposed simplification
		Compact Exp.	Range of Negligible terms	
TTS-V2	$-\frac{1-\nu}{2}\left(1+\kappa\gamma\zeta^{-1}\cos\theta\right)$	$-\frac{1-\nu}{2}(1+\alpha)$	$-\frac{1}{4800}\le\alpha\le\frac{1}{14400}$	$-\frac{1-\nu}{2}$
Sanders	$-\frac{1-\nu}{2}\left[1-\kappa\left(\frac{3}{4}-\frac{5}{2}\gamma\zeta^{-1}\cos\theta+\frac{3}{4}\gamma^2\zeta^{-2}\cos^2\theta\right)\right]$	$-\frac{1-\nu}{2}(1+\alpha)$	$-\frac{1}{1200}\le\alpha\le 0$	
TTS-V3	$-\frac{1-\nu}{2}$	-	-	

Coefficient d_9				
Theory	Expression	Numeric evaluation of negligible terms		Proposed simplification
		Compact Exp.	Range of Negligible terms	
TTS-V2	$-\frac{1}{R}\left(\frac{1-\nu}{2}\right)\gamma\zeta^{-1}\sin\theta\times\left[1-\kappa\left(2-\gamma\zeta^{-1}\cos\theta\right)\right]$	$-\frac{1}{R}\left(\frac{1-\nu}{2}\right)\gamma\zeta^{-1}\times\sin\theta(1+\alpha)$	$-\frac{1}{1600}\le\alpha\le-\frac{1}{2880}$	$-\frac{1}{R}\left(\frac{1-\nu}{2}\right)\gamma\zeta^{-1}\sin\theta$
Sanders	$-\frac{1}{R}\left(\frac{1-\nu}{2}\right)\gamma\zeta^{-1}\sin\theta\times\left[1-\kappa\left(\frac{3}{4}-\frac{5}{2}\gamma\zeta^{-1}\cos\theta+\frac{3}{4}\gamma^2\zeta^{-2}\cos^2\theta\right)\right]$	$-\frac{1}{R}\left(\frac{1-\nu}{2}\right)\gamma\zeta^{-1}\times\sin\theta(1+\alpha)$	$-\frac{1}{1200}\le\alpha\le 0$	
TTS-V3	$-\frac{1}{R}\left(\frac{1-\nu}{2}\right)\gamma\zeta^{-1}\sin\theta$	-	-	

Coefficient d_{10}				
Theory	Expression	Numeric evaluation of negligible terms		Proposed simplification
		Compact Exp.	Range of Negligible terms	
TTS-V2	$-\frac{1-\nu}{2}\zeta^{-1}\left(1-3\kappa\gamma\zeta^{-1}\cos\theta\right)$	$-\frac{1-\nu}{2}\zeta^{-1}(1+\alpha)$	$-\frac{1}{4800}\le\alpha\le\frac{1}{1600}$	$-\frac{1-\nu}{2}\zeta^{-1}$
Sanders	$-\frac{1-\nu}{2}\zeta^{-1}\left[1+\kappa\left(\frac{9}{4}-\frac{3}{2}\gamma\zeta^{-1}\cos\theta+\frac{1}{4}\gamma^2\zeta^{-2}\cos^2\theta\right)\right]$	$-\frac{1-\nu}{2}\zeta^{-1}(1+\alpha)$	$\frac{1}{2700}\le\alpha\le\frac{1}{1200}$	
TTS-V3	$-\frac{1-\nu}{2}\zeta^{-1}$	-	-	

Table 6.7 - Comparison of d_i coefficients in various toroidal thin shell theories (continued)

Coefficient d_{11}				
Theory	Expression	Numeric evaluation of negligible terms		Proposed simplification
		Compact Exp.	Range of Negligible terms	
TTS-V2	$R\frac{1-\nu}{2}\kappa\zeta^{-1}\left(3-\gamma\zeta^{-1}\cos\theta\right)$	-	-	$R\frac{1-\nu}{2}\kappa\zeta^{-1}\left(3-\gamma\zeta^{-1}\cos\theta\right)$
Sanders	$R\frac{1-\nu}{2}\kappa\zeta^{-1}\left(3-\gamma\zeta^{-1}\cos\theta\right)$	-	-	
TTS-V3	0	-	-	

Coefficient d_{12}				
Theory	Expression	Numeric evaluation of negligible terms		Proposed simplification
		Compact Exp.	Range of Negligible terms	
TTS-V2	$\frac{1-\nu}{2}\kappa\gamma\zeta^{-2}\sin\theta\left(3-\gamma\zeta^{-1}\cos\theta\right)$	-	-	$\frac{1-\nu}{2}\kappa\gamma\zeta^{-2}\sin\theta\left(3-\gamma\zeta^{-1}\cos\theta\right)$
Sanders	$\frac{1-\nu}{2}\kappa\gamma\zeta^{-2}\sin\theta\left(3-\gamma\zeta^{-1}\cos\theta\right)$	-	-	
TTS-V3	$-\frac{1-\nu}{2}\kappa\gamma\zeta^{-3}\sin\theta$	-	-	

Coefficient d_{13}				
Theory	Expression	Numeric evaluation of negligible terms		Proposed simplification
		Compact Exp.	Range of Negligible terms	
TTS-V2	$-R\kappa\zeta^{-2}$	-	-	$-R\kappa\zeta^{-2}$
Sanders	0	-	-	
TTS-V3	0	-	-	

Table 6.7 - Comparison of d_i coefficients in various toroidal thin shell theories (continued)

Coefficient d_{14}				
Theory	Expression	Numeric evaluation of negligible terms		Proposed simplification
		Compact Exp.	Range of Negligible terms	
TTS-V2	$R\frac{1-\nu}{2}\kappa\left(1-3\gamma\zeta^{-1}\cos\theta\right)$	-	-	$R\frac{1-\nu}{2}\kappa\left(1-3\gamma\zeta^{-1}\cos\theta\right)$
Sanders	$R\frac{1-\nu}{2}\kappa\left(1-3\gamma\zeta^{-1}\cos\theta\right)\times\frac{1}{2}$	-	-	
TTS-V3	0	-	-	

Coefficient d_{15}				
Theory	Expression	Numeric evaluation of negligible terms		Proposed simplification
		Compact Exp.	Range of Negligible terms	
TTS-V2	$3\frac{1-\nu}{2}\kappa\gamma\zeta^{-1}\sin\theta\times\left(1-\gamma\zeta^{-1}\cos\theta\right)$	-	-	$3\frac{1-\nu}{2}\kappa\gamma\zeta^{-1}\sin\theta\left(1-\gamma\zeta^{-1}\cos\theta\right)$
Sanders	$3\frac{1-\nu}{2}\kappa\gamma\zeta^{-1}\sin\theta\times\left[\frac{1}{3}+\frac{1}{3}\zeta^{-3}\left(1-3\gamma^2\cos^2\theta-2\gamma^3\cos^3\theta\right)\right]$	-	-	
TTS-V3	$3(1-\nu)\kappa\gamma\zeta^{-1}\sin\theta$	-	-	

Although, the uncommon parts in TTS-V2, TTS-V3 and Sanders have significantly different expressions, Figure 6.2 shows that they have the same trend.

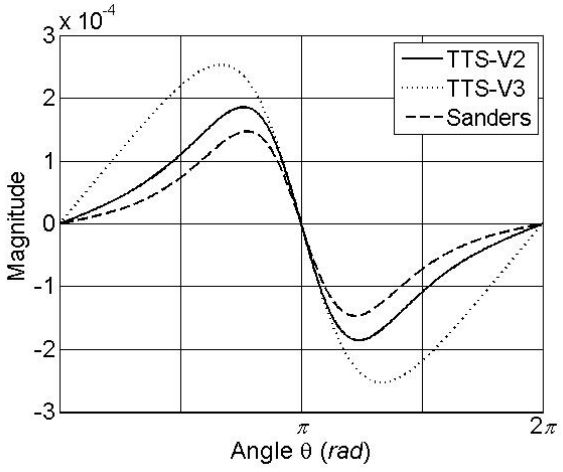

Figure 6.2 – Comparing coefficient d_{15} from various theories

Table 6.7 - Comparison of d_i coefficients in various toroidal thin shell theories (continued)

Coefficient d_{16}				
Theory	Expression	Numeric evaluation of negligible terms		Proposed simplification
		Compact Exp.	Range of negligible terms	
TTS-V2	$\frac{1}{R}\frac{1-\nu}{2}\kappa\gamma\zeta^{-1}\left[\cos\theta+3\gamma\zeta^{-1}\left(\sin^2\theta-\cos^2\theta-\gamma\zeta^{-1}\sin^2\theta\cos\theta\right)\right]$	-	-	$\frac{1}{R}\frac{1-\nu}{2}\kappa\gamma\zeta^{-1}\left[\cos\theta+3\gamma\zeta^{-1}\left(\sin^2\theta-\cos^2\theta-\gamma\zeta^{-1}\sin^2\theta\cos\theta\right)\right]$
Sanders	$\frac{1}{R}\frac{1-\nu}{2}\kappa\gamma\zeta^{-1}\left[\cos\theta+3\gamma\zeta^{-1}\left(\sin^2\theta-\cos^2\theta-\gamma\zeta^{-1}\sin^2\theta\cos\theta\right)\right]$	-	-	
TTS-V3	$\frac{1}{R}(1-\nu)\kappa\gamma\zeta^{-3}\left(2\gamma+2\cos\theta+\gamma\sin^2\theta\right)$	-	-	

Table 6.7 - Comparison of d_i coefficients in various toroidal thin shell theories (continued)

Coefficient d_{17}				
Theory	Expression	Numeric evaluation of negligible terms		Proposed simplification
		Compact Exp.	Range of negligible terms	
TTS-V2	$-R\kappa\zeta^{-1}\left(\frac{3-\nu}{2}-\frac{1-\nu}{2}\gamma\zeta^{-1}\cos\theta\right)$	-	-	$-R\kappa\zeta^{-1}\left(\frac{3-\nu}{2}-\frac{1-\nu}{2}\gamma\zeta^{-1}\cos\theta\right)$
Sanders	$-R\frac{1-\nu}{2}\kappa\zeta^{-1}\left(\frac{3}{2}-\frac{1}{2}\gamma\zeta^{-1}\cos\theta\right)$	-	-	
TTS-V3	0	-	-	

Although, the expressions from TTS-V2 and Sanders are different, Figure 6.3 shows that they have the same trend with a shift.

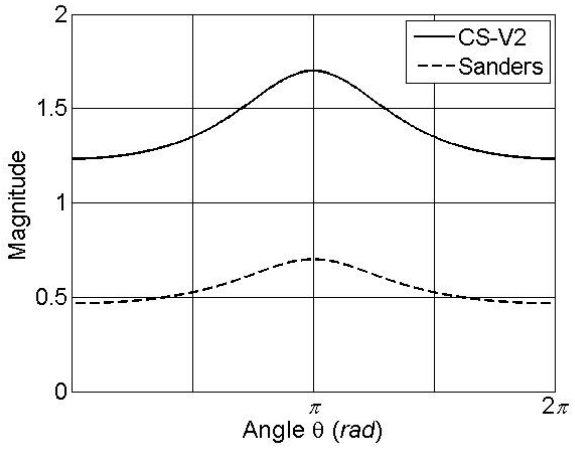

Figure 6.3 - Comparing coefficient d_{17} from various theories

Coefficient d_{18}				
Theory	Expression	Numeric evaluation of negligible terms		Proposed simplification
		Compact Exp.	Range of negligible terms	
TTS-V2	$\kappa\gamma\zeta^{-2}\sin\theta\left(1+\frac{1+\nu}{2}\zeta^{-1}\right)$	-	-	$\kappa\gamma\zeta^{-2}\sin\theta\left(1+\frac{1+\nu}{2}\zeta^{-1}\right)$
Sanders	$\frac{1-\nu}{2}\kappa\gamma\zeta^{-2}\sin\theta\left(1+\zeta^{-1}\right)$	-	-	
TTS-V3	0	-	-	

Table 6.7 - Comparison of d_i coefficients in various toroidal thin shell theories (continued)

Coefficient d_{19}				
Theory	Expression	Numeric evaluation of negligible terms		Proposed simplification
		Compact Exp.	Range of Negligible terms	
TTS-V2	$R^2\kappa\zeta^{-3}$	-	-	$R^2\kappa\zeta^{-3}$
Sanders	0	-	-	
TTS-V3	$R^2\kappa\zeta^{-3}$	-	-	

Coefficient d_{20}				
Theory	Expression	Numeric evaluation of negligible terms		Proposed simplification
		Compact Exp.	Range of negligible terms	
TTS-V2	$R^2\left(2-\nu\right)\kappa\zeta^{-1}$	-	-	$R^2\left(2-\nu\right)\kappa\zeta^{-1}$
Sanders	$R^2\left(1-\nu\right)\kappa\zeta^{-1}$	-	-	
TTS-V3	$R^2\left(2-\nu\right)\kappa\zeta^{-1}$	-	-	

Coefficient d_{21}				
Theory	Expression	Numeric evaluation of negligible terms		Proposed simplification
		Compact Exp.	Range of Negligible terms	
TTS-V2	$R\left(1-2\nu\right)\kappa\gamma\zeta^{-2}\sin\theta$	-	-	$R\left(1-2\nu\right)\kappa\gamma\zeta^{-2}\sin\theta$
Sanders	$R\left(2-2\nu\right)\kappa\gamma\zeta^{-2}\sin\theta$	-	-	
TTS-V3	$R\left(1-2\nu\right)\kappa\gamma\zeta^{-2}\sin\theta$	-	-	

Table 6.7 - Comparison of d_i coefficients in various toroidal thin shell theories (continued)

Coefficient d_{22}				
Theory	Expression	Numeric evaluation of negligible terms		Proposed simplification
		Compact Exp.	Range of Negligible terms	
TTS-V2	$2(1-\nu)\kappa\gamma\zeta^{-3}\times\left(\gamma+\frac{1-2\nu}{2-2\nu}\cos\theta\right)$	-	-	$2(1-\nu)\kappa\gamma\zeta^{-3}\left(\gamma+\frac{1-2\nu}{2-2\nu}\cos\theta\right)$
Sanders	$2(1-\nu)\kappa\gamma\zeta^{-3}\times\left(\gamma+\frac{1}{2}\cos\theta-\frac{1}{2}\gamma\cos^2\theta\right)$	-	-	
TTS-V3	$2(1-\nu)\kappa\gamma\zeta^{-3}\times(\gamma+\cos\theta)$	-	-	

Coefficient d_{23}				
Theory	Expression	Numeric evaluation of negligible terms		Proposed simplification
		Compact Exp.	Range of negligible terms	
TTS-V2	$R\kappa\zeta^{-2}$	-	-	$R\kappa\zeta^{-2}$
Sanders	$R\kappa\zeta^{-2}(\gamma\cos\theta)$	-	-	
TTS-V3	0	-	-	

Coefficient d_{24}				
Theory	Expression	Numeric evaluation of negligible terms		Proposed simplification
		Compact Exp.	Range of Negligible terms	
TTS-V2	$R\nu\kappa\zeta^{-1}$	-	-	$R\nu\kappa\zeta^{-1}$
Sanders	$R\nu\kappa$	-	-	
TTS-V3	0	-	-	

Coefficient d_{25}				
Theory	Expression	Numeric evaluation of negligible terms		Proposed simplification
		Compact Exp.	Range of Negligible terms	
TTS-V2	$-\kappa\gamma\zeta^{-2}\sin\theta\left(2-\gamma\zeta^{-1}\cos\theta\right)$	-	-	$-\kappa\gamma\zeta^{-2}\sin\theta\left(2-\gamma\zeta^{-1}\cos\theta\right)$
Sanders	$-\kappa\gamma\zeta^{-1}\sin\theta$	-	-	
TTS-V3	0	-	-	

Table 6.7 - Comparison of d_i coefficients in various toroidal thin shell theories (continued)

Coefficient d_{26}				
Theory	Expression	Numeric evaluation of negligible terms		Proposed simplification
		Compact Exp.	Range of negligible terms	
TTS-V2	$-R^2\kappa\zeta^{-3}$	-	-	$-R^2\kappa\zeta^{-3}$
Sanders	$-R^2\kappa\zeta^{-2}$	-	-	
TTS-V3	$-R^2\kappa\zeta^{-3}$	-	-	

Coefficient d_{27}				
Theory	Expression	Numeric evaluation of negligible terms		Proposed simplification
		Compact Exp.	Range of Negligible terms	
TTS-V2	$-R^2\nu\kappa\zeta^{-1}$	-	-	$-R^2\nu\kappa\zeta^{-1}$
Sanders	$-R^2\nu\kappa$	-	-	
TTS-V3	$-R^2\nu\kappa\zeta^{-1}$	-	-	

Coefficient d_{28}				
Theory	Expression	Numeric evaluation of negligible terms		Proposed simplification
		Compact Exp.	Range of Negligible terms	
TTS-V2	$R\kappa\gamma\zeta^{-2}\sin\theta$	-	-	$R\kappa\gamma\zeta^{-2}\sin\theta$
Sanders	$R\kappa\gamma\zeta^{-1}\sin\theta$	-	-	
TTS-V3	$R\kappa\gamma\zeta^{-2}\sin\theta$	-	-	

Coefficient d_{29}				
Theory	Expression	Numeric evaluation of negligible terms		Proposed simplification
		Compact Exp.	Range of Negligible terms	
TTS-V2	$\kappa\gamma\zeta^{-2}\cos\theta\left(1-\gamma\zeta^{-1}\cos\theta\right)$	-	-	$\kappa\gamma\zeta^{-2}\cos\theta\left(1-\gamma\zeta^{-1}\cos\theta\right)$
Sanders	0	-	-	
TTS-V3	0	-	-	

Table 6.8 – Comparison of l_i^I coefficients in various toroidal thin shell theories

Coefficient l_4^I				
Theory	Expression	Numeric evaluation of negligible terms		Proposed simplification
		Compact Exp.	Range of Negligible terms	
TTS-V2	$-\frac{1-\nu^2}{E}\rho\{1+(3+\kappa)\gamma\cos\theta + (3+2\kappa)\gamma^2\cos^2\theta+(1+\kappa)\gamma^3\cos^3\theta\}$	-	-	$-\frac{1-\nu^2}{E}\rho\zeta^3$
TTS-V3	$-\frac{1-\nu^2}{E}\rho\zeta^3$	-	-	

Coefficient l_{16}^I				
Theory	Expression	Numeric evaluation of negligible terms		Proposed simplification
		Compact Exp.	Range of Negligible terms	
TTS-V2	$-\frac{1-\nu^2}{E}\rho\zeta\left(1+3\kappa\gamma\zeta^{-1}\cos\theta\right)$	$-\frac{1-\nu^2}{E}\rho\zeta(1+\alpha)$	$-\frac{1}{1600}\le\alpha\le\frac{1}{4800}$	$-\frac{1-\nu^2}{E}\rho\zeta$
TTS-V3	$-\frac{1-\nu^2}{E}\rho\zeta$	-	-	

Coefficient l_{41}^I				
Theory	Expression	Numeric evaluation of negligible terms		Proposed simplification
		Compact Exp.	Range of Negligible terms	
TTS-V2	$-\frac{1-\nu^2}{E}\rho\zeta(1+\kappa\gamma\cos\theta)$	$-\frac{1-\nu^2}{E}\rho\zeta(1+\alpha)$	$-\frac{1}{9600}\le\alpha\le\frac{1}{9600}$	$-\frac{1-\nu^2}{E}\rho\zeta$
TTS-V3	$-\frac{1-\nu^2}{E}\rho\zeta$	-	-	

Chapter 7

Finite Element Formulation for Toroidal Thin Shells

7.1 Abstract

Using the generalized thin shell theory developed in Chapter 6, the governing field equations and corresponding boundary conditions of the toroidal thin shells is expressed in the variational form of the Hamiltonian of the system. The method of separation of variables in conjunction with the Fourier expansion of the unknown displacement fields and applied forces with respect to circumferential coordinate is used to formulate the ordinary differential equations of the system in terms of longitudinal coordinate. A set of exact shape functions is developed based on the exact solution of the field equations of the system and led to formulation of a quasi-exact toroidal finite element. Numerical results are compared with those based on conventional finite element methods.

7.2 Introduction

Toroidal shells are commonly used as elbow piping components in petrochemical refineries and power plants. Due to their relatively complex geometry, they exhibit more complex behaviours than straight pipes. Within this context, this chapter aims at developing a toroidal finite element that accurately captures membrane and flexural effects for these segments which is compatible with the cylindrical element developed in Chapter 5 for straight

segments. The combination of both toroidal and cylindrical finite elements should provide the necessary tool to analyze most piping systems with much fewer degrees of freedom compared to conventional finite element methods.

7.3 Literature Review

Mackerle [7.1]-[7.4] provided a comprehensive literature review on the general field of finite element formulations for pressure vessels and piping in four consequent papers. Also, Qatu [7.5]-[7.6] collected a summary of recent research advances on the dynamic behaviour of Shells. The following review focuses on shell based curved pipe finite elements and analytical solutions relevant to the present work. In general, various studies have used different interpolation schemes for the variation of the displacement fields in the longitudinal directions and a number of harmonic modes in the circumferential direction.

Based on the principle of virtual work, Ohtsubo and Watanabe [7.7] developed a ring element for small strains for torus elements. Displacement components are interpolated by Hermitian polynomials along the elbow. Their model captures both ovalization and warping effects. Takeda et al. [7.8] modified the work of Ohtsubo and Watanabe [7.7] by including the transverse shear effects in their formulation and adopting 2D Lagrangian bilinear functions to interpolate the circumferential, radial displacements, and rotations. The longitudinal displacement is interpolated using Fourier series in the circumferential direction and linear functions in the longitudinal direction.

Bathe and Almeida [7.9] developed a four node elbow finite element for in-plane flexure analysis. Based on a Lagrangian cubic interpolation of the displacement fields, their model captured circumferential shear deformation and ovalization effects and neglectesd warping

effects. They extended their model to investigate interaction effects between elbow elements and straight pipe segments [7.10]. Also, they added geometric non-linear effects to the formulation [7.11]. Militello and Huespe [7.12] extended the model by Bathe and Almeida [7.9] to capture warping deformations by adopting a Lagrangian cubic interpolation for the longitudinal displacement. The tangential and radial displacements were interpolated using harmonic functions. Abo-Elkhier [7.13] generalized the model by Bathe and Almeida [7.9] by adopting more complete displacement-strain relations into the formulation.

Zhang and Redekop [7.14] developed an analytical displacement-based solution for a simply supported toroidal shell using Sanders linear shell theory. A double Fourier expansion series, modified for simply supported boundary conditions, is used in the meridional and longitudinal directions.

In a ring formulation, Melo and Castro [7.15] used a simple linear interpolation for displacements which captures both in-plane and out-of-plane flexure of curved pipes. Yan et al. [7.16] developed an element for elasto-plastic limit load of pipe elbows by relaxing the pipe inextensibility assumption in the radial direction adopted in the model by Militello and Huespe [7.12]. They used cubic Lagrangian interpolation for the longitudinal displacement and Hermitian polynomials for the tangential and radial displacements.

Based on the work of Melo and Castro [7.15], Fonseca et al. [7.17] presented a semi-analytical formulation by using Fourier trigonometric series in circumferential direction for the problem of pure bending in curved pipes. The system of differential equations was numerically solved.

Karamanos [7.18] formulated an element to model buckling instability of pipes. Subsequent extension of the model involved adding plasticity and internal pressure effects (Karamanos et al. [7.19]). Carneiro et al. [7.20] developed a semi-analytic finite ring element to study the natural frequencies and associated eigenmodes of a pipe elbow with end flanges or tangent terminations. They used Fourier expansions along the meridional direction combined with linear polynomials along the longitudinal direction. The model is based on a Reissner-Mindlin two node beam element on which superimposed are the shell distortion displacements including ovalization and warping. The study involved an experimental.

Redekop and Chang [7.21] studied the linear vibration of mitred and smooth pipe bends and their cylindrical and toroidal shell components using differential quadrature method based on classical shell theory.

7.4 Assumptions

The main assumptions of the formulation are:

- A straight fibre normal to the shell mid-surface before deformation remains straight, un-stretched and normal to the mid-surface throughout deformation.
- All displacements are small compared to the radius of curvature of the middle surface.
- Normal stresses perpendicular to the middle surface are negligible compared to the in-plane stresses.
- The through thickness shear strains are negligible.
- Material is elastic isotropic.

- Only the steady state response is sought

- $\zeta^{-i} \simeq \sum_{j=0}^{5} R_{ij} \cos(j\theta) \qquad ; i = 1,2,3$

7.5 Hamilton's Principle for Toroidal Thin Shells

Recalling the variational form of the Hamiltonian functional of the system developed in Chapter 6 (Eq. 6.21), one has

$$\delta\Pi = \left[\left[\int_0^{2\pi R} \left(\begin{array}{l} \left\langle \delta u(x,s) \;\; \delta v(x,s) \;\; \delta w(x,s) \;\; \delta w_{,1}(x,s) \right\rangle \\ \quad \times \left(\left[\begin{array}{c|c|c} D_{11} & D_{12} & D_{13} \\ \hline D_{21} & D_{22} & D_{23} \\ \hline D_{31} & D_{32} & D_{33} \\ \hline D_{41} & D_{42} & D_{43} \end{array}\right] \left\{\begin{array}{c} u(x,s) \\ v(x,s) \\ w(x,s) \end{array}\right\} + \left\{\begin{array}{c} 0 \\ 0 \\ F_{BC}^{w} \\ 0 \end{array}\right\} \right) \end{array} \right) ds \right]\right]_0^L \right.$$

$$+ \int_0^L \int_0^{2\pi R} \left(\begin{array}{l} \left\langle \delta u(x,s) \;\; \delta v(x,s) \;\; \delta w(x,s) \right\rangle \\ \quad \times \left(\left[\begin{array}{c|c|c} L_{11} & L_{12} & L_{13} \\ \hline L_{21} & L_{22} & L_{23} \\ \hline L_{31} & L_{32} & L_{33} \end{array}\right] \left\{\begin{array}{c} u(x,s) \\ v(x,s) \\ w(x,s) \end{array}\right\} + \left\{\begin{array}{c} F_{FE}^{u} \\ F_{FE}^{v} \\ F_{FE}^{w} \end{array}\right\} \right) \end{array} \right) ds dx = 0 \tag{7.1}$$

where the differential operators D_{ij} in boundary condition equations are

$$\begin{aligned} D_{11} &= d_1 \frac{\partial}{\partial x} \\ D_{12} &= d_2 \frac{\partial}{\partial s} + d_3 \\ D_{13} &= d_4 \frac{\partial^2}{\partial x^2} + d_5 \frac{\partial^2}{\partial s^2} + d_6 \frac{\partial}{\partial s} + d_7 \end{aligned} \tag{7.2}$$

$$\begin{aligned} D_{21} &= d_8 \frac{\partial}{\partial s} + d_9 \\ D_{22} &= d_{10} \frac{\partial}{\partial x} \\ D_{23} &= d_{11} \frac{\partial^2}{\partial x \partial s} + d_{12} \frac{\partial}{\partial x} \end{aligned} \tag{7.3}$$

$$
\begin{aligned}
D_{31} &= d_{13}\frac{\partial^2}{\partial x^2} + d_{14}\frac{\partial^2}{\partial s^2} + d_{15}\frac{\partial}{\partial s} + \left(d_{16} + d_{16}^I \frac{\partial^2}{\partial t^2} \right) \\
D_{32} &= d_{17}\frac{\partial^2}{\partial x \partial s} + d_{18}\frac{\partial}{\partial x} \\
D_{33} &= d_{19}\frac{\partial^3}{\partial x^3} + d_{20}\frac{\partial^3}{\partial x \partial s^2} + d_{21}\frac{\partial^2}{\partial x \partial s} + \left(d_{22} + d_{22}^I \frac{\partial^2}{\partial t^2} \right)\frac{\partial}{\partial x}
\end{aligned}
\tag{7.4}
$$

$$
\begin{aligned}
D_{41} &= d_{23}\frac{\partial}{\partial x} \\
D_{42} &= d_{24}\frac{\partial}{\partial s} + d_{25} \\
D_{43} &= d_{26}\frac{\partial^2}{\partial x^2} + d_{27}\frac{\partial^2}{\partial s^2} + d_{28}\frac{\partial}{\partial s} + d_{29}
\end{aligned}
\tag{7.5}
$$

and the differential operators L_{ij} in the field equations are

$$
\begin{aligned}
L_{11} &= l_1\frac{\partial^2}{\partial x^2} + l_2\frac{\partial^2}{\partial s^2} + l_3\frac{\partial}{\partial s} + \left(l_4 + l_4^I \frac{\partial^2}{\partial t^2} \right) \\
L_{12} &= l_5\frac{\partial^2}{\partial x \partial s} + l_6\frac{\partial}{\partial x} \\
L_{13} &= l_7\frac{\partial^3}{\partial x^3} + l_8\frac{\partial^3}{\partial x \partial s^2} + l_9\frac{\partial^2}{\partial x \partial s} + \left(l_{10} + l_{10}^I \frac{\partial^2}{\partial t^2} \right)\frac{\partial}{\partial x}
\end{aligned}
\tag{7.6}
$$

$$
\begin{aligned}
L_{21} &= l_{11}\frac{\partial^2}{\partial x \partial s} + l_{12}\frac{\partial}{\partial x} \\
L_{22} &= l_{13}\frac{\partial^2}{\partial x^2} + l_{14}\frac{\partial^2}{\partial s^2} + l_{15}\frac{\partial}{\partial s} + \left(l_{16} + l_{16}^I \frac{\partial^2}{\partial t^2} \right) \\
L_{23} &= l_{17}\frac{\partial^3}{\partial s^3} + l_{18}\frac{\partial^3}{\partial x^2 \partial s} + l_{19}\frac{\partial^2}{\partial x^2} + l_{20}\frac{\partial^2}{\partial s^2} + \left(l_{21} + l_{21}^I \frac{\partial^2}{\partial t^2} \right)\frac{\partial}{\partial s} + l_{22}
\end{aligned}
\tag{7.7}
$$

$$
\begin{aligned}
L_{31} &= l_{23}\frac{\partial^3}{\partial x^3} + l_{24}\frac{\partial^3}{\partial x \partial s^2} + l_{25}\frac{\partial^2}{\partial x \partial s} + \left(l_{26} + l_{26}^I \frac{\partial^2}{\partial t^2} \right)\frac{\partial}{\partial x} \\
L_{32} &= l_{27}\frac{\partial^3}{\partial s^3} + l_{28}\frac{\partial^3}{\partial x^2 \partial s} + l_{29}\frac{\partial^2}{\partial x^2} + l_{30}\frac{\partial^2}{\partial s^2} + \left(l_{31} + l_{31}^I \frac{\partial^2}{\partial t^2} \right)\frac{\partial}{\partial s} + \left(l_{32} + l_{32}^I \frac{\partial^2}{\partial t^2} \right) \\
L_{33} &= l_{33}\frac{\partial^4}{\partial x^4} + l_{34}\frac{\partial^4}{\partial s^4} + l_{35}\frac{\partial^4}{\partial x^2 \partial s^2} + l_{36}\frac{\partial^3}{\partial s^3} + l_{37}\frac{\partial^3}{\partial x^2 \partial s} + \left(l_{38} + l_{38}^I \frac{\partial^2}{\partial t^2} \right)\frac{\partial^2}{\partial x^2} \\
&\quad + \left(l_{39} + l_{39}^I \frac{\partial^2}{\partial t^2} \right)\frac{\partial^2}{\partial s^2} + \left(l_{40} + l_{40}^I \frac{\partial^2}{\partial t^2} \right)\frac{\partial}{\partial s} + \left(l_{41} + l_{41}^I \frac{\partial^2}{\partial t^2} \right)
\end{aligned}
\tag{7.8}
$$

The generic force terms F_{BC}^w, F_{FE}^u, F_{FE}^v and F_{FE}^w are defined as

$$
\begin{aligned}
F_{BC}^{w} &= f_1^F f_1^{xw} + f_2^F f_2^{xw} \\
F_{FE}^{u} &= f_3^F f_1^{xu} + f_4^F f_2^{xu} \\
F_{FE}^{v} &= f_5^F f_1^{sv} + f_6^F f_2^{sv} \\
F_{FE}^{w} &= f_7^F f_1^{zw} + f_8^F f_2^{zw} + f_9^F \frac{\partial}{\partial x} f_1^{xw} + f_{10}^F \frac{\partial}{\partial x} f_2^{xw} + \left(f_{11}^F \frac{\partial}{\partial s} + f_{12}^F \right) f_1^{sw} + f_{13}^F \frac{\partial}{\partial s} f_2^{sw}
\end{aligned}
\tag{7.9}
$$

Coefficients d_i, d_i^I, l_i, l_i^I, f_i^F, which are functions of circumferential coordinate θ $(= s/R)$, and forces f_1^{xu}, f_2^{xu}, f_1^{sv}, f_2^{sv}, f_1^{zw}, f_2^{zw}, f_1^{xw}, f_2^{xw}, f_1^{sw} and f_2^{sw} are based on the TTS-V2 theory developed in Chapter 6 and are provided in Appendix 7.A .

7.6 Overview of the Formulation

Knowing that the steady-state response of the structure is harmonic allows the elimination of the time dependency of the response by integrating over the variational Hamiltonian of the system (Eq. 7.1) with respect to time t. Also, using the orthogonal properties of the trigonometric functions allows us to eliminate the dependency of the response on the circumferential coordinate s. However, it is noted that the curvature of the torus significantly increases the complexity of the differential equations of the system in two respects: a) It significantly increases the number of the terms involved and b) The coefficients of the governing equations become no longer constant and consist of trigonometric functions of the circumferential coordinate θ $(= s/R)$. The combination of these two complexities makes the integration with respect to θ difficult. These difficulties and proposed solutions are detailed in the subsections 7.6.1 through 7.6.4 .

7.6.1 Displacement Function Expressions

Similar to CCTSs, the method of separation of variables is used. Since only the steady-state response of the structure is sought, the applied body forces are assumed to take the form

$$\bar{p}^x(x,s,z,t)=\sum_{n=-\infty}^{+\infty}\bar{p}_n^x(x,z)e^{ins/R}e^{i\bar{\omega}t}$$
$$\bar{p}^s(x,s,z,t)=\sum_{n=-\infty}^{+\infty}\bar{p}_n^s(x,z)e^{ins/R}e^{i\bar{\omega}t} \qquad (7.10a\text{-}c)$$
$$\bar{p}^z(x,s,z,t)=\sum_{n=-\infty}^{+\infty}\bar{p}_n^z(x,z)e^{ins/R}e^{i\bar{\omega}t}$$

Subsequently, unknown mid-surface displacement fields are assumed to take the form

$$\bar{u}(x,s,t)=\sum_{n=-\infty}^{+\infty}A_n(x)e^{ins/R}e^{i\bar{\omega}t}$$
$$\bar{v}(x,s,t)=\sum_{n=-\infty}^{+\infty}B_n(x)e^{ins/R}e^{i\bar{\omega}t} \qquad (7.11a\text{-}c)$$
$$\bar{w}(x,s,t)=\sum_{n=-\infty}^{+\infty}C_n(x)e^{ins/R}e^{i\bar{\omega}t}$$

7.6.2 Approximations for Coefficients Dependent on Circumferential Coordinate

One of the difficulties in the process of integration with respect to circumferential coordinate θ $(=s/R)$ is the presence of $\cos\theta$ terms in the denominator of some of the coefficients in the form of $\zeta^{-i}=1/(1+\gamma\cos\theta)^i$ $(i=1,2,3)$. This issue is treated by introducing the following approximation.

$$\zeta^{-i}=\frac{1}{(1+\gamma\cos\theta)^i}\simeq\sum_{j=0}^{5}R_{ij}\cos(j\theta) \quad , \quad R_{ij}=\int_0^{2\pi}(1+\gamma\cos\theta)^{-i}\cos(j\theta)\,d\theta \qquad (7.12a,b)$$

where, R_{ij} are constants to be determined from Eq. 7.12b. It is observed that by taking six terms ($j=0,...,5$) in Eq. 7.12 the approximation is quite accurate for the practical range of

torus geometries (i.e. $\gamma = R/\Re \le 0.5$). Function $\zeta(\theta)$ and its approximate truncated Fourier series are compared in Figure 7.1 for the worst case of $\gamma = 0.5$ and $i = 3$.

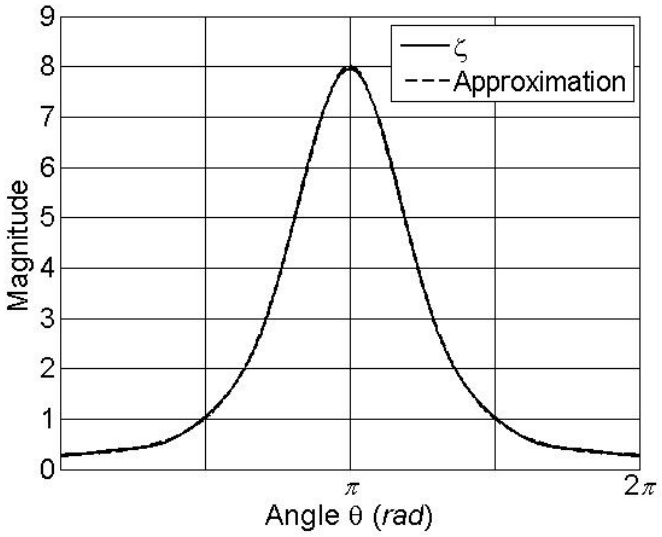

Figure 7.1 – Comparison of coefficients ζ^{-3} and corresponding approximate Fourier series

7.6.3 Truncation of Intermodal Coupling

The approximation introduced in Eq. 7.12 enables us to express all the coefficients in Eq. 7.1 in the unified generic form

$$l_i = \alpha_i \sin^p \theta \cos^q \theta \cos(j\theta) \qquad ;\begin{cases} p = 0,1,2 \\ q = 0,1,2 \\ j = 1,...,5 \end{cases} \qquad (7.13a\text{-}c)$$

in which symbols α_i represents constant values as defined in Appendix 7.A . Considering the generic expression in Eq. 7.13 for l_i coefficients and after substituting the mid-surface displacement fields as expressed in the form of the Fourier expansion series (Eq. 7.11) into Eq. 7.1, the x independent part of the coefficients in Eq. 7.1 is found to take the generic form

$$\overline{l_i} = \alpha_{in} \sin^p \theta \cos^q \theta \cos(j\theta) e^{i(n+l)\theta} \quad ; \begin{cases} p = 0,1,2 \\ q = 0,1,2 \\ j = 1,...,5 \\ n = -\infty,...,+\infty \\ l = -\infty,...,+\infty \end{cases} \tag{7.14a-c}$$

The generic expression in Eq. 7.14 shows that, depending on the values of p, q j n and l, each set of equations for each mode n is in general coupled to some other modes $m \neq n$. The coupling between modes leads to an infinite number of inter-coupled equations. Unlike the case of CCTSs, in which the set of equations related to each mode n were completely uncoupled from the other modes $m \neq n$, a similar separation is found no longer possible for toroidal thin shells. However, the farther apart modes m and n are, the less significant the coupling becomes. If modes m and n are far apart, one may assume their interdependency to be negligible. Thus, in practice this interdependency of each mode n is limited to M higher and M lower modes and any coupling with other modes beyond this range is neglected.

7.6.4 Equilibrium Condition in Terms of Longitudinal Coordinate

From Eq. 7.11 and 7.12, by substituting into Eq. 7.1 and integrating with circumferential coordinate, the dependency of the variational Hamiltonian functional on circumferential coordinate s is eliminated and one obtains

$$
\begin{aligned}
&\frac{Eh}{1-\nu^2}\sum_{n=-N}^{+N}\Bigg[\Big\langle \delta A_{-n}(x)\ \delta B_{-n}(x)\ \delta C_{-n}(x)\ \delta C'_{-n}(x)\Big\rangle_{1\times 4}\times \\
&\qquad\Big[{}^0\mathbf{H}_n+{}^1\mathbf{H}_n D+{}^2\mathbf{H}_n D^2+{}^3\mathbf{H}_n D^3\Big]_{4\times 3(2M+1)}\big\{\mathbf{\Lambda}_n\big\}_{3(2M+1)\times 1} \\
&\qquad+\delta C_{-n}(x)\sum_{j=1}^{2}\Big[\mathbf{H}_{jn}^{xw}\Big]_{1\times(2M+1)}\Big\{\mathbf{f}_{jn}^{xw}(x)\Big\}_{(2M+1)\times 1}\Bigg]_0^L \\
&+\int_0^L\frac{Eh}{1-\nu^2}\Bigg(\sum_{n=-N}^{+N}\Bigg[\Big(\Big\langle \delta A_{-n}(x)\ \delta B_{-n}(x)\ \delta C_{-n}(x)\Big\rangle_{1\times 3}\times \\
&\qquad\Big[{}^0\mathbf{G}_n+{}^1\mathbf{G}_n D+{}^2\mathbf{G}_n D^2+{}^3\mathbf{G}_n D^3+{}^4\mathbf{G}_n D^4\Big]_{3\times 3(2M+1)}\big\{\mathbf{\Lambda}_n\big\}_{3(2M+1)\times 1}\Big) \\
&\qquad+\sum_{j=1}^{2}\Bigg(\delta A_{-n}(x)\Big[\mathbf{G}_{jn}^{xu}\Big]_{1\times(2M+1)}\Big\{\mathbf{f}_{jn}^{xu}(x)\Big\}_{(2M+1)\times 1} \\
&\qquad\quad+\delta B_{-n}(x)\Big[\mathbf{G}_{jn}^{sv}\Big]_{1\times(2M+1)}\Big\{\mathbf{f}_{jn}^{sv}(x)\Big\}_{(2M+1)\times 1} \\
&\qquad\quad+\delta C_{-n}(x)\Big\langle\Big[\mathbf{G}_{jn}^{zw}\Big]_{1\times(2M+1)}\Big\{\mathbf{f}_{jn}^{zw}(x)\Big\}_{(2M+1)\times 1} \\
&\qquad\quad+\Big[\mathbf{G}_{jn}^{xw}D\Big]_{1\times(2M+1)}\Big\{\mathbf{f}_{jn}^{xw}(x)\Big\}_{(2M+1)\times 1} \\
&\qquad\quad+\Big[\mathbf{G}_{jn}^{sw}\Big]_{1\times(2M+1)}\Big\{\mathbf{f}_{jn}^{sw}(x)\Big\}_{(2M+1)\times 1}\Big\rangle\Bigg)\Bigg]\Bigg)dx=0
\end{aligned}
\tag{7.15}
$$

where

$$
\big\{\mathbf{\Lambda}_n\big\}=\begin{Bmatrix}\big\{\widehat{\mathbf{\Lambda}}_{n-M}\big\}\\ \vdots\\ \big\{\widehat{\mathbf{\Lambda}}_{n}\big\}\\ \vdots\\ \big\{\widehat{\mathbf{\Lambda}}_{n+M}\big\}\end{Bmatrix}_{3(2M+1)\times 1}\qquad;\qquad \big\{\widehat{\mathbf{\Lambda}}_n\big\}=\begin{Bmatrix}A_n(x)\\ B_n(x)\\ C_n(x)\end{Bmatrix}_{3\times 1}
\tag{7.16}
$$

and the force vector contributions are given by

$$\left(\left\{\mathbf{f}_{jn}^{xu}(x)\right\},\left\{\mathbf{f}_{jn}^{sv}(x)\right\},\left\{\mathbf{f}_{jn}^{zw}(x)\right\},\left\{\mathbf{f}_{jn}^{xw}(x)\right\},\left\{\mathbf{f}_{jn}^{sw}(x)\right\}\right)_{(2M+1)\times 5} = \tag{7.17}$$

$$\left(\begin{Bmatrix} f_{j.n-M}^{xu}(x) \\ \vdots \\ f_{j.n}^{xu}(x) \\ \vdots \\ f_{j.n+M}^{xu}(x) \end{Bmatrix},\begin{Bmatrix} f_{j.n-M}^{sv}(x) \\ \vdots \\ f_{j.n}^{sv}(x) \\ \vdots \\ f_{j.n+M}^{sv}(x) \end{Bmatrix},\begin{Bmatrix} f_{j.n-M}^{zw}(x) \\ \vdots \\ f_{j.n}^{zw}(x) \\ \vdots \\ f_{j.n+M}^{zw}(x) \end{Bmatrix},\begin{Bmatrix} f_{j.n-M}^{xw}(x) \\ \vdots \\ f_{j.n}^{xw}(x) \\ \vdots \\ f_{j.n+M}^{xw}(x) \end{Bmatrix},\begin{Bmatrix} f_{j.n-M}^{sw}(x) \\ \vdots \\ f_{j.n}^{sw}(x) \\ \vdots \\ f_{j.n+M}^{sw}(x) \end{Bmatrix}\right)_{(2M+1)\times 5}$$

In Eq. 7.15, symbol D denotes the first derivative of the argument function and symbols D^i $(i=2,3,4)$ denote the ith derivative of the argument functions with respect to x. Symbol N denotes the maximum number of higher/lower modes involved in the analysis and the exact solution is obtained as $N\to\infty$. Symbol M $(\gg 1)$ denotes the number of higher/lower modes that are considered to be coupled to a given mode n. Coefficient matrices ${}^{i}\mathbf{H}_n$ $(i=0,...,3)$, ${}^{i}\mathbf{G}_n$ $(i=0,...,4)$, $\mathbf{H}_{jn}^{xw}$, $\mathbf{G}_{jn}^{xu}$, $\mathbf{G}_{jn}^{sv}$, $\mathbf{G}_{jn}^{zw}$, $\mathbf{G}_{jn}^{xw}$ and $\mathbf{G}_{jn}^{sw}$ $j=1,2$, include all contributions to a given mode n of all M higher and M lower modes of interest in the analysis that are coupled to mode n (to be explained in the following paragraphs). Appendix 7.A provides the explicit expressions for coefficient matrices ${}^{i}\mathbf{H}_n$, ${}^{i}\mathbf{G}_n$, $\mathbf{H}_{jn}^{xw}$, $\mathbf{G}_{jn}^{xu}$, $\mathbf{G}_{jn}^{sv}$, $\mathbf{G}_{jn}^{zw}$, $\mathbf{G}_{jn}^{xw}$ and $\mathbf{G}_{jn}^{sw}$, for the case $M=7$. Expressions $f_{j.n}^{xu}(x)$, $f_{j.n}^{sv}(x)$, $f_{j.n}^{zw}(x)$, $f_{j.n}^{xw}(x)$ and $f_{j.n}^{sw}(x)$ represent the x dependent component of the nth term of the across thickness integrated traction functions $f_j^{xu}(x,s)$, $f_j^{sv}(x,s)$, $f_j^{zw}(x,s)$, $f_j^{xw}(x,s)$ and $f_j^{sw}(x,s)$ already defined in Appendix 6.A.3 .

$$f_{1.n}^{xu}=\int_{-\frac{h}{2}}^{\frac{h}{2}}\overline{p}_n^{x}\left(1+\frac{z}{R}\right)dz \qquad , \qquad f_{2.n}^{xu}=\int_{-\frac{h}{2}}^{\frac{h}{2}}\overline{p}_n^{x}z\left(1+\frac{z}{R}\right)dz$$

$$f_{1.n}^{xw} = \int_{-\frac{h}{2}}^{\frac{h}{2}} \overline{p}_n^x z\left(1+\frac{z}{R}\right)dz \quad , \quad f_{2.n}^{xw} = \int_{-\frac{h}{2}}^{\frac{h}{2}} \overline{p}_n^x z^2\left(1+\frac{z}{R}\right)dz$$

$$f_{1.n}^{sv} = \int_{-\frac{h}{2}}^{\frac{h}{2}} \overline{p}_n^s \left(1+2\frac{z}{R}\right)dz \quad , \quad f_{2.n}^{sv} = \int_{-\frac{h}{2}}^{\frac{h}{2}} \overline{p}_n^s \left(1+3\frac{z}{R}\right)dz$$

$$f_{1.n}^{sw} = \int_{-\frac{h}{2}}^{\frac{h}{2}} \overline{p}_n^s z\left(1+2\frac{z}{R}\right)dz \quad , \quad f_{2.n}^{sw} = \int_{-\frac{h}{2}}^{\frac{h}{2}} \overline{p}_n^s z\left(1+\frac{z}{R}\right)dz$$

$$f_{1.n}^{zw} = \int_{-\frac{h}{2}}^{\frac{h}{2}} \overline{p}_n^z \left(1+\frac{z}{R}\right)dz \quad , \quad f_{2.n}^{zw} = \int_{-\frac{h}{2}}^{\frac{h}{2}} \overline{p}_n^z \left(1+2\frac{z}{R}\right)dz \qquad (7.18)$$

Although the coupling of each mode n was assumed to be limited to the M higher and M lower modes, there remains an infinite number of sets of equations, yet to be solved simultaneously. In practicality, N will be a finite number. The larger N is the more accurate the solution will be. $N = 7$ is found reasonable for most practical loadings. Thus, without losing the generality of the number of modes included in the solution, the system of equations is truncated to the first N higher and N lower modes.

Numerical evaluation showed that the contribution of any mode beyond the first seven higher and the first lower modes is less than 0.1% of the maximum contribution of any other modes within the range $-M \le n \le M$. Thus, $M = 7$ is a reasonable assumption for a reliable analysis.

It is noted that, in contrast to the case of CCTSs, the number of modes to be taken should be determined a-priori. In the event the convergence attained is not satisfactory, the whole solution should be redone with more terms. Figure 7.2a schematically shows the non-zero terms of the operator matrix resulting from an uncoupled sets of ODEs resulting from a CCST while Figure 7.2b shows the non-zero terms of the operator matrix of coefficients

resulting from a coupled set of ODEs for the case of a toroidal shell. As shown in Figure 7.2, in both cases, the matrices are banded about the diagonal.

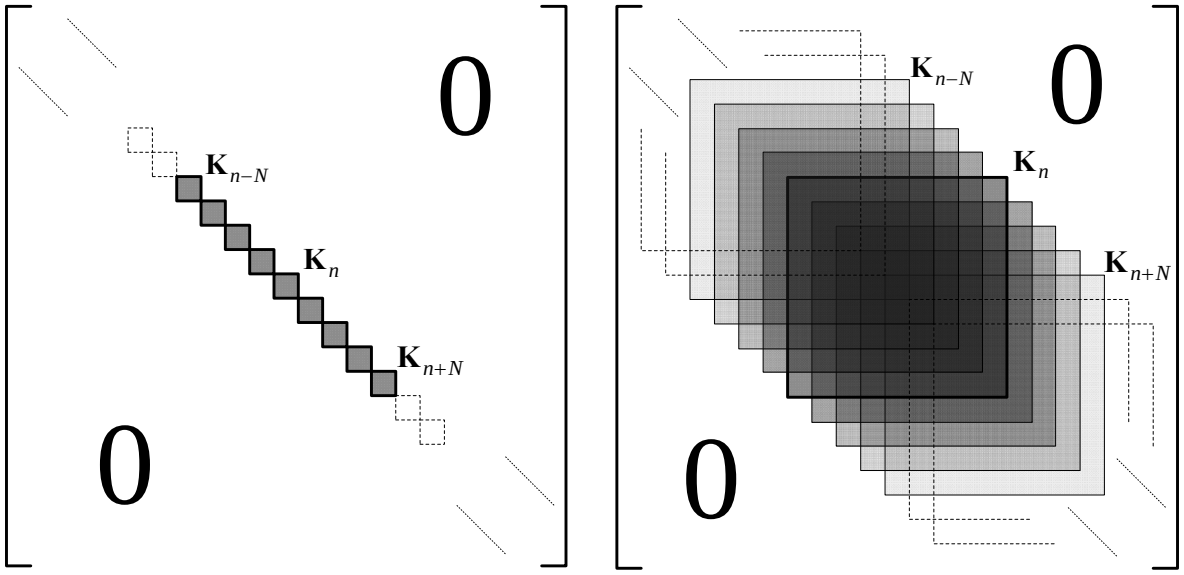

Figure 7.2 – Schematic matrices of coefficients a) Matrix of coefficients of the uncoupled system of a CCTS, b) Matrix of coefficients of the coupled system of a toroidal thin shell

7.7 Formulation of the Field Equations

The objective of this section is to express the governing field equations, given in Eq. 7.15, into a consolidated system of size $3(2N+1)\times 3(2N+2M+1)$ for the whole structure. From Eq. 7.15, the homogeneous part of the field equations yields $(2N+1)$ sets of equations for $-N \le n \le N$ in the form

$$\left[{}^{0}\mathbf{G}_n + {}^{1}\mathbf{G}_n D + {}^{2}\mathbf{G}_n D^2 + {}^{3}\mathbf{G}_n D^3 + {}^{4}\mathbf{G}_n D^4 \right]_{3\times 3(2M+1)} \{\mathbf{\Lambda}_n\}_{3(2M+1)\times 1} = \{\mathbf{0}\}_{3(2M+1)\times 1} \qquad (7.19)$$

Equations 7.19 can be consolidated into a single matrix equation in the form

$$\left[{}^{0}\overline{\mathbf{G}} + {}^{1}\overline{\mathbf{G}}\ D + {}^{2}\overline{\mathbf{G}}\ D^2 + {}^{3}\overline{\mathbf{G}}\ D^3 + {}^{4}\overline{\mathbf{G}}\ D^4 \right]_{3(2N+1)\times 3(2N+2M+1)} \left\{ \overline{\mathbf{\Lambda}} \right\}_{3(2N+2M+1)\times 1} = \left\{ \mathbf{0} \right\}_{3(2N+1)\times 1} \tag{7.20}$$

where the rectangular coefficient matrices ${}^{i}\overline{\mathbf{G}}$ $(i = 0,...,4)$ are schematically shown in Figure 7.3. Also, the unknown displacement vector $\overline{\mathbf{\Lambda}}$ is defined as

$$\left\{ \overline{\mathbf{\Lambda}} \right\} = \begin{Bmatrix} \left\{ \widehat{\mathbf{\Lambda}}_{n-2N} \right\} \\ \vdots \\ \left\{ \widehat{\mathbf{\Lambda}}_{n} \right\} \\ \vdots \\ \left\{ \widehat{\mathbf{\Lambda}}_{n+2N} \right\} \end{Bmatrix}_{3(2N+2M+1)\times 1} \tag{7.21}$$

where its constructing blocks $\widehat{\mathbf{\Lambda}}_n$ were defined in Eq. 7.16 as $\left\{ \widehat{\mathbf{\Lambda}}_n \right\}^T = \left\langle A_n(x)\ B_n(x)\ C_n(x) \right\rangle$.

Figure 7.3 schematically shows how each matrix ${}^{i}\mathbf{G}_n$ corresponding to mode n is related to those of modes $m \neq n$. Considering a certain mode $\overline{n}$, Figure 7.3 illustrates how each horizontal block ${}^{i}\mathbf{G}_n$ includes the contributions from modes $n-M$ to $n+M$ on mode n and the vertical block matrix ${}^{i}_{\mathbf{v}}\mathbf{G}_n$, defined in Appendix 7.B , includes the contributions of mode n on modes $n-M$ to $n+M$.

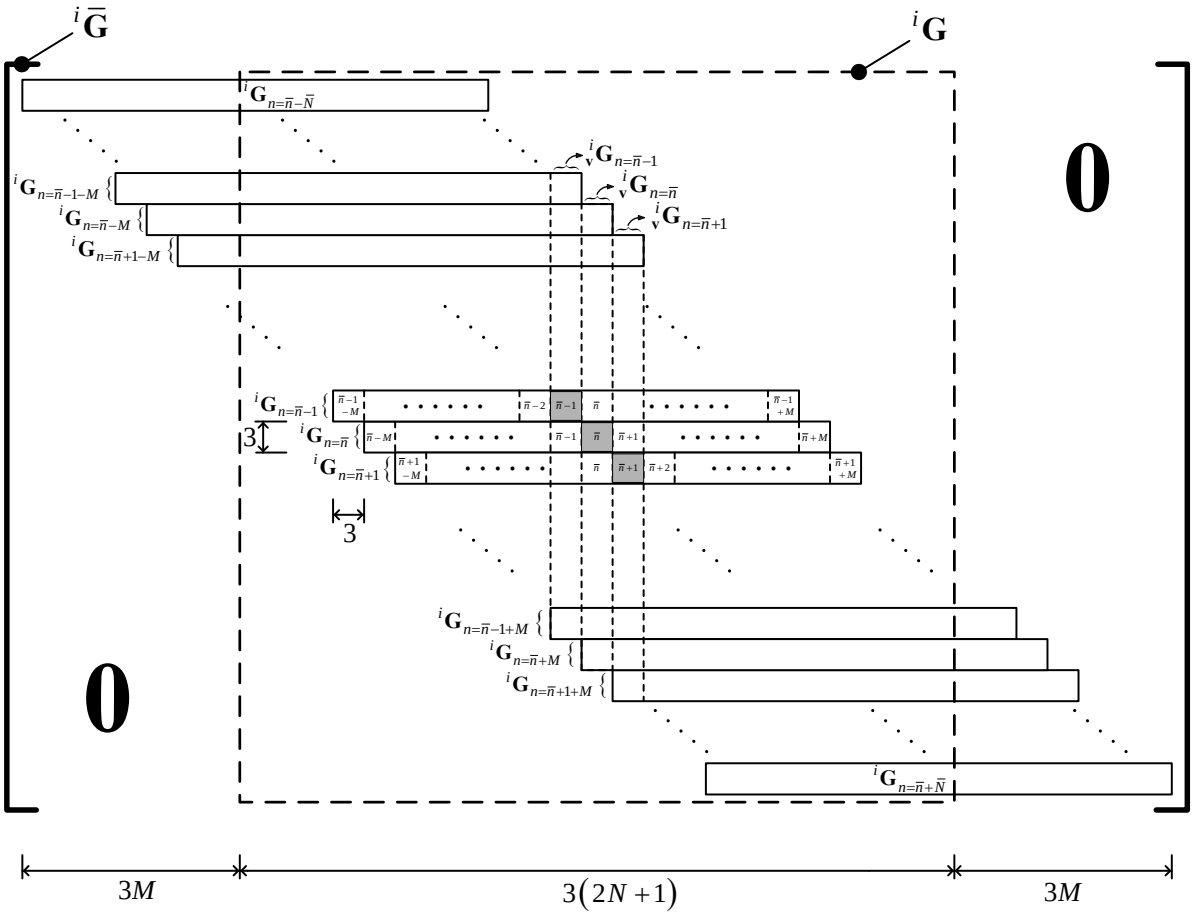

Figure 7.3 – Schematic presentation of matrices $^{i}\bar{\mathbf{G}}$ and $^{i}\mathbf{G}$ and their constructing blocks $^{i}\mathbf{G}_{n}$ and $^{i}_{\mathrm{v}}\mathbf{G}_{n}$

It is noted that all blocks can be defined in terms of a certain mode $\bar{n}$. In order to relate the horizontal block matrix $^{i}\mathbf{G}_{n}$ and the vertical block matrix $^{i}_{\mathrm{v}}\mathbf{G}_{n}$, they are partitioned into $2M+1$ blocks as

$$\left[{}^{i}\mathbf{G}_{n} \right]_{3\times 3(2M+1)} = \left[\left[{}^{i}\widehat{\mathbf{G}}_{\substack{n \\ k=-M}} \right]_{3\times 3} \cdots \left[{}^{i}\widehat{\mathbf{G}}_{\substack{n \\ k=0}} \right]_{3\times 3} \cdots \left[{}^{i}\widehat{\mathbf{G}}_{\substack{n \\ k=M}} \right]_{3\times 3} \right]$$

$$\left[{}^{i}_{\mathbf{v}}\mathbf{G}_{n} \right]_{3(2M+1)\times 3} = \begin{bmatrix} \left[{}^{i}_{\mathbf{v}}\mathbf{G}_{\substack{n \\ k=-M}} \right]_{3\times 3} \\ \vdots \\ \left[{}^{i}_{\mathbf{v}}\mathbf{G}_{\substack{n \\ k=0}} \right]_{3\times 3} \\ \vdots \\ \left[{}^{i}_{\mathbf{v}}\mathbf{G}_{\substack{n \\ k=M}} \right]_{3\times 3} \end{bmatrix} \tag{7.22a,b}$$

Considering a certain mode $\bar{n}$, square block matrices ${}^{i}\widehat{\mathbf{G}}_{\substack{n \\ k}}$ and ${}^{i}_{\mathbf{v}}\widehat{\mathbf{G}}_{\substack{n \\ k}}$ of size 3×3 are related through

$${}^{i}_{\mathbf{v}}\widehat{\mathbf{G}}_{\substack{n=\bar{n} \\ k=-\bar{k}}} = {}^{i}\widehat{\mathbf{G}}_{\substack{n=\bar{n}-\bar{k} \\ k=\bar{k}}} \tag{7.23}$$

Since the unknown displacement fields are truncated (i.e. $\langle A_n(x), B_n(x), C_n(x) \rangle = \langle 0,0,0 \rangle$ for $|n| > N$), the first $3M$ and the last $3M$ rows of the unknown displacement vector $\bar{\mathbf{\Lambda}}$ are null i.e.,

$$\left\{ \bar{\mathbf{\Lambda}} \right\} = \begin{Bmatrix} \{\mathbf{0}\}_{3M\times 1} \\ \{\mathbf{\Lambda}\}_{3(2N+1)\times 1} \\ \{\mathbf{0}\}_{3M\times 1} \end{Bmatrix}_{3(2N+2M+1)\times 1} \tag{7.24}$$

where the unknown displacement vector $\mathbf{\Lambda}$ is defined as

$$\left\{ \mathbf{\Lambda} \right\} = \begin{Bmatrix} \{\widehat{\mathbf{\Lambda}}_{n-N}\} \\ \vdots \\ \{\widehat{\mathbf{\Lambda}}_{n}\} \\ \vdots \\ \{\widehat{\mathbf{\Lambda}}_{n+N}\} \end{Bmatrix}_{3(2N+1)\times 1} \tag{7.25}$$

This makes the first $3M$ and the last $3M$ columns of operator matrix $\bar{\mathbf{G}}$ irrelevant to the solution. Thus, the system of ODEs in Eq. 7.20 is simplified to

$$\left(\left[{}^{4}\mathbf{G}\right]D^4+\left[{}^{3}\mathbf{G}\right]D^3+\left[{}^{2}\mathbf{G}\right]D^2+\left[{}^{1}\mathbf{G}\right]D+\left[{}^{0}\mathbf{G}\right]\right)_{3(2N+1)\times 3(2N+1)}\{\mathbf{\Lambda}\}_{3(2N+1)\times 1}=0 \qquad (7.26)$$

where coefficient matrices ${}^{i}\mathbf{G}$ $(i=0,...,4)$ are square of size $3(2N+1)\times 3(2N+1)$. Matrices ${}^{i}\mathbf{G}$ are obtained by truncating the first $3M$ and the last $3M$ columns of matrices ${}^{i}\bar{\mathbf{G}}$ (the area enclosed by dashed line in Figure 7.3).

7.8 Homogeneous Solution

Seeking the homogeneous solution of the system of ODEs (Eq. 7.26) in an exponential form

$$A_n(x)=A_n e^{mx} \quad , \quad B_n(x)=B_n e^{mx} \quad , \quad C_n(x)=C_n e^{mx} \qquad (7.27)$$

yields the polynomial eigenvalue problem (PEP)

$$\mathbf{\Omega}(m)\hat{A}=0 \qquad (7.28)$$

where, $\mathbf{\Omega}(m)$ is a matrix polynomial defined as

$$\mathbf{\Omega}(m)=m^4\left[{}^{4}\mathbf{G}\right]+m^3\left[{}^{3}\mathbf{G}\right]+m^2\left[{}^{2}\mathbf{G}\right]+m\left[{}^{1}\mathbf{G}\right]+\left[{}^{0}\mathbf{G}\right] \qquad (7.29)$$

It is noted that mode coupling gives rise to an $8(2N+1)th$ order characteristic equation. This eliminates the possibility of providing an analytical solution to the characteristic equation in search of its eigenvalues and corresponding eigenvectors.

The solution of the 4th order PEP of size $3(2N+1)$ can be transformed into an equivalent first order generalized eigenvalue problem (GEP) of size $12(2N+1)$ in the form

$$m\begin{bmatrix} {}^{4}\mathbf{G} & \mathbf{0} & \mathbf{0} & \mathbf{0} \\ \mathbf{0} & \mathbf{I}_n & \mathbf{0} & \mathbf{0} \\ \mathbf{0} & \mathbf{0} & \mathbf{I}_n & \mathbf{0} \\ \mathbf{0} & \mathbf{0} & \mathbf{0} & \mathbf{I}_n \end{bmatrix} + \begin{bmatrix} {}^{3}\mathbf{G} & {}^{2}\mathbf{G} & {}^{1}\mathbf{G} & {}^{0}\mathbf{G} \\ -\mathbf{I}_n & \mathbf{0} & \mathbf{0} & \mathbf{0} \\ \mathbf{0} & -\mathbf{I}_n & \mathbf{0} & \mathbf{0} \\ \mathbf{0} & \mathbf{0} & -\mathbf{I}_n & \mathbf{0} \end{bmatrix} = 0 \tag{7.30}$$

where, $\mathbf{I}_n$ denotes a $3(2N+1)\times 3(2N+1)$ identity matrix. The solution of Eq. 7.30, yields $8(2N+1)$ eigenvalues m_j ($j=1,...,8(2N+1)$) and corresponding eigenvectors $\{\tilde{\mathrm{v}}_j\}$. The j th eigenvector of the equivalent GEP is denoted $\{\tilde{\mathrm{v}}_j\}$ and the corresponding eigenvector of the original PEP is $\hat{\mathbf{A}}_\mathbf{j}$. Both vectors are related through $\{\tilde{\mathbf{v}}_j\} = \left\langle m^3\hat{\mathbf{A}}_j^T, m^2\hat{\mathbf{A}}_j^T, m\hat{\mathbf{A}}_j^T, \hat{\mathbf{A}}_j^T \right\rangle^T$. Thus, one obtains

$$\begin{aligned} A_n(x) &= \sum_{j=1}^{8(2N+1)} \tilde{A}_j \bar{A}_{nj} e^{m_j x} \\ B_n(x) &= \sum_{j=1}^{8(2N+1)} \tilde{A}_j \bar{B}_{nj} e^{m_j x} \\ C_n(x) &= \sum_{j=1}^{8(2N+1)} \tilde{A}_j \bar{C}_{nj} e^{m_j x} \end{aligned} \tag{7.31}$$

In Eq. 7.31, m_j is the jth eigenvalue of the system. Recalling the order of x dependent components of displacement fields within the displacement function vector $\mathbf{\Lambda}$ (Eq. 7.19), constants $\bar{A}_{nj}$, $\bar{B}_{nj}$ and $\bar{C}_{nj}$ are the $\left[3(N+n)+1\right]th$, $\left[3(N+n)+2\right]th$ and $\left[3(N+n)+3\right]th$ rows of the eigenvector $\hat{\mathbf{A}}_j$, respectively. Constants $\tilde{A}_j$ are unknowns to be determined from the boundary conditions of the system. It is noted that the eigenvalues and eigenvectors of the system are independent of the length of the pipe.

7.9 Finite Element Development

A complete analytical solution of the system is tedious and cumbersome. Thus, only a finite element formulation is developed. The shape functions will be based on the exact solution of the homogenous part of the field equations of the system.

7.9.1 Formulation of Shape Functions

From Eq. 7.31, by substituting into Eq. 7.11, one obtains

$$\begin{aligned}
\bar{u}(x,s) &= \sum_{n=-N}^{+N} A_n(x) e^{ins/R} = \sum_{n=-N}^{+N} \left(\sum_{j=1}^{8(2N+1)} \tilde{A}_j \bar{A}_{nj} e^{m_j x} \right) e^{ins/R} \\
\bar{v}(x,s) &= \sum_{n=-N}^{+N} B_n(x) e^{ins/R} = \sum_{n=-N}^{+N} \left(\sum_{j=1}^{8(2N+1)} \tilde{A}_j \bar{B}_{nj} e^{m_j x} \right) e^{ins/R} \\
\bar{w}(x,s) &= \sum_{n=-N}^{+N} C_n(x) e^{ins/R} = \sum_{n=-N}^{+N} \left(\sum_{j=1}^{8(2N+1)} \tilde{A}_j \bar{C}_{nj} e^{m_j x} \right) e^{ins/R}
\end{aligned} \tag{7.32a-c}$$

The displacements in Eq. 7.32 can be expressed in the following form

$$\begin{aligned}
\bar{u}(x,s) &= \sum_{n=-N}^{+N} \langle \mathbf{S}_{An}(x) \rangle_{1\times 8(2N+1)} \{ \tilde{\mathbf{A}} \}_{8(2N+1)\times 1} e^{ins/R} \\
\bar{v}(x,s) &= \sum_{n=-N}^{+N} \langle \mathbf{S}_{Bn}(x) \rangle_{1\times 8(2N+1)} \{ \tilde{\mathbf{A}} \}_{8(2N+1)\times 1} e^{ins/R} \\
\bar{w}(x,s) &= \sum_{n=-N}^{+N} \langle \mathbf{S}_{Cn}(x) \rangle_{1\times 8(2N+1)} \{ \tilde{\mathbf{A}} \}_{8(2N+1)\times 1} e^{ins/R}
\end{aligned} \tag{7.33a-c}$$

where

$$\begin{aligned}
\langle \mathbf{S}_{An}(x) \rangle_{1\times 8(2N+1)} &= \left\langle \bar{A}_{n.1} e^{m_1 x} \ \cdots \ \bar{A}_{n.8(2N+1)} e^{m_{8(2N+1)} x} \right\rangle_{1\times 8(2N+1)} \\
\langle \mathbf{S}_{Bn}(x) \rangle_{1\times 8(2N+1)} &= \left\langle \bar{B}_{n.1} e^{m_1 x} \ \cdots \ \bar{B}_{n.8(2N+1)} e^{m_{8(2N+1)} x} \right\rangle_{1\times 8(2N+1)}
\end{aligned} \tag{7.34a-c}$$

$$\left\langle \mathbf{S}_{Cn}(x) \right\rangle_{1\times 8(2N+1)} = \left\langle \bar{C}_{n.1} e^{m_1 x} \ \cdots \ \bar{C}_{n.8(2N+1)} e^{m_{8(2N+1)} x} \right\rangle_{1\times 8(2N+1)}$$

$$\left\{ \tilde{\mathbf{A}} \right\}^T = \left\langle \tilde{A}_1 \ \cdots \ \tilde{A}_{8(2N+1)} \right\rangle_{1\times 8(2N+1)} \tag{7.35}$$

By comparing Eqs. 7.33-7.35, one recovers the following expressions for $A_n(x)$, $B_n(x)$ and $C_n(x)$ functions.

$$\begin{aligned} A_n(x) &= \left\langle \mathbf{S}_{An}(x) \right\rangle_{1\times 8(2N+1)} \left\{ \tilde{\mathbf{A}} \right\}_{8(2N+1)\times 1} \\ B_n(x) &= \left\langle \mathbf{S}_{Bn}(x) \right\rangle_{1\times 8(2N+1)} \left\{ \tilde{\mathbf{A}} \right\}_{8(2N+1)\times 1} \\ C_n(x) &= \left\langle \mathbf{S}_{Cn}(x) \right\rangle_{1\times 8(2N+1)} \left\{ \tilde{\mathbf{A}} \right\}_{8(2N+1)\times 1} \end{aligned} \tag{7.36a-c}$$

In a finite element context, all unknown coefficients should be expressed in terms of the nodal displacements, which are $A_n(0)$, $B_n(0)$, $C_n(0)$, $C'_n(0)$, $A_n(L)$, $B_n(L)$, $C_n(L)$ and $C'_n(L)$. From Eqs. 7.36a-c, one obtains

$$\left\{ \mathbf{\Delta}_n \right\}_{8\times 1} = \left[\mathbf{L}_n \right]_{8\times 8(2N+1)} \left\{ \tilde{\mathbf{A}} \right\}_{8(2N+1)\times 1}$$

where

$$\left\{ \mathbf{\Delta}_n \right\}_{8\times 1} = \begin{Bmatrix} A_n(0) \\ B_n(0) \\ C_n(0) \\ C'_n(0) \\ A_n(L) \\ B_n(L) \\ C_n(L) \\ C'_n(L) \end{Bmatrix}_{8\times 1} \quad , \quad \left[\mathbf{L}_n \right] = \begin{bmatrix} \left\langle \mathbf{S}_{An}(0) \right\rangle \\ \left\langle \mathbf{S}_{Bn}(0) \right\rangle \\ \left\langle \mathbf{S}_{Cn}(0) \right\rangle \\ \left\langle \mathbf{S}'_{Cn}(0) \right\rangle \\ \left\langle \mathbf{S}_{An}(L) \right\rangle \\ \left\langle \mathbf{S}_{Bn}(L) \right\rangle \\ \left\langle \mathbf{S}_{Cn}(L) \right\rangle \\ \left\langle \mathbf{S}'_{Cn}(L) \right\rangle \end{bmatrix}_{8\times 8(2N+1)} \tag{7.37}$$

Assembling the displacement contributions of all terms in the range of $-N \le n \le N$ yields

$$\left\{ \mathbf{\Delta} \right\}_{8(2N+1)\times 1} = \left[\mathbf{L} \right]_{8(2N+1)\times 8(2N+1)} \left\{ \tilde{\mathbf{A}} \right\}_{8(2N+1)\times 1} \tag{7.38}$$

where

$$\left\{\boldsymbol{\Delta}\right\}_{8(2k+1)\times 1}=\left\{\begin{array}{c}\left\{\boldsymbol{\Delta}_{-N}\right\}\\ \vdots\\ \left\{\boldsymbol{\Delta}_{0}\right\}\\ \vdots\\ \left\{\boldsymbol{\Delta}_{N}\right\}\end{array}\right\}_{8(2k+1)\times 1} \quad , \quad \left[\mathbf{L}\right]=\left[\begin{array}{c}\left[\mathbf{L}_{-N}\right]\\ \vdots\\ \left[\mathbf{L}_{0}\right]\\ \vdots\\ \left[\mathbf{L}_{N}\right]\end{array}\right]_{8(2N+1)\times 8(2N+1)}$$

Solving Eq. 7.38 for the unknown coefficients $\left\{\tilde{\mathbf{A}}\right\}_{8(2N+1)\times 1}$ yields

$$\left\{\tilde{\mathbf{A}}\right\}_{8(2N+1)\times 1}=\left[\mathbf{L}\right]^{-1}_{8(2N+1)\times 8(2N+1)}\left\{\boldsymbol{\Delta}\right\}_{8(2N+1)\times 1} \tag{7.39}$$

From Eq. 7.39, by substituting into Eqs. 7.36a-c yields

$$\begin{aligned}A_n(x)&=\left\langle\mathbf{N}_{An}(x)\right\rangle_{1\times 8(2N+1)}\left\{\boldsymbol{\Delta}\right\}_{8(2N+1)\times 1}\\ B_n(x)&=\left\langle\mathbf{N}_{Bn}(x)\right\rangle_{1\times 8(2N+1)}\left\{\boldsymbol{\Delta}\right\}_{8(2N+1)\times 1}\\ C_n(x)&=\left\langle\mathbf{N}_{Cn}(x)\right\rangle_{1\times 8(2N+1)}\left\{\boldsymbol{\Delta}\right\}_{8(2N+1)\times 1}\end{aligned} \tag{7.40}$$

where

$$\left\langle\mathbf{N}_{An}(x)\right\rangle_{1\times 8(2N+1)}=\left\langle\mathbf{S}_{An}(x)\right\rangle_{1\times 8(2N+1)}\left[\mathbf{L}\right]^{-1}_{8(2N+1)\times 8(2N+1)} \tag{7.41}$$

$$\left\langle\mathbf{N}_{Bn}(x)\right\rangle_{1\times 8(2N+1)}=\left\langle\mathbf{S}_{Bn}(x)\right\rangle_{1\times 8(2N+1)}\left[\mathbf{L}\right]^{-1}_{8(2N+1)\times 8(2N+1)} \tag{7.42}$$

$$\left\langle\mathbf{N}_{Cn}(x)\right\rangle_{1\times 8(2N+1)}=\left\langle\mathbf{S}_{Cn}(x)\right\rangle_{1\times 8(2N+1)}\left[\mathbf{L}\right]^{-1}_{8(2N+1)\times 8(2N+1)} \tag{7.43}$$

It is noted that $\left\langle\mathbf{N}_{An}(x)\right\rangle_{1\times 8(2N+1)}$, $\left\langle\mathbf{N}_{Bn}(x)\right\rangle_{1\times 8(2N+1)}$ and $\left\langle\mathbf{N}_{Cn}(x)\right\rangle_{1\times 8(2N+1)}$ are the exact shape function matrices.

7.9.2 Discretized Equilibrium Equations

In this section a methodology similar to that in Section 7.7 is adopted to express the discretized equilibrium equations of the system into a consolidated form.

From Eq. 7.15, the homogeneous part of the boundary condition equations yields $(2N+1)$ sets of equations for $-N \le n \le N$ in the form

$$\left[{}^{0}\mathbf{H}_n + {}^{1}\mathbf{H}_n D + {}^{2}\mathbf{H}_n D^2 + {}^{3}\mathbf{H}_n D^3 \right]_{4\times 3(2M+1)} \left\{ \mathbf{\Lambda}_n \right\}_{3(2M+1)\times 1} = \left\{ \mathbf{0} \right\}_{4\times 1} \tag{7.44}$$

Equations 7.44 can be consolidated into a single matrix equation in the form

$$\left[{}^{0}\overline{\mathbf{H}} + {}^{1}\overline{\mathbf{H}}\ D + {}^{2}\overline{\mathbf{H}}\ D^2 + {}^{3}\overline{\mathbf{H}}\ D^3 \right]_{4(2N+1)\times 3(2N+2M+1)} \left\{ \overline{\mathbf{\Lambda}} \right\}_{3(2N+2M+1)\times 1} = \left\{ \mathbf{0} \right\}_{4(2N+1)\times 1} \tag{7.45}$$

where the rectangular coefficient matrices ${}^{i}\overline{\mathbf{H}}$ $(i = 0,...,3)$ and their constructing blocks ${}^{i}\mathbf{H}_n$ are schematically shown in Figure 7.4. Considering a certain mode $\overline{n}$, Figure 7.4 shows how each horizontal block ${}^{i}\mathbf{H}_n$ includes the contributions from modes $n-M$ to $n+M$ on mode n and the vertical block matrix ${}^{i}_{\mathbf{v}}\mathbf{H}_n$, defined in Appendix 7.B , includes the contributions of mode n on modes $n-M$ to $n+M$.

In the same manner as in Eq. 7.22, in order to relate the vertical block matrices ${}^{i}_{\mathbf{v}}\mathbf{H}_n$ to the horizontal block matrices ${}^{i}\mathbf{H}_n$, both matrices are partitioned as

$$\left[{}^{i}\mathbf{H}_n \right]_{4\times 3(2M+1)} = \left[\left[{}^{i}\widehat{\mathbf{H}}_{\substack{n \\ k=-M}} \right]_{4\times 3} \middle| \cdots \middle| \left[{}^{i}\widehat{\mathbf{H}}_{\substack{n \\ k=0}} \right]_{4\times 3} \middle| \cdots \middle| \left[{}^{i}\widehat{\mathbf{H}}_{\substack{n \\ k=M}} \right]_{4\times 3} \right]$$

$$\left[{}^{i}_{\mathbf{v}}\mathbf{H}_n \right]_{4(2M+1)\times 3} = \left[\begin{array}{c} \left[{}^{i}_{\mathbf{v}}\widehat{\mathbf{H}}_{\substack{n \\ k=-M}} \right]_{4\times 3} \\ \hdashline \vdots \\ \hdashline \left[{}^{i}_{\mathbf{v}}\widehat{\mathbf{H}}_{\substack{n \\ k=0}} \right]_{4\times 3} \\ \hdashline \vdots \\ \hdashline \left[{}^{i}_{\mathbf{v}}\widehat{\mathbf{H}}_{\substack{n \\ k=M}} \right]_{4\times 3} \end{array} \right] \tag{7.46a,b}$$

Similar to Eq. 7.23, by considering a certain mode $\bar{n}$, rectangular block matrices ${}^{i}\widehat{\mathbf{H}}_{\substack{n\\k}}$ and ${}^{i}_{\mathbf{v}}\widehat{\mathbf{H}}_{\substack{n\\k}}$ of size 4×3 are related through

$$ {}^{i}_{\mathbf{v}}\widehat{\mathbf{H}}_{\substack{n=\bar{n}\\k=-\bar{k}}} = {}^{i}\widehat{\mathbf{H}}_{\substack{n=\bar{n}-\bar{k}\\k=\bar{k}}} \tag{7.47} $$

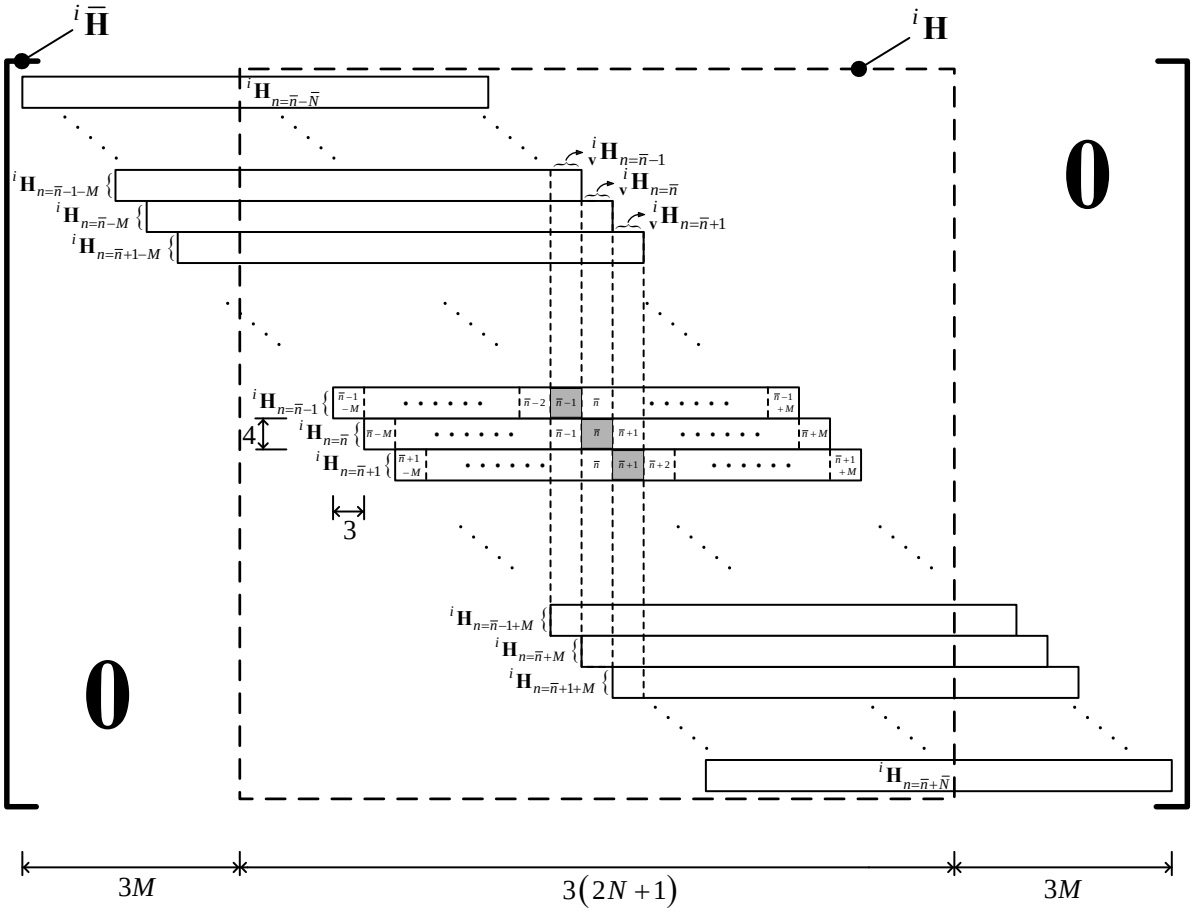

Figure 7.4 - Schematic presentation of matrices ${}^{i}\bar{\mathbf{H}}$ and ${}^{i}\mathbf{H}$ and their constructing blocks ${}^{i}\mathbf{H}_{n}$ and ${}^{i}_{\mathbf{v}}\mathbf{H}_{n}$

Due to the fact that the unknown displacement fields are truncated (i.e. $\langle A_n(x), B_n(x), C_n(x)\rangle = \langle 0,0,0\rangle$ for $|n| > N$), the first $3M$ and the last $3M$ columns of

coefficient matrices ${}^{i}\bar{\mathbf{H}}$ are irrelevant to the solution. Thus, the system of ODEs in Eq. 7.45 is simplified to

$$\left[{}^{0}\mathbf{H} + {}^{1}\mathbf{H}\, D + {}^{2}\mathbf{H}\, D^2 + {}^{3}\mathbf{H}\, D^3 \right]_{4(2N+1)\times 3(2N+1)} \left\{ \mathbf{\Lambda} \right\}_{3(2N+1)\times 1} = \left\{ \mathbf{0} \right\}_{4(2N+1)\times 1} \tag{7.48}$$

where the rectangular coefficient matrices ${}^{i}\mathbf{H}$ $(i = 0,...,3)$ are of size $4(2N+1)\times 3(2N+1)$. Matrices ${}^{i}\mathbf{H}$ are obtained by truncating the first $3M$ and the last $3M$ columns of matrices ${}^{i}\bar{\mathbf{H}}$ (the area enclosed by dashed line in Figure 7.4).

Similarly, matrices $\bar{\mathbf{H}}_j^{xw}$, $\bar{\mathbf{G}}_j^{xu}$, $\bar{\mathbf{G}}_j^{sv}$, $\bar{\mathbf{G}}_j^{zw}$, $\bar{\mathbf{G}}_j^{xw}$ and $\bar{\mathbf{G}}_j^{sw}$ of dimension $(2N+2M+1)\times(2N+1)$ are obtained by summing over n $(-N \le n \le N)$ in Eq. 7.15 and represent the consolidated form of contribution of row force vectors $\mathbf{H}_{jn}^{xw}$, $\mathbf{G}_{jn}^{xu}$, $\mathbf{G}_{jn}^{sv}$, $\mathbf{G}_{jn}^{zw}$, $\mathbf{G}_{jn}^{xw}$ and $\mathbf{G}_{jn}^{sw}$, respectively. The term $\bar{\mathbf{X}}_j^{\mathbf{xx}}$ (where $\bar{\mathbf{X}}$ takes the values $\mathbf{G}$, $\mathbf{H}$ as applicable and superscript $\mathbf{xx}$ takes the values xu, sv, zw, xw, sw as applicable) is introduced here as a generic representation of matrices $\bar{\mathbf{H}}_j^{xw}$, $\bar{\mathbf{G}}_j^{xu}$, $\bar{\mathbf{G}}_j^{sv}$, $\bar{\mathbf{G}}_j^{zw}$, $\bar{\mathbf{G}}_j^{xw}$ and $\bar{\mathbf{G}}_j^{sw}$. Also the term $\mathbf{X}_{jn}^{\mathbf{xx}}$ (where $\mathbf{X}$ takes the values $\mathbf{G}$, $\mathbf{H}$ as applicable and superscript $\mathbf{xx}$ takes the values xu, sv, zw, xw, sw as applicable) is introduced as another generic representation of matrices $\mathbf{H}_{jn}^{xw}$, $\mathbf{G}_{jn}^{xu}$, $\mathbf{G}_{jn}^{sv}$, $\mathbf{G}_{jn}^{zw}$, $\mathbf{G}_{jn}^{xw}$ and $\mathbf{G}_{jn}^{sw}$. Figure 7.5 schematically shows how consolidated matrices $\bar{\mathbf{X}}_j^{\mathbf{xx}}$ are assembled by $\mathbf{X}_{jn}^{\mathbf{xx}}$.

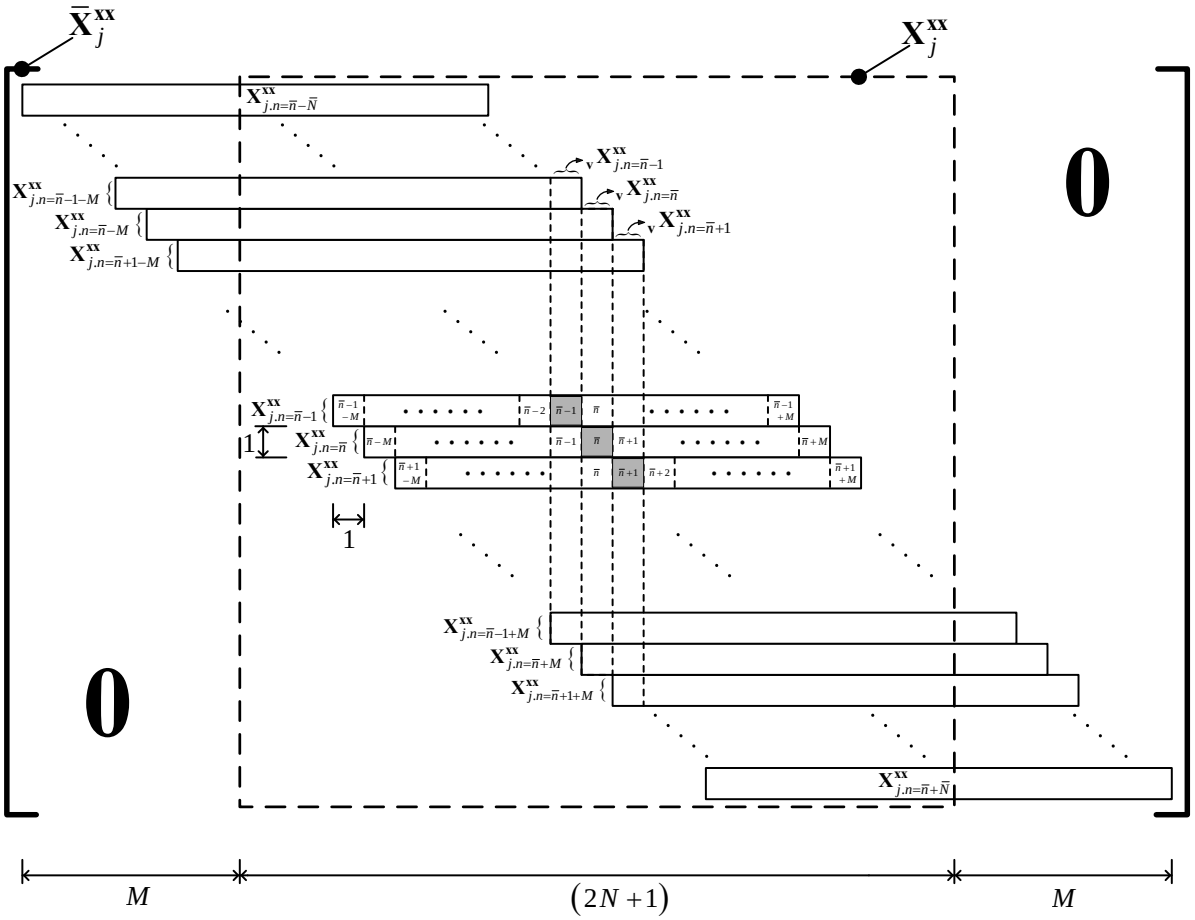

Figure 7.5 - Schematic presentation of matrices $\bar{\mathbf{X}}_j^{\mathbf{xx}}$ and $\mathbf{X}_j^{\mathbf{xx}}$ and their constructing blocks $\mathbf{X}_{jn}^{\mathbf{xx}}$ and ${}_{\mathbf{v}}\mathbf{X}_{jn}^{\mathbf{xx}}$

Square matrices $\mathbf{H}_j^{xw}$, $\mathbf{G}_j^{xu}$, $\mathbf{G}_j^{sv}$, $\mathbf{G}_j^{zw}$, $\mathbf{G}_j^{xw}$ and $\mathbf{G}_j^{sw}$ of dimension $(2N+1)\times(2N+1)$ are obtained by truncating the first M and the last M columns of matrices $\bar{\mathbf{H}}_j^{xw}$, $\bar{\mathbf{G}}_j^{xu}$, $\bar{\mathbf{G}}_j^{sv}$, $\bar{\mathbf{G}}_j^{zw}$, $\bar{\mathbf{G}}_j^{xw}$ and $\bar{\mathbf{G}}_j^{sw}$, respectively. Horizontal row vectors $\mathbf{X}_{jn}^{\mathbf{xx}}$ include the contributions from modes $n-M$ to $n+M$ on mode n. Also, column vectors ${}_{\mathbf{v}}\mathbf{X}_{jn}^{\mathbf{xx}}$ are introduced, which include the contributions of mode n on modes $n-M$ to $n+M$. By partitioning row vectors $\mathbf{X}_{jn}^{\mathbf{xx}}$ and column vectors ${}_{\mathbf{v}}\mathbf{X}_{jn}^{\mathbf{xx}}$ as

$$\left\langle \mathbf{X}_n^{\mathbf{xx}} \right\rangle_{1\times(2M+1)} = \left\langle \widehat{\mathbf{X}}_{n\ k=-M}^{\mathbf{xx}} \;\middle|\; \cdots \;\middle|\; \widehat{\mathbf{X}}_{n\ k=0}^{\mathbf{xx}} \;\middle|\; \cdots \;\middle|\; \widehat{\mathbf{X}}_{n\ k=M}^{\mathbf{xx}} \right\rangle \tag{7.49a,b}$$

$$\left\{ {}_{\mathbf{v}}\mathbf{X}_n^{\mathbf{xx}} \right\}_{(2M+1)\times 1} = \begin{Bmatrix} {}_{\mathbf{v}}\widehat{\mathbf{X}}_{n\ k=-M}^{\mathbf{xx}} \\ \hline \vdots \\ \hline {}_{\mathbf{v}}\widehat{\mathbf{X}}_{n\ k=0}^{\mathbf{xx}} \\ \hline \vdots \\ \hline {}_{\mathbf{v}}\widehat{\mathbf{X}}_{n\ k=M}^{\mathbf{xx}} \end{Bmatrix}$$

one concludes that

$${}_{\mathbf{v}}\widehat{\mathbf{X}}_{n=\bar{n}\ k=-\bar{k}}^{\mathbf{xx}} = \widehat{\mathbf{X}}_{n=\bar{n}-\bar{k}\ k=\bar{k}}^{\mathbf{xx}} \tag{7.50a,b}$$

and consequently

$$\begin{aligned}
&{}_{\mathbf{v}}\widehat{\mathbf{H}}_{j.n=\bar{n}\ k=-\bar{k}}^{xw} = \widehat{\mathbf{H}}_{j.n=\bar{n}-\bar{k}\ k=\bar{k}}^{xw} \quad , \quad {}_{\mathbf{v}}\widehat{\mathbf{G}}_{j.n=\bar{n}\ k=-\bar{k}}^{xu} = \widehat{\mathbf{G}}_{j.n=\bar{n}-\bar{k}\ k=\bar{k}}^{xu} \\
&{}_{\mathbf{v}}\widehat{\mathbf{G}}_{j.n=\bar{n}\ k=-\bar{k}}^{sv} = \widehat{\mathbf{G}}_{j.n=\bar{n}-\bar{k}\ k=\bar{k}}^{sv} \quad , \quad {}_{\mathbf{v}}\widehat{\mathbf{G}}_{j.n=\bar{n}\ k=-\bar{k}}^{zw} = \widehat{\mathbf{G}}_{j.n=\bar{n}-\bar{k}\ k=\bar{k}}^{zw} \\
&{}^{i}_{\mathbf{v}}\widehat{\mathbf{G}}_{j.n=\bar{n}\ k=-\bar{k}}^{xw} = \widehat{\mathbf{G}}_{j.n=\bar{n}-\bar{k}\ k=\bar{k}}^{xw} \quad , \quad {}_{\mathbf{v}}\widehat{\mathbf{G}}_{j.n=\bar{n}\ k=-\bar{k}}^{sw} = \widehat{\mathbf{G}}_{j.n=\bar{n}-\bar{k}\ k=\bar{k}}^{sw}
\end{aligned} \tag{7.51}$$

The non zero entries of matrices ${}_{\mathbf{v}}\mathbf{H}_n^i$, ${}_{\mathbf{v}}\mathbf{H}_{jn}^{xw}$, ${}_{\mathbf{v}}\mathbf{G}_{jn}^{xu}$, ${}_{\mathbf{v}}\mathbf{G}_{jn}^{sv}$, ${}_{\mathbf{v}}\mathbf{G}_{jn}^{zw}$, ${}_{\mathbf{v}}\mathbf{G}_{jn}^{xw}$ and ${}_{\mathbf{v}}\mathbf{G}_{jn}^{sw}$ are provided in Appendix 7.B .

From Eq. 7.40, by substituting into Eq. 7.15, and summing over n, $(2N+1)$ sets of equations for $-N \le n \le N$ of the system are expressed in the consolidated form

$$\frac{Eh}{1-\nu^2}\left[\delta\left\{\mathbf{\Lambda}^*\right\}^T\left({}^0\mathbf{H}+{}^1\mathbf{H}D+{}^2\mathbf{H}D^2+{}^3\mathbf{H}D^3\right)\{\mathbf{\Lambda}\}+\delta\left\{\mathbf{C}^*\right\}^T\sum_{j=1}^{2}\left[\mathbf{H}_j^{xw}\right]\left\{\mathbf{f}_j^{xw}\right\}\right]_0^L$$
$$+\frac{Eh}{1-\nu^2}\int_0^L\sum_{j=1}^{2}\Big[\delta\left\{\mathbf{A}^*\right\}^T\left[\mathbf{G}_j^{xu}\right]\left\{\mathbf{f}_j^{xu}\right\}+\delta\left\{\mathbf{B}^*\right\}^T\left[\mathbf{G}_j^{sv}\right]\left\{\mathbf{f}_j^{sv}\right\} \tag{7.52}$$
$$+\delta\left\{\mathbf{C}^*\right\}^T\left(\left[\mathbf{G}_j^{zw}\right]\left\{\mathbf{f}_j^{zw}\right\}+\left[\mathbf{G}_j^{xw}D\right]\left\{\mathbf{f}_j^{xw}\right\}+\left[\mathbf{G}_j^{sw}\right]\left\{\mathbf{f}_j^{sw}\right\}\right)\Big]dx=0$$

where

$$\{\mathbf{\Lambda}\}_{3(2N+1)\times1}=[\mathbf{Q}][\mathbf{L}]^{-1}\{\mathbf{\Delta}\}\quad,\quad\left\{\mathbf{\Lambda}^*\right\}_{4(2N+1)\times1}=\left[\mathbf{Q}^*\right][\mathbf{L}]^{-1}\{\mathbf{\Delta}\}$$
$$\left\{\mathbf{A}^*\right\}_{(2N+1)\times1}=\left[\mathbf{Q}_A^*\right][\mathbf{L}]^{-1}\{\mathbf{\Delta}\}\quad,\quad\left\{\mathbf{B}^*\right\}_{(2N+1)\times1}=\left[\mathbf{Q}_B^*\right][\mathbf{L}]^{-1}\{\mathbf{\Delta}\} \tag{7.53}$$
$$\left\{\mathbf{C}^*\right\}_{(2N+1)\times1}=\left[\mathbf{Q}_C^*\right][\mathbf{L}]^{-1}\{\mathbf{\Delta}\}$$

in which

$$[\mathbf{Q}]=\begin{bmatrix}\left[\mathbf{Q}_{-N}\right]\\ \vdots\\ \left[\mathbf{Q}_0\right]\\ \vdots\\ \left[\mathbf{Q}_N\right]\end{bmatrix}_{3(2N+1)\times8(2N+1)}\quad;\quad\left[\mathbf{Q}_n\right]=\begin{bmatrix}\langle\mathbf{S}_{An}(x)\rangle\\ \langle\mathbf{S}_{Bn}(x)\rangle\\ \langle\mathbf{S}_{Cn}(x)\rangle\end{bmatrix}_{3\times8(2N+1)} \tag{7.54}$$

$$\left[\mathbf{Q}^*\right]=\begin{bmatrix}\left[\mathbf{Q}_N^*\right]\\ \vdots\\ \left[\mathbf{Q}_0^*\right]\\ \vdots\\ \left[\mathbf{Q}_{-N}^*\right]\end{bmatrix}_{4(2N+1)\times8(2N+1)}\quad;\quad\left[\mathbf{Q}_n^*\right]=\begin{bmatrix}\langle\mathbf{S}_{An}(x)\rangle\\ \langle\mathbf{S}_{Bn}(x)\rangle\\ \langle\mathbf{S}_{Cn}(x)\rangle\\ \langle\mathbf{S}'_{Cn}(x)\rangle\end{bmatrix}_{4\times8(2N+1)} \tag{7.55}$$

and

$$\left[\mathbf{Q}_A^*\right]=\begin{bmatrix}\langle\mathbf{S}_{A.N}(x)\rangle\\ \vdots\\ \langle\mathbf{S}_{A.0}(x)\rangle\\ \vdots\\ \langle\mathbf{S}_{A.-N}(x)\rangle\end{bmatrix}_{(2N+1)\times8(2N+1)}\quad,\quad\left[\mathbf{Q}_B^*\right]=\begin{bmatrix}\langle\mathbf{S}_{B.N}(x)\rangle\\ \vdots\\ \langle\mathbf{S}_{B.0}(x)\rangle\\ \vdots\\ \langle\mathbf{S}_{B.-N}(x)\rangle\end{bmatrix}_{(2N+1)\times8(2N+1)} \tag{7.56}$$

$$\left[\mathbf{Q}_C^*\right]=\begin{bmatrix}\langle \mathbf{S}_{C.N}(x)\rangle \\ \vdots \\ \langle \mathbf{S}_{C.0}(x)\rangle \\ \vdots \\ \langle \mathbf{S}_{C.-N}(x)\rangle\end{bmatrix}_{(2N+1)\times 8(2N+1)} \tag{7.57}$$

It is noted that since the shape functions were obtained based on the quasi-exact solution of the homogeneous form of the truncated field equations, the homogenous part of the field equations in the second integral term in Eq. 7.15 vanishes.

7.10 Example

A fixed-free pipe bend (Figure 7.6) with cross-sectional radius $R=0.25m$, radius of curvature $\Re=2m$ and thickness $h=0.01m$ and centerline length L is to be analyzed under the following scenarios provided in Table 7.1. It is required to obtain the response of the structure at free end. In all cases the modulus of elasticity and Poisson's ratio are $200Gpa$ and 0.3, respectively. The sign convention in Figure 6.1 is adopted.

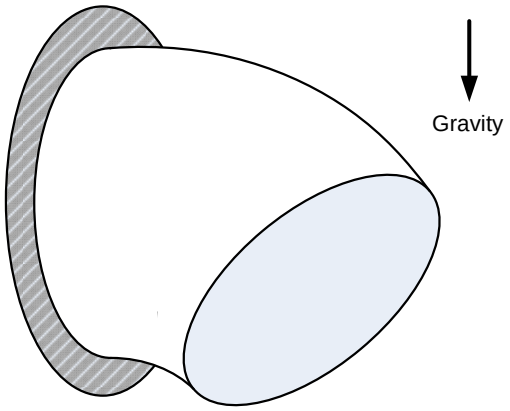

Figure 7.6 – Fixed-free pipe bend in the Example

Table 7.1 – Scenarios in the Example

Case	Load	Torus length
a	Uniform axial traction $F_a = 1,000\, kN/m^2$	$L = 0.15\, m$
b	Uniform circumferential traction $F_c = 1,000\, kN/m^2$	$L = 0.15\, m$
c	Uniform radial traction $F_r = 1,000\, kN/m^2$	$L = 0.05\, m$
d	Self weight, $\rho = 7850\, kg/m^3$	$L = 0.10\, m$
e	Harmonic ring load $F_a = 1,000 \sin\theta \cos\bar{\omega}t \;\; kN/m^2$ at free end, where $\bar{\omega} = 1000 \;\; rad/s$	$L = 0.05\, m$

For all cases (a-e), the solutions were provided by a single finite element, which involves 120 DOFs. For comparison, a solution based on the commercial software Abaqus is provided and the results from both methods are provided in Figure 7.7 to Figure 7.11. All figures show the magnitude of the total displacement vector along the edge of the free end of the pipe bend. In the solutions based on the Abaqus, the shell element used is S4R (4-node doubly curved shell element with five integration points across the thickness and 6 DOFs at each node) and the number of elements is given in the figures. Excellent agreement is achieved in all cases and the difference between the results based on the current study and those based on the Abaqus are within a few percents.

Also, all cases are repeated for a straight pipe of the same geometry (except $\Re \to \infty$). The result based on both elements (i.e., straight element developed in Chapter 5 and Curved element developed in the present chapter) are indistinguishable. These are provided in each figure for comparison.

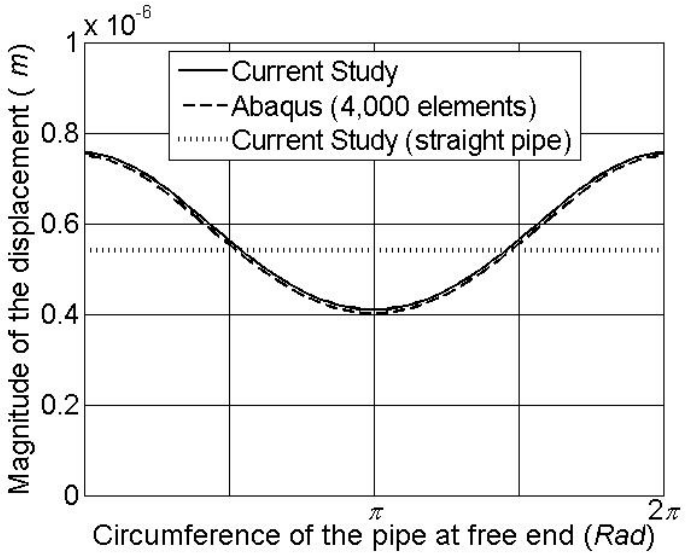

Figure 7.7 – Pipe bend under axial traction (Scenario a), $L = 0.15\,m$

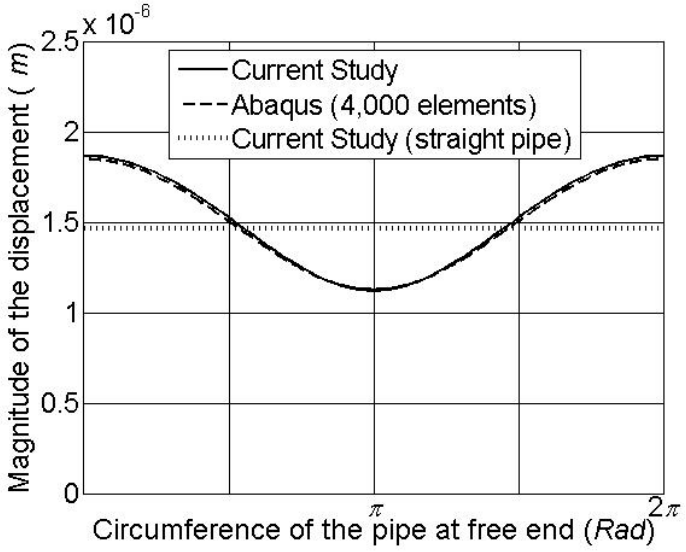

Figure 7.8 – Pipe bend under uniform torsion (Scenario b), $L = 0.15\,m$

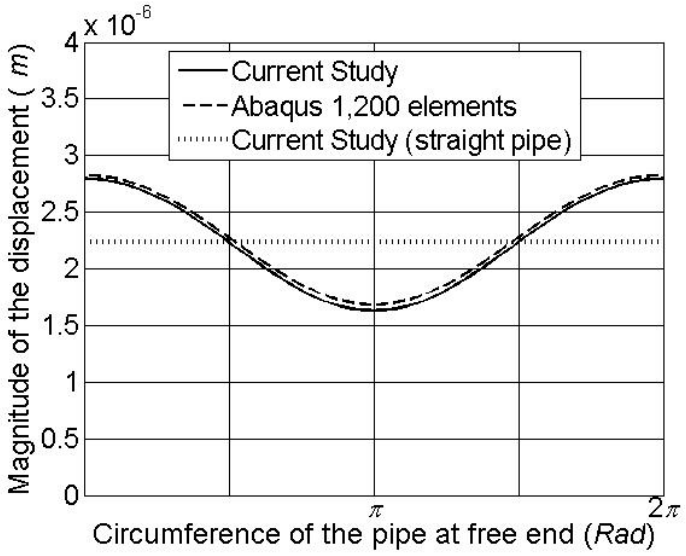

Figure 7.9 – Pipe bend under uniform radial traction (Scenario c), $L = 0.05\,m$

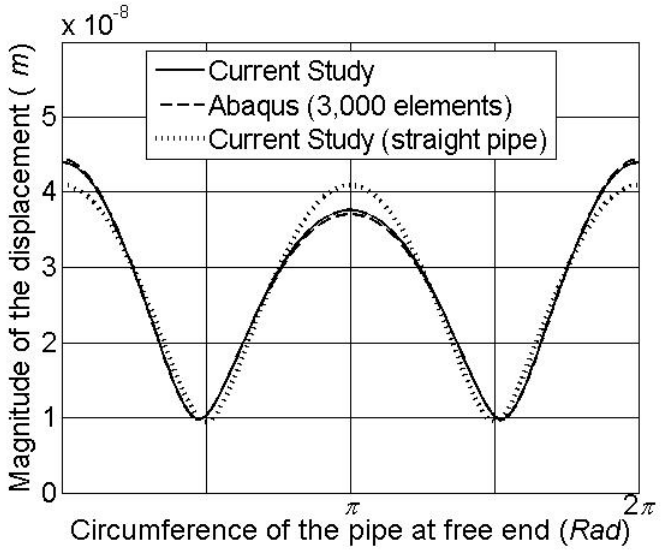

Figure 7.10 – Pipe bend under self weight (Scenario d), $L = 0.10\,m$

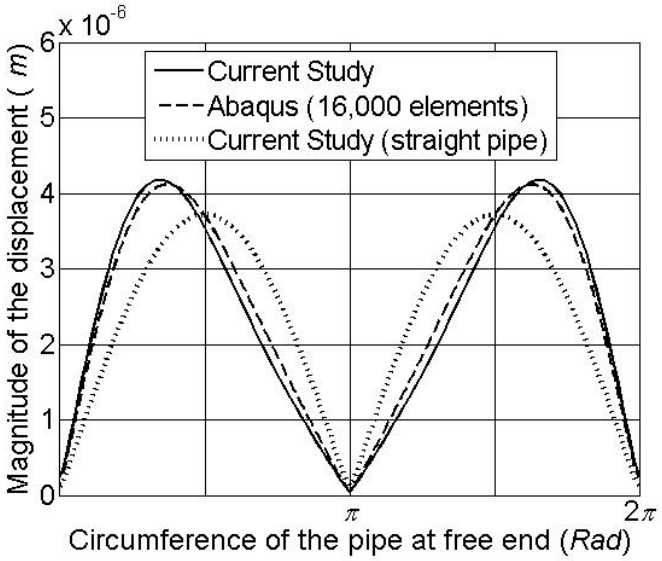

Figure 7.11 – Pipe bend under out-of-plain harmonic moment (Scenario e), $L = 0.05\,m$

It is noted that all previous examples showed excellent agreement with Abaqus for pipe bends of relatively short length. Theoretically, the model developed was intended to achieve satisfactory convergence to the solution for any given range of practical length. However, numerical problems were encountered when applying the longer length of pipe bends. This is believed to be caused by the lack of enough number of machine precision. It is noted that when $\Re \to \infty$ the solution converges to the solution of the straight pipes.

7.11 Summary and Conclusion

Using the method of separation of variables in conjunction with the Fourier expansion of the unknown displacement fields and applied forces with respect to circumferential coordinate, the variational form of Hamiltonian functional of toroidal thin shells transformed into an infinite system of ordinary differential equation with respect to longitudinal coordinate. A set of exact shape functions is developed based on the exact solution of the field equations of

the system and led to formulation of an exact toroidal finite element. It is observed that there is excellent agreement between the results based on the proposed toroidal finite element and those based on the Abaqus for short pipe bends. For the case of longer pipe bends, although using more refined and sensitive numerical solution methods is recommended, it is expected to achieve satisfactory results by using higher precision.

7.12 References

[7.1] J. Mackerle, Finite elements in the analysis of pressure vessels and piping - a bibliography (1976-1996), Int. J. Press. Vessel. Pip. 69 (1996) 279-339.

[7.2] J. Mackerle, Finite elements in the analysis of pressure vessels and piping, an addendum (1996-1998)", Int. J. Press. Vessel. Pip. 76 (1999) 461-485.

[7.3] J. Mackerle, Finite elements in the analysis of pressure vessels and piping, an addendum: a bibliography (1998-2001), Int. J. Press. Vessel. Pip. 79 (2002) 1-26.

[7.4] J. Mackerle, Finite elements in the analysis of pressure vessels and piping, an addendum: a bibliography (2001-2004), Int. J. Press. Vessel. Pip. 82 (2005) 571-592.

[7.5] M.S. Qatu, Recent Research Advances in the Dynamic Behaviour of Shells: 1989-2000, Part 1: Laminated Composite Shells. ASME, Appl. Mech. Rev. 55 (2002) 325-350.

[7.6] M.S. Qatu, Recent Research Advances in the Dynamic Behaviour of Shells: 1989-2000, Part 2: Homogeneous Shells. ASME, Appl. Mech. Rev. 55 (2002) 415-434.

[7.7] H. Ohtsubo, O. Watanabe, Stress analysis of pipe bends by ring elements, J. Press. Vessel. Technol. 100 (1978) 112-122.

[7.8] H. Takeda, S. Asai, K. Kwata, A New Finite Element for Structural Analysis of Piping Systems, Proc. Fifth SMIRT Conf. Berlin, 1979.

[7.9] K.J. Bathe, C. A. Almeida, A Simple and Effective Pipe Elbow Element-Linear Analysis, Trans. ASME, J. Appl. Mech. 47 (1980) 93-100.

[7.10] K.J. Bathe, C. Almeida, A simple and effective pipe elbow element – interaction effects, J. Appl. Mech. 49 (1982) 165-171.

[7.11] K.J. Bathe, C. Almeida, A simple and effective pipe elbow element – some non-linear capabilities, Comput. Struct. 17 (1983) 659-667.

[7.12] C. Militello, A.E. Huespe, A displacement-based pipe elbow element, Comput. Struct. 29 (1988) 339-343.

[7.13] M. Abo-Elkhier, Analysis of pipe bends using pipe elbow element, Comput. Struct. 37 (1990) 9-15.

[7.14] F. Zhang, D. Redecop, Surface Loading of a Thin-Walled Toroidal Shell, Comp. Struct. 43 (1992) 1019-1028.

[7.15] F.J.M.Q. Melo, P.M.S.T. de Castro, The Linear Elastic Stress Analysis of curved pipes under generalized loads using a reduced integration finite element, J. Strain Anal. Eng. Des. 32 (1997) 47-59.

[7.16] A.M. Yan, R.J. Jospin, D.H. Nguyen, An enhanced pipe elbow element - application in plastic limit analysis of pipe structures, International Journal for Numerical Methods in Engineering, 46 (1999) 409-431.

[7.17] E.M.M. Fonseca, F.J.M.Q. de Melo, C.A.M. Oliveira, Determination of flexibility factors in curved pipes with end restraints using a semi-analytical formulation, Int. J. Press. Vessel. Pip, 79 (2002) 829-840

[7.18] S.A. Karamanos, Bending Instabilities of Elastic Tubes, Int. J. Solid. and Struct. 39 (2002) 2059-2085.

[7.19] S.A. Karamanos, E. Giakoumatos, A.M. Gresnigt, Nonlinear Response and Failure of Steel Elbows under In-Plane Bending and Pressure, J. Press. Vessel Technol. 125 (2003) 393-402.

[7.20] J.O. Carneiro, F.J.Q. de Melo, J.F.D. Rodrigues, H. Lopes, V. Teixeira, The Modal Analysis of Pipe Elbow with Realistic Boundary Conditions, Int. J. Press. Vessel. Piping. 82 (2005) 593-601.

[7.21] D. Redekop, D. Chang, Vibration of Mitred and Smooth Pipe Bends and Their Components, Struct. Eng. Mech., 33 (2009) 747-763.

[7.22] J.P. Dedieu and F. Tisseur, Perturbation theory for homogeneous polynomial eigenvalue problems, Linear Algebra Appl. 358 (2003) 71-94.

7.13 List of Symbols

$A_n(x), B_n(x), C_n(x)$	Contributions of circumferential mode n to mid-surface displacements u, v, w, respectively
$\bar{A}_{nj}, \bar{B}_{nj}, \bar{C}_{nj}$	Constants relating the rows of the eigenvector $\hat{\mathbf{A}}_j$
$\tilde{A}_j$	Unknown constants to be determined from the boundary conditions of the system
D, D^i	Differentiation with respect to x and ith differential with respect to x, respectively
D_{ij}, L_{ij}	Differential operators in boundary condition and field equations, respectively
E	Modulus of elasticity
$F^u_{FE}, F^v_{FE}, F^w_{FE}, F^w_{BC}$	Generic force terms in the functional
R	Cross-sectional radius of torus
R_{ij} $(i=1,...,3)$, $(j=0,...,5)$	Fourier constants in approximating ζ^{-i}
f_i^F $(i=1,...,13)$	Constants in defining the generic force terms F^u_{FE}, F^v_{FE}, F^w_{FE}, F^w_{BC} in the functional
$f_j^{xu}, f_j^{sv}, f_j^{xw}, f_j^{sw}, f_j^{zw}$ $(j=1,2)$	Tractions in defining the generic force terms F^u_{FE}, F^v_{FE}, F^w_{FE}, F^w_{BC} in the functional as a function of x and s
$f_{jn}^{xu}(x)$ $f_{jn}^{sv}(x)$ $f_{jn}^{zw}(x)$ $f_{jn}^{xw}(x)$ $f_{jn}^{sw}(x)$	Respective force contributions of f_j^{xu}, f_j^{xw}, f_j^{sv}, f_j^{sw} and f_j^{zw} based on mode n as functions of coordinate x

$\bar{p}^x\ \bar{p}^s\ \bar{p}^z$	Axial, circumferential and radial components of applied body forces, respectively, as functions of coordinates x, s, z
$\bar{p}_n^x\ \bar{p}_n^s\ \bar{p}_n^z$	n th component of applied body forces $\bar{p}^x$, $\bar{p}^s$, $\bar{p}^z$, respectively,
u, v, w	Covariant components of the displacement of a point on the middle surface along axes x, s and w, respectively
$\bar{u}, \bar{v}, \bar{w}$	Physical components of the covariant displacement components u, v, w, respectively
x, s, z	Coordinates of the system
$\mathbf{A}^*, \mathbf{B}^*, \mathbf{C}^*$	Unknown displacement vector, including longitudinal, circumferential and radial components, respectively
$\tilde{\mathbf{A}}$	Integration constant vector
$\hat{\mathbf{A}}_\mathbf{j}$	Eigenvector of the original PEP
$\mathbf{f}_{jn}^{xu}(x)\ \mathbf{f}_{jn}^{sv}(x)$ $\mathbf{f}_{jn}^{zw}(x)\ \mathbf{f}_{jn}^{xw}(x)$ $\mathbf{f}_{jn}^{sw}(x)$	Vectors representing the contributions from mode n of the force components f_{jn}^{xu}, f_{jn}^{xw}, f_{jn}^{sv}, f_{jn}^{sw}, f_{jn}^{zw}, respectively, on modes $n-M$ to $n+M$
${}^i\bar{\mathbf{G}}$	Consolidated coefficient matrix of differential operator D^i
${}^i\mathbf{G}$	Truncated coefficient matrix of differential operator D^i
${}^i\mathbf{G}_n$	Horizontal constructing block matrix of matrix ${}^i\bar{\mathbf{G}}$, representing the contributions from modes $n-M$ to $n+M$ on mode n
${}^i_\mathbf{v}\mathbf{G}_n$	Vertical constructing block matrix of matrix ${}^i\bar{\mathbf{G}}$ for mode n, representing the contributions from mode n on modes $n-M$ to $n+M$
${}^i\hat{\mathbf{G}}_{n\ k}$, ${}^i_\mathbf{v}\hat{\mathbf{G}}_{n\ k}$	k th constructing blocks of matrices ${}^i\mathbf{G}_n$ and ${}^i_\mathbf{v}\mathbf{G}_n$, respectively

$\bar{\mathbf{G}}_j^{xu}, \bar{\mathbf{G}}_j^{sv}, \bar{\mathbf{G}}_j^{zw},$ $\bar{\mathbf{G}}_j^{xw}, \bar{\mathbf{G}}_j^{sw}$	Consolidated coefficient matrix of j th component of the applied forces in homogeneous form of the field equations
$\mathbf{G}_j^{xu}, \mathbf{G}_j^{sv}, \mathbf{G}_j^{zw},$ $\mathbf{G}_j^{xw}, \mathbf{G}_j^{sw}$	Truncated coefficient matrix of j th component of the applied forces in homogeneous form of the field equations
$\mathbf{G}_{jn}^{xu}, \mathbf{G}_{jn}^{sv}, \mathbf{G}_{jn}^{zw},$ $\mathbf{G}_{jn}^{xw}, \mathbf{G}_{jn}^{sw}$	Horizontal constructing block matrices of matrices $\bar{\mathbf{G}}_j^{xu}$, $\bar{\mathbf{G}}_j^{sv}$, $\bar{\mathbf{G}}_j^{zw}$, $\bar{\mathbf{G}}_j^{xw}$ and $\bar{\mathbf{G}}_j^{sw}$, respectively, representing the contributions from modes $n-M$ to $n+M$ on mode n
${}_{\mathbf{v}}\mathbf{G}_{jn}^{xu}, {}_{\mathbf{v}}\mathbf{G}_{jn}^{sv}, {}_{\mathbf{v}}\mathbf{G}_{jn}^{zw},$ ${}_{\mathbf{v}}\mathbf{G}_{jn}^{xw}, {}_{\mathbf{v}}\mathbf{G}_{jn}^{sw}$	Vertical constructing block matrices of matrices $\bar{\mathbf{G}}_j^{xu}$, $\bar{\mathbf{G}}_j^{sv}$, $\bar{\mathbf{G}}_j^{zw}$, $\bar{\mathbf{G}}_j^{xw}$ and $\bar{\mathbf{G}}_j^{sw}$, respectively, representing the contributions from mode n on modes $n-M$ to $n+M$
$\underset{k}{\hat{\mathbf{G}}}_{jn}^{xu}, \underset{k}{\hat{\mathbf{G}}}_{jn}^{sv}, \underset{k}{\hat{\mathbf{G}}}_{jn}^{zw},$ $\underset{k}{\hat{\mathbf{G}}}_{jn}^{xw}, \underset{k}{\hat{\mathbf{G}}}_{jn}^{sw}$	k th constructing blocks of matrices $\mathbf{G}_{jn}^{xu}$, $\mathbf{G}_{jn}^{sv}$, $\mathbf{G}_{jn}^{zw}$, $\mathbf{G}_{jn}^{xw}$ and $\mathbf{G}_{jn}^{sw}$, respectively
${}_{\mathbf{v}}\underset{k}{\hat{\mathbf{G}}}_{jn}^{xu}, {}_{\mathbf{v}}\underset{k}{\hat{\mathbf{G}}}_{jn}^{sv}, {}_{\mathbf{v}}\underset{k}{\hat{\mathbf{G}}}_{jn}^{zw},$ ${}_{\mathbf{v}}\underset{k}{\hat{\mathbf{G}}}_{jn}^{sw}, {}_{\mathbf{v}}\underset{k}{\hat{\mathbf{G}}}_{jn}^{xw}$	k th constructing blocks of matrices ${}_{\mathbf{v}}\mathbf{G}_{jn}^{xu}$, ${}_{\mathbf{v}}\mathbf{G}_{jn}^{sv}$, ${}_{\mathbf{v}}\mathbf{G}_{jn}^{zw}$, ${}_{\mathbf{v}}\mathbf{G}_{jn}^{xw}$ and ${}_{\mathbf{v}}\mathbf{G}_{jn}^{sw}$, respectively
${}^{i}\bar{\mathbf{H}}$	Consolidated coefficient matrix of differential operator D^i in homogeneous form of boundary condition equations
${}^{i}\mathbf{H}$	Truncated coefficient matrix of differential operator D^i in homogeneous form of the boundary condition equations
${}^{i}\mathbf{H}_n$	Horizontal constructing block matrix of matrix ${}^{i}\bar{\mathbf{H}}$, representing the contributions from modes $n-M$ to $n+M$ on mode n

${}_{\mathrm{v}}^{i}\mathbf{H}_n$	vertical constructing block matrix of matrix ${}^{i}\bar{\mathbf{H}}$, representing the contributions from mode n on modes $n-M$ to $n+M$
${}^{i}\widehat{\mathbf{H}}_{\underset{k}{n}}$, ${}^{i}\widehat{\mathbf{H}}_{\underset{k}{n}}$	k th constructing blocks of matrices ${}^{i}\mathbf{H}_n$ and ${}_{\mathrm{v}}^{i}\mathbf{H}_n$, respectively
$\bar{\mathbf{H}}_j^{xw}$	Consolidated coefficient matrix of j th component of the applied forces in homogeneous form of the boundary condition equations
$\mathbf{H}_j^{xw}$	Truncated coefficient matrix of j th component of the applied forces in homogeneous form of the boundary condition equations
$\mathbf{H}_{jn}^{xw}$	Horizontal constructing block matrix of matrix $\bar{\mathbf{H}}_j^{xw}$, representing the contributions from modes $n-M$ to $n+M$ on mode n
${}_{\mathrm{v}}\mathbf{H}_{jn}^{xw}$	Vertical constructing block matrix of matrix $\bar{\mathbf{H}}_j^{xw}$, representing the contributions from mode n on modes $n-M$ to $n+M$
${}_{\mathrm{v}}\widehat{\mathbf{H}}_{\underset{k}{jn}}^{xw}$, $\widehat{\mathbf{H}}_{\underset{k}{jn}}^{xw}$	k th constructing blocks of matrices $\mathbf{H}_{jn}^{xw}$ and ${}_{\mathrm{v}}\mathbf{H}_{jn}^{xw}$, respectively
$\mathbf{L}$	Matrix relating the integration constants vector $\tilde{\mathbf{A}}$ to nodal displacement vector $\boldsymbol{\Delta}$
$\mathbf{L}_n$	Matrix relating the integration constants vector $\tilde{\mathbf{A}}$ to nodal displacement vector $\boldsymbol{\Delta}_n$
$\mathbf{N}_{An}(x)$	Quasi-exact shape functions defining the axial, circumferential and radial displacements corresponding to mode n, respectively
$\mathbf{N}_{Bn}(x)$	
$\mathbf{N}_{Cn}(x)$	
$\mathbf{Q}_A^*, \mathbf{Q}_B^*, \mathbf{Q}_C^*,$	Matrices relating the nodal displacement vector $\boldsymbol{\Delta}$ to unknown displacement vectors $\mathbf{A}^*$, $\mathbf{B}^*$, $\mathbf{C}^*$, $\boldsymbol{\Lambda}$, $\boldsymbol{\Lambda}^*$
$\mathbf{Q}, \mathbf{Q}^*$	
$\mathbf{Q}_n, \mathbf{Q}_n^*$	Constructing block matrices of matrices $\mathbf{Q}$ and $\mathbf{Q}^*$, respectively
$\tilde{\mathrm{v}}_j$	j th eigenvector of the equivalent GEP

$\bar{\mathbf{X}}_{jn}^{\mathbf{xx}}$	Generic expression for matrices $\bar{\mathbf{H}}_j^{xw}$, $\bar{\mathbf{G}}_j^{xu}$, $\bar{\mathbf{G}}_j^{sv}$, $\bar{\mathbf{G}}_j^{zw}$, $\bar{\mathbf{G}}_j^{xw}$, $\bar{\mathbf{G}}_j^{sw}$
$\mathbf{X}_{jn}^{\mathbf{xx}}$	Generic expression for matrices $\mathbf{H}_j^{xw}$, $\mathbf{G}_j^{xu}$, $\mathbf{G}_j^{sv}$, $\mathbf{G}_j^{zw}$, $\mathbf{G}_j^{xw}$, $\mathbf{G}_j^{sw}$
$\mathbf{X}_{jn}^{\mathbf{xx}}$	Generic expression for matrices $\mathbf{G}_{jn}^{xu}$, $\mathbf{G}_{jn}^{sv}$, $\mathbf{G}_{jn}^{zw}$, $\mathbf{G}_{jn}^{xw}$, $\mathbf{G}_{jn}^{sw}$
${}_{\mathbf{v}}\mathbf{X}_{jn}^{\mathbf{xx}}$	Generic expression for matrices ${}_{\mathbf{v}}\mathbf{G}_{jn}^{xu}$, ${}_{\mathbf{v}}\mathbf{G}_{jn}^{sv}$, ${}_{\mathbf{v}}\mathbf{G}_{jn}^{zw}$, ${}_{\mathbf{v}}\mathbf{G}_{jn}^{xw}$, ${}_{\mathbf{v}}\mathbf{G}_{jn}^{sw}$
$\underset{k}{\widehat{\mathbf{X}}}_{jn}^{\mathbf{xx}}$	Generic expression for matrices $\underset{k}{\widehat{\mathbf{G}}}_{jn}^{xu}$, $\underset{k}{\widehat{\mathbf{G}}}_{jn}^{sv}$, $\underset{k}{\widehat{\mathbf{G}}}_{jn}^{zw}$, $\underset{k}{\widehat{\mathbf{G}}}_{jn}^{xw}$, $\underset{k}{\widehat{\mathbf{G}}}_{jn}^{sw}$
${}_{\mathbf{v}}\underset{k}{\widehat{\mathbf{X}}}_{jn}^{\mathbf{xx}}$	Generic expression for matrices ${}_{\mathbf{v}}\underset{k}{\widehat{\mathbf{G}}}_{jn}^{xu}$, ${}_{\mathbf{v}}\underset{k}{\widehat{\mathbf{G}}}_{jn}^{sv}$, ${}_{\mathbf{v}}\underset{k}{\widehat{\mathbf{G}}}_{jn}^{zw}$, ${}_{\mathbf{v}}\underset{k}{\widehat{\mathbf{G}}}_{jn}^{sw}$, ${}_{\mathbf{v}}\underset{k}{\widehat{\mathbf{G}}}_{jn}^{xw}$
$\mathbf{\Delta}$	Nodal displacement vector of the whole system
$\mathbf{\Delta}_n$	Nodal displacement vector for mode n
$\bar{\mathbf{\Lambda}}$	Consolidated nodal displacement vector
$\mathbf{\Lambda}$	Unknown displacement vector, including translational components
$\mathbf{\Lambda}^*$	Unknown displacement vector, including translational and rotational components
$\mathbf{\Lambda}_n$	Nodal displacement vector including displacement components from modes $n-M$ to $n+M$
$\widehat{\mathbf{\Lambda}}_n$	Displacement vector corresponding to mode n
$\mathbf{\Omega}(m)$	Polynomial eigenproblem of the system
γ	$R/\Re$
$\prod$	Mechanical energy of the system
ρ	Density of the mass
$\Re$	Torus radius
θ	s/R

ν	Poisson's ratio
χ	$1+z/R$
ζ	$1+\gamma\cos\theta$
ξ	$1+\gamma\chi\cos\theta$

Appendix 7.A Coefficients for the TTS-V2 Theory

Coefficients d_i and d_i^I were introduced in Eqs. 7.2-7.5 when defining the differential operators of the boundary condition equations based on the TTS-V2 theory. Unlike the CCTSs, these coefficients are functions of the circumferential coordinate θ

$$d_1 = -\zeta^{-1}\left(1+\kappa\gamma\zeta^{-1}\cos\theta\right) \quad , \quad d_2 = -\nu\left(1+\kappa\gamma\zeta^{-1}\cos\theta\right)$$
$$d_3 = \frac{1}{R}\gamma\zeta^{-1}\sin\theta \quad , \quad d_4 = R\kappa\zeta^{-2}$$
$$d_5 = R\nu\kappa\gamma\zeta^{-1}\cos\theta \quad , \quad d_6 = -\kappa\gamma\zeta^{-1}\sin\theta$$
$$d_7 = -\frac{1}{R}\left(\nu+\gamma\zeta^{-1}\cos\theta\right)$$

$$d_8 = -\frac{1-\nu}{2}\left(1+\kappa\gamma\zeta^{-1}\cos\theta\right)$$
$$d_9 = -\frac{1}{R}\frac{1-\nu}{2}\gamma\zeta^{-1}\sin\theta\left[1-\kappa\left(2-\gamma\zeta^{-1}\cos\theta\right)\right]$$
$$d_{10} = -\frac{1-\nu}{2}\zeta^{-1}\left(1-3\kappa\gamma\zeta^{-1}\cos\theta\right) \quad , \quad d_{11} = R\frac{1-\nu}{2}\kappa\zeta^{-1}\left(3-\gamma\zeta^{-1}\cos\theta\right)$$
$$d_{12} = \frac{1-\nu}{2}\kappa\gamma\zeta^{-2}\sin\theta\left(3-\gamma\zeta^{-1}\cos\theta\right)$$

$$d_{13} = -R\kappa\zeta^{-2} \quad , \quad d_{14} = R\frac{1-\nu}{2}\kappa\left(1-3\gamma\zeta^{-1}\cos\theta\right)$$
$$d_{15} = 3\frac{1-\nu}{2}\kappa\gamma\zeta^{-1}\sin\theta\left(1-\gamma\zeta^{-1}\cos\theta\right)$$
$$d_{16} = \frac{1}{R}\frac{1-\nu}{2}\kappa\gamma\zeta^{-1}\left[\cos\theta+3\gamma\zeta^{-1}\left(\sin^2\theta-\cos^2\theta-\gamma\zeta^{-1}\sin^2\theta\cos\theta\right)\right]$$
$$d_{16}^I = \frac{1-\nu^2}{E}R\rho\kappa\left(1+4\gamma\cos\theta+3\gamma^2\cos^2\theta\right)$$

$$d_{17} = -R\kappa\zeta^{-1}\left(\frac{3-\nu}{2}-\frac{1-\nu}{2}\gamma\zeta^{-1}\cos\theta\right)$$
$$d_{18} = \kappa\gamma\zeta^{-2}\sin\theta\left(\frac{3+\nu}{2}-\frac{1+\nu}{2}\gamma\zeta^{-1}\sin\theta\cos\theta\right)$$
$$d_{19} = R^2\kappa\zeta^{-3} \quad , \quad d_{20} = R^2\left(2-\nu\right)\kappa\zeta^{-1}$$
$$d_{21} = R\left(1-2\nu\right)\kappa\gamma\zeta^{-2}\sin\theta$$
$$d_{22} = 2\left(1-\nu\right)\kappa\gamma\zeta^{-3}\left(\gamma+\frac{1-2\nu}{2-2\nu}\cos\theta\right)$$
$$d_{22}^I = -\frac{1-\nu^2}{E}R^2\rho\kappa\zeta$$

$$d_{23} = R\kappa\zeta^{-2} \quad , \quad d_{24} = R\nu\kappa\zeta^{-1}$$
$$d_{25} = -\kappa\gamma\zeta^{-2}\sin\theta\left(2-\gamma\zeta^{-1}\cos\theta\right) \quad , \quad d_{26} = -R^2\kappa\zeta^{-3}$$
$$d_{27} = -R^2\nu\kappa\zeta^{-1} \quad , \quad d_{28} = R\kappa\gamma\zeta^{-2}\sin\theta$$
$$d_{29} = \kappa\gamma\zeta^{-2}\cos\theta\left(1-\gamma\zeta^{-1}\cos\theta\right)$$

The coefficients l_i and l_i^I introduced in Eqs. 7.6-7.8 in defining the differential operators of the field equations of the TTS-V2 theory are defined as

$$l_1 = \left(\zeta^{-1} + \kappa\gamma\zeta^{-2}\sin\theta\cos^2\theta\right) \quad , \quad l_2 = \left(\frac{1-\nu}{2}\right)\left[1+(1-3\kappa)\gamma\cos\theta\right]$$
$$l_3 = \frac{1}{R}\left(\frac{1-\nu}{2}\right)\left[(-1+4\kappa)\gamma\sin\theta - 6\kappa\gamma^2\zeta^{-1}\sin\theta\cos\theta + 8\kappa\gamma^3\zeta^{-2}\sin\theta\cos^2\theta\right]$$
$$l_4 = \frac{1}{R^2}\left(\frac{1-\nu}{2}\right)\left[(1+2\kappa)\gamma\cos\theta - (1-2\kappa)\gamma^2\zeta^{-1}\sin^2\theta - 3\kappa\gamma^2\zeta^{-1}\cos^2\theta \right.$$
$$\left. +4\kappa\gamma^3\zeta^{-2}\cos\theta - 10\kappa\gamma^3\zeta^{-2}\sin^2\theta\cos\theta + 4\kappa\gamma^4\zeta^{-3}\sin^2\theta\cos^2\theta\right]$$
$$l_4^I = -\frac{1-\nu^2}{E}\rho\left\{1+\left[2+(1+\kappa)\left(1+\gamma^2\right)\right]\gamma\cos\theta + (3+2\kappa)\gamma^2\cos^2\theta \right.$$
$$\left. -(1+\kappa)\gamma^3\sin^2\theta\cos\theta \right\}$$
$$l_5 = \left(\frac{1+\nu}{2}\right)\left(1+\kappa\gamma\zeta^{-1}\cos\theta\right) \quad , \quad l_6 = -\left(\frac{3-\nu}{2}\right)\frac{\gamma}{R}\zeta^{-1}\sin\theta$$
$$l_7 = -R\kappa\zeta^{-2} \quad , \quad l_8 = R\left[\left(\frac{1-\nu}{2}\right)\kappa\zeta^{-1} - \kappa\gamma\zeta^{-1}\cos\theta\right]$$
$$l_9 = \left(\frac{5-3\nu}{2}\right)\kappa\gamma\zeta^{-2}\sin\theta + \kappa\gamma^2\zeta^{-2}\sin\theta\cos\theta$$
$$l_{10} = \frac{1}{R}\left[\nu + \left(1+\kappa\frac{1-\nu}{2}\right)\gamma\zeta^{-1}\cos\theta + 3\left(\frac{1-\nu}{2}\right)\kappa\gamma^2\zeta^{-2}\sin^2\theta - 3\left(\frac{1-\nu}{2}\right)\kappa\gamma^2\zeta^{-2}\cos^2\theta \right.$$
$$\left. -3\left(\frac{1-\nu}{2}\right)\kappa\gamma^3\zeta^{-3}\sin^2\theta\cos\theta\right]$$
$$l_{10}^I = \frac{1-\nu^2}{E}R\rho\kappa\left(1+4\gamma\cos\theta+3\gamma^2\cos^2\theta\right)$$

$$l_{11} = \left(\frac{1+\nu}{2}\right)\left(1+\kappa\gamma\zeta^{-1}\cos\theta\right)$$

$$l_{12} = \frac{1}{R}\left[\left(\frac{3-\nu}{2}\right)\gamma\zeta^{-1}\sin\theta - (1+\nu)\kappa\gamma\zeta^{-2}\sin\theta - \left(\frac{1+\nu}{2}\right)\kappa\gamma^2\zeta^{-2}\sin\theta\cos\theta\right]$$

$$l_{13} = \left(\frac{1-\nu}{2}\right)\left(\zeta^{-1} - 3\kappa\gamma\zeta^{-2}\cos\theta\right) \quad , \quad l_{14} = \left[1+(1+\kappa)\gamma\cos\theta\right]$$

$$l_{15} = -\frac{\gamma}{R}\sin\theta$$

$$l_{16} = -\frac{1}{R^2}\left(\nu\gamma\cos\theta + \gamma^2\zeta^{-1}\sin^2\theta - 3\kappa\gamma^3\zeta^{-2}\sin^2\theta\cos\theta\right)$$

$$l_{16}^I = -\frac{1-\nu^2}{E}\rho\left[1+(1+3\kappa)\gamma\cos\theta\right] \quad , \quad l_{17} = -R\kappa\gamma\cos\theta$$

$$l_{18} = -R\left[\left(\frac{3-\nu}{2}\right)\kappa\zeta^{-1} - \left(\frac{1-\nu}{2}\right)\kappa\gamma\zeta^{-2}\cos\theta\right]$$

$$l_{19} = -\left[\left(\frac{7-\nu}{2}\right)\kappa\gamma\zeta^{-3}\sin\theta + 2\kappa\gamma^2\zeta^{-3}\sin\theta\cos\theta\right]$$

$$l_{20} = \kappa\gamma\sin\theta$$

$$l_{21} = \frac{1}{R}\left\{1+\left[1+\nu(1+\kappa)\right]\gamma\cos\theta + 2\kappa\gamma^2\zeta^{-1}\sin^2\theta - \kappa\gamma^3\zeta^{-2}\sin^2\theta\cos\theta\right\}$$

$$l_{21}^I = \frac{1-\nu^2}{E}R\rho\kappa\left(2+3\gamma\cos\theta\right)$$

$$l_{22} = -\frac{1}{R^2}\left(\nu\gamma\zeta^{-1}\sin\theta - \nu\kappa\gamma^2\zeta^{-2}\sin\theta\cos\theta\right)$$

$$l_{23} = R\kappa\zeta^{-2} \quad , \quad l_{24} = R\left[-\left(\frac{1-\nu}{2}\right)\kappa + \left(\frac{3-\nu}{2}\right)\kappa\gamma\zeta^{-1}\cos\theta\right]$$

$$l_{25} = \left[-\left(\frac{1+\nu}{2}\right)\kappa\gamma\zeta^{-1}\sin\theta + \left(\frac{3+\nu}{2}\right)\kappa\gamma^2\zeta^{-2}\sin\theta\cos\theta\right]$$

$$l_{26} = \frac{1}{R}\left\{-\nu - \left[1+\left(\frac{1-\nu}{2}\right)\kappa\right]\gamma\zeta^{-1}\cos\theta + \left(\frac{3-\nu}{2}\right)\kappa\gamma^2\zeta^{-2} + 2\kappa\gamma^2\zeta^{-2}\sin^2\theta + \left(\frac{3+\nu}{2}\right)\kappa\gamma^3\zeta^{-3}\sin^2\theta\cos\theta\right\}$$

$$l_{26}^I = -\frac{1-\nu^2}{E}R\rho\kappa\left(1+4\gamma\cos\theta+3\gamma^2\cos^2\theta\right) \quad , \quad l_{27} = R\kappa\gamma\cos\theta$$

$$l_{28} = R\left[\left(\frac{3-\nu}{2}\right)\kappa\zeta^{-1} - \left(\frac{1-\nu}{2}\right)\kappa\gamma\zeta^{-2}\cos\theta\right]$$

$$l_{29} = \left[-\left(\frac{3+\nu}{2}\right)\kappa\gamma\zeta^{-2}\sin\theta + \left(\frac{1+\nu}{2}\right)\kappa\gamma^2\zeta^{-3}\sin\theta\cos\theta\right]$$

$$l_{30} = -2\kappa\gamma\sin\theta$$

$$l_{31} = \frac{1}{R}\left[-1-(1+\nu)(1+\kappa)\gamma\cos\theta - 2\kappa\gamma^2\zeta^{-1}\sin^2\theta + \kappa\gamma^3\zeta^{-2}\sin^2\theta\cos\theta\right]$$

$$l_{31}^I = -\frac{1-\nu^2}{E}R\rho\kappa\left(2+3\gamma\cos\theta\right)$$

$$l_{32}=\frac{1}{R^2}\Big[\nu\left(1+\kappa\right)\gamma\sin\theta+\left(1-4\kappa\right)\gamma^2\zeta^{-1}\sin\theta\cos\theta-\kappa\gamma^3\zeta^{-2}\sin\theta$$
$$+\kappa\gamma^3\zeta^{-2}\sin\theta\cos^2\theta-2\kappa\gamma^3\zeta^{-3}\sin\theta+2\kappa\gamma^3\zeta^{-3}\sin\theta\cos^2\theta\Big]$$
$$l_{32}^I=\frac{1-\nu^2}{E}3\rho\kappa\gamma\sin\theta \quad , \quad l_{33}=-R^2\kappa\zeta^{-3}$$
$$l_{34}=-R^2\kappa\zeta \quad , \quad l_{35}=-2R^2\kappa\zeta^{-1}$$
$$l_{36}=2R\kappa\gamma\sin\theta \quad , \quad l_{37}=-2R\kappa\gamma\zeta^{-2}\sin\theta$$
$$l_{38}=\Big[-\left(1-\nu\right)\kappa\gamma\zeta^{-2}\cos\theta-2\kappa\gamma^2\zeta^{-3}-2\kappa\gamma^2\zeta^{-3}\sin^2\theta\Big]$$
$$l_{38}^I=\frac{1-\nu^2}{E}R^2\rho\kappa\zeta$$
$$l_{39}=\Big[-2\kappa+\left(1+\nu\right)\kappa\gamma\cos\theta+\kappa\gamma^2\zeta^{-1}\sin^2\theta\Big] \quad , \quad l_{39}^I=\frac{1-\nu^2}{E}R^2\rho\kappa\zeta$$
$$l_{40}=\frac{1}{R}\left(-\nu\kappa\gamma\sin\theta+\kappa\gamma^2\zeta^{-1}\sin\theta\cos\theta+\kappa\gamma^3\zeta^{-2}\sin\theta+\nu\kappa\gamma^2\zeta^{-2}\sin\theta\cos\theta\right)$$
$$l_{40}^I=-\frac{1-\nu^2}{E}R\rho\kappa\gamma\sin\theta$$
$$l_{41}=\frac{1}{R^2}\Big[-1-\left(1+2\nu-\kappa\right)\gamma\cos\theta-\gamma^2\zeta^{-1}\cos^2\theta-\nu\kappa\gamma^2\zeta^{-2}+2\nu\kappa\gamma^2\zeta^{-2}\cos^2\theta$$
$$+\kappa\gamma^3\zeta^{-2}\cos\theta-\kappa\gamma^3\zeta^{-2}\sin^2\theta\cos\theta+2\nu\kappa\gamma^3\zeta^{-3}\sin^2\theta\cos\theta\Big]$$
$$l_{41}^I=-\frac{1-\nu^2}{E}\rho\Big[1+\left(1+\kappa\right)\gamma\cos\theta\Big]$$

The coefficients f_i^F and forces f_1^{xu}, f_2^{xu}, f_1^{sv}, f_2^{sv}, f_1^{zw}, f_2^{zw}, f_1^{xw}, f_2^{xw}, f_1^{sw} and f_2^{sw} introduced in Eq. 7.9 in defining the differential operators of the applied forces of the TTS-V2 theory are defined as

$$f_1^F=-\frac{1-\nu^2}{Eh} \quad , \quad f_2^F=-\frac{1-\nu^2}{Eh}\frac{1}{R}\gamma\zeta^{-1}\cos\theta$$
$$f_3^F=\frac{1-\nu^2}{Eh}\zeta \quad , \quad f_4^F=\frac{1-\nu^2}{Eh}\frac{2}{R}\gamma\cos\theta$$
$$f_5^F=\frac{1-\nu^2}{Eh} \quad , \quad f_6^F=\frac{1-\nu^2}{Eh}\gamma\cos\theta$$
$$f_7^F=\frac{1-\nu^2}{Eh} \quad , \quad f_8^F=\frac{1-\nu^2}{Eh}\gamma\cos\theta$$
$$f_9^F=\frac{1-\nu^2}{Eh} \quad , \quad f_{10}^F=\frac{1-\nu^2}{Eh}\frac{1}{R}\gamma\zeta^{-1}\cos\theta$$
$$f_{11}^F=\frac{1-\nu^2}{Eh}\gamma\cos\theta \quad , \quad f_{12}^F=-\frac{1-\nu^2}{Eh}\frac{1}{R}\gamma\sin\theta$$
$$f_{13}^F=\frac{1-\nu^2}{Eh}$$

$$f_1^{xu} = \int_{-\frac{h}{2}}^{\frac{h}{2}} p^x \left(1+\frac{z}{R}\right) dz \quad , \quad f_2^{xu} = \int_{-\frac{h}{2}}^{\frac{h}{2}} p^x z \left(1+\frac{z}{R}\right) dz$$

$$f_1^{xw} = \int_{-\frac{h}{2}}^{\frac{h}{2}} p^x z \left(1+\frac{z}{R}\right) dz \quad , \quad f_2^{xw} = \int_{-\frac{h}{2}}^{\frac{h}{2}} p^x z^2 \left(1+\frac{z}{R}\right) dz$$

$$f_1^{sv} = \int_{-\frac{h}{2}}^{\frac{h}{2}} p^s \left(1+2\frac{z}{R}\right) dz \quad , \quad f_2^{sv} = \int_{-\frac{h}{2}}^{\frac{h}{2}} p^s \left(1+3\frac{z}{R}\right) dz$$

$$f_1^{sw} = \int_{-\frac{h}{2}}^{\frac{h}{2}} p^s z \left(1+2\frac{z}{R}\right) dz \quad , \quad f_2^{sw} = \int_{-\frac{h}{2}}^{\frac{h}{2}} p^s z \left(1+\frac{z}{R}\right) dz$$

$$f_1^{zw} = \int_{-\frac{h}{2}}^{\frac{h}{2}} p^z \left(1+\frac{z}{R}\right) dz \quad , \quad f_2^{zw} = \int_{-\frac{h}{2}}^{\frac{h}{2}} p^z \left(1+2\frac{z}{R}\right) dz$$

Appendix 7.B Coefficient Matrices in the Functional

In the following subsections all non-zero entries of matrices ${}^{i}_{\mathrm{v}}\mathbf{H}_{n}$, ${}^{i}_{\mathrm{v}}\mathbf{G}_{n}$, ${}_{\mathrm{v}}\mathbf{H}^{xw}_{j.n}$, ${}_{\mathrm{v}}\mathbf{G}^{xu}_{j.n}$, ${}_{\mathrm{v}}\mathbf{G}^{sv}_{j.n}$, ${}_{\mathrm{v}}\mathbf{G}^{zw}_{j.n}$, ${}_{\mathrm{v}}\mathbf{G}^{xw}_{j.n}$ and ${}_{\mathrm{v}}\mathbf{G}^{sw}_{j.n}$, introduced in Sections 7.6.4 and 7.9.2 , are explicitly defined for $M = 7$. The block diagram in Figure 7.12 schematically illustrates the whole process of evaluating these Matrices.

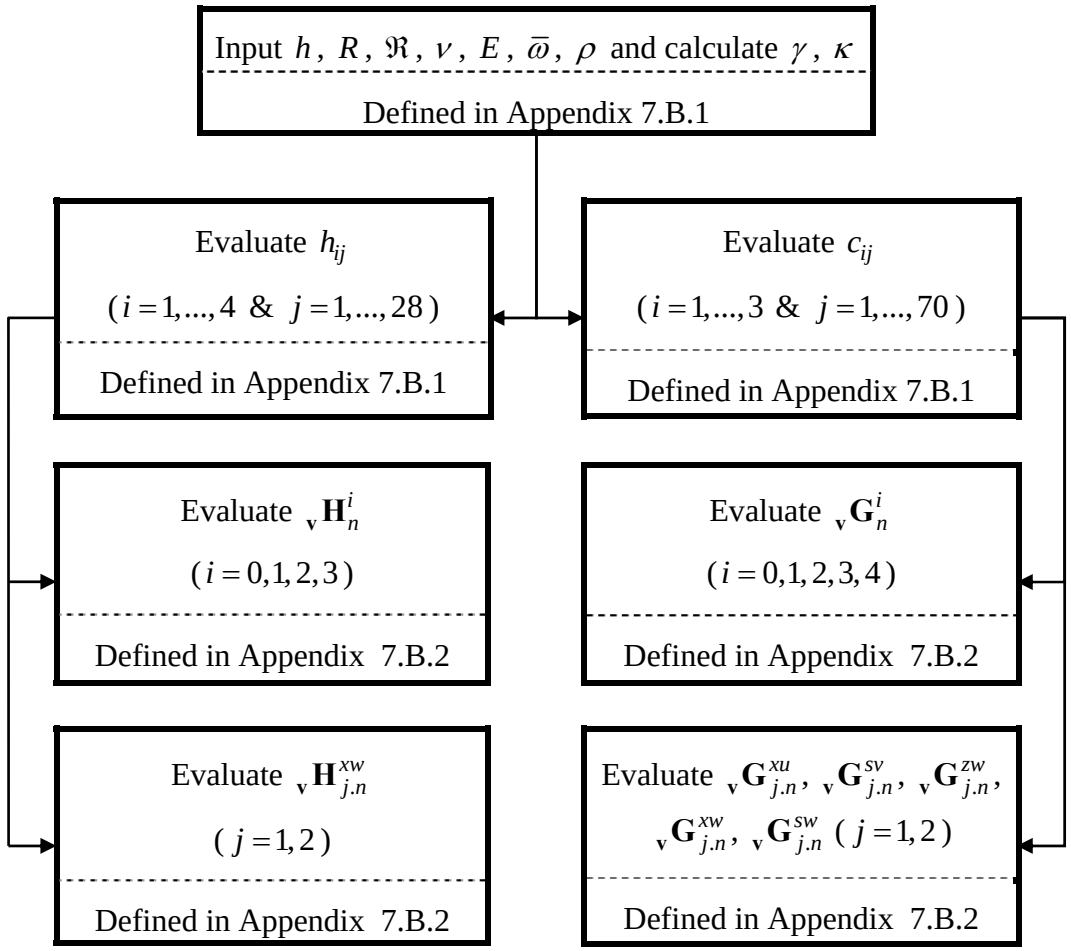

Figure 7.12 – Block diagram of the evaluation of constant matrices ${}_{\mathrm{v}}\mathbf{H}^{i}_{n}$, ${}_{\mathrm{v}}\mathbf{G}^{i}_{n}$, ${}_{\mathrm{v}}\mathbf{H}^{xw}_{j.n}$, ${}_{\mathrm{v}}\mathbf{G}^{xu}_{j.n}$, ${}_{\mathrm{v}}\mathbf{G}^{sv}_{j.n}$, ${}_{\mathrm{v}}\mathbf{G}^{zw}_{j.n}$, ${}_{\mathrm{v}}\mathbf{G}^{xw}_{j.n}$ and ${}_{\mathrm{v}}\mathbf{G}^{sw}_{j.n}$

7.B.1 Explicit Expressions for c_{ij} and h_{ij}

In this section the constants c_{ij} and h_{ij} are explicitly defined. Constants c_{ij} are related to the field equations of the system where $i=1,2,3$ denotes the equation number and $j=1,...,70$ denotes the term number within each equation. Constants h_{ij} are related to the boundary condition equations of the system where $i=1,2,3,4$ denotes the equation number and $j=1,...,28$ denotes the term number within each equation. Since these constants and the other constants to be explicitly defined in the following sections are generated by codes written in MATLAB, the font conversions in Table 7.2 are introduced.

Table 7.2 – Geometric and mechanical properties of the toroid and their equivalent in MATLAB codes

Symbol in the text	R	κ	γ	E	ν	$\bar{\omega}$	ρ	c_{ij}	h_{ij}
Equivalent in MATLAB	**R**	**kapa**	**gama**	**E**	**nu**	**omega**	**Ro**	**cij**	**hij**

7.B.1.1 Explicit Expressions for h_{ij}

The following constants appear in the first natural boundary condition equation of the system, D_{1j}.

```
h11=-1
h12=-kapa*gama
h13=1/R*gama
h14=-nu
h15=-nu*kapa*gama
h16=-1/R*nu
```

```
h17=-1/R*gama

h18=-kapa*gama

h19=R*kapa

h110=R*nu*kapa*gama
```

The following constants appear in the first natural boundary condition equation of the system, D_{2j}.

```
h21=-(1-nu)/2/R*(1-2*kapa)*gama

h22=-(1-nu)/2/R*kapa*gama^2

h23=-(1-nu)/2

h24=-(1-nu)/2*kapa*gama

h25=-(1-nu)/2

h26=+(1-nu)/2*3*kapa*gama

h27=+(1-nu)/2*3*kapa*gama

h28=-(1-nu)/2*kapa*gama^2

h29=+(1-nu)/2*R*3*kapa

h210=-(1-nu)/2*R*kapa*gama
```

The following constants appear in the first natural boundary condition equation of the system, D_{3j}.

```
h31=+1/R*(1-nu)/2*kapa*gama

h32=+1/R*(1-nu)/2*kapa*gama^2

h33=+1/R*(1-nu)/2*2*kapa*gama^2

h34=-1/R*(1-nu)/2*4*kapa*gama^2

h35=-1/R*(1-nu)/2*3*kapa*gama^3

h36=+(1-nu)/2*3*kapa*gama

h37=-(1-nu)/2*3*kapa*gama^2

h38=-R*kapa
```

```
h39=+R*(1-nu)/2*kapa

h310=-R*(1-nu)/2*3*kapa*gama

h311=+(3+nu)/2*kapa*gama

h312=-(1+nu)/2*kapa*gama^2

h313=-R*(3-nu)/2*kapa

h314=+R*(1-nu)/2*kapa*gama

h315=+(1-2*nu)*kapa*gama

h316=+(3-2*nu)/2*kapa*gama^2

h317=+(1-nu)/2*kapa*gama^2

h318=-(1-nu)/2*kapa*gama^2

h319=+R*(1-2*nu)*kapa*gama

h320=+R^2*kapa

h321=+R^2*(2-nu)*kapa

h322=-(1-nu^2)/E*Ro*omega^2*R*kapa

h323=-(1-nu^2)/E*Ro*omega^2*R*kapa*4*gama

h324=-(1-nu^2)/E*Ro*omega^2*R*kapa*3*gama^2

h325=+(1-nu^2)/E*Ro*omega^2*R^2*kapa

h326=+(1-nu^2)/E*Ro*omega^2*R^2*kapa*gama

h327=-(1-nu^2)/E/h

h328=-(1-nu^2)/E/h/R*gama
```

The following constants appear in the first natural boundary condition equation of the system, D_{4j}.

```
h41=R*kapa

h42=-2*kapa*gama

h43=kapa*gama^2

h44=R*nu*kapa

h45=kapa*gama
```

```
h46=-kapa*gama^2

h47=R*kapa*gama

h48=-R^2*kapa

h49=-R^2*nu*kapa
```

7.B.1.2 Explicit Expressions for c_{ij}

The following constants appear in the first field equation of the system, L_{1j}.

```
c11=+1/R^2*(1-nu)/2*gama * (1+2*kapa)

c12=-1/R^2*(1-nu)/2*(1-2*kapa)*gama^2

c13=-1/R^2*(1-nu)/2*3*kapa*gama^2

c14=+1/R^2*(1-nu)/2*4*kapa*gama^3

c15=-1/R^2*(1-nu)/2*10*kapa*gama^3

c16=+1/R^2*(1-nu)/2*4*kapa*gama^4

c17=+1/R*(1-nu)/2*(-1+4*kapa)*gama

c18=-1/R*(1-nu)/2*6*kapa*gama^2

c19=+1/R*(1-nu)/2*8*kapa*gama^3

c110=1

c111=kapa*gama

c112=(1-nu)/2

c113=(1-nu)/2*(1-3*kapa)*gama

c114=-(3-nu)/2*gama/R

c115=(1+nu)/2

c116=(1+nu)/2*kapa*gama

c117=nu/R

c118=+1/R*(1+(1-nu)/2*kapa)*gama

c119=+1/R*3*(1-nu)/2*kapa*gama^2

c120=-1/R*3*(1-nu)/2*kapa*gama^2
```

```
c121=-1/R*3*(1-nu)/2*kapa*gama^3

c122=(5-3*nu)/2*kapa*gama

c123=kapa*gama^2

c124=-R*kapa

c125=R*(1-nu)/2*kapa

c126=-R*kapa*gama

c127=+(1-nu^2)/E*Ro*omega^2

c128=+(1-nu^2)/E*Ro*omega^2*(2+(1+kapa)*(1+gama^2))*gama

c129=+(1-nu^2)/E*Ro*omega^2*(3+2*kapa)*gama^2

c130=-(1-nu^2)/E*Ro*omega^2*(1+kapa)*gama^3

c131=-(1-nu^2)/E*Ro*omega^2*R*kapa

c132=-(1-nu^2)/E*Ro*omega^2*R*kapa*4*gama

c133=-(1-nu^2)/E*Ro*omega^2*R*kapa*3*gama^2

c134=+(1-nu^2)/E/h

c135=+(1-nu^2)/E/h*gama

c136=+(1-nu^2)/E/h*2/R*gama
```

The following constants appear in the first field equation of the system, L_{2j}.

```
c21=+1/R*(3-nu)/2*gama

c22=-1/R*(1+nu)*kapa*gama

c23=-1/R*(1+nu)/2*kapa*gama^2

c24=(1+nu)/2

c25=(1+nu)/2*kapa*gama

c26=-1/R^2*nu*gama

c27=-1/R^2*gama^2

c28=+1/R^2*3*kapa*gama^3

c29=-gama/R

c210=(1-nu)/2
```

```
c211=-(1-nu)/2*3*kapa*gama

c212=1

c213=(1+kapa)*gama

c214=-1/R^2*nu*gama

c215=1/R^2*nu*kapa*gama^2

c216=1/R

c217=1/R*(1+nu*(1+kapa))*gama

c218=1/R*2*kapa*gama^2

c219=-1/R*kapa*gama^3

c220=-(7-nu)/2*kapa*gama

c221=-2*kapa*gama^2

c222=kapa*gama

c223=-R*(3-nu)/2*kapa

c224=R*(1-nu)/2*kapa*gama

c225=-R*kapa*gama

c226=+(1-nu^2)/E*Ro*omega^2

c227=+(1-nu^2)/E*Ro*omega^2*(1+3*kapa)*gama

c228=-(1-nu^2)/E*Ro*omega^2*R*kapa*2

c229=-(1-nu^2)/E*Ro*omega^2*R*kapa*3*gama

c230=+(1-nu^2)/E/h

c231=(1-nu^2)/E/h*gama
```

The following constants appear in the first field equation of the system, L_{3j}.

```
c31=-1/R*nu

c32=-1/R*(1+(1-nu)/2*kapa)*gama

c33=+1/R*(3-nu)/2*kapa*gama^2

c34=+1/R*2*kapa*gama^2

c35=+1/R*(3+nu)/2*kapa*gama^3
```

```
c36=-(1+nu)/2*kapa*gama

c37=(3+nu)/2*kapa*gama^2

c38=R*kapa

c39=-R*(1-nu)/2*kapa

c310=R*(3-nu)/2*kapa*gama

c311=+1/R^2*nu*(1+kapa)*gama

c312=+1/R^2*(1-4*kapa)*gama^2

c313=-1/R^2*kapa*gama^3

c314=+1/R^2*kapa*gama^3

c315=-1/R^2*2*kapa*gama^3

c316=+1/R^2*2*kapa*gama^3

c317=-1/R

c318=-1/R*(1+nu)*(1+kapa)*gama

c319=-1/R*2*kapa*gama^2

c320=+1/R*kapa*gama^3

c321=-(3+nu)/2*kapa*gama

c322=+(1+nu)/2*kapa*gama^2

c323=-2*kapa*gama

c324=R*(3-nu)/2*kapa

c325=-R*(1-nu)/2*kapa*gama

c326=R*kapa*gama

c327=-1/R^2

c328=-1/R^2*(1+2*nu-kapa)*gama

c329=-1/R^2*gama^2

c330=-1/R^2*nu*kapa*gama^2

c331=+1/R^2*2*nu*kapa*gama^2

c332=+1/R^2*kapa*gama^3

c333=-1/R^2*kapa*gama^3
```

```
c334=+1/R^2*2*nu*kapa*gama^3

c335=-1/R*nu*kapa*gama

c336=+1/R*kapa*gama^2

c337=+1/R*kapa*gama^3

c338=+1/R*2*nu*kapa*gama^2

c339=-(1-nu)*kapa*gama

c340=-2*kapa*gama^2

c341=-2*kapa*gama^2

c342=-2*kapa

c343=(1+nu)*kapa*gama

c344=kapa*gama^2

c345=-2*R*kapa*gama

c346=2*R*kapa*gama

c347=-R^2*kapa

c348=-2*R^2*kapa

c349=-R^2*kapa

c350=-R^2*kapa*gama

c351=+(1-nu^2)/E*Ro*omega^2

c352=+(1-nu^2)/E*Ro*omega^2*(1+kapa)*gama

c353=-(1-nu^2)/E*Ro*omega^2*3*kapa*gama

c354=+(1-nu^2)/E*Ro*omega^2*R*kapa

c355=+(1-nu^2)/E*Ro*omega^2*R*kapa*4*gama

c356=+(1-nu^2)/E*Ro*omega^2*R*kapa*3*gama^2

c357=+(1-nu^2)/E*Ro*omega^2*R*kapa*2

c358=+(1-nu^2)/E*Ro*omega^2*R*kapa*3*gama

c359=+(1-nu^2)/E*Ro*omega^2*R*kapa*gama

c360=-(1-nu^2)/E*Ro*omega^2*R^2*kapa

c361=-(1-nu^2)/E*Ro*omega^2*R^2*kapa*gama
```

```
c362=-(1-nu^2)/E*Ro*omega^2*R^2*kapa

c363=-(1-nu^2)/E*Ro*omega^2*R^2*kapa*gama

c364=+(1-nu^2)/E/h

c365=+(1-nu^2)/E/h*gama

c366=+(1-nu^2)/E/h

c367=+(1-nu^2)/E/h/R*gama

c368=-(1-nu^2)/E/h/R*gama

c369=+(1-nu^2)/E/h*gama

c370=-(1-nu^2)/E/h
```

7.B.2 Entries of Matrices ${}_{\mathrm{v}}\mathbf{H}_{n}^{i}$, ${}_{\mathrm{v}}\mathbf{G}_{n}^{i}$, ${}_{\mathrm{v}}\mathbf{H}_{j.n}^{xw}$, ${}_{\mathrm{v}}\mathbf{G}_{j.n}^{xu}$, ${}_{\mathrm{v}}\mathbf{G}_{j.n}^{sv}$, ${}_{\mathrm{v}}\mathbf{G}_{j.n}^{zw}$, ${}_{\mathrm{v}}\mathbf{G}_{j.n}^{xw}$ and ${}_{\mathrm{v}}\mathbf{G}_{j.n}^{sw}$

In this section the entries of matrices ${}_{\mathrm{v}}\mathbf{H}_{n}^{i}$, ${}_{\mathrm{v}}\mathbf{G}_{n}^{i}$, ${}_{\mathrm{v}}\mathbf{H}_{j.n}^{xw}$, ${}_{\mathrm{v}}\mathbf{G}_{j.n}^{xu}$, ${}_{\mathrm{v}}\mathbf{G}_{j.n}^{sv}$, ${}_{\mathrm{v}}\mathbf{G}_{j.n}^{zw}$, ${}_{\mathrm{v}}\mathbf{G}_{j.n}^{xw}$ and ${}_{\mathrm{v}}\mathbf{G}_{j.n}^{sw}$, where $j=1,2$, are explicitly defined. In this regard, the new symbol $a=i\frac{n}{R}$, in which the symbol "i" is the imaginary unit vector, is introduced. Also symbols R_{ij} are introduced, where constants R_{ij} are defined in the Fourier expansion series $\zeta^{-i}=\sum_{j=0}^{5}R_{ij}\cos\left(j\theta\right)$, where $i=1,2,3$. Similar to the previous section the font conversions in Table 7.3 are introduced to relate MATLAB generated expressions to symbols adopted in the text.

Table 7.3 – Font conversion between the text symbols and their equivalent in MATLAB codes

Symbol in the text	i	a	R_{ij}	${}_{\mathbf{v}}\mathbf{H}_{n}^{i}$	${}_{\mathbf{v}}\mathbf{G}_{n}^{i}$	${}_{\mathbf{v}}\mathbf{H}_{j.n}^{xw}$	${}_{\mathbf{v}}\mathbf{G}_{j.n}^{xu}$	${}_{\mathbf{v}}\mathbf{G}_{j.n}^{sv}$	${}_{\mathbf{v}}\mathbf{G}_{j.n}^{zw}$	${}_{\mathbf{v}}\mathbf{G}_{j.n}^{xw}$	${}_{\mathbf{v}}\mathbf{G}_{j.n}^{sw}$
Equivalent in MATLAB	`i`	`a`	`Rij`	`Hni`	`Gni`	`Hjnxw`	`Gjnxu`	`Gjnsv`	`Gjnzw`	`Gjnxw`	`Gjnsw`

7.B.2.1 Entries of ${}_{\mathbf{v}}\mathbf{H}_{n}^{0}$

```
Hn0(2,1)=0.125*R25*h22*i

Hn0(3,1)=0.125*R25*h34    -    0.125*R25*h33    -    0.0625*R34*h35    +
         0.125*R25*a*h37*i

Hn0(4,2)=0.125*R35*h43*i

Hn0(4,3)=0.125*R35*h46

Hn0(5,2)=0.25*R15*a*h15 + 0.25*R15*h13*i

Hn0(5,3)=0.25*R15*h110*a^2 + 0.25*R15*h18*i*a + 0.25*R15*h17

Hn0(6,1)=0.25*R15*a*h24 + 0.25*R15*h21*i + 0.125*R24*h22*i

Hn0(7,1)=0.25*R15*h31 - 0.125*R24*h33 + 0.125*R24*h34 - 0.0625*R33*h35 +
         0.0625*R35*h35   +   0.25*R15*a^2*h310   +   0.25*R15*a*h36*i   +
         0.125*R24*a*h37*i

Hn0(8,2)=0.25*R25*h42*i + 0.125*R34*h43*i

Hn0(8,3)=0.25*R25*h45 + 0.125*R34*h46 + 0.25*R25*a*h47*i

Hn0(9,2)=0.25*R14*a*h15 + 0.25*R14*h13*i

Hn0(9,3)=0.25*R14*h110*a^2 + 0.25*R14*h18*i*a + 0.25*R14*h17

Hn0(10,1)=0.25*R14*a*h24 + 0.25*R14*h21*i + 0.125*R23*h22*i

Hn0(11,1)=0.25*R14*h31 - 0.125*R23*h33 + 0.125*R23*h34 + 0.5*R25*h32 +
         0.25*R25*h33 + 0.25*R25*h34 - 0.0625*R32*h35 + 0.0625*R34*h35 +
         0.25*R14*a^2*h310 + 0.25*R14*a*h36*i + 0.125*R23*a*h37*i

Hn0(12,2)=0.5*R15*a*h44 + 0.25*R24*h42*i + 0.125*R33*h43*i

Hn0(12,3)=0.5*R15*h49*a^2    +    0.25*R24*h47*i*a    +    0.25*R24*h45    +
         0.125*R33*h46 + 0.25*R35*h46
```

```
Hn0(13,2)=0.25*R13*a*h15    +    0.25*R15*a*h15    +    0.25*R13*h13*i    -
         0.25*R15*h13*i

Hn0(13,3)=0.25*R13*h17    +    0.25*R15*h17    +    0.25*R13*a^2*h110    +
         0.25*R15*a^2*h110 + 0.25*R13*a*h18*i - 0.25*R15*a*h18*i

Hn0(14,1)=0.25*R13*a*h24    +    0.25*R15*a*h24    +    0.25*R13*h21*i    -
         0.25*R15*h21*i + 0.125*R22*h22*i

Hn0(15,1)=0.25*R13*h31 + 0.25*R15*h31 - 0.125*R22*h33 + 0.125*R22*h34 +
         0.5*R24*h32 + 0.25*R24*h33 + 0.25*R24*h34 - 0.0625*R31*h35 +
         0.0625*R33*h35    +    0.0625*R35*h35    +    0.25*R13*a^2*h310    +
         0.25*R15*a^2*h310   +   0.25*R13*a*h36*i   -   0.25*R15*a*h36*i   +
         0.125*R22*a*h37*i

Hn0(16,2)=0.5*R14*a*h44    +    0.25*R23*h42*i    -    0.25*R25*h42*i    +
         0.125*R32*h43*i

Hn0(16,3)=0.25*R23*h45 + 0.25*R25*h45 + 0.125*R32*h46 + 0.25*R34*h46 +
         0.5*R14*a^2*h49 + 0.25*R23*a*h47*i - 0.25*R25*a*h47*i

Hn0(17,2)=0.25*R12*a*h15    +    0.25*R14*a*h15    +    0.25*R12*h13*i    -
         0.25*R14*h13*i

Hn0(17,3)=0.25*R12*h17    +    0.25*R14*h17    +    0.25*R12*a^2*h110    +
         0.25*R14*a^2*h110 + 0.25*R12*a*h18*i - 0.25*R14*a*h18*i

Hn0(18,1)=0.25*R12*a*h24    +    0.25*R14*a*h24    +    0.25*R12*h21*i    -
         0.25*R14*h21*i + 0.125*R21*h22*i - 0.125*R25*h22*i

Hn0(19,1)=0.25*R12*h31 + 0.25*R14*h31 - 0.125*R21*h33 + 0.125*R21*h34 +
         0.5*R23*h32 + 0.25*R23*h33 + 0.25*R23*h34 - 0.125*R25*h33 +
         0.125*R25*h34 - 0.125*R30*h35 + 0.0625*R32*h35 + 0.0625*R34*h35 +
         0.25*R12*a^2*h310   +   0.25*R14*a^2*h310   +   0.25*R12*a*h36*i   -
         0.25*R14*a*h36*i + 0.125*R21*a*h37*i - 0.125*R25*a*h37*i

Hn0(20,2)=0.5*R13*a*h44    +    0.25*R22*h42*i    -    0.25*R24*h42*i    +
         0.125*R31*h43*i - 0.125*R35*h43*i

Hn0(20,3)=0.25*R22*h45 + 0.25*R24*h45 + 0.125*R31*h46 + 0.25*R33*h46 +
         0.125*R35*h46    +    0.5*R13*a^2*h49    +    0.25*R22*a*h47*i    -
         0.25*R24*a*h47*i

Hn0(21,2)=0.25*R11*a*h15    +    0.25*R13*a*h15    +    0.25*R11*h13*i    -
         0.25*R13*h13*i

Hn0(21,3)=0.25*R11*h17    +    0.25*R13*h17    +    0.25*R11*a^2*h110    +
         0.25*R13*a^2*h110 + 0.25*R11*a*h18*i - 0.25*R13*a*h18*i

Hn0(22,1)=0.25*R11*a*h24    +    0.25*R13*a*h24    +    0.25*R11*h21*i    -
         0.25*R13*h21*i + 0.25*R20*h22*i - 0.125*R24*h22*i

Hn0(23,1)=0.25*h324  +  0.25*R11*h31  +  0.25*R13*h31  -  0.25*R20*h33  +
         0.25*R20*h34  +  0.5*R22*h32  +  0.25*R22*h33  +  0.25*R22*h34  -
         0.125*R24*h33 + 0.125*R24*h34 + 0.0625*R33*h35 - 0.0625*R35*h35 +
```

```
        0.25*R11*a^2*h310  +  0.25*R13*a^2*h310  +  0.25*R11*a*h36*i  -
        0.25*R13*a*h36*i + 0.25*R20*a*h37*i - 0.125*R24*a*h37*i

Hn0(24,2)=0.5*R12*a*h44 + 0.25*R21*h42*i - 0.25*R23*h42*i + 0.25*R30*h43*i
        - 0.125*R34*h43*i

Hn0(24,3)=0.25*R21*h45  +  0.25*R23*h45  +  0.25*R30*h46  +  0.25*R32*h46  +
        0.125*R34*h46   +   0.5*R12*a^2*h49   +   0.25*R21*a*h47*i   -
        0.25*R23*a*h47*i

Hn0(25,2)=0.5*R10*a*h15 + 0.25*R12*a*h15 + 0.5*R10*h13*i - 0.25*R12*h13*i

Hn0(25,3)=0.5*R10*h17    +    0.25*R12*h17    +    0.5*R10*a^2*h110    +
        0.25*R12*a^2*h110 + 0.5*R10*a*h18*i - 0.25*R12*a*h18*i

Hn0(26,1)=0.5*R10*a*h24 + 0.25*R12*a*h24 + 0.5*R10*h21*i - 0.25*R12*h21*i
        + 0.125*R21*h22*i - 0.125*R23*h22*i

Hn0(27,1)=0.5*h323  +  0.5*R10*h31  +  0.25*R12*h31  +  0.5*R21*h32  +
        0.125*R21*h33 + 0.375*R21*h34 - 0.125*R23*h33 + 0.125*R23*h34 +
        0.125*R30*h35   -   0.0625*R34*h35   +   0.5*R10*a^2*h310   +
        0.25*R12*a^2*h310  +  0.5*R10*a*h36*i  -  0.25*R12*a*h36*i  +
        0.125*R21*a*h37*i - 0.125*R23*a*h37*i

Hn0(28,2)=0.5*R11*a*h44 + 0.5*R20*h42*i - 0.25*R22*h42*i + 0.125*R31*h43*i
        - 0.125*R33*h43*i

Hn0(28,3)=0.5*R20*h45  +  0.25*R22*h45  +  0.375*R31*h46  +  0.125*R33*h46  +
        0.5*R11*a^2*h49 + 0.5*R20*a*h47*i - 0.25*R22*a*h47*i

Hn0(29,2)=a*h14 + 0.5*R11*a*h15

Hn0(29,3)=0.5*R11*h110*a^2 + h16 + 0.5*R11*h17

Hn0(30,1)=a*h23 + 0.5*R11*a*h24

Hn0(31,1)=h322  +  0.5*h324  +  0.5*R11*h31  +  R20*h32  +  0.5*R20*h33  +
        0.5*R20*h34  -  0.25*R22*h33  +  0.25*R22*h34  +  0.125*R31*h35  -
        0.125*R33*h35 + a^2*h39 + 0.5*R11*a^2*h310

Hn0(32,2)=R10*a*h44

Hn0(32,3)=R10*h49*a^2 + 0.5*R21*h45 + 0.5*R30*h46 + 0.25*R32*h46

Hn0(33,2)=0.5*R10*a*h15 + 0.25*R12*a*h15 - 0.5*R10*h13*i + 0.25*R12*h13*i

Hn0(33,3)=0.5*R10*h17    +    0.25*R12*h17    +    0.5*R10*a^2*h110    +
        0.25*R12*a^2*h110 - 0.5*R10*a*h18*i + 0.25*R12*a*h18*i

Hn0(34,1)=0.5*R10*a*h24 + 0.25*R12*a*h24 - 0.5*R10*h21*i + 0.25*R12*h21*i
        - 0.125*R21*h22*i + 0.125*R23*h22*i

Hn0(35,1)=0.5*h323  +  0.5*R10*h31  +  0.25*R12*h31  +  0.5*R21*h32  +
        0.125*R21*h33 + 0.375*R21*h34 - 0.125*R23*h33 + 0.125*R23*h34 +
        0.125*R30*h35   -   0.0625*R34*h35   +   0.5*R10*a^2*h310   +
```

```
        0.25*R12*a^2*h310  -  0.5*R10*a*h36*i  +  0.25*R12*a*h36*i  -
        0.125*R21*a*h37*i + 0.125*R23*a*h37*i

Hn0(36,2)=0.5*R11*a*h44 - 0.5*R20*h42*i + 0.25*R22*h42*i - 0.125*R31*h43*i
        + 0.125*R33*h43*i

Hn0(36,3)=0.5*R20*h45 + 0.25*R22*h45 + 0.375*R31*h46 + 0.125*R33*h46 +
        0.5*R11*a^2*h49 - 0.5*R20*a*h47*i + 0.25*R22*a*h47*i

Hn0(37,2)=0.25*R11*a*h15   +   0.25*R13*a*h15   -   0.25*R11*h13*i   +
        0.25*R13*h13*i

Hn0(37,3)=0.25*R11*h17   +   0.25*R13*h17   +   0.25*R11*a^2*h110   +
        0.25*R13*a^2*h110 - 0.25*R11*a*h18*i + 0.25*R13*a*h18*i

Hn0(38,1)=0.25*R11*a*h24   +   0.25*R13*a*h24   -   0.25*R11*h21*i   +
        0.25*R13*h21*i - 0.25*R20*h22*i + 0.125*R24*h22*i

Hn0(39,1)=0.25*h324 + 0.25*R11*h31 + 0.25*R13*h31 - 0.25*R20*h33 +
        0.25*R20*h34 + 0.5*R22*h32 + 0.25*R22*h33 + 0.25*R22*h34 -
        0.125*R24*h33 + 0.125*R24*h34 + 0.0625*R33*h35 - 0.0625*R35*h35 +
        0.25*R11*a^2*h310  +  0.25*R13*a^2*h310  -  0.25*R11*a*h36*i  +
        0.25*R13*a*h36*i - 0.25*R20*a*h37*i + 0.125*R24*a*h37*i

Hn0(40,2)=0.5*R12*a*h44 - 0.25*R21*h42*i + 0.25*R23*h42*i - 0.25*R30*h43*i
        + 0.125*R34*h43*i

Hn0(40,3)=0.25*R21*h45 + 0.25*R23*h45 + 0.25*R30*h46 + 0.25*R32*h46 +
        0.125*R34*h46   +   0.5*R12*a^2*h49   -   0.25*R21*a*h47*i   +
        0.25*R23*a*h47*i

Hn0(41,2)=0.25*R12*a*h15   +   0.25*R14*a*h15   -   0.25*R12*h13*i   +
        0.25*R14*h13*i

Hn0(41,3)=0.25*R12*h17   +   0.25*R14*h17   +   0.25*R12*a^2*h110   +
        0.25*R14*a^2*h110 - 0.25*R12*a*h18*i + 0.25*R14*a*h18*i

Hn0(42,1)=0.25*R12*a*h24   +   0.25*R14*a*h24   -   0.25*R12*h21*i   +
        0.25*R14*h21*i - 0.125*R21*h22*i + 0.125*R25*h22*i

Hn0(43,1)=0.25*R12*h31 + 0.25*R14*h31 - 0.125*R21*h33 + 0.125*R21*h34 +
        0.5*R23*h32 + 0.25*R23*h33 + 0.25*R23*h34 - 0.125*R25*h33 +
        0.125*R25*h34 - 0.125*R30*h35 + 0.0625*R32*h35 + 0.0625*R34*h35 +
        0.25*R12*a^2*h310  +  0.25*R14*a^2*h310  -  0.25*R12*a*h36*i  +
        0.25*R14*a*h36*i - 0.125*R21*a*h37*i + 0.125*R25*a*h37*i

Hn0(44,2)=0.5*R13*a*h44   -   0.25*R22*h42*i   +   0.25*R24*h42*i   -
        0.125*R31*h43*i + 0.125*R35*h43*i

Hn0(44,3)=0.25*R22*h45 + 0.25*R24*h45 + 0.125*R31*h46 + 0.25*R33*h46 +
        0.125*R35*h46   +   0.5*R13*a^2*h49   -   0.25*R22*a*h47*i   +
        0.25*R24*a*h47*i

Hn0(45,2)=0.25*R13*a*h15   +   0.25*R15*a*h15   -   0.25*R13*h13*i   +
        0.25*R15*h13*i
```

```
Hn0(45,3)=0.25*R13*h17    +    0.25*R15*h17    +    0.25*R13*a^2*h110    +
         0.25*R15*a^2*h110 - 0.25*R13*a*h18*i + 0.25*R15*a*h18*i

Hn0(46,1)=0.25*R13*a*h24    +    0.25*R15*a*h24    -    0.25*R13*h21*i    +
         0.25*R15*h21*i - 0.125*R22*h22*i

Hn0(47,1)=0.25*R13*h31 + 0.25*R15*h31 - 0.125*R22*h33 + 0.125*R22*h34 +
         0.5*R24*h32 + 0.25*R24*h33 + 0.25*R24*h34 - 0.0625*R31*h35 +
         0.0625*R33*h35    +    0.0625*R35*h35    +    0.25*R13*a^2*h310    +
         0.25*R15*a^2*h310   -   0.25*R13*a*h36*i   +   0.25*R15*a*h36*i   -
         0.125*R22*a*h37*i

Hn0(48,2)=0.5*R14*a*h44    -    0.25*R23*h42*i    +    0.25*R25*h42*i    -
         0.125*R32*h43*i

Hn0(48,3)=0.25*R23*h45 + 0.25*R25*h45 + 0.125*R32*h46 + 0.25*R34*h46 +
         0.5*R14*a^2*h49 - 0.25*R23*a*h47*i + 0.25*R25*a*h47*i

Hn0(49,2)=0.25*R14*a*h15 - 0.25*R14*h13*i

Hn0(49,3)=0.25*R14*h110*a^2 - 0.25*R14*h18*i*a + 0.25*R14*h17

Hn0(50,1)=0.25*R14*a*h24 - 0.25*R14*h21*i - 0.125*R23*h22*i

Hn0(51,1)=0.25*R14*h31 - 0.125*R23*h33 + 0.125*R23*h34 + 0.5*R25*h32 +
         0.25*R25*h33 + 0.25*R25*h34 - 0.0625*R32*h35 + 0.0625*R34*h35 +
         0.25*R14*a^2*h310 - 0.25*R14*a*h36*i - 0.125*R23*a*h37*i

Hn0(52,2)=0.5*R15*a*h44 - 0.25*R24*h42*i - 0.125*R33*h43*i

Hn0(52,3)=0.5*R15*h49*a^2    -    0.25*R24*h47*i*a    +    0.25*R24*h45    +
         0.125*R33*h46 + 0.25*R35*h46

Hn0(53,2)=0.25*R15*a*h15 - 0.25*R15*h13*i

Hn0(53,3)=0.25*R15*h110*a^2 - 0.25*R15*h18*i*a + 0.25*R15*h17

Hn0(54,1)=0.25*R15*a*h24 - 0.25*R15*h21*i - 0.125*R24*h22*i

Hn0(55,1)=0.25*R15*h31 - 0.125*R24*h33 + 0.125*R24*h34 - 0.0625*R33*h35 +
         0.0625*R35*h35   +   0.25*R15*a^2*h310   -   0.25*R15*a*h36*i   -
         0.125*R24*a*h37*i

Hn0(56,2)=- 0.25*R25*h42*i - 0.125*R34*h43*i

Hn0(56,3)=0.25*R25*h45 + 0.125*R34*h46 - 0.25*R25*a*h47*i

Hn0(58,1)=(-0.125)*R25*h22*i

Hn0(59,1)=0.125*R25*h34    -    0.125*R25*h33    -    0.0625*R34*h35    -
         0.125*R25*a*h37*i

Hn0(60,2)=(-0.125)*R35*h43*i

Hn0(60,3)=0.125*R35*h46
```

7.B.2.2 Entries of ${}_{\mathbf{v}}\mathbf{H}_n^1$

```
Hn1(2,3)=0.125*R35*h28*i

Hn1(3,2)=0.125*R35*h312*i

Hn1(3,3)=0.125*R35*h318 - 0.125*R35*h317

Hn1(5,1)=0.25*R25*h12

Hn1(6,2)=0.25*R25*h26

Hn1(6,3)=0.25*R25*a*h210 + 0.25*R25*h27*i + 0.125*R34*h28*i

Hn1(7,2)=0.25*R25*a*h314 + 0.25*R25*h311*i + 0.125*R34*h312*i

Hn1(7,3)=0.25*R25*h315    -    0.125*R34*h317    +    0.125*R34*h318    +
         0.25*R25*a*h319*i

Hn1(9,1)=0.5*R15*h11 + 0.25*R24*h12

Hn1(10,2)=0.5*R15*h25 + 0.25*R24*h26

Hn1(10,3)=0.5*R15*a*h29    +    0.25*R24*a*h210    +    0.25*R24*h27*i    +
         0.125*R33*h28*i

Hn1(11,2)=0.5*R15*a*h313    +    0.25*R24*a*h314    +    0.25*R24*h311*i    +
         0.125*R33*h312*i

Hn1(11,3)=0.5*R15*h321*a^2    +    0.25*R24*h319*i*a    +    0.25*R24*h315    -
         0.125*R33*h317 + 0.125*R33*h318 + 0.5*R35*h316 + 0.25*R35*h317 +
         0.25*R35*h318

Hn1(12,1)=0.5*R25*h41

Hn1(13,1)=0.5*R14*h11 + 0.25*R23*h12 + 0.25*R25*h12

Hn1(14,2)=0.5*R14*h25 + 0.25*R23*h26 + 0.25*R25*h26

Hn1(14,3)=0.5*R14*a*h29    +    0.25*R23*a*h210    +    0.25*R25*a*h210    +
         0.25*R23*h27*i - 0.25*R25*h27*i + 0.125*R32*h28*i

Hn1(15,2)=0.5*R14*a*h313    +    0.25*R23*a*h314    +    0.25*R25*a*h314    +
         0.25*R23*h311*i - 0.25*R25*h311*i + 0.125*R32*h312*i

Hn1(15,3)=0.25*R23*h315 + 0.25*R25*h315 - 0.125*R32*h317 + 0.125*R32*h318
         + 0.5*R34*h316 + 0.25*R34*h317 + 0.25*R34*h318 + 0.5*R14*a^2*h321
         + 0.25*R23*a*h319*i - 0.25*R25*a*h319*i

Hn1(16,1)=0.5*R24*h41

Hn1(17,1)=0.5*R13*h11 + 0.25*R22*h12 + 0.25*R24*h12
```

```
Hn1(18,2)=0.5*R13*h25 + 0.25*R22*h26 + 0.25*R24*h26

Hn1(18,3)=0.5*R13*a*h29    +    0.25*R22*a*h210    +    0.25*R24*a*h210    +
          0.25*R22*h27*i    -    0.25*R24*h27*i    +    0.125*R31*h28*i    -
          0.125*R35*h28*i

Hn1(19,2)=0.5*R13*a*h313    +    0.25*R22*a*h314    +    0.25*R24*a*h314    +
          0.25*R22*h311*i    -    0.25*R24*h311*i    +    0.125*R31*h312*i    -
          0.125*R35*h312*i

Hn1(19,3)=0.25*R22*h315 + 0.25*R24*h315 - 0.125*R31*h317 + 0.125*R31*h318
          + 0.5*R33*h316 + 0.25*R33*h317 + 0.25*R33*h318 - 0.125*R35*h317 +
          0.125*R35*h318   +   0.5*R13*a^2*h321   +   0.25*R22*a*h319*i   -
          0.25*R24*a*h319*i

Hn1(20,1)=0.5*R23*h41

Hn1(21,1)=0.5*R12*h11 + 0.25*R21*h12 + 0.25*R23*h12

Hn1(22,2)=0.5*R12*h25 + 0.25*R21*h26 + 0.25*R23*h26

Hn1(22,3)=0.5*R12*a*h29    +    0.25*R21*a*h210    +    0.25*R23*a*h210    +
          0.25*R21*h27*i    -    0.25*R23*h27*i    +    0.25*R30*h28*i    -
          0.125*R34*h28*i

Hn1(23,2)=0.5*R12*a*h313    +    0.25*R21*a*h314    +    0.25*R23*a*h314    +
          0.25*R21*h311*i    -    0.25*R23*h311*i    +    0.25*R30*h312*i    -
          0.125*R34*h312*i

Hn1(23,3)=0.25*R21*h315 + 0.25*R23*h315 - 0.25*R30*h317 + 0.25*R30*h318 +
          0.5*R32*h316 + 0.25*R32*h317 + 0.25*R32*h318 - 0.125*R34*h317 +
          0.125*R34*h318   +   0.5*R12*a^2*h321   +   0.25*R21*a*h319*i   -
          0.25*R23*a*h319*i

Hn1(24,1)=0.5*R22*h41

Hn1(25,1)=0.5*R11*h11 + 0.5*R20*h12 + 0.25*R22*h12

Hn1(26,2)=0.5*R11*h25 + 0.5*R20*h26 + 0.25*R22*h26

Hn1(26,3)=0.5*R11*a*h29 + 0.5*R20*a*h210 + 0.25*R22*a*h210 + 0.5*R20*h27*i
          - 0.25*R22*h27*i + 0.125*R31*h28*i - 0.125*R33*h28*i

Hn1(27,2)=0.5*R11*a*h313    +    0.5*R20*a*h314    +    0.25*R22*a*h314    +
          0.5*R20*h311*i    -    0.25*R22*h311*i    +    0.125*R31*h312*i    -
          0.125*R33*h312*i

Hn1(27,3)=0.5*h326  +  0.5*R20*h315  +  0.25*R22*h315  +  0.5*R31*h316  +
          0.125*R31*h317 + 0.375*R31*h318 - 0.125*R33*h317 + 0.125*R33*h318
          + 0.5*R11*a^2*h321 + 0.5*R20*a*h319*i - 0.25*R22*a*h319*i

Hn1(28,1)=0.5*R21*h41

Hn1(29,1)=R10*h11 + 0.5*R21*h12

Hn1(30,2)=R10*h25 + 0.5*R21*h26
```

```
Hn1(30,3)=R10*a*h29 + 0.5*R21*a*h210

Hn1(31,2)=R10*a*h313 + 0.5*R21*a*h314

Hn1(31,3)=R10*h321*a^2 + h325 + 0.5*R21*h315 + R30*h316 + 0.5*R30*h317 +
         0.5*R30*h318 - 0.25*R32*h317 + 0.25*R32*h318

Hn1(32,1)=R20*h41

Hn1(33,1)=0.5*R11*h11 + 0.5*R20*h12 + 0.25*R22*h12

Hn1(34,2)=0.5*R11*h25 + 0.5*R20*h26 + 0.25*R22*h26

Hn1(34,3)=0.5*R11*a*h29 + 0.5*R20*a*h210 + 0.25*R22*a*h210 - 0.5*R20*h27*i
         + 0.25*R22*h27*i - 0.125*R31*h28*i + 0.125*R33*h28*i

Hn1(35,2)=0.5*R11*a*h313    +    0.5*R20*a*h314    +    0.25*R22*a*h314    -
         0.5*R20*h311*i    +    0.25*R22*h311*i    -    0.125*R31*h312*i    +
         0.125*R33*h312*i

Hn1(35,3)=0.5*h326  +  0.5*R20*h315  +  0.25*R22*h315  +  0.5*R31*h316  +
         0.125*R31*h317 + 0.375*R31*h318 - 0.125*R33*h317 + 0.125*R33*h318
         + 0.5*R11*a^2*h321 - 0.5*R20*a*h319*i + 0.25*R22*a*h319*i

Hn1(36,1)=0.5*R21*h41

Hn1(37,1)=0.5*R12*h11 + 0.25*R21*h12 + 0.25*R23*h12

Hn1(38,2)=0.5*R12*h25 + 0.25*R21*h26 + 0.25*R23*h26

Hn1(38,3)=0.5*R12*a*h29    +    0.25*R21*a*h210    +    0.25*R23*a*h210    -
         0.25*R21*h27*i    +    0.25*R23*h27*i    -    0.25*R30*h28*i    +
         0.125*R34*h28*i

Hn1(39,2)=0.5*R12*a*h313    +    0.25*R21*a*h314    +    0.25*R23*a*h314    -
         0.25*R21*h311*i    +    0.25*R23*h311*i    -    0.25*R30*h312*i    +
         0.125*R34*h312*i

Hn1(39,3)=0.25*R21*h315 + 0.25*R23*h315 - 0.25*R30*h317 + 0.25*R30*h318 +
         0.5*R32*h316 + 0.25*R32*h317 + 0.25*R32*h318 - 0.125*R34*h317 +
         0.125*R34*h318    +    0.5*R12*a^2*h321    -    0.25*R21*a*h319*i    +
         0.25*R23*a*h319*i

Hn1(40,1)=0.5*R22*h41

Hn1(41,1)=0.5*R13*h11 + 0.25*R22*h12 + 0.25*R24*h12

Hn1(42,2)=0.5*R13*h25 + 0.25*R22*h26 + 0.25*R24*h26

Hn1(42,3)=0.5*R13*a*h29    +    0.25*R22*a*h210    +    0.25*R24*a*h210    -
         0.25*R22*h27*i    +    0.25*R24*h27*i    -    0.125*R31*h28*i    +
         0.125*R35*h28*i

Hn1(43,2)=0.5*R13*a*h313    +    0.25*R22*a*h314    +    0.25*R24*a*h314    -
         0.25*R22*h311*i    +    0.25*R24*h311*i    -    0.125*R31*h312*i    +
         0.125*R35*h312*i
```

```
Hn1(43,3)=0.25*R22*h315 + 0.25*R24*h315 - 0.125*R31*h317 + 0.125*R31*h318
         + 0.5*R33*h316 + 0.25*R33*h317 + 0.25*R33*h318 - 0.125*R35*h317 +
         0.125*R35*h318   +   0.5*R13*a^2*h321   -   0.25*R22*a*h319*i   +
         0.25*R24*a*h319*i

Hn1(44,1)=0.5*R23*h41

Hn1(45,1)=0.5*R14*h11 + 0.25*R23*h12 + 0.25*R25*h12

Hn1(46,2)=0.5*R14*h25 + 0.25*R23*h26 + 0.25*R25*h26

Hn1(46,3)=0.5*R14*a*h29    +    0.25*R23*a*h210    +    0.25*R25*a*h210    -
         0.25*R23*h27*i + 0.25*R25*h27*i - 0.125*R32*h28*i

Hn1(47,2)=0.5*R14*a*h313    +    0.25*R23*a*h314    +    0.25*R25*a*h314    -
         0.25*R23*h311*i + 0.25*R25*h311*i - 0.125*R32*h312*i

Hn1(47,3)=0.25*R23*h315 + 0.25*R25*h315 - 0.125*R32*h317 + 0.125*R32*h318
         + 0.5*R34*h316 + 0.25*R34*h317 + 0.25*R34*h318 + 0.5*R14*a^2*h321
         - 0.25*R23*a*h319*i + 0.25*R25*a*h319*i

Hn1(48,1)=0.5*R24*h41

Hn1(49,1)=0.5*R15*h11 + 0.25*R24*h12

Hn1(50,2)=0.5*R15*h25 + 0.25*R24*h26

Hn1(50,3)=0.5*R15*a*h29    +    0.25*R24*a*h210    -    0.25*R24*h27*i    -
         0.125*R33*h28*i

Hn1(51,2)=0.5*R15*a*h313    +    0.25*R24*a*h314    -    0.25*R24*h311*i    -
         0.125*R33*h312*i

Hn1(51,3)=0.5*R15*h321*a^2   -   0.25*R24*h319*i*a   +   0.25*R24*h315   -
         0.125*R33*h317 + 0.125*R33*h318 + 0.5*R35*h316 + 0.25*R35*h317 +
         0.25*R35*h318

Hn1(52,1)=0.5*R25*h41

Hn1(53,1)=0.25*R25*h12

Hn1(54,2)=0.25*R25*h26

Hn1(54,3)=0.25*R25*a*h210 - 0.25*R25*h27*i - 0.125*R34*h28*i

Hn1(55,2)=0.25*R25*a*h314 - 0.25*R25*h311*i - 0.125*R34*h312*i

Hn1(55,3)=0.25*R25*h315    -    0.125*R34*h317    +    0.125*R34*h318    -
         0.25*R25*a*h319*i

Hn1(58,3)=(-0.125)*R35*h28*i

Hn1(59,2)=(-0.125)*R35*h312*i

Hn1(59,3)=0.125*R35*h318 - 0.125*R35*h317
```

7.B.2.3 Entries of ${}_{\mathbf{v}}\mathbf{H}_n^2$

```
Hn2(9,3)=0.5*R25*h19
Hn2(11,1)=0.5*R25*h38
Hn2(12,3)=0.5*R35*h48
Hn2(13,3)=0.5*R24*h19
Hn2(15,1)=0.5*R24*h38
Hn2(16,3)=0.5*R34*h48
Hn2(17,3)=0.5*R23*h19
Hn2(19,1)=0.5*R23*h38
Hn2(20,3)=0.5*R33*h48
Hn2(21,3)=0.5*R22*h19
Hn2(23,1)=0.5*R22*h38
Hn2(24,3)=0.5*R32*h48
Hn2(25,3)=0.5*R21*h19
Hn2(27,1)=0.5*R21*h38
Hn2(28,3)=0.5*R31*h48
Hn2(29,3)=R20*h19
Hn2(31,1)=R20*h38
Hn2(32,3)=R30*h48
Hn2(33,3)=0.5*R21*h19
Hn2(35,1)=0.5*R21*h38
Hn2(36,3)=0.5*R31*h48
Hn2(37,3)=0.5*R22*h19
Hn2(39,1)=0.5*R22*h38
Hn2(40,3)=0.5*R32*h48
Hn2(41,3)=0.5*R23*h19
Hn2(43,1)=0.5*R23*h38
```

```
Hn2(44,3)=0.5*R33*h48

Hn2(45,3)=0.5*R24*h19

Hn2(47,1)=0.5*R24*h38

Hn2(48,3)=0.5*R34*h48

Hn2(49,3)=0.5*R25*h19

Hn2(51,1)=0.5*R25*h38

Hn2(52,3)=0.5*R35*h48
```

7.B.2.4 Entries of ${}_{\mathrm{v}}\mathbf{H}_n^3$

```
Hn3(11,3)=0.5*R35*h320

Hn3(15,3)=0.5*R34*h320

Hn3(19,3)=0.5*R33*h320

Hn3(23,3)=0.5*R32*h320

Hn3(27,3)=0.5*R31*h320

Hn3(31,3)=R30*h320

Hn3(35,3)=0.5*R31*h320

Hn3(39,3)=0.5*R32*h320

Hn3(43,3)=0.5*R33*h320

Hn3(47,3)=0.5*R34*h320

Hn3(51,3)=0.5*R35*h320
```

7.B.2.5 Entries of ${}_{\mathrm{v}}\mathbf{G}_n^0$

```
Gn0(1,1)=0.125*R15*c13 - 0.125*R15*c12 - 0.0625*R24*c15 - 0.03125*R33*c16
         + 0.125*R15*a*c18*i + 0.0625*R24*a*c19*i

Gn0(2,2)=- 0.125*R15*c27 - 0.0625*R24*c28

Gn0(2,3)=0.125*R25*c215*i - 0.0625*R24*a*c219 - 0.125*R15*a*c218

Gn0(3,2)=0.125*R15*c312*i   -   0.0625*R24*a*c320   -   0.125*R15*a*c319   +
         0.0625*R24*c314*i + 0.0625*R34*c316*i
```

```
Gn0(3,3)=0.125*R15*c329    -    0.0625*R24*c333    +    0.125*R25*c331    -
         0.0625*R34*c334   -   0.125*R15*a^2*c344   +   0.125*R15*a*c336*i   +
         0.125*R25*a*c338*i

Gn0(4,1)=0.125*R14*c13 - 0.125*R14*c12 - 0.0625*R23*c15 + 0.25*R25*c14 +
         0.0625*R25*c15    -    0.03125*R32*c16    +    0.125*R14*a*c18*i    +
         0.0625*R23*a*c19*i + 0.0625*R25*a*c19*i

Gn0(5,2)=0.0625*R25*c28 - 0.0625*R23*c28 - 0.125*R14*c27

Gn0(5,3)=0.0625*R25*a*c219   -   0.0625*R23*a*c219   -   0.125*R14*a*c218   +
         0.25*R15*c214*i + 0.125*R24*c215*i

Gn0(6,2)=0.0625*R25*a*c320   -   0.0625*R23*a*c320   -   0.125*R14*a*c319   +
         0.125*R14*c312*i   +   0.0625*R23*c314*i   +   0.25*R25*c313*i   +
         0.0625*R25*c314*i   +   0.0625*R33*c316*i   +   0.25*R35*c315*i   +
         0.0625*R35*c316*i

Gn0(6,3)=0.125*R14*c329 - 0.0625*R23*c333 + 0.125*R24*c331 + 0.25*R25*c332
         +   0.0625*R25*c333   -   0.0625*R33*c334   +   0.0625*R35*c334   -
         0.125*R14*a^2*c344  +  0.125*R14*a*c336*i  +  0.125*R24*a*c338*i  +
         0.25*R25*a*c337*i

Gn0(7,1)=0.125*R13*c13  -  0.125*R13*c12  +  0.25*R15*c12  +  0.25*R15*c13  -
         0.0625*R22*c15 + 0.25*R24*c14 + 0.0625*R24*c15 - 0.03125*R31*c16
         +  0.0625*R35*c16  +  0.125*R13*a*c18*i  +  0.0625*R22*a*c19*i  +
         0.0625*R24*a*c19*i

Gn0(8,2)=0.25*R15*c27 - 0.125*R13*c27 - 0.0625*R22*c28 + 0.0625*R24*c28

Gn0(8,3)=0.25*R15*a*c218   -   0.125*R13*a*c218   -   0.0625*R22*a*c219   +
         0.0625*R24*a*c219 + 0.25*R14*c214*i + 0.125*R23*c215*i

Gn0(9,2)=0.25*R15*a*c319   -   0.125*R13*a*c319   -   0.0625*R22*a*c320   +
         0.0625*R24*a*c320   +   0.125*R13*c312*i   +   0.0625*R22*c314*i   +
         0.25*R24*c313*i   +   0.0625*R24*c314*i   +   0.0625*R32*c316*i   +
         0.25*R34*c315*i + 0.0625*R34*c316*i

Gn0(9,3)=0.125*R13*c329 + 0.25*R15*c329 - 0.0625*R22*c333 + 0.125*R23*c331
         + 0.25*R24*c332 + 0.0625*R24*c333 + 0.5*R25*c330 + 0.25*R25*c331
         -  0.0625*R32*c334   +   0.0625*R34*c334   -   0.125*R13*a^2*c344   +
         0.25*R15*a^2*c344  +  0.125*R13*a*c336*i  +  0.125*R23*a*c338*i  +
         0.25*R24*a*c337*i

Gn0(10,1)=0.125*R12*c13  -  0.125*R12*c12  +  0.25*R14*c12  +  0.25*R14*c13  -
         0.0625*R21*c15 + 0.25*R23*c14 + 0.0625*R23*c15 + 0.25*R25*c14 +
         0.0625*R25*c15    -    0.0625*R30*c16    +    0.0625*R34*c16    +
         0.125*R12*a*c18*i  +  0.0625*R21*a*c19*i  +  0.0625*R23*a*c19*i  -
         0.0625*R25*a*c19*i

Gn0(11,2)=0.25*R14*c27 - 0.125*R12*c27 - 0.0625*R21*c28 + 0.0625*R23*c28 +
         0.0625*R25*c28

Gn0(11,3)=0.25*R14*a*c218   -   0.125*R12*a*c218   -   0.0625*R21*a*c219   +
         0.0625*R23*a*c219   +   0.0625*R25*a*c219   +   0.25*R13*c214*i   -
         0.25*R15*c214*i + 0.125*R22*c215*i
```

```
Gn0(12,2)=0.25*R14*a*c319  -  0.125*R12*a*c319  -  0.0625*R21*a*c320  +
         0.0625*R23*a*c320  +  0.0625*R25*a*c320  +  0.125*R12*c312*i  +
         0.0625*R21*c314*i  +  0.25*R23*c313*i  +  0.0625*R23*c314*i  -
         0.25*R25*c313*i  -  0.0625*R25*c314*i  +  0.0625*R31*c316*i  +
         0.25*R33*c315*i  +  0.0625*R33*c316*i  -  0.25*R35*c315*i  -
         0.0625*R35*c316*i

Gn0(12,3)=0.125*R12*c329  +  0.25*R14*c329  -  0.0625*R21*c333  +
         0.125*R22*c331 + 0.25*R23*c332 + 0.0625*R23*c333 + 0.5*R24*c330 +
         0.25*R24*c331 + 0.25*R25*c332 + 0.0625*R25*c333 - 0.0625*R31*c334
         +  0.0625*R33*c334  +  0.0625*R35*c334  -  0.125*R12*a^2*c344  +
         0.25*R14*a^2*c344  +  0.125*R12*a*c336*i  +  0.125*R22*a*c338*i  +
         0.25*R23*a*c337*i - 0.25*R25*a*c337*i

Gn0(13,1)=0.125*R11*c13  -  0.125*R11*c12  -  0.125*c130  +  0.25*R13*c12  +
         0.25*R13*c13  -  0.125*R15*c12 + 0.125*R15*c13 - 0.125*R20*c15 +
         0.25*R22*c14 + 0.0625*R22*c15 + 0.25*R24*c14 + 0.0625*R24*c15 -
         0.03125*R31*c16  +  0.0625*R33*c16  +  0.125*R11*a*c18*i  -
         0.125*R15*a*c18*i  +  0.125*R20*a*c19*i  +  0.0625*R22*a*c19*i  -
         0.0625*R24*a*c19*i

Gn0(14,2)=0.25*R13*c27 - 0.125*R11*c27 - 0.125*R15*c27 - 0.125*R20*c28 +
         0.0625*R22*c28 + 0.0625*R24*c28

Gn0(14,3)=0.25*R13*a*c218  -  0.125*R11*a*c218  -  0.125*R15*a*c218  -
         0.125*R20*a*c219  +  0.0625*R22*a*c219  +  0.0625*R24*a*c219  +
         0.25*R12*c214*i  -  0.25*R14*c214*i  +  0.125*R21*c215*i  -
         0.125*R25*c215*i

Gn0(15,2)=0.25*R13*a*c319  -  0.125*R11*a*c319  -  0.125*R15*a*c319  -
         0.125*R20*a*c320  +  0.0625*R22*a*c320  +  0.0625*R24*a*c320  +
         0.125*R11*c312*i  -  0.125*R15*c312*i  +  0.125*R20*c314*i  +
         0.25*R22*c313*i  +  0.0625*R22*c314*i  -  0.25*R24*c313*i  -
         0.0625*R24*c314*i  +  0.125*R30*c316*i  +  0.25*R32*c315*i  +
         0.0625*R32*c316*i - 0.25*R34*c315*i - 0.0625*R34*c316*i

Gn0(15,3)=0.125*R11*c329 + 0.25*R13*c329 + 0.125*R15*c329 - 0.125*R20*c333
         + 0.125*R21*c331 + 0.25*R22*c332 + 0.0625*R22*c333 + 0.5*R23*c330
         +  0.25*R23*c331  +  0.25*R24*c332  +  0.0625*R24*c333  +
         0.125*R25*c331  -  0.125*R30*c334  +  0.0625*R32*c334  +
         0.0625*R34*c334  -  0.125*R11*a^2*c344  +  0.25*R13*a^2*c344  -
         0.125*R15*a^2*c344  +  0.125*R11*a*c336*i  -  0.125*R15*a*c336*i  +
         0.125*R21*a*c338*i  +  0.25*R22*a*c337*i  -  0.25*R24*a*c337*i  -
         0.125*R25*a*c338*i

Gn0(16,1)=0.25*c129  -  0.25*R10*c12  +  0.25*R10*c13  +  0.25*R12*c12  +
         0.25*R12*c13  -  0.125*R14*c12 + 0.125*R14*c13 + 0.25*R21*c14 +
         0.25*R23*c14 + 0.0625*R23*c15 - 0.0625*R25*c15 + 0.03125*R32*c16
         +  0.25*R10*a*c18*i  -  0.125*R14*a*c18*i  +  0.125*R21*a*c19*i  -
         0.0625*R23*a*c19*i - 0.0625*R25*a*c19*i

Gn0(17,2)=0.25*R12*c27 - 0.25*R10*c27 - 0.125*R14*c27 + 0.0625*R23*c28 -
         0.0625*R25*c28
```

```
Gn0(17,3)=0.25*R12*a*c218   -   0.25*R10*a*c218   -   0.125*R14*a*c218   +
         0.0625*R23*a*c219   -   0.0625*R25*a*c219   +   0.25*R11*c214*i   -
         0.25*R13*c214*i + 0.25*R20*c215*i - 0.125*R24*c215*i

Gn0(18,2)=0.25*R12*a*c319   -   0.25*R10*a*c319   -   0.125*R14*a*c319   +
         0.0625*R23*a*c320   -   0.0625*R25*a*c320   +   0.25*R10*c312*i   -
         0.125*R14*c312*i   +   0.25*R21*c313*i   +   0.125*R21*c314*i   -
         0.25*R23*c313*i   -   0.0625*R23*c314*i   -   0.0625*R25*c314*i   +
         0.25*R31*c315*i   +   0.125*R31*c316*i   -   0.25*R33*c315*i   -
         0.0625*R33*c316*i - 0.0625*R35*c316*i

Gn0(18,3)=0.25*R10*c329 + 0.25*R12*c329 + 0.125*R14*c329 + 0.25*R20*c331 +
         0.25*R21*c332 + 0.5*R22*c330 + 0.25*R22*c331 + 0.25*R23*c332 +
         0.0625*R23*c333   +   0.125*R24*c331   -   0.0625*R25*c333   +
         0.0625*R33*c334   -   0.0625*R35*c334   -   0.25*R10*a^2*c344   +
         0.25*R12*a^2*c344  -  0.125*R14*a^2*c344  +  0.25*R10*a*c336*i  -
         0.125*R14*a*c336*i  +  0.25*R20*a*c338*i  +  0.25*R21*a*c337*i  -
         0.25*R23*a*c337*i - 0.125*R24*a*c338*i

Gn0(19,1)=0.5*c11 + 0.5*c128 + 0.125*c130 + 0.125*R11*c12 + 0.375*R11*c13
         - 0.125*R13*c12 + 0.125*R13*c13 + 0.5*R20*c14 + 0.125*R20*c15 +
         0.25*R22*c14 - 0.0625*R24*c15 + 0.0625*R31*c16 - 0.03125*R33*c16
         -   0.03125*R35*c16   +   0.5*a^2*c113   +   0.5*a*c17*i   +
         0.125*R11*a*c18*i  -  0.125*R13*a*c18*i  +  0.125*R20*a*c19*i  -
         0.0625*R24*a*c19*i

Gn0(20,2)=0.5*c213*a^2 + 0.5*c29*i*a + 0.5*c227 + 0.5*c26 + 0.125*R11*c27
         - 0.125*R13*c27 + 0.125*R20*c28 - 0.0625*R24*c28

Gn0(20,3)=0.5*a*c217  +  0.5*a*c229  +  0.5*a^3*c225  +  0.125*R11*a*c218  -
         0.125*R13*a*c218   +   0.125*R20*a*c219   -   0.0625*R24*a*c219   +
         0.5*R10*c214*i   -   0.25*R12*c214*i   +   0.125*R21*c215*i   -
         0.125*R23*c215*i + 0.5*a^2*c222*i

Gn0(21,2)=0.5*a*c318 + 0.5*a*c358 + 0.5*c311*i + 0.5*c353*i + 0.5*a^3*c326
         +  0.125*R11*a*c319  -  0.125*R13*a*c319  +  0.125*R20*a*c320  -
         0.0625*R24*a*c320   +   0.125*R11*c312*i   -   0.125*R13*c312*i   +
         0.5*R20*c313*i   +   0.125*R20*c314*i   -   0.25*R22*c313*i   -
         0.0625*R24*c314*i   +   0.5*R30*c315*i   +   0.125*R30*c316*i   -
         0.25*R32*c315*i - 0.0625*R34*c316*i + 0.5*a^2*c323*i

Gn0(21,3)=0.5*c328  +  0.5*c352  +  0.375*R11*c329  +  0.125*R13*c329  +
         0.5*R20*c332 + 0.125*R20*c333 + 0.5*R21*c330 + 0.375*R21*c331 +
         0.25*R22*c332 + 0.125*R23*c331 - 0.0625*R24*c333 + 0.125*R30*c334
         - 0.0625*R34*c334 + 0.5*a^2*c343 + 0.5*a^4*c350 + 0.5*a^2*c363 +
         0.5*a*c335*i   +   0.5*a*c359*i   +   0.125*R11*a^2*c344   -
         0.125*R13*a^2*c344  +  0.5*a^3*c346*i  +  0.125*R11*a*c336*i  -
         0.125*R13*a*c336*i  +  0.5*R20*a*c337*i  +  0.125*R21*a*c338*i  -
         0.25*R22*a*c337*i - 0.125*R23*a*c338*i

Gn0(22,1)=c112*a^2  +  c127  +  0.5*c129  +  0.5*R10*c12  +  0.5*R10*c13  -
         0.25*R12*c12  +  0.25*R12*c13  +  0.5*R21*c14  +  0.125*R21*c15  -
         0.125*R23*c15 + 0.125*R30*c16 - 0.0625*R34*c16

Gn0(23,2)=c212*a^2 + c226 + 0.5*R10*c27 - 0.25*R12*c27 + 0.125*R21*c28 -
         0.125*R23*c28
```

```
Gn0(23,3)=a*c216 + a*c228 + 0.5*R10*a*c218 - 0.25*R12*a*c218 +
        0.125*R21*a*c219 - 0.125*R23*a*c219

Gn0(24,2)=a*c317 + a*c357 + 0.5*R10*a*c319 - 0.25*R12*a*c319 +
        0.125*R21*a*c320 - 0.125*R23*a*c320

Gn0(24,3)=c327 + c351 + 0.5*R10*c329 + 0.25*R12*c329 + R20*c330 +
        0.5*R20*c331 + 0.5*R21*c332 + 0.125*R21*c333 + 0.25*R22*c331 -
        0.125*R23*c333 + 0.125*R31*c334 - 0.125*R33*c334 + a^2*c342 +
        a^4*c349 + a^2*c362 + 0.5*R10*a^2*c344 - 0.25*R12*a^2*c344

Gn0(25,1)=0.5*c11 + 0.5*c128 + 0.125*c130 + 0.125*R11*c12 + 0.375*R11*c13
        - 0.125*R13*c12 + 0.125*R13*c13 + 0.5*R20*c14 + 0.125*R20*c15 +
        0.25*R22*c14 - 0.0625*R24*c15 + 0.0625*R31*c16 - 0.03125*R33*c16
        - 0.03125*R35*c16 + 0.5*a^2*c113 - 0.5*a*c17*i -
        0.125*R11*a*c18*i + 0.125*R13*a*c18*i - 0.125*R20*a*c19*i +
        0.0625*R24*a*c19*i

Gn0(26,2)=0.5*c213*a^2 - 0.5*c29*i*a + 0.5*c227 + 0.5*c26 + 0.125*R11*c27
        - 0.125*R13*c27 + 0.125*R20*c28 - 0.0625*R24*c28

Gn0(26,3)=0.5*a*c217 + 0.5*a*c229 + 0.5*a^3*c225 + 0.125*R11*a*c218 -
        0.125*R13*a*c218 + 0.125*R20*a*c219 - 0.0625*R24*a*c219 -
        0.5*R10*c214*i + 0.25*R12*c214*i - 0.125*R21*c215*i +
        0.125*R23*c215*i - 0.5*a^2*c222*i

Gn0(27,2)=0.5*a*c318 + 0.5*a*c358 - 0.5*c311*i - 0.5*c353*i + 0.5*a^3*c326
        + 0.125*R11*a*c319 - 0.125*R13*a*c319 + 0.125*R20*a*c320 -
        0.0625*R24*a*c320 - 0.125*R11*c312*i + 0.125*R13*c312*i -
        0.5*R20*c313*i - 0.125*R20*c314*i + 0.25*R22*c313*i +
        0.0625*R24*c314*i - 0.5*R30*c315*i - 0.125*R30*c316*i +
        0.25*R32*c315*i + 0.0625*R34*c316*i - 0.5*a^2*c323*i

Gn0(27,3)=0.5*c328 + 0.5*c352 + 0.375*R11*c329 + 0.125*R13*c329 +
        0.5*R20*c332 + 0.125*R20*c333 + 0.5*R21*c330 + 0.375*R21*c331 +
        0.25*R22*c332 + 0.125*R23*c331 - 0.0625*R24*c333 + 0.125*R30*c334
        - 0.0625*R34*c334 + 0.5*a^2*c343 + 0.5*a^4*c350 + 0.5*a^2*c363 -
        0.5*a*c335*i - 0.5*a*c359*i + 0.125*R11*a^2*c344 -
        0.125*R13*a^2*c344 - 0.5*a^3*c346*i - 0.125*R11*a*c336*i +
        0.125*R13*a*c336*i - 0.5*R20*a*c337*i - 0.125*R21*a*c338*i +
        0.25*R22*a*c337*i + 0.125*R23*a*c338*i

Gn0(28,1)=0.25*c129 - 0.25*R10*c12 + 0.25*R10*c13 + 0.25*R12*c12 +
        0.25*R12*c13 - 0.125*R14*c12 + 0.125*R14*c13 + 0.25*R21*c14 +
        0.25*R23*c14 + 0.0625*R23*c15 - 0.0625*R25*c15 + 0.03125*R32*c16
        - 0.25*R10*a*c18*i + 0.125*R14*a*c18*i - 0.125*R21*a*c19*i +
        0.0625*R23*a*c19*i + 0.0625*R25*a*c19*i

Gn0(29,2)=0.25*R12*c27 - 0.25*R10*c27 - 0.125*R14*c27 + 0.0625*R23*c28 -
        0.0625*R25*c28

Gn0(29,3)=0.25*R12*a*c218 - 0.25*R10*a*c218 - 0.125*R14*a*c218 +
        0.0625*R23*a*c219 - 0.0625*R25*a*c219 - 0.25*R11*c214*i +
        0.25*R13*c214*i - 0.25*R20*c215*i + 0.125*R24*c215*i
```

```
Gn0(30,2)=0.25*R12*a*c319   -   0.25*R10*a*c319   -   0.125*R14*a*c319   +
         0.0625*R23*a*c320   -   0.0625*R25*a*c320   -   0.25*R10*c312*i   +
         0.125*R14*c312*i   -   0.25*R21*c313*i   -   0.125*R21*c314*i   +
         0.25*R23*c313*i   +   0.0625*R23*c314*i   +   0.0625*R25*c314*i   -
         0.25*R31*c315*i   -   0.125*R31*c316*i   +   0.25*R33*c315*i   +
         0.0625*R33*c316*i + 0.0625*R35*c316*i

Gn0(30,3)=0.25*R10*c329 + 0.25*R12*c329 + 0.125*R14*c329 + 0.25*R20*c331 +
         0.25*R21*c332 + 0.5*R22*c330 + 0.25*R22*c331 + 0.25*R23*c332 +
         0.0625*R23*c333   +   0.125*R24*c331   -   0.0625*R25*c333   +
         0.0625*R33*c334   -   0.0625*R35*c334   -   0.25*R10*a^2*c344   +
         0.25*R12*a^2*c344  -  0.125*R14*a^2*c344  -  0.25*R10*a*c336*i  +
         0.125*R14*a*c336*i  -  0.25*R20*a*c338*i  -  0.25*R21*a*c337*i  +
         0.25*R23*a*c337*i + 0.125*R24*a*c338*i

Gn0(31,1)=0.125*R11*c13  -  0.125*R11*c12  -  0.125*c130  +  0.25*R13*c12  +
         0.25*R13*c13  -  0.125*R15*c12 + 0.125*R15*c13 - 0.125*R20*c15 +
         0.25*R22*c14 + 0.0625*R22*c15 + 0.25*R24*c14 + 0.0625*R24*c15 -
         0.03125*R31*c16   +   0.0625*R33*c16   -   0.125*R11*a*c18*i   +
         0.125*R15*a*c18*i  -  0.125*R20*a*c19*i  -  0.0625*R22*a*c19*i  +
         0.0625*R24*a*c19*i

Gn0(32,2)=0.25*R13*c27 - 0.125*R11*c27 - 0.125*R15*c27 - 0.125*R20*c28 +
         0.0625*R22*c28 + 0.0625*R24*c28

Gn0(32,3)=0.25*R13*a*c218   -   0.125*R11*a*c218   -   0.125*R15*a*c218   -
         0.125*R20*a*c219   +   0.0625*R22*a*c219   +   0.0625*R24*a*c219   -
         0.25*R12*c214*i   +   0.25*R14*c214*i   -   0.125*R21*c215*i   +
         0.125*R25*c215*i

Gn0(33,2)=0.25*R13*a*c319   -   0.125*R11*a*c319   -   0.125*R15*a*c319   -
         0.125*R20*a*c320   +   0.0625*R22*a*c320   +   0.0625*R24*a*c320   -
         0.125*R11*c312*i   +   0.125*R15*c312*i   -   0.125*R20*c314*i   -
         0.25*R22*c313*i   -   0.0625*R22*c314*i   +   0.25*R24*c313*i   +
         0.0625*R24*c314*i   -   0.125*R30*c316*i   -   0.25*R32*c315*i   -
         0.0625*R32*c316*i + 0.25*R34*c315*i + 0.0625*R34*c316*i

Gn0(33,3)=0.125*R11*c329 + 0.25*R13*c329 + 0.125*R15*c329 - 0.125*R20*c333
         + 0.125*R21*c331 + 0.25*R22*c332 + 0.0625*R22*c333 + 0.5*R23*c330
         +   0.25*R23*c331   +   0.25*R24*c332   +   0.0625*R24*c333   +
         0.125*R25*c331   -   0.125*R30*c334   +   0.0625*R32*c334   +
         0.0625*R34*c334   -   0.125*R11*a^2*c344   +   0.25*R13*a^2*c344   -
         0.125*R15*a^2*c344  -  0.125*R11*a*c336*i  +  0.125*R15*a*c336*i  -
         0.125*R21*a*c338*i  -  0.25*R22*a*c337*i  +  0.25*R24*a*c337*i  +
         0.125*R25*a*c338*i

Gn0(34,1)=0.125*R12*c13  -  0.125*R12*c12  +  0.25*R14*c12  +  0.25*R14*c13  -
         0.0625*R21*c15 + 0.25*R23*c14 + 0.0625*R23*c15 + 0.25*R25*c14 +
         0.0625*R25*c15   -   0.0625*R30*c16   +   0.0625*R34*c16   -
         0.125*R12*a*c18*i  -  0.0625*R21*a*c19*i  -  0.0625*R23*a*c19*i  +
         0.0625*R25*a*c19*i

Gn0(35,2)=0.25*R14*c27 - 0.125*R12*c27 - 0.0625*R21*c28 + 0.0625*R23*c28 +
         0.0625*R25*c28
```

```
Gn0(35,3)=0.25*R14*a*c218   -   0.125*R12*a*c218   -   0.0625*R21*a*c219   +
         0.0625*R23*a*c219   +   0.0625*R25*a*c219   -   0.25*R13*c214*i   +
         0.25*R15*c214*i - 0.125*R22*c215*i

Gn0(36,2)=0.25*R14*a*c319   -   0.125*R12*a*c319   -   0.0625*R21*a*c320   +
         0.0625*R23*a*c320   +   0.0625*R25*a*c320   -   0.125*R12*c312*i   -
         0.0625*R21*c314*i   -   0.25*R23*c313*i   -   0.0625*R23*c314*i   +
         0.25*R25*c313*i   +   0.0625*R25*c314*i   -   0.0625*R31*c316*i   -
         0.25*R33*c315*i   -   0.0625*R33*c316*i   +   0.25*R35*c315*i   +
         0.0625*R35*c316*i

Gn0(36,3)=0.125*R12*c329    +    0.25*R14*c329    -    0.0625*R21*c333    +
         0.125*R22*c331 + 0.25*R23*c332 + 0.0625*R23*c333 + 0.5*R24*c330 +
         0.25*R24*c331 + 0.25*R25*c332 + 0.0625*R25*c333 - 0.0625*R31*c334
         +   0.0625*R33*c334   +   0.0625*R35*c334   -   0.125*R12*a^2*c344   +
         0.25*R14*a^2*c344   -   0.125*R12*a*c336*i   -   0.125*R22*a*c338*i   -
         0.25*R23*a*c337*i + 0.25*R25*a*c337*i

Gn0(37,1)=0.125*R13*c13   -   0.125*R13*c12   +   0.25*R15*c12   +   0.25*R15*c13   -
         0.0625*R22*c15 + 0.25*R24*c14 + 0.0625*R24*c15 - 0.03125*R31*c16
         +   0.0625*R35*c16   -   0.125*R13*a*c18*i   -   0.0625*R22*a*c19*i   -
         0.0625*R24*a*c19*i

Gn0(38,2)=0.25*R15*c27 - 0.125*R13*c27 - 0.0625*R22*c28 + 0.0625*R24*c28

Gn0(38,3)=0.25*R15*a*c218   -   0.125*R13*a*c218   -   0.0625*R22*a*c219   +
         0.0625*R24*a*c219 - 0.25*R14*c214*i - 0.125*R23*c215*i

Gn0(39,2)=0.25*R15*a*c319   -   0.125*R13*a*c319   -   0.0625*R22*a*c320   +
         0.0625*R24*a*c320   -   0.125*R13*c312*i   -   0.0625*R22*c314*i   -
         0.25*R24*c313*i   -   0.0625*R24*c314*i   -   0.0625*R32*c316*i   -
         0.25*R34*c315*i - 0.0625*R34*c316*i

Gn0(39,3)=0.125*R13*c329    +    0.25*R15*c329    -    0.0625*R22*c333    +
         0.125*R23*c331 + 0.25*R24*c332 + 0.0625*R24*c333 + 0.5*R25*c330 +
         0.25*R25*c331    -    0.0625*R32*c334    +    0.0625*R34*c334    -
         0.125*R13*a^2*c344   +   0.25*R15*a^2*c344   -   0.125*R13*a*c336*i   -
         0.125*R23*a*c338*i - 0.25*R24*a*c337*i

Gn0(40,1)=0.125*R14*c13 - 0.125*R14*c12 - 0.0625*R23*c15 + 0.25*R25*c14 +
         0.0625*R25*c15   -   0.03125*R32*c16   -   0.125*R14*a*c18*i   -
         0.0625*R23*a*c19*i - 0.0625*R25*a*c19*i

Gn0(41,2)=0.0625*R25*c28 - 0.0625*R23*c28 - 0.125*R14*c27

Gn0(41,3)=0.0625*R25*a*c219   -   0.0625*R23*a*c219   -   0.125*R14*a*c218   -
         0.25*R15*c214*i - 0.125*R24*c215*i

Gn0(42,2)=0.0625*R25*a*c320   -   0.0625*R23*a*c320   -   0.125*R14*a*c319   -
         0.125*R14*c312*i   -   0.0625*R23*c314*i   -   0.25*R25*c313*i   -
         0.0625*R25*c314*i   -   0.0625*R33*c316*i   -   0.25*R35*c315*i   -
         0.0625*R35*c316*i

Gn0(42,3)=0.125*R14*c329    -    0.0625*R23*c333    +    0.125*R24*c331    +
         0.25*R25*c332    +    0.0625*R25*c333    -    0.0625*R33*c334    +
```

```
        0.0625*R35*c334  -  0.125*R14*a^2*c344  -  0.125*R14*a*c336*i  -
        0.125*R24*a*c338*i - 0.25*R25*a*c337*i

Gn0(43,1)=0.125*R15*c13 - 0.125*R15*c12 - 0.0625*R24*c15 - 0.03125*R33*c16
        - 0.125*R15*a*c18*i - 0.0625*R24*a*c19*i

Gn0(44,2)=- 0.125*R15*c27 - 0.0625*R24*c28

Gn0(44,3)=- 0.125*R15*a*c218 - 0.0625*R24*a*c219 - 0.125*R25*c215*i

Gn0(45,2)=-  0.125*R15*a*c319  -  0.0625*R24*a*c320  -  0.125*R15*c312*i  -
        0.0625*R24*c314*i - 0.0625*R34*c316*i

Gn0(45,3)=0.125*R15*c329   -   0.0625*R24*c333   +   0.125*R25*c331   -
        0.0625*R34*c334  -  0.125*R15*a^2*c344  -  0.125*R15*a*c336*i  -
        0.125*R25*a*c338*i
```

7.B.2.6 Entries of ${}_{\mathrm{v}}\mathbf{G}_n^1$

```
Gn1(1,3)=0.125*R25*c120   -   0.125*R25*c119   -   0.0625*R34*c121   +
        0.125*R25*a*c123*i

Gn1(2,1)=0.125*R25*c23*i

Gn1(3,1)=0.125*R25*a*c37*i - 0.0625*R34*c35 - 0.125*R25*c34

Gn1(4,2)=0.25*R15*a*c116 + 0.25*R15*c114*i

Gn1(4,3)=0.25*R15*c118 - 0.125*R24*c119 + 0.125*R24*c120 - 0.0625*R33*c121
        +  0.0625*R35*c121  +  0.25*R15*a^2*c126  +  0.125*R24*a*c123*i  +
        0.25*R25*a*c122*i

Gn1(5,1)=0.25*R15*a*c25   +   0.25*R15*c21*i   +   0.125*R24*c23*i   +
        0.25*R25*c22*i

Gn1(6,1)=0.25*R15*c32 - 0.125*R24*c34 - 0.0625*R33*c35 + 0.0625*R35*c35 +
        0.25*R15*a^2*c310 + 0.25*R15*a*c36*i + 0.125*R24*a*c37*i

Gn1(7,2)=0.25*R14*a*c116 + 0.25*R14*c114*i

Gn1(7,3)=0.25*R14*c118 - 0.125*R23*c119 + 0.125*R23*c120 + 0.25*R25*c119 +
        0.25*R25*c120   -   0.0625*R32*c121   +   0.0625*R34*c121   +
        0.25*R14*a^2*c126  +  0.5*R15*a^2*c125  +  0.125*R23*a*c123*i  +
        0.25*R24*a*c122*i

Gn1(8,1)=0.25*R14*a*c25   +   0.25*R14*c21*i   +   0.125*R23*c23*i   +
        0.25*R24*c22*i

Gn1(9,1)=0.25*R14*c32  -  0.125*R23*c34  +  0.5*R25*c33  +  0.25*R25*c34  -
        0.0625*R32*c35   +   0.0625*R34*c35   +   0.25*R14*a^2*c310   +
        0.25*R14*a*c36*i + 0.125*R23*a*c37*i
```

```
Gn1(10,2)=0.25*R13*a*c116   +   0.25*R15*a*c116   +   0.25*R13*c114*i   -
         0.25*R15*c114*i

Gn1(10,3)=0.25*R13*c118 + 0.25*R15*c118 - 0.125*R22*c119 + 0.125*R22*c120
         +   0.25*R24*c119   +   0.25*R24*c120   -   0.0625*R31*c121   +
         0.0625*R33*c121   +   0.0625*R35*c121   +   0.25*R13*a^2*c126   +
         0.5*R14*a^2*c125  +  0.25*R15*a^2*c126  +  0.125*R22*a*c123*i  +
         0.25*R23*a*c122*i - 0.25*R25*a*c122*i

Gn1(11,1)=0.25*R13*a*c25    +    0.25*R15*a*c25    +    0.25*R13*c21*i    -
         0.25*R15*c21*i    +    0.125*R22*c23*i    +    0.25*R23*c22*i    -
         0.25*R25*c22*i

Gn1(12,1)=0.25*R13*c32  +  0.25*R15*c32  -  0.125*R22*c34  +  0.5*R24*c33  +
         0.25*R24*c34 - 0.0625*R31*c35 + 0.0625*R33*c35 + 0.0625*R35*c35 +
         0.25*R13*a^2*c310   +   0.25*R15*a^2*c310   +   0.25*R13*a*c36*i   -
         0.25*R15*a*c36*i + 0.125*R22*a*c37*i

Gn1(13,2)=0.25*R12*a*c116   +   0.25*R14*a*c116   +   0.25*R12*c114*i   -
         0.25*R14*c114*i

Gn1(13,3)=0.25*R12*c118 + 0.25*R14*c118 - 0.125*R21*c119 + 0.125*R21*c120
         + 0.25*R23*c119 + 0.25*R23*c120 - 0.125*R25*c119 + 0.125*R25*c120
         -   0.125*R30*c121   +   0.0625*R32*c121   +   0.0625*R34*c121   +
         0.25*R12*a^2*c126   +   0.5*R13*a^2*c125   +   0.25*R14*a^2*c126   +
         0.125*R21*a*c123*i  +  0.25*R22*a*c122*i  -  0.25*R24*a*c122*i  -
         0.125*R25*a*c123*i

Gn1(14,1)=0.25*R12*a*c25    +    0.25*R14*a*c25    +    0.25*R12*c21*i    -
         0.25*R14*c21*i    +    0.125*R21*c23*i    +    0.25*R22*c22*i    -
         0.25*R24*c22*i - 0.125*R25*c23*i

Gn1(15,1)=0.25*R12*c32  +  0.25*R14*c32  -  0.125*R21*c34  +  0.5*R23*c33  +
         0.25*R23*c34 - 0.125*R25*c34 - 0.125*R30*c35 + 0.0625*R32*c35 +
         0.0625*R34*c35   +   0.25*R12*a^2*c310   +   0.25*R14*a^2*c310   +
         0.25*R12*a*c36*i   -   0.25*R14*a*c36*i   +   0.125*R21*a*c37*i   -
         0.125*R25*a*c37*i

Gn1(16,2)=0.25*R11*a*c116   +   0.25*R13*a*c116   +   0.25*R11*c114*i   -
         0.25*R13*c114*i

Gn1(16,3)=0.25*c133  +  0.25*R11*c118  +  0.25*R13*c118  -  0.25*R20*c119  +
         0.25*R20*c120 + 0.25*R22*c119 + 0.25*R22*c120 - 0.125*R24*c119 +
         0.125*R24*c120    +    0.0625*R33*c121    -    0.0625*R35*c121    +
         0.25*R11*a^2*c126   +   0.5*R12*a^2*c125   +   0.25*R13*a^2*c126   +
         0.25*R20*a*c123*i  +  0.25*R21*a*c122*i  -  0.25*R23*a*c122*i  -
         0.125*R24*a*c123*i

Gn1(17,1)=0.25*R11*a*c25    +    0.25*R13*a*c25    +    0.25*R11*c21*i    -
         0.25*R13*c21*i + 0.25*R20*c23*i + 0.25*R21*c22*i - 0.25*R23*c22*i
         - 0.125*R24*c23*i

Gn1(18,1)=0.25*c356  +  0.25*R11*c32  +  0.25*R13*c32  -  0.25*R20*c34  +
         0.5*R22*c33  +  0.25*R22*c34  -  0.125*R24*c34  +  0.0625*R33*c35  -
         0.0625*R35*c35   +   0.25*R11*a^2*c310   +   0.25*R13*a^2*c310   +
```

```
        0.25*R11*a*c36*i   -   0.25*R13*a*c36*i   +   0.25*R20*a*c37*i   -
        0.125*R24*a*c37*i

Gn1(19,2)=0.5*R10*a*c116    +    0.25*R12*a*c116    +    0.5*R10*c114*i    -
        0.25*R12*c114*i

Gn1(19,3)=0.5*c132  +  0.5*R10*c118  +  0.25*R12*c118  +  0.125*R21*c119  +
        0.375*R21*c120 - 0.125*R23*c119 + 0.125*R23*c120 + 0.125*R30*c121
        -  0.0625*R34*c121  +  0.5*R10*a^2*c126  +  0.5*R11*a^2*c125  +
        0.25*R12*a^2*c126  +  0.5*R20*a*c122*i  +  0.125*R21*a*c123*i  -
        0.25*R22*a*c122*i - 0.125*R23*a*c123*i

Gn1(20,1)=0.5*R10*a*c25 + 0.25*R12*a*c25 + 0.5*R10*c21*i - 0.25*R12*c21*i
        +   0.5*R20*c22*i   +   0.125*R21*c23*i   -   0.25*R22*c22*i   -
        0.125*R23*c23*i

Gn1(21,1)=0.5*c355   +   0.5*R10*c32   +   0.25*R12*c32   +   0.5*R21*c33   +
        0.125*R21*c34 - 0.125*R23*c34 + 0.125*R30*c35 - 0.0625*R34*c35 +
        0.5*R10*a^2*c310   +   0.25*R12*a^2*c310   +   0.5*R10*a*c36*i   -
        0.25*R12*a*c36*i + 0.125*R21*a*c37*i - 0.125*R23*a*c37*i

Gn1(22,2)=a*c115 + 0.5*R11*a*c116

Gn1(22,3)=c117  +  c131  +  0.5*c133  +  0.5*R11*c118  +  0.5*R20*c119  +
        0.5*R20*c120 - 0.25*R22*c119 + 0.25*R22*c120 + 0.125*R31*c121 -
        0.125*R33*c121 + R10*a^2*c125 + 0.5*R11*a^2*c126

Gn1(23,1)=a*c24 + 0.5*R11*a*c25

Gn1(24,1)=c31 + c354 + 0.5*c356 + 0.5*R11*c32 + R20*c33 + 0.5*R20*c34 -
        0.25*R22*c34  +  0.125*R31*c35  -  0.125*R33*c35  +  a^2*c39  +
        0.5*R11*a^2*c310

Gn1(25,2)=0.5*R10*a*c116    +    0.25*R12*a*c116    -    0.5*R10*c114*i    +
        0.25*R12*c114*i

Gn1(25,3)=0.5*c132  +  0.5*R10*c118  +  0.25*R12*c118  +  0.125*R21*c119  +
        0.375*R21*c120 - 0.125*R23*c119 + 0.125*R23*c120 + 0.125*R30*c121
        -  0.0625*R34*c121  +  0.5*R10*a^2*c126  +  0.5*R11*a^2*c125  +
        0.25*R12*a^2*c126  -  0.5*R20*a*c122*i  -  0.125*R21*a*c123*i  +
        0.25*R22*a*c122*i + 0.125*R23*a*c123*i

Gn1(26,1)=0.5*R10*a*c25 + 0.25*R12*a*c25 - 0.5*R10*c21*i + 0.25*R12*c21*i
        -   0.5*R20*c22*i   -   0.125*R21*c23*i   +   0.25*R22*c22*i   +
        0.125*R23*c23*i

Gn1(27,1)=0.5*c355   +   0.5*R10*c32   +   0.25*R12*c32   +   0.5*R21*c33   +
        0.125*R21*c34 - 0.125*R23*c34 + 0.125*R30*c35 - 0.0625*R34*c35 +
        0.5*R10*a^2*c310   +   0.25*R12*a^2*c310   -   0.5*R10*a*c36*i   +
        0.25*R12*a*c36*i - 0.125*R21*a*c37*i + 0.125*R23*a*c37*i

Gn1(28,2)=0.25*R11*a*c116   +   0.25*R13*a*c116   -   0.25*R11*c114*i   +
        0.25*R13*c114*i

Gn1(28,3)=0.25*c133  +  0.25*R11*c118  +  0.25*R13*c118  -  0.25*R20*c119  +
        0.25*R20*c120 + 0.25*R22*c119 + 0.25*R22*c120 - 0.125*R24*c119 +
```

```
        0.125*R24*c120   +   0.0625*R33*c121   -   0.0625*R35*c121   +
        0.25*R11*a^2*c126  +  0.5*R12*a^2*c125  +  0.25*R13*a^2*c126  -
        0.25*R20*a*c123*i  -  0.25*R21*a*c122*i  +  0.25*R23*a*c122*i  +
        0.125*R24*a*c123*i

Gn1(29,1)=0.25*R11*a*c25   +   0.25*R13*a*c25   -   0.25*R11*c21*i   +
        0.25*R13*c21*i - 0.25*R20*c23*i - 0.25*R21*c22*i + 0.25*R23*c22*i
        + 0.125*R24*c23*i

Gn1(30,1)=0.25*c356  +  0.25*R11*c32  +  0.25*R13*c32  -  0.25*R20*c34  +
        0.5*R22*c33 + 0.25*R22*c34 - 0.125*R24*c34 + 0.0625*R33*c35 -
        0.0625*R35*c35   +   0.25*R11*a^2*c310   +   0.25*R13*a^2*c310   -
        0.25*R11*a*c36*i   +   0.25*R13*a*c36*i   -   0.25*R20*a*c37*i   +
        0.125*R24*a*c37*i

Gn1(31,2)=0.25*R12*a*c116   +   0.25*R14*a*c116   -   0.25*R12*c114*i   +
        0.25*R14*c114*i

Gn1(31,3)=0.25*R12*c118 + 0.25*R14*c118 - 0.125*R21*c119 + 0.125*R21*c120
        + 0.25*R23*c119 + 0.25*R23*c120 - 0.125*R25*c119 + 0.125*R25*c120
        -   0.125*R30*c121   +   0.0625*R32*c121   +   0.0625*R34*c121   +
        0.25*R12*a^2*c126  +  0.5*R13*a^2*c125  +  0.25*R14*a^2*c126  -
        0.125*R21*a*c123*i  -  0.25*R22*a*c122*i  +  0.25*R24*a*c122*i  +
        0.125*R25*a*c123*i

Gn1(32,1)=0.25*R12*a*c25   +   0.25*R14*a*c25   -   0.25*R12*c21*i   +
        0.25*R14*c21*i   -   0.125*R21*c23*i   -   0.25*R22*c22*i   +
        0.25*R24*c22*i + 0.125*R25*c23*i

Gn1(33,1)=0.25*R12*c32  +  0.25*R14*c32  -  0.125*R21*c34  +  0.5*R23*c33  +
        0.25*R23*c34 - 0.125*R25*c34 - 0.125*R30*c35 + 0.0625*R32*c35 +
        0.0625*R34*c35   +   0.25*R12*a^2*c310   +   0.25*R14*a^2*c310   -
        0.25*R12*a*c36*i   +   0.25*R14*a*c36*i   -   0.125*R21*a*c37*i   +
        0.125*R25*a*c37*i

Gn1(34,2)=0.25*R13*a*c116   +   0.25*R15*a*c116   -   0.25*R13*c114*i   +
        0.25*R15*c114*i

Gn1(34,3)=0.25*R13*c118 + 0.25*R15*c118 - 0.125*R22*c119 + 0.125*R22*c120
        +   0.25*R24*c119   +   0.25*R24*c120   -   0.0625*R31*c121   +
        0.0625*R33*c121   +   0.0625*R35*c121   +   0.25*R13*a^2*c126   +
        0.5*R14*a^2*c125  +  0.25*R15*a^2*c126  -  0.125*R22*a*c123*i  -
        0.25*R23*a*c122*i + 0.25*R25*a*c122*i

Gn1(35,1)=0.25*R13*a*c25   +   0.25*R15*a*c25   -   0.25*R13*c21*i   +
        0.25*R15*c21*i   -   0.125*R22*c23*i   -   0.25*R23*c22*i   +
        0.25*R25*c22*i

Gn1(36,1)=0.25*R13*c32  +  0.25*R15*c32  -  0.125*R22*c34  +  0.5*R24*c33  +
        0.25*R24*c34 - 0.0625*R31*c35 + 0.0625*R33*c35 + 0.0625*R35*c35 +
        0.25*R13*a^2*c310   +   0.25*R15*a^2*c310   -   0.25*R13*a*c36*i   +
        0.25*R15*a*c36*i - 0.125*R22*a*c37*i

Gn1(37,2)=0.25*R14*a*c116 - 0.25*R14*c114*i
```

```
Gn1(37,3)=0.25*R14*c118 - 0.125*R23*c119 + 0.125*R23*c120 + 0.25*R25*c119
         +   0.25*R25*c120   -   0.0625*R32*c121   +   0.0625*R34*c121   +
         0.25*R14*a^2*c126  +  0.5*R15*a^2*c125  -  0.125*R23*a*c123*i  -
         0.25*R24*a*c122*i

Gn1(38,1)=0.25*R14*a*c25    -    0.25*R14*c21*i    -    0.125*R23*c23*i    -
         0.25*R24*c22*i

Gn1(39,1)=0.25*R14*c32  -  0.125*R23*c34  +  0.5*R25*c33  +  0.25*R25*c34  -
         0.0625*R32*c35   +   0.0625*R34*c35   +   0.25*R14*a^2*c310   -
         0.25*R14*a*c36*i - 0.125*R23*a*c37*i

Gn1(40,2)=0.25*R15*a*c116 - 0.25*R15*c114*i

Gn1(40,3)=0.25*R15*c118    -    0.125*R24*c119    +    0.125*R24*c120    -
         0.0625*R33*c121   +   0.0625*R35*c121   +   0.25*R15*a^2*c126   -
         0.125*R24*a*c123*i - 0.25*R25*a*c122*i

Gn1(41,1)=0.25*R15*a*c25    -    0.25*R15*c21*i    -    0.125*R24*c23*i    -
         0.25*R25*c22*i

Gn1(42,1)=0.25*R15*c32 - 0.125*R24*c34 - 0.0625*R33*c35 + 0.0625*R35*c35 +
         0.25*R15*a^2*c310 - 0.25*R15*a*c36*i - 0.125*R24*a*c37*i

Gn1(43,3)=0.125*R25*c120    -    0.125*R25*c119    -    0.0625*R34*c121    -
         0.125*R25*a*c123*i

Gn1(44,1)=(-0.125)*R25*c23*i

Gn1(45,1)=- 0.125*R25*c34 - 0.0625*R34*c35 - 0.125*R25*a*c37*i
```

7.B.2.7 Entries of ${}_{\mathrm{v}}\mathbf{G}_n^2$

```
Gn2(1,1)=0.0625*R24*c111*i

Gn2(2,3)=0.125*R35*c221*i

Gn2(3,2)=0.125*R35*c322*i

Gn2(3,3)=(-0.125)*R35*c341

Gn2(4,1)=0.0625*R23*c111*i + 0.0625*R25*c111*i

Gn2(5,2)=0.25*R25*c211

Gn2(5,3)=0.25*R25*a*c224 + 0.125*R34*c221*i + 0.25*R35*c220*i

Gn2(6,2)=0.25*R25*a*c325 + 0.25*R25*c321*i + 0.125*R34*c322*i

Gn2(6,3)=0.25*R25*c339 - 0.125*R34*c341 + 0.25*R25*a*c345*i

Gn2(7,1)=0.5*R15*c110 + 0.0625*R22*c111*i + 0.0625*R24*c111*i
```

```
Gn2(8,2)=0.5*R15*c210 + 0.25*R24*c211

Gn2(8,3)=0.5*R15*a*c223   +   0.25*R24*a*c224   +   0.125*R33*c221*i   +
         0.25*R34*c220*i

Gn2(9,2)=0.5*R15*a*c324   +   0.25*R24*a*c325   +   0.25*R24*c321*i   +
         0.125*R33*c322*i

Gn2(9,3)=0.5*R15*c348*a^2   +   0.25*R24*c345*i*a   +   0.25*R24*c339   -
         0.125*R33*c341 + 0.5*R35*c340 + 0.25*R35*c341

Gn2(10,1)=0.5*R14*c110   +   0.0625*R21*c111*i   +   0.0625*R23*c111*i   -
         0.0625*R25*c111*i

Gn2(11,2)=0.5*R14*c210 + 0.25*R23*c211 + 0.25*R25*c211

Gn2(11,3)=0.5*R14*a*c223   +   0.25*R23*a*c224   +   0.25*R25*a*c224   +
         0.125*R32*c221*i + 0.25*R33*c220*i - 0.25*R35*c220*i

Gn2(12,2)=0.5*R14*a*c324   +   0.25*R23*a*c325   +   0.25*R25*a*c325   +
         0.25*R23*c321*i - 0.25*R25*c321*i + 0.125*R32*c322*i

Gn2(12,3)=0.25*R23*c339 + 0.25*R25*c339 - 0.125*R32*c341 + 0.5*R34*c340 +
         0.25*R34*c341   +   0.5*R14*a^2*c348   +   0.25*R23*a*c345*i   -
         0.25*R25*a*c345*i

Gn2(13,1)=0.5*R13*c110   +   0.125*R20*c111*i   +   0.0625*R22*c111*i   -
         0.0625*R24*c111*i

Gn2(14,2)=0.5*R13*c210 + 0.25*R22*c211 + 0.25*R24*c211

Gn2(14,3)=0.5*R13*a*c223   +   0.25*R22*a*c224   +   0.25*R24*a*c224   +
         0.125*R31*c221*i   +   0.25*R32*c220*i   -   0.25*R34*c220*i   -
         0.125*R35*c221*i

Gn2(15,2)=0.5*R13*a*c324   +   0.25*R22*a*c325   +   0.25*R24*a*c325   +
         0.25*R22*c321*i   -   0.25*R24*c321*i   +   0.125*R31*c322*i   -
         0.125*R35*c322*i

Gn2(15,3)=0.25*R22*c339 + 0.25*R24*c339 - 0.125*R31*c341 + 0.5*R33*c340 +
         0.25*R33*c341   -   0.125*R35*c341   +   0.5*R13*a^2*c348   +
         0.25*R22*a*c345*i - 0.25*R24*a*c345*i

Gn2(16,1)=0.5*R12*c110   +   0.125*R21*c111*i   -   0.0625*R23*c111*i   -
         0.0625*R25*c111*i

Gn2(17,2)=0.5*R12*c210 + 0.25*R21*c211 + 0.25*R23*c211

Gn2(17,3)=0.5*R12*a*c223   +   0.25*R21*a*c224   +   0.25*R23*a*c224   +
         0.25*R30*c221*i   +   0.25*R31*c220*i   -   0.25*R33*c220*i   -
         0.125*R34*c221*i

Gn2(18,2)=0.5*R12*a*c324   +   0.25*R21*a*c325   +   0.25*R23*a*c325   +
         0.25*R21*c321*i   -   0.25*R23*c321*i   +   0.25*R30*c322*i   -
         0.125*R34*c322*i
```

```
Gn2(18,3)=0.25*R21*c339 + 0.25*R23*c339 - 0.25*R30*c341 + 0.5*R32*c340 +
         0.25*R32*c341    -    0.125*R34*c341    +    0.5*R12*a^2*c348    +
         0.25*R21*a*c345*i - 0.25*R23*a*c345*i

Gn2(19,1)=0.5*R11*c110 + 0.125*R20*c111*i - 0.0625*R24*c111*i

Gn2(20,2)=0.5*R11*c210 + 0.5*R20*c211 + 0.25*R22*c211

Gn2(20,3)=0.5*R11*a*c223    +    0.5*R20*a*c224    +    0.25*R22*a*c224    +
         0.5*R30*c220*i    +    0.125*R31*c221*i    -    0.25*R32*c220*i    -
         0.125*R33*c221*i

Gn2(21,2)=0.5*R11*a*c324    +    0.5*R20*a*c325    +    0.25*R22*a*c325    +
         0.5*R20*c321*i    -    0.25*R22*c321*i    +    0.125*R31*c322*i    -
         0.125*R33*c322*i

Gn2(21,3)=0.5*c361  +  0.5*R20*c339  +  0.25*R22*c339  +  0.5*R31*c340  +
         0.125*R31*c341    -    0.125*R33*c341    +    0.5*R11*a^2*c348    +
         0.5*R20*a*c345*i - 0.25*R22*a*c345*i

Gn2(22,1)=R10*c110

Gn2(23,2)=R10*c210 + 0.5*R21*c211

Gn2(23,3)=R10*a*c223 + 0.5*R21*a*c224

Gn2(24,2)=R10*a*c324 + 0.5*R21*a*c325

Gn2(24,3)=R10*c348*a^2 + c360 + 0.5*R21*c339 + R30*c340 + 0.5*R30*c341 -
         0.25*R32*c341

Gn2(25,1)=0.5*R11*c110 - 0.125*R20*c111*i + 0.0625*R24*c111*i

Gn2(26,2)=0.5*R11*c210 + 0.5*R20*c211 + 0.25*R22*c211

Gn2(26,3)=0.5*R11*a*c223    +    0.5*R20*a*c224    +    0.25*R22*a*c224    -
         0.5*R30*c220*i    -    0.125*R31*c221*i    +    0.25*R32*c220*i    +
         0.125*R33*c221*i

Gn2(27,2)=0.5*R11*a*c324    +    0.5*R20*a*c325    +    0.25*R22*a*c325    -
         0.5*R20*c321*i    +    0.25*R22*c321*i    -    0.125*R31*c322*i    +
         0.125*R33*c322*i

Gn2(27,3)=0.5*c361  +  0.5*R20*c339  +  0.25*R22*c339  +  0.5*R31*c340  +
         0.125*R31*c341    -    0.125*R33*c341    +    0.5*R11*a^2*c348    -
         0.5*R20*a*c345*i + 0.25*R22*a*c345*i

Gn2(28,1)=0.5*R12*c110    -    0.125*R21*c111*i    +    0.0625*R23*c111*i    +
         0.0625*R25*c111*i

Gn2(29,2)=0.5*R12*c210 + 0.25*R21*c211 + 0.25*R23*c211

Gn2(29,3)=0.5*R12*a*c223    +    0.25*R21*a*c224    +    0.25*R23*a*c224    -
         0.25*R30*c221*i    -    0.25*R31*c220*i    +    0.25*R33*c220*i    +
         0.125*R34*c221*i
```

```
Gn2(30,2)=0.5*R12*a*c324   +   0.25*R21*a*c325   +   0.25*R23*a*c325   -
         0.25*R21*c321*i   +   0.25*R23*c321*i   -   0.25*R30*c322*i   +
         0.125*R34*c322*i

Gn2(30,3)=0.25*R21*c339 + 0.25*R23*c339 - 0.25*R30*c341 + 0.5*R32*c340 +
         0.25*R32*c341   -   0.125*R34*c341   +   0.5*R12*a^2*c348   -
         0.25*R21*a*c345*i + 0.25*R23*a*c345*i

Gn2(31,1)=0.5*R13*c110   -   0.125*R20*c111*i   -   0.0625*R22*c111*i   +
         0.0625*R24*c111*i

Gn2(32,2)=0.5*R13*c210 + 0.25*R22*c211 + 0.25*R24*c211

Gn2(32,3)=0.5*R13*a*c223   +   0.25*R22*a*c224   +   0.25*R24*a*c224   -
         0.125*R31*c221*i   -   0.25*R32*c220*i   +   0.25*R34*c220*i   +
         0.125*R35*c221*i

Gn2(33,2)=0.5*R13*a*c324   +   0.25*R22*a*c325   +   0.25*R24*a*c325   -
         0.25*R22*c321*i   +   0.25*R24*c321*i   -   0.125*R31*c322*i   +
         0.125*R35*c322*i

Gn2(33,3)=0.25*R22*c339 + 0.25*R24*c339 - 0.125*R31*c341 + 0.5*R33*c340 +
         0.25*R33*c341   -   0.125*R35*c341   +   0.5*R13*a^2*c348   -
         0.25*R22*a*c345*i + 0.25*R24*a*c345*i

Gn2(34,1)=0.5*R14*c110   -   0.0625*R21*c111*i   -   0.0625*R23*c111*i   +
         0.0625*R25*c111*i

Gn2(35,2)=0.5*R14*c210 + 0.25*R23*c211 + 0.25*R25*c211

Gn2(35,3)=0.5*R14*a*c223   +   0.25*R23*a*c224   +   0.25*R25*a*c224   -
         0.125*R32*c221*i - 0.25*R33*c220*i + 0.25*R35*c220*i

Gn2(36,2)=0.5*R14*a*c324   +   0.25*R23*a*c325   +   0.25*R25*a*c325   -
         0.25*R23*c321*i + 0.25*R25*c321*i - 0.125*R32*c322*i

Gn2(36,3)=0.25*R23*c339 + 0.25*R25*c339 - 0.125*R32*c341 + 0.5*R34*c340 +
         0.25*R34*c341   +   0.5*R14*a^2*c348   -   0.25*R23*a*c345*i   +
         0.25*R25*a*c345*i

Gn2(37,1)=0.5*R15*c110 - 0.0625*R22*c111*i - 0.0625*R24*c111*i

Gn2(38,2)=0.5*R15*c210 + 0.25*R24*c211

Gn2(38,3)=0.5*R15*a*c223   +   0.25*R24*a*c224   -   0.125*R33*c221*i   -
         0.25*R34*c220*i

Gn2(39,2)=0.5*R15*a*c324   +   0.25*R24*a*c325   -   0.25*R24*c321*i   -
         0.125*R33*c322*i

Gn2(39,3)=0.5*R15*c348*a^2   -   0.25*R24*c345*i*a   +   0.25*R24*c339   -
         0.125*R33*c341 + 0.5*R35*c340 + 0.25*R35*c341

Gn2(40,1)=- 0.0625*R23*c111*i - 0.0625*R25*c111*i

Gn2(41,2)=0.25*R25*c211
```

```
Gn2(41,3)=0.25*R25*a*c224 - 0.125*R34*c221*i - 0.25*R35*c220*i

Gn2(42,2)=0.25*R25*a*c325 - 0.25*R25*c321*i - 0.125*R34*c322*i

Gn2(42,3)=0.25*R25*c339 - 0.125*R34*c341 - 0.25*R25*a*c345*i

Gn2(43,1)=(-0.0625)*R24*c111*i

Gn2(44,3)=(-0.125)*R35*c221*i

Gn2(45,2)=(-0.125)*R35*c322*i

Gn2(45,3)=(-0.125)*R35*c341
```

7.B.2.8 Entries of ${}_{\mathrm{v}}\mathbf{G}_n^3$

```
Gn3(7,3)=0.5*R25*c124

Gn3(9,1)=0.5*R25*c38

Gn3(10,3)=0.5*R24*c124

Gn3(12,1)=0.5*R24*c38

Gn3(13,3)=0.5*R23*c124

Gn3(15,1)=0.5*R23*c38

Gn3(16,3)=0.5*R22*c124

Gn3(18,1)=0.5*R22*c38

Gn3(19,3)=0.5*R21*c124

Gn3(21,1)=0.5*R21*c38

Gn3(22,3)=R20*c124

Gn3(24,1)=R20*c38

Gn3(25,3)=0.5*R21*c124

Gn3(27,1)=0.5*R21*c38

Gn3(28,3)=0.5*R22*c124

Gn3(30,1)=0.5*R22*c38

Gn3(31,3)=0.5*R23*c124

Gn3(33,1)=0.5*R23*c38

Gn3(34,3)=0.5*R24*c124
```

```
Gn3(36,1)=0.5*R24*c38
Gn3(37,3)=0.5*R25*c124
Gn3(39,1)=0.5*R25*c38
```

7.B.2.9 Entries of ${}_{\mathbf{v}}\mathbf{G}_{n}^{4}$

```
Gn4(9,3)=0.5*R35*c347
Gn4(12,3)=0.5*R34*c347
Gn4(15,3)=0.5*R33*c347
Gn4(18,3)=0.5*R32*c347
Gn4(21,3)=0.5*R31*c347
Gn4(24,3)=R30*c347
Gn4(27,3)=0.5*R31*c347
Gn4(30,3)=0.5*R32*c347
Gn4(33,3)=0.5*R33*c347
Gn4(36,3)=0.5*R34*c347
Gn4(39,3)=0.5*R35*c347
```

7.B.2.10 Entries of ${}_{\mathbf{v}}\mathbf{H}_{j.n}^{xw}$

```
H1nxw(8,1)=h327
H2nxw(7,1)=0.5*h328
H2nxw(9,1)=0.5*h328
```

7.B.2.11 Entries of ${}_{\mathbf{v}}\mathbf{G}_{j.n}^{xu}$

```
G1nxu(7,1)=0.5*c135
G1nxu(8,1)=c134
G1nxu(9,1)=0.5*c135
```

```
G2nxu(7,1)=0.5*c136

G2nxu(9,1)=0.5*c136
```

7.B.2.12 Entries of ${}_{\mathrm{v}}\mathbf{G}_{j.n}^{sv}$

```
G1nsv(8,1)=c230


G2nsv(7,1)=0.5*c231

G2nsv(9,1)=0.5*c231
```

7.B.2.13 Entries of ${}_{\mathrm{v}}\mathbf{G}_{j.n}^{zw}$

```
G1nzw(8,1)=c364


G2nzw(7,1)=0.5*c365

G2nzw(9,1)=0.5*c365
```

7.B.2.14 Entries of ${}_{\mathrm{v}}\mathbf{G}_{j.n}^{xw}$

```
G1nxw(8,1)=c366


G2nxw(2,1)=0.25*R15*c367

G2nxw(3,1)=0.25*R14*c367

G2nxw(4,1)=0.25*R13*c367 + 0.25*R15*c367

G2nxw(5,1)=0.25*R12*c367 + 0.25*R14*c367

G2nxw(6,1)=0.25*R11*c367 + 0.25*R13*c367

G2nxw(7,1)=0.5*R10*c367 + 0.25*R12*c367

G2nxw(8,1)=0.5*R11*c367

G2nxw(9,1)=0.5*R10*c367 + 0.25*R12*c367

G2nxw(10,1)=0.25*R11*c367 + 0.25*R13*c367
```

```
G2nxw(11,1)=0.25*R12*c367 + 0.25*R14*c367

G2nxw(12,1)=0.25*R13*c367 + 0.25*R15*c367

G2nxw(13,1)=0.25*R14*c367

G2nxw(14,1)=0.25*R15*c367
```

7.B.2.15 Entries of ${}_{\mathbf{v}}\mathbf{G}_{j.n}^{sw}$

```
G1nsw(7,1)=0.5*a*c369

G1nsw(9,1)=0.5*a*c369


G2nsw(8,1)=a*c370
```

Chapter 8

Conclusions and Remarks

8.1 Summary and Conclusions

Starting with tensor calculus and the variational form of the dynamic form of the Hamiltonian functional, a generalized theory was formulated for doubly curved thin shells of general geometry. The formulation avoids geometric approximations commonly adopted in other formulations.

The generalized thin shell theory was specialized to circular cylinders and toroids. In case of circular cylindrical thin shells, beside the original theory, three additional theories were recovered by applying different sets of consistent approximations in line with those in existing simplified theories. Two of the simplified theories happened to coincide with those of the Flugge and DMV theories for CCTSs. Several comparisons are made with other theories. In the case of toroidal thin shells, by applying two different sets of consistent approximations two more simplified theories were recovered. The more accurate version happens to be comparable to the Sanders theory and the other one is found nearly identical to the DMV theory for TTSs. By applying further simplifying geometric assumptions, for common geometries in pipe elbows, a third toroidal thin shell theory is also recovered. The theory preserves the accuracy of the formulation while involving simpler expressions.

An exact closed form solution was developed for circular cylindrical thin shells. Also, a quasi closed form solution was developed for toroidal thin shells. The closed form solutions provided were successfully used to formulate a family of exact shape functions and the formulation of super convergent elements.

Excellent agreement was obtained between the results predicted by the proposed finite elements, in which only a single element is used, and those based on Abaqus, in which thousands of shell elements were used.

Using the alternative form of the variational form of the Hamiltonian functional, in which the field equations and corresponding boundary condition equations are explicitly present, in conjunction with the exact shape functions decreases the number of numerical operations required by vanishing the field integral, thus eliminating integrals over displacement fields with respect to longitudinal coordinate. Also, using the Fourier series expansion of the displacement fields and applied forces in circumferential direction eliminates the need of all numerical integrations with respect to circumferential coordinate.

Through several examples, it is shown that the proposed analytical and finite element formulations are able to model static, in-phase and out-of-phase harmonic forces of general spatial distributions including body forces, surface forces, tractions, ring loads, patch loads, line loads, as well as support excitations.

The accuracy and efficiency of the proposed finite elements provide a powerful and reliable tool for analysis of long pipeline systems. With the models developed, pipelines can be modelled accurately while keeping the DOFs as a minimum.

8.2 Proposed Future Work

1. The proposed generalized shell theory can be modified to include the through thickness shear strains. Thus, making it applicable to thicker shells.

2. A generalized thin shell theory capturing large deformation effects by retaining the non-linear strain displacement terms can be formulated.

3. The proposed generalized thin shell theory can be specialized to other geometries. In a piping system this includes annular flanges, frustums, hemispherical and ellipsoidal caps. In a more general context, the generalized thin shell theory could be specialized to plates, panels, spherical, parabolic and hyperbolic domes, and shells of revolutions.

4. For circular cylindrical and toroidal shells, the present theory can be applied to free vibration analysis. Also, modal analysis of both systems, consistent with the present theories, is a possible avenue of interest.

5. While the solution provided for toroidal shells is conceptually correct, the numerical difficulties associated with the presence of close eigenvalues obtained is of interest in future research. These could be resolved by considering close roots to coincide and modifying the algebraic form of the postulated exponential solution to account for repeated roots.

Appendix A

Mathematical Preliminaries

A.1 Objective and Scope

This chapter aims at providing background material on tensor calculus with emphasis on continuum mechanics and more specifically to shells. Most of the material is extracted from the classical book by Sokolnikoff [A.1]. Additional information was drawn from three other classical references by Mercier [A.2], Flugge [A.3] and Niordson [A.4].

A.2 Introduction

A tensor is an object beyond the scalar, vector and matrix. According to Mercier [A.2] “Since physical phenomena are independent of the man-made measuring instruments such as coordinate systems, which may be introduced to describe them, it is desirable to develop a symbolism which is independent of any particular reference”.

Tensor Calculus was first developed around 1890 by Gregorio Ricci-Curbastro under the title “Absolute Differential Calculus” and later on came to be known as tensor analysis [A.5]. In tensor notation, indicial notation is used, in which the coordinate systems and all corresponding parameters have the same literal form in any coordinate system. The mathematical concept of tensor is based on the transformation between arbitrary coordinate systems.

A.3 Conventions

The following conventions are applied throughout this chapter unless mentioned otherwise.

1) *Einstein's summation convention:* Whenever an index appears twice in a product, once as a superscript and once as a subscript, summation on all terms of this kind over the whole range of the index is implied. For example:

$$A_i B^i = \sum_{i=1}^{n} A_i B^i = A_1 B^1 + ... + A_n B^n$$

2) All vectors and tensors are shown in bold face.

A.4 Coordinate Transformation

A.4.1 Contravariant Law of Transformation

Consider two generalized curvilinear coordinate systems of n dimensions x^i and $\hat{x}^i$ (Figure A. 1 illustrates the special case where $n = 3$). Here we assume that the transformation from one coordinate system to the other one is real, one-to-one and reversible. Thus, the generalized coordinates of an arbitrary point P_0 in coordinate system $\hat{x}^i$ can be expressed in terms of its coordinates in coordinate system x^i and vice-versa:

$$\hat{x}^i = \hat{x}^i \left(x^1, x^2, ... , x^n \right) \tag{A.1}$$

$$x^i = x^i \left(\hat{x}^1, \hat{x}^2, ... , \hat{x}^n \right) \tag{A.2}$$

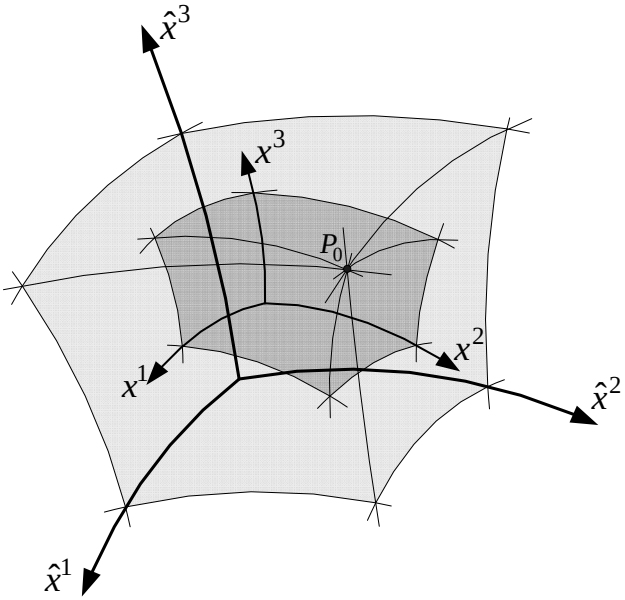

Figure A. 1 - A point defined in Two 3D curvilinear coordinate systems

Differentiating Eq. A.1, one obtains

$$d\hat{x}^i = \frac{\partial \hat{x}^i}{\partial x^j} dx^j \tag{A.3}$$

Eq. A.3 describes how the differentials dx^j transform to $d\hat{x}^j$ when the coordinate system is changed from x^i to $\hat{x}^i$. The transformation described in Eqs. A.3 is called the *contravariant law of transformation*, which can be written as:

$$\hat{A}^i = \frac{\partial \hat{x}^i}{\partial x^j} A^j \tag{A.4}$$

Any set of n quantities, represented by A^j, which is transformed according to Eq.A.4 is called a contravariant vector.

A.4.2 Covariant Law of Transformation

Now, let us consider the multi-variable continuously differentiable function y defined within the same space. It can be defined in terms of both coordinate systems as

$$y = \hat{f}\left(\hat{x}^1, \hat{x}^2, \ldots, \hat{x}^n\right) \tag{A.5}$$

$$y = f\left(x^1, x^2, \ldots, x^n\right) \tag{A.6}$$

In general, the incremental change of functions y can be written as:

$$dy = \frac{\partial \hat{f}}{\partial \hat{x}^i} d\hat{x}^i \tag{A.7}$$

$$dy = \frac{\partial f}{\partial x^i} dx^i \tag{A.8}$$

Considering Eq. A.2, $x^i = x^i\left(\hat{x}^1, \hat{x}^2, \ldots, \hat{x}^n\right)$, the incremental change of coordinate variables x^i can be written as:

$$dx^i = \frac{\partial x^i}{\partial \hat{x}^j} d\hat{x}^j \tag{A.9}$$

From Eq. A.9, by substituting into Eq. A.8, one obtains

$$dy = \frac{\partial f}{\partial x^k} \frac{\partial x^k}{\partial \hat{x}^j} d\hat{x}^j \tag{A.10}$$

Equality of Eqs. A.7 and A.10 gives

$$\frac{\partial \hat{f}}{\partial \hat{x}^i} = \frac{\partial x^j}{\partial \hat{x}^i} \frac{\partial f}{\partial x^j} \tag{A.11}$$

As $\frac{\partial \hat{f}}{\partial \hat{x}^i}$ and $\frac{\partial f}{\partial x^j}$ are general vectors, Eq. A.11 can be written in the following general form:

$$\hat{A}_i = \frac{\partial x^j}{\partial \hat{x}^i} A_j \tag{A.12}$$

where, in lieu of a subscript, the superscript in denominator is considered as subscript. Eq. A.12 is called the *covariant law of transformation*. Any set of m quantities, represented by vector A_j, which are transformed according to Eq. A.12, is called a covariant vector.

A.5 Tensors

The previous section dealt with vectors (i.e, quantities defined by a single index). In mechanics, there are quantities defined by more multiple indices. These are called tensors. For examples, tensors of the second, third, and forth orders are defined by two, three, and four indices, respectively. Since vectors are defined by a single index, they can be conceived as first order tensors.

A.5.1 Contravariant Tensors

Now, the concept of vector transformation can be generalized to tensors. The entity $T^{ij\ldots}$ with n upper indices is called a *contravariant tensor* of rank n if it transforms according to the contravariant law of transformation, Eq. A.4, generalized for the nth rank

$$\hat{T}^{kl\ldots} = \frac{\partial \hat{x}^k}{\partial x^i}\frac{\partial \hat{x}^l}{\partial x^j} \ \ldots \ T^{ij\ldots} \tag{A.13}$$

A.5.2 Covariant Tensors

Similarly, the entity $T_{ij\ldots}$ with n lower indices is called a *covariant tensor* of rank n, if it transforms according to the covariant law of transformation, Eq. A.12, generalized for the nth rank

$$\hat{T}_{kl\ldots} = \frac{\partial x^i}{\partial \hat{x}^k}\frac{\partial x^j}{\partial \hat{x}^l} \ \ldots \ T_{ij\ldots} \tag{A.14}$$

A.5.3 Mixed Tensors

Finally, combining the concepts introduced in Eqs. A.13 and A.14, the entity $T_{pq}^{ij...}$ with a total number of n upper and lower indices is called a *mixed tensor* of rank n, if it transforms according to the following rule:

$$\hat{T}_{st...}^{kl...} = \frac{\partial \hat{x}^k}{\partial x^i}\frac{\partial \hat{x}^l}{\partial x^j} \ \cdots \ \frac{\partial x^p}{\partial \hat{x}^s}\frac{\partial x^q}{\partial \hat{x}^t} \ \cdots \ T_{pq}^{ij...} \tag{A.15}$$

A special case of mixed tensors that is commonly used in tensor calculus is the second order tensor Kronecker Delta function defined as

$$\delta_i^j = \begin{cases} 1 & ; i = j \\ 0 & ; i \neq j \end{cases} \tag{A.16}$$

The generalized nth order Kronecker Delta function is defined as

$$\delta_{i_1...i_n}^{j_1...j_n} = \begin{cases} -1 & \text{, if the set of distinct integers } j_1...j_n \text{ is obtained from the set of distinct integers } i_1...i_n \text{ by an odd permutation.} \\ 0 & \text{, if any two of the integers in the sets } j_1...j_n \text{ or } i_1...i_n \text{ are not distinct.} \\ +1 & \text{, if the set of distinct integers } i_1...i_n \text{ is obtained from the set of distinctintegers } i_1...i_n \text{ by an even permutation.} \end{cases} \tag{A.17}$$

in which, $i_1,...,i_n, j_1,..., j_n \in 1...n$

A.6 Covariant Base Vectors

The position of a generic point with respect to an arbitrary fixed origin O can be defined by the position vector $\mathbf{R}\left(x^1, x^2, x^3\right) = \hat{\mathbf{R}}\left(\hat{x}^1, \hat{x}^2, \hat{x}^3\right)$. This concept can be generalized to an n-dimensional hyper-space in which $\mathbf{R}\left(x^1, x^2, \ldots, x^n\right) = \hat{\mathbf{R}}\left(\hat{x}^1, \hat{x}^2, \ldots, \hat{x}^n\right)$. Since, to each point

of the hyper-space, there exists a unique vector $\mathbf{R}$, the position vector in the n-dimensional space is invariant. The incremental change of vector $\mathbf{R}$ is:

$$d\mathbf{R} = \frac{\partial \mathbf{R}}{\partial x^i} dx^i = \mathbf{g}_i dx^i = \hat{\mathbf{g}}_i d\hat{x}^i = \frac{\partial \hat{\mathbf{R}}}{\partial x^i} d\hat{x}^i = d\hat{\mathbf{R}} \tag{A.18}$$

in which

$$\mathbf{g}_i = \frac{\partial \mathbf{R}}{\partial x^i} \quad , \quad \hat{\mathbf{g}}_i = \frac{\partial \hat{\mathbf{R}}}{\partial \hat{x}^i} \tag{A.19}$$

Symbols $\mathbf{g}_i$ and $\hat{\mathbf{g}}_i$ are called the *covariant base vectors* of the coordinate system x^i and $\hat{x}^i$, respectively. The term "covariant" reminds that they transform under the covariant law of transformation, (i.e., Eq. A.12). It should be noted that as x^i are independent coordinates, the corresponding base vectors $\mathbf{g}_i$ are independent. The argument is equally valid for $\hat{\mathbf{g}}_i$. As evidenced by Eq. A.18, the invariant vector $d\mathbf{R}$ has the same expression in any other coordinate system. Generalizing this concept, the arbitrary invariant vector $\mathbf{V}$ (displacement, velocity, acceleration, …) in a given space can be constructed (or resolved) on the base vectors $\mathbf{g}_i$ of the coordinate systems x^i. For example:

$$\mathbf{V} = V^i \mathbf{g}_i \tag{A.20}$$

In the same manner:

$$\hat{\mathbf{V}} = \hat{V}^i \hat{\mathbf{g}}_i \tag{A.21}$$

As vector $\mathbf{V}$ is invariant, one has

$$\mathbf{V} = \hat{\mathbf{V}} \quad \Rightarrow \quad \mathbf{V} = V^i \mathbf{g}_i = \hat{V}^i \hat{\mathbf{g}}_i = \hat{\mathbf{V}} \tag{A.22}$$

A.7 Reciprocal Contravariant Base Vectors

A second set of mutually independent base vectors in contravariant form can be defined by the means of Kronecker Delta function:

$$\mathbf{g}_i \cdot \mathbf{g}^j = \delta_i^j \tag{A.23}$$

where the symbol "$\cdot$" denotes the dot product and the symbols $\mathbf{g}^j$ are called the *contravariant base vectors*. The term "contravariant" reminds that they transform under the contravariant law of transformation (i.e. Eq. A.4). Therefore, any invariant vector embedded in the same space can also be constructed on the contravariant base vectors $\mathbf{g}^i$, $\hat{\mathbf{g}}^i$ of the coordinate systems x^i, $\hat{x}^i$, respectively. For example:

$$\mathbf{V} = V_i \mathbf{g}^i \tag{A.24}$$

In the same manner:

$$\hat{\mathbf{V}} = \hat{V}_i \hat{\mathbf{g}}^i \tag{A.25}$$

As vector $\mathbf{V}$ is invariant, one has

$$\mathbf{V} = \hat{\mathbf{V}} \qquad \Rightarrow \qquad \mathbf{V} = V_i \mathbf{g}^i = \hat{V}_i \hat{\mathbf{g}}^i = \hat{\mathbf{V}} \tag{A.26}$$

Equality of Eqs. A.22 and A.26 gives:

$$\mathbf{V} = V^i \mathbf{g}_i = V_i \mathbf{g}^i = \hat{V}^i \hat{\mathbf{g}}_i = \hat{V}_i \hat{\mathbf{g}}^i = \hat{\mathbf{V}} \tag{A.27}$$

A.8 Algebra of Tensors

A.8.1 Addition and Subtraction

The sum or difference of two tensors with the same number of covariant and the same number of contravariant indices is a tensor of the same type and rank, i.e.,

$$\mathbf{A} \pm \mathbf{B} = \mathbf{C}$$

$$A_{k\ldots l}^{i\ldots j} \mathbf{g}_i \ldots \mathbf{g}_j \mathbf{g}^k \ldots \mathbf{g}^l \pm B_{k\ldots l}^{i\ldots j} \mathbf{g}_i \ldots \mathbf{g}_j \mathbf{g}^k \ldots \mathbf{g}^l = C_{k\ldots l}^{i\ldots j} \mathbf{g}_i \ldots \mathbf{g}_j \mathbf{g}^k \ldots \mathbf{g}^l \tag{A.28}$$

$$\Rightarrow \qquad A_{k\ldots l}^{i\ldots j} \pm B_{k\ldots l}^{i\ldots j} = C_{k\ldots l}^{i\ldots j}$$

In general, any linear combination of tensors of the same type and rank is a tensor of the same type and rank.

A.8.2 Outer Product

The outer product of two tensors is a tensor with a contravariant order equal to the sum of the contravariant orders of the two tensors and a covariant order equal to the sum of the covariant orders of the two tensors:

$$\mathbf{AB} = \mathbf{C}$$

$$\left(A^{i\ldots j}_{k\ldots l}\mathbf{g}_i\ldots\mathbf{g}_j\mathbf{g}^k\ldots\mathbf{g}^l\right)\left(B^{p\ldots q}_{r\ldots s}\mathbf{g}_p\ldots\mathbf{g}_q\mathbf{g}^r\ldots\mathbf{g}^s\right) = C^{i\ldots jp\ldots q}_{k\ldots lr\ldots s}\mathbf{g}_i\ldots\mathbf{g}_j\mathbf{g}^k\ldots\mathbf{g}^l\mathbf{g}_p\ldots\mathbf{g}_q\mathbf{g}^r\ldots\mathbf{g}^s \tag{A.29}$$

$$\Rightarrow \qquad \left(A^{i\ldots j}_{k\ldots l}\right)\left(B^{p\ldots q}_{r\ldots s}\right) = C^{i\ldots jp\ldots q}_{k\ldots lr\ldots s}$$

It should be noted that the outer product has the distributive property on addition and subtraction, i.e.,

$$\left(A^{\cdots}_{\cdots} \pm B^{\cdots}_{\cdots}\right)C^{\cdots}_{\cdots} = A^{\cdots}_{\cdots}C^{\cdots}_{\cdots} \pm B^{\cdots}_{\cdots}C^{\cdots}_{\cdots} \tag{A.30}$$

A.8.3 Contraction

In mixed tensors, whenever an index appears twice, the summation convention is implied and the resulting tensor is contracted by two orders. This process is called contraction.

$$A^{i\ldots j}_{k\ldots m\ldots l}B^{p\ldots m\ldots q}_{r\ldots s} = C^{i\ldots jp\ldots q}_{k\ldots lr\ldots s} \tag{A.31}$$

A.8.4 Inner Product

The inner product of two tensors, one of them with at least one contravariant index and the other one with at least one covariant index is a tensor of two orders less (one contravariant and one covariant).

$$\mathbf{A}\cdot\mathbf{B}=\mathbf{C}$$

$$\begin{aligned}
&\left(A^{i\ldots j}_{k\ldots m\ldots l}\mathbf{g}_i\ldots\mathbf{g}_j\mathbf{g}^k\ldots\mathbf{g}^m\ldots\mathbf{g}^l\right)\cdot\left(B^{p\ldots n\ldots q}_{r\ldots s}\mathbf{g}_p\ldots\mathbf{g}_n\ldots\mathbf{g}_q\mathbf{g}^r\ldots\mathbf{g}^s\right)=\\
&\quad A^{i\ldots j}_{k\ldots m\ldots l}B^{p\ldots n\ldots q}_{r\ldots s}\mathbf{g}_i\ldots\mathbf{g}_j\mathbf{g}^k\ldots\mathbf{g}^l\left(\mathbf{g}^m\cdot\mathbf{g}_n\right)\mathbf{g}_p\ldots\mathbf{g}_q\mathbf{g}^r\ldots\mathbf{g}^s=\\
&\quad A^{i\ldots j}_{k\ldots m\ldots l}B^{p\ldots n\ldots q}_{r\ldots s}\mathbf{g}_i\ldots\mathbf{g}_j\mathbf{g}^k\ldots\mathbf{g}^l\delta^m_n\mathbf{g}_p\ldots\mathbf{g}_q\mathbf{g}^r\ldots\mathbf{g}^s=\\
&\quad A^{i\ldots j}_{k\ldots m\ldots l}B^{p\ldots m\ldots q}_{r\ldots s}\mathbf{g}_i\ldots\mathbf{g}_j\mathbf{g}^k\ldots\mathbf{g}^l\mathbf{g}_p\ldots\mathbf{g}_q\mathbf{g}^r\ldots\mathbf{g}^s=\\
&\quad =C^{i\ldots jp\ldots q}_{k\ldots lr\ldots s}\mathbf{g}_i\ldots\mathbf{g}_j\mathbf{g}^k\ldots\mathbf{g}^l\mathbf{g}_p\ldots\mathbf{g}_q\mathbf{g}^r\ldots\mathbf{g}^s
\end{aligned}\tag{A.32}$$

$$\Rightarrow\qquad A^{i\ldots j}_{k\ldots m\ldots l}B^{p\ldots m\ldots q}_{r\ldots s}=C^{i\ldots jp\ldots q}_{k\ldots lr\ldots s}$$

A.8.5 Scalar Product

The scalar product is a special case of the inner product of two first rank tensors, in which an index is repeated once as contravariant and once as covariant:

$$\mathbf{A}\cdot\mathbf{B}=c$$

$$\begin{aligned}
&A^i\mathbf{g}_i\cdot B_j\mathbf{g}^j=\\
&A^iB_j\mathbf{g}_i\cdot\mathbf{g}^j=\\
&\quad A^iB_j\delta^j_i=\\
&\quad\ A^iB_i=c
\end{aligned}\tag{A.33}$$

A.9 Invariant Formulation

In a particular coordinate system, by applying the addition, subtraction, multiplication and contraction rules described above to tensors yields a tensor. If this tensor happens to vanish in a particular coordinate system, it should vanish in all other coordinate systems. By setting a tensor expression to zero in one coordinate system, the expression will be valid in all other coordinate systems.

A.10 The First Fundamental Tensor

Consider two neighbouring points in space. The distance ds between them, which is an invariant quantity, is equal to the length of the line element $d\mathbf{R}$ that connects the two points. The square of the length of the line element can be calculated by Pythagoras' theorem:

$$ds^2 = d\mathbf{R}\cdot d\mathbf{R} = \mathbf{g}_i dx^i \cdot \mathbf{g}_j dx^j = \mathbf{g}_i \cdot \mathbf{g}_j dx^i dx^j = g_{ij} dx^i dx^j \tag{A.34}$$

in which

$$g_{ij} = \mathbf{g}_i \cdot \mathbf{g}_j \tag{A.35}$$

The quantity g_{ij} is called the *first fundamental* or *metric tensor*. The word fundamental is used here because some fundamental properties of space can be retrieved from this tensor. Also, the word metric is because the metrification of the space is related to this tensor. Similarly, the quantities g^{ij} and g^i_j are called *fundamental contravariant* and *fundamental mixed tensors*, respectively, and are defined as

$$g^{ij} = \mathbf{g}^i \cdot \mathbf{g}^j \tag{A.36}$$

$$g^i_j = \mathbf{g}^i \cdot \mathbf{g}_j \tag{A.37}$$

The following definition is of use in the following sections.

$$g = \det\left(g_{ij}\right) = \begin{vmatrix} g_{11} & \cdots & g_{1n} \\ \vdots & \ddots & \vdots \\ g_{n1} & \cdots & g_{nn} \end{vmatrix} \tag{A.38}$$

A.11 Lowering and Raising of indices

Using the fundamental tensor, two new operations can be defined:

$$\begin{aligned} \mathbf{A} &= A_j \mathbf{g}^j = A^i \mathbf{g}_i \\ A_j \mathbf{g}^j \cdot \mathbf{g}_k &= A^i \mathbf{g}_i \cdot \mathbf{g}_k \\ A_j \delta^j_k &= A^i g_{ik} \\ A_k &= g_{ik} A^i \end{aligned} \tag{A.39}$$

Similarly:

$$A^k = g^{ik} A_i \tag{A.40}$$

The operations defined in Eqs. A.39 and A.40 are called *the lowering and raising of an index*, respectively, which are applicable to tensors of any type and rank. In general,

$$A^{i\ldots j}_{k\ldots t\ldots l} = g_{nt} A^{i\ldots n\ldots j}_{k\ldots l} \tag{A.41}$$

$$A^{i\ldots t\ldots j}_{k\ldots l} = g^{nt} A^{i\ldots j}_{k\ldots n\ldots l} \tag{A.42}$$

A.12 Permutation Tensor

The permutation symbol in an n-dimensional coordinate system is defined using the generalized Kronecker Delta function (defined in Eq. A.17) through

$$e^{i\ldots j} = \delta^{i\ldots j}_{1\ldots n} \quad , \quad e_{i\ldots j} = \delta^{1\ldots n}_{i\ldots j} \tag{A.43}$$

which are valid only in Cartesian coordinate systems and result in magnitudes -1, 0 or $+1$ depending on the order of the $i\ldots j$. For a general coordinate system, the *permutation tensor* is defined as

$$\mathbf{e}^{i\ldots j} = \frac{1}{\sqrt{g}} e^{i\ldots j} = \frac{1}{\sqrt{g}} \delta^{i\ldots j}_{1\ldots n} \quad , \quad \mathbf{e}_{i\ldots j} = \sqrt{g}\, e_{i\ldots j} = \sqrt{g}\, \delta^{1\ldots n}_{i\ldots j} \tag{A.44}$$

Permutation tensors are called *pseudo scalar*, because every time they transform from one coordinate system to another, they are multiplied by a factor. In three-dimensional coordinate systems ($n = 3$), Eqs. A.43 and A.44 take the form

$$e^{ijk} = \delta^{ijk}_{123} \quad , \quad e_{ijk} = \delta^{123}_{ijk} \tag{A.45}$$

$$\mathbf{e}^{ijk} = \frac{1}{\sqrt{g}} e^{ijk} = \frac{1}{\sqrt{g}} \delta^{ijk}_{123} \quad , \quad \mathbf{e}_{ijk} = \sqrt{g}\, e_{ijk} = \sqrt{g}\, \delta^{123}_{ijk} \tag{A.46}$$

A.13 Determinant

The determinant A of second order covariant and contravariant tensors is defined as

$$Ae^{i\ldots j} = A^i_k \ldots A^j_l e^{k\ldots l} \qquad , \qquad Ae_{i\ldots j} = A^k_i \ldots A^l_j e_{k\ldots l} \tag{A.47}$$

A.14 Cross Product

The cross product of two first rank tensors A and B is a first rank tensor C, defined by

$$\begin{aligned} A^i \mathbf{g}_i \otimes B^j \mathbf{g}_j &= \\ A^i B^j \mathbf{g}_i \otimes \mathbf{g}_j &= \\ A^i B^j e_{ijk} \mathbf{g}^k &= C_k \mathbf{g}^k \\ &= \mathbf{C} \end{aligned} \tag{A.48}$$

$$\Rightarrow \mathbf{A} \otimes \mathbf{B} = \mathbf{C} \qquad \text{where} \qquad C_k = e_{ijk} A^i B^j \tag{A.49}$$

In general, for higher order tensors,

$$\mathbf{A} \otimes \mathbf{B} = \mathbf{C} \;\; ; \; C^{i\ldots jtp\ldots q}_{k\ldots lr\ldots s} = e^{mnt} A^{i\ldots j}_{k\ldots m\ldots l} B^{p\ldots q}_{r\ldots n\ldots s} \quad \text{or} \quad C^{i\ldots jp\ldots q}_{k\ldots ltr\ldots s} = e_{mnt} A^{i\ldots m\ldots j}_{k\ldots l} B^{p\ldots n\ldots q}_{r\ldots s} \tag{A.50}$$

A.15 Surface and Volume Elements

The area dA of an infinitesimal element defined by base vectors $\mathbf{g}_1$ and $\mathbf{g}_2$ as its edges (Figure A. 2) can be represented by the cross product of both base vectors. The product yields a vector normal to the area (vectors $d\mathbf{r}$, $d\mathbf{s}$ and $d\mathbf{t}$ are the base vectors and their magnitude is unity). Also, we recall that the contravariant base vector $\mathbf{g}^3$ is normal to the covariant base vectors $\mathbf{g}_1$ and $\mathbf{g}_2$ (refer to Eq. A.23)).

$$d\mathbf{r} \otimes d\mathbf{s} = dr^1 \mathbf{g}_1 \otimes ds^2 \mathbf{g}_2 = dA_3 \mathbf{g}^3 \qquad ; dA_3 = e_{123} dr^1 ds^2 = \sqrt{g}\, dr^1 ds^2 \tag{A.51}$$

If vector $\mathbf{g}^3$ is as unit base vector, the component dA_3 represents the area of the parallelepiped whose sides are $d\mathbf{r}$ and $d\mathbf{s}$.

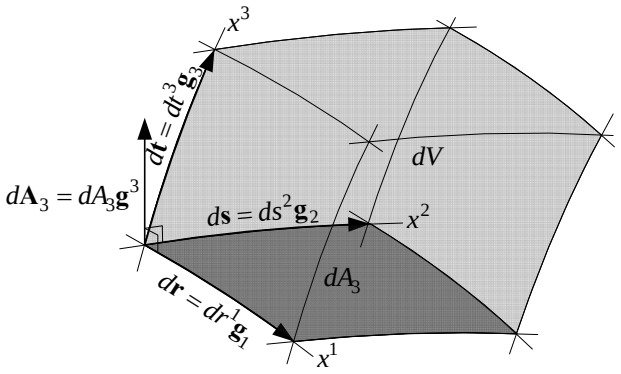

Figure A. 2 - Infinitesimal volume element

Also, the volume dV of the infinitesimal block constructed by base vectors $\mathbf{g}_1$, $\mathbf{g}_2$ and $\mathbf{g}_3$ as its edges (Figure A. 2) is given by the cross product of two of them dot-multiplied by the third one, i.e.,

$$\begin{aligned} dV &= d\mathbf{r} \otimes d\mathbf{s} \cdot d\mathbf{t} = dr^1\mathbf{g}_1 \otimes ds^2\mathbf{g}_2 \cdot dt^3\mathbf{g}_3 \\ dV &= \mathsf{e}_{123} dr^1 ds^2 dt^3 = \sqrt{g}\, dr^1 ds^2 dt^3 \end{aligned} \tag{A.52}$$

A.16 Christoffel Symbol

In Eq. A.18, base vectors $\mathbf{g}_i$ or $\hat{\mathbf{g}}_i$ at an arbitrary point are respectively defined in curvilinear coordinate systems x^i and $\hat{x}^i$. In general, their differentials with respect to coordinates x^i or $\hat{x}^i$ are non-zero. Thus, the derivative of a first rank tensor (vector) with respect to coordinate x^j can be written as

$$\mathbf{U}_{,j} = \left(U^i\mathbf{g}_i\right)_{,j} = U^i_{,j}\mathbf{g}_i + U^i\mathbf{g}_{i,j} \tag{A.53}$$

In obtaining Eq. A.53, one recalls that vectors $\mathbf{g}_i$ are functions only of coordinates x^i. Thus, their partial derivatives are also vectors, which may be decomposed along base vectors $\mathbf{g}_i$ or $\mathbf{g}^i$, i.e.,

$$\mathbf{g}_{i,j} = \Gamma_{ijk}\mathbf{g}^k = \Gamma^k_{ij}\mathbf{g}_k \tag{A.54}$$

where the third rank tensors Γ_{ijk} and Γ_{ij}^{k} are respectively called the Christoffel symbols of the first and second kind, and are a measure of the curvature of the space. At this stage, the Christoffel symbols are newly defined symbols. Later on, more explicit expressions will be formulated for these symbols.

By dot-multiplying Eq. A.54 by the base vector $\mathbf{g}_k$ and using of the identity $\mathbf{g}_i \cdot \mathbf{g}^j = \delta_i^j$ and $g_{ij} = \mathbf{g}_i \cdot \mathbf{g}_j$ (Eq. A.35), one obtains:

$$\begin{aligned} \mathbf{g}_{i,j} \cdot \mathbf{g}_k &= \Gamma_{ijl}\mathbf{g}^l \cdot \mathbf{g}_k = \Gamma_{ij}^l \mathbf{g}_l \cdot \mathbf{g}_k \\ &= \Gamma_{ijl}\delta_k^l \quad = \Gamma_{ij}^l g_{lk} \\ &= \Gamma_{ijk} \quad = \Gamma_{ij}^l g_{lk} \end{aligned} \tag{A.55}$$

Also, by multiplying Eq. A.54 by $\mathbf{g}^k$, one obtains:

$$\begin{aligned} \mathbf{g}_{i,j} \cdot \mathbf{g}^k &= \Gamma_{ijl}\mathbf{g}^l \cdot \mathbf{g}^k = \Gamma_{ij}^l \mathbf{g}_l \cdot \mathbf{g}^k \\ &= \Gamma_{ijl}g^{lk} \quad = \Gamma_{ij}^l \delta_l^k \\ &= \Gamma_{ijk}g^{lk} \quad = \Gamma_{ij}^k \end{aligned} \tag{A.56}$$

Eqs. A.55 and A.56 provide the relationships between the Christoffel symbols of the first and second kinds. By differentiating both sides of the identity $\mathbf{g}_i \cdot \mathbf{g}^j = \delta_i^j$ (Eq. A.23), one obtains

$$\mathbf{g}_{i,k} \cdot \mathbf{g}^j + \mathbf{g}_i \cdot \mathbf{g}_{,k}^j = 0 \tag{A.57}$$

Using the identity in the first line of Eq. A.56, i.e., $\mathbf{g}_{i,k} \cdot \mathbf{g}^j = \Gamma_{ik}^j$, one obtains

$$\mathbf{g}_i \cdot \mathbf{g}_{,k}^j = -\Gamma_{ik}^j \tag{A.58}$$

Multiplying both sides of Eq. A.58 by $\mathbf{g}^n$, one obtains

$$\mathbf{g}_{,k}^j = -\Gamma_{nk}^j \mathbf{g}^n \tag{A.59}$$

After changing indices, one obtains

$$\mathbf{g}^{i}_{,j} = -\Gamma^{i}_{jk}\mathbf{g}^{k} \tag{A.60}$$

A.16.1 Symmetry Property

The Christoffel symbols are symmetric with respect to the first two indices. Recalling the Eq. A.19, $\mathbf{g}_i = \dfrac{\partial \mathbf{R}}{\partial x^i} = \mathbf{R}_{,i}$, and differentiating its both sides, one obtains

$$\mathbf{g}_{i,j} = \mathbf{R}_{,ij} = \mathbf{R}_{,ji} = \mathbf{g}_{j,i} \tag{A.61}$$

From Eqs. A.54 and A.61, one obtains

$$\mathbf{g}_{i,j} = \mathbf{g}_{j,i} = \Gamma_{ijk}\mathbf{g}^{k} = \Gamma_{jik}\mathbf{g}^{k} \quad , \quad \mathbf{g}_{i,j} = \mathbf{g}_{j,i} = \Gamma^{k}_{ij}\mathbf{g}_{k} = \Gamma^{k}_{ji}\mathbf{g}_{k} \tag{A.62}$$

Now, by dot-multiplying both sides by base vector $\mathbf{g}_l$ or $\mathbf{g}^l$, one obtains

$$\begin{aligned} \Gamma_{ijk}\mathbf{g}^{k}\cdot\mathbf{g}_{l} &= \Gamma_{jik}\mathbf{g}^{k}\cdot\mathbf{g}_{l} & \qquad \Gamma^{k}_{ij}\mathbf{g}_{k}\cdot\mathbf{g}^{l} &= \Gamma^{k}_{ji}\mathbf{g}_{k}\cdot\mathbf{g}^{l} \\ \Gamma_{ijl} &= \Gamma_{jil} & \qquad \Gamma^{l}_{ij} &= \Gamma^{l}_{ji} \end{aligned} \tag{A.63}$$

Eq. A.63 shows that the Christoffel symbols are symmetric with respect to the first two subscripts.

A.16.2 Evaluation of the Christoffel Symbol

Recalling the definition of the fundamental tensor $g_{ij} = \mathbf{g}_i \cdot \mathbf{g}_j$ (Eq. A.35) and differentiating both sides with respect to x^j, one obtains

$$\begin{aligned} g_{ij,k} &= \mathbf{g}_{i,k}\cdot\mathbf{g}_{j} + \mathbf{g}_{i}\cdot\mathbf{g}_{j,k} \\ &= \mathbf{g}_{i,k}\cdot\mathbf{g}_{j} + \mathbf{g}_{j,k}\cdot\mathbf{g}_{i} \end{aligned} \tag{A.64}$$

From Eq. A.55, by substituting into Eq. A.64, one obtains

$$g_{ij,k} = \Gamma_{ikj} + \Gamma_{ijk} \tag{A.65}$$

By writing Eq. A.65 three times while permuting subscripts each time, one obtains

$$\begin{aligned} g_{ij,k} &= \Gamma_{kij} + \Gamma_{jki} \\ g_{ki,j} &= \Gamma_{jki} + \Gamma_{ijk} \\ g_{jk,i} &= \Gamma_{kij} + \Gamma_{ijk} \end{aligned} \qquad \text{(A.66a-c)}$$

Subtracting Eq. A.66a from the sum of Eqs A.66b-c, one obtains

$$\Gamma_{ijk} = \frac{1}{2}\left(g_{ki,j} + g_{jk,i} - g_{ij,k}\right) \qquad \text{(A.67)}$$

Also, from Eq. A.67 by substituting into Eq. A.56, one obtains:

$$\Gamma^k_{ij} = \frac{1}{2} g^{kl}\left(g_{li,j} + g_{lj,i} - g_{ij,l}\right) \qquad \text{(A.68)}$$

Equations A.67 and A.68 relate the Christoffel symbols Γ_{ijk} and Γ^k_{ij} to the derivatives of the fundamental tensor g_{ij}

A.17 Covariant Derivatives

A.17.1 Covariant Derivative of First Order Tensors

From Eq. A.54, by substituting into Eq. A.53, one obtains:

$$\mathbf{U}_{,j} = \left(U^i \mathbf{g}_i\right)_{,j} = U^i_{,j}\mathbf{g}_i + U^i \Gamma^k_{ij}\mathbf{g}_k \qquad \text{(A.69)}$$

As i and k are dummy indices, they can be interchanged in the second term yielding

$$\mathbf{U}_{,j} = \left(U^i_{,j} + U^k \Gamma^i_{kj}\right)\mathbf{g}_i = U^i\,|_j\ \mathbf{g}_i \qquad \text{(A.70)}$$

in which

$$U^i\,|_j = \left(U^i_{,j} + U^k \Gamma^i_{kj}\right) \qquad \text{(A.71)}$$

where the symbol "$U^i\,|_j$" denotes the covariant derivative of contravariant first order tensor U^i with respect to x^j. In the same manner, the covariant derivative of a covariant first order tensor U_i with respect to x^j, $U_i\,|_j$, is defined as

$$\mathbf{U}_{,j} = \left(U_{i,j} - U_k \Gamma^k_{ij}\right)\mathbf{g}^i = U_i\,|_j\ \mathbf{g}^i \tag{A.72}$$

in which

$$U_i\,|_j = U_{i,j} - U_k \Gamma^k_{ij} \tag{A.73}$$

A.17.2 Covariant Derivative of Second Order Tensors

The covariant derivative of a second rank covariant tensor is

$$\mathbf{U}_{,k} = \left(U_{ij}\mathbf{g}^i\mathbf{g}^j\right)_{,k} = U_{ij,k}\mathbf{g}^i\mathbf{g}^j + U_{ij}\mathbf{g}^i_{,k}\mathbf{g}^j + U_{ij}\mathbf{g}^i\mathbf{g}^j_{,k} \tag{A.74}$$

Recalling the identity $\mathbf{g}^i_{,j} = -\Gamma^i_{jk}\mathbf{g}^k$ in Eq. A.60, and substituting into Eq. 1.74, one obtains

$$\begin{aligned}\mathbf{U}_{,k} &= U_{ij,k}\mathbf{g}^i\mathbf{g}^j - U_{ij}\Gamma^i_{km}\mathbf{g}^m\mathbf{g}^j - U_{ij}\mathbf{g}^i\Gamma^j_{km}\mathbf{g}^m \\ &= U_{ij,k}\mathbf{g}^i\mathbf{g}^j - U_{lj}\Gamma^l_{ki}\mathbf{g}^i\mathbf{g}^j - U_{il}\Gamma^l_{kj}\mathbf{g}^i\mathbf{g}^j \\ &= \left(U_{ij,k} - U_{lj}\Gamma^l_{ki} - U_{il}\Gamma^l_{kj}\right)\mathbf{g}^i\mathbf{g}^j \\ &= U_{ij}\,|_k\ \mathbf{g}^i\mathbf{g}^j\end{aligned} \tag{A.75}$$

in which

$$U_{ij}\,|_k = U_{ij,k} - U_{lj}\Gamma^l_{ik} - U_{il}\Gamma^l_{kj} \tag{A.76}$$

In the same manner, one obtains

$$U^{ij}\,|_k = U^{ij}_{\ \ ,k} + U^{lj}\Gamma^i_{kl} + U^{il}\Gamma^j_{kl} \tag{A.77}$$

$$U^i_j\,|_k = U^i_{j,k} + U^l_j\Gamma^i_{kl} - U^i_l\Gamma^l_{jk} \tag{A.78}$$

A.17.3 Second Covariant Derivative of First Order Covariant Tensors

It is observed that $U_i\,|_j = U_{i,j} - U_m\Gamma^m_{ij}$ is a second order covariant tensor. Applying the operator $U_{ij}\,|_k$ defined in Eq. A.76 to tensor $U_i\,|_j$, one obtains

$$\begin{aligned} U_i\,|_j|_k &= \left(U_{i,j} - U_m\Gamma^m_{ij}\right)|_k \\ &= \left(U_{i,j} - U_m\Gamma^m_{ij}\right)_{,k} - \left(U_{l,j} - U_m\Gamma^m_{lj}\right)\Gamma^l_{ik} - \left(U_{i,l} - U_m\Gamma^m_{il}\right)\Gamma^l_{kj} \\ &= U_{i,jk} - U_{m,k}\Gamma^m_{ij} - U_m\Gamma^m_{ij,k} - U_{l,j}\Gamma^l_{ik} + U_m\Gamma^m_{lj}\Gamma^l_{ik} - U_{i,l}\Gamma^l_{kj} + U_m\Gamma^m_{il}\Gamma^l_{kj} \\ &= U_i\,|_{jk} \end{aligned} \tag{A.79}$$

In the same manner, the second covariant derivative of a contravariant tensor is:

$$\begin{aligned} U^i\,|_j|_k &= \left(U^i_{,j} + U^m\Gamma^i_{mj}\right)|_k \\ &= \left(U^i_{,j} + U^m\Gamma^i_{mj}\right)_{,k} + \left(U^l_{,j} + U^m\Gamma^l_{mj}\right)\Gamma^i_{lk} - \left(U^i_{,l} + U^m\Gamma^i_{ml}\right)\Gamma^l_{kj} \\ &= U^i_{,jk} + U^m_{,k}\Gamma^i_{mj,k} + U^m\Gamma^i_{mj,k} + U^l_{,j}\Gamma^i_{lk} + U^m\Gamma^l_{mj}\Gamma^i_{lk} - U^i_{,l}\Gamma^l_{kj} - U^m\Gamma^i_{ml}\Gamma^l_{kj} \\ &= U^i\,|_{jk} \end{aligned} \tag{A.80}$$

A.18 Strain Expressions for a Continuum

A.18.1 Strains in Terms of First Fundamental Tensor

The convected coordinate system x^i is affixed to the un-deformed continuum. This implies that after deformation, the coordinate system x^i is transformed to the new coordinate system $\hat{x}^i$. In convected coordinate systems, the media and the coordinate system undergo the same deformation so that the position of a point in the media, before and after deformation, can be expressed through the same sets of coordinates $x^i\,(=\hat{x}^i)$. In a coordinate system x^i, the distance between two neighbouring points within a shell before deformation is:

$$d\mathbf{s} = \frac{\partial \mathbf{R}}{\partial x^i}dx^i = \mathbf{g}_i dx^i \tag{A.81}$$

The distance between the same two points after a time step dt, during which the continuum is subjected to the deformation, in the new coordinate system $\hat{x}^i$ is:

$$d\hat{\mathbf{s}} = \frac{\partial \hat{\mathbf{R}}}{\partial \hat{x}^i}d\hat{x}^i = \hat{\mathbf{g}}_i d\hat{x}^i \tag{A.82}$$

The Lagrangian strain $\boldsymbol{\eta}$ can be extracted from the normalized difference between the differential vectors $d\mathbf{s}$ and $d\hat{\mathbf{s}}$ as

$$\boldsymbol{\eta} = \frac{1}{2}\frac{d\hat{\mathbf{s}}\cdot d\hat{\mathbf{s}} - d\mathbf{s}\cdot d\mathbf{s}}{d\mathbf{s}\cdot d\mathbf{s}} \tag{A.83}$$

From Eqs. A.81 and A.82, by substituting into Eq. A.83, and noting that $\hat{x}^i = x^i$ (or $d\hat{x}^i = dx^i$), one obtains:

$$\boldsymbol{\eta} = \frac{1}{2}\frac{\left(\hat{g}_{ij} - g_{ij}\right)dx^i dx^j}{|d\mathbf{s}|^2} = \frac{1}{2}\left(\hat{g}_{ij} - g_{ij}\right)\frac{dx^i}{ds}\frac{dx^j}{ds} = \frac{1}{2}\left(\hat{g}_{ij} - g_{ij}\right)L^i L^j \tag{A.84}$$

in which $L^i = \frac{dx^i}{ds}$ and $L^j = \frac{dx^j}{ds}$ are the contravariant components of the unit vector $\mathbf{L} = L^i\mathbf{g}_i$ representing the direction of $d\mathbf{s}$. We introduce the definition

$$\eta_{ij} = \frac{1}{2}\left(\hat{g}_{ij} - g_{ij}\right) \tag{A.85}$$

in which η_{ij} is the Lagrangian strain tensor.

A.18.2 Strain Tensor In Terms of Displacements

The strain tensor defined in Eq. A.85 has been expressed in terms of the metric tensor. We need to express it in terms of the displacements. The displacement of an arbitrary point within the continuum is

$$\mathbf{U} = \hat{\mathbf{R}} - \mathbf{R} \tag{A.86}$$

where $\mathbf{R}$ and $\hat{\mathbf{R}}$ are the position vectors of the arbitrary point before and after deformation in coordinate systems x^i and $\hat{x}^i$, respectively. Taking the differential of Eq. A.86, one obtains

$$d\mathbf{U} = d\hat{\mathbf{R}} - d\mathbf{R} \tag{A.87}$$

Expanding Eq. A.87, one obtains

$$\left(\frac{\partial \mathbf{U}}{\partial x^i}dx^i + \frac{\partial \mathbf{U}}{\partial t}dt\right) = \left(\frac{\partial \hat{\mathbf{R}}}{\partial x^i}dx^i + \frac{\partial \hat{\mathbf{R}}}{\partial t}dt\right) - \left(\frac{\partial \mathbf{R}}{\partial x^i}dx^i + \frac{\partial \mathbf{R}}{\partial t}dt\right) \tag{A.88}$$

Grouping terms with the same differentials yields

$$\frac{\partial \mathbf{U}}{\partial x^i}dx^i = \frac{\partial \hat{\mathbf{R}}}{\partial x^i}dx^i - \frac{\partial \mathbf{R}}{\partial x^i}dx^i \tag{A.89}$$

From Eqs. A.71 and A.73, the derivative of displacement vector $\mathbf{U}$ with respect to x^i can be written as

$$\frac{\partial \mathbf{U}}{\partial x^j} = \mathbf{U}_{,j} = U_i\,|_j\ \mathbf{g}^i = U^i\,|_j\ \mathbf{g}_i \tag{A.90}$$

From Eq. A.90, by substituting into Eq. A.89, one obtains

$$U^k\,|_i\ \mathbf{g}_k dx^i = \hat{\mathbf{g}}_i dx^i - \mathbf{g}_i dx^i \tag{A.91}$$

Or,

$$\hat{\mathbf{g}}_i = \mathbf{g}_i + U^k\,|_i\ \mathbf{g}_k \tag{A.92}$$

Using Eq. A.92, the metric tensor in the deformed coordinate system can be written as:

$$\begin{aligned}\hat{g}_{ij} = \hat{\mathbf{g}}_i \cdot \hat{\mathbf{g}}_j &= \left(\mathbf{g}_i + U^k\,|_i\ \mathbf{g}_k\right)\cdot\left(\mathbf{g}_j + U^l\,|_j\ \mathbf{g}_l\right) \\ &= g_{ij} + U^k\,|_i\ g_{kj} + U^l\,|_j\ g_{jl} + U^k\,|_i\ U^l\,|_j\ g_{kl}\end{aligned} \tag{A.93}$$

By evoking the operation of lowering indices (A.11) to the last three terms of the right hand side of the Eq. A.93, one obtains

$$\hat{g}_{ij} = g_{ij} + U_i\,|_j + U_j\,|_i + U^k\,|_i\ U_k\,|_j \tag{A.94}$$

From Eq. A.94, by substituting into Eq. A.85, one obtains:

$$\eta_{ij} = \tfrac{1}{2}\left(U_i\,|_j + U_j\,|_i + U^k\,|_i\ U_k\,|_j\right) \tag{A.95}$$

A.19 Hamilton's Principle in Tensor Form

In general, Hamilton's principle is expressed as

$$\delta \prod = \int_{t_1}^{t_2} \delta(T^* - V^*)dt + \int_{t_1}^{t_2} \delta W^* dt = 0 \tag{A.96}$$

where $\prod$ is the mechanical energy of the system, T^*, V^* and W^* are the kinetic energy, potential energy and external work in the system, respectively. Symbol δ denotes the variation operator and integration is performed over an arbitrary period starting from time t_1 to time t_2 [A.6]. In the following subsections it will be shown that the variation of different entities of Eq. A.96 can be written as

$$\delta T^* = \int_V \rho \dot{U}^i \delta \dot{U}_i dV \tag{A.97}$$

$$\delta V^* = \int_V E^{ijkl} \eta_{kl} \delta \eta_{ij} dV \tag{A.98}$$

and

$$\delta W^* = \int_V F^i \delta U_i dV \tag{A.99}$$

A.19.1 Kinetic Energy

The kinetic energy is expressed as

$$\begin{aligned} T^* &= \int_V \tfrac{1}{2}\rho \dot{\mathbf{U}} \cdot \dot{\mathbf{U}} dV = \int_V \tfrac{1}{2}\rho \left(\dot{U}^i \mathbf{g}_i\right) \cdot \left(\dot{U}_j \mathbf{g}^j\right) dV = \int_V \tfrac{1}{2}\rho \dot{U}^i \dot{U}_j \left(\mathbf{g}_i \cdot \mathbf{g}^j\right) dV \\ &= \int_V \tfrac{1}{2}\rho \dot{U}^i \dot{U}_j \delta_i^j dV = \int_V \tfrac{1}{2}\rho \dot{U}^i \dot{U}_i dV \end{aligned} \tag{A.100}$$

By taking the variation of kinetic energy, one obtains

$$\delta T^* = \delta \int_V \tfrac{1}{2}\dot{U}^i \rho \dot{U}_i dV = \int_V \tfrac{1}{2}\left(\delta \dot{U}^i \rho \dot{U}_i + \dot{U}^i \rho \delta \dot{U}_i\right) dV \tag{A.101}$$

By applying the identity $g_{ij}g^{ij}=1$ which is valid in any orthogonal coordinate system to the first term of the integral and using the operations of lowering and raising the indices, $\dot{U}_j = g_{ij}\dot{U}^i$ and $\dot{U}^j = g^{ij}\dot{U}_i$ for first rank tensors $\dot{U}^i$ and $\dot{U}_i$, one can write

$$\begin{aligned}\delta T^* &= \int_V \tfrac{1}{2}\left[\left(\delta\dot{U}^i g_{ij}\right)\rho\left(\dot{U}_i g^{ij}\right)+\dot{U}^i\rho\delta\dot{U}_i\right]dV \\ &= \int_V \tfrac{1}{2}\left[\left(\delta\dot{U}_j\right)\rho\left(\dot{U}^j\right)+\dot{U}^i\rho\delta\dot{U}_i\right]dV\end{aligned} \tag{A.102}$$

Changing the dummy indices j in the first term and simplifying yields

$$\delta T^* = \delta\int_V \tfrac{1}{2}\dot{U}^i\rho\dot{U}_i dV = \int_V \dot{U}^i\rho\delta\dot{U}_i dV \tag{A.103}$$

A.19.2 Internal Strain Energy

The internal strain energy V^* is

$$\begin{aligned}V^* &= \int_V \tfrac{1}{2}\boldsymbol{\sigma}\cdot\cdot\boldsymbol{\eta}dV = \int_V \tfrac{1}{2}\left(\sigma^{\alpha\beta}\mathbf{g}_\alpha\mathbf{g}_\beta\right)\cdot\cdot\left(\eta_{\gamma\kappa}\mathbf{g}^\gamma\mathbf{g}^\kappa\right)dV \\ &= \int_V \tfrac{1}{2}\sigma^{\alpha\beta}\eta_{\gamma\kappa}\left(\mathbf{g}_\alpha\cdot\mathbf{g}^\gamma\right)\left(\mathbf{g}_\beta\cdot\mathbf{g}^\kappa\right)dV = \int_V \tfrac{1}{2}\sigma^{\alpha\beta}\eta_{\gamma\kappa}\delta_\alpha^\gamma\delta_\beta^\kappa dV = \int_V \tfrac{1}{2}\sigma^{\alpha\beta}\eta_{\alpha\beta}dV\end{aligned} \tag{A.104}$$

By taking the variation of the internal strain energy, one obtains

$$\begin{aligned}\delta V^* &= \delta\int_V \tfrac{1}{2}E^{\alpha\beta\lambda\delta}\eta_{\lambda\delta}\eta_{\alpha\beta}dV \\ &= \int_V \tfrac{1}{2}E^{\alpha\beta\lambda\delta}\left(\delta\eta_{\lambda\delta}\eta_{\alpha\beta}+\eta_{\lambda\delta}\delta\eta_{\alpha\beta}\right)dV \\ &= \int_V \left(\tfrac{1}{2}E^{\alpha\beta\lambda\delta}\delta\eta_{\lambda\delta}\eta_{\alpha\beta}+\tfrac{1}{2}E^{\alpha\beta\lambda\delta}\eta_{\lambda\delta}\delta\eta_{\alpha\beta}\right)dV\end{aligned} \tag{A.105}$$

Recalling Eqs. 2.B.1 and 2.B.6, one can write

$$E^{\alpha\beta\lambda\delta} = E^{\beta\alpha\lambda\delta} = E^{\beta\alpha\delta\lambda} = E^{\alpha\beta\delta\lambda} \quad , \quad E^{\alpha\beta\lambda\delta} = E^{\lambda\delta\alpha\beta} \tag{A.106}$$

Based on the above equalities and using the identity $E^{\alpha\beta\lambda\delta} = E^{\lambda\delta\alpha\beta}$ and interchanging the dummy indices $\alpha\beta$ and $\lambda\delta$ in the first term of Eq. A.105, one obtains

$$\begin{aligned}\delta V^* &= \int_V \left(\tfrac{1}{2}E^{\alpha\beta\lambda\delta}\delta\eta_{\lambda\delta}\eta_{\alpha\beta} + \tfrac{1}{2}E^{\alpha\beta\lambda\delta}\eta_{\lambda\delta}\delta\eta_{\alpha\beta}\right)dV \\ &= \int_V \left(\tfrac{1}{2}E^{\lambda\delta\alpha\beta}\eta_{\alpha\beta}\delta\eta_{\lambda\delta} + \tfrac{1}{2}E^{\alpha\beta\lambda\delta}\eta_{\lambda\delta}\delta\eta_{\alpha\beta}\right)dV \\ &= \int_V \left(\tfrac{1}{2}E^{\alpha\beta\lambda\delta}\eta_{\lambda\delta}\delta\eta_{\alpha\beta} + \tfrac{1}{2}E^{\alpha\beta\lambda\delta}\eta_{\lambda\delta}\delta\eta_{\alpha\beta}\right)dV \\ &= \int_V E^{\alpha\beta\lambda\delta}\eta_{\lambda\delta}\delta\eta_{\alpha\beta}dV\end{aligned} \tag{A.107}$$

A.19.3 External Work

The external work W^* is

$$\begin{aligned}W^* &= \int_V \mathbf{F}\cdot\mathbf{U}dV = \int_V \left(F^i g_i\right)\cdot\left(U_i g^i\right)dV = \int_V F^i U_i\left(\mathbf{g}_i\cdot\mathbf{g}^i\right)dV \\ &= \int_V F^i U_j \delta_i^j dV = \int_V F^i U_i dV\end{aligned} \tag{A.108}$$

Considering that the external forces are specified, the variation of the external work is

$$\delta W^* = \delta\int_V F^i U_i dV = \int_V F^i \delta U_i dV \tag{A.109}$$

A.20 Physical Components of Tensors

Defining tensors in terms of base vectors gives them power and flexibility in conducting mathematical derivations. Nevertheless, their physical components are frequently sought in order to provide more concrete and more realistic quantities. When this is the case, one needs to express them in terms of the unit vectors rather than the base vectors. Recalling the first rank tensor relation $\mathbf{V} = V^i\mathbf{g}_i$ expressed in Eq. A.27 and multiplying and dividing the right hand side by $\sqrt{g_{kk}}$, ($\sqrt{g_{kk}}$ being the length of the base vector $\mathbf{g}_i$), one obtains

$$\mathbf{V} = V^i \mathbf{g}_i = \sqrt{g_{ii}}\, V^i \frac{\mathbf{g}_i}{\sqrt{g_{ii}}} = \bar{V}^i \mathbf{e}_i \text{, (no sum on } k\text{)} \tag{A.110}$$

In Eq. A.110, $\mathbf{e}_i = \mathbf{g}_i \big/ \sqrt{g_{ii}}$ are unit vectors along the base vectors $\mathbf{g}_i$ and the quantities $\bar{V}^i = \sqrt{g_{ii}}\, V^i$ are the physical components of the first order tensor $\mathbf{V}$. In the same manner,

$$\mathbf{V} = V_i \mathbf{g}^i = \sqrt{g^{ii}}\, V_i \frac{\mathbf{g}^i}{\sqrt{g^{ii}}} = \bar{V}_i \mathbf{e}^i \text{, (no sum on } i\text{)} \tag{A.111}$$

where $\mathbf{e}^i = \mathbf{g}^i \big/ \sqrt{g^{ii}}$ are unit vectors along the base vectors $\mathbf{g}^i$ and the quantities $\bar{V}_i = \sqrt{g^{ii}}\, V_i$ are the physical components of the first rank tensor $\mathbf{V}$. In general for a higher rank mixed tensor $\mathbf{A}$,

$$\begin{aligned} \mathbf{A} &= A^{i\ldots j}_{k\ldots l} \mathbf{g}_i \ldots \mathbf{g}_j \mathbf{g}^k \ldots \mathbf{g}^l \\ &= \sqrt{g_{ii}} \ldots \sqrt{g_{jj}} \sqrt{g^{kk}} \ldots \sqrt{g^{ll}}\, A^{i\ldots j}_{k\ldots l} \frac{\mathbf{g}_i}{\sqrt{g_{ii}}} \ldots \frac{\mathbf{g}_j}{\sqrt{g_{jj}}} \frac{\mathbf{g}^k}{\sqrt{g^{kk}}} \ldots \frac{\mathbf{g}^l}{\sqrt{g^{ll}}} \\ &= \bar{A}^{i\ldots j}_{k\ldots l} \mathbf{e}_i \ldots \mathbf{e}_j \mathbf{e}^k \ldots \mathbf{e}^l \end{aligned} \tag{A.112}$$

(no summation on i, j, k and l)

where vectors $\mathbf{e}_i = \frac{\mathbf{g}_i}{\sqrt{g_{ii}}}, \ldots, \mathbf{e}^l = \frac{\mathbf{g}^l}{\sqrt{g^{ll}}}$ are unit vectors along the base vectors $\mathbf{g}_i, \ldots, \mathbf{g}^l$ respectively, and the quantities $\bar{A}^{i\ldots j}_{k\ldots l} = \sqrt{g_{ii}} \ldots \sqrt{g_{jj}} \sqrt{g^{kk}} \ldots \sqrt{g^{ll}}\, A^{i\ldots j}_{k\ldots l}$ are the physical components of tensor $\mathbf{A}$.

A.21 References

[A.1] I. S. Sokolnikoff, Tensor Analysis Theory And Applications To Geometry And Mechanics Of Continua, Second Edition, John Wiley & Sons, Inc., New York, 1965.

[A.2] J.L. Mercier, An Introduction To Tensor Calculus, Wolters-Noordhoff Publishing, Groningen, The Netherlands, 1971.

[A.3] W. Flugge, Tensor Analysis And Continuum Mechanics, Springer-Verlag, New York, 1972.

[A.4] F.I. Niordson, Shell Theory, North-Holland Series In Applied Mathematics and Mechanics, North-Holland Amsterdam, 1985.

[A.5] Wikipedia: http://en.wikipedia.org/wiki/Tensor (accessed 2009-11-26)

[A.6] A. Bedford, Hamilton's principle in continuum mechanics, Pitman Advanced Publishing Program, Boston, 1985.

A.22 List of symbols

$\mathbf{a}_i$	Covariant base vectors of the middle surface
a_{ij}	First fundamental tensor defined on the middle surface of a thin shell
a	Determinant of the first fundamental tensor a_{ij}
$b_{\alpha\beta}$	Curvature tensor of the surfaces parallel and adjacent to the middle surface
$\overline{b}_{\alpha\beta}$	Second fundamental tensor or curvature tensor defined on the middle surface of a thin shell
$\mathbf{a}^i$	Contravariant base vectors of the middle surface
a^{ij}	First fundamental tensor of the second kind defined on the middle surface of a thin shell
$\mathbf{g}_i$	Covariant base vectors of any surface parallel and adjacent to the middle surface
g_{ij}	First fundamental tensor defined within the shell
g	Determinant of the first fundamental tensor g_{ij}
$\mathbf{g}^i$	Contravariant base vectors of any surface parallel and adjacent to the middle surface

g^{ij}	First fundamental tensor of the second kind defined within the shell
$\mathbf{U}$	Displacement of a point within the shell
U_i	Covariant components of the displacement of a point on a surface parallel and adjacent to the middle surface along axis x^i
u_i	Covariant components of the displacement of a point on the middle surface along axis x^i
u, v, w	Components of the displacement of a point on the middle surface along axes x^1, x^2 and x^3, respectively
X^i	Coordinate system/Coordinates of the system
x^i	Coordinate system/Coordinates of the system
x, s, z	Coordinates of the system, equivalent to x^1, x^2 and x^3, respectively
$^{\alpha}, _{\alpha}, ...$	All Greek superscripts or subscripts range from 1 to 2
$^{i}, _{i}, ...$	All Italic superscripts or subscripts range from 1 to 3
$\vec{\mathbf{i}}_i, \vec{\mathbf{j}}_i$	Covariant unit vectors along axis x^i in middle surface and adjacent surfaces, respectively

$\vec{\mathbf{i}}^i, \vec{\mathbf{j}}^i$	Contravariant unit vectors along axis x^i in middle surface and adjacent surfaces, respectively
Γ_{ij}^k	Christoffel symbols in terms of g_i and g_{ij}
$\overline{\Gamma}_{ij}^k$	Christoffel symbols in terms of a_i and a_{ij} (defined for the middle surface)
$\cdot$	Inner product
$\otimes$	Cross product
$\vert$	Covariant derivative
$\Vert$	Covariant derivative in two dimensional spaces
T^*	Kinetic energy
V^*	Potential energy
V	Volume
W^*	External work
Π	Mechanical energy of the system
ε_{ij}	Components of the strain tensor on the middle surface
η_{ij}	Components of the strain tensor adjacent to the middle surface

$\eta_{\alpha\beta}$	In-plane components of the Strain tensor
σ^{ij}	Stress tensor
$\sigma^{\alpha\beta}$	In-plane components of the stress tensor
E^{ijlm}	Generalized Hooke's Law
$E^{\alpha\beta\lambda\delta}$	In-plane components of the generalized Hooke's Law
$\cdots_{,i}$	Partial derivative with respect to x^i
δ^{α}_{β}	Kronecker delta function
μ^{α}_{β}	The covariant tensor which connects the base vectors of two different points
$\lambda^{\gamma}_{\alpha}$	Contravariant counterpart of μ^{α}_{β}
ρ	Density of the mass
E	Modulus of elasticity
ν	Poisson's ratio